Cardiff School of Pharmacy and Pharmaceutical Sciences, Cardiff University

Computer-aided design, synthesis and evaluation of novel antiviral compounds

A thesis submitted in accordance with the conditions governing candidates for the degree of

Philosophiae Doctor in Cardiff University

Michela Cancellieri

Supervisor: Dr. Andrea Brancale

October 2014

Ringraziamenti

La prima persona a cui vanno i miei ringraziamenti e' Andrea, un invidiabile supervisor, a cui devo la possibilita' di aver lavorato a questo progetto e di aver contribuito alla mia crescita professionale. Grazie Andrea per i consigli non solo di lavoro, ma anche personali e per avermi sempre permesso di essere me stessa, senza bisogno di formalismi, con il mio linguaggio colorito e i miei modi a volte bruschi ma sinceri.

La piu' bella cosa che questa esperienza potesse regalarmi e' l'aver conosciuto delle persone molto speciali che non smettero' di vedere e sentire una volta chiusa questa parentesi. Immensa gratitudine va alla persona di cui piu' sentiro' piu' la mancanza, Marcella, con la quale si e' stretta una bellissima complicita' ed amicizia. Grazie Marcella per essere stata mia guida e sostenitrice, per la pazienza che hai avuto e il tuo preziosissimo aiuto. Il continuo entusiasmo e i sorrisi con cui mi hai sempre accolto e confortato sono ineguagliabili, sei davvero la migliore compagna di viaggio che potessi desiderare e la piu' bella scoperta di questa avventura.

I miei ringraziamenti vanno anche a te, caro Salvotto, il burbero dal cuore dolce e tenero, sempre pronto ad aiutarmi e con cui sono libera di esprimere il mio essere a volte un po' maschiaccio.

Un pensiero va anche anche a Samia con le sue pillole di saggezza, a Gilda, per aver portato un' aria di giovialita' in laboratorio, a Francy, Silvi, Lucy, Rulli, Eli e Patz, per aver accorciato le distanze che ci separavano con il fedele diario di bordo e alla mia migliore amica Lola, per aver detto sempre le parole giuste al momento giusto, senza il bisogno di cercarsi.

Impossibile non ringraziare la mia famiglia, per avermi sempre incoraggiato nelle mie scelte e, in particolar modo, mia madre, confidente ed amica, l'unica a riconoscere solo da uno sguardo i miei altalenanti stati d'animo, nonostante i 1.557,49 km che ci separano. Profonda riconoscenza per la mia adorabile zia, che anche in questa circostanza si e' rivelata la migliore dispensiera di consigli di vita. In ultimo, ma non per importanza, Daniele: nonostante la paura e i timori inziali, ti sei lasciato convincere da questa folle ragazza che ti ha scelto come uomo e compagno di vita. Grazie per saper domare il mio animo ribelle, per i tuoi ''non preoccuparti, bensi' occupati'', per prenderti cura amorevole di me, ma soprattutto per aver sconvolto la tua quotidianita' ed avere seguito/inseguito me e i miei sogni.

Abstract

RNA viruses are a major cause of disease that in the last fifteen years counted for frequent outbreaks, infecting both humans and animals. Examples of emerging or ri-emerging viral pathogens are the Foot-and-Mouth disease virus (FMDV) for animals, Chikungunya virus (CHIKV), Coxsackie virus B3 (CVB3) and Respiratory Syncytial virus (RSV) for humans, all responsible for infections associated with mild to severe complications. Although both vaccines and small-molecule compounds are at different stages of development, no selective antiviral drugs have been approved so far, therefore for all four these viruses improved treatment strategies are required. Promising targets are the viral non-structural proteins, which are commonly evaluated for the identification of new antivirals. Starting from the study of different viral proteins, several computer-aided techniques were applied, aiming to identify hit molecules first, and secondly to synthesise new series of potential antiviral compounds. The available crystal structures of some of the proteins that play a role in viral replication were used for structure- and ligand-based virtual screenings of commercially available compounds against CVB3, FMDV and RSV. New families of potential anti-CHIKV compounds were rationally designed and synthesized, in order to establish a structure-activity relationship study on a lead structure previously found in our group. Finally, a *de-novo* drug design approach was performed to find a suitable scaffold for the synthesis of a series of zinc-ejecting compounds against RSV. Inhibition of virus replication was evaluated for all the new compounds, of which different showed antiviral potential.

Table of contents

Chapter 1: Molecular Modelling in drug discovery

1.1 The drug discovery ‘game’ 2

1.2 Introduction to Molecular Modelling 3
- 1.2.1 Quantum mechanics 3
- 1.2.2 Molecular mechanics 4
- 1.2.3 Energy minimization 5
- 1.2.4 Conformational analysis 6

1.3 Computational approaches in drug discovery 7
- 1.3.1 Homology modelling 7
- 1.3.2 Ligand-based drug design 8
- 1.3.3 Pharmacophore models 8
- 1.3.4 Structure-based drug design 9
- 1.3.5 Docking and Scoring 10

1.4 Aims of the study 12

References 13

Chapter 2: Coxsackie Virus B3

Introduction to the virus 17

2.1 Coxsackie virus B3 17
- 2.1.1 Virion structure 18
- 2.1.2 Genome organization 18
- 2.1.3 Viral proteins 19
- 2.1.4 Viral life cycle 20
- 2.1.5 Current treatment 21

2.2 3A protein and 3D polymerase as antiviral targets 22
- 2.2.1 3A protein 22
- 2.2.2 RNA-dependent RNA polymerase 23

Results and discussion **27**

2.3 Structure-based Virtual Screening on the 3A protein **27**
2.3.1 Homology model 27
2.3.2 Pharmacophore models 27
2.3.3 Molecular docking and consensus scoring 30

2.4 Design and synthesis of tetrazole derivatives **31**
2.4.1 (Benzylthio)-1-aryl-1*H*-tetrazoles 31
2.4.2 Biological evaluation 40

2.5 Computer-aided approaches on the 3D polymerase **41**
2.5.1 Structure-based Virtual Screening 41
2.5.2 Model of the GPC-N114 bound to the polymerase 44
2.5.3 Design of new GPC-N114 analogues 45

2.6 Synthesis of GPC-N114 analogues **49**
2.6.1 2,5-bis-Aryl-1,3,4-oxadiazoles 49
2.6.2 1,3-bis-Aryl-1*H*-benzo[*d*]imidazol-2(3*H*)-ones 51
2.6.3 1-Methyl-3,4-bis(phenylamino)-1*H*-pyrrole-2,5-dione 54
2.6.4 1-Methyl-3,4-bis(4-nitrophenylamino)-1*H*-pyrrole-2,5 dione 58
2.6.5 N^1-Phenylbenzene-1,2-diamine 60
2.6.6 N^1,N^2-Diphenylbenzene-1,2-diamine 61
2.6.7 Biological evaluation 62

2.7 Design and docking validation of new GPC-N114 analogues **64**
2.7.1 Bis-Aryl sulfonamides 65
2.7.2 bis-Aryl amides 66
2.7.3 Biological evaluation 67

2.8 Ligand-based Virtual Screening **70**
2.8.1 Shape complementarity search with ROCS 70

Conclusions **72**

References **75**

Chapter 3: Foot-and-mouth Disease Virus

Introduction to the virus **82**

3.1 Foot-and-mouth Disease Virus **82**
3.1.1 Diversity and similarity to other Picornaviruses 82
3.1.2 Current treatment 83

Results and discussion **84**

3.2 Structure-based Virtual Screening on the FMDV polymerase **84**

3.3 *De novo* drug design approach **87**

3.4 Synthesis of coumarin-based structures **88**
3.4.1 7-((1*H*-Benzo[*d*]imidazol-2-*yl*)methoxy)-2*H*-chromen-2-one 88
3.4.2 *N*-(2-Oxo-2*H*-chromen-7-*yl*)-1*H*-Benzo[*d*]imidazole-2-carboxamide 89
3.4.3 7-Aryl thio methyl-2*H*-chromen-2-ones 91
3.4.4 7-Aryl sulfinyl methyl-2*H*-chromen-2-ones 93
3.4.5 7-Aryl sulfonyl methyl-2*H*-chromen-2-ones 94
3.4.6 Biological evaluation 97

Conclusions **98**

References **99**

Chapter 4: Chikungunya Virus

Introduction to the virus **103**

4.1 Chikungunya Virus **103**
4.1.1 Virion structure 103
4.1.2 Genome organization 104
4.1.3 Viral proteins 104
4.1.4 Viral life cycle 105
4.1.5 Current treatment 106

4.2 nsP2 protease **107**
4.2.1 Structure 107
4.2.2 Mechanism of action 108

Results and discussion **109**

4.3 nsP2 Protease as a target for the identification of new antivirals **109**
4.3.1 Project background 109
4.3.2 Design and synthesis of novel derivatives 112

4.4 Synthesis of (2*E*)-*N*'-benzylidene aryl acrylohydrazides **113**
4.4.1 (2*E*)-*N*'-Benzylidene aryl acrylohydrazides 114
4.4.2 (2*E*)-*N*'-(4-Hydroxybenzylidene)-3-(4-isopropylphenyl)acrylohydrazide 117
4.4.3 Biological evaluation 119

4.5 Synthesis of *N*-(1*H*-benzo[*d*]imidazol-2-*yl*)aryl amides **121**
4.5.1 *N*-(1*H*-Benzo[*d*]imidazol-2-*yl*)-3-(4-*tert*-butylphenyl)propanamides 122
4.5.2 (*N*-)1*H*-Benzo[*d*]imidazol-2-*yl*)-3-(4-*tert*-butylphenyl)propanamides 124
4.5.3 Biological evaluation 126

4.6 Synthesis of 1-phenethyl-4-phenyl-1*H*-1,2,3-triazole **128**
4.6.1 Biological evaluation 131

4.7 Synthesis of (*E*)-2-benzylidene-*N*-(4-*tert*-butylstyryl)hydrazinecarboxamides **132**
4.7.1 *N*-((*E*)-(4-*tert*-Butyl)styryl)-2-(benzylidene) hydrazinecarboxamides 133
4.7.2 Biological evaluation 135

4.8 Synthesis of 2-(benzylidene)-*N*-aryl hydrazinecarbothiamides **136**
4.8.1 2-(Benzylidene)-*N*-aryl hydrazinecarbothiamides 137
4.8.2 Biological evaluation 139

Conclusions **140**

References **141**

Chapter 5: Respiratory syncytial virus

Introduction to the virus **150**

5.1 Respiratory Syncytial Virus **150**
5.1.1 Virion structure 150
5.1.2 Genome organization 151
5.1.3 Viral proteins 152
5.1.4 Viral life cycle 153
5.1.5 Current treatment 154
5.1.6 New treatments under development 154
5.1.7 Vaccines under development 156

5.2 M2-1 protein **157**
5.2.1 Structure 157
5.2.2 Mechanism of action 159

5.3 Fusion protein **160**
5.3.1 Structure 160
5.3.2 RSV entry inhibitors targeting F protein 162

Results and discussion **164**

5.4 M2-1 protein as a target for drug design of new antivirals **164**
5.4.1 Zinc-binding domain of M2-1 protein as a target for *de novo* design 164
5.4.2 *De novo* drug design 165

5.5 Synthesis of aryl dithiocarbamates **167**
5.5.1 2-Chloromethyl benzoimidazol carbodithioates 167
5.5.2 2-Chloromethyl benzoxazol carbodithioates 169
5.5.3 2-Chloromethyl benzothiazole carbodithioates 171
5.5.4 Aryl dithioates 172
5.5.5 Dithiocarbamate methyl aryl acids 174
5.5.6 Biological evaluation 176

5.6 Structure-based Virtual Screening on the M2-1 protein 179
5.6.1 Pharmacophoric filter and docking methods 179

5.7 Ligand-based Virtual Screening on the F protein 182

Conclusions 184

References 186

Conclusions 197

Chapter 6: Experimental part

6.1 General information 202
6.1.1 Molecular Modelling 202

6.2 Synthesis of tetrazoles derivatives 203
6.2.1 General procedures 1-5 203
6.2.2 Aryl isothiocyanates 207
6.2.3 Aryl mercaptotetrazoles 211
6.2.4 Benzylthio-1-aryl-1*H*-tetrazoles 215
6.2.5 (5-(Benzylthio)-1*H*-tetrazol-1-*yl*)benzoic acids 223
6.2.6 Ethyl 4-(5-(benzylthio)-1*H*-tetrazol-1-*yl*)benzoates 226

6.3 Synthesis of 2,5-bis-aryl-1,3,4-oxadiazoles 228
6.3.1 General procedures 6-7 228
6.3.2 2-Phenylacetic acid 229
6.3.3 Ethyl 2-(4-nitrophenyl)acetate 229
6.3.4 Aryl acetohydrazides 231
6.3.5 2,5-bis-Aryl-1,3,4-oxadiazoles 233

6.4 1,3-bis-Aryl-1*H*-benzo[*d*]imidazol-2(3*H*)-ones 235
6.4.1 General procedure 8: synthesis of 1,3-bis-aryl-1*H*-benzo[*d*]imidazol-2(3*H*)-ones 235
6.4.2 1,3-1*H*-Benzo[*d*]imidazol-2(3*H*)-one 235
6.4.3 1,3-bis-Aryl benzoimidazol-2-ones 237

6.5 Methyl-3,4-bis(phenylamino)-1*H*-pyrrole-2,5-dione 239
6.5.1 *N*-Methyl-3,4-dibromomaleimide 239

6.5.2 3-Bromo-1-methyl-4-(phenylamino)-1*H*-pyrrole-2,5-dione 239
6.5.3 1-Methyl-3,4-bis(phenylamino)-1*H*-pyrrole-2,5-dione 240

6.6 Synthesis of *N*[1]-phenylbenzene-1,2-diamine 241

6.7 Synthesis of arylsulfonamides 243
6.7.1 General procedure 9: synthesis of bis-sulfonamido derivatives 243

6.8 Aryl amides 255
6.8.1 General procedure 10: synthesis of bis-amido derivatives 255

6.9 Synthesis of aryl coumarin structures 267
6.9.1 General procedures 11-13 267
6.9.2 Synthesis of 7-bromomethyl coumarin 268
6.9.3 Synthesis of 6-amino coumarin 269
6.9.4 Synthesis of 7-((1*H*-benzo[*d*]imidazol-2-*yl*)methoxy)-2*H*-chromen-2-one 270
6.9.5 Synthesis of *N*-(2-oxo-2*H*-chromen-7-*yl*)-1*H*-benzo[*d*]imidazole-2-carboxamide 271
6.9.6 Aryl thio methyl 2*H*-chromen-2-ones 272
6.9.7 Aryl sulfinyl methyl-2*H*-chromen-2-ones 271
6.9.8 Aryl sulfonyl methyl-2*H*-chromen-2-ones 276

6.10 Synthesis of (2*E*)-*N*'-benzylidene aryl acrylohydrazides 278
6.10.1 General procedures14-17 278
6.10.2 Aryl acrylic acids 280
6.10.3 Aryl acryloyl chlorides 283
6.10.4 Aryl hydrazones 286
6.10.5 *N*'-Benzylideneacrylohydrazides 289
6.10.6 *E*)-3-(4-Isopropylphenyl)acrylohydrazide 301
6.10.7 *N*'-(4-Hydroxybenzylidene)-3-(4-isopropylphenyl)acrylohydrazide 302

6.11 (*E*)-*N*-(1*H*-Benzo[*d*]imidazol-2-*yl*)-3-(4-*tert*-butylphenyl)acrylamides 303
6.11.1 General procedures 18-19 303
6.11.2 (*E*)-3-(4-*tert*-Butylphenyl)acrylic acid 305
6.11.3 Substituted 2-aminobenzimidazoles 306

6.11.4 (*E*)-*N*-(1*H*-Benzo[*d*]imidazol-2-yl)-3-(4-*tert*-butylphenyl)acrylamides 308

6.12 Synthesis of *N*-(1*H*-benzo[*d*]imidazol-2-*yl*)-3-(4-*tert*-butylphenyl)propanamides 310

6.12.1 General procedure 20: synthesis of *N*-(1*H*-benzo[*d*]imidazol-2-*yl*)-3-(4-*tert*-butylphenyl)propanamides 310

6.12.2 3-(4-*tert*-Butylphenyl)propanoic acid 310

6.12.3 3-(4-*tert*-Butylphenyl)propanoyl chloride 311

6.12.4 Benzoimidazol-4-*tert*-butylphenyl)propanamides 312

6.13 Synthesis of 1-phenethyl-4-*p*-tolyl-1*H*-1,2,3-triazole 314

6.13.1 2-(Azidoethyl)benzene 314

6.13.2 1-Phenethyl-4-*p*-tolyl-1*H*-1,2,3-triazole 314

6.14 Synthesis of (*E*)-2-benzylidene-*N*-(4-*tert*-butylstyryl)hydrazinecarboxamides 316

6.14.1 General procedure 21: synthesis of -2-benzylidene-*N*-(4-*tert*-butylstyryl)hydrazinecarboxamides 316

6.14.2 (*E*)-3-(4-*tert*-Butylphenyl)acryloyl azide 317

6.14.3 2-Benzylidene-*N*-(4-*tert*-butylstyryl) hydrazinecarboxamides 318

6.15 Synthesis of 2-arylidene-*N*-phenetylhydrazine carbothioamides 322

6.15.1 General procedure 22: synthesis of 2-arylidene-*N*-phenetyl hydrazine carbothioamides 322

6.15.2 (2-Isothiocyanatoethyl)benzene 322

6.15.3 2-Arylidene-*N*-phenetylhydrazinecarbothioamides 324

6.16 Synthesis of dithiocarbamate structures 327

6.16.1 General procedures 23-24 327

6.16.2 Benzyl piperazine 328

6.16.3 2-(Bromomethyl)benzo[*d*]oxazole 328

6.16.4 2-(Chloromethyl)benzo[*d*]thiazole 329

6.16.5 Methyl 4-bromo-3-nitrobenzoate 330

6.16.6 2-Chloromethyl benzoimidazol carbodithioates 331

6.16.7 2-Chloromethyl benzo[*d*]oxazol carbodithioates 335

6.16.8 2-Chloromethyl benzo[*d*]thiazol carbodithioates 338
6.16.9 Aryl carbodithioates 342
6.16.10 Dithiocarbamate methyl aryl acids 354

References **358**

Appendix

Structure and biological evaluation for purchased compounds **365**

Abbreviations and Acronyms

3D	Three-dimensional
3Dpol	3D polymerase
Å	Angstrom
ALRI	Acute lower respiratory infection
Anhyd.	Anhydrous
Arg	Arginine
Asn	Asparagine
Asp	Aspartic acid
CADD	Computer-aided drug design
CC50	Cytotoxic concentration to observe 50% adverse effect
CPE	Cytopathic effect
CNS	Central nervous system
CP	Capsid protein
Cys	Cysteine
DCM	Dichloromethane
DIPEA	N,N-Diisopropylethylamine
DMF	Dimethylformamide
DMSO	Dimethylsulfoxide
EC50	Effective concentration to observe 50% activity
EC90	Effective concentration to observe 90% activity
ER	Endoplasmic reticulum
FDA	Food and Drug Administration
F	Fusion
GE	Gene end
Glu	Glutamic acid
Gly	Glycine
GS	Gene start
h	Hour
His	Histidine
HTS	High-throughput screening
HTVS	High-throughput virtual screening
Hz	Hertz
kb	Kilobases
Ile	Isoleucine
IC50	Inhibitory concentration to observe 50% effect
IRES	Internal ribosomal entry site
Le	Leader

LogP	Partition coefficient
Lys	Lysine
Leu	Leucine
LBDD	Ligand-based drug design
MOE	Molecular operating environment
MS	Mass Spectroscopy
mRNA	Messenger ribonucleic acid
NMR	Nuclear magnetic resonance
NS	Non-structural
NTP	Nucleoside triphosphate
NS	Non-structural protein
ORF	Open reading frame
O.n.	Over night
PDB	Protein Data Bank
PV	Poliovirus
Phe	Phenylalanine
RdRp	RNA-dependent RNA polymerase
r.t.	Room temperature
Rf	Retention factor
RMSD	Root-mean-square deviation
RNA	Ribonucleic acid
ROCS	Rapid Overlay of Chemical Structures
SAR	Structure-activity relationship
SBVS	Structure-Based Virtual Screening
Ser	Serine
Ss	Single-stranded
TBTU	O-(Benzotriazol-1-yl)-N,N,N',N'-tetramethyluronium tetrafluoroborate
THF	Tetrahydrofuran
Thr	Threonine
TLC	Thin layer chromatography
Tr	Trailer
Trp	Tryptophan
UTR	Untranslated region
Val	Valine
VP	Viral protein
VPg	Viral Protein genome-linked
ZBD	Zinc binding domain

Chapter I

Molecular modelling in drug discovery

1.1 The drug discovery 'game'

Drug discovery is a long and complex process through which novel drugs are identified. Figure 1.1 shows the typical workflow of drug discovery and development over the time. The process is not so linear as represented: most of the time, it is a random sequence of events, driven by uncertainty and highly-dependent on knowledge about human biological systems which are still not completely known.[1,2,3]

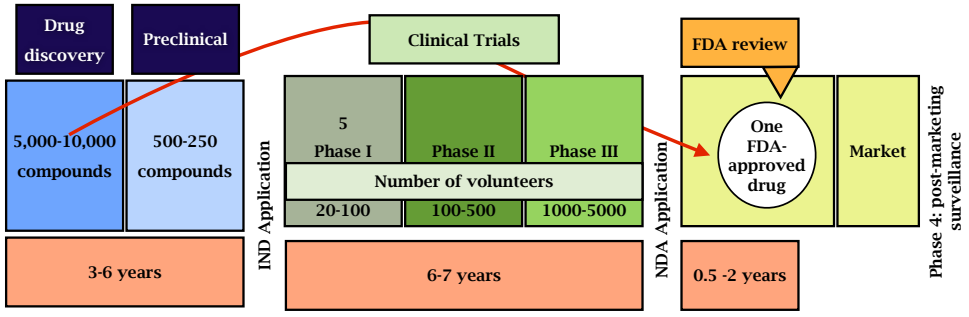

Figure 1.1: States of the drug discovery process

There is no formula that can be applied to define if a molecule will be a drug candidate. It is more an 'exercise' of trial-and-error that takes between 10 and 15 years for a potential new drug to move from the early drug discovery to the market. According to a recent article published in Forbes in 2013, 95% of experimental medicines fail. Moreover, the price for developing a new drug has increased to $5b, which includes the cost to bring a drug from discovery to clinical trials (around $800 thousand per drug) and the loss of money for those drugs that fail during the overall process.[4,5]

The early discovery research is one of the most consuming phases in terms of time and cost, along with preclinical and clinical development.[6] Different strategies can be applied for lead identification: first of all, high-throughput screenings (HTS) of synthetic chemical libraries or natural products are commonly used to find a hit molecule; secondly, working with compounds that already have some desired properties. Another methodology that has played an important role since its beginnings in the 1970s is the use of computational approaches. Computer-aided drug design (CADD) has been demonstrated to be successful in the discovery of

several drugs when the 3D crystal structure of a target protein is available. The first drug on the market that was discovered through a structure-based drug design approach was the carbonic anhydrase inhibitor dorzolamide.[7] Another example of drug developed by rational drug design is imatinib, a tyrosine kinase inhibitor, marketed by Novartis as Glivec®. This anticancer drug was designed to target the bcr-abl fusion protein by chemical modification of a starting lead compound found through a virtual screening.[8] Among antiviral compounds, there are few examples that can be cited: saquinavir (Invirase®), a HIV protease inhibitor, designed on the basis of a crystal structure between the protein and a peptidic inhibitor,[9] and zanamivir, marketed as Relenza®, which is the first neuraminidase inhibitor for the treatment of influenza. This drug was discovered through studies conducted on the binding site of the target 3D structure that led to modifications aiming to improve the binding mode of a first inhibitor in the active site.[10] All these examples are a proof that computer-aided techniques have contributed in the recent years for the discovery of several compounds that are on the market and represent an important tool for the development of new target-based drugs.

1.2 Introduction to Molecular Modelling

Molecular modelling is regarded as a set of computational techniques based on theoretical methods and experimental data that can be used to understand molecules and molecular systems or to predict molecular, chemical and biochemical properties.[11] Programs or algorithms are used to calculate the energetic aspects of a molecular system. There are two main approaches to compute the energy: quantum mechanics and molecular mechanics.

1.2.1 Quantum mechanics

Quantum mechanics methods allow to calculate the electronic properties by considering the interactions between electrons and nuclei of the molecule. Electrons are explicitly considered to be moving around a fixed nucleus, therefore it is possible to consider properties that depend on the electrostatic distribution. Quantum mechanics can be divided into *ab initio* and *semi-empirical* methods. The first one is able to reproduce experimental data but does not employ stored empirical parameters; it is rigorous and restricted to small molecules. *Semi-empirical* methods are

quicker and less accurate than the previous ones and can be used for larger molecules. They differ from *ab initio* methods for the use of empirical parameters in order to reduce the high costs of computer time necessary.[11] The core of quantum mechanics is the Schroëdinger equation, which is a wave function that can be exactly solved for the hydrogen atom. For atoms with more than one electron, simplifications of this equation need to be applied, like the Born-Oppenheimer approximation. Since the nuclei are much heavier than the electrons, this approximation considers the nuclear and electronic motions separately, therefore the system total energy is considered as composed by the nuclear energy and the electronic energy, which is calculated by solving the Schroëdinger equation:[12]

$$E_{tot} = E_{electrons} + E_{nuclei}$$

Quantum mechanics is suitable for calculating a vast range of properties, such as the molecular orbital energies and coefficients, heat of formation for specific conformations, partial atomic charges, electrostatic potentials, bond dissociation energies, transition state geometries and energies[13].

1.2.2 Molecular mechanics

For large biomolecules, quantum mechanics cannot be applied; in these cases, molecular mechanics can be used to study their structures and behaviors. This method is fast and less time consuming than quantum mechanics because it does not consider the electronic motions. Nuclei and electrons are treated as a unit, with no distinction. Therefore, the major limit is the impossibility of calculating properties that depends on the electronic distribution.[14] The energy of the molecule is represented by the equation:

$$E_{tot} = E_{bend} + E_{str} + E_{tors} + E_{vdw} + E_{elec} + \ldots$$

The total energy of a molecule has to be seen in terms of deviations from reference “unstrained” bond lengths, angles, torsions and non-bonded interactions. To these elements, additional components can be added in more complex calculations. The *force field* is a collection of these values. The energies obtained by such calculations have no physical meaning if considered by themselves. They can be considered as deviations from the standard values defined in the force field (denoted as *force field*

parameters). Each deviation will result in an increase of the total energy of the molecule, therefore the total energy derives from a comparison between the intramolecular strain of the molecule and a hypothetical molecule with an ideal geometry.[28] AMBER, MMFF and OPLS force fields are examples of common force fields used for drug design applications. The first one is primarily used for molecular dynamics of macromolecules but it is also applied for energy minimization. MMFF force field may be considered the most widely used, as it has been integrated into a number of different software packages (e.g. MOE), and gives reasonable results in a wide range of chemical systems.[15] The concept of atom type is one of the basis of molecular mechanics. The atom type describes a particular chemical situation of each atom. Behind the concept of atom type is the idea that an atom, within a molecule, does not have the same behavior. In fact, an atom is described by hybridization, formal charge and it also depends on the bonded atoms. Thus, molecular mechanics considers interactions between atom types and not elements, and the number of atom-types respects the number of possible chemical situations in which an atom can be found in building different molecular structures. A brief example of atom types for AMBER force field is reported below.

hydrogen types	H	amide or imino hydrogen
	HC	explicit hydrogen attached to carbon
	HO	hydrogen or hydroxyl oxygen
	HS	hydrogen attached to sulfur
	HW	hydrogen water
	H2	amido hydrogen in NH2
	H3	hydrogen of lysine or arginine (positively charged)

1.2.3 Energy minimisation

Energy minimization is a method that allows finding the (global) minimum energy conformation of a molecule by locating all the local minima of the function describing the potential energy surface. Energy minimization is useful for bringing a molecule to, or close to, its equilibrium conformation. The process consists of calculating the energy of a starting molecule, then variating the bond lengths, bond angles, and torsion angles to create a new configuration. The energy associated is measured to see whether the generated configuration is more stable or not in terms of energy. The program carries out more changes and is able to recognize these

conformations which lead to stabilisation and those which do not.[30] This analysis is commonly performed in molecular modelling, as well as related procedures like conformational analysis, with the aim of avoiding any unfavorable interaction in the system.

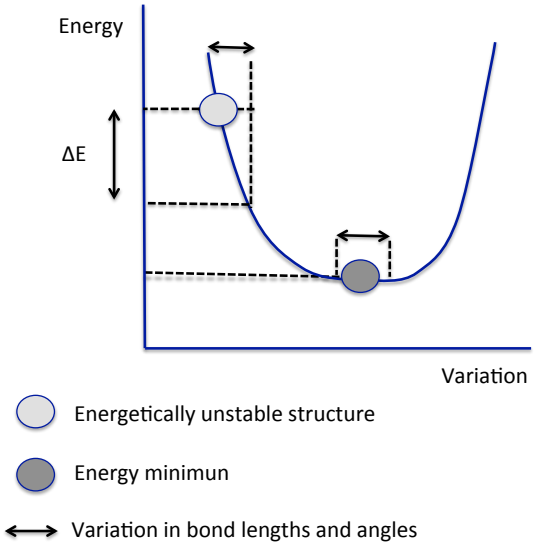

Figure 1.2: Energy minimization graph

1.2.4 Conformational analysis

The energy minimization is able to produce a stable conformation for a 3D structure. However, the product obtained could not be the most stable conformation. In fact, the energy minimisation stops as soon as it reaches the first stable conformation it finds, closest in structure to the starting one. This may represent a local energy minimum, far away from the most stable conformation. Even if the bioactive conformation of a drug molecule is not necessarily identical to the lowest-energy conformation, it cannot be high in energy. Thus, the identification of low-energy conformations is an important task to understand the relationship between the structure and the biological activity of a molecule.[16] Conformational analysis is able to identify the preferred conformations of a molecule and evaluate their influence on its properties.

1.3 Computational approaches in drug discovery

Computer-aided techniques are useful tools for new hit identification, as already described. In this section, the techniques that were applied in the project will be discussed. Computer-aided methods can be classified in two main categories: structure-based drug design (SBDD) and ligand-based drug design (LBDD). Structure-based approaches depend on the availability of information on the target protein, and are used to predict interaction energies of screened compounds with the given binding pocket. Ligand-based methods focus instead on the chemical structure of known active molecules through chemical or shape similarity searches, or quantitative structure-activity relationship (QSAR) analyses. Depending on the information available on the specific drug targets or known active compounds, the most suitable computational method can be applied.

1.3.1 Homology Modelling

In a drug design project, the best ideal condition is to have X-ray crystallographic data of the protein structure to study. In this case, a structure-based drug design approach (SBDD) can be applied.[17] Additional information about the conformational changes of the protein can be derived if structures of the protein with and without a ligand are available. Unfortunately, proteins are known to be difficult to crystallize. In addition to this, crystal structures, in some cases, might not be entirely exact. When 3D structures or 2D NMR models are not available, homology modelling is the best way of predicting the actual three-dimensional structure of a protein. This tool is used to build this putative structure for an unknown protein using its amino acid sequence and a comparative three-dimensional crystal structure.[18] An alignment is required between the two amino acid sequences of the target protein and the template (carrying the 3D information). This strategy is based on the assumption that in two homologous proteins the most relevant structural and functional sites tend to remain conserved and that the tertiary structure of a protein is more conserved than the amino acid sequence.[19,20] Therefore, two proteins that diverge from the primary sequence can have some similarity in terms of structural properties, such as the overall fold.

1.3.2 Ligand-based drug design

When the protein target is unknown, designing an innovative compound can become a difficult task. In this case, the approach to use is called ligand-based drug design (LBDD): it enables to study a collection of active compounds, in order to understand their structural and physico-chemical properties that are in correlation with their pharmacological activity. Several studies have shown that the molecular shape is an important indicator for protein-ligand recognition.[21] The majority of docking programs generates a number of poses for a ligand within the active site and gives a score to the docked conformation according to its binding energy with the target. On the other hand, shape comparison, for which more accurate results have been demonstrated rather than docking algorithms, focuses on the occupational volume associated with each molecule.[22] In ligand docking, the binding site area is the centre of attention, while shape-based similarity methods dismiss the protein and focus only on the conformation of the ligand.

1.3.3 Pharmacophore models

The basic idea of pharmacophore models is to identify the common structural features that are necessary for binding a certain target or are essential for biological activity (e.g. disposition of hydrogen bond acceptors or donors, hydrophobic and ionic groups). A pharmacophore is a representation of points in 3D space surrounded by a spherical region: a molecule must place these relevant features within restricted spatial portions. One of the advantages of building a pharmacophore is that it can be generated also when no information about the binding site is available. A better result would be obtained if the active conformation of the ligand is known and a good combination of pharmacophoric groups is found. If the pharmacophore is generated starting from the geometry of the binding site, it is important that it contains features able to mimic the presence of the receptor: these are represented by exclusion volumes that indicate those regions within the pharmacophore where the ligand should not place any of its parts (fig.13).[32]

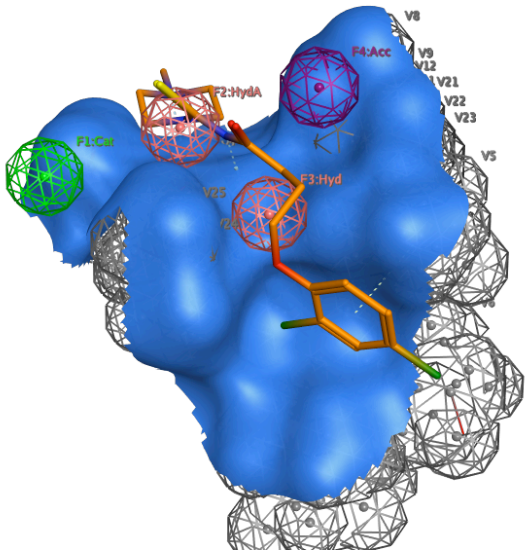

Figure1.3: Example of pharmacophore model. Coloured spheres are the pharmacophoric features. Grey spheres represent the exclusion volumes

1.3.4 Structure-based drug design

Structure-based drug design is the preferred method in a the drug design process because it can give a prediction of how a drug works, thus allowing to improve activity, pharmacokinetics and other properties concerning the molecule. *In silico* virtual screening using docking techniques enables to screen electronic libraries of known chemical structures to find those that might fit the active site. A pharmacophore search, at this step, may be useful because it has the advantage of not requiring a particular backbone. It only needs molecule annotations related to ligand-receptor binding, like H-bond donor, H-bond acceptor, etc. A second strategy that can be carried out is to design new structures rather than screen libraries. This approach is named *de novo* drug design and it also depends on the available information of the targeted protein binding site.

1.3.5 Docking and Scoring

Docking techniques are commonly used in hit identification and lead optimisation with the scope to predict the potential binding mode of a ligand in the target site of a protein as well as estimate the strength of the interactions between the ligand and the protein. Thanks to the increasing improvements in techniques for structure determination, the number of 3D structures is increasing over the years and, as a consequence, structure-based approach in drug design has become very common.[23] Two steps are typically involved in all docking programs, the first of which is the generation of many ligand conformations in the active site and the second one is the evaluation of the protein-ligand affinity, a process known as scoring.[24] It is very challenging to satisfy all these tasks: in fact, even the simplest organic molecules can have many conformational degrees of freedom originating from the presence of rotatable bonds, flexibility of ring structures in the ligand molecule, as well as the flexibility of the protein structure.[25] There are several algorithms that can be used to generate ligand conformations, while the receptor is assumed to be rigid. In order to consider also the receptor conformational space, the most common analysis is to perform a molecular dynamics simulation of the ligand-receptor complex. However, these calculations are computer demanding and can be useful only to refine structures produced by docking methods as they are not able to explore all the possible binding modes, except for small flexible ligands. Docking algorithms predict several poses for a ligand within the binding site, but it is crucial to evaluate and rank the results in order to identify the most interesting ones. Scoring functions are mathematical methods used to find the docked orientation that represents the most probable structure. Many scoring functions evaluate the binding free energy between a protein and a ligand by considering various elements:

$$\Delta G_{bind} = \Delta G_{solvent} + \Delta G_{conf} + \Delta G_{int} + \Delta G_{motion}$$

$\Delta G_{solvent}$ is the contribution due to solvent effects, ΔG_{conf} takes into account the conformational changes in the ligand and the receptor, ΔG_{int} is the free energy variation related to specific protein-ligand interactions and, finally,

ΔG_{rot} takes into account the motions (rotational, translational and vibrational) during the formation of the ligand-receptor complex. One limit of scoring functions is that they result from ligands that are bound very tightly to their receptors, while docking usually identifies ligands of a moderate potency. For this reason, it is more appropriate to combine the results of different scoring functions such that a molecule is scored by different scoring functions rather than use only a single one. This procedure is called Consensus Scoring (CS) and compensates the possible errors or lacks of each scoring function.[26,27]

1.4 Aims of the study

In the 21st century, there are still viruses that have a dramatic socio-economical impact worldwide and for which no efficient antiviral therapy has been approved so far. This project aims to apply different molecular modelling techniques to design and synthesise small molecules against four RNA viruses. In particular, some of the non-structural proteins required for viral replication of Coxsackie virus B3, Foot-and-Mouth Disease and Chikungunya viruses, all positive-strand RNA viruses will be targeted by structure-based or ligand-based virtual screenings for the identification and synthesis of potential inhibitors of viral replication. Molecular modelling studies, such as *de novo* drug design, will be performed for the synthesis of small-molecule compounds against Respiratory Syncytial Virus, a negative-strand RNA virus. All of the molecules synthesized will be evaluated for their antiviral activity and cytotoxicity in cell-based assays and the biological results will be used to direct further investigations.

References

1 Chen, Y.-T.; van den Ven, A.H. Learning the innovation journey: order out of chaos. *Organ. Sci.* **1996**, 7, 593–614.

2 Gittins, J. Quantitative methods in the planning of pharmaceutical research. *Drug Inf. J.* **1996**, 30, 479–87.

3 Pisano, G.P. Can science be a business? Lessons from biotech. *Harvard Bus. Rev.* **2006**, 84 (10), 114–25.

4 Herper, M. How much does pharmaceutical innovation cost? a look at 100 companies. *Pharma & Healthcare*, November 8, 2013. [accessed online 9/10/2014].

5 Earl, J. What makes a good forecaster? *Nature Rev. Drug Discovery* **2003**, 2, 83.

6 DiMasi, J.A.; Hansen, R.W.; Grabowski, H.G. The price of innovation: new estimates of drug development costs. *J. Health Economics* **2003**, 22(2), 151-185.

7 Greer, J.; Erickson, J.W.; Baldwin, J.J.; Varney, M.D. Application of the three-dimensional structures of protein target molecules in structure-based drug design. *J.Med.Chem.* **1994**, 37 (8), 1035-1054.

8 Capdeville, R.; Buchdunger, E.; Zimmermann, J.; Matter, A. Glivec (STI571, Imatinib), a rationally developed, targeted anticancer drug. *Nature Rev. Drug Discovery* **2002**, 1, 493-502.

9 Roberts, N.A. Rational design of peptide-based HIV proteinase inhibitors. *Science* **1990**, 248, 358-361.

10 Wood, J.M.; Bethell, R.C.; Coates, J.A.; Healy, N.; Hiscox, S.A.; Pearson, B.A.; Ryan, D.M.; Ticehurst, J.; Tilling, J.; Walcott, S.M. 4-Guanidino-2,4-dideoxy-2,3-dehydro-*N*-acetylneuraminic acid is a highly effective inhibitor both of the sialidase (neuraminidase) and of growth of a wide range of influenza A and B viruses in vitro. *Antimicrob. Agents Chemother.* **1993**, 37, 1473-1479.

11 Holtje, H-D.; Folkers, G. *Molecular Modeling: Basic Principles and Applications*; Mannhold, R., Kubinyi, H., Timmerman, H., Eds.; VCH publishers, New York, 1997.

12 Lewars, E. *Computational Chemistry: Introduction to the Theory and Applications of Molecular and Quantum Mechanics*. Springer Ed.; 2nd edition, 2010

13 Patrick, G.L., Computers in medicinal chemistry. In: *An introduction to medicinal chemistry*. 3rd edition; Oxford University Press Inc.: New York, 2005; 319-323.

14 Vinter, J.G. Optimisation Extended electron distributions applied to molecular mechanics of some intermolecular interactions. *J. Comput. Aid. Mol. Des.* **1994,** 8, 653- 668.

15 Young, D.C. Molecular mechanics. In: *Computational drug design: a guide for computational and medicinal chemists*. John Wiley & Sons: New Jersey, 2009; DOI: 10.1002/9780470451854.ch10

16 Goodman, J.M; Still, W.C. An unbounded systematic search of conformational space. *J. Comput. Chem.* **1991,** 12, 1110-1117.

17 Kapetanovic, I.M. Computer-aided drug discovery and development (CADD): in silico chemico-biological approach. *Current computer-aided drug design* **2008**, 3 (2), 165-176.

18 Marti-Renom, M.A., Stuart, A. C., Fiser, A., Sanchez, R., Melo, F., Sali, A. Comparative protein structure modeling of genes and genomes. *Annu. Rev. Biophys. Biomol. Struct.* **2000**, 29, 291–325.

19 Xu, D.; Xu, Y.; Uberbacher, E.C. Computational tools for protein modelling. *Curr. Protein Pept. Sci.* **2000**, 1, 1–21.

20 Johnson, M.S.; Srinivasan, N.; Sowdhamini, R.; Blundell, T.L. Knowledge-based protein modelling. *CRC Crit. Rev. Biochem. Mol. Biol.* **1994**, 29, 1–68.

21 Mezey, P.G. *Shape in Chemistry*, VCH Publishers Inc; 1993.

22 McGaughey, G.B.; Sheridan, R.P.; Bayly, C.I.; Culberson, J.C.; Kreatsoulas, C.; Lindsley, S.; Maiorov, V.; Truchon, J.; Cornell, W.D. Comparison of topological, shape, and docking methods in virtual screening. *J. Chem. Inf. Model.* **2007**, 47, 1504- 1519.

23 Plewczynski, D.; Lazniewski, M.; Augustyniak, R.; Ginalski, K. Can we trust docking results? Evaluation of seven commonly used programs on PDBbind database. *J. Comput. Chem.* **2011**, 32 (4), 742-755.

24 Teramoto, R.; Fukunishi, H. Supervised consensus scoring for docking and virtual screening'. *J Chem Inf. Model.* **2007**, 47 (2), 526-534.

25 Novikov, F.N.; Chilov, G.G. Molecular docking: theoretical background, practical applications and perspectives. *Mendeleev Commun.* **2009**, 19, 237-242.

26 Kitchen, D.B.; Decornez, H.; Furr, J.R., Bajorath, J. Docking and scoring in virtual screening for drug discovery: methods and applications. *Nature Reviews* **2004**, 3, 935-949.

27 Teramoto, R.; Fukunishi, H. Supervised Consensus Scoring for Docking and Virtual Screening. *J. Chem. Inf. Model.* **2007,** 47, 526-534.

Chapter 2

Coxsackie Virus B3

Introduction to the virus

2.1 Coxsackie Virus B3

Coxsackie Virus B3 (CVB3) is a subgroup of the Coxsackievirus, a member of the Enterovirus genus, of the family *Picornaviridae*, which is responsible for viral myocarditis that mostly affects children.[1] Although most of the time infections caused by this virus are characterized by mild symptoms, e.g. gastrointestinal distress, fever, headache, sore throat, CVB3 is also associated to pancreatitis, meningitis and encephalitis.[2] The greatest risk is in the case of congenital infection,[3] when the illness develops in the first days of life and is often associated with high mortality due to the involvement of several organs (liver, heart, brain and lungs). In some cases, the myocardial inflammation may persist producing a chronic state that can progress to dilated cardiomyopathy (DCM), which involves the enlargement of the heart muscle. The incidence of infections, which is seasonal between June and October, is more frequent in males than females. Epidemiological studies of the Centers for Disease Control and Prevention accounted for approximately 5.9 % of neonatal enterovirus infections related to CVB3 from 1983 to 2003 in USA only. Outbreaks of aseptic meningitis caused by CVB3 have also been reported between 2001 and 2008 in Taiwan,[4] Argentine,[5] Korea,[6] France[7] and in a region of China.[8] CVB3 can be transmitted by four modes: fecal-oral, vertical (maternal-fetal) respiratory and inoculation; the first one is, by far, the major mode of transmission. The lack of adequate hygienic condition in developing countries contribute to this mode of transmission. After the virus entries via oral cavity and/or respiratory tract, it invades and replicates in pharynx and in the lower gastrointestinal tract, especially in the lymphoid tissue (e.g. tonsils). Then, it enters the bloodstream, resulting in a 'minor viraemia' and spreads to a vast number of target organs, like heart, liver, pancreas, skin, leading to the typical signs and symptoms.[9] A 'major viraemia' occurs during this infection, involving the central nervous system (CNS).

2.1.1 Virion Structure

The crystal structure of CVB3 virion has been resolved at 3.5 Å resolution.[10] Figure 2.1 shows a general model of virion structure for Picornaviruses. The virion particles are spherical, with a diameter of 30 nm and do not have a lipid envelope. They are surrounded by a shell called capsid formed by four structural proteins, VP1, VP2, VP3 and VP4. VP4 is in the inner surface and anchors the capsid to the RNA genome, while VP1, VP2 and VP3 are on the outer surface where there is a deep depression, called canyon, which corresponds to the receptor-binding site.

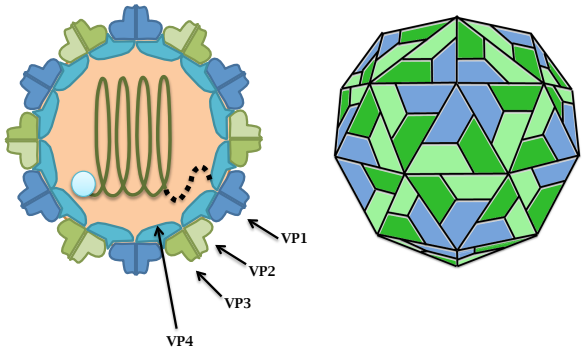

Figure 2.1: Picornavirus virion structure

2.1.2 Genome organization

Virion particles contain a single, positive strand RNA from 7 to 8.5 kb in length, with similar organization across the Picornavirus family (Figure 2.2).

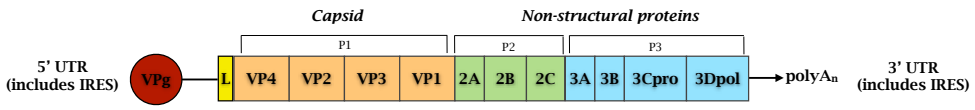

Figure 2.2: Picornavirus genome organization

The genome is divided in three regions: a 5'-untranslated region (5'-UTR), a central open reading frame (ORF) encoding a single large polyprotein and a 3'-untranslated region (3'-UTR) which contains a poly-adenine tail. 5'-UTR contains the internal ribosome entry sites (IRES), an element responsible for the translation of the mRNA. A small protein called VPg (Virion Protein genome linked) is covalently attached at the 5' end and takes part in the

RNA initiation replication. The coding region of the viral genome contains the precursors of structural and non-structural proteins (P1, P2, P3). The P1 portion comprises the structural proteins of the capsid (VP1-VP4), while P2 and P3 regions encode non-structural proteins.

2.1.3 Viral proteins

Viral particles are classified as structural and non structural proteins, the former being part of the viral particle, while the second ones do not form the virion structure but take part in several processes of viral replication. Non-structural proteins are are produced by the translation of a single open reading frame (ORF) that is followed by cleavage of the polyprotein through proteinases encoded in the viral genome. Most of the members of Picornavirus family encode for 2A and 3C proteinases. The 2A protease has been associated with multiple roles. First of all, its proteolytic function at the junction between the P1 and P2 domains. Secondly, it cleaves the eukaryotic initiation factor polypeptide eIF4F which is required for the attachment of mRNAs to the ribosome.[11] Cleavage of this factor impairs this process, leading to the so-called 'host cells shut off' which means that the synthesis of host cell proteins is blocked. Finally, 2A may directly be involved in the pathogenesis of viral-induced dilated cardiomyopathy in coxsackievirus B3 through its ability to cleave dystrophin and glycoproteins associated to this protein.[12] 2B protein is a small, hydrophobic membrane-associated protein that is localized at endoplasmic reticulum (ER) and Golgi membranes. The precise role is yet poorly understood, but several studies have demonstrated that it is responsible for disassembly of Golgi complex, causing the release of virus from cells.[13,14] 2C protein is one of the most conserved proteins in the *Picornaviridae* family with multiple roles in viral replication.[15] It has a nucleoside triphosphatase (NTPase) activity, it is also involved in the formation of membrane vesicles and it may direct the formation of the replication complex.[12] P3 region encodes for 3A, 3B (also called VPg), 3C protease and 3D polymerase. The 3A is a small protein that forms homodimers. It has an hydrophobic region that is important for its binding to membranes. This protein is able to alter the structures of host-cell membranes[16] and to inhibit the protein transport from the endoplasmic reticulum to the Golgi complex, a phenomenon that is thought to have a

link with the suppression of the immune response.[17] 3C is a chemotrypsine-like serine protease that cleaves between 2C and 3A proteins and also the P1 and P2 precursors.[12] The non-structural protein 3D is a viral RNA-dependent RNA polymerase (RdRP) that catalyses both negative and positive-strand RNA synthesis. It takes part also in the VPg uridylylation, which is the first step in the RNA replication.[18]

2.1.4 Viral life cycle

The replication of picornaviruses consists of several steps that entirely takes place in the cell cytoplasm (Figure 2.3).

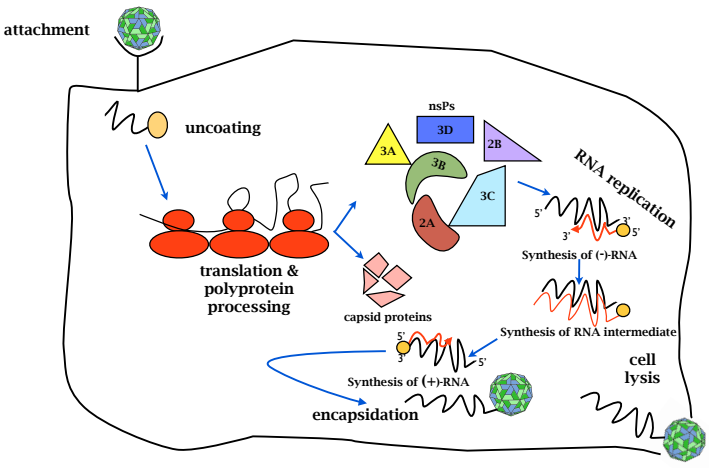

Figure 2.3: Picornavirus life cycle

The first step in the infection of target cells is the attachment to the host cell membrane through host receptors.[12] CVB3 viruses attach the cells through binding to the canyon.[10] Once the virus particle has attached to its cellular receptor, the viral RNA is released into the cytoplasm, which is the site of the genome replication. Since the RNA is positive sense it can be used as mRNA and can be translated into a single polyprotein, which is subsequently cleaved to produce viral proteins by encoded proteases 2A and 3C. Negative strand RNA is synthesized using the parental positive-strand RNA as a template. The resulting minus RNA is subsequently used in order to produce new positive-strand RNAs via multi-stranded replicative intermediate structures. When sufficient genome is made, virion assembly occurs: a single molecule of new viral RNA is inserted in the so-called procapsid, which is a preformed, empty capsid. The new virus particle can finally be released through cell lysis.[12]

2.1.5 Current treatment

There is no approved antiviral therapy for the treatment of CVB3 infections, nor an efficient vaccine is at hand. Only supportive treatment is used. Patients with dilated cardiomyopathy are treated with agents commonly used for heart failure as their symptoms are similar.[19] In the case of viral meningitis, patients recover in the majority of cases within 7 to 10 days. Sometimes, a hospital stay could be necessary, especially for people with a weak immune system.

2.2 3A protein and 3D polymerase as antiviral targets

In this project, two proteins were taken into account for computer-aided studies. The first one is the 3A protein that has been explored to a less extent as antiviral target. The second one is the 3D polymerase, which is typically considered as a good target for the identification of potential antivirals, as demonstrated by several examples among viral RdRPs.

2.2.1 3A protein

3A protein is a homodimer involved in the formation of the replication complex on the surface of membranous vesicles in infected cells, along with other non-structural proteins. So far, the 3A protein has not been taken into account as a target for drug design. There is no crystal structure available for CVB3 3A protein, only a soluble N domain (1-59 aa) of the protein has been determined by NMR spectroscopy for Poliovirus (PV), member of the Enterovirus genus (figure 2.4).[20]

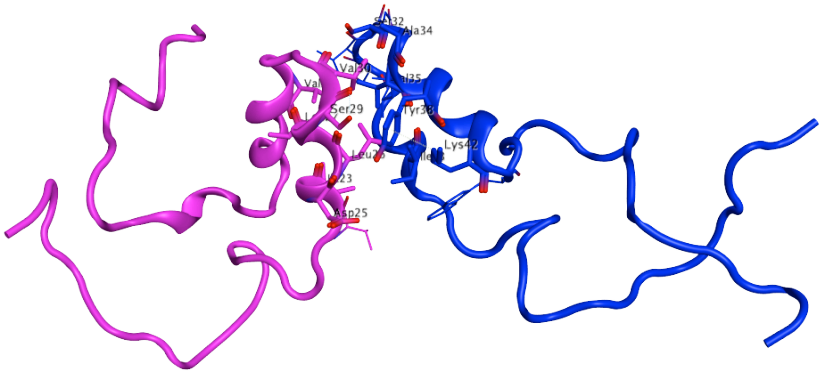

Figure 2.4: NMR solution structure of PV 3A protein

3A protein, as formerly said, is responsible for the inhibition of protein transport from the ER to the Golgi complex, a process that might have some relevance in viral evasion from the host immune response. Mutational studies in the 3A region of the 3AB precursor have indicated a loss of virus replication and resistance to enviroxime, a known inhibitor of viral replication. This information supported the idea that 3A has a role in the replication complex that is still not completely understood.[25] Based on

these information, CVB3 3A protein was chosen as a target for the identification of potential antivirals. An homology model of this protein for CVB3 3A was built in 2006,[21] using as a template the NMR resolution structure of PV 3A. With a similar sequence identity to PV 3A, the model has 60 aa and is membrane-associated via the C-terminal hydrophobic domain. In addition, CVB3 3A protein was predicted to form a homodimer, with the two helical monomers connected each other via a hydrophobic interface. In vitro mutational analysis showed the ability of the protein to dimerize and, like PV 3A, the dimerization of the 3A protein was demonstrated to be important for protein function. In the same study,[21] the amino acids involved in the dimerization process were determined: when mutating the amino acids that were predicted to form the hydrophobic interactions between the two monomers, dimerization was lost and the replication process was reduced. Two main regions seem to be essential for the homodimerization: the hydrophobic interface between the helical regions of the two monomers, formed by residues Ile22, Leu25, Leu26, Val29 and Val34 and an intermolecular salt bridge between Asp24 of one monomer and Lys41 of the other one.[26]

2.2.2 RNA-dependent RNA Polymerase

The RNA-dependent RNA polymerase (RdRP), also named 3Dpol, is a multi-functional protein, responsible for chain elongation during the RNA synthesis, RNA binding and nucleotidyl transfer. In addition, it participates in the uridylylation process of VPg, which is the first step in the genome replication. The PV 3Dpol was the first complete crystal structure determined and has a similar structure observed in other nucleic acid polymerases. To date, several crystal structures of RdRPs from the Picornavirus family are available. Despite the little sequence identity shared, they adopt a similar fold that resembles a cupped right hand with 'fingers', 'palm' and 'thumb' domains (figure 2.5). The 'palm' domain is composed of 5 sub-domains (A-E), four of which (A-D) are highly conserved among polymerases and fold into a structure that generates the core of this domain. This core is composed of two α-helices that pack under a four-stranded antiparallel β-sheet. Motif C of 'palm' domain has a relevant importance: it contains the 'GDD' motif active site (Gly-Asp-Asp) found in all RdRPs. The 'thumb' domain is the most different feature among the

RdRPs and is mainly composed of C-terminal amino acid residues. The 'fingers' domain is composed of four separate sub-domains, 'index', 'middle', 'ring' and 'pinky' fingers. 'Fingers' and 'thumb' domains, interconnecting each other, generate the so-called 'closed-hand conformation' of the protein and completely encircle the active site of the enzyme.[22]

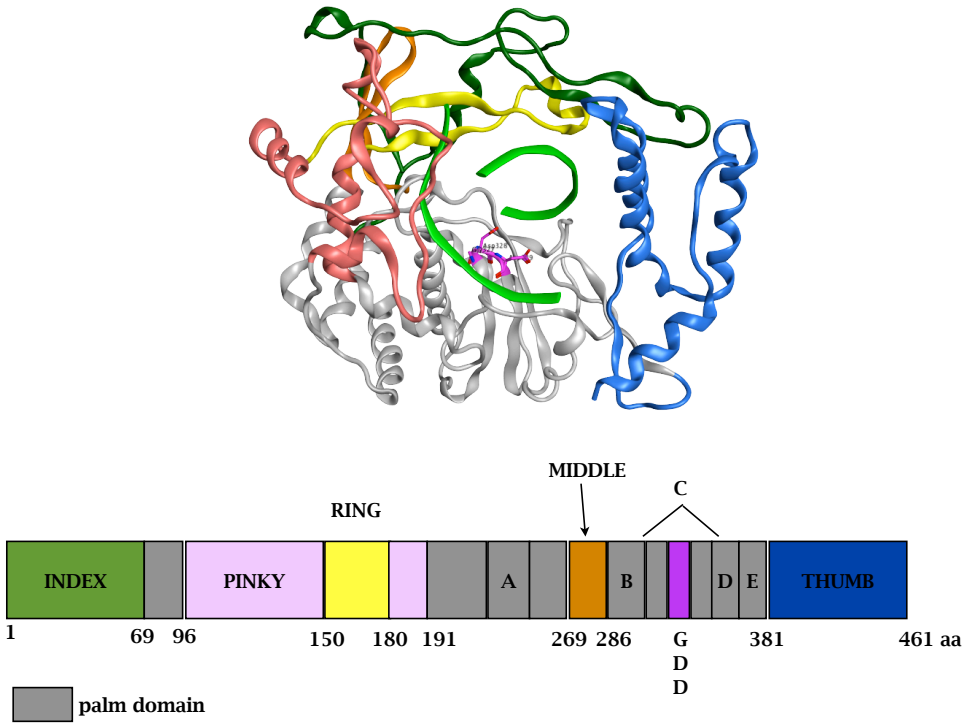

Figure 2.5: Top view of the 3D structure of Picornavirus polymerase and 3Dpol sequence differently colored according to the structural elements. Ribbon of the RNA is represented in green

These interactions also create a small tunnel, positively charged, where the template-primer RNA binds.[23] The crystal structure of the FMDV 3Dpol in complex with the template-primer RNA has confirmed the function of this channel which is also used by a new incoming nucleotide; for this reason, it is also called NTP entry tunnel.[24] It is believed that all the five motifs of 'palm' domain are involved in several steps of the replication process: for example, motifs A and B participate in the nucleotide recognition and binding, motifs A and C in the phosphoryl transfer, motif D in structural integrity of the 'palm' domain and finally motif E in priming nucleotide binding.[23]

A new binding site into the polymerase

A small molecule that inhibits RNA replication by targeting the 3D polymerase in a region near the active binding site was recently discovered (unpublished data kindly received from our collaborator at Utrecht University, Dr. Frank van Kuppeveld). This compound, named GPC-N114, has been found active against a broad spectrum of Enteroviruses and Encephalomyocarditis virus (EMCV), a member of Cardiovirus genus, of the family *Picornaviridae*. The activity of the compound extends from 0.1μM to 1.7μM. No inhibitory effect was detected, by contrast, against two Aphthoviruses, FMDV and equine rhinitis A virus (ERAV), also belonging to the Picornavirus family. According to biochemical studies, the elongation activity was inhibited by this compound, which was crysallized with the CVB3 3Dpol (figure 2.6).

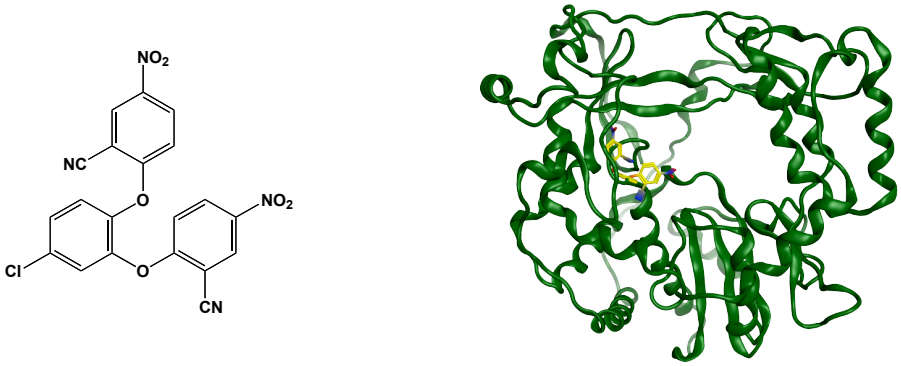

Figure 2.6: Chemical structure of GPC-N114 and crystal structure of CVB3 3Dpol-GPC-N114 complex

The binding region is located at the bottom of the RNA template site, according to the X-ray crystallographic analysis, where the compound seems to mimic the position of the template acceptor nucleotide. In the crystal structure, the inhibitor makes contacts, mainly, with three different regions of the polymerase: the template entry channel, regarding residues Leu110, Thr114 and Lys127, an hydrophobic area where this molecule strongly interacts with His199 and makes stacking interactions between its central ring and Tyr195. Additional interactions with residues Gly290, Cys291, Ser292, Gly293, Thr294, Ile296 have also been individuated. The resolved crystal structure of the FMDV 3Dpol with GPC-N114 (figure 2.7) has also explained why the virus in not sensitive to the inhibitor. Despite

the fact that GPC-N114 binds FMDV 3Dpol in a relatively similar pocket found for CVB3, the conformation assumed and the binding mode are completely different. It is, therefore, likely that the very few contacts of GPC-N114 with the polymerase have an influence on the polymerase activity.

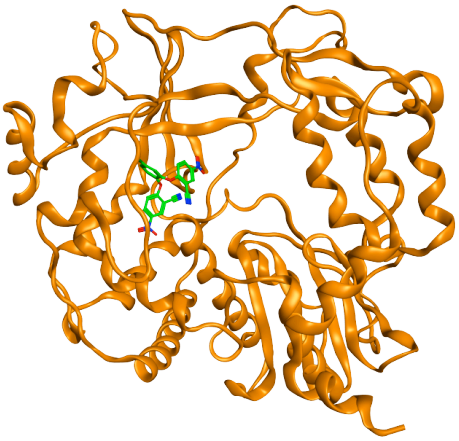

Figure 2.7: Crystal structure of FMDV-GPC-N114 complex

A close up of the two different conformations of GPC-N114 found in the resolved crystal structures of CVB3 and FMDV polymerases is represented in figure 2.8.

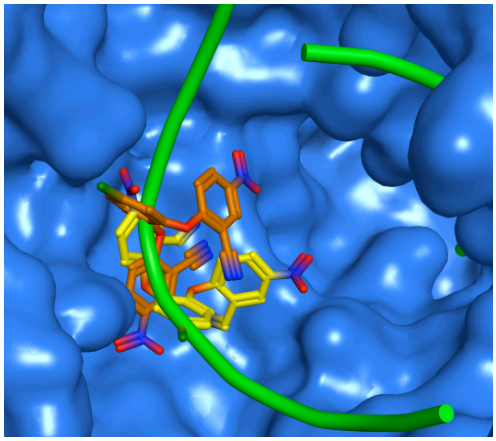

Figure 2.8: Representation of GPC-N114 in two conformations. The jellow one is the ligand conformation in the CVB3 3Dpol, the orange one is the one observed in the FMDV 3Dpol. The predicted position of the RNA template was determined using the FMDV 3Dpol-RNA complex (PDB ID: 1WNE) as a guide

Results and discussion

2.3 Structure based Virtual Screening on 3A protein

The non-structural protein 3A of CVB3 was investigated and a structure-based virtual screening approach (SBVS) was applied. So far, no antiviral compound is known to prevent protein dimerization.[25] Having information on the essential residues that are responsible for the 3A protein function, the scope of this study was to identify molecules that could bind on the interface of the protein, thus competing with the protein-protein interaction.

2.3.1 Homology model

Since no crystal structure of the CVB3 3A protein is available, an homology model was constructed using the solution structure of PV 3A protein soluble domain (PDB ID: 1NG7).[26] Figure 2.9 shows the sequence alignment between the model generated and PV 3A protein used as a template: the structures share 47% sequence identity and a common fold, with an RMSD value of 1.822 Å observed when they were superposed. Moreover, the RMSD value at the level of the dimeric interface is significantly lower (0.56 Å), confirming the accuracy of the model.

```
1NG7.A          MGPLQYKDLKIDIK-TSPPPECINDLLQAVDSQEVRDYCEKKGWIVN-ITSQVQTERNIN
1NG7.B          MGPLQYKDLKIDIKTS-PPPECINDLLQAVDSQEVRDYCEKKGWIV-NITSQVQTERNIN
model_1.pdb     QGPPVYREIKISVAPETPPPPVIADLLKSVDSEAVREYCKEKGWLVPEINSTLQIEKHVS
model_2.pdb     QGPPVYREIKISVAPETPPPPVIADLLKSVDSEAVREYCKEKGWLVPEINSTLQIEKHVS
                 **  *:::**.:    ***  * ***:.***: **:**:.***:*  *.* :* *:.:.

1NG7.A          RA-
1NG7.B          -RA
model_1.pdb     RA-
model_2.pdb     RA-
```

Figure 2.9: Sequence alignment of PV 3A protein (PDB ID: 1NG7) and the model generated. Identity between amino acid sequences are shown with an asterisks. Conservative substitutions are represented by a colon and semiconservative substitutions are indicated by a period

2.3.2 Pharmacophore models

The model generated, like the template, has two monomers; each one consists of two α-helices (amino acids 20-27 and 31-42) connected by a loop. The two helical hairpins have a hydrophobic interface with residues

Ile22, Leu25, Leu26, Val29, Val34 which are fundamental for the intermolecular interactions responsible for the homodimerization. Similarly to the PV 3A protein,[26] four amino acids are in the right position to contribute to the dimerization: Asp24 and Lys41 are supposed to form an intermolecular salt bridge, together with Ser28 and Tyr37, which could interact by an intermolecular hydrogen bond. Since these residues are essential for the dimerization process, they were taken into account for the generation of two pharmacophoric models. In figure 2.10, an alignment of the 3A structures of PV and CVB3 is reported, with a close up of the dimer interface.

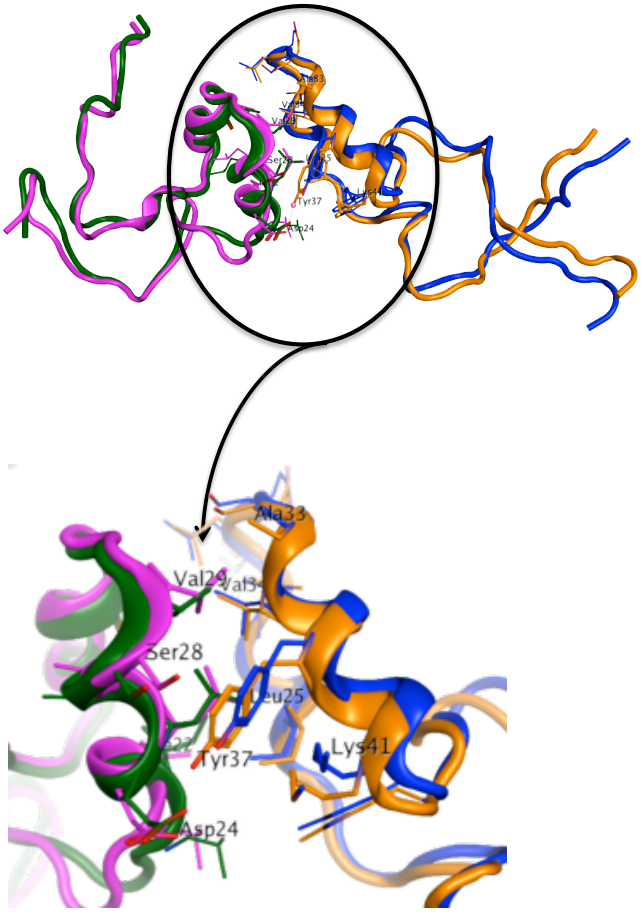

Figure 2.10: PV 3A structure aligned (purple and blue ribbon) with the model created (green and orange ribbon). A close up of the dimer interface is represented below

The Specs database[27] is a public library of around 450,000 commercially available compounds that was used in this search. These structures were downloaded and analysed with MOE 2010.10 conformational search tool, setting 500 low-energy conformations to be for each input molecule.[28] For

each chain, a pharmacophore model was built, with all the necessary features in correspondence to the key residues important for the dimerisation. For chain 1, an anionic group (F1:Ani), adjacent to Lys41 was kept as essential for the pharmacophoric search; a donor group (F2:Don) was added to interact with Glu40, along with three hydrophobic features (F3:Hyd, F4:HydA and F5:Hyd) in close proximity to the aromatic rings of Tyr37 and Trp42, but also in correspondence to Leu25 of chain 2, which is known to take part in the hydrophobic packing essential for the homodimerization. An additional hydrophobic interaction (F5:Hyd) was added and set as essential since it is in a cleft where ligands could be anchored. Finally, a donor group (F6: Don) was introduced to create a possible repulsive interaction with the carbonyl group of Leu25, in the opposite monomer (figure 2.11). Exclusion volumes corresponding to the protein surface were added to the pharmacophoric model, with the scope to prevent that any compound could fit to this region of exclusion. The pharmacophoric search, which is able to pre-filter a large molecular database, was run requiring a partial match of at least 2 features. 6760 molecules were found to respond to the chosen criteria and were used for the following docking step.

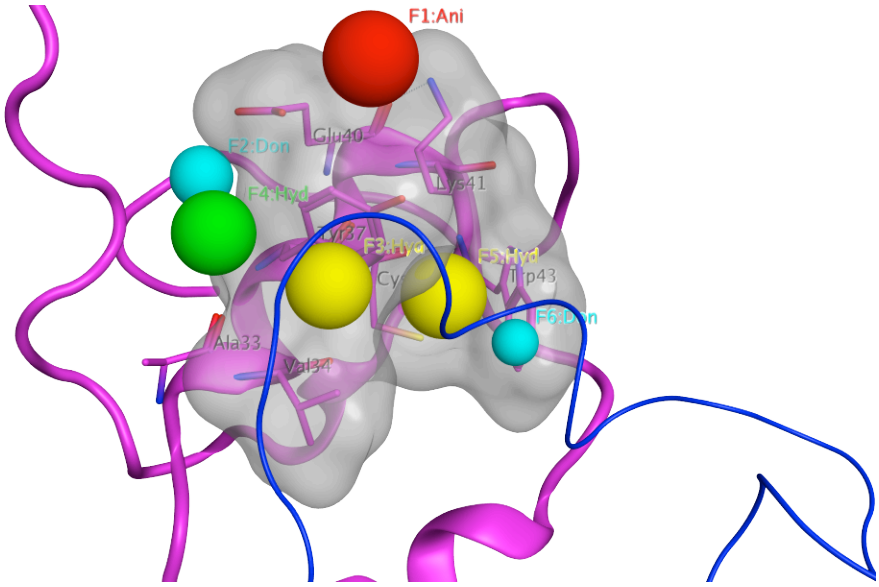

Figure 2.11: Pharmacophoric model of chain 1. Backbone of chain 2 is represented as blue ribbon

In a similar way, a second pharmacophore was created using the chain 2 of the dimeric protein. The target site is represented by several residues: Asp24, a key residue for the formation of a salt bridge essential for protein

dimerization, Ile22, Leu25 and 26, Val29 and Val34 predicted to be part of the hydrophobic packing. Finally, Ser28 which forms an intermolecular hydrogen bond with Tyr37 of chain 2 in the PV 3A structure. The pharmacophore model was made by four features: a donor group (F1:Don), in correspondence to the carbonyl group of Val34, a cationic group (F2:Cat), which is one of the essential features set in proximity of Asp24, and, finally, two hydrophobic features (F3:Hyd and F4:Hyd) to interact with amino acids Ile22, Leu25, Leu26, Val29 and Val34 (figure 2.12). At least two partial matches were enabled in the pharmacophoric search panel, with two features (F2 and F4) kept as essential. 4157 entries were found and used for docking calculations.

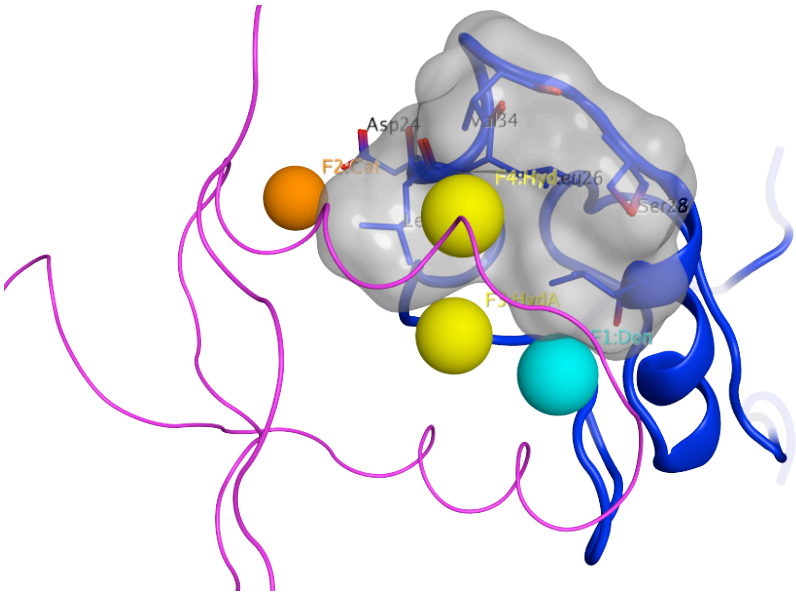

Figure 2.12: Pharmacophoric model of chain 2. Backbone of chain 1 is represented as purple ribbon

2.3.3 Molecular docking and consensus scoring

Those molecules matching the search criteria in both pharmacophores were analysed within the putative binding site of the homologous model with Glide docking under the Standard Precision (SP) screening mode.[29] This docking program generates a series of docked poses, which correspond to the minimum energy conformations, and calculates for them the predicted binding free energies. The conformational database produced by docking was successively evaluated with the scoring functions implemented in two programs: Plants[30] and FlexX.[31] Using only one scoring function is not recommended, since every scoring function gives different

relevance to diverse aspects that may be irrelevant to evaluate the binding potential of a compound.[32,33] A good strategy is to use multiple scoring functions and to combine all the results obtained through a consensus scoring, aiming to give the same relevance to the three scoring algorithms (section 1.3.5). Those structures belonging to the best 25 % according to all the functions applied to elaborate the consensus scoring were subjected to a more precise docking analysis using Glide under an Extra Precision (XP) screening mode. All the poses identified were subsequently minimized in order to avoid potential steric clashes within the protein. To make a selection of the best molecules coming from the extra precision docking, cluster of different groups were defined according to the diversity of their chemical structure. For each cluster, only the conformation with the highest score was retained. A visual inspection of the best poses allowed to select 20 compounds (see Appendix I) that were purchased and tested in *in vitro* assays. One compound (**1**, figure 2.13) was found to inhibit RNA replication of CVB3 in Vero cells (subtype A) with EC_{50} value of 129 µM. From a molecular modelling point of view, this relatively high value can be still taken into account, therefore it represented a starting point for a structure-activity relationship (SAR) evaluation.

2.4 Design and synthesis of tetrazole derivatives

2.4.1 (Benzylthio)-1-aryl 1*H*-tetrazoles (1, 21-23, 25-31)

A small series of tetrazole derivatives was prepared in order to confirm and improve the activity of the hit compound. The structure of the hit compound **1** is characterized by a central tetrazole moiety that is linked to a benzylthio ring in position 5 and has a benzoic acid in position 1 of the tetrazole (figure 2.13). Different aromatic substitutions were introduced to explore their effect on the activity of the molecule. In addition, the original compound was prepared in order to confirm the first activity results.

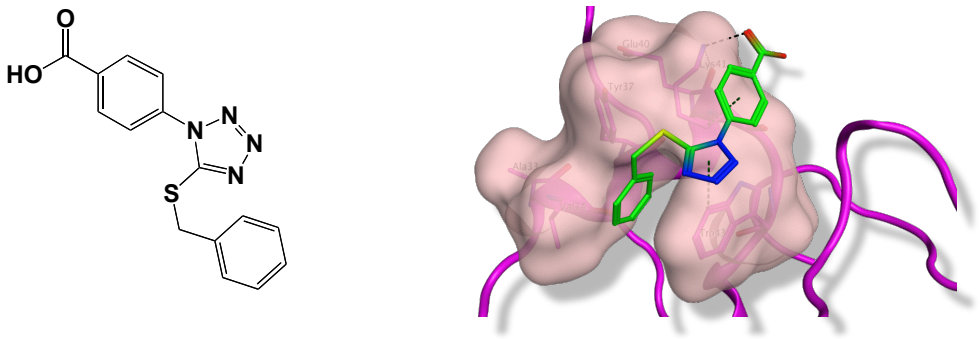

Figure 2.13: Chemical structure of compound **1** and its predicted binding mode

Scheme 2.1 shows the synthetic pathway used to prepare analogues **20-25**, while in scheme 2.2 is reported the procedure followed for the synthesis of the original hit compound **1**, its ester derivative **30** and the synthesis of compounds **29, 31**.

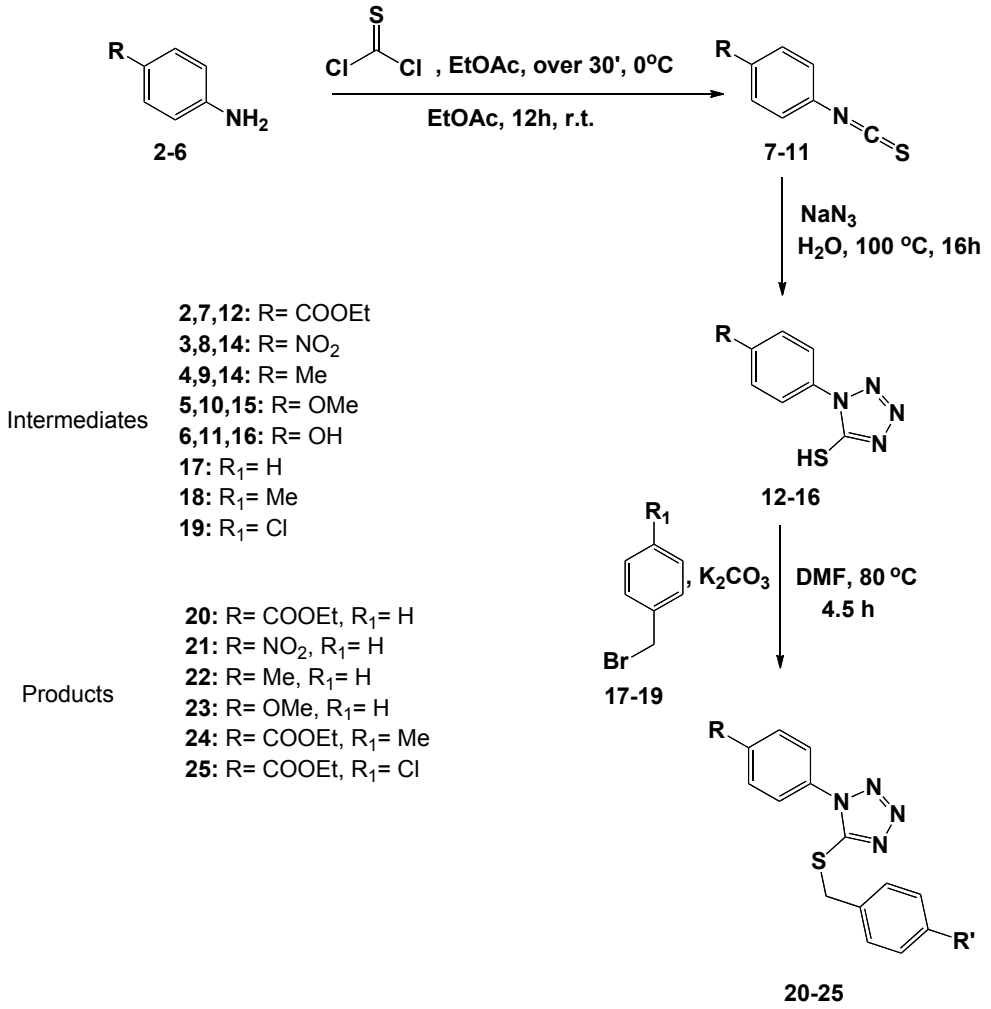

Scheme 2.1: Synthetic pathway for compounds **20-25**

Isothiocyanate intermediates **7-11** (Scheme 2.3) were synthesized through the reaction between a primary aromatic amine and thiophosgene. By treating them with a solution of sodium azide in water, tetrazole-5-thiones **12-16** (Scheme 2.5) were obtained. Compounds **20-25** (Scheme 2.5) were prepared through a nucleophilic substitution by the thiol group on the aryl bromide leaving group. Ethyl 4-(5-(benzylthio)4,5-dihydro-1*H*-tetrazol-1-*yl*)benzoate **20** was used for the synthesis of hit compound **1** through hydrolysis of the ester moiety with a solution of lithium hydroxide monohydrate. The same reaction was applied for the synthesis of acid derivatives **28**, **29** (Scheme 2.9) by conversion of, respectively, intermediates **24**, **25**.

Since it was not possible to obtain the pure ester compounds **24**, **25**, they were re-synthesised by a Fisher esterification of the correspondent acids **1, 28 (**scheme 2.2**)**.

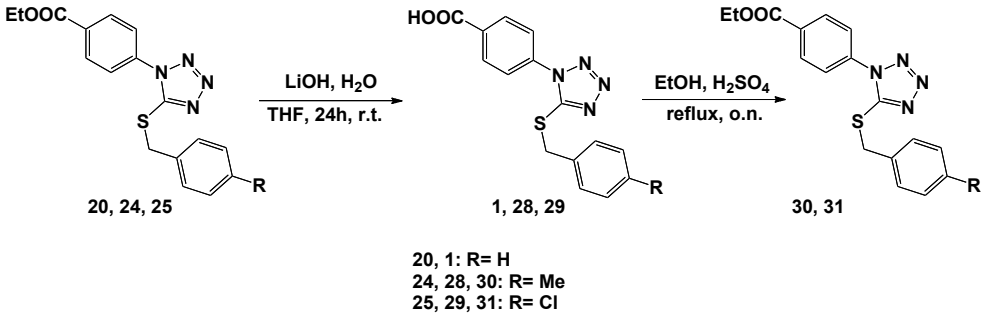

Scheme 2.2: Synthetic pathway for compounds **1, 29, 30, 31**

Synthesis of aryl isothiocyanates (7-11)

Aryl isothiocyanates were prepared by acylation of amines with thiophosgene in the presence of a base, according to the reported procedure.[34]

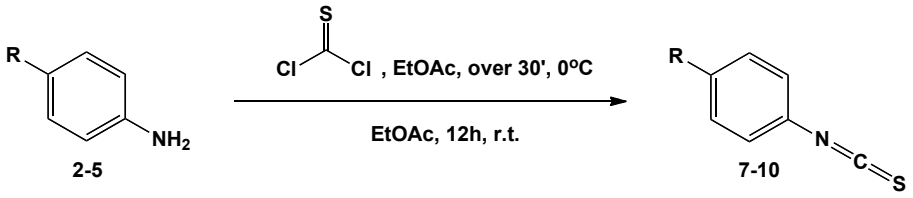

Aryl amine	R	Product	Yield %
2	COOEt	**7**	99
3	NO_2	**8**	90
4	Me	**9**	91
5	OMe	**10**	98

Scheme 2.3: Synthesis of compounds **7-10**

A different strategy was applied for the synthesis of the intermediate **11**, 4-hydroxyl isothiocyanate, because the product was obtained in low yield using the reaction conditions above described. According to a different reported procedure,[35] *p*-aminophenol **6** was treated with thiophosgene and 1M HCl solution, the latter one being responsible for the protonation of the

hydroxyl group, thus preventing any undesired reaction with thiophosgene. The modified conditions were helpful for the acylation of the amine group only the yield of the reaction (scheme 2.4).

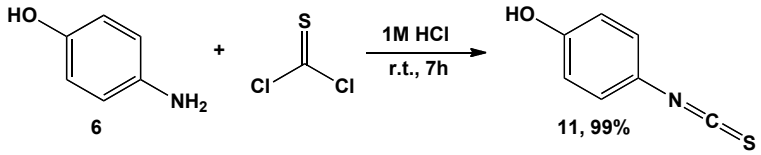

Scheme 2.4: Synthesis of compound **11**

Synthesis of 1-aryl-1*H*-tetrazole-5(4*H*)-thiones (12-16)

1-Aryl-1*H*-tetrazole-5(4*H*)-thiones **12-16** were obtained by treating the isothiocyanate intermediates **7-11** with sodium azide in water at 100 °C. The reaction was quenched with 1M HCl solution to obtain tetrazole derivatives **12-16** (scheme 2.5).[36]

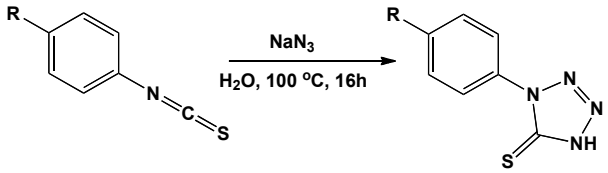

Aryl isothiocyanate	R	Product	Yield %
7	COOEt	**12**	40
8	NO_2	**13**	38
9	Me	**14**	58
10	OMe	**15**	70
11	OH	**16**	78

Scheme 2.5: Synthesis of compounds **12-16**

The postulated mechanism for the formation of the tetrazole ring can be described as a nucleophilic attack of the azide ion on the carbon atom of the isothiocyano group, followed by electrocyclization.

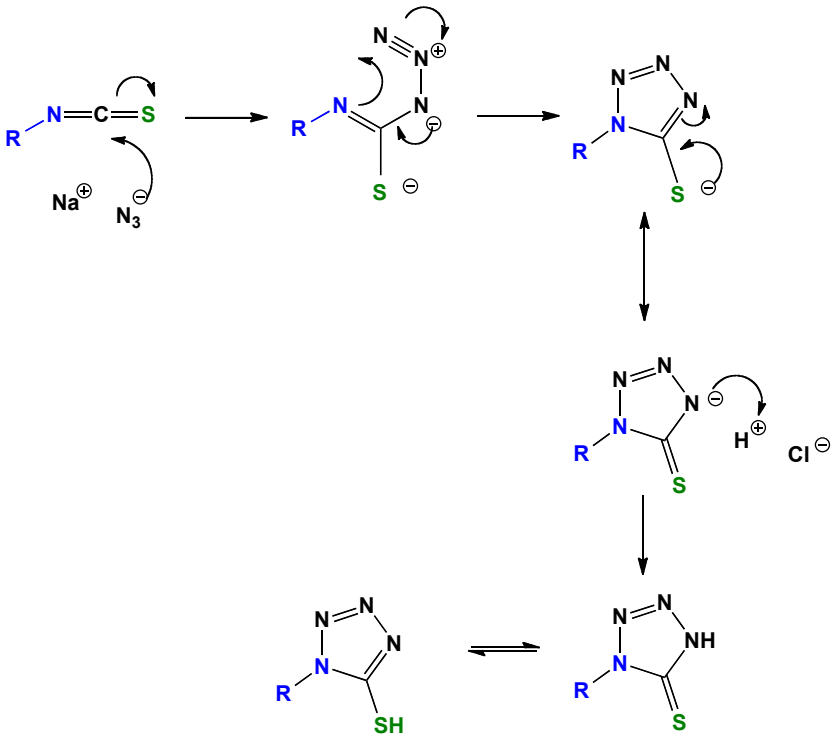

Scheme 2.6: Postulated mechanism for the tetrazole formation

Synthesis of 5-(benzylthio)-1-aryl-1*H*-tetrazoles (21-23, 25)

Final products **21-23** and **25** were obtained through a nucleophilic substitution between the aryl mercapto tetrazole intermediate and aryl bromides under basic reaction conditions (scheme 2.7).[37] Ethyl 4-(5-((4-methylbenzyl)thio)-1*H*-tetrazol-1-yl)benzoate **24** was not obtained as pure product after standard purification techniques, therefore was first converted to the acid derivative **28.** By Fisher esterification, compound **28** was converted to the final ester product **31**.

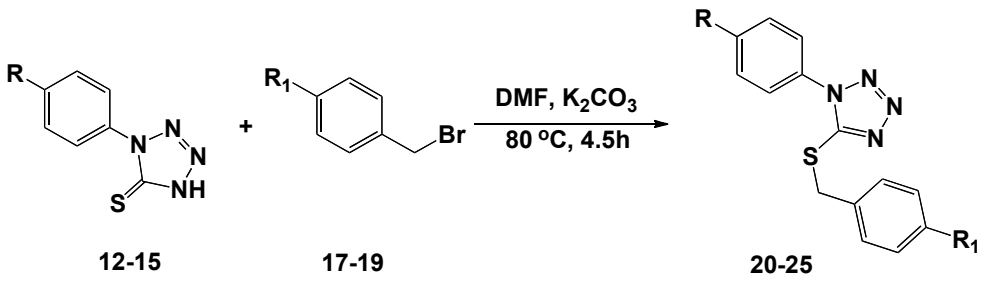

12-15 17-19 20-25

Aryl mercapto tetrazole intermediates	R	Aryl bromide	R_1	Product	Yield %
12	COOEt	**17**	H	**20**	83
13	NO_2	**17**	H	**21**	39
14	Me	**17**	H	**22**	57
15	OMe	**17**	H	**23**	60
12	COOEt	**18**	Me	**24**	48
12	COOEt	**19**	Cl	**25**	15

Scheme 2.7: Synthesis of compounds **20-25**

The reaction between benzyl bromide and 1-(4-hydroxyphenyl)-1*H*-tetrazole-5(4*H*)-thione **16** gave two products in one-step synthesis, the desired compound **26** and the disubstituted derivative **27**, as a product of bis nucleophilic substitution on two positions, the hydroxyl group and the thione group. Compounds **26** and **27** were successfully isolated by flash column chromatography (scheme 2.8).

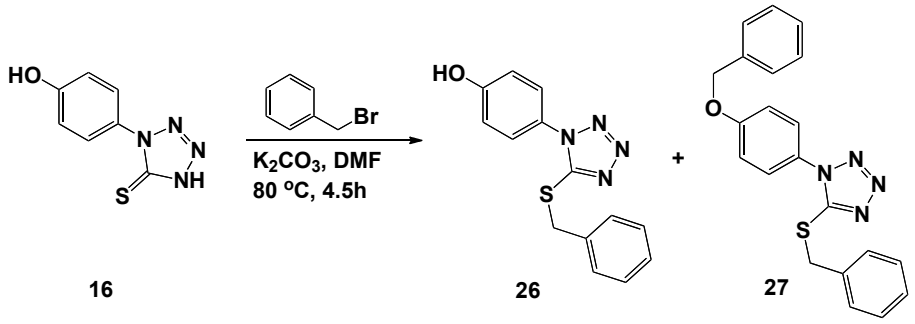

Aryl mercapto tetrazole	Product	Yield %
16	**26**	21.5
16	**27**	28.5

Scheme 2.8: Synthesis of compounds **26, 27**

Synthesis of 4-(5-(Arylthio)-1*H*-tetrazol-1-*yl*)benzoic acids (1, 28-29)

Hit compound **1** and final products **28, 29** were synthesised by a base-catalysed hydrolysis reaction of intermediate**s 20, 24** and **25** (scheme 2.9). Ethyl ester groups were hydrolyzed into the free carboxylic acids with lithium hydroxide, stirring the reaction mixture at r.t. over night. Final products **1, 28, 29** were precipitated after removal of the organic solvent and subsequent acidification of the water residue to pH 5.[38]

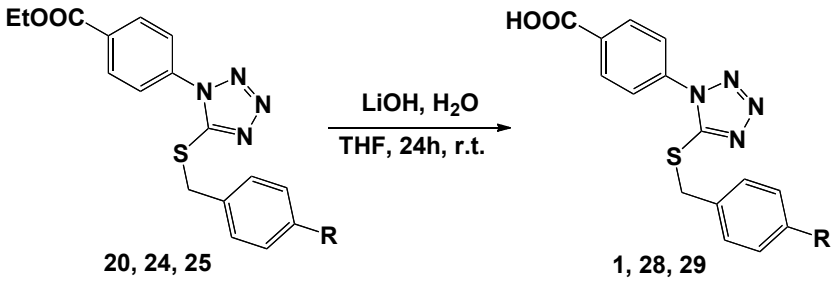

5-(Benzylthio)-1-aryl-1*H*-tetrazoles	R	Product	Yield %
20	H	**1**	32
24	Me	**28**	34
25	Cl	**29**	33

Scheme 2.9: Synthesis of compounds **1, 28, 29**

Synthesis of ethyl 4-(5-(benzylthio)-1*H*-tetrazol-1-*yl*)benzoates (30, 31)

Compounds **30**, **31** were synthesised following a Fisher esterification by refluxing over night compounds **1, 28** with ethanol and sulfuric acid. Upon reaction completion, $NaHCO_3$ was added to neutralize the excess of acid used (scheme 2.10).[39]

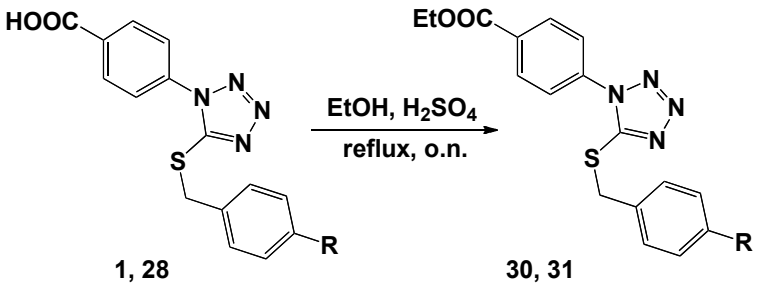

Ethyl 4-(5-(benzylthio)-1*H*-tetrazol-1-*yl*)benzoate	R	Product	Yield %
1	H	**30**	88
28	Me	**31**	26

Scheme 2.10: Synthesis of compounds **30, 31**

2.4.2 Biological evaluation

All compounds prepared were tested in a cell-based assay at Rega Institute for Medical Research in Leuven, under the supervision of Dr. Johan Neyts. Activity is expressed for each compound in terms of EC_{50}, that is the effective concentration (μM) of compound required to reduce viral replication by 50%, and EC_{90}, that is the effective concentration (μM) of compound required to reduce CVB3 replication by 90%. Cytotoxicity is evaluated in terms of CC_{50}, that is the cytostatic/cytotoxic concentration (μM) required to observe 50% of adverse effect on the host cell. The selectivity index, SI, is evaluated by calculating the ratio CC_{50}/EC_{50}.

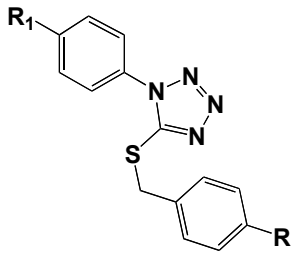

Compound	R_1	R	EC_{50} (μM)	EC_{90} (μM)	CC_{50} (μM)
1	COOH	H	130	130	-
21	NO_2	H	>239	>239	-
22	Me	H	>266	>266	-
23	OMe	H	>251.6	>251.6	-
25	COOEt	Cl	>33.4	>33.4	-
26	OH	H	>264	>264	-
27	OCH_2Ph	H	>66.8	>66.8	-
28	COOH	Me	>306	>306	-
29	COOH	Cl	>216	>216	-
30	COOEt	H	>220	>220	-
31	COOEt	Me	>211	>211	-

Table 2.1: Activity and cytotoxicity data for compounds **1**, **21-23, 25-31**

The biological evaluation shows that the activity of the re-synthesised hit compound **1** is confirmed. However, the data for new derivatives show a loss of antiviral activity associated to the modifications applied.

2.5 Computer-aided approaches on the 3D polymerase

One of the most common targets for the identification of novel antivirals is the RNA-dependent RNA polymerase. Using the available crystal structure of the CVB3 polymerase, different computer-aided approaches were applied.

2.5.1 Structure-based Virtual Screening

As already mentioned in section 2.2.2, a small molecule, GPC-N114, was recently identified as a new non-nucleoside inhibitor with a broad spectrum of activity against several members of the Picornavirus family. Although the activity data were very promising, this compound encountered poor bioavailability issues when tested in animals, therefore the aim of this study was to identify new scaffolds with an improved solubility and a similar or better biological activity. The structure of GPC-N114 was not accessible for our project at the beginning, therefore, using the available information on the binding region of GPC-N114, a structure based virtual screening was performed. The area within the polymerase is a tight pocket, near the nucleotide entry tunnel. GPC-N114 was found to make contacts with Leu110, Thr114 and Lys127. It strongly interacts with Arg188, His199 and Tyr195 and it is close to residues Gly290, Cys291, Gly293 and Ile296.

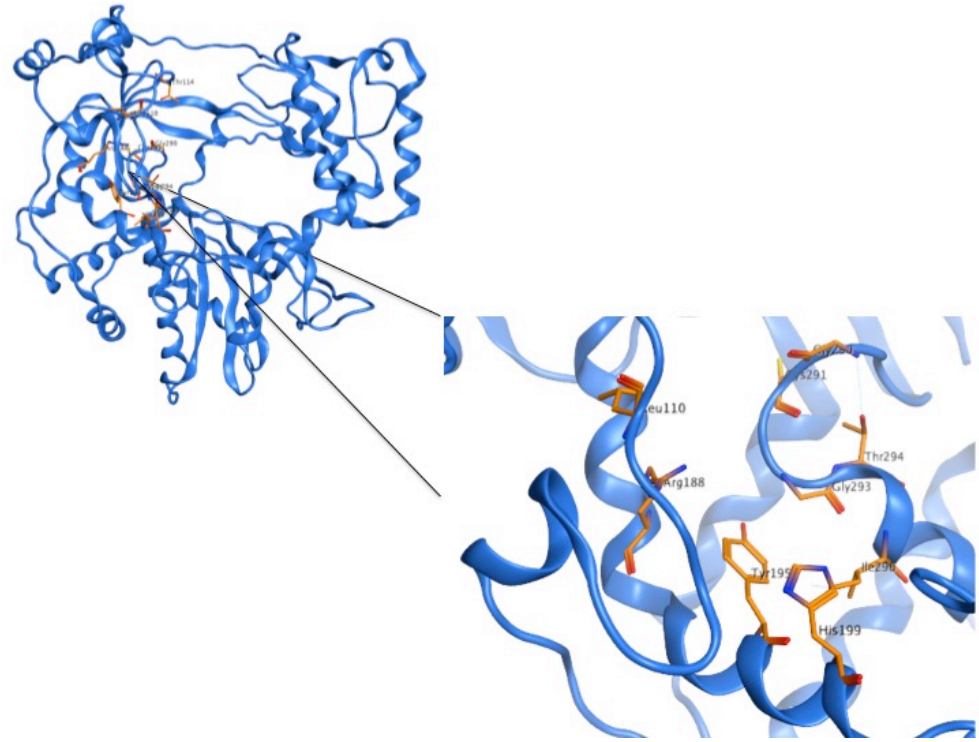

Figure 2.14: Crystal structure of the CVB3 3D polymerase and close-up of the binding site of GPC-N114

Using the available crystal structure of CVB3 RNA-dependent RNA polymerase in complex with a pyrophosphate (PDB ID: 3CDU),[40] a pharmacophore model of six features was built: a hydrogen bond acceptor, (F1:Acc), near Ser115, two hydrogen bond donors, (F2/F3:Don) to interact, respectively, with Thr114 and Gly290, a hydrogen bond acceptor (F4:Acc) in close vicinity to Arg188, a hydrophobic feature to interact with Tyr195 (F5:Hyd) and finally an additional hydrogen bond acceptor (F6:Acc), near Gly293. F5 was kept as essential due to the essential stacking interactions for the ligand binding with the aromatic ring of Tyr195 (figure 2.15). Exclusion volumes corresponding to the protein occupational space were added before the first pre-filtration of the conformational database of the SPECS compounds. Around 3000 molecules matched these criteria.

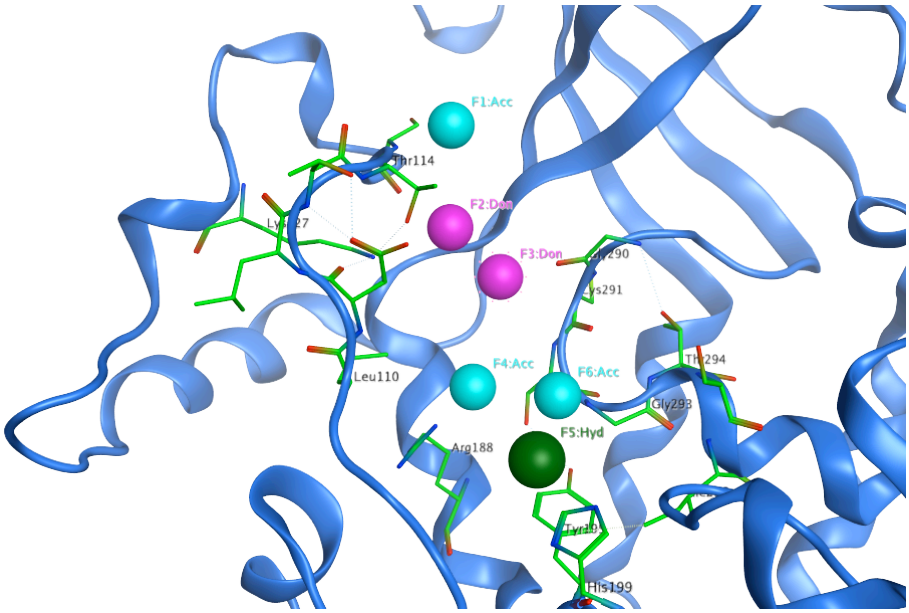

Figure 2.15: Pharmacophoric model built on 3CDU

These molecules were evaluated by a docking procedure using Glide SP mode which produced a conformational database of docked poses for each molecule. A re-scoring process was finally performed for all the conformations obtained, using FlexX and Plants. By a consensus scoring method, described in section 1.3.5, the best 25% results were selected, reducing the number of the molecules to 410. These compounds underwent to an extra precision docking (XP) mode. A final visual inspection allowed to select 18 compounds that were purchased for biological testing (Appendix I). Unfortunately, none of these compounds showed antiviral activity on a cell-based assay.

2.5.2 Model of the GPC-N114 bound to the polymerase

A second approach was carried out when the chemical structure of the ligand GPC-N114 was revealed (figure 216).

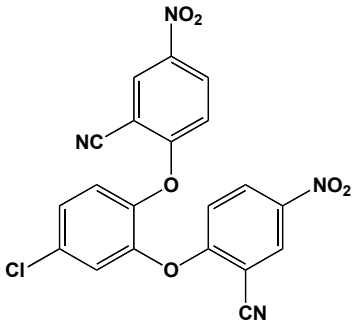

Figure 2.16: Chemical structure of GPC-N114

The 3D structure of the co-crystallized ligand in the polymerase was not accessible yet, therefore a model of the complex between the polymerase and the inhibitor was generated, using the information on the ligand interactions that were obtained. The compound is bound in a cavity of the polymerase located at the bottom of the template channel, mimicking the template acceptor nucleotide. Both hydrophobic and polar interactions are responsible for the inhibitor binding. One of the 2-cyano-4-nitrophenyl rings is involved in van der Waals contacts with side chains of residues Leu110 and Asp111; it also interacts with Arg188 and makes contacts with Gly290, Cys291 and Gly292. One nitro group is hydrogen-bonded to the amide group of Asp111 and Thr114, while the central chlorophenyl ring makes van der Waals contacts with Leu107, Tyr195, Cys293 and Ile296. Furthermore, the chloride atom is hydrogen-bonded to the side chain of His199. The second 2-cyano-4-nitrophenyl ring seems to occupy the position expected for the template acceptor base, with the nitro group hydrogen bonded with Ser295 and Tyr327. This moiety also interacts with residues from Gly293 to Ile296. Finally, the oxygen atom linkers are involved in contacts with amino acids Ser292 and Gly293. The model created contains a RNA chain, the coordinates of which were taken from the crystal structure of the FMDV 3Dpol-RNA complex (PDB ID: 1WNE).[41] The scope of this model is to reproduce the active conformation of the inhibitor GPC-N114. After energy minimization of the complex created, *in silico* approaches were applied (figure 2.17).

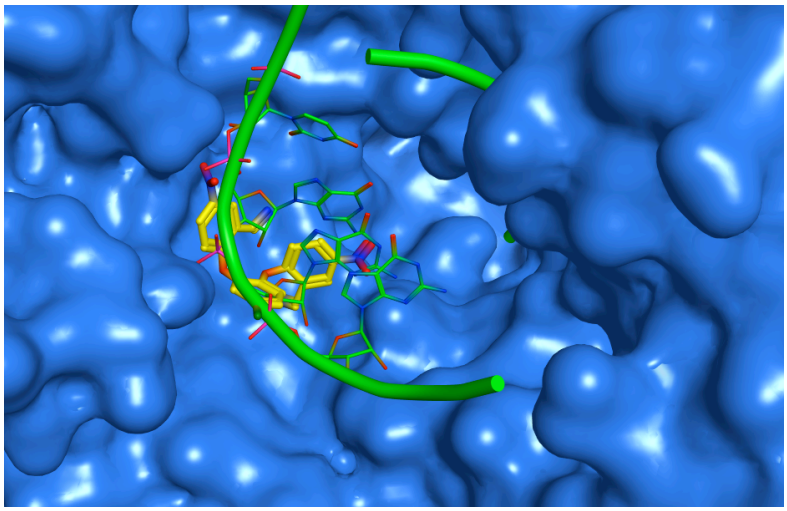

Figure 2.17: Model of GPC-N114 in its binding site. The predicted position of the RNA template was determined using the FMDV 3Dpol -RNA complex (PDB ID: 1WNE) as a guide

2.5.3 Design of new GPC-N114 analogues

Aiming to identify new scaffolds active against CVB3 replication, the GPC-N114 structure was taken into account for structural modifications that allowed the design and synthesis of six new scaffolds. Figure 2.18 shows the positions modified for the preparation of the new derivatives that were all analysed with the flexible alignment technique, available in MOE 2010.10, to compare them with the known inhibitor.[42]

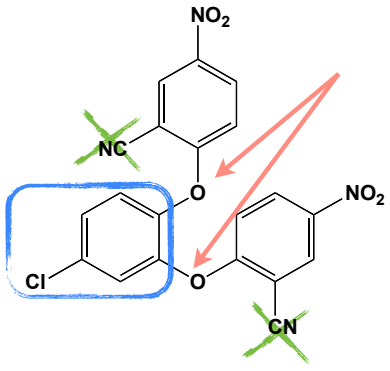

Figure 2.18: Chemical structure of GPC-N114.
The applied modifications were also represented: cyano groups were removed, the oxygen linker was replaced with a C or a N and the central ring was substituted with several new groups

This application is able to align two molecules by maximising steric and feature overlap and minimising the internal ligand strain. A score is produced for each alignment which is an evaluation of how good the alignment is. Different parameters, in particular, can be generated: the average internal strain energy, U, the total mutual similarity score, F which, for a good alignment, should be a low value and the function S, which corresponds to the sum of U and F values. Two molecules are well aligned when the S value is low, together with the dU that, ideally, should be lower than 1 kcal/mol. Four new scaffolds were designed with the aim to explore a different central ring and a diverse atom linker between the two aromatic moieties. All the structures designed had good scoring when aligned to the modelled conformation of the GPC-N114. Figures 2.19 shows the chemical structure and alignment of the derivative bearing nitro groups like the reference molecule.

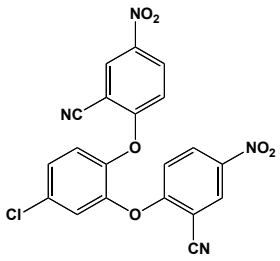

LogP = 3.41

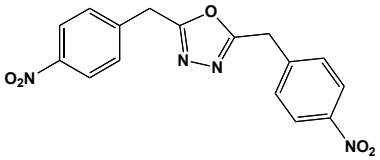

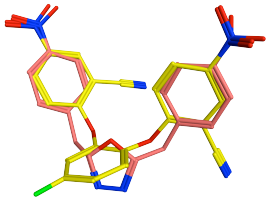

Compound **32**: dU=0 kcal/mol

LogP= 3.83

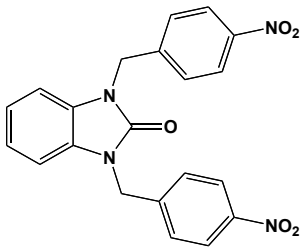

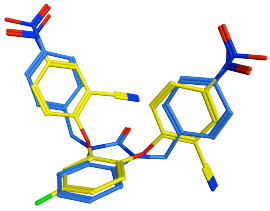

Compound **33**: dU= 0 kcal/mol

LogP= 4.36

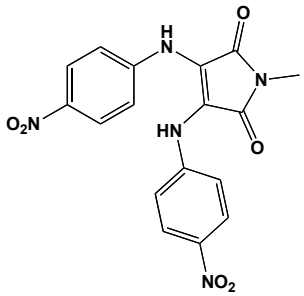

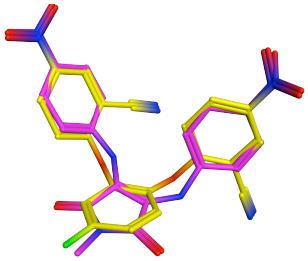

Compound **34**: dU= 0 kcal/mol

LogP= 2.54

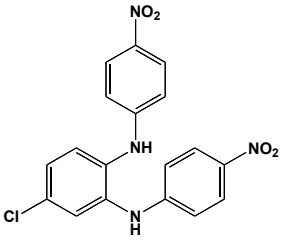

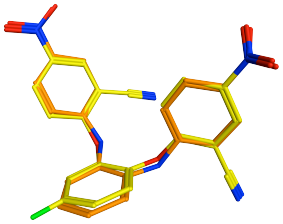

Compound **35**: dU= 0 kcal/mol

LogP= 5.16

Figure 2.19: Structure and alignment results of designed compounds **32-35**

The new derivatives present a good overlapping to the known inhibitor, with the central ring and the two nitro groups well aligned to the GPC-N114 ligand. The good superimposition was also confirmed by energy strain values that were all lower than 1 kcal/mol. Apart from compound **35**, for which a border line LogP (partition coefficient) value was predicted (5.16), all the other compounds showed an acceptable LogP value. A better calculated value was reported for compound **34**, compared to GPC-N114. For each scaffold, two derivatives, the unsubstituted and the one bearing two nitro groups, were synthesised. Cyano groups were not kept in the new structures, as they were not related to GPC-N114 activity (data not shown, personal communication with Dr. Gherard Purstinger). The reason behind the synthesis of the unsubstituted compound was to confirm the relevance of the nitro groups, as already observed being essential features of the reference inhibitor.

2.6 Synthesis of GPC-N114 analogues

2.6.1 2,5-bis-Aryl-1,3,4-oxadiazoles (32, 40)

The first designed chemical scaffold is characterized by a central oxadiazole ring and a carbon linker between the two lateral benzene moieties and the central part.

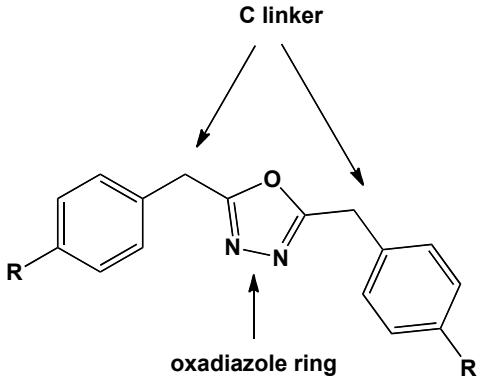

Figure 2.20: Chemical features of the oxadiazole scaffold

The followed chemical pathway is a condensation between aryl acetohydrazides and aryl acetic acids in the presence of phosphorus oxychloride ($POCl_3$).

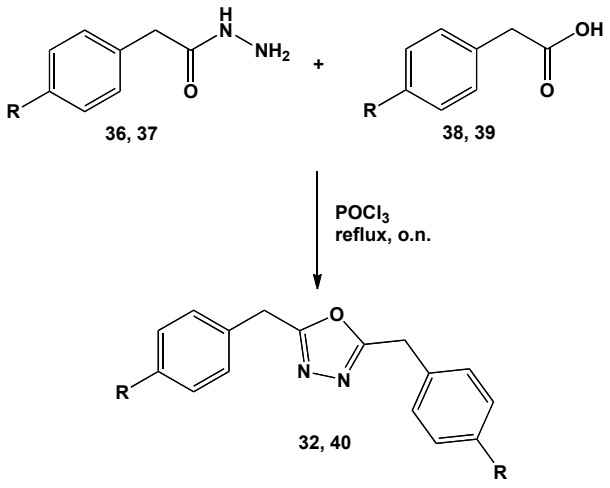

Scheme 2.11: Synthetic pathway for compounds **32, 40**

Synthesis of 4-(nitrophenyl)acetohydrazide (36)

Starting materials were not commercially available and were, therefore, prepared. For the synthesis of final product bis-(4-nitrophenyl)-1,3,4-oxadiazole **32**, the available 4-nitro phenyl acetic acid **38** was first converted to the correspondent ethyl ester by a Fisher esterification using EtOH and sulfuric acid. The ester derivative **41** was then converted to 4-(nitrophenyl)acetohydrazide intermediate **36** by nucleophilic addition of hydrazine monohydrate (scheme 2.12).

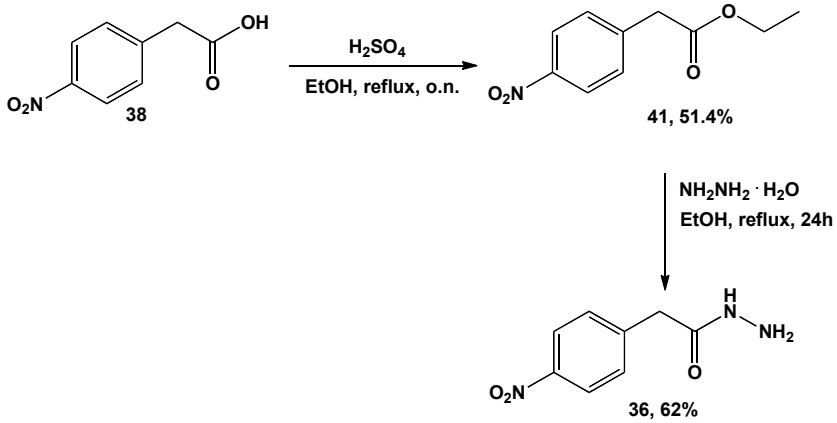

Scheme 2.12: Synthetic pathway for the synthesis of intermediate **36**

Synthesis of 2-phenylacetohydrazide (37) and 2-phenyl acetic acid (39)

In order to obtain the unsubstituted derivative **40**, starting material 2-phenylacetohydrazide **37** was synthesized by reaction of the commercially available ethyl phenyl acetate **42** with hydrazine monohydrate, following reported procedure.[43] Ethyl phenyl acetate was also used to prepare 2-phenyl acetic acid **39** by a base-catalyzed hydrolysis in the presence of lithium hydroxide monohydrate (scheme 2.13).

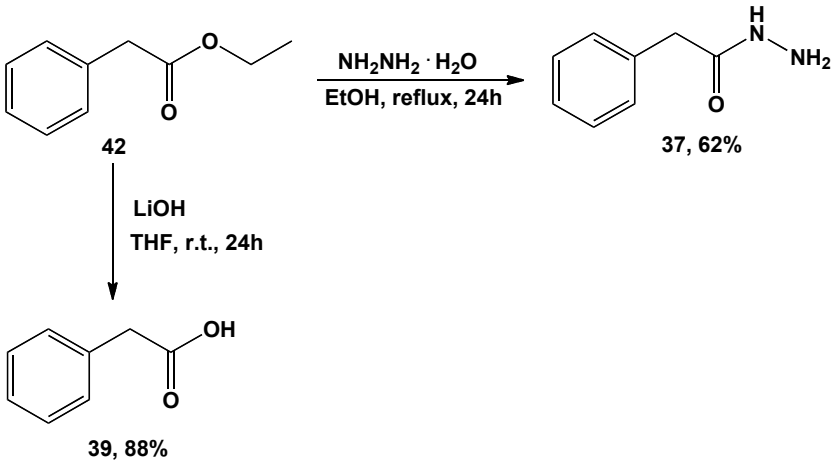

Scheme 2.13: Synthetic pathway for the synthesis of intermediates **37, 39**

Synthesis of ethyl 2,5-bis-aryl-1,3,4-oxadiazoles (32, 40)

Following a reported procedure, the desired products were synthesized by cyclodehyrogenation of aryl acetohydrazide and aryl acetic acid using phosphorus oxychloride ($POCl_3$).[44]

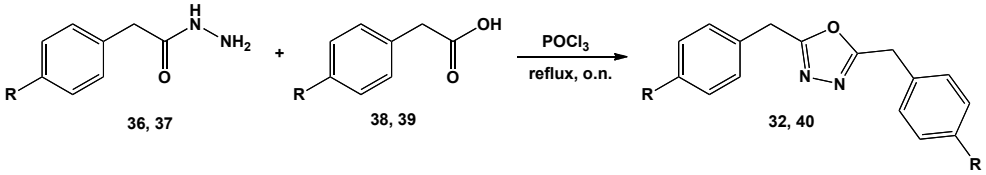

Aryl acetohydrazide	Aryl acetic acid	R	Product	Yield %
36	38	NO_2	32	53
37	39	H	40	54

Scheme 2.24: Synthesis of compounds **32, 40**

2.6.2 1,3-bis-Aryl-1*H*-benzo[*d*]imidazol-2(3*H*)-ones (33, 46)

A second selected scaffold, according to the flexible alignment analysis, was used for the synthesis of two new analogues of the GPC-N114. In this case, the central 4-chlorobenzene was replaced with a benzoimidazol-2-one and a C-linker was inserted in place of the original O atom, as already seen in the previous family of compounds (figure 2.21). Also in this case, two derivatives were prepared, the unsubstituted and the nitro ones.

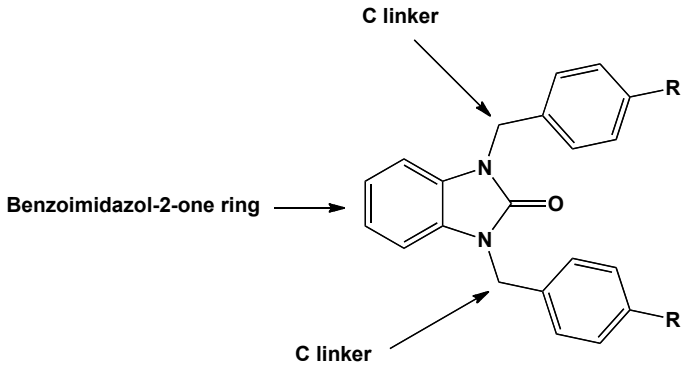

Fig. 2.21: Structure and features of benzoimidazol-2-one scaffold

The synthetic strategy applied is a two-step synthesis that starts with the formation of the central ring, by treating *o*-phenylendiamine with the carbonylating agent carbonyl diimidazole. Final products were obtained through nucleophilic displacement of bromide leaving group by the 1*H*-benzo[*d*]imidazol-2(3*H*)-one intermediate.

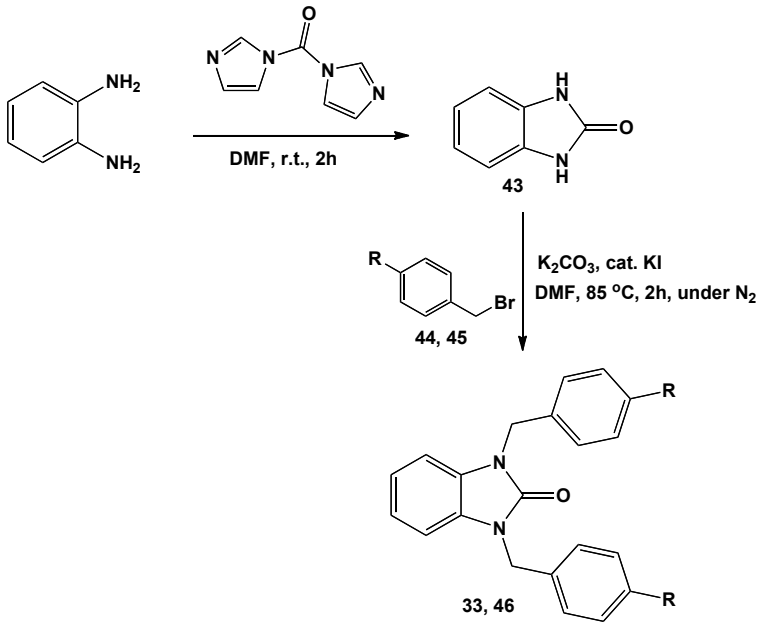

Scheme 2.15: Synthetic pathway for the synthesis of compounds **33, 46**

Synthesis of 1*H*-benzo[*d*]imidazol-2-(3*H*)-one (43)

In a first attempt to prepare intermediate **43**, *o*-phenylendiamine was dissolved in THF and then carbonyl diimidazole was added to the reaction mixture, according to a reported procedure (scheme 2.16).[45] After stirring at room temperature for 22 h, the reaction mixture was heated at 50°C for additional 6 h, due to the presence of unreacted starting material. From the

reaction, a mixture of products was formed, from which the desired product **43** could not be isolated by standard purification techniques.

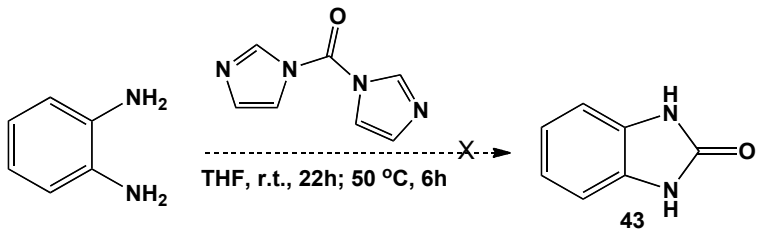

Scheme2.16: First attempt for the synthesis of compound **43**

A second attempt was made using a different procedure that allowed to obtain the desired intermediate (scheme 2.17).[46] The title compound was obtained by carrying out the reaction in dimethyl formamide and stirring at room temperature for 2 hours. The title compound was obtained without purification in 50 % yield.

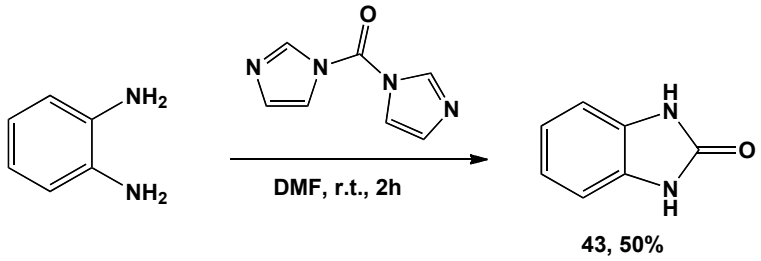

Scheme 2.17: Second attempt for the synthesis of compound **43**

Synthesis of 1,3-bis-aryl-1*H*-benzo[*d*]imidazol-2(3*H*)-ones (33, 46)

Final products **33**, **46** were obtained with a one-step synthesis through nucleophilic substitution between intermediate benzoimidazol-2-one **43** and aryl bromides.

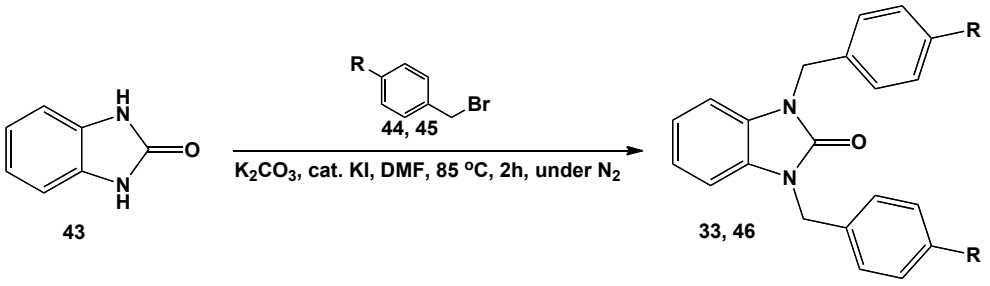

Aryl bromide	R	Product	Yield %
44	NO_2	**33**	16
45	H	**46**	11

Scheme 2.18: Synthesis of final products **33, 46**

2.6.3 1-Methyl-3,4-bis-(phenylamino)-1*H*-pyrrole-2,5-dione (47)

A third modification made on the query molecule, GPC-N114, was the introduction of a maleimide ring. From docking studies, this ring is predicted to establish similar interactions observed for the reference molecule and an additional hydrogen bond between one carbonyl group and Arg 188 (figure 2.22). The oxygen linker was replaced by a nitrogen atom. Two derivatives were planned for the synthesis, as previously seen for the other two families of compounds.

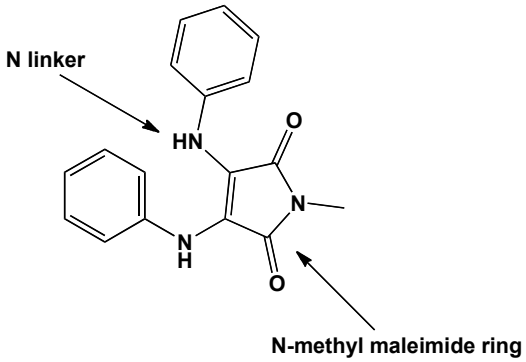

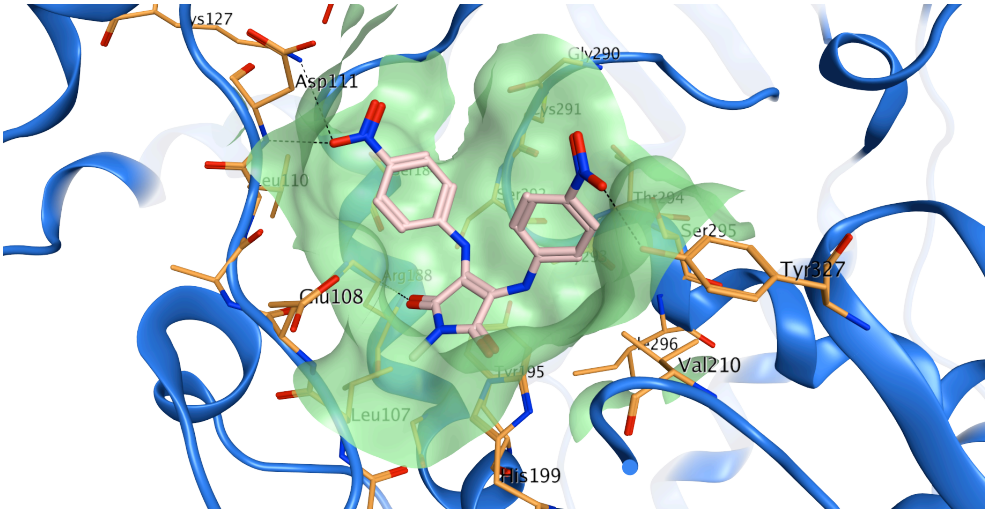

Figure 2.22: Chemical scaffold of compound **47** and its predicted binding mode

According to the literature, the synthetic pathway consists of a 3-step reaction, with the synthesis of the central maleimide ring intermediate that reacts by two conjugate addition/elimination reactions with the aryl aniline (scheme 2.19).

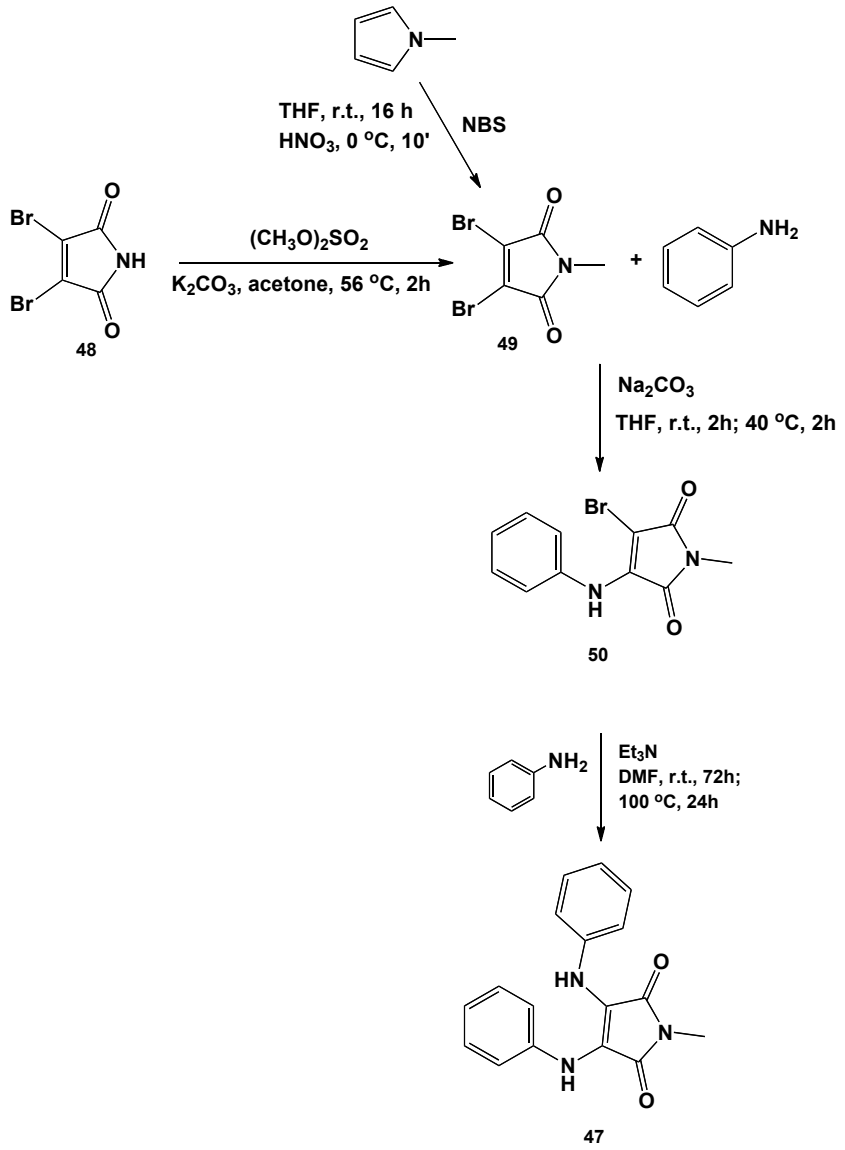

Scheme 2.19: Synthetic pathway for compound **47**

Synthesis of *N*-methyl-3,4-dibromomaleimide (49)

The initial method adopted to synthesise maleimide **49** was to obtain *N*-substituted 2,5-dibromopyrrole by a reaction between *N*-methyl pyrrole and two equivalents of *N*-dibromosuccinimide. The following oxidation of the intermediate allowed to obtain the desired product, according to a reported procedure (scheme 2.20).[47]

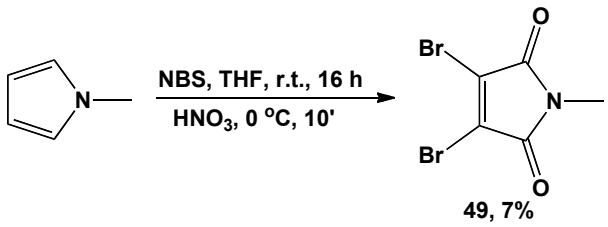

Scheme 2.20: Synthesis of intermediate **49**

Scheme 2.21 shows the suggested mechanism. According to the literature, this reaction is described as a transposition of both bromides to the 3,4-positions, followed by the oxidation with nitric acid at 0 °C.

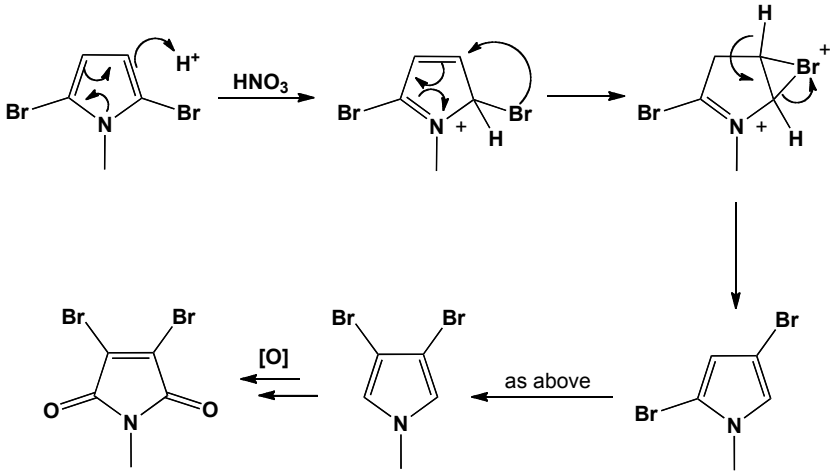

Scheme 2.21: Mechanism of *N*-methyl maleimide formation

Due to the low yield of the reaction linked to the difficulty of obtaining the only dibrominated product, it was decided to start from the 3,4-dibromomaleimide **48** to synthesize *N*-methyl-3,4-dibromomaleimide **49** by *N*-alkylation with dimethyl sulfate (scheme 2.22).[48] The reaction went to completion after 2 h and the product was obtained without purification and with a increased yield (54.4%).

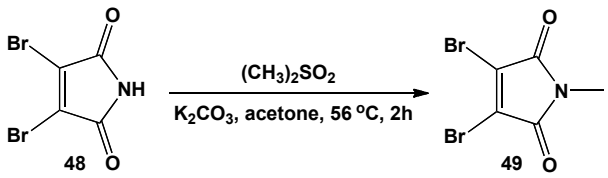

Scheme 2.22: Second procedure for the synthesis of intermediate **49**

2.6.4 1-Methyl-3,4-bis-(4-nitrophenylamino)-1*H*-pyrrole-2,5-dione (34)

The designed compound **34**, bis-(4-nitrophenylamino)-maleimide, was not obtained after trying several reaction conditions (scheme 2.23). In a first attempt, a solution of *N*-methyl-3,4-dibromomaleimide **49** in dimethylformamide was treated with an excess of 4-nitroaniline, under basic condition with Et_3N for 24 h.[49] After that time, the starting material was still present, therefore the reaction mixture was heated at 90°C for 24 h. Flash column chromatography was performed to separate a mixture of new species formed, but it was not possible to isolate the desired intermediate. A second attempt was made prolonging the reaction time to 7 total days, stirring the mixture at room temperature and then heating it at 80°C for 6 days. The reaction was constantly monitored by TLC. Starting materials were still present, together with a mixture of new species. Also in this case, purification by flash column chromatography did not allow to isolate the desired product.

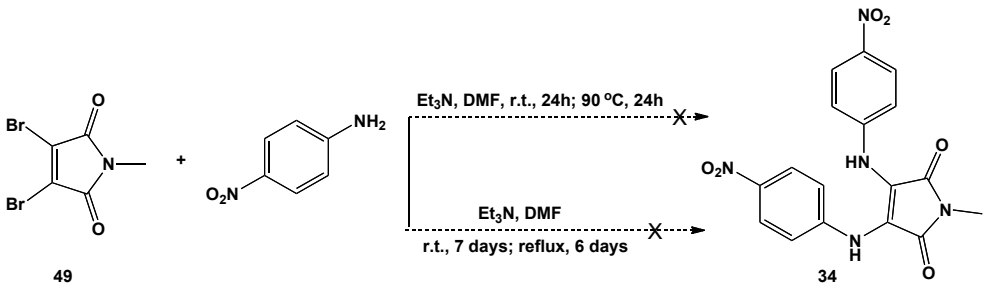

Scheme 2.23: Attempts for the synthesis of bis-(4-nitrophenylamino)-maleimide **34**

A probable explanation is the poor reactivity of 4-nitroaniline: the electron withdrawing and inductive effects of the nitro group deactivate the aromatic ring, rendering the amine a poor nucleophile and thus explaining the failure of the coupling reaction. However, it was possible to obtain the unsubstituted product, 1-methyl-3,4-bis-(4-nitrophenyl)amino)-1*H*-pyrrole-2,5-dione **47**.

Synthesis of 1-methyl-3,4-bis-(phenylamino)-1*H*-pyrrole-2,5-dione (47)

The unsubstituted derivative **47** was obtained by two coupling reactions with aniline. While milder conditions were followed for the first step of the synthesis, the second conjugation reaction required a longer reaction time and heating to boost the formation of the designed product.

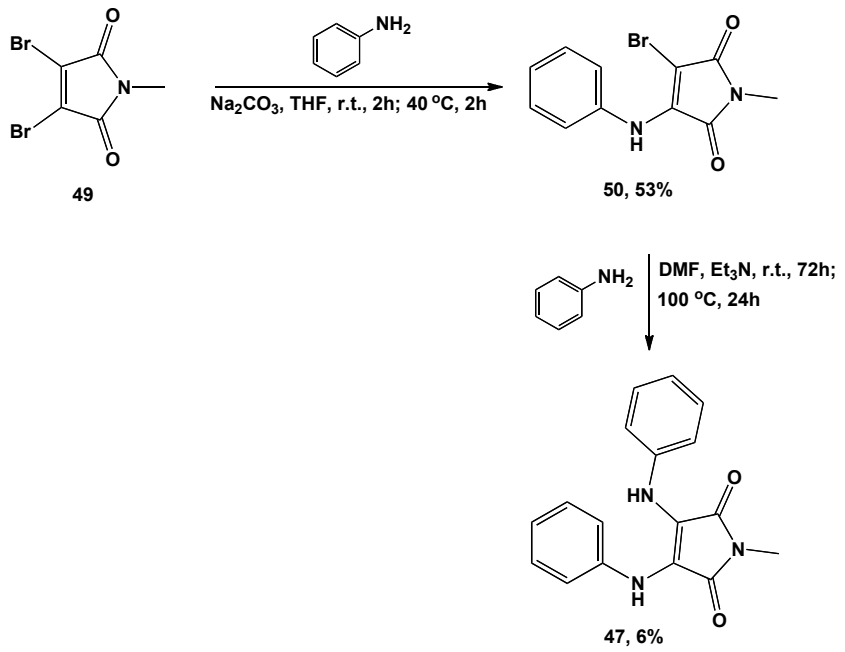

Scheme 2.24: Synthetic pathway for the synthesis of compound **47**

Synthesis of 3-bromo-1-methyl-4-(phenylamino)-1*H*-pyrrole-2,5-dione (50)

According to a reported procedure, *N*-methylmaleimide **49** was treated with an excess of sodium carbonate and aniline (scheme 2.25).[9] The reaction was stirred for 2 hours at r.t. in THF and heated at 40°C for 2 h in order to enhance the formation of the probable product. The crude mixture was purified by chromatography and the monosubstituted intermediate **50** was obtained with 53 % yield.

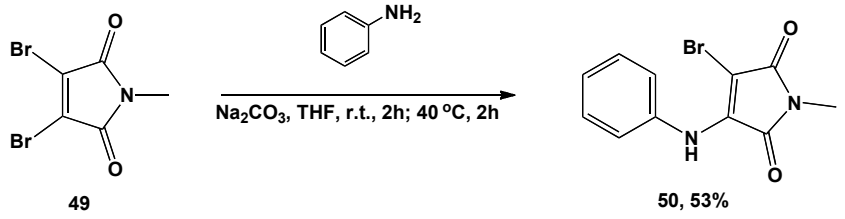

Scheme 2.25: Synthesis of intermediate **50**

Synthesis of 1-methyl-3,4-bis(phenylamino)-1*H*-pyrrole-2,5-dione (47)

Following a reported procedure, the symmetrical unsubstituted maleimide was finally obtained despite the discouraging discussion presented in the referred paper.[50] It is suggested, in fact, that the coupling of the second amine could be achieved only forcing the reaction conditions and using an amine with a more nucleophilic profile. In the monoaminated intermediate,

the carbon bearing the Br group has a reduced electrophilicity, thus preventing the addition of a second aniline molecule. Final product **47** was obtained using 3 equivalents of both, the aniline and triethylamine (scheme 2.26). The reaction was stirred at r.t. for 3 days in dimethyl formamide. To enhance the formation of the product, the reaction was heated to 100°C for additional 24h. The title compound was finally isolated as a pure product in low yield (6 %) by flash column chromatography and recrystallization purification.

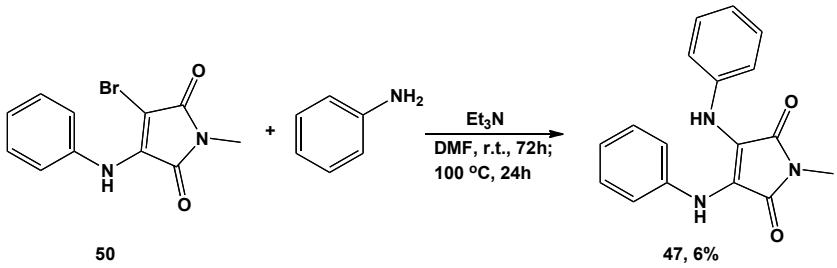

Scheme 2.26: Synthesis of compound **47**

2.6.5 *N*^{1}-Phenylbenzene-1,2-diamine (52)

Bearing a nitrogen atom in place of the oxygen linker, a series of two compounds was designed.

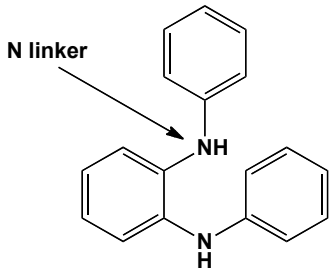

Figure 2.23: Chemical scaffold for compound **52**

As in the reference molecule, the central phenyl ring was kept, while the cyano groups were not conserved on the new derivatives. The synthetic pathway planned was a variation of Ullmann reaction between aryl 1,2-diamine and iodobenzene, according to a reported procedure.[51] A first attempt was made starting from *o*-phenylenediamine and iodobenzene to get the formation of the unsubstituted derivative **51** (scheme 2.27). Formation of the desired disubstituted product was confirmed by NMR experiment, but it was not possible to purify it, due to the simultaneous

formation of a mixture of products. However, from chromatographic purification, the mono substituted compound, N^1-phenylbenzene-1,2-diamine **52**, was obtained as pure product and evaluated for its antiviral activity.

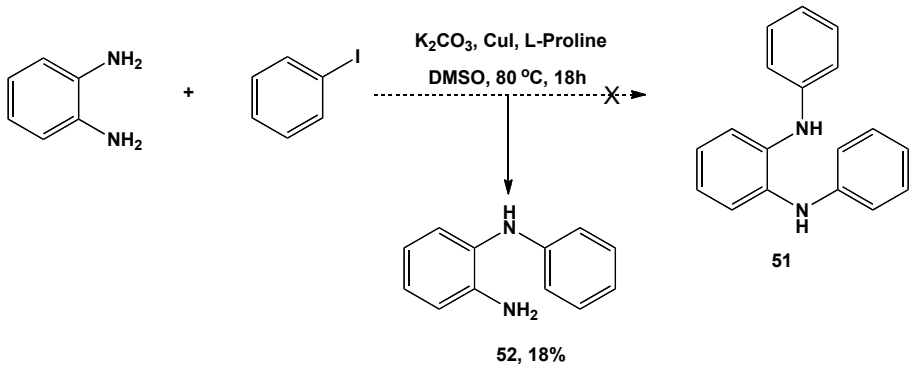

Scheme 2.27: First attempt for the synthesis of compound **51**

2.6.6 N^1,N^2-Diphenylbenzene-1,2-diamine (51)

Another attempt to obtain the disubstituted derivative was carried out with a second procedure, where *o*-phenylenediamine and iodobenzene were stirred in DMF with copper as a catalyst, CuI, Pyr and Et_3N (scheme 2.28). Only unreacted starting materials were recovered, therefore it was decided not to make further effort to get the desired products, as it would have been even more difficult to obtained the planned nitroderivative **35**.

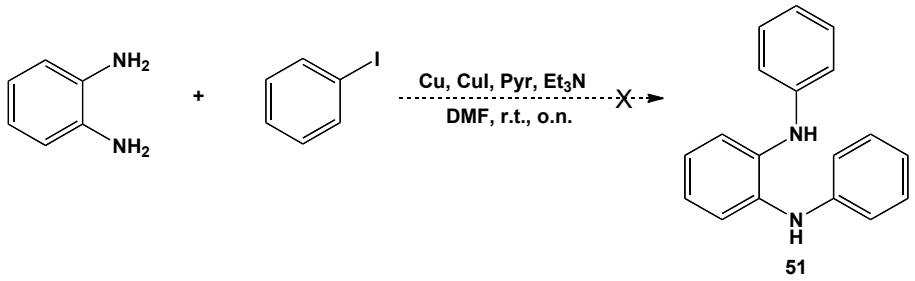

Scheme 2.28: Second attempt for the synthesis of compound **51**

2.6.7 Biological evaluation

Compounds **32-33, 40, 46-47** and **52** were evaluated for their antiviral activity and cytotoxicity in a virus-cell-based assay (tables 2.2, 2.3).

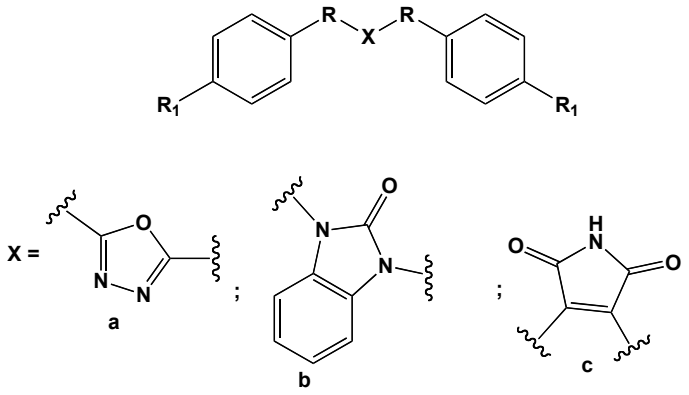

Compound	X	R	R_1	EC_{50} (µM)	EC_{90} (µM)	CC_{50} (µM)
32	a	CH_2	NO_2	>300	>300	-
40	a	CH_2	H	>294	>294	-
33	b	CH_2	NO_2	>238	>238	-
46	b	CH_2	H	>30.9	>30.9	-
47	c	N	H	>300	>300	-

Table 2.2: Activity and cytotoxicity data for compounds **32-33, 40, 46-47**

The biological evaluation for the new derivatives suggests that there is no correlation between the modifications applied and the antiviral activity. It is not possible to speculate if the absence of the activity for compounds **32**, **40**, bearing a central oxadiazole ring, is linked to the presence of a smaller central moiety. A second series of compounds was designed by introducing a benzoimidazol-2one ring and maintaining the C atom as linker between the central and the two lateral aromatic moieties. Also in this case, the biological results highlight the absence of antiviral effect against CVB3 replication for compounds **33, 46**. A third planned scaffold was based on the replacement of the oxygen atom with a nitrogen linker and on a new central ring that, according to the putative docking mode, seems to maintain the essential interaction with residues of the binding site. Unfortunately, no antiviral activity was observed for the new

derivative **47**, leading to the conclusion that the modifications applied were not successful. Due to the impossibility to understand the relation between the loss of activity and the new chemical structures, a final scaffold was designed with the scope to maintain the overall structure of the reference inhibitor GPC-N114 and to change only the oxygen atom linker with a nitrogen. In a first attempt to synthesise the unsubstituted derivative **51**, it was not possible to obtain the desired compound. However, a side product, the mono-substituted derivative **52** was isolated and tested in *in vitro* assays.

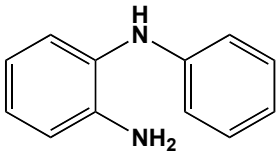

Compound	**EC_{50} (µM)**	**EC_{90} (µM)**	**CC_{50} (µM)**	**SI**
52	42.5	55.4	170	4

Table 2.3: Activity and cytotoxicity data for compound **52**

Compound **52** is associated with a certain activity in terms of EC_{50}, but the antiviral effect is reduced if compared to the the original GPC-N114. The low selectivity index also emphasizes poor antiviral properties for this compound, of which the chemical scaffold was not taken in consideration for further studies.

2.7 Design and docking validation of new GPC-N114 analogues

In an attempt to find a new chemical structure with a similar or better antiviral activity of the reference GPC-N114, a further modification was made. The collected data from the four new families of compounds analysed so far suggest that the replacement of either the central ring or the atom linker was not associated to any activity improvement. It was decided, therefore, to change only one position (the atom linker), maintaining the overall structure close to the reference molecule. The oxygen linker was substituted with two functional groups that were never explored before, a sulphonamido and an amido moieties (figure 2.24).

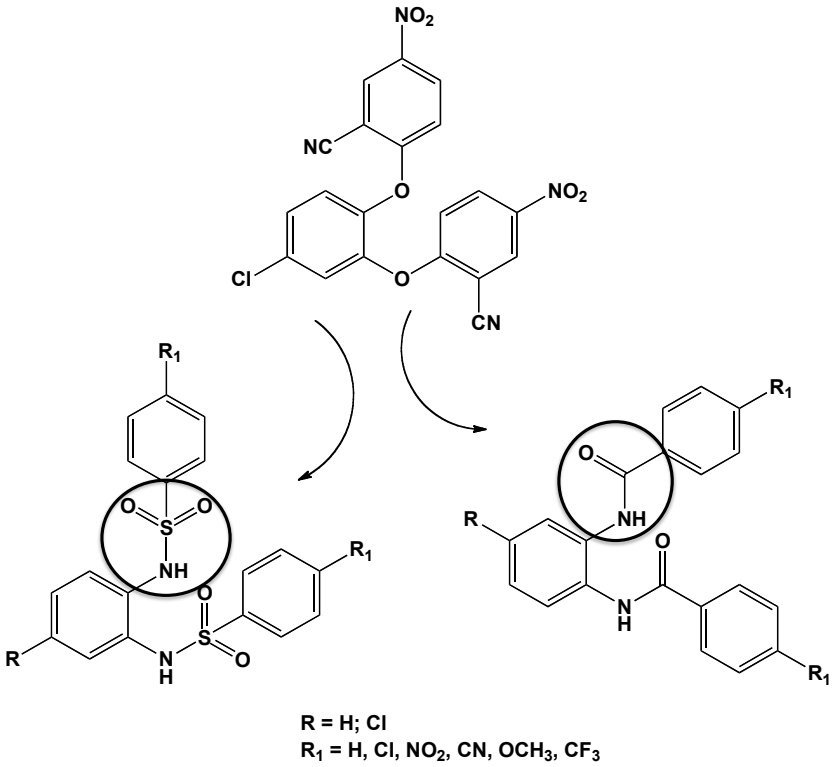

Figure 2.24: Chemical structure of GPC-N114 (above) and scaffolds of the new derivatives (below)

For each family of the new compounds, two sub-structures were considered, a symmetrical one, having a central benzene ring, and a non symmetrical scaffold, bearing a chlorine atom on the central moiety, like the reference GPC-N114 compound. In addition, different chemical groups were explored in *para* position of the two lateral moieties, based on a previous SAR study on a series of GPC-N114 analogues made elsewhere (unpublished data kindly received by Dr. Gherard Purstinger, from Innsbruck University). In particular, only those substituents that showed

antiviral activity were introduced on the new chemical scaffolds. Docking studies were performed on the new compounds using the Glide Docking standard precision SP mode. Figure 2.25 shows an example of the predicted binding mode of the sulphonamido structures: compound **63** nicely fits the binding pocket of the CVB3 polymerase, maintaining the essential interactions observed for GPC-N114. Although the sulphonamido linker contains two atoms in comparison with the oxygen in the reference molecule, additional interactions were observed between the oxygen atoms of the new linker and the hydroxyl group of Tyr195.

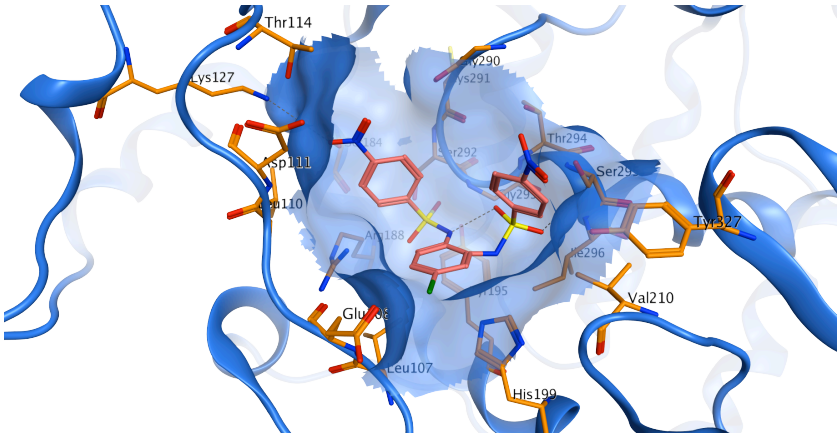

Figure 2.25: Predicted binding pose of compound **58**

An analogous situation was found for the amido derivatives, where docking studies gave a valid predicted binding mode, similar to the one described above.

2.7.1 bis-Aryl sulfonamides (61-72)

Two families of arylsulfonamido derivatives were designed and synthesized through a nucleophilic displacement by the amine groups of *o*-phenylenediamine **53** or 4-chloro-*o*-phenylenediamine **54** (Scheme 2.29) on the electrophilic site of the sulfonyl chloride.[52] The reaction conditions allowed a bis nucleophilic substitution in a one step synthesis that was monitored by TLC. The new derivatives were obtained as pure product by recrystallization, with reasonable yields that are reported in scheme 2.29.

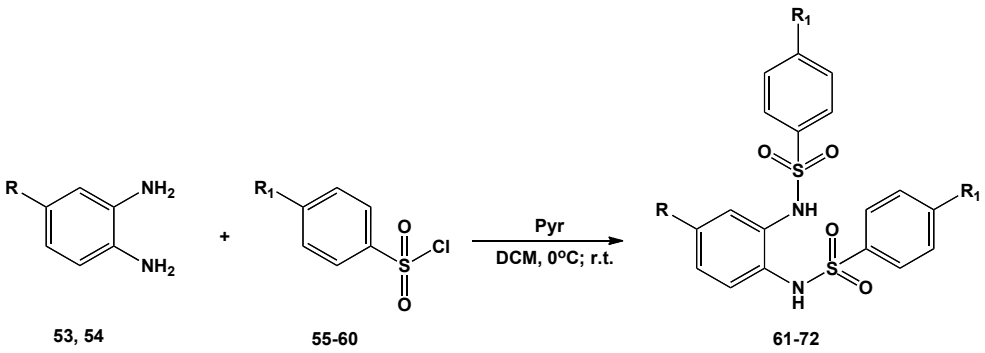

Aryl 1,2-diamine	R	Aryl sulfonylchloride	R_1	Product	Yield %
53	H	**55**	H	**61**	67.5
53	H	**56**	Cl	**62**	45
53	H	**57**	NO_2	**63**	51
53	H	**58**	CN	**64**	30
53	H	**59**	OMe	**65**	73
53	H	**60**	CF_3	**66**	21
54	Cl	**55**	H	**67**	21
54	Cl	**56**	Cl	**68**	29
54	Cl	**57**	NO_2	**69**	46
54	Cl	**58**	CN	**70**	24
54	Cl	**59**	OMe	**71**	39
54	Cl	**60**	CF_3	**72**	28

Scheme 2.29: Synthesis of compounds **61-72**

2.7.2 bis-Aryl amides (79-90)

A further modification applied on the level of the oxygen linker was the introduction of an amido group. Twelve new derivatives were prepared, according to a reported procedure.[53] The chemical pathway chosen consists in a one-step reaction that was carried out with a bis nucleophilic displacement of the chloride leaving group by the amine groups of *o*-phenylenediamine **53** or 4-chloro-*o*-phenylenediamine **54** (scheme 2.30).

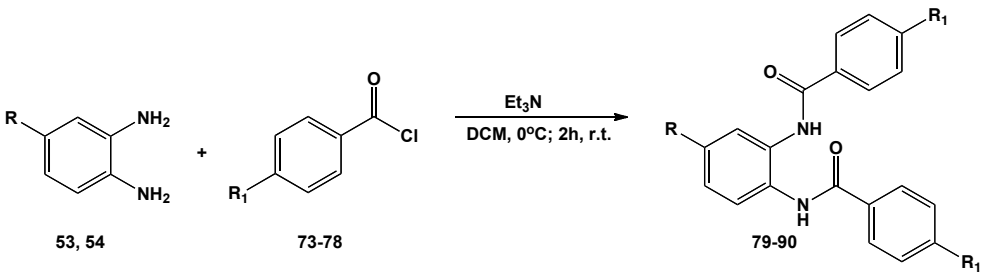

53, 54 73-78 79-90

Aryl 1,2-diamine	R	Aryl chloride	R_1	Product	Yield %
53	H	**73**	H	**79**	59
53	H	**74**	Cl	**80**	41
53	H	**75**	NO_2	**81**	84
53	H	**76**	CN	**82**	65
53	H	**77**	OMe	**83**	53
53	H	**78**	CF_3	**84**	33
54	Cl	**73**	H	**85**	27
54	Cl	**74**	Cl	**86**	80
54	Cl	**75**	NO_2	**87**	71
54	Cl	**76**	CN	**88**	48
54	Cl	**77**	OMe	**89**	70
54	Cl	**78**	CF_3	**90**	30

Scheme 2.30: Synthesis of compounds **79-90**

2.7.3 Biological evaluation

Bis arylsulfonamides **61-72** and bis aryl amides **79-90** were evaluated for their antiviral activity and cytotoxicity in a virus-cell-based assay (table 2.4).

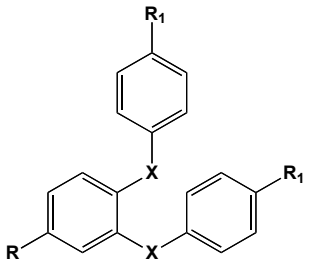

Compound	R	R_1	X	EC_{50} (µM)	CC_{50} (µM)	SI
61	H	H	$NHSO_2$	>100	>100	-
62	H	Cl	$NHSO_2$	>100	>100	-
63	H	NO_2	$NHSO_2$	>100	>100	-
64	H	CN	$NHSO_2$	>100	>100	-
65	H	OMe	$NHSO_2$	>100	>100	-
66	H	CF_3	$NHSO_2$	>100	>100	-
67	Cl	H	$NHSO_2$	>100	>100	-
68	Cl	Cl	$NHSO_2$	>100	>100	-
69	Cl	NO_2	$NHSO_2$	>100	>100	-
70	Cl	CN	$NHSO_2$	>100	>100	-
71	Cl	OMe	$NHSO_2$	>100	>100	-
72	Cl	CF_3	$NHSO_2$	>100	>100	-
79	H	H	NHCO	>100	>100	-
80	H	Cl	NHCO	>100	>100	-
81	H	NO_2	NHCO	>100	>100	-
82	H	CN	NHCO	>100	>100	-
83	H	OMe	NHCO	>100	>100	-
84	H	CF_3	NHCO	>100	>100	-
85	Cl	H	NHCO	>100	>100	-
86	Cl	Cl	NHCO	>100	>100	-
87	Cl	NO_2	NHCO	>100	>100	-
88	Cl	CN	NHCO	>100	>100	-
89	Cl	OMe	NHCO	>100	>100	-
90	Cl	CF_3	NHCO	>100	>100	-

Table 2.4: Activity and cytotoxicity data for compounds **61-72** and **79-90**

A clear outcome can be drawn: the modifications applied were not tolerated, there was no observed antiviral activity, therefore these scaffolds were not object of further studies. At this stage of the study, the crystal structure of CVB3 polymerase with the ligand GPC-N114 co-crystallized was accessible and was used as a target for a ligand-based virtual screening approach.

2.8 Ligand-Based Virtual Screening

A final attempt for the identification of new, potential hit compounds was applied when the crystal structure of CVB3 3Dpol in complex with the non-nucleoside inhibitor GPC-N114. With the accessible crystal structure, a shape comparison was performed using the active conformation of the molecule.

2.8.1 Shape complementarity search with ROCS

ROCS (Rapid Overlay of Chemical Structures) is an efficient software that was used for a ligand-based virtual screening approach. The principle behind ROCS is to find those molecules that have a well volume overlapping with the query target in its active conformation.[54] This program has also the advantage to integrate the information about the bioactive conformation with the chemical features that are essential for ligand-receptor recognition. The volume of screened compounds is superimposed to the target query and each shape density overlapping is quantified on the basis of a shape Tanimoto value which would be equal to 1 if two shapes are identical, and 0 if they are different. It is therefore evident that the conformation of the query molecule has a primary role for the screening. The fact that only shape complementarity is considered, could be of advantage in finding new, different chemical scaffolds that have a similar shape to the query. However, it was found that the results obtained from a virtual screening can be more accurate if the overlapping of groups with a certain chemical relevance is also considered.[55] The evaluation of the alignment of groups having binding properties (for example, donor, acceptor, hydrophobic features) is made by the so-called Combo score. Ranking molecules considering the sum of the shape-Tanimoto and Combo score considerably improve the reliability of the screening performed. In this study, the conformation of GPC-N114 was used as the query target and the conformational database of Specs compounds was analysed with vROCS 3.1.2 version. Both shape and electrostatics properties were used for the evaluation and all conformations found (max limit of 20000) were ranked according to their value of similarity using Combo-shape and Tanimoto score. Four features were considered essential: the three aromatic rings as hydrophobic groups and one of the nitro group as acceptor group. In this manner, those conformations with the highest values of shape similarity and those that

have the major number of different conformation overlapping the query molecule were taken into account.

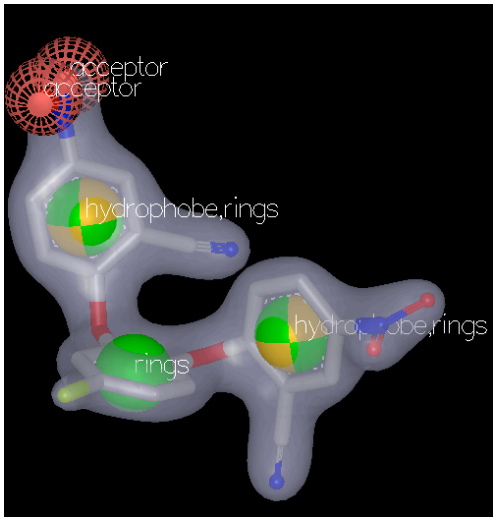

Figure 2.26: Shape and selected electrostatic features for GPC-N114

Around 6000 molecules were found to match the set parameters; all the ligands were preprocessed using LigPrep (Maestro, package version 2.3, Schrödinger, LLC, New York, NY, 2009),[56] which enables to make corrections to the structures, optimise or eliminate unwanted structures. The general *iter* described for docking procedures (see section 1.3.5) was applied also in this case: Glide standard precision (SP) docking mode was performed and the output database was re-scored with three scoring functions (Glide XP, Plants and FlexX). After a visual inspection of the best 25% from docking results, 10 compounds were selected and purchased from the Specs company to be tested (Appendix I). Unfortunately, none of the selected molecules showed an interesting antiviral profile.

Conclusions

In this study, different computer-based methods were used for the identification of potential inhibitors against CVB3 replication.
A structure-based virtual screening performed on the homodimer 3A protein guided the identification of a hit structure active against viral replication at 129 μM. Its chemical scaffold was taken for the design and synthesis of 11 tetrazole-based analogues that explored several aromatic substitutions.

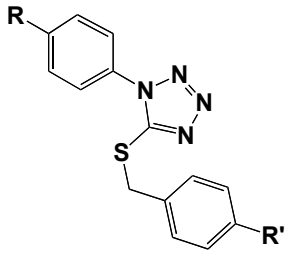

Biological data revealed no antiviral effect of the new derivatives. The preliminary data obtained for the hit compound, however, were confirmed. Targeting the surface of a protein, which is water exposed, could represent an issue to design inhibitors of protein-protein interactions, such as in the case of the 3A protein of CVB3. The lack of information on this target and the difficulties that should be faced led to the conclusion that this protein is not feasible enough from a computer-aided approach, therefore a different target was chosen for the identification of potential antivirals.

Starting from the available information on a novel inhibitor, GPC-N114, targeting the polymerase of CVB3, a series of molecular modelling techniques were applied.

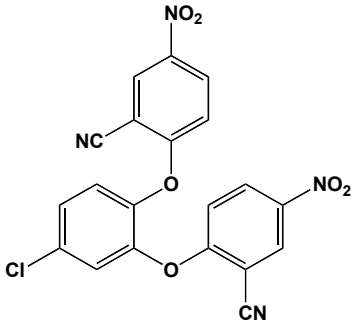

GPC-N114

Ligand-based optimisation using flexible alignment method led to the design of new chemical structures. Data obtained so far suggest the essential role of the oxygen linker which is associated to a loss of antiviral activity when replaced. A first series of compounds was designed in order to explore the oxygen atom and the central moiety. On the level of the linker, a C or N atoms were introduced, while the central moiety was modified by inserting a maleimido, a benzoimidazol-2-one and an oxadiazole groups.

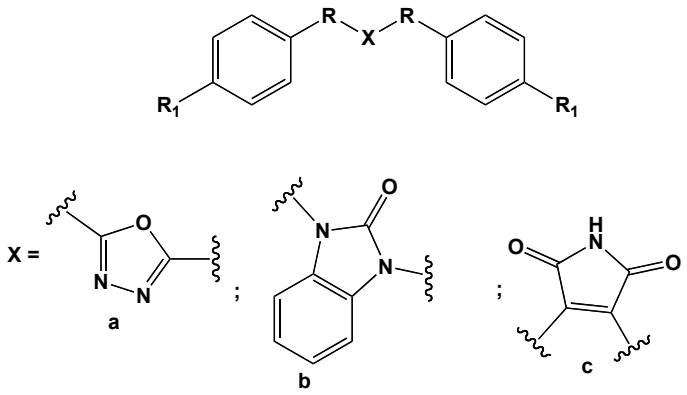

R = CH_2, NH, SO_2NH, NHCO

R' = H, NO_2

For the first two families having the oxadiazole and the benzoimidazol-2-one rings in the centre, the derivative bearing nitro groups on the two lateral benzene ring was prepared, as the activity of GPC-N114 was linked to the presence of these functional groups. As a useful comparison, the unsubstituted molecule was also prepared. All the modifications were not associated to antiviral activity and it is not possible to understand from these data wether one or both modifications were not tolerated. A third scaffold with a central maleimide ring was also validated with docking techniques and used for the synthesis of the unsubstituted product, for which no antiviral activity was observed.The only derivative that was obtained in an attempt to synthesize the N^1, N^2-disubstituted compound **51** was N^1-phenylbenzene-1,2-diamine **52**, that showed a EC_{50} of 40 µM but also cytotoxic effects on the cells.

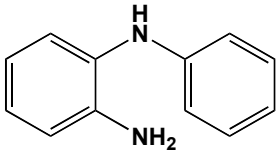

Compound **52**

Based on the first series of results, a second family of compounds was planned by changing the atom linker only: a sulfonamido and an amido groups were introduced in this position, while maintaining those aromatic substituents that were linked to biological activity on the reference compound. A total of 24 compounds were synthesised and tested against viral replication. Unfortunately, no antiviral activity was observed for the new derivatives. A possible explanation could be the conformation of the reference molecule on the crystal structure, which is highly strained and impossible to reproduce with docking studies. As a consequence of that, using a model which is not completely reliable increases the probabilities to fail in identifying new active compounds. Nevertheless, no interesting outcomes were achieved when a ligand-based virtual screening was performed, using the crystal structure of GPC-N114 within the CVB3 polymerase that was finally accessible. In conclusion, no interesting scaffold was found using computer-aided techniques. Further studies are required in order to establish clear structure-activity relationships of the reference molecule that could be used as a starting point for lead optimisation.

References

1 Bowles, N.E.; Richardson, P.J.; Olsen, E.G.; Archard, L.C. Detection of Coxsackie-B-virus-specific RNA sequences in myocardial biopsy samples from patients with myocarditis and dilated cardiomyopathy. *Lancet* **1986**, 1, 1120–1123.

2 Rotbart, H.A. Treatment of picornavirus infections. *Antiviral Res.* **2002**, 53 (2), 83-98.

3 Overall, J.C.Jr. Intrauterine virus infections and congenital heart diseases. *American Heart J.* **1972**, 84 (6), 823-833.

4 Mirand, A.; Archimbaud, C.; Henquell, C.; Michel, Y.; Chambon, M.; Peigue-Lafeuille, H.; Bailly, J.L. Prospective identification of HEV-B enteroviruses during the 2005 outbreak. *J.Med. Virol.* **2006**, 78, 1624– 1634.

5 Mistchenko, A.S.; Viegas, M.; Latta, M.P.D.; Barrero, P.R. Molecular and epidemiolgic analysis of EV B neurological infection in Argentine children. *J. Clin. Virol.* **2006**, 37, 293–299.

6 Lee, S.T.; Ki, C.S.; Lee, N.Y. Molecular characterization of enteroviruses isolated from patients with aseptic meningitis in Korea, 2005. *Arch. Virol.* **2007**, 152, 963–970.

7 Antona, D.; Lévêque, N.; Chomel, J.J.; Dubrou, S.; Lévy-Bruhl, D.; Lina, B. Surveillance of enteroviruses in France, 2000–2004. *Eur. J. Clin. Microbiol. Infect. Dis.* **2007**, 26, 403–412.

8 Tao, Z.; Song, Y.; Li, Y.; Liu, Y.; Jiang, P.; Lin, X.; Liu, G.; Song, L.; Wang, H.; Xu, A. Coxsackievirus B3, Shandong Province, China, 1990–2010. *Emerg. Infect. Dis.* **2012**, 18 (11), 1865-1867.

9 Romero, J.R. Enteroviruses in Humans. In: eLS. John Wiley & Sons Ltd, Chichester. http://www.els.net [doi: 10.1002/9780470015902.a0002230.pub2] (accessed July 25, 2012).

10 Muckelbaurer, J.K.; Kremer, M.; Minor, I.; Diana, G.; Dutko, F.J.; Groarke, J.; Pevear, D.C.; Rossmann, M.G. The structure of coxsackievirus B3 at 3.5 Å resolution. *Structure* **1995**, 3 (7), 653-667.

11 Kräusslich, H.G.; Nicklin, M.J.H.; Toyoda, H.; Etchison, D.; Wimmer, E. Poliovirus proteinase 2A induces cleavage of Eucaryotic initiation factor 4F polypeptide p220. *J. Virol.* **1998**, 61 (9), 2711-2718.

12 Badorff, C.; Lee, G.H.; Lamphear, B.J.; Martone, M.E.; Campbell, K.P.; Rhoads, R.E.; Knowlton, K.U. Enteroviral protease 2A cleaves dystrophin: evidence of cytoskeletal disruption in an acquired cardiomyopathy. *Nat. Med.* **1999**, 5, 320-326.

13 Jong, A.S.; Melchers, W.J.G.; Glaudemans, D.H.R.F.; Kuppeveld, F.J.M. Mutational analysis of different regions in the Coxsackievirus 2B protein: requirements for homo-multimerization, membrane permeabilization, subcellular localization, and virus replication. *J.Biol.Chem.* **2004**, 279, 19924-19935.

14 Kuppeveld, F.J.M.; Melchers, W.J.G.; Kirkegaard, K.; Doedens, J.R. Structure–Function Analysis of Coxsackie B3 Virus Protein 2B. *Virology* **1997**, 227, 111-118.

15 Gorbalenya, A.E.; Lauber, C. Origin and Evolution of the Picornaviridae Proteome. In: *The Picornaviruses*. Ehrenfeld, E., Domingo, E., Roos, R.P. Eds.; ASM Press, Washington DC, 2010; 253-270.

16 Strauss, D.N.; Wuttke, D.S. Characterization of Protein-protein interactions critical for polio replication: 3AB and VPg binding to the RNA-dependent RNA pol. *J. Virol.* **2007**, 81 (12), 6369-6378.

17 Wessels, E.; Duijsings, D.; Niu, T-K.; Neumann, S.; Oorschot, V.M.; Lange, F.; Lanke, K.H.W.; Klumperman, J.; Henke, A.; Jackson, C.L.; Melchers, W.J.G.; Kuppeveld, F.J.M. A viral protein that blocks Arf1-mediated COP-I assembly by inhibiting the guanine nucleotide exchange factor GBF1. *Developmental Cell* **2006**, 11, 191-201.

18 Paul, A.V.; Yin, J.; Mugavero, J.; Rieder, E.; Liu, Y.; Wimmer, E. A “slide-back” mechanism for the initiation of protein-primed RNA synthesis by the RNA polymerase of poliovirus. *J. Bio. Chem.* **2003**, 278 (45), 43951-60.

19 Brunetti, L.; De Santis, E.R. Treatment of viral myocarditis caused by coxsackievirus B. *Am. J. Health Syst. Pharm.* **2008**, 65(2). 132-137.

20 Strauss, D.M.; Glustrom, L.W.; Wuttke, D.S. Towards an understanding of the poliovirus replication complex: the solution structure of the soluble domain of the poliovirus 3A protein. *J. Mol. Biol.* **2003**, 330, 225-234.

21 Wessels, E.; Notebaart, A.R.; Duijsing, D.; Lanke, K.; Vergeer, B.; Melchers, W.J.G.; van Kuppeveld, F.J.M. Structure-function analysis of the coxsackievirus protein 3A-Identification of residues important for dimerization, viral RNA replication, and transport inhibition. *J. Biol. Chem.* **2006**, 281 (38), 28232-28243.

22 Kok, C.C.; McMinn, P. Picornavirus RNA-dependent polymerase. *The International Journal of Biochemistry & Cell Biology* **2009**, 41, 498-502.

23 Ferrer-Orta, C. A comparison for viral RNA-dependent RNA polymerase. *Curr. Opin. Struct. Biol.* **2006**, 16, 27-34.

24 Ferrer-Orta, C.; Arias, A.; Perez-Luque, R.; Escamìs, C.; Domingo, E.; Verdarguer, N. Structure of foot-and-mouth- disease with RNA-dependent RNA polymerase and its complex with a template-primer RNA. *J. Biol. Chem. 2004*, 279, 47212-47221.

25 Wessels, E.; Notebaart, R.A.; Duijsings, D.; Lanke, K.; Vergeer, B.; Melchers, W.J.; van Kuppeveld, F.J. Structure-Function Analysis of the Coxsackievirus Protein 3A: identification of residues important for dimerization, viral RNA replication, and transport inhibition. *J. Biol. Chem.* **2006**, 281(38), 28232-43.

26 Strauss, D.M.; Glustrom, L.W.; Wuttke, D.S. Towards an understanding of the poliovirus replication complex: the solution structure of the soluble domain of the poliovirus 3A protein. *J. Mol. Biol.* **2003**, 330: 225-234.

27 Specs. www.specs.net (accessed May, 2012).

28 Chemical Computing Group, Montreal, Canada. www.chemcomp.com (accessed May, 2012).

29 Schrödinger, Cambridge, MA. http://www.schrodinger.com (accessed May, 2012).

30 Korb, O.; Stützle, T.; Exner, T.E. An ant colony optimization approach to flexible protein–ligand docking. *Swarm Intell.* **2007,** 1, 115-134.

31 BioSolveIT GmbH, Sankt Augustin, Germany. www.biosolveit.de (accessed July, 2012).

32 Charifson, P.S.; Corkery, J.J.; Murcko, M.A.; Walters, W.P. Consensus scoring: a method for obtaining improved hit rates from docking databases of three-dimensional structures into proteins. *J. Med. Chem.* **1999**, 42, 5100-5109.

33 Plewczynski, D.; Lazniewski, M.; Augustyniak, R.; Ginalski, K. Can we trust docking results? Evaluation of seven commonly used programs on PDBbind database. *J. Comput. Chem.* **2011**, 32 (4),742-755.

34 Carpenter, R.D.; Andrei, M.; Aina, O.H.; Lau, Y.; Lightstone, F.C.; Liu, R.; Lam, K.S.; Kurth, M. Selectively targeting T- and B-cell Lymphomas: a benzothiazole antagonist of $\alpha_4\beta_1$ Integrin. *J. Med. Chem.* **2009**, 52 (1), 14-19.

35 Humeres, E.; Zucco, C.; Nunes, M.; Debacher, N.A.; Nunes, R.J. Hydrolysis of N-aryl thioncarbamate esters. Modified Marcus equation for reactions with asymmetric intrinsic barriers. *J. Phys. Org. Chem.* **2002**, 15, 570–575.

36 Lee, H.H.; Han, S.; Gyoung, S.; Kim, Y.; Lee, K.; Jang, Y.; Lee, S. Bis(phosphine)-Pd(II) and -Pt(II) complexes containing chiral tetrazole-thiolato rings: synthesis, structures, and reactivity toward some electrophiles. *Inorg. Chem. Acta* **2011**, 378 (1),174-185.

37 Pellecchia, M. Inhibitors of JNK and methods for identifying inhibitors of JNK. Patent WO, 2008118626, Oct 02, 2008.

38 Matos, M-C.; Murphy, P.V. Synthesis of macrolide-saccharide hybrids by ring-closing metathesis of precursors derived from glycitols and benzoic acids. *J. Org. Chem.* **2007**, 72 (5), 1803-1806.

39 Amalendu, B.; Saumitra, S.; Mohan, A.M.; Chandra, B.G. Use of phosphorus pentoxide: esterification of organic acids. *J. Org. Chem.* **1983**, 48(18), 3106-3108.

40 Gruez, A.; Selisko, B.; Roberts, M.; Bricogne, G.; Bussetta, C.; Jabafi, I.; Coutard, B.; De Palma, A.M.; Neyts, J.; Canard, B. The crystal structure of coxsackievirus B3 RNA-dependent RNA polymerase in complex with its protein primer VPg confirms the existence of a second VPg binding site on Picornaviridae polymerases. *J. Virol.* **2008**, 82 (19), 9577-9590.

41 Ferrer-Orta, C.; Arias, A.; Perez-Luque, R.; Escarmis, C.; Domingo, E.; Verdaguer, N. Structure of foot-and-mouth disease virus RNA-dependent RNA polymerase and its complex with a template-primer RNA. *J. Biol. Chem.* **2004**, 279 (45), 47212-47221.

42 Chemical Computing Group, Montreal, Canada. www.chemcomp.com (accessed September, 2012).

43 Manjunatha, K.; Poojary, B.; Lobo, P.L.; Fernandes, J.; Suchetha Kumari, N. Synthesis and biological evaluation of some 1,3,4-oxadiazole derivatives. *Eur. J. Med. Chem.* **2010**, 45 (11), 5225-5233.

44 Patel, N. B.; Patel, J. C. Synthesis and antimicrobial activity of novel 1,3,4-oxadiazolyl-quinazolin-4(3*H*)ones. *J. Heterocyclic Chem.* **2010**, 47 (4), 923-931.

45 Kornberg, B. E.; Lewthwaite, R. A.; Manning, D. D.; Nikam, S. S.; Scott, I. L. Preparation of piperidine derivatives as subtype selective n-methyl-d-aspartate antagonists useful in the treatment of cerebral vascular disorders. Patent WO 2002050070, Jun 27, 2002.

46 Woodhead, S. J.; Frederickson, M.; Hamlett, C.; Woodhead, A. J.; Verdonk, M.; Leendert, S.; Hannah, F.; Walker, D. W.; Blurton, P.; Collins, I.; Chenug, K. M.; Caldwell, J.; Da Fonseca M.T.F.; Luke, R. W. A.; Matusiak, Z., S.; Leach, A.; Morris, J. J. Preparation of substituted purine and purine analogs having protein kinase inhibiting activity. PatentWO 2008075109, Jun 26, 2008.

47 Choi, D.; Huang, S.; Huang, M.; Barnard, T.S.; Adams, R.D.; Seminario, J.M.; Tour, J.M. Revised structures of N-substituted dibrominated pyrrole derivatives and their polymeric products. Termaleimide models with low optical band gaps. *J. Org. Chem.* **1998**, 63, 2646-2655.

48 Brenner, M.; Rexhausen, H.; Steffan, B.; Steglich, W. Synthesis of arcyriarubin B and related bisindolylmaleimides. *Tetrahedron* **1988**, 44 (10), 2887-2892.

49 Lakatosh, S.A.; Luzikov, Y.N.; Preobrazhenskaya, M. Synthesis of 6*H*-pyrrolo[3',4':2,3][1,4]diazepino[6,7,1-*hi*]indole-8,10 (7*H*,9*H*)-diones using 3-bromo-4-(indol-1-yl) maleimide scaffold. *Org. Biomol. Chem.* **2003**, 1, 826-833.

50 Awuah, E.; Capretta, A. Development of methods for the synthesis of libraries of substituted maleimides and α,β-unsaturated-γ-butyrolactams. *J. Org. Chem.* **2011**, 76, 3122-3130.

51 Huang, G.; Guo, J.; Zhu, M.; Gang, Z.; Tang, J. Palladium-benzimidazolium salt catalyst systems for Suzuki coupling: development of a practical and highly active palladium catalyst system for coupling of aromatic halides with arylboronic acids. *Tetrahedron* **2005**, 61 (41), 9783-9790.

52 Proust, N.; Gallucci, J. C.; Paquette, L. A. Effect of sulfonyl protecting groups on the neighboringgroup participation ability of sulfonamido nitrogen. *J. Org. Chem.* **2009**, 74 (7), 2897-2900.

53 Abdel-Aziz, Mo.; Matsuda, K.; Otsuka, M.; Uyeda, M.; Okawara, T.; Suzuki, K. Inhibitory activities against topoisomerase I & II by polyhydroxybenzoyl amide derivatives and their structure-activity relationship. *Bioorg. Med Chem. Lett.* **2004**, 14 (7), 1669-1672.

54 Rush III, T.S.; Grant, J.A.; Mosyak, L., Nicholls, A. A shape-based 3-D scaffold hopping method and its application to bacterial protein-protein interaction. *J. Med. Chem.* **2005**, 48, 1489-1495.

55 OpenEye Scientific Software, Santa Fe, NM. www.eyesopen.com (accessed October, 2012).

56 LigPrep, version 2.3, Schrödinger, LLC, New York, NY, 2009 (accessed Sept, 2012).

Chapter 3

Foot-and-Mouth-Disease Virus

Introduction to the virus

3.1 Foot-and-mouth disease virus

Foot-and-mouth disease virus (FMDV) has been considered one of the most economically devastating animal diseases mainly affecting cattle, pigs, sheep, goats and occurring throughout the world.[1,2] The disease causes high fever, blisters inside the mouth and on the feet that can lead to lameness. Animals could loose weight and milk production may decline. FMDV is highly contagious and is transmitted animal-to-animal by close contact. For this reason, a way to eradicate the virus and control epidemics is to kill infected animals and those that have been in contact with them. Several outbreaks have been reported during the last decade in many countries in East Asia and in South Africa. In 2001, the virus expanded also in Europe, in particular Britain was affected by a serious outbreak: over 10 million sheep and cattle were killed to stop the virus spreading, with an estimated cost of £8billion ($16bn).[3] Other cases of FMDV were also reported in Ireland, France and The Netherlands during the same period[4] and, more recently, in 2010, in Japan.[5]

3.1.1 Diversity and similarity to other Picornaviruses

FMDV is the prototype of the *Aphthovirus* genus that belongs to the *Picornaviridae* family.[6] It is a positive, single-strand RNA virus, for which seven different serotypes have been identified, named O, A, C, SAT1, SAT2, SAT3 and Asia-1, according to the place where they were discovered. Many sub-types are also present that can be different from other strains of the same serotype. FMDV shares common functional and structural analogies with other Picornaviruses, e.g. CVB3. For this reason, the virion structure, genome organization and life cycle will not described in this section, but can be referred to the previous sections 2.1.1-2.2.4. However, some differences that distinguish the virus are reported here:

1) while Enteroviruses, Cardioviruses, Hepatoviruses and Parechoviruses are acid stable and are infectious at pH of 3 and lower, Aphthoviruses are less resistant to pH values less than 6.0. This is due to the different sites of virus replication: the former ones replicate in the intestine, therefore they have to pass through the stomach and must

be acid stable. Aphthoviruses, on the other hand, replicate in the respiratory tract, therefore they don't need to be acid-resistant.[7]

2) FMDV is the only Picornavirus member to encode in the genome three VPg genes required for replication in cell culture[8] and for infectivity and pathogenicity in host cells.[9] It has also a proteinase, named L protein, at the 5'-end of the genome that is responsible for protein cleavage.

3) There is no canyon on the surface of the viral particle for FMDV. It is believed that the attach to cell receptors is through surface loops.[7]

4) FMDV has been shown to have resistance to the Golgi disruption by brefeldin A, an inhibitor of viral replication in some Picornaviruses, and to induce a different membrane reorganization in infected cells.[10]

5) FMDV is the only one to evade the innate and acquired immune responses through 2B and 2BC, instead of 3A protein, as already seen for CVB3 (section 2.2.1).[11]

3.1.2 Current treatment

Currently, no antiviral therapy is available for the treatment of FMDV. Although the frequency of outbreaks have been reduced in the past by the use of a vaccine,[12,13] there are some issues to overcome, like the high variability of FMDV serotypes and subtypes that make it difficult the animal immunization. In addition, it seems that some FMDV episodes have derived from a vaccine due to incomplete inactivation of the live virus.[14] A valid alternative to the vaccine is the use of drugs against FMDV replication which are not present at the moment on the market.

Results and discussion

3.2 Structure-Based Virtual Screening of the FMDV polymerase

As already mentioned in section 2.2.2, GPC-N114 showed a broad spectrum of activity against several members of the genus *Enterovirus* and EMCV. On the contrary, this compound did not prove any activity against FMDV. A possible explanation for that derived from the observation made on the crystal structure of FMDV 3Dpol with the co-crystallized ligand. Interestingly, the binding area of the ligand in FMDV 3Dpol is approximately the same individuated for the polymerase of CVB3, but the ligand assumed different conformations in the two complexes.

Figure 3.1: Binding site of GPC-N114 in CVB3 3Dpol (blue ribbon) and FMDV 3Dpol (orange ribbon)

In FMDV, the central ring pointed towards the template entry channel, while one of the 2-cyano-4-nitrophenyl groups is exposed to the solvent (Fig. 3.2). It is likely that the lack of activity is due to the different fit of the molecule, if compared with the binding mode in the CVB3 3Dpol.

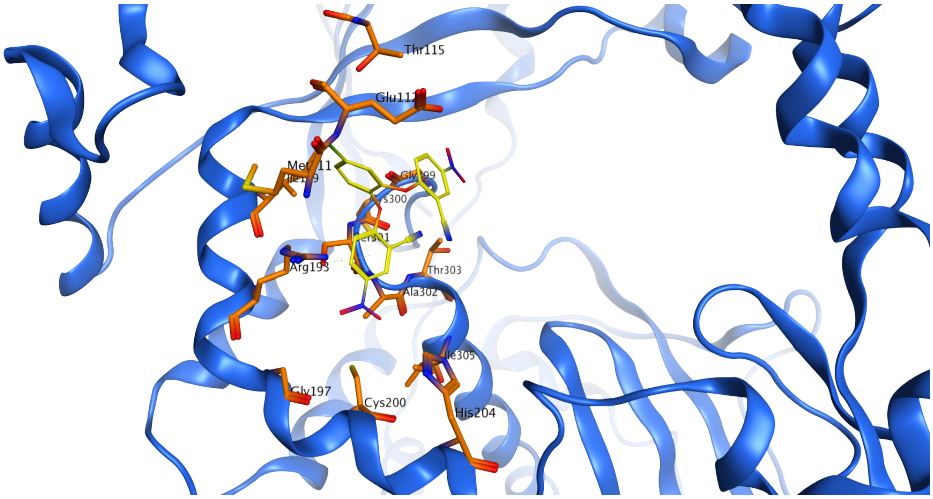

Figure 3.2: Close up of GPC-N114 binding pose in FMDV 3Dpol

Few residues differ from FMDV and CVB3 polymerases; one of these residues is supposed to be relevant for ligand binding in CVB3, hence, for the activity of the compound. As already mentioned, it is believed that stacking interactions between Tyr195 and the central chlorophenyl ring of the inhibitor play an essential role in the GPC-N114 binding. The presence of a cysteine in the FMDV 3Dpol and, therefore, the absence of the bulky aromatic ring of the tyrosine residue, alters the modality of the ligand binding. As a result, there is a reduction of contacts between the ligand and the binding site of the protein.

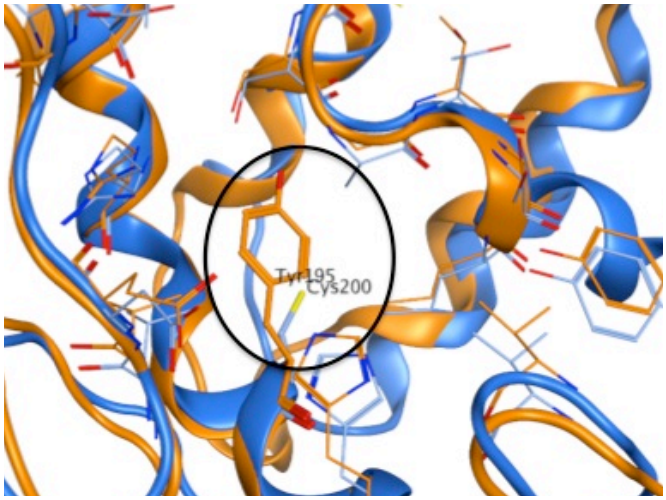

Figure 3.3: Ribbon representation of the superposed structures of CVB3 3Dpol (orange) and FMDV 3Dpol (blu)

The available crystal structure of the complex between GPC-N114 and FMDV 3Dpol was taken as a starting point for a structure-based virtual screening that was performed with the aim to find molecules that could better fit the binding pocket, making more interactions with the amino acids present in this area. FMDV RNA-dependent RNA polymerase crystal structure in complex with a template-primer RNA (PDB ID: 1WNE)[15] was used for the virtual screening. Due to the high level of the program, Glide was used with the scope to search for favorable interactions between the receptor and the ligand molecules in the database. The strategy planned in this case was to perform a docking-based virtual screening using the high-throughput virtual screening (HTVS) mode that is able to roughly screen a very large number of molecules without using a pharmacophore. The initial filtration was performed by using a grid in the area of the binding site, where three amino acids (Arg188, Cys200, Ser301) were selected to delimitate the site. The Specs database was used after pre-processing all the molecules with the LigPrep step.[24] Conformations with a positive value of docking score (which indicates a bad docking pose) were discarded. Around 117,000 conformations were obtained, of which the best 10% were taken for the standard precision Glide docking (SP) mode. The output database was used for re-scoring the results using Glide Extra Precision (XP) mode, Plants and FlexX scoring functions. The predicted poses were evaluated using the already described consensus scoring process (see section 1.3.5). A final visual inspection allowed us to select 17 compounds that were purchased and were evaluated in *in vitro* tests (Appendix I). From the biological results, however, no interesting results came out, therefore a different approach was tried.

3.3 *De novo* drug design approach

A second study performed for the identification of selective inhibitors of FMDV 3D polymerase was a *de novo* drug design approach, which involves the design of novel structures based on the geometry of the binding site. In this study, a multi-fragment search using a list of ligands available from MOE 2010.10 and a in-house selection of small fragments was carried out within the binding site in order to target Cys200. Among all, the coumarin ring represented an interesting fragment to use for the design of new compounds: it acts by irreversible binding to the cysteine residue through Michael addition reaction. In order to fit the pocket, 2-benzimidazole and 4,5-diphenyl-1*H*-imidazole were found to be suitable groups. To link these chemical entities with the coumarin ring, five linkers were used according to chemical feasibility.

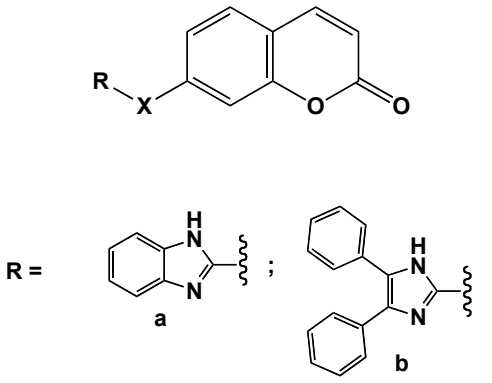

Figure 3.4: General chemical scaffold for compounds **91, 94, 99-100, 105-108**

3.4 Synthesis of coumarin-based structures

3.4.1 7-((1*H*-Benzo[*d*]imidazol-2-*yl*)methoxy)-2*H*-chromen-2-one (91)

The first scaffold prepared was a 2-benzimidazole group linked to the coumarin ring by a methoxy function. The predicted binding mode, shown in figure 3.5, highlights three hydrogen bonds, the first one between Cys200 and the carbonyl group of the coumarin moiety and two others between the nitrogen atom of benzimidazole and residues Met111 and Glu112.

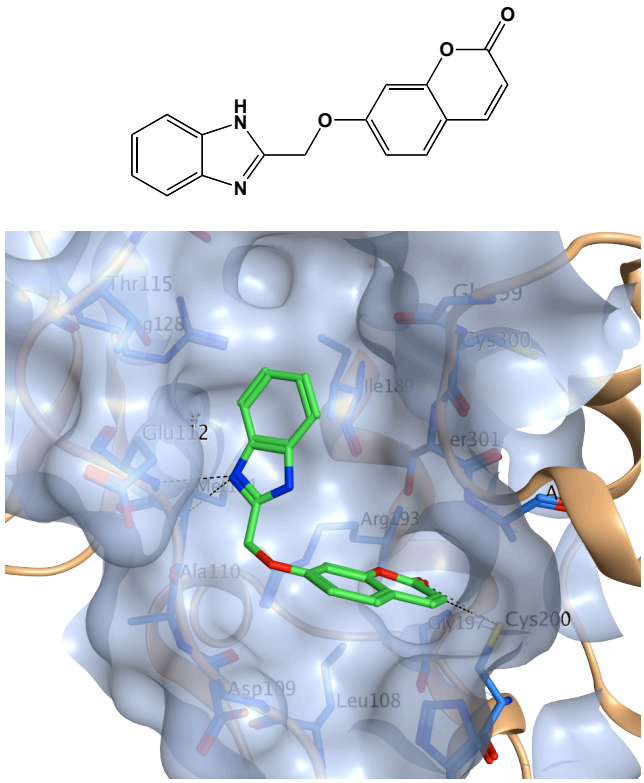

Figure 3.5: Chemical structure of compound **91** and its predicted binding mode

A first attempt was made by mixing 7-hydroxyl coumarin **92** and 2-chloromethyl benzimidazole **93** in the presence of potassium carbonate (Scheme 3.1). The designed product was not obtained and it could be speculated that the base reacted with 2-chloromethyl benzimidazole by deprotonating the nitrogen, instead of acting on the hydroxyl group of the coumarin moiety.

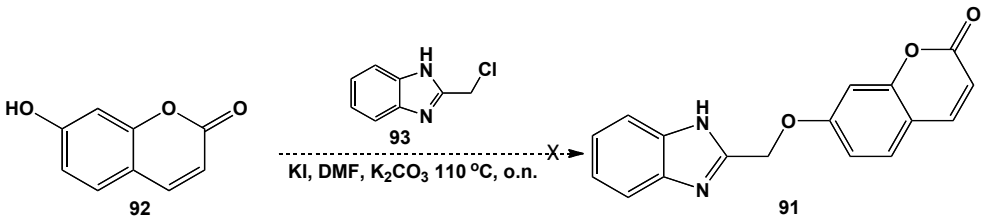

Scheme 3.1: First attempt for the synthesis of compound **91, 94, 99**

A different procedure was, therefore, applied (scheme 3.2): the proton of the 7-hydroxyl coumarin was first removed by treating it with 1 equivalent of NaH in anhydrous DMF, followed by the addition of 2-chloromethyl benzimidazole to the reaction mixture in order to obtain the displacement of the chloride by the oxygen lone pair.[16] The compound was obtained as pure product after chromatographic purification with a 10 % of yield.

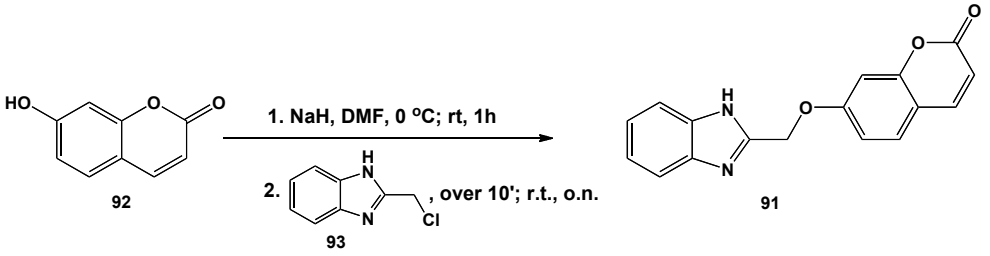

Scheme 3.2: Synthetic pathway for compound **91**

3.4.2 *N*-(2-Oxo-2*H*-chromen-7-*yl*)-1*H*-Benzo[*d*]imidazole-2-carboxamide (94)

A second linker introduced between the coumarin ring and the benzimidazole function was the amido group (e.g., compound **94**, Figure 3.6).

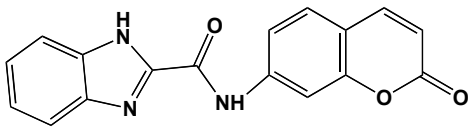

Figure 3.6: Chemical structure of compound **94**

Several attempts were made before finding the right conditions to obtain the desired product (scheme 3.3). At first, DMAP and Et_3N were added to a solution of DCM and 6-aminocoumarin **96** (previously obtained by reducing 6-nitrocoumarin **95** with hydrogen and palladium on carbon as catalyst).[17] 1*H*-Benzo[*d*]imidazole-2-carbonyl chloride **98**, synthesised from the

correspondent acid **97**, was added and the mixture was stirred at 0 ºC for 2h. Unreacted starting acid was the major component of the reaction mixture, therefore the reaction conditions were adjusted by using toluene as solvent and stirring the reaction for 48 h (scheme 3.3). Desired product **94** was not the main species formed, starting material was still present, therefore this procedure was discarded due to the very low yield obtained. A third attempt was tried following reported procedure.[18] 1*H*-Benzimidazole-2-carboxylic acid **97** was refluxed with carbonyldiimidazole for 30'. After cooling down to r.t., 6-aminocoumarin was added to the reaction mixture that was stirred for 16 h at reflux. Unfortunately, in this case, the formation of the desired product was not observed, only starting materials were isolated.

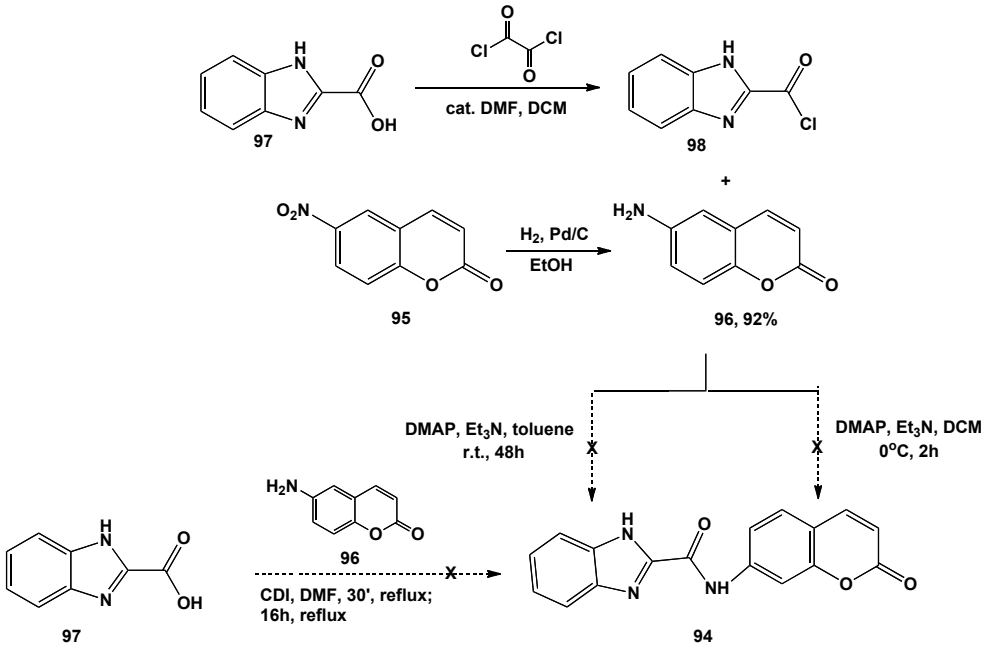

Scheme 3.3: First three attempts for the synthesis of compound **94**

A fourth attempt, finally, led to the synthesis of the desired product (scheme 3.4). According to a reported procedure,[19] the amido derivative was obtained with a 18% of yield by a coupling reaction between 6-aminocoumarin **96** and 1*H*-benzimidazole-2-carboxylic acid **97**, using TBTU as a coupling reagent.

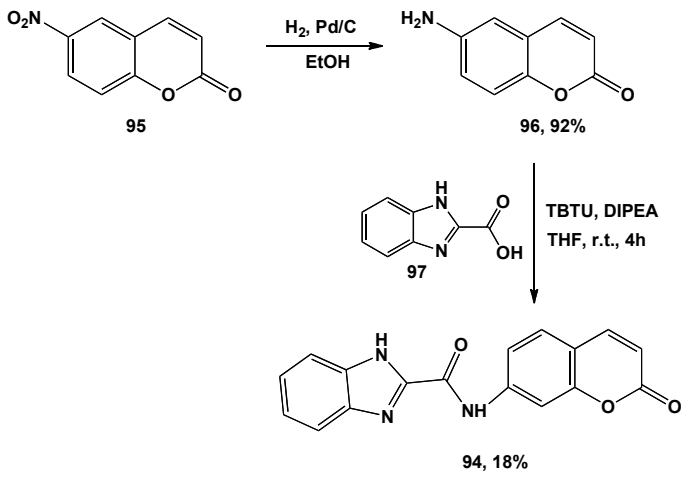

Scheme 3.4: Synthetic pathway for compound **92**

3.4.3 7-Aryl thio methyl-2*H*-chromen-2-ones (99, 100)

Another series of compounds, aiming to bind the pocket of the FMDV polymerase, was characterised by a thiol moiety that links together the coumarin ring and two types of aryl substituents, a 2-benzimidazole and 4,5-diphenyl-1*H*-imidazole (e.g., compounds **99** and **100**, Scheme 3.7).

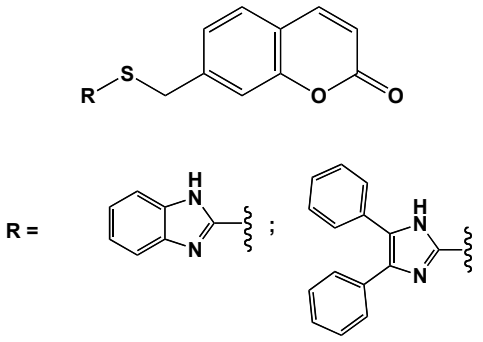

Figure 3.7: Chemical scaffold of compounds **99, 100**

The synthetic pathway followed is a one step synthesis that started from the preparation of intermediate 7-bromomethyl coumarin **102** (Scheme 3.5). According to a reported procedure,[20] the designed molecules were obtained by nucleophilic displacement of the bromide leaving group.

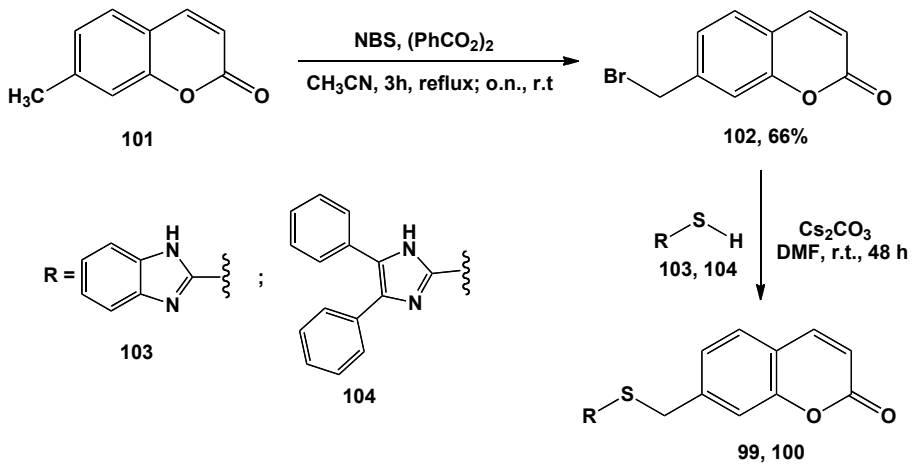

Scheme3.5: Synthetic pathway for the synthesis of compounds **99, 100**

Synthesis of 7-bromomethyl coumarin (102)

Intermediate 7-bromomethyl coumarin was obtained by bromination of 7-methylcoumarin **101** with N-bromosuccinimide in presence of a catalytic amount of benzoyl peroxide (Scheme 3.5).[21] The product was obtained with 66% yield.

Synthesis of aryl thio methyl-2*H*-chromen-2-ones (99, 100)

Aryl thiol derivatives **99, 100** (Scheme 3.6) were obtained through a nucleophilic substitution by the thiol group on the methyl bromide portion of 7-methyl bromocoumarin in basic conditions. The reaction was carried out at r.t. for 48 h. From the reaction mixture, the product was isolated from unreacted starting material through flash column chromatography.

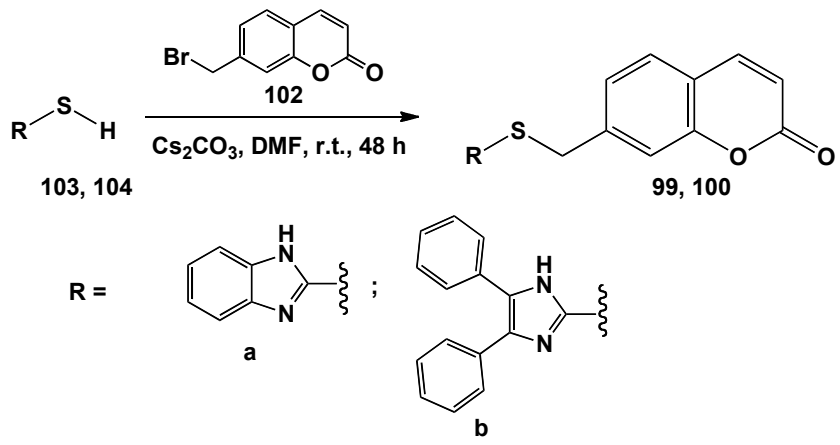

Starting aryl thiol compounds	R	Product	Yield %
103	a	**99**	42
104	b	**100**	8.5

Scheme 3.6: Synthesis of compounds **99, 100**

3.4.4 7-Aryl sulfinyl methyl-2*H*-chromen-2-ones (105, 106)

Another small series of sulfinyl compounds was prepared in order to be tested against FMDV replication (e.g. compounds **105** and **106**, Scheme 3.8).

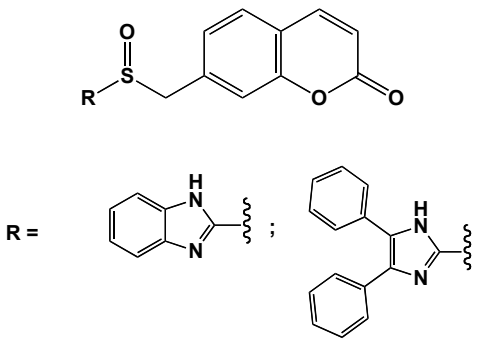

Figure 3.8: Chemical scaffold of compounds **105, 106**

Following a reported procedure,[22] aryl thio methyl-2*H*-chromen-2-ones **99, 100**, previously synthesised, were converted to the sulfoxide derivatives **105, 106** by oxidation through *m*-CPBA at -20 ºC, that was neutralised with $NaHCO_3$ (Scheme 3.7).

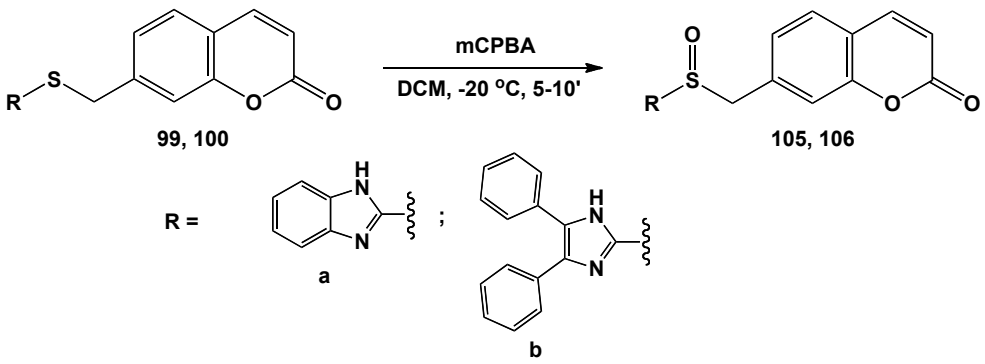

Starting aryl thio methyl-2*H*-chromen-2-ones	R	Product	Yield %
99	a	**105**	59
100	b	**106**	20

Scheme 3.7: Synthesis of compounds **105, 106**

3.4.5 7-Aryl sulfonyl methyl-2H-chromen-2-ones (107, 108)

The last family of derivatives designed as potential inhibitors of FMDV polymerase was made by sulfonyl compounds obtained by oxidation of the previously described thiol derivatives **99, 100** (Scheme 3.6). Docking studies were performed to validate this scaffold, for which two derivatives were prepared, the one bearing a 2-benzimidazole and the other one with a 4,5-diphenyl-1*H*-imidazole group. For the 2-benzimidazole derivative, two main interactions were predicted: one hydrogen bond between Cys200 and the coumarin ring and another one between Glu112 and an oxygen of the sulfonyl group. The second derivative, not only contains the same interactions, but has an additional hydrogen bond with Arg189 and better fills the occupational space thanks to the two benzene substituents.

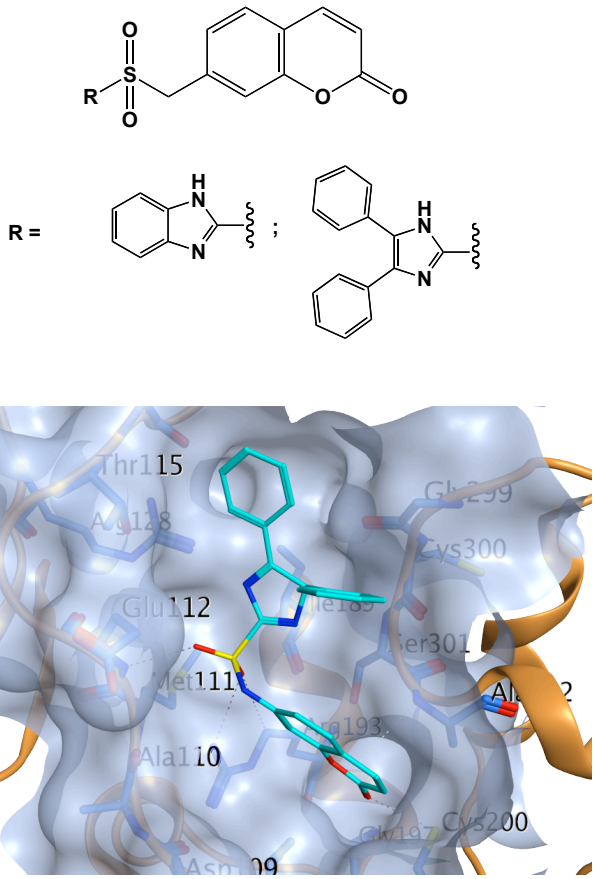

Figure 3.9: Chemical scaffold of compounds **107, 108** (above)**.** Predicted binding mode for compound **108** (below)

The synthetic pathway applied is the one previously described for the synthesis of sulfinyl derivatives, consisting in an oxidation reaction through *m*-CPBA (Scheme 3.8). The conditions were adjusted by stirring the mixture at r.t. and keeping the reaction longer (o.n.).

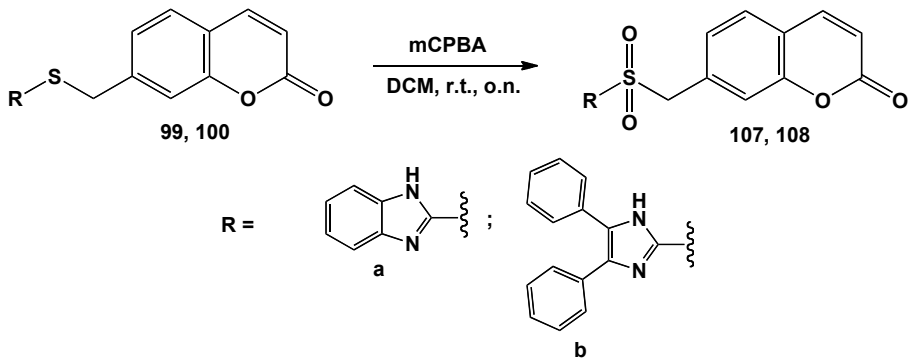

Starting aryl thio methyl-2*H*-chromen-2-ones	R	Product	Yield %
99	a	**107**	13
100	b	**108**	39

Scheme 3.8: Synthetic pathway for the synthesis of compounds **107, 108**

3.4.6 Biological evaluation

Eight new coumarin-based structures were tested for their antiviral activity and cytotoxicity in a MTT cell viability assay against three strains of FMDV (FMDV 01 Manisa, FMDV A22 Iraq, FMDV A96 Iran) and ERAV, Equine rhinitis A virus, a serotype of Aphthovirus, which is very similar to FMDV genome (table 3.1). Biological tests were carried out at Aratana Therapeutics in Leuven, Belgium under the supervision of Dr. Nesya Goris.

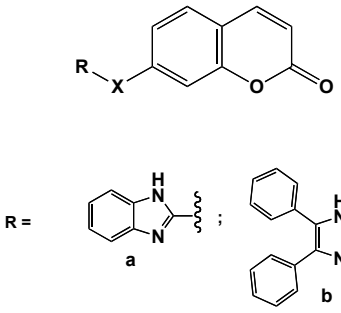

Compound	R	X	EC_{50} (µM) (FMDV)	EC_{50} (µM) (ERAV)	CC_{50} (µM)	SI
91	a	O	>50	>50	>250	-
94	a	NC=O	>50	>50	>250	-
99	a	CH_2S	>50	>50	>250	-
100	b	CH_2S	>50	>50	111	-
105	a	CH_2S=O	>50	>50	170	-
106	b	CH_2S=O	>50	>50	81	-
107	a	CH_2SO_2	>50	>50	>250	-
108	b	CH_2SO_2	>50	>50	>250	-

Table 3.1: Activity and cytotoxicity data of compounds **91, 94, 99-100, 105-108**

All the new compounds were tested with the highest concentration of 50 µM and were found inactive against FMDV and ERAV replication. However, from the CC_{50} values, it could be speculated a possible Michael adduct formation, known to be a mechanism of toxicity. In conclusion, the modifications applied were not successful for the identification of a new FMDV inhibitors and further studies are required.

Conclusions

In an attempt to identify a new scaffold with a selective activity against FMDV replication, molecular modelling techniques were applied. A structure-based virtual screening was carried out on the region where GPC-N114 binds the polymerase of FMDV without inhibiting the viral replication. Selected molecules were evaluated for their activity, but no interesting antiviral profile emerged from that batch of molecules. A *de novo* drug design approach was then applied. Taking into account the geometry of the binding site and the available information on the ligand binding within the polymerase, a multi-fragment search was performed in order to find which molecules could fit the target where Cys200 is located.

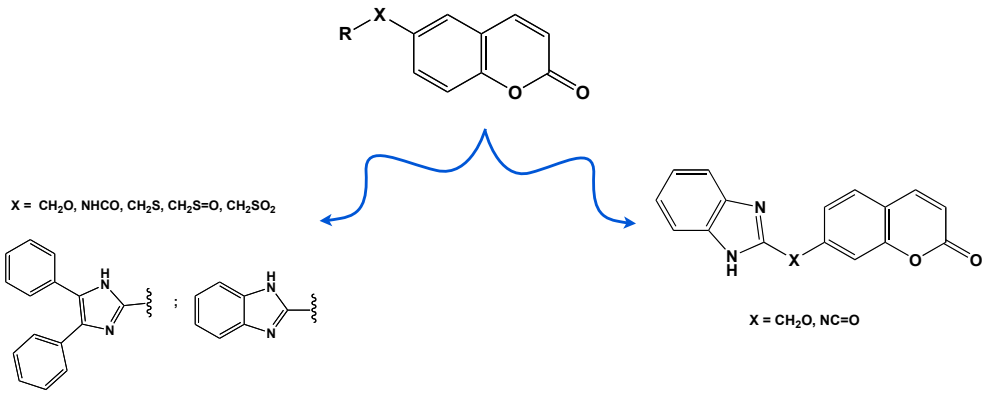

The coumarin ring was chosen as the best one to interact with this key residue. Two functional groups were chosen to be linked to this moiety in order to fill the empty space of the active site and improve the binding. Five linkers were also analysed to connect the two main portions of the molecule. According to the biological results obtained, this scaffold is not associated to antiviral activity. The lack of activity may be due to the fact that these compounds, like GPC-N114, bind but do not inhibit the enzymatic activity. One other possibility of course is that these tested compounds are inactive because they do not bind to the enzyme. Not knowing whether the test compounds bind as intended or not, it is not possible to learn much.

References

1 Thomson, G. Foot and mouth disease: facing the new dilemmas. *Rev. Sci. Tech.* **2002**, 21 (3), 425-428.

2 Thomson, G.R.; Vosloo, W.; Bastos, A.D. Foot and mouth disease in wildlife. *Virus Res.* **2003**, 91 (1), 145-161.

3 Knowles, N.J.; Samuel, A.R.; Davies, P.R.; Kitching, R.P.; Donaldson, A.I. Outbreak of foot-and-mouth disease virus serotype O in the UK caused by a pandemic strain. *Vet. Rec.* **2001**, 148, 258 –259.

4 Leforban, Y.; Gerbier, G. Review of the status of foot and mouth disease and approach to control/eradication in Europe and Central Asia. *Rev. Sci. Tech.* **2002**, 21 (3), 477-492.

5 Nishiuram H.; Omori, R. An epidemiological analysis of the foot-and-mouth disease epidemic in Miyazaki, Japan, 2010. *Transboundary Emerg. Dis.* **2010**, 57, 396-403.

6 Bachrach, H.L. Foot-and-mouth disease virus, properties, molecular biology and immunogenicity. In: Romberger J.A. ed., Beltsville symposia in agricultural research. Vol I, Virology in agriculture, Allanheld, Osmund, Monclair, NJ, 1977; 3-32.

7 Racaniello, V.R. Picornaviridae: the virus and their replication. In: *Fields Virology*, Fields, B.N.; Knipe, B.N.; Howley,P.M. eds., Vol.I, 4th edition, Philadelphia: Lippincott Williams & Wilkins, 2001; 685-722.

8 Falk, M.M.; Grigeran P.R.; Bergamm, I.E.; Zibert, A.; Multhaup, G.; Beck, E. Foot-and-mouth disease virus protease 3C induces specific proteolytic cleavage of host cell histone H3. *J. Virol.* **1990**, 64 (2), 748-756.

9 Pacheco, J.M.; Henry, T.M.; O'Donnell, V.K.; Gregory, J.B.; Mason, P.W. Role of nonstructural proteins 3A and 3B in host range and pathogenicity of foot-and-mouth disease virus. *J. Virol.* **2003**, 77,13017–13027.

10 Monaghan, P.; Cook, H.; Jackson, T.; Ryan, M.; Wileman, T. The ultrastructure of the developing replication site in foot-and-mouth disease virus-infected BHK-38 cells. *J. Gen. Virol.* **2004**, 85 (4), 933-946.

11 Moffat, K.; Howell, G.; Knox, C.; Beisham, G.J.; Monaghan, P.; Ryan, M.D.; Wileman, T. Effect of foot-an-mouth disease viruse nonstructural proteins on the structure and function of the early secretory pathway: 2BC but not 3A blocks endoplasmic reticulum-to-Golgi transport. *J. Virol.* **2005**, 79 (7), 4382-4395.

12 Brown, F. New approaches to vaccination against foot-and-mouth disease. *Vaccine* **1992**, 10 (14), 1022-1026.

13 Doel, T.R. FMD vaccines. *Virus Res.* **2003**, 91(1), 81-99.

14 Sobrino, F.; Saiz, M.; Jimenez-Clavero, M.A.; Nunez, J.I.; Rosas, M.F.; Baranowski, E.; Ley, V. Foot-and-mouth disease virus: a long known virus, but a current threat. *Vet. Res.* **2001**, 32(1), 1-30.

15 Ferrer-Orta, C.; Arias, A.; Perez-Luque, R.; Escarmis, C.; Domingo, E.; Verdaguer, N. Structure of foot-and-mouth disease virus RNA-dependent RNA polymerase and its complex with a template-primer RNA. *J. Biol. Chem.* **2004**, 279 (45), 47212-47221.

16 Zhang, Y.; Biqun, Z.; Zhenfeng, C.; Yingming, P.; Hengshan, W.; Hong, L.; Xianghui, Y. Synthesis and antioxidant activities of novel 4-Schiff base-7-benzyloxy-coumarin derivatives. *Bioorg. Med. Chem. Lett.* **2011**, 21 (22), 6811-6815.

17 Majumdar, K.C.; Chattopadhyay, B.; Sanjay, N. New Heck coupling strategies for the arylation of secondary and tertiary amides via palladium-catalyzed intramolecular cyclization. *Tetrahedron Lett.* **2008**, 49 (10), 1609-1612.

18 Flohr, A.; Jakob-Roetne, R.; Norcross, R.D.; Riemer, C. Imidazo-benzothiazoles. Patent WO 20040229862, November 18, 2004.

19 Venkatraj, M.; Messagie, J.; Joossens, J.; Lambeir, A-M.; Haemers, A.; van der Veken, P.; Augustyns, K. Synthesis and evaluation of non-basic inhibitors of urokinase-type plasminogen activator (uPA). *Bioorg. Med. Chem.* **2013**, 20 (4), 1557-1568

20 Moore, T.W.; Sana, K.; Yan, D.; Krumm, S.A.; Thepchatri, P.; Synder, J.P.; Marengo, J.; Arrendale, R.F.; Prussia, A.J.; Natchus, M.G.; Liotta, D.C.; Plemper, R.K.; Sun, A. Synthesis and Metabolic Studies of Host-Directed Inhibitors for Anti-Viral Therapy. *ACS Med. Chem. Lett.* **2013**, 4 (8), 762-767.

21 Ouellet, S.G.; Gauvreau, D.; Cameron, M.; Dolma, S.; Campeau, L-C.; Hughes, G.; O'Shea, P.D.; Davies, I.W. Convergent, fit-for-purpose, kilogram-scale synthesis of a 5-lipoxygenase inhibitor. *Org. Process Dev.* **2012**, 16 (2), 214-219.

22 Barry, N.; Brondel, N.; Lawrence, S.E.; Maguire, A.R. Synthesis of aryl benzyl NH-sulfoximines. *Tetrahedron* **2009**, 65 (51), 10660-10670.

Chapter 4

Chikungunya Virus

Introduction to the virus

4.1 Chikungunya virus

Chikungunya is a re-emerging viral disease that is transmitted to humans by infected mosquitoes. This viral pathogen causes a serious socio-economical impact, being responsible for an acute febrile illness characterized by joint pain and rush.[1,2] Febrile symptoms usually last 3-4 days, but arthralgia may persist for months, involving knees, elbows, ankles. Cases of eye, neurologic and heart complications have been also reported to happen occasionally, as well as other non-specific symptoms, like headache and gastrointestinal upset.[3] Chikungunya has been reported in many countries of Asia[4] and Africa.[5] From 2001 and 2007, major outbreaks occurred in the Mauritius, Mayotte, Madagascar; in the Reunion Island, one third of the population was infected and 235 cases of death were registered.[6] In 2007, CHIKV virus spread also in Europe for the first time, in Italy.[7] Cases of viral infections have been reported in the Americas[8] and, more recently, in Venenzuela.[9] Two ways of transmission are described for CHIKV: the sylvatic cycle, limited within Africa, where forest-dwelling mosquitoes are the principal vectors that transmit the virus to primates[6] and the human-mosquito-human urban cycle, common in Asia, where *Aedes Aegypti* and, more recently, *Aedes Albopictus*, are the main responsible for virus spreading.[10] The transmission is mediated by the salivary glands of the mosquito. The virus directly enters the bloodstream of humans through mosquito bites and combines with the cells of the nose, throat and mouth.

4.1.1 Virion structure

The Chikungunya viral particle is spherical, icosahedral, of about 70-100 nm in diameters. It has a lipid bilayer that is formed by 80 flower-like structures made of three subunits. These heterodimers are formed by glycoproteins E1 and E2. The envelope represents the outer surface that surrounds the nucleocapsid, which is made of 240 copies of capsid proteins and contains one molecule of RNA.

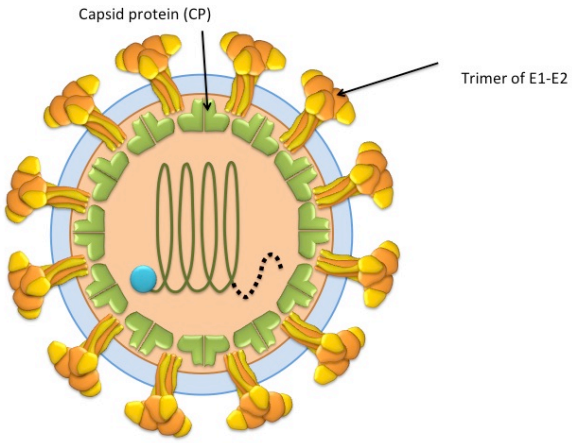

Figure 4.1: Structure of the Chikungunya virion particle

4.1.2 Genome organization

Chikungunya is an Arbovirus that belongs to the *Alphavirus* genus, of the family *Togaviridae.*[11] Viruses of the *Alphavirus* genus are divided in two main groups: the Old and the New World viruses. The genus is composed of three subgroups, the Semliki Forest virus (SFV), the Eastern Equine Encephalitis virus (EEEV) and the Sinbis virus. Taxonomically, CHIKV is part of the first complex, SFV.[12] CHIKV is an enveloped, single strand RNA virus. The genome, 11.8 kb in length, is formed by a 5' cap-untranslated region (UTR), non-structural proteins (nsP1-4), structural proteins (C-E3-E2-6K-E1) and a 3' terminal poly-A tail.[13]

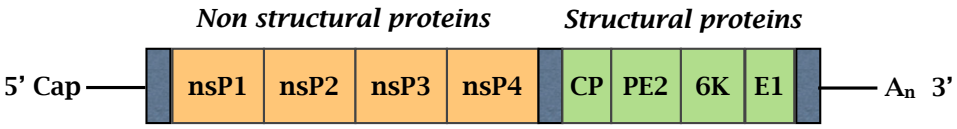

Figure 4.2: Chikungunya genome organization

4.1.3 Viral proteins

The role of the non-structural proteins, nsP1, nsP2, nsP3 and nsP4 is to carry out the synthesis of viral RNAs. nsP1 participates in the anchorage of replicase complex on the plasma membrane and has a methyltransferase activity.[14,15] nsP2 is a multifunctional enzyme: while the N-terminal part has NTPase, RNA triphosphatase and helicase properties, the C-terminal section has protease activity.[16,17,18] A more detail description is given

below. The function of nsP3 is not well known, but it is thought to be a phosphoprotein responsible for recruiting several cellular proteins to the replicase complex.[19] Finally, nsP4 has RNA-dependent RNA polymerase activity and replicates genomic and antigenomic RNA through specific signals.[20] Among the structural proteins, capsid protein (CP) forms the nucleocapsid and has a protease activity that makes an autocatalytic cleavage of itself from the polyprotein.[21] Capsid protein is also able to associate with ribosomes and to bind the genome RNA, thus forming viral particles.[22] E3 protein is the amino-terminal part of the E2 precursor (PE2) and is able to provide the signal sequence for the translocation of PE2 into the ER.[23] E2 protein is involved in viral attachment to target host cells,[24] while 6K is responsible for virus assembly and budding of viral proteins.[25] Finally, E1 protein, a type I transmembrane glycoprotein, takes part in the viral nucleocapsid release in cytoplasm after endosome and viral membrane fusion.[26]

4.1.4 Viral life cycle

Virus uptake, for CHIKV, is a receptor-mediated endocytosis process. The attachment is mediated by E2 protein that binds cellular receptors of different type. Once in the endosomal vesicles, the genomic RNA is released into the cytoplasm by fusion to the endosomal membranes and the replication process can start.[27,28] The first step, after releasing the RNA from the nucleocapsid, is the translation of the genome by cellular ribosomes. From this process, the P1234 polyprotein is initially cleaved in a P123 complex and nsP4, then a second complex made by nsP1, nsP23 and nsP4 is formed (Figure 4.3).[29]

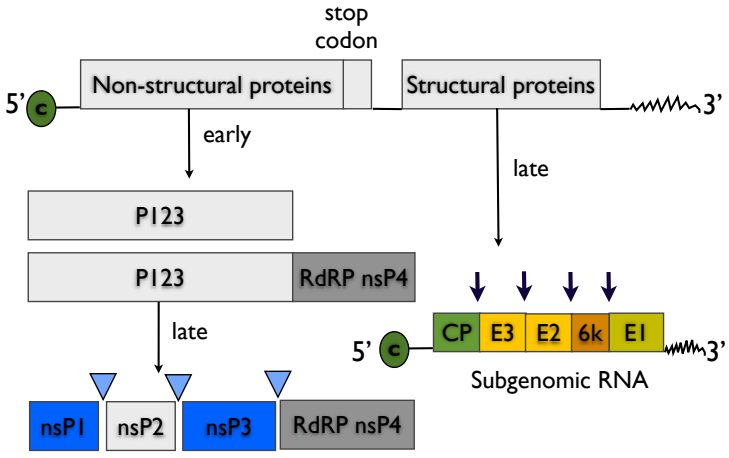

Figure 4.3: Translation of the genome

In the early phase of infection, full-length negative strand antigenome RNA is synthesized by the complex formed between P123 and nsP4. The antigenome is the template for the synthesis of full-length RNA and also subgenomic mRNAs. After final cleavage to nsP1, nsP2, nsP3 and nsP4 the switch from synthesis of negative to positive strands occurs. The replication process starts, along with the translation of proteins that eventually encapsidate nascent genome RNA before viral release by budding through the cell membrane (figure 4.4).[30]

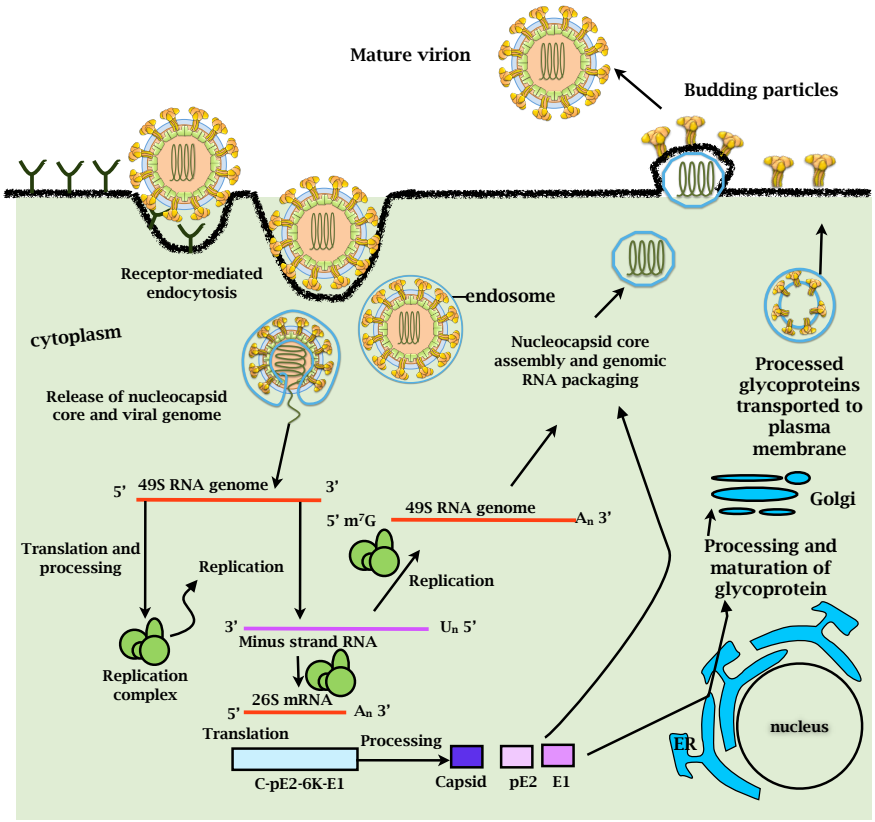

Figure 4.4: Chikungunya life cycle

4.1.5 Current treatment

At the moment, there is no antiviral therapy nor a vaccine available. Treatment of chikungunya disease is only symptomatic, by using non-steroidal anti-inflammatory analgesics and fluids. Corticosteroids are used to decrease the inflammation.[31] The antimalarial drug chloroquine and other examples of compounds, like ammonium chloride, amantadine and methylamine have been used against *Alphaviruses*, but only for their anti-inflammatory properties.[31] Chloroquine entered phase 3 clinical trials in France in 2006, but was stopped in 2007 because of no antiviral results.[32]

In the literature, several examples of active compounds against viral replication have been described. They all range from well-known antivirals, like ribavirin[33] and arbidol,[34] to natural sources, like prostatin, 12-O-tetradecanoyl- phorbol 13-acetate [35] and the antitumor compound harringtonine.[36] Bassetto et al. identified for the first time through a *in silico* approach one hit compound active at low micromolar range (EC_{50} of 5 μM) that was the starting point of further optimization studies which will described in section 4.3.[37] Many efforts have been done in the past 30 years to develop a vaccine against CHIKV. Potential candidates were obtained using live inactivated or attenuated strains, but they were stopped due to lack of funding or no commercial potential.[38] Some of them are still under evaluation.[39] Recently, a very promising vaccine candidate that uses a virus-like particle is in the early stages of preclinical development.[40]

4.2 nsP2 protease

4.2.1 Structure

The nsP2 protease has an essential function in the viral replication and propagation. Its crystal structure has been solved in 2011 with a 2.40 Å resolution (PDB ID: 3TRK).[41] Two main domains characterise nsP2 protease: the N-terminal domain (aa 1-470) has NTPase[42,43] and RNA triphosphatase activities, involved in viral RNA capping. It has also an important RNA helicase activity.[44] The C-terminal domain (aa 471-798) exhibits protease activity, with the presence of the catalytic dyad cystein and histidine residues.[45,46] The active site is at the interface between the two main domains that are involved in substrate recognition. Among *Alphavirus* nsP2 protease, there is little sequence similarity, but the catalytic residues are conserved. In addition, the three residues that follow each catalytic residue do not vary and one of them, Trp has been shown to be important for proteolytic activity. The proteolytic processing happens at three different cleavage sites, nsP1-2, nsP2-3 and nsP3-4, with a preference for nsP3-4> nsP1-2>> nsP2-3. Studies on the Venezuelan Equine Encephalitis Virus (VEEV) revealed the essential residues for cleavage site recognition. Homology modelling studies carried out for different members of the Aphavirus genus demonstrated common characteristics that may be present also in the case of CHIKV.[47]

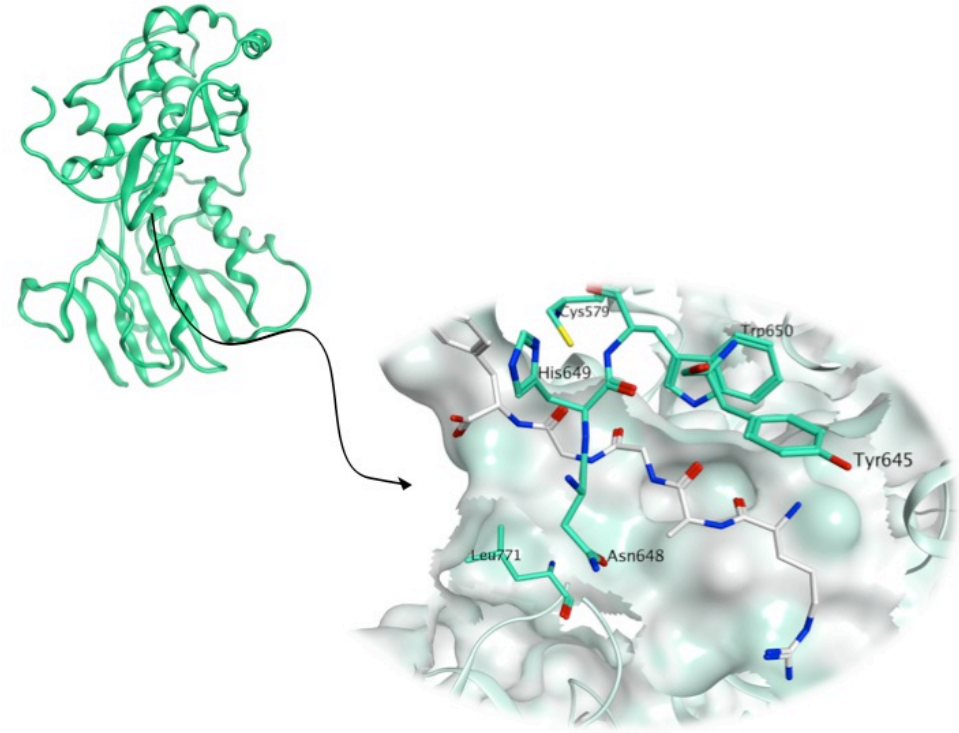

Figure 4.4: Ribbon representation of Chikungunya nsP2 protease. Close up of the nsP2 protease binding site in presence of a model of nsP3-4 junction peptide

4.2.2 Mechanism of action

The catalytic mechanism of nsP2 proteases is similar to the one proposed for papain-like proteases.[48,49] The protease cleft can accommodate a substrate of five residues, defined P1'-P1-P2-P3-P4. To each residue corresponds a protein subsite. They are termed S1', S1, S2, S3 and S4. The cleavage occurs between P1' and P1 and the mechanism consists in the formation of a thiolate-imidazolium ion pair of the catalytic dyad. The substrate is ready to bind the active site: the P1 carbonyl can be attacked by the deprotonated thiol and the reaction can proceed.[47]

Results and discussion

4.3 nsP2 Protease as a target for the identification of new antivirals

The nsP2 protease is one of the most promising targets since it is responsible for the formation of the four mature nsPs that are required for virus replication. Potential inhibitors can be identified by targeting the critical residues for the proteolytic cleavage.

4.3.1 Project background

Previous work done in our lab explored the nsP2 protease as a target for the development of selective inhibitors of CHIKV replication. A structure-based virtual screening on the active site of a homology model of the nsP2 protein was performed using a library of ~5 million compounds. The original database was pre-filtered using a pharmacophore model set on the nsP2 binding site. Nine compounds were purchased and their antiviral activity was assessed in a cell-based assay. Compound **109 (**Figure 4.5**)** selectively inhibited CHIKV-induced cell death at low µM concentration, with an EC_{50} value of 5.0 µM in the cytophatic effect (CPE) reduction assay. This molecule was chosen as a starting point for the development of novel potential nsP2 protease inhibitors.[37]

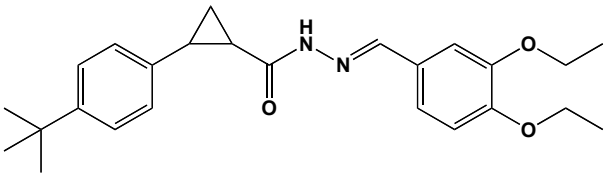

Figure 4.5: Chemical structure of hit compound **109**

The predicted binding mode is shown in figure 4.6. This compound nicely fits in the central portion of the nsP2 protease active site, with the hydrazone group placed near the catalytic dyad, Cys579 and His649, and in close proximity to Trp650. Several interactions have been identified by docking studies as essential: a hydrophobic bond between the *t*-butylic group of **109** and His649, two hydrogen-bonds between the hydrazide function and the backbone amido groups of Tyr645 and Asn648, and

another hydrophobic contact between the 3,4-diethoxyphenyl ring and the lateral chain of Trp650.

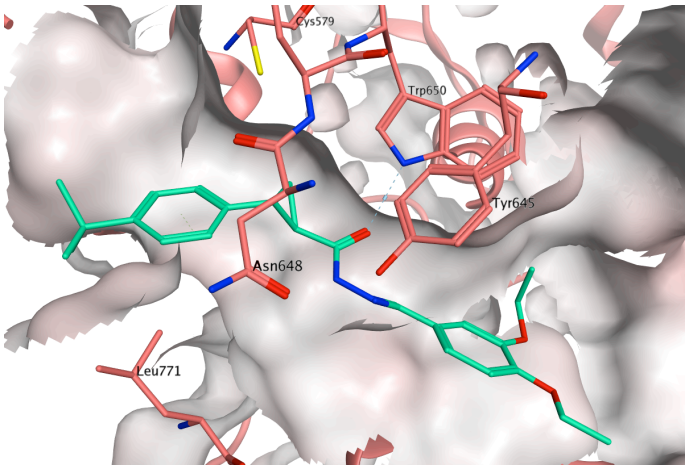

Figure 4.6: Predicted binding mode of compound **109** in the nsP2 binding site

The chemical scaffold of compound **109** was explored to investigate its potential for the design of new anti-CHIKV compounds. First of all, 23 analogues were directly purchased from the SPECS library and tested for their antiviral activity. From the biological data, two structural elements seemed essential for antiviral activity: the cyclopropylic ring and the presence of an aliphatic group in *para* position of the benzylidene portion. The data obtained guided the design and synthesis of a first series of compounds aimed to optimise the identified hit structure. The main modification regarded the cyclopropylic moiety, that was replaced by a *trans*-ethenylic group, as the presence of two chiral centers on this ring represented an issue for the preparation and purification of new analogues. The double bond in its *trans* configuration had the advantage of avoiding the presence of chiral centers while maintaining the length and geometry of the original cyclopropylic ring. Compound **110** (Figure 4.7) was prepared and tested in *in vitro* assays. Interestingly, the biological evaluation showed retained antiviral activity, which proofed that the replacement of the cyclopropylic ring with a *trans*-ethenylic bond was acceptable. The new derivative showed a EC_{50} value of 3.2 µM and was taken as a starting point for SAR studies.[35]

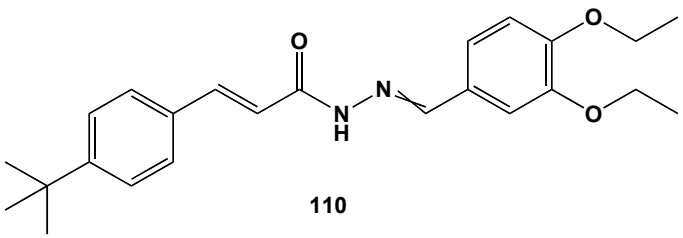

Figure 4.7: Chemical structure of compound **110**

Docking analysis of compound **110** in the nsP2 binding site (Figure 4.8) showed great similarities with the hit structure **109**: the *t*-butyl group has maintained its position and makes hydrophobic interaction with His649; the hydrogen-bonds between the hydrazone group and residues Tyr613 and Asn648 are also present, along with hydrophobic contacts between the second aromatic ring and Trp650.

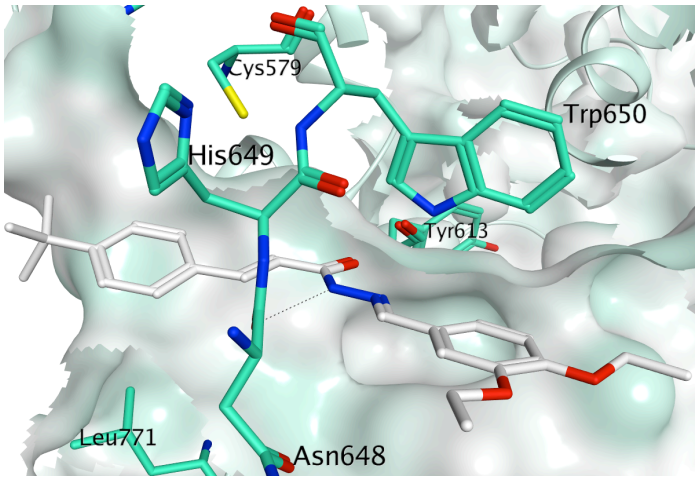

Figure 4.8: Predicted binding pose of compound **110** in the nsP2 binding site

4.3.2 Design and synthesis of novel derivatives

The chemical structure of compound **110** was taken as a lead compound for this study, with the aim to improve the activity of the original molecule and better understand its structure-activity relationships. Four families of compounds were designed, validated with docking techniques and finally prepared in order to be tested.

1) A first series of compounds was synthesized in order to explore different substituents in place of the *t*-butyl group;

2) Another series of compounds was designed with the aim to protect the overall molecule from chemical instability, by introducing a benzimidazole ring on the level of the hydrazone group. Furthermore, a new scaffold bearing a triazole ring was designed in place of the hydrazide group;

3) An additional modification was the introduction of a urea and, successively, a thiourea group in place of the hydrazide moiety, in order to increase the hydrophilicity of the molecule.

4.4 Synthesis of (2*E*)-*N*'-benzylidene aryl acrylohydrazides

With the purpose to better understand the importance of the *t*-butylic moiety, four different functional groups were introduced in place of it.

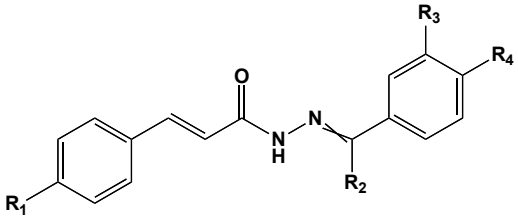

Phenyl and isopropyl groups were chosen to explore the effect of similar or bulkier substituents and analyse activity related to their steic effect. To evaluate the influence of electronic contributions on the original molecule, a methoxy and a trifluoromethyl groups were also introduced, while on positions R_3 and R_4 the most active groups (*m,p*-diethoxy, *p*-methyl, *p*-hydroxyl and *p*-cyclohexyl groups) were maintained, based on previous SAR studies. Figure 4.9 shows the predicted binding mode of compound **137** as a representative example, which is consistent with the one previously described for the lead compound, showing an hydrogen bond between the carbonyl group and the indole of Trp650.

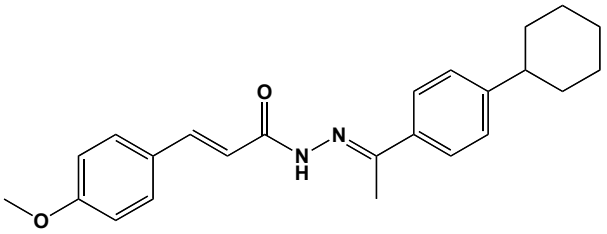

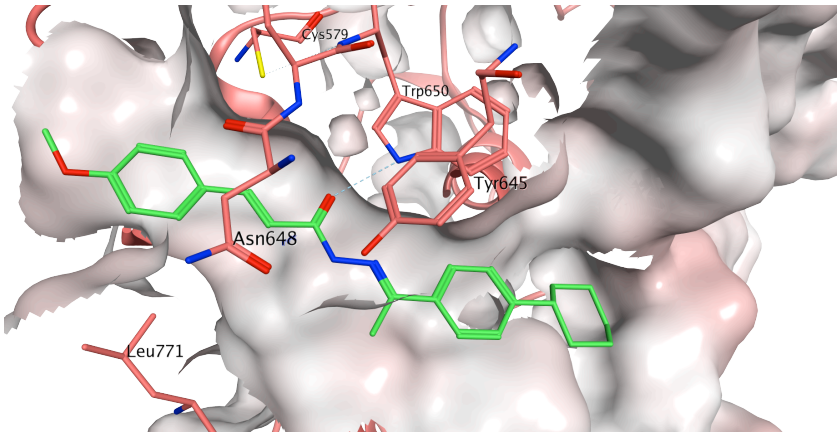

Figure 4.9: Chemical structure and predicted binding mode of compound **137** as a representative example

4.4.1 (2*E*)-*N'*-Benzylidene aryl acrylohydrazides

The planned strategy for the synthesis of the new derivatives was a three step synthetic pathway, that begins with the formation of substituted acrylic acids, successively converted to their correspondent chloride forms. Final compounds were obtained by a condensation reaction between the acryloyl chloride intermediates and aryl hydrazones previously synthesized.

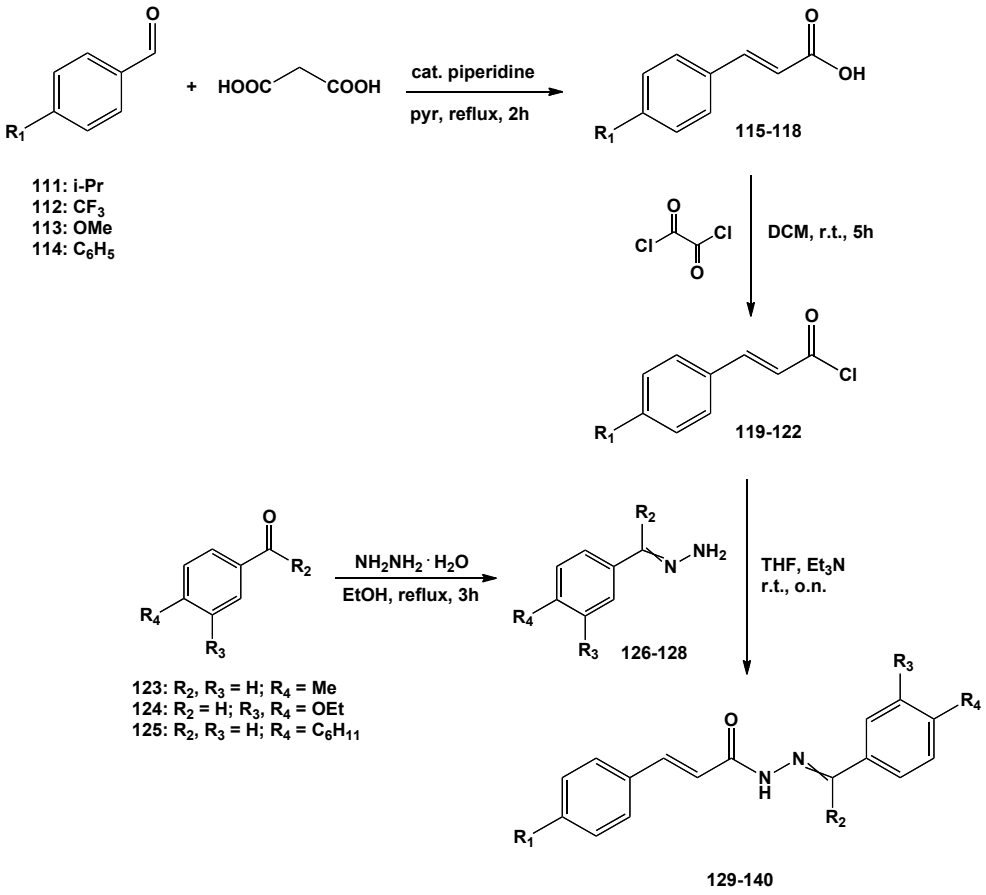

Scheme 4.1: Common synthetic strategy applied for compounds **129-140**

Synthesis of aryl acrylic acids (115-118)

The first step is a Knoevenagel condensation between malonic acid and the appropriate aldehyde to give aryl acrylic acid derivatives **115-118** (Scheme 4.2).[50] All the four intermediates were obtained as pure products by flash chromatographic purification with high yields.

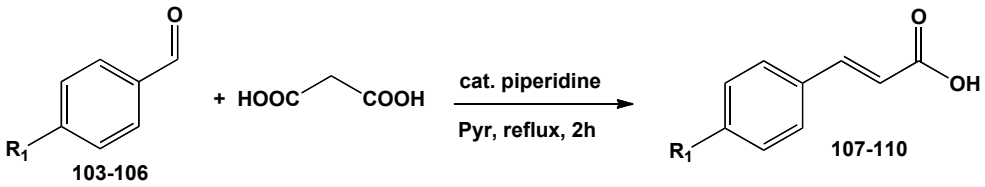

Starting aldehyde	R_1	Product	Yield %
111	i-Pr	**115**	91
112	CF_3	**116**	91
113	OMe	**117**	80
114	C_6H_5	**118**	92

Scheme 4.2: First step synthesis for compounds **115-118**

Synthesis of acryloyl chlorides (119-122)

The correspondent aryl acrylic acids **115-118** (Scheme 4.3) were chlorinated, according to reported procedures, with oxalyl chloride to prepare acryloyl chloride intermediates **119-122**.[51]

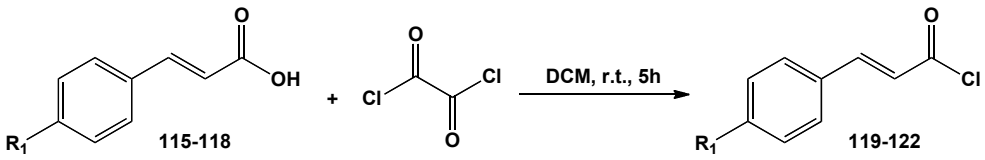

Acryloyl acid intermediate	R_1	Product	Yield %
115	i-Pr	**119**	100
116	CF_3	**120**	91
117	OMe	**121**	94
118	C_6H_5	**122**	98

Scheme 4.3: Second step synthesis for compounds **119-122**

Synthesis of aryl hydrazones (126-128)

Aryl hydrazone intermediates **126-128** (Scheme 4.4) were synthesized through the formation of a Schiff base between the aldehydes **123-125** with hydrazine monohydrate.[52] All products were obtained with good yields and used for the following step without further purification.

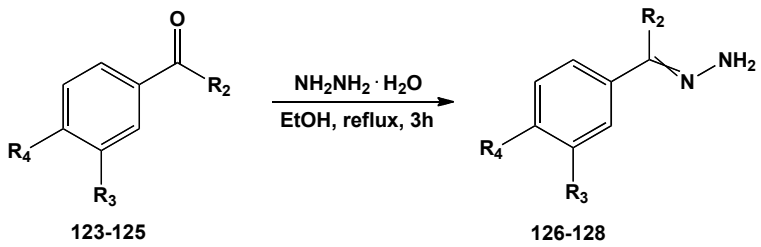

123-125 126-128

Starting aldehyde	R_2	R_3	R_4	Product	Yield %
123	H	H	Me	**126**	76
124	H	OEt	OEt	**127**	91
125	Me	H	C_6H_{11}	**128**	94

Scheme 4.4: Third step synthesis for compounds **126-128**

Synthesis of (2*E*)-*N*'-benzylidene aryl acrylohydrazides (129-140)

Final compounds **129-140** (Scheme 4.5) were prepared by adding the hydrazone intermediates **126-128** to a solution of acryloyl chlorides **119-122** in anhydrous THF and triethylamine, which was used to neutralize the hydrochloric acid formed.[53]

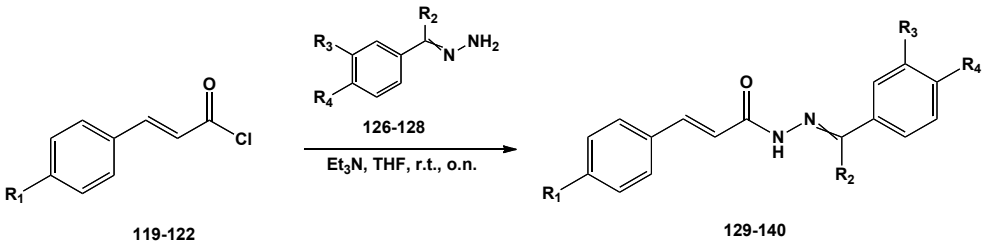

Acryloyl chloride	R_1	Aryl hydrazones	R_2	R_3	R_4	Product	Yield %
119	i-Pr	**126**	H	H	Me	**129**	58
119	i-Pr	**127**	H	OEt	OEt	**130**	13
119	i-Pr	**128**	Me	H	C_6H_{11}	**131**	18
120	CF_3	**126**	H	H	Me	**132**	6
120	CF_3	**127**	H	OEt	OEt	**133**	5
120	CF_3	**128**	Me	H	C_6H_{11}	**134**	12
121	OMe	**126**	H	H	Me	**135**	55
121	OMe	**127**	H	OEt	OEt	**136**	35
121	OMe	**128**	Me	H	C_6H_{11}	**137**	9
122	C_6H_5	**126**	H	H	Me	**138**	10
122	C_6H_5	**127**	H	OEt	OEt	**139**	6
122	C_6H_5	**128**	Me	H	C_6H_{11}	**140**	5

Scheme 4.5: Synthesis of compounds **129-140**

4.4.2 (2*E*)-*N*'-(4-Hydroxybenzylidene)-3-(4-isopropylphenyl)acrylohydrazide (143)

The described procedure for the synthesis of (2*E*)-*N*'-benzylidene aryl acrylohydrazides was also applied for the preparation of derivatives bearing a hydroxyl group on the aryl hydrazone moiety. In these conditions, a complex mixture of multiple products was obtained and it was not possible to purify the designed compounds by chromatographic or recrystallisation techniques. This might be due to the presence of the triethylamine base in the reaction mixture, that might deprotonate the hydroxyl group causing the formation of a nucleophile center able to react with the acryloyl chloride, thus preventing the condensation with the hydrazones. A different synthetic pathway was attempted. By a one-pot

reaction, acryloyl acid derivatives were converted to the correspondent acrylohydrazides without isolating the intermediate acryloyl chlorides.[54] Unfortunately, the only acrylohydrazide obtained from this reaction was the one bearing the i-Pr group, **141**, which was finally used to obtain the Schiff base with 4-hydroxyaldehyde **142**, following a modified procedure.[55] The desired compound **143** was purified by recrystallization from EtOH and obtained with a 7% of yield.

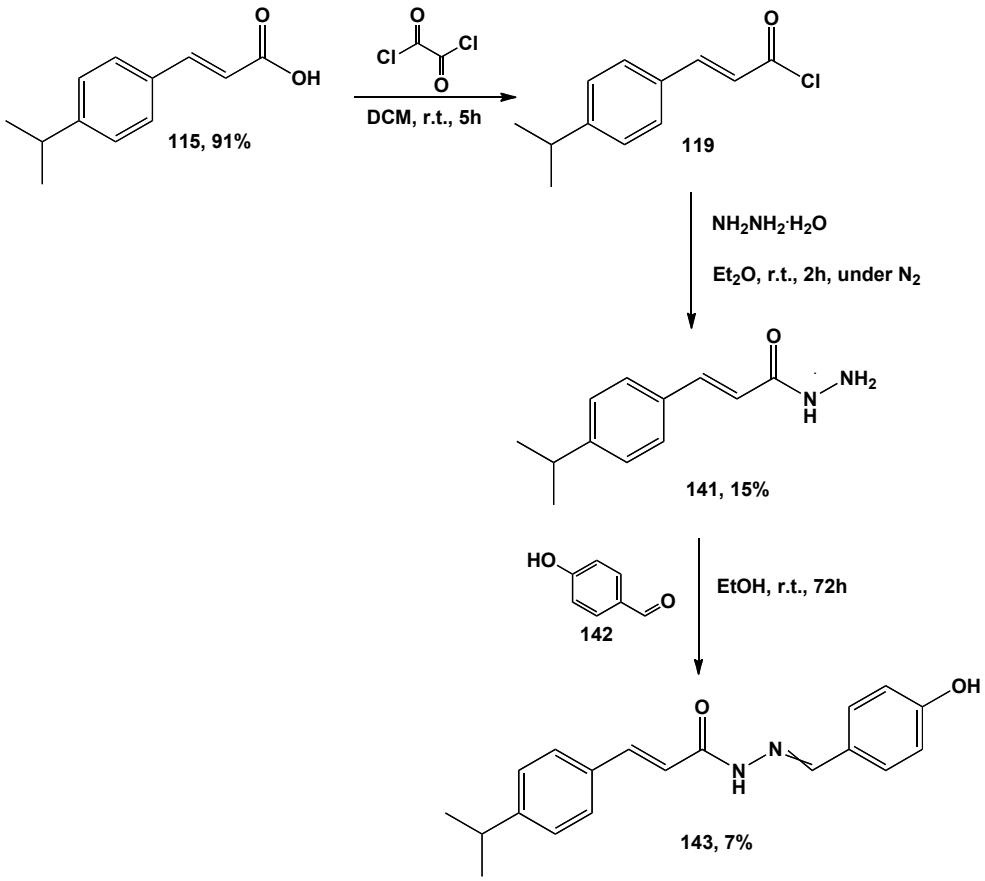

Scheme 4.6: Synthetic pathway applied for compound **143**

Synthesis of (*E*)-3-(4-isopropylphenyl)acryloyl chloride (119)

Intermediate **119** (Scheme 4.6) was obtained through chlorination of acrylic acid **115** by oxalyl chloride, in DCM, at r.t., for 5 h, according to the same procedure previously described.[3] The product was not isolated and directly used for the following step.

Synthesis of (*E*)-3-(4-isopropylphenyl)acrylohydrazide (143)

Nucleophilic displacement of the chloride leaving group with aqueous hydrazine was carried out to obtain the correspondent acrylohydrazide **141.** The intermediate was used for the final step as crude product, as it was not possible to purify it from a mixture of impurities that could not be identified by column chromatography or recrystallization.

Synthesis of (2*E*)-*N'*-(4-hydroxybenzylidene)-3-(4-isopropylphenyl)acrylohydrazide (143)

The desired product bearing a hydroxyl group at the level of the hydrazone moiety was obtained through the formation of a Schiff base between acrylohydrazide **141** and 4-hydroxylaldehyde **142**. Although from the crude mixture multiple products were observed by T.L.C., final compound **142** was isolated through flash column chromatography and further purified by recrystallization from ethanol with a 7% of yield.

4.4.3 Biological evaluation

Thirteen new derivatives were evaluated for their antiviral activity and cytotoxicity in a virus-cell-based assay (table 4.1).
The evaluation was performed at the Rega Institute for Medical Research in Leuven, Belgium, under the supervision of Professor Johan Neyts. Activity is espressed as EC_{50} and EC_{90} and cytotoxicity as CC_{50}, as already described in section 2.4.2

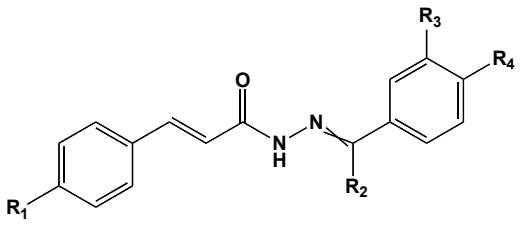

Compound	R_1	R_2	R_3	R_4	EC_{50} (µM)	EC_{90} (µM)	CC_{50} (µM)	SI
110 (lead compound)	t-But	H	OEt	OEt	3.2	11	101	32
129	i-Pr	H	H	Me	25.9	-	25	0
130	i-Pr	H	OEt	OEt	>29.2	>29.2	-	-
131	i-Pr	Me	H	C_6H_{11}	>193	>193	-	-
132	CF_3	H	H	Me	96.3	>150	203	2
133	CF_3	H	OEt	OEt	48.9	84.2	84.1	2
134	CF_3	Me	H	C_6H_{11}	>241	>241	-	-
135	OMe	H	H	Me	>112	>112	-	-
136	OMe	H	OEt	OEt	>271	>271	-	-
137	OMe	Me	H	C_6H_{11}	>87.7	>87.7	-	-
138	C_6H_5	H	H	Me	230	>294	>294	-
139	C_6H_5	H	OEt	OEt	>80.2	>80.2	-	-
140	C_6H_5	Me	H	C_6H_{11}	>29.6	>29.6	-	-
143	i-Pr	H	H	OH	>324	>324	-	-

Table 4.1: activity and cytotoxicity data for compounds **129-140, 143**

As can be deduced from the biological data shown above, the new derivatives bearing four different functional groups in place of the *t*-butylic group are associated to loss of antiviral activity. Compound **129**, with an isopropyl group in *para* position of the acrylic moiety, is the only one that shows a certain activity at higher concentration than the original compound, but it is also associated to an increased toxicity against the cell. These data, therefore, confirmed previous indications of the essential role occupied by the *t*-butyl group.

4.5 Synthesis of *N*-(1*H*-benzo[*d*]imidazol-2-yl)aryl amides

A first attempt to replace the hydrazone linker, known to be poorly stable in aqueous systems, was the introduction of a benzimidazole ring.

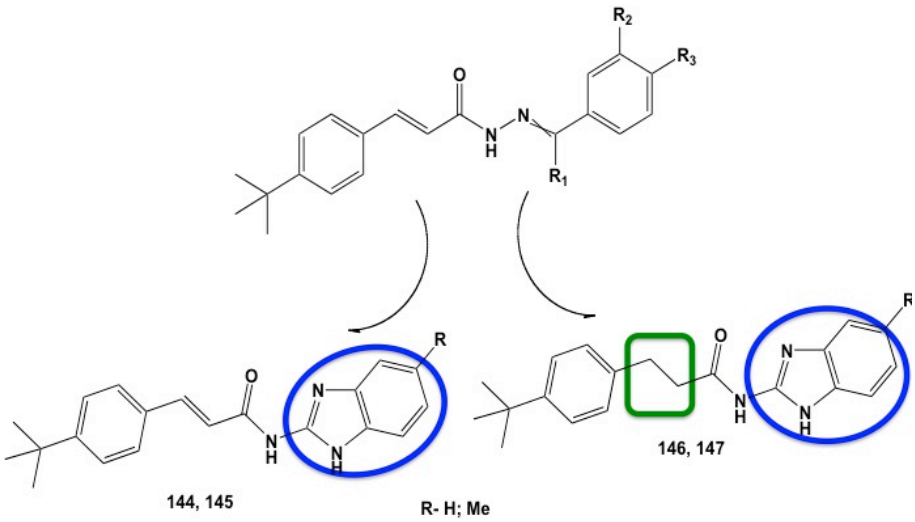

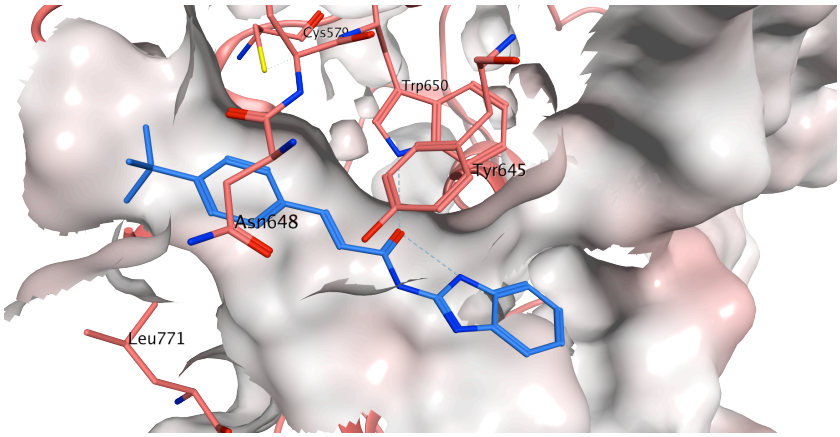

Figure 4.10: Chemical scaffold of *N*-(1*H*-benzo[*d*]imidazol-2-*yl*)aryl amides. The predicted binding pose of compound **144** is a representative example

For this series of compounds, a total of four derivatives were designed and synthesised. As previously said, the general approach in this drug optimisation study is to prepare new derivatives while maintaining the aromatic substituents that were associated to antiviral activity on the hit structure. In this case, the *t*-butyl group on the aromatic acryloyl moiety was kept, but it was not possible to purchase or prepare the benzimidazole moiety with 3,4-diethoxy, *p*-hydroxyl and *p*-cyclohexyl functional groups.

Following reported procedures and according to the starting materials commercially available, the unsubstituted and *para* methyl derivatives were prepared. The introduction of the benzimidazole ring increases the rigidity of the overall structure, therefore the double bond at the level of the acryloyl moiety was reduced in two of the four derivatives, in order to understand the effect of this modification on the activity of the new compounds. Figure 4.10 shows the predicted binding mode for compound **144** as a representative example. Docking studies for the two scaffolds exhibit a similar occupational space comparable to lead structure **110**, with all the key interactions maintained.

4.5.1 *N*-(1*H*-Benzo[*d*]imidazol-2-*yl*)-3-(4-*tert*-butylphenyl)acrylamides (144, 145)

The synthetic pathway toward the synthesis of 144 and 145 (Scheme 4.7) consists in a coupling reaction between (*E*)-3-(4-*tert*-butylphenyl)acrylic acid **153** and substituted 2-aminobenzimidazoles **150, 151** using TBTU as coupling agent.[56] (*E*)-3-(4-*tert*-butylphenyl)acrylic acid **153** was synthesized from 4-*tert*-butylbenzaldehyde **152**, following the procedure described above for compounds **119-122**, while substituted 2-aminobenzimidazoles **150, 151** were obtained by cyclization of aryl 1,2-diamines **148, 149** using cyanogen bromide.

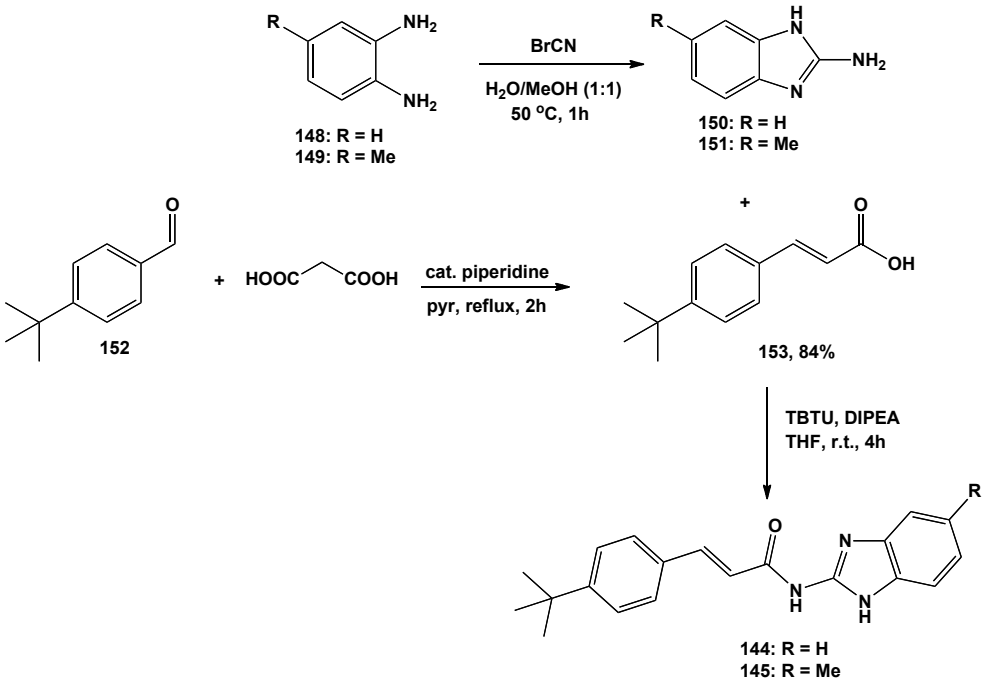

Scheme 4.7: Synthetic pathway for compounds **144, 145**

Synthesis of substituted 2-aminobenzimidazoles (150, 151)

Following reported procedures, compounds **150, 151** (Scheme 4.8) were obtained by addition of cyanogen bromide to a 1:1 solution of MeOH and water where the aryl 1,2-diamine was previously dissolved.[57] The mechanism of this reaction is a nucleophilic addition between one amino group of the aryl 1,2-diamine and the electrophilic carbon of the cyanogen bromide. Final substituted 2-aminobenzimidazoles **150, 151** were obtained by ring closure of the *N*-(2-aminoaryl)cyanamide intermediate formed.[58]

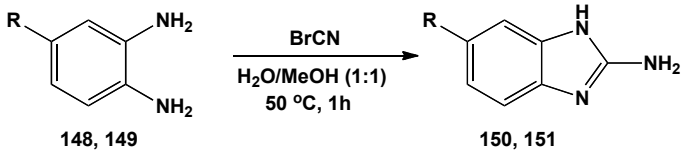

148, 149 150, 151

Aryl 1,2-diamine	R	Product	Yield %
148	H	**150**	87
149	Me	**151**	87

Scheme 4.8: First step synthesis for compounds **150, 151**

(*E*)-3-(4-*tert*-butylphenyl)acrylic acid (153)

Intermediate **153** (Scheme 4.9) was synthesised according to a Knoevenagel reaction, previously described for compounds **119-122**, starting from 4-*tert*-butyl benzaldehyde **152**. The crude product was purified through flash column chromatography to obtain the pure product with a 84 % of yield.

Synthesis of (*E*)-*N*-(1*H*-benzo[*d*]imidazol-2-*yl*)-3-(4-*tert*-butylphenyl)acrylamides (144, 145)

Final amide derivatives were prepared by a coupling reaction between substituted 2-aminobenzimidazoles **150, 151** and (*E*)-3-(4-*tert*-butylphenyl)acrylic acid **153** using TBTU as a coupling reagent (Scheme 4.9). O-(Benzotriazol-1-*yl*)-*N,N,N',N'*-tetramethyluronium tetrafluoroborate is a member of the uronium-type reagents used for efficient amide bond formation under mild reaction conditions. Like most coupling agents, uronium reagents are able to enhance the electrophilic characteristic of the

carbonyl carbon towards nucleophilic substitution by the formation of a highly reactive intermediate ester.[59]

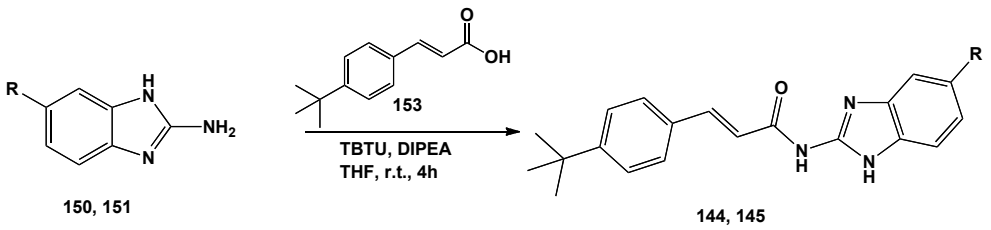

Aryl 1,2-diamine intermediate	R	Product	Yield %
150	H	**144**	12
151	Me	**145**	10

Scheme 4.9: Final step synthesis for compounds **144, 145**

4.5.2 (*N*-)1*H*-Benzo[*d*]imidazol-2-*yl*)-3-(4-*tert*-butylphenyl)propanamides (146, 147)

A second series of derivatives bearing the benzimidazole ring at the level of the hydrazone group was designed with an additional modification: the C-C double bond was reduced in order to decrease the rigidity of the molecule, that was intensified by the introduction of the ring. For the preparation of compounds **146, 147** a different synthetic pathway was followed (Scheme 4.10). (*E*)-3-(4-*tert*-Butylphenyl)acrylic acid **153** was first reduced to 3-(4-*tert*-butylphenyl)propanoic acid **154** that was successively converted to the correspondent aryl propanoyl chloride **155**. Final compounds **146, 147** were obtained by a nucleophlic substitution between 2-aminobenzimidazoles **150, 151** and 3-(4-*tert*-butylphenyl)propanoyl chloride **155**.

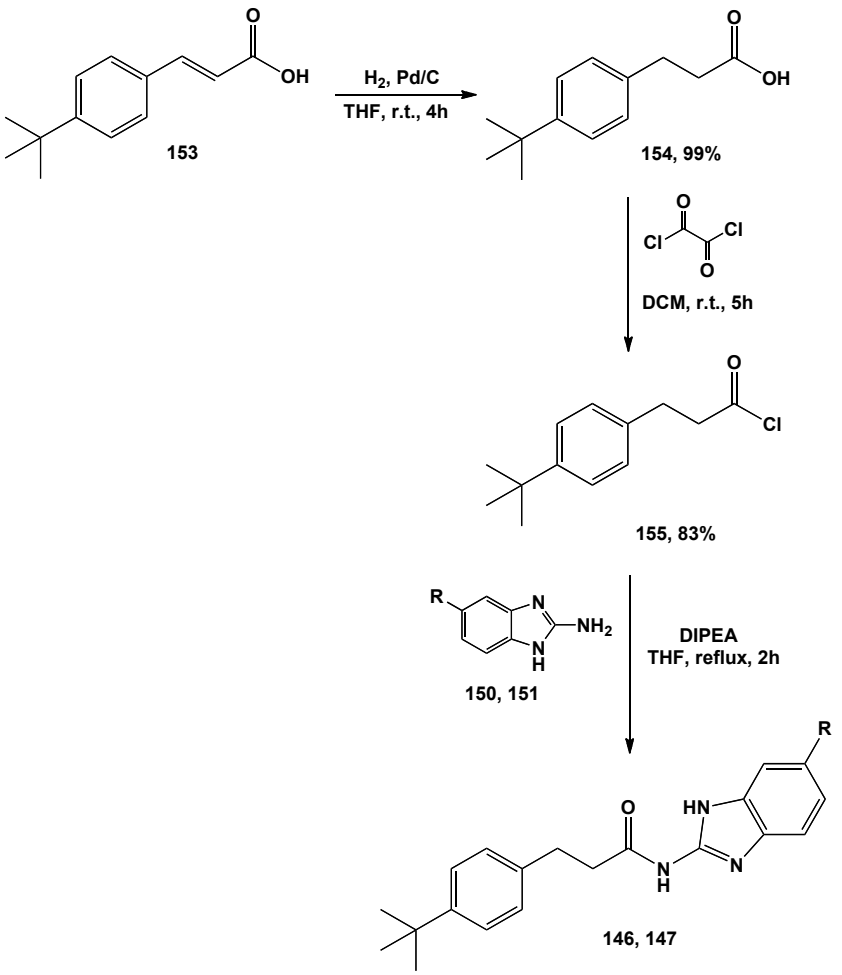

Scheme 4.10: Synthetic pathway for compounds **146, 147**

Synthesis of 3-(4-*tert*-butylphenyl)propanoic acid (154)

Following reported procedures, the C-C double bound in (E)-3-(4-*tert*-butylphenyl)acrylic acid **153** (Scheme 4.10) was reduced by a Pd/C-catalyzed hydrogenation in THF. The desired product was obtained without further purification with a 99 % of yield.[60]

Synthesis of 3-(4-*tert*-butylphenyl)propanoyl chloride (155)

3-(4-*tert*-Butylphenyl)propanoyl chloride **155** (Scheme 4.10) was synthesized by a chlorination reaction with oxalyl chloride in DCM, following reported procedures.[61] Final compound **155** was obtained with 83% of yield and was used for the following step without further purification.

Synthesis of benzoimidazol-3-(4-*tert*-butylphenyl)propanamides (146, 147)

Final amide derivatives **146, 147** were prepared by nucleophilic displacement of the chloride leaving group by primary amino function of substituted 2-aminobenzimidazoles **150, 151** in anhydrous conditions, using DIPEA to neutralize the hydrochloric acid formed.[62]

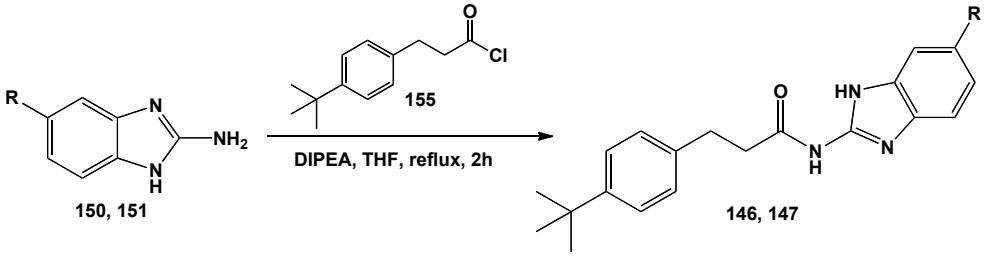

Aryl 1,2-diamine intermediate	R	Product	Yield %
150	H	**146**	5
151	Me	**147**	5

Scheme 4.11: Final step synthesis for compounds **146, 147**

4.5.3 Biological evaluation

New derivatives **144-147** were evaluated for their antiviral activity and cytotoxicity in a virus-cell-based assay (table 4.2).

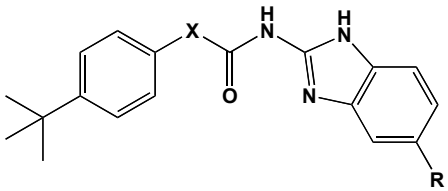

Compound	X	R	EC_{50} (µM)	EC_{90} (µM)	CC_{50} (µM)	SI
110 (lead compound)			3.2	11	101	32
144	CH=CH	H	>157	>157	-	-
145	CH=CH	Me	>300	>300	-	-
146	CH_2CH_2	H	>311	>311	-	-
146	CH_2CH_2	Me	>298	>298	-	-

Table 4.2: activity and cytotoxicity data for compounds **144, 145**

None of the new four derivatives was related to activity improvement. It could be speculated that the increased rigidity of the overall molecule by the introduction of a benzimidazole ring has affected the activity of the molecules. For the derivatives bearing the reduced C-C bond, it is not possible to hypothesize if one or both modifications affected the activity of the molecule. Different new modifications were planned aiming to improve the stability of the overall structure.

4.6 Synthesis of 1-phenethyl-4-phenyl-1*H*-1,2,3-triazole (157)

A second attempt to reduce the instability of the molecule due to the presence of the hydrazone group was the introduction of a triazole ring. The design of this compound was also supported by the biological data on derivative **156** (Scheme 4.11), that was previously synthesized in our lab. The rational behind the design of this compound was to replace the hydrazide group with an oxadiazole ring. Derivative **156** was found to have a retained antiviral activity. Based on these results, compound **157** designed and prepared in order to see the effect of a different 5-heterocyclic ring on the biological activity.

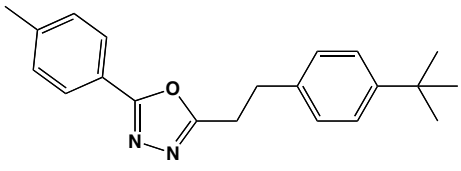

156

EC_{50} = 17 μM
EC_{90} = 21 μM

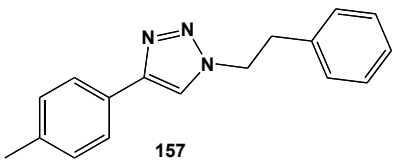

157

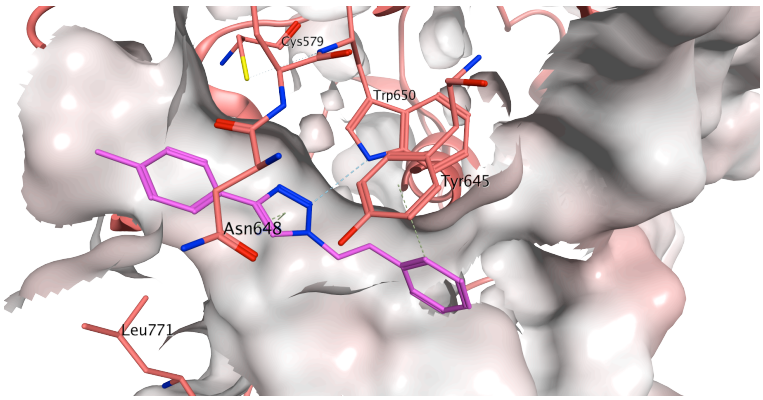

Figure 4.11: Chemical scaffold of triazole-based structures and predicted binding mode of compound **157**. Key interactions with the residues of the binding site were maintained

A three-step synthetic pathway was planned for the preparation of compound **157** (Scheme 4.12), starting with the synthesis of 2-(azidoethyl)benzene **159** that was used for a regiospecific copper(I)-

catalyzed reaction with the formation of the only 1,4-disubstituted 1,2,3-triazole **159**.[63]

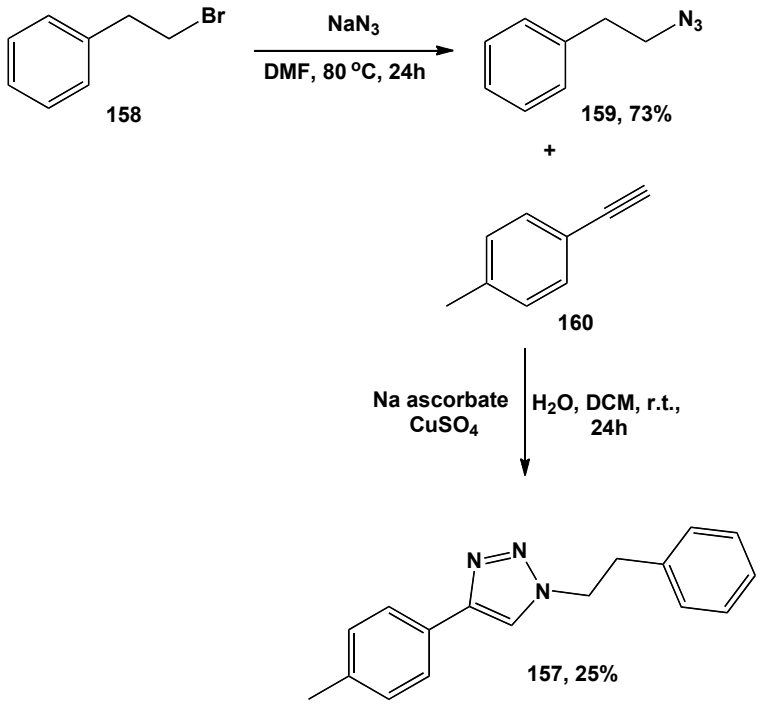

Scheme 4.12: Synthetic pathway applied for the synthesis of compound **157**

Synthesis of 2-(Azidoethyl)benzene (159)

Intermediate **159** was prepared by a nucleophilic displacement of the bromide leaving group by sodium azide.[64] The desired product was obtained with a 73 % yield and was used for the following step without further purification.

Synthesis of 1-phenethyl-4-*p*-tolyl-1*H*-1,2,3-triazole (157)

Final compound **157** was prepared by a variant of the Huisgen 1,3-dipolar cycloaddition, which enables the formation of 1,4-disubstituted 1,2,3-triazole in a regiospecific manner by a copper(I)-catalyzed reaction between a terminal acetylene and an azide. The reaction was performed according to a referred procedure, preparing the catalyst *in situ* by reduction of Cu^{II} salts.[65] $CuSO_4 \cdot 5\ H_2O$ was used as a source of Cu^{II} and sodium ascorbate as the reducing agent. The reaction can be carried out at r.t. and in different solvents with no base or co-solvent needed. The mechanism of reaction was postulated by Vsevolod et al. and it is shown in scheme 4.13. It is believed that the stepwise catalytic process starts with the formation of a

Cu (I) acetylide intermediate and successively with the formation of a six-membered copper-containing intermediate. Protonation then takes place followed by dissociation of the product and regeneration of the catalyst-ligand complex.[66] Final product **157** was obtained pure after recrystallization, in acceptable yield (25 %).

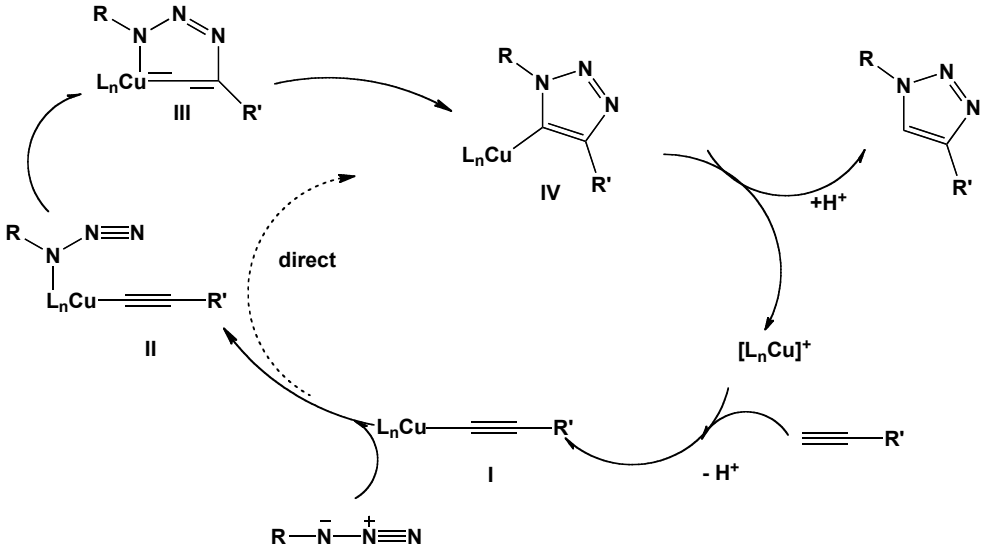

Scheme 4.13: Proposed mechanism of triazole formation

4.6.1 Biological evaluation

1-Phenethyl-4-*p*-tolyl-1*H*-1,2,3-triazole was evaluated for its antiviral activity and cytotoxicity in a virus-cell-based assay (table 4.4).

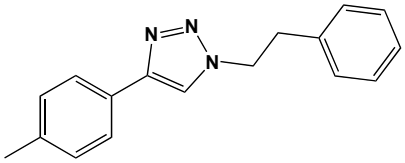

Compound	EC_{50} (µM)	EC_{90} (µM)	CC_{50} (µM)	SI
110 (lead compound)	3.2	11	101	32
157	122	189	200	1.6

Table 4.3: activity and cytotoxicity data for compound **157**

The biological result revealed a loss of antiviral activity for compound **157** compared to the lead compound **110**. It is not possible to infer if the loss of activity is related to the ring introduced or to the absence of the *t*-butyl group. Based on these preliminary data, no additional modifications were planned on this scaffold. Further improvement studies led to the design and preparation of new classes of compounds that will be described below.

4.7 Synthesis of *N*-((*E*)-(4-*tert*-butyl)styryl)-2-(benzylidene)hydrazinecarboxamides

Based on previous results obtained from a series of semicarbazone-based compound (e.g. compound **161**, Figure 4.12), the aim of this series of compounds was to introduce this group on the structure of the lead compound **110**. The rational behind the preparation of compound **161** was to replace the hydrazide group of the lead compound **110** with a new moiety that could decrease the liposolubility (LogP **110**= 5.94; LogP **161**= 4.18). The new derivatives **162-165** would benefit from the presence of the semicarbazone moiety, since it is a more chemically stable functional group. The essential functional groups on the two aromatic moieties, which are the *t*-butyl group on one benzene ring and four groups (3,4-OEt, 4-OH, 4-Me, 4-C_6H_{11}) on the level of the benzene ring, were kept as already known to be the most relevant for the antiviral activity.

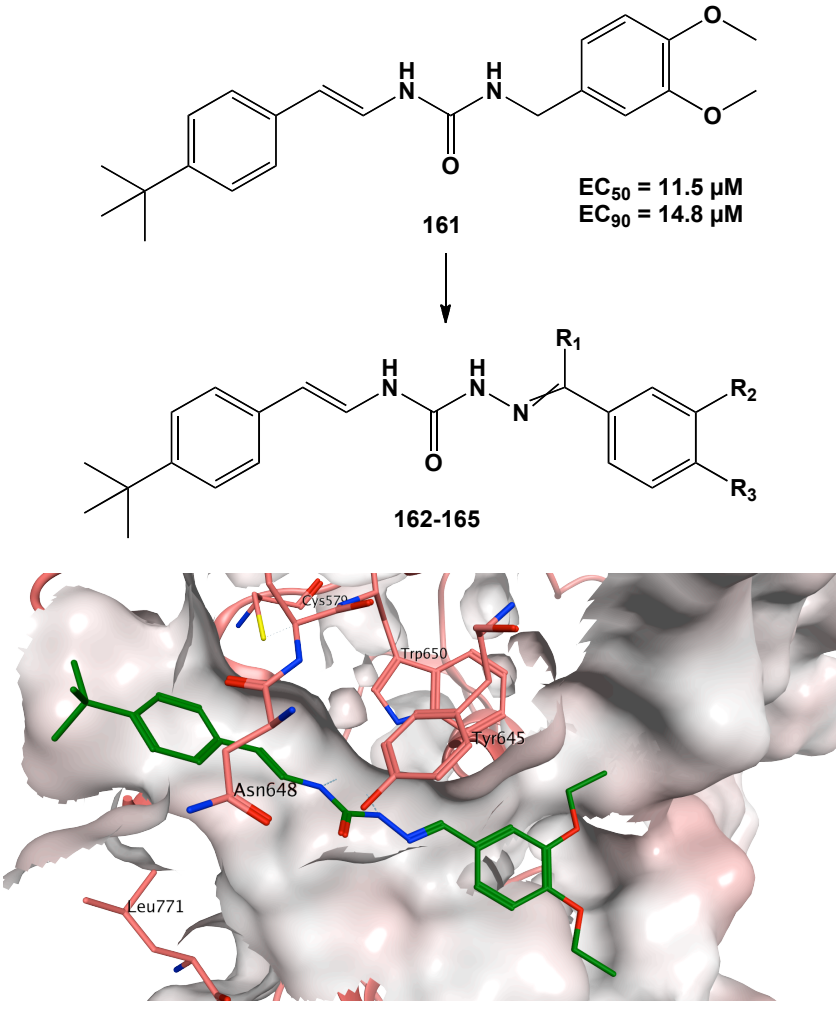

Figure 4.12: Chemical scaffold of semicarbazone derivatives and predicted binding mode for compound **163** as a representative example

4.7.1 *N*-((*E*)-(4-*tert*-Butyl)styryl)-2-(benzylidene)hydrazinecarboxamides

The synthetic pathway followed (Scheme 4.14) consists of three steps, starting from the preparation of (*E*)-3-(4-*tert*-butylphenyl)acrylic acid **153**, according to described procedures,[67] that was used for the synthesis of the correspondent azide **166**. Through Curtis rearrangement, intermediate **166** was converted to (*E*)-1-(*tert*-butyl)-4-(2-isocyanatovinyl)benzene **167**, that was not isolated and used for the condensation with aryl hydrazones **126-128** and **168** to finally obtain the designed compounds **162-165**.

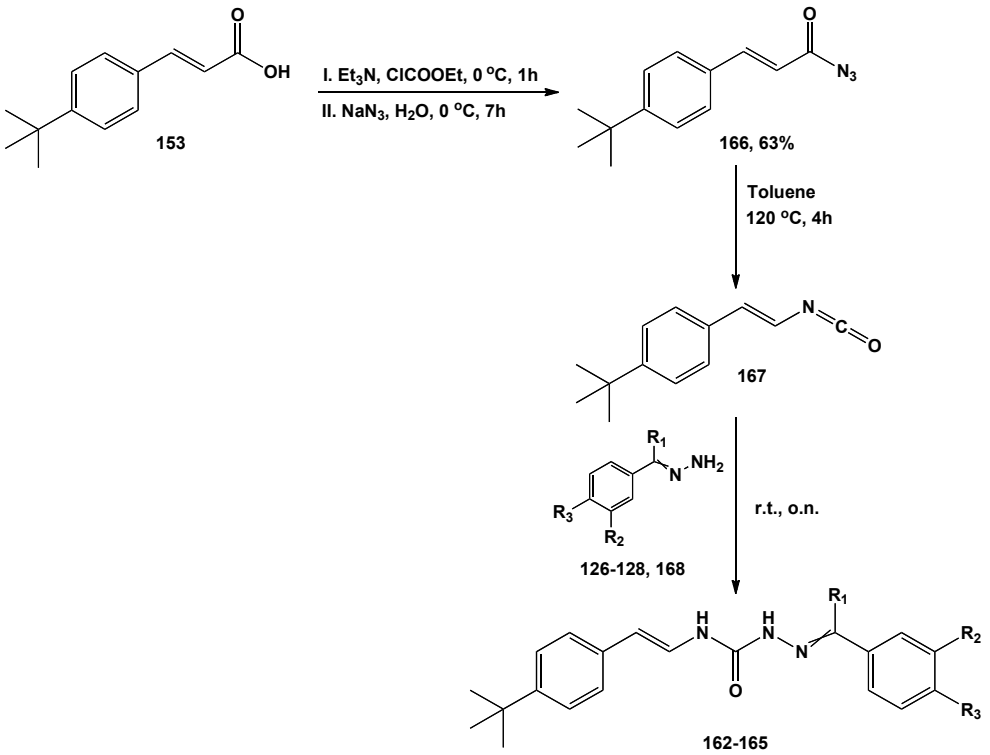

Scheme 4.14: Synthetic pathway applied for the synthesis of compounds **162-165**

Synthesis of (*E*)-3-(4-*tert*-butylphenyl)acryloyl azide (166)

The synthesis of the azide intermediate **166** (Scheme 4.14) was carried out following a reported procedure.[68] (*E*)-3-(4-*tert*-Butylphenyl)acrylic acid **153**, synthesized by Knoevenagel reaction, was converted to the corresponding anhydride (which was not isolated) by reaction with ethyl chloroformate in the presence of a base (triethylamine).[69] The azide ion was then attached to the most electrophilic carbonyl which gave the desired product in a 63 % yield.

Synthesis of 4-(hydrazonomethyl)phenol (168)

Intermediate **168** (Scheme 4.15) was synthesized through the formation of a Schiff base between 4-hydroxybenzaldehyde **169** and hydrazine monohydrate.[70]

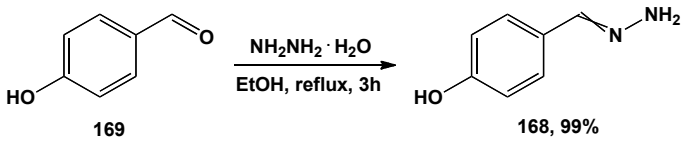

Scheme 4.15: Synthesis of compound **168**

Synthesis of *N*-((*E*)-(4-*tert*-butyl)styryl)-2-(benzylidene)hydrazinecarboxamides (162-165)

Final compounds **162-165** (Scheme 4.16) were prepared by reaction between the isocyanate derivative **167**, formed by the azide intermediate **166**, and aryl hydrazones. The isocyanate derivative **167** was prepared by a Curtius rearrangement that was not isolated. Curtius rearrangement is a concerted two-step reaction. Nitrogen gas is lost with heating, forming an acyl nitrene derivative which is unstable. The second step is a thermal decomposition of acyl nitrene to form the desired isocyanate. Aryl hydrazones **126-128** and **168**, previously prepared by reported procedures, were added to the reaction mixtures to react with the electrophilic carbon of the isocyanate group to give the final products.

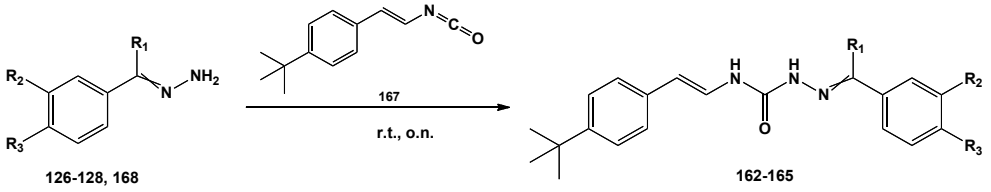

Aryl hydrazones	R_1	R_2	R_3	Product	Yield %
126	H	H	Me	**162**	43
127	H	OEt	OEt	**163**	11
128	Me	H	C_6H_{11}	**164**	29
168	H	H	OH	**165**	40

Scheme 4.16: Final step synthesis for compounds **162-165**

4.7.2 Biological evaluation

Newly synthesized derivatives were evaluated for their antiviral activity and cytotoxicity in a virus-cell-based assay (table 4.4).

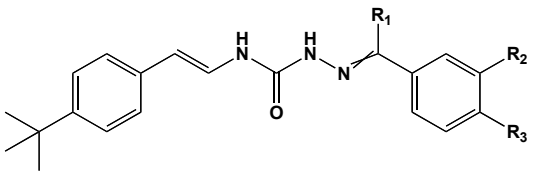

Compound	R_1	R_2	R_3	EC_{50} (µM)	EC_{90} (µM)	CC_{50} (µM)	SI
110 (lead compound)				3.2	11	101	32
162	H	H	Me	246	>298	192	0.8
163	H	OEt	OEt	>100	>100	-	-
164	Me	H	C_6H_{11}	42.3	78.7	123	2.9
165	H	H	OH	5.63	7.48	10.4	1.8

Table 4.4: Biological data for compounds **162-165**

From the biological data, it can be inferred that this modification has not improved the activity of the original compound **110.** From a EC_{50} point of view, **165** has a retained activity but this compound is mainly associated with an adverse effect against cells (low CC_{50}). Compound **164** is linked to a certain activity but at higher concentrations than the lead compound, while the other two derivatives were associated to loss of antiviral activity.

4.8 Synthesis of 2-(benzylidene)-*N*-aryl hydrazinecarbothiamides

Similarly to the semicarbazone derivatives, a second attempt to increase the solubility of the original hit structure was the introduction of a thiosemicarbazone (LogP **170**= 8.41; LogP **172**= 6.21). This modification was also supported by biological results of a previous compound, **170** (data not shown, Scheme 4.13), bearing the thiourea linker that showed antiviral activity at low micromolar concentration, even if it was associated also to cytotoxicity effect (unpublished data).

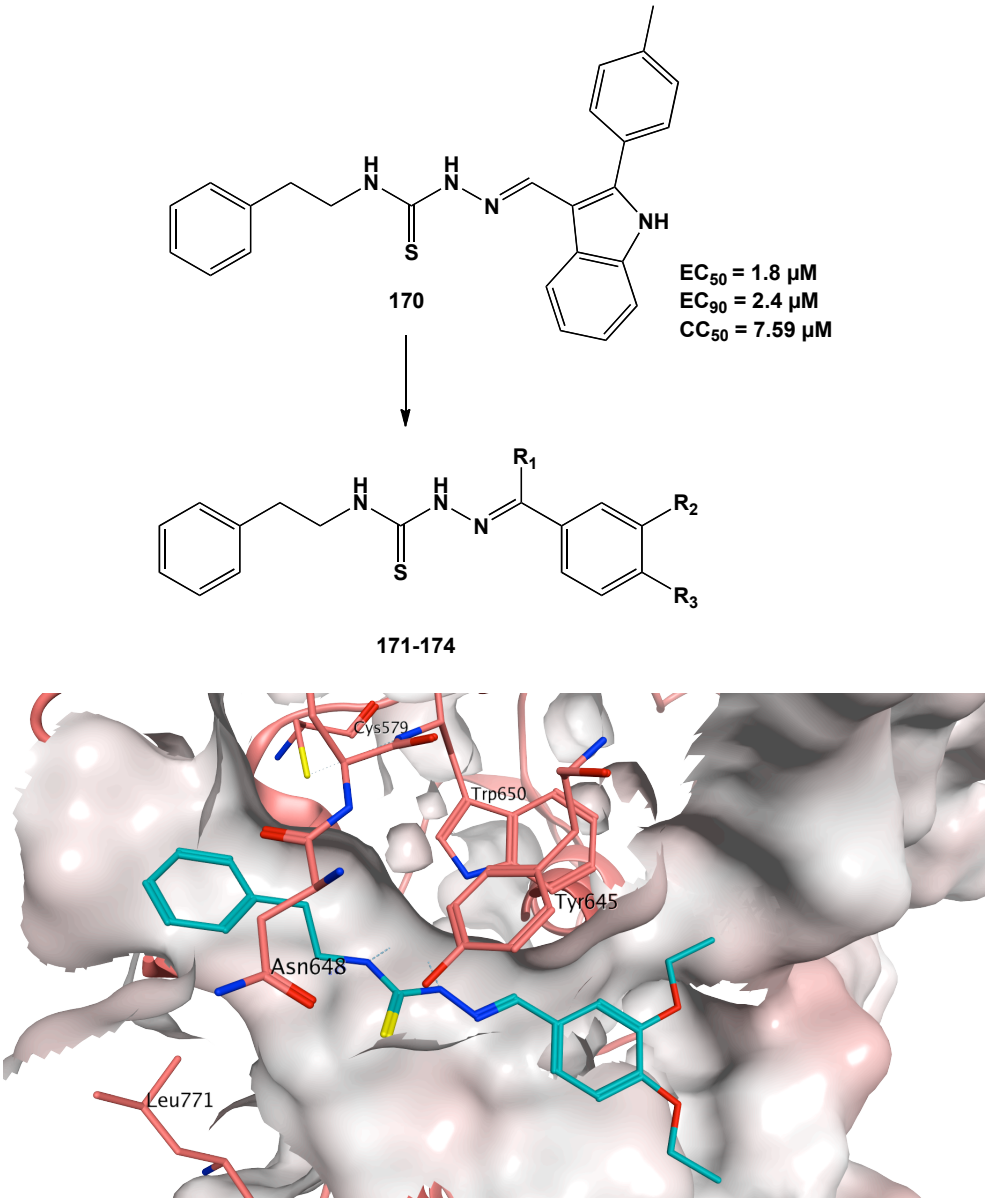

Figure 4.13: Chemical scaffold of the thiosemicarbazone derivatives and predicted binding mode of compound **172** as a representative example. Key interactions are maintained

4.8.1 2-(Benzylidene)-*N*-aryl hydrazinecarbothiamides

The chemical pathway followed (Scheme 4.17) consists of a two step synthesis starting from the formation of (2-isothiocyanatoethyl)benzene, that gives final compounds **171-174** by condensation reaction with aryl hydrazones, previously synthesized according to reported procedures.[71]

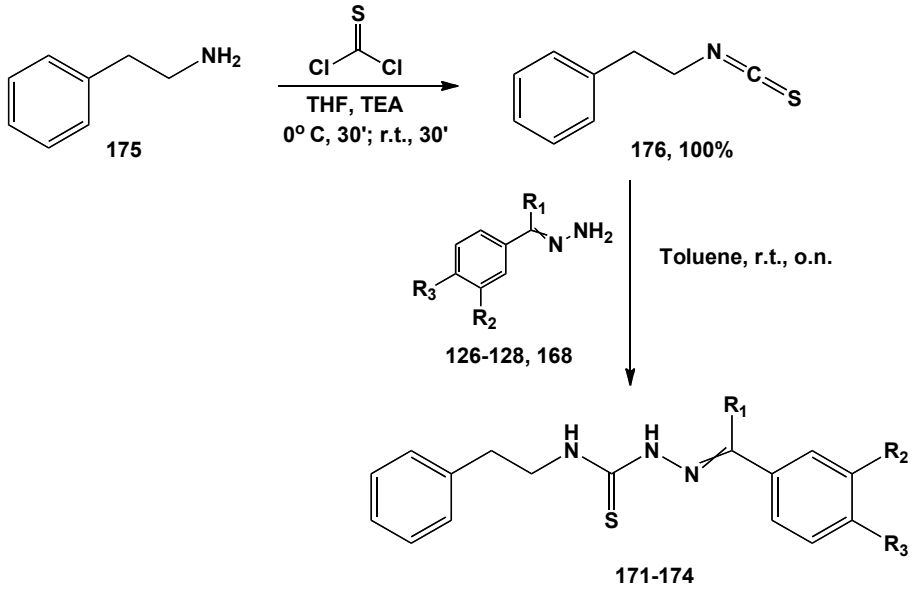

Scheme 4.17: Synthetic pathway applied for the synthesis of compounds **171-174**

Synthesis of (2-isothiocyanatoethyl)benzene (176)

The synthesis of (2-isothiocyanatoethyl)benzene **176** (Scheme 4.17) was realized by nucleophilic attack of 2-phenylethanamine **175** and thiophosgene in THF, in the presence of triethylamine that neutralizes the hydrochloric acid formed.[72] The product was obtained with 100 % yield and was used for the following step without further purification.

2-(Benzylidene)-*N*-aryl hydrazinecarbothiamides (171-174)

Final derivatives **171-174** (Scheme 4.18) were obtained by a condensation reaction between (2-isothiocyanatoethyl)benzene **175** and the substituted hydrazones **118-120** and **168**, using toluene as solvent and stirring the reaction at r.t., o.n.

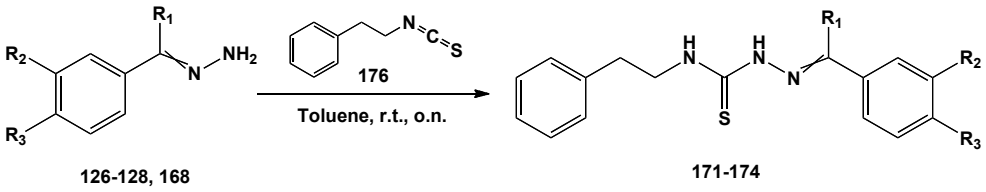

Aryl hydrazone intermediates	R_1	R_2	R_3	Product	Yield %
118	H	H	Me	**171**	15
119	H	OEt	OEt	**172**	10.5
120	Me	H	C_6H_{11}	**173**	10
168	H	H	OH	**174**	16

Scheme 4.18: Final step synthesis for compounds **171-174**

4.8.2 Biological evaluation

Four derivatives were prepared and evaluated for their antiviral activity and cytotoxicity in a virus-cell-based assay (table 4.6).

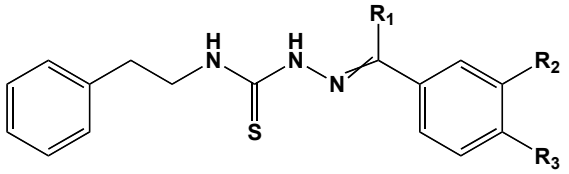

Compound	R_1	R_2	R_3	EC_{50} (µM)	EC_{90} (µM)	CC_{50} (µM)	SI
110 (lead compound)				3.2	11	101	32
171	H	H	Me	>336	>336	-	-
172	H	OEt	OEt	5.91	9.82	109	18
173	Me	H	C_6H_{11}	4.32	5.95	52.9	12.2
174	H	H	OH	48.3	51.8	87.8	1.8

Table 4.5: Antiviral activity and cytotoxicity of compounds **171-174**

Among the new scaffolds, compounds **172** and **173** were associated with a positive antiviral effect against CHIKV replication, with an EC_{50} value that indicated activity retention compared to lead compound **110.** Considering the biological data, it is possible to assume that the antiviral activity is correlated with the presence of a bulky group in *para* position of the aryl hydrazone, as it was already seen for the reference compound **102**. While compound **171** shows to a loss of antiviral activity, compound **174** is associated mainly to a cytotoxic effect.

Conclusions

A structure-activity relationship approach was applied in this study, where several modifications were made on the lead structure **110,** previously identified in our lab. 26 compounds were synthesized and evaluated for their antiviral activity against CHIKV replication.

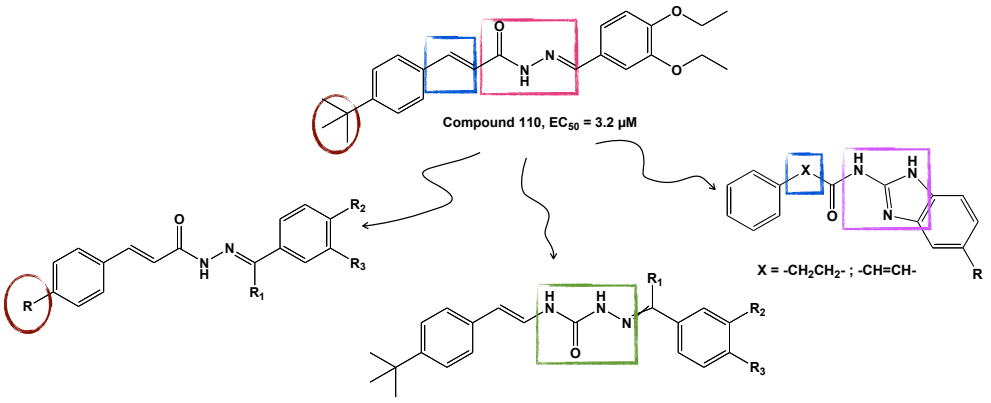

From the biological results, it can be inferred that the removal of *t*-butyl group is detrimental for antiviral activity, since its replacement with bulkier and smaller groups is associated to loss of activity. Many attempts were made to replace the poorly water stable hydrazide group. From the data obtained so far, the introduction of a group that increases the rigidity of the molecule, such as benzimidazole, is linked to loss of activity, while an increased cytotoxic effect was observed for the semicarbazone derivatives that were synthesized not only to contribute to the stability of the structure, but also to increase the solubility in water of the new derivatives.

Two new scaffolds were explored, based on previous compounds showing antiviral activity. While for the triazole derivative **157** no interesting activity profile was observed, two compounds bearing a thiosemicarbazone linker, derivatives **172, 173** were associated to a retained biological activity. This scaffold could be subject of further development to confirm these preliminary data.

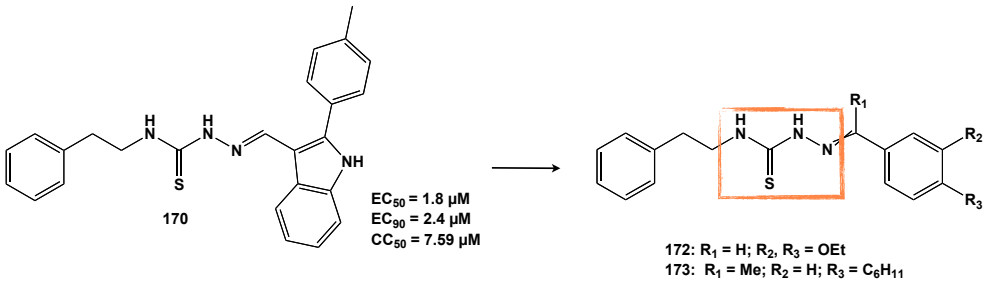

References

1 Suhrbier, A.; Jaffar-Bandjee, M. C.; Gasque, P. Arthritogenic alphaviruses–An overview. *Nat. Rev. Rheumatol.* **2012**, 8, 420–429.

2 Jain, M.; Chakravarti, A. Chikungunya: a review. *Trop. Doct.* **2008**, 38, 70-72.

3 Thiberville, S.D.; Moyen, N.; Dupuis-Maguiraga, L.; Nougairede, A.; Gould, E.A.; Roques, P.; de Lamballerie, X. Chikungunya fever: Epidemiology, clinical syndrome, pathogenesis and therapy. *Antiviral Res.* **2013,** 99, 345–370.

4 Lam, S.K.; Chua, K.B.; Hooi, P.S.; Rahimah, M.A.; Kumari, M.; Tharmaratnam, S.K.; Chuah, D.W.; Smith, I.A.; Sampson, I.A. Chijunguya infection- an emerging disease in Malayisia. Southern Asian J. Trop. Med. Public Health 2001, 32, 447-451.

5 Diallo,M.J.; Thonnon, J.; Traore-Lamizana, M.; Fontenille, D. Vectors of Chikungunya virus in Senegal: current data and transmission cycles. *Am J. Trop. Med. Hyg.* **1999**, 60, 281-86.

6 Reiter, P.; Fontenille, C.; Paupy, C. Aedes Alopictus as an endemic vector of Chikungunya virus: another emerging problem? *Lancet Infect. Dis.* **2006**, 6, 463-464.

7 Lamballerie, X.D.; Leroy, E.; Charrel, R.N.; Tsetsarkin, K.; Higgs, S.; Gould, E.A. Chikungunya virus adapts to tiger mosquito via evolutionary convergence: a sign of things to come? *J. Virol.* **2008**, 5, 1-5.

8 Leparc-Goffart, I.; Nougairede, A.; Cassadou, S.; Prat, C.; de Lamballerie, X. Chikungunya in the Americas. *Lancet* **2014**, 383, 514.

9 Venenzuela reports 94 events of Chikungunya fever. *El Universal*, Caracas, August 5, 2014.

10 Gould, E.A.; Higgs, S. Impact of climate change and other factors on emerging arbovirus diseases. *Trans. R. Soc. Trop. Med. Hyg.* **2009**, 103, 109-121.

11 Weaver, S.C.; Frey, T.K.; Huang, H.V.; Kinney, R.M.; Rice, C.M.; Roehrig, J.T.; Shope, R.E.; Strauss, E.G. Togaviridae. In: *Virus Taxonomy. Eighth Report of the International Committee on Taxonomy of Viruses.* Fauquet, C. M.; Mayo, M. A.; Maniloff, J.; Desselberger, U. Ball, L. A. Eds.; London: Elsevier/Academic Press, 2005; 999–1008.

12 Powers, A.M.; Brault, A.C.; Shirako, Y.; Strauss, E.G.; Kang, W.; Strauss, J.H.; Weaver, S.C. Evolutionary relationships and systematics of the alphaviruses. *J. Virol.* **2001**, 75 (21), 10118–31.

13 Strauss, J.H.; Strauss, E.G. The Alphaviruses: gene expression, replication and evolution. *Microbiol. Mol. Biol. Rev.* **1994**, 58, 621-633.

14 Laakkonen, P., Hyvonen, M., Peranen, J., Kaariainen, L. Expression of Semliki Forest virus nsP1-specific methyltransferase in insect cells and in Escherichia coli. *J. Virol.* **1994**, 68,7418–7425.

15 Ahola T, Lampio A, Auvien P, Kaariainen L. Semliki Forest virus mRNA capping enzyme requires association with anionic membrane phospholipids for activity. *EMBO J.* **1999**, 18, 3164–3172.

16 Rikkonen, M., Peranen, J., Kaariainen, L. ATPase and GTPase activities associated with Semliki Forest virus nonstructural protein nsP2. *J. Virol.* **1994**, 68,5804–5810.

17 Vasiljeva L, Mertis A, Auvinen P, Kaariainen L. Identification of a novel function of the alphavirus capping apparatus. *J. Biol. Chem.* **2000**, 275, 17281–17287.

18 de Cedron, M.G.; Ehsani, N.; Mikkola, M.L.; Garcia, J.A.; Kaariainen, L. RNA helicase activity of Semliki Forest virus replicase protein nsP2. *FEBS Lett.* **1999**, 448, 19–22.

19 Peranen J, Takkinen K, Kalkkinen N, Kaariainen L. Semliki Forest virus-specific nonstructural protein nsP3 is a phosphoprotein. *J. Gen. Virol.* **1988**, 69, 2165–2178.

20 Sawicki DL, Barkhimer DB, Sawicki SG, Rice CM, Schlesinger S. Temperature sensitive shut-off of alphavirus minus strand RNA synthesis maps to a nonstructural protein, nsP4. *Virology* **1990**, 174, 43–52.

21 Choi, H.K.; Lu, G.; Lee, S.; Wengler, G.; Rossmann, M.G. Structure of Semliki Forest virus core protein. *Proteins* **1997**, 27, 345-359.

22 Thomas, S.; Rai, J.; John, L.; Günther, S.; Drosten, C.; Pützer, B.M.; Schaefer, S. Functional dissection of the alphavirus capsid protease: sequence requirements for activity. *J. Virol.* **2010**, 7, 327.

23 Kuhn R.J. Togaviridae: The Viruses and Their Replication. In: *Fields virology*, Knipe DM, Howley PM, Griffin DE, Lamb RA, Martin MA, Roizman B, Straus SE Eds., 5th edition; Lippincott Williams & Wilkins, Philadelphia, PA, 2007; 1001–1022.

24 Asnet, J.M.; Paramasivan, R.; Tyagi, B.K.; Surender, M.; Shenbagarathai, R. Identification of structural motifs in the E2 glycoprotein of Chikungunya involved in virus–host interaction *J. Biomol. Struct. Dyn.* **2013**, 31 (10), 1077-1085.

25 Gaedigk-Nitschko, K. Schlesinger, M. J. The Sindbis virus 6K protein can be detected in virions and is acylated with fatty acids. *Virology* **1990**, 175 (1), 274–281.

26 Spyr, C.; Käsermann, F.; Kempf, C. Identification of the pore forming element of Semliki Forest virus spikes. *FEBS Lett.* **1995**, 375 (1-2), 134–136.

27 Soutisseau, M.; Vanlandingham, D.L.; McGee, C.E.; Higgs, S. A single mutation in chikungunya virus affects vector specificity and epidemic potential. *PLoS Pathog.* **2007**, 3 (12), 1895-1906.

28 Singh, I.; Helenius, A. Role of ribosomes in Semliki Forest virus nucleocapsid uncoating. *J. Virol.* **1992**, 66 (12), 7049-7058.

29 Shirako, Y.; Strauss, J.H. Regulation of Sindbis virus RNA replication: uncleaved P123 and nsP4 function in minus-strand RNA synthesis, whereas cleaved products from P123 are required for efficient plus-strand RNA synthesis. *J. Virol.* **1994**, 68 (3), 1874-1885.

30 Perera, R.; Owen, K.E.; Tellinghuisen, T.L.; Gorbalenya, A.E.; Kuhn, R.J. Alphavirus nucleocapsid protein contains a putative coiled coil alpha-helix important for core assembly. *J. Virol.* **2001**, 75 (1), 1-10.

31 de Lamballerie, X.; Ninove, L.; Charrel, R. N. Antiviral treatment of chikungunya virus infection. *Infect. Disord.: Drug Targets* **2009**, 9, 101–104.

32 Brighton, S. Chloroquine phosphate treatment of chronic Chikungunya arthritis. An open study. *S. Afr. Med. J.* **1984**, 66, 217-218.

33 Briolant, S.; Garin, D.; Scaramozzino, N.; Jouan, A.; Crance, J. M. In vitro inhibition of chikungunya and Semliki Forest viruses replication by antiviral compounds: synergistic effect of interferon- alpha and ribavirin combination. *Antiviral Res.* **2004**, 61, 111–117.

34 Delogu, I.; Pastorino, B.; Baronti, C.; Nougairede, A.; Bonnet, E.; de Lamballerie, X. In vitro antiviral activity of arbidol against chikungunya virus and characteristics of a selected resistant mutant. *Antiviral Res.* **2011**, 90, 99–107.

35 Bourjot, M.;Delang, L.;Nguyen, V.H.;Neyts, J.;Gueitte, F.; Leyssen, P.; Litaudon, M. Prostratin and 12-O-tetradecanoylphorbol 13-acetate are potent and selective inhibitors of chikungunya virus replication. *J. Nat. Prod.* **2012**, 75, 2183–2187.

36 Kaur, P.; Thiruchelvan, M.; Lee, R. C.; Chen, H.; Chen, K. C.; Ng, M. L.; Chu, J. J. Inhibition of chikungunya virus replication by harringtonine, a novel antiviral that suppresses viral protein expression. *Antimicrob. Agents Chemother.* **2013**, 57, 155–167.

37 Bassetto, M.; de Burghgraeve, T.; Delang, L.; Massarotti, A.; Coluccia, A.; Zonta, N.; Gatti, V.; Colombano, G.; Sorba, G.; Silvestri, R.; Tron, G.C.; Neyts, J.; Leyssen, P.; Brancale, A. Computer-aided identification, design and synthesis of a novel series of compounds with selective antiviral activity against chikungunya virus. *Antiviral Res.* **2013**, 98, 12-18.

38 Edelman, R.; Tacket, C.O.; Wasserman, S.S.; Bodison, S.A.; Perry, J.G.; Mangiafico, J.A. Phase II safety and immunogenicity study of live chikungunya virus vaccine TSI-GSD-218. *Am. J. Trop. Med. Hyg.* **2000**, 62 (6), 681-685.

39 Plante, K.; Wang, E. Y.; Partidos, C. D.; Weger, J.; Gorchakov, R.; Tsetsarkin, K.; Borland, E. M.; Powers, A. M.; Seymour, R.; Stinchcomb, D. T.; Osorio, J. E.; Frolov, I.; Weaver, S. C. Novel chikungunya vaccine candidate with an IRES-based attenuation and host range alteration mechanism. *PLoS Pathog.* **2011**, 7, 1-11.

40 Chang, L-J.; Dowd, K.A.; Mendoza, F.H.; Saunders, J.G.; Sitar, S.; Plummer, S.H.; Yamshchikov, G.; Sarwar, U.N.; Hu, Z.; Enama, M.E.; Bailer, R.T.; Koup, R.A.; Schwartz, R.M.; Akahata, W.; Nabel, G.J.; Mascola, J.R.; Pierson, T.C.; Graham, B.S.; Ledgerwood, J.E. Safety and tolerability of chikungunya virus-like particle vaccine in healthy adults: a phase 1 dose-escalation trial. *The Lancet*, in press.

41 Cheung, J.; Franklin, M.; Mancia, F.; Rudolph, M.; Cassidy, M.; Gary, E.; Burshteyn, F.; Love, J. Structure of the Chikungunya virus nsP2 protease. doi: 10.2210/pdb3trk/pdb.

42 Rikkonen, M.; Peränen, J.; Kääriäinen, L. ATPase and GTPase activities associated with Semliki Forest virus nonstructural protein nsP2. *J. Virol.* **1994**, 68, 5804 –5810.

43 Karpe, Y. A.; Aher, P. P.; Lole, K. S. NTPase and 5'-RNA triphosphatase activities of Chikungunya virus nsP2 protein. *PLoS One* **2011**, 6(7), 1-8.

44 Gomez de Cedrón, M.; Ehsani, N.; Mikkola, M. L.; García, J. A.; Kääriäinen, L. RNA helicase activity of Semliki Forest virus replicase protein nsP2. *FEBS Lett.* **1999**, 448, 19 –22.

45 Hardy, W.R.; Strauss, J.H. Processing the nonstructural polyproteins of Sindbis virus: nonstructural proteinase is in the C-terminal half of nsP2 and functions both in cis and in trans. *J. Virol.* **1989**, 63, 4653-4664.

46 Vasiljeva, L.; Valmu, L.; Kääriäinen, L.; Merits, A. Site-specific protease activity of the carboxyl-terminal domain of Semliki Forest virus replicase protein nsP2. *J. Biol. Chem.* **2001**, 276, 30786-30793.

47 Russo, A.T.; Malmstrom, R.D.; White, M.A.; Watowich, S.J. Structural basis for substrate specificity of Alphavirus nsP2 proteases. *J. Mol. Graph. Model.* **2010**, 29 (1), 46-53.

48 Beveridge, A.J. A theoretical study of the active sites of papain and S195C rat trypsin: implications for the low reactivity of mutant serine proteinases, *Protein Sci.* **1996**, 5, 1355–1365.

49 Polgar,L. Mercaptide-imidazoliumion-pair: the reactive nucleophile in papain catalysis, *FEBS Lett.* **1974**, 47, 15–18.

50 Zhang, P.; HU, H-R.; Bian, S-H.; Huang, Z-H.; Chu, Y.; Ye, D-Y. Design, synthesis and biological evaluation of benzothiazepinones (BTZs) as novel non-ATP competitive inhibitors of glycogen synthase kinase-3β (GSK-3β). *Eur. J. Med. Chem.* **2013**, 61, 95-103.

51 Chuang, T-H.; Chen, Y-C.; Someshwar, P. Use of the Curtius rearrangement of acryloyl azides in the synthesis of 3,5-disubstituted pyridines: mechanicistic studies. *J. Org. Chem.* **2010**, 75 (19), 6625-6630.

52 Butler, R.N.; Hanniffy, J.M.; Stephens, J.C.; Burke, L.A. A ceric ammonium nitrate N-dearylation of N-p-anylazoles applied to pyrazole, triazole, tetrazole, and pentazole rings: release of parent azoles. Generation of unstable pentazole, HN%/N%-, in solution. *J.Org. Chem.* **2008**, 73 (4), 1354-1364.

53 Liao, C-T.; Wang, Y-J.; Huang, C-S.; Sheu, H-S.; Lee, G-H.; Lai, C.K. New metallomesogens derived from unsymmetric 1,3,4-thiodiazoles: synthesis, single crystal structure, mesomorphism, and optical properties. *Tetrahedron* **2007**, 63, 12437-12443.

54 Narasimhan, B.; Belsare, D.; Pharande, D.;Mourya, V.; Dhake, A. Esters, amides and substituted derivatives of cinnamic acid: synthesis, antimicrobial activity and QSAR investigations. *Eur. J. Med. Chem.* **2004**, 39(10), 827-834.

55 Sellamuthu, A.; Subban, K.; Chelliah, J.; Partha, S.M. Naphthalene carbohydrazone based dizinc(II) chemosensor for a pyrophosphate ion and its DNA assessment application in polymerase chain reaction products. *Inorg. Chem.* **2013**, 52 (15), 8294-8296.

56 Wadhwani, P.; Afonin, S.; Ieronimo, M.; Buerck, J.; Ulrich, A.S. Optimised protocol for synthesis of cyclic gramicidin S: starting amine acid is key to high yield. *J. Org. Chem.* **2006,** 71, 55-61.

57 Blackwell, H.; Frei, R.; Breitbach, A.; Lynn, D.M.; Broderick, A.H. Inhibition and dispersion of bacterial biofilms with 2-aminobenzimidazole derivatives. Patent WO 20130136782, 30 May, 2013.

58 Rastogi, R.; Sharma, S. 2-Aminobenzimidazoles in organic syntheses. *Synthesis* **1983**, 1983 (11), 861-882.

59 Carpino, L.A.; Henklein, P.; Foxman, B.M.; Abdelmoty, I.; Costisella, B.; Wray, V.; Domke, T.; El-Faham, A.; Mugge, C. The solid state and solution structure of HAPyU. *J. Org. Chem.* **2001,** 66, 5245-5247.

60 Suh, Y-G.; Kim, H-D.; Oh, U.T.; Park, H-G.; Seung, H.S.; Park, S.R.; Kim, J.H.; Nam, Y.H.; Park, Y-H.; Shin, S.S.; Kim, S-Y.; Kim, J.K.; Jeong, Y.S.; Joo, Y.H.; Lee, K-W.; Choi, J.K.; Lim, K.M.; Koh, H.J.; Moh, J.H.; Woo, B.Y. Preparation of thioamides as vanilloid receptor antagonist. Patent WO 2006098554, 21 Sept, 2006.

61 Codd, E.; Dax, S.; Flores, C.; Jetter, M.; Youngman, M. Biaryl derived amides as modulators of vanilloid VR1 receptor and their preparation, pharmaceutical compositions and use in treatment and prevention of diseases. Patent WO 2006102645, 28 Sept, 2006.

62 Knust, H.; Nettekoven, M.; Pinard, E.; Roche, O.; Rogers-Evans, M. Preparation of heteroaromatic monoamides as orexin receptor antagonists. Patent WO 20090312314, 17 Dec, 2009.

63 Vsevolod, V.; R.; Luke, G.G.; Valery, F.; Sharpless, K.B. A stepwise Huisgen cycloaddition process: copper(I)-catalyzed regioselective ''ligation'' of azides and terminal alkynes. *Angew. Chem. Int. Ed.* **2002**, 41 (14), 2596-2599.

64 Diaz, L.; Bujons, J.; Casas, J.; Llebaria, A.; Delgado, A. Click chemistry approach to new N-substituted aminocyclitols as potential pharmacological chaperones for Gaucher disease. *J. Med. Chem.* **2010**, 53 (14), 5248-5255.

65 Creary, X.; Andreson, A.; Brophy, C.; Crowell, F.; Funk, Z. Method for assigning structure of 1,2,3-triazoles. *J. Org. Chem.* **2012**, 77 (19), 8756-8761.

66 Bock, V.D.; Hiemstra, H.; van Maarseveen, J.H. CU^{1}-catalyzed alkyne-azide ''click'' cycloadditions from a mechanicistic and synthetic perspective. *Eur. J. Org. Chem.* **2006,** 51–68.

67 Zhang, P.; HU, H-R.; Bian, S-H.; Huang, Z-H.; Chu, Y.; Ye, D-Y. Design, synthesis and biological evaluation of benzothiazepinones (BTZs) as novel non-ATP competitive inhibitors of glycogen synthase kinase-3β (GSK-3β). Eur. *J. Med. Chem.* **2013**, 61, 95-103.

68 Chai, L-Q.; Chen, W-P.; Wang, X-Q.; Ge, J-L. One-pot synthesis of phenylallyl substituted unsymmetrical ureas under microwave irradiation. *Phosphorus, Sulfur and Silicon and the Related Elements*, **2007**, 182 (11), 2491-2496.

69 Chai, L-Q.; Zhang, H-S.; Liu, G.; Huang, J-J.; Cheng, Q-Q. Synthesis of styryl substituted semicarbazides under microwave irradiation. *J. Chem. Res.* **2013**, 37 (6), 356-358.

70 Butler, R.N.; Hanniffy, J.M.; Stephens, J.C.; Burke, L.A. A ceric ammonium nitrate N-dearylation of N-p-anylazoles applied to pyrazole, triazole, tetrazole, and pentazole rings: release of parent azoles. Generation of unstable pentazole, $HN_5/N5^-$, in solution. *J.Org. Chem.* **2008**, 73 (4), 1354-1364.

71 Hearn, M.; Chen, M.; Cynamon, M.; Wang'Ondu, R.; Webster, E. Preparation and properties of new antitubercular thioureas and thiosemicarbazides . *J. Sulfur Chem.* **2006**, 27 (2), 149-164

72 Poitout, L.; Brault, V.; Sackur, C.; Pierre, R.; Plas, P. Novel derivatives of benzimidazole and imidazo-pyridine as MCR receptors modulators and their preparation, pharmaceutical compositions and use in the treatment of MC4R. Patent WO 20090270372, Jan 21, 2009.

Chapter 5

Respiratory Syncytial Virus

Introduction

5.1 Respiratory Syncytial virus

Respiratory syncytial virus (RSV) is considered as the major cause of lower respiratory tract infections in infants and young children.[1] Worldwide, RSV is responsible for nearly 34 million episodes of acute lower respiratory tract infections yearly and 3.4 million episodes that required hospitalization.[2] The risk of death is not even rare: about 66,000 to 199,000 deaths per year of children younger than 5 years old were estimated to be caused by RSV infection.[1,3] RSV is highly contagious and can infect people multiple times. RSV is transmitted in humans via the nasopharynx and the eyes; it spreads through contact with infected individuals or through coughing and sneezing. Period of incubation is around 3-5 days. RSV can cause a variety of symptoms: mild upper tract illness, like rhinitis, cough, ear infection that can progress to acute otitis, apnoea, but also more severe diseases, like pneumonia and bronchiolitis, that are indication of the virus spreading into the lower respiratory tract. Older adults and children with pathologies like congenital heart disease, lung malformations and neuromuscular disease are at risk for severe infections.[4] The virus replicates in the superficial layer of the respiratory epithelial cells and is shed from the apical surface to get into the lumen of the respiratory tract.[5]

5.1.1 Virion structure

The RSV virus particle has a diameter ranging from 150 to 350 nm that is surrounded by a lipid bilayer envelope. Two proteins are inserted into the envelope, forming spikes on it: the glycoprotein (G), responsible for binding of the virus to receptors on the host cell surface and the fusion (F) glycoprotein that participates in the fusion event between the viral particle and the host cell membrane.[6,7] An additional small hydrophobic (SH) glycoprotein is also made by the virus, for which the function is unknown.

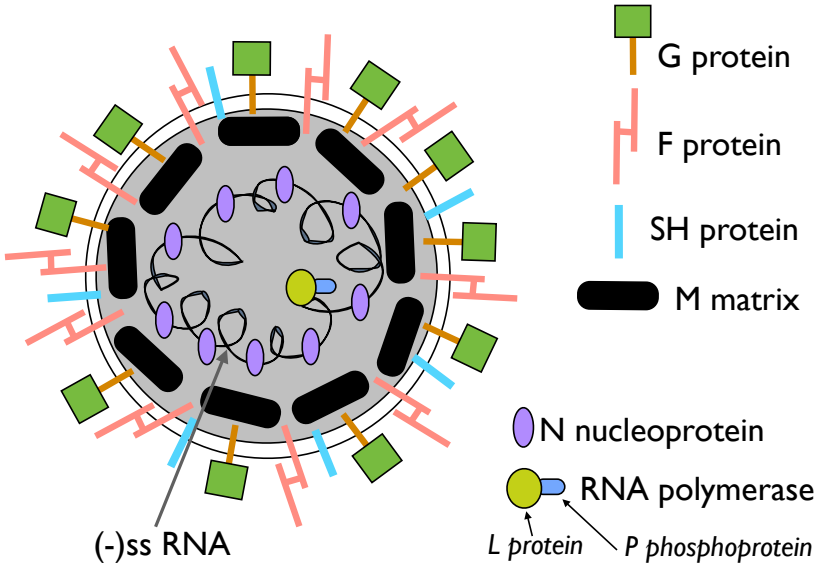

Figure 5.1: Schematic representation of RSV virion structure

5.1.2 Genome organization

RSV is a enveloped, negative, single strand RNA virus that belongs to the *Paramyoxiviridae* family (*Pneumovirinae* subfamily of the *Mononegavirales* order).[8] It is divided in two groups: 10 genotypes are in the subgroup A, while 13 have been designated in group B.[9] Its genome is 5.2 kb and encodes 10 genes that are transcribed into ten separate mRNAs.[10] Two extragenic sites are present at both extremities of the genome: at the 3'-end, a leader region (Le) contains promoter sequences essential for transcription of subgenomic mRNAs and RNA replication of a full-length antigenome intermediate;[11] at the 5'-end, a trailer (Tr) region that contains the promoter that signals the synthesis of genome RNA in the antigenome intermediate.[12]

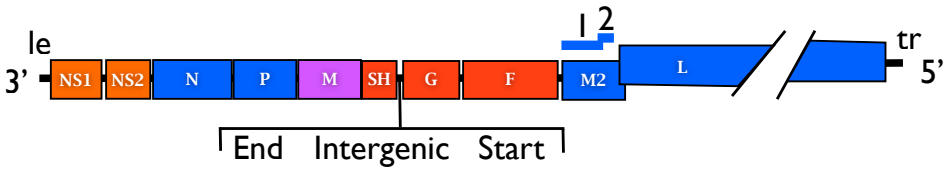

Figure 5.2: Representation of the eleven viral genes, including one example of intergenic sequence, with end (GE) and start (SG) genes

Downstream of the Le region are NS1-NS2-N-P-M-SH-F-G-M2-L genes. Between two sequential genes, there is an intergenic sequence composed of a gene start (GS) and a gene end (GE) sequences that regulates transcription termination, polyadenylation and reinitiation.[13]

5.1.3 Viral proteins

RSV is one of the most complex virus of the *Paramyxoviridae* family with its ten proteins that can be divided into two groups. The first group is made by structural proteins, which are the polymerase L, the nucleoprotein N, the phosphoprotein P, the matrix, the transmembrane proteins G, the F, SH and M2-1 proteins. The second group is characterized by NS1, NS2 which are defined as non-structural proteins, while M2-2 is a regulatory factor. As in most of the RNA viruses, the L polymerase has a crucial role. It takes part in the synthesis of complementary, positive-sense RNA that must occur before the translation of the RNA genome, once the virus has entered into the cell. This event distinguishes the RNA process between positive and negative RNA viruses. Positive RNA genome is infectious itself when introduced to host cells and does not package an RNA polymerase. It can be directly translated into several proteins, including the RNA polymerase that will replicate the viral genome and synthesize mRNAs. Negative RNA viruses are not infectious themselves, they need to be transcribed into positive-sense mRNAs and, for this reason, they require the polymerase which is packaged in the virion. Once it enters the host cell with the genome RNA, it uses cellular ribonucleoside triphosphates for the mRNA synthesis. L polymerase is also responsible for capping, methylation at the 5'-end and polyadenylation at the 3'-end.[14] The nucleoprotein N, encoded in the N gene, is a protein bound to the genome responsible for the formation of the helical nucleocapsid and it is relevant for genome replication and transcription.[15,16,17,18] The phosphoprotein P coordinates binding between L and N proteins[19] and affects the functionality of M2-1 protein by interacting with it.[20] Furthermore, it participates in the assembly of the N protein on RNA chains for the formation of nucleocapsid.[21] While M2-1 protein is an antitermination trasnscription factor,[22] for which a detailed description will be provided, M2-2 protein is responsible for switching the RNA transcription step to the RNA replication.[23] Three glycoproteins form the envelope of the virion: protein G, a type II transmembrane glycoprotein, responsible for the virus attachment, the fusion F protein, which mediates the viral entry by a mechanism of fusion between the virion and the host cell membrane and, finally, the small SH

glycoprotein that increases the function of G and F proteins.[24,25,26] G, F and SH proteins, all together, form the typical spikes of RSV virions. Finally, the matrix M protein, which is on the inner surface of the viral envelope, seems responsible for virus assembly and budding,[27] but also inhibits the host-cell transcription.[28] Non-structural proteins NS1 and NS2 are multifunctional accessory proteins. It has been suggested that they could have a role in the RNA synthesis, but they also seem to interfere with the induction of interferon (IFN) transcription.[29,30]

5.1.4 Viral life cycle

The life cycle of RSV starts, as in most of the cases, with the recognition of cellular receptors that allows the attachment of the viral particle. Upon binding to the receptor mediated by the G protein, F protein is activated and the fusion process between the envelope and the host cell membrane occurs. The viral nucleocapsid then enters the cell and transcription is activated. This event, that leads to the synthesis of 10 subgenomic mRNAs, occurs by a sequential mechanism named 'stop and re-start process': when RdRP locates a gene start (GS), it starts synthesizing mRNA; when it comes across to a gene end (GE), it polyadenylates and releases the new mRNA.[31,32,33] The transcription is then (re)initiated when RdRP scans the template and finds a new GS signal. On the contrary, when the polymerase replicates the full genome, GS and GE are ignored and a full length positive sense, the antigenome, is produced.[34] Eventually, newly nucleocapsids migrate from the cytoplasm to the plasma membrane and will interact with the M protein. Viral particles are then assembled and released from the infected cells by budding from the plasma membrane.[35]

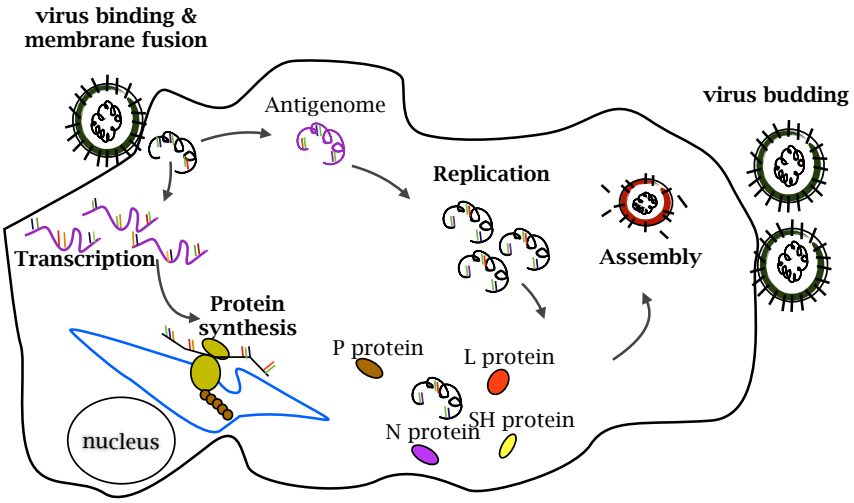

Figure 5.3: RSV life cycle

5.1.5 Current treatment

There is no specific cure for treating viral RSV infection at the moment, although RSV is considered one of the most common pathogens among children worldwide.[36] Current treatment is mainly supportive and is focused on curing symptoms and avoiding complications.[37,38] The major actions consist in providing adequate oxygenation, hydration and ventilation, mechanical and through the use of broncodilators. Corticosteroids, nebulized agents, like albuterol and epinephrine are commonly used.[39] Prevention is limited to a humanized monoclonal antibody, Palizumab (Synagis®) that is used only in pediatric patients with risk for developing acute lower respiratory infection (ALRI) due to the high cost of the product.[40,41] The only available drug approved in 1986 from FDA for the treatment of RSV is ribavirin (Virazole®) that can be used intravenously, orally and as aerosol.[42] However, for safety and economical reasons, its clinical use is limited to people at high risk for developing complication.[43]

5.1.6 New treatments under development

At the moment, there are several compounds in clinical trials for the treatment of RSV infection. Two drugs targeting the nucleocapsid N protein are currently in Phase II clinical trials: ALN-RSV01,[44] a siRNA that could represent a new class of agents to treat human disease and the small molecule RSV-604 (Figure 5.4).[45] Many efforts have been spent on the development of molecules targeting F protein. No clinical studies have been reported for BMS433771, a promising molecule discovered by Bristol-Meyer Squibb.[46] In other cases, the clinical development has been stopped, as was for BTA9881 produced by Biota Holdings Ltd. Only two molecules under clinical development are reported: MDT-637, developed by MicroDose Therapeutic, is currently in phase I[47] and GS-5806 in Phase 2.[48] Among entry inhibitors, MBX-300, a sulphated sialyl lipid, has been developed as an attachment inhibitor active against G protein. This agent has been evaluated in preclinical studies, but no further studies have been recently announced. Finally, nucleoside analogues were developed by Chimerix and are currently under preclinical studies.

Therapeutic description	Company/Istitution	Development stage
ALN-RSV01	Alnylam/Kyowa	Phase II
ALN-RSV second generation	Alnylam/Kyowa/cubist	Phase II
RSV-604	Arrow Therapeutics/ Novartis	Phase II
GS-5806	Gilead Sciences	Phase II
MDT-637(VP-14637)	MicroDose Therapeutix	Phase I
MBX-300	Microbiotix	Preclinical
Small-molecule nucleoside analogues	Chimerix	Preclinical

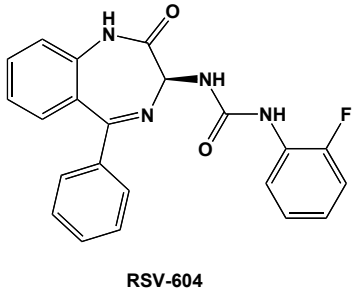

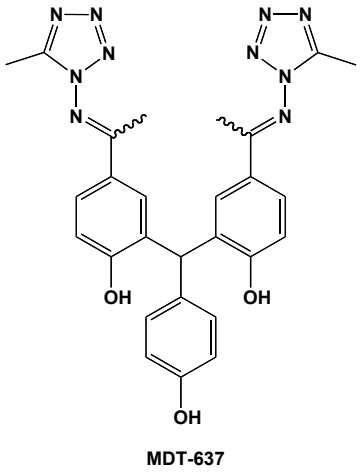

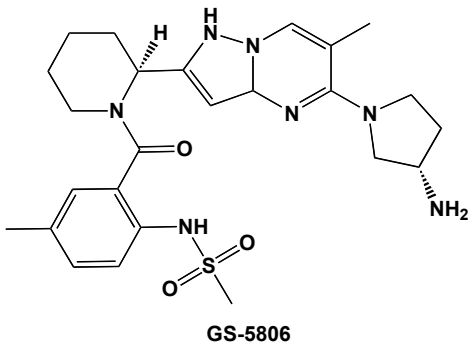

Figure 5.4: Overview of the RSV therapeutic agents currently in clinical evaluation and chemical structures of RSV-604, MDT-637 and GS-5806

5.1.7 Vaccines under development

Despite the socio-economical impact of RSV infections, no vaccine is available so far. Several strategies have been made in the past and are currently under studies.[49] Figure 5.5 shows an overview of vaccines that are now in clinical evaluation.

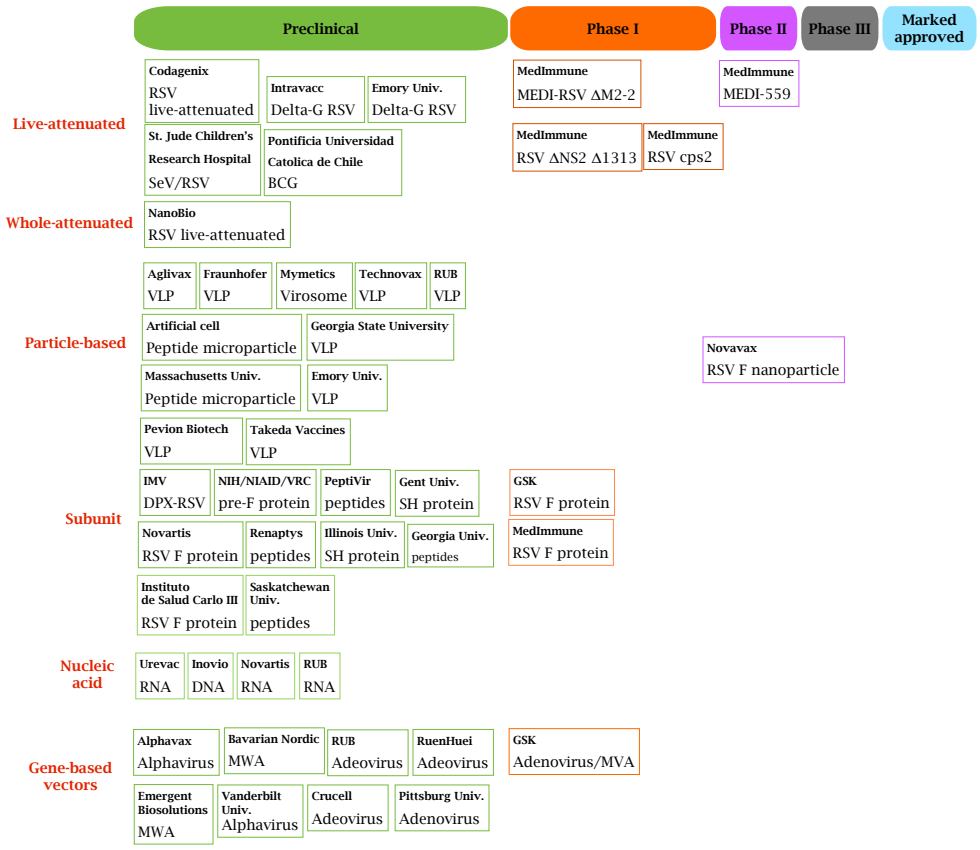

Figure 5.5: Overview of vaccines currently under clinical evaluation[50]

5.2 M2-1 Protein

The HRSV M2-1 protein is an essential transcription antitermination cofactor of the viral RNA-dependent RNA polymerase (RdRP) complex that increases the polymerase function. It is important for the synthesis of full-length mRNAs but also enhances the synthesis of polycistronic mRNAs.[51,52,53] More specifically, the functional activity of this protein is to prevent the termination of the transcription event, which has been already described. Furthermore, M2-1 protein is important for HRSV replication, but the role is still unknown. All these important functions makes the M2-1 protein a good target for the design of antiviral compounds.[54]

5.2.1 Structure

The crystal structure of the M2-1 protein has been recently released (PDB ID: 4C3B).[54] M2-1 has been classified as a RNA binding protein that is associated to the viral genome, together with three other proteins (the nucleoprotein N, the phosphoprotein P and the polymerase subunit L). These four proteins form the holonucleocapsid.[55] M2-1 protein is formed by 194 amino acid and it assumes a tetrameric structure in solution (figure 5.6).[56]

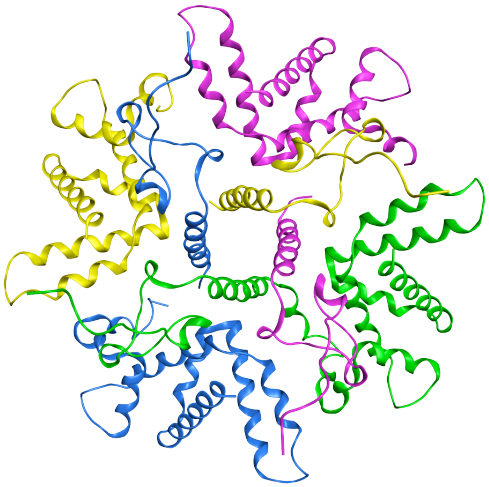

Figure 5.6: Ribbon model of HRSV M2-1 tetramer. Each monomer has a different color

Previous studies have predicted four functionally important domains of the M2-1 protein: an N-terminal zinc-binding domain (ZBD, residues 7-25), with a Cys_3-His_1 motif that is thought to be involved in RNA binding; an

oligomerization domain (residues 33-45); a central part, or core domain (residues 53-177), that is related to RNA and phosphoprotein P binding and, finally, a C-terminal tail which is less structured.[57,58,59] The only stable form of this protein is the tetramer: each monomer has extensive contact regions with other protomers. The structure of the core domain reveals a 4-helix bundle at its center (α1, α2, α5, α6) and an hairpin (α3-α4).[54] Extensive interactions have been identified between the ZBD and the N-terminal face of the core of the neighboring monomer, which confirms the importance of the zinc motif for the tetramer integrity. In addition, it is possible that ZBD is involved in RNA binding due to its close proximity to the RNA binding surface.

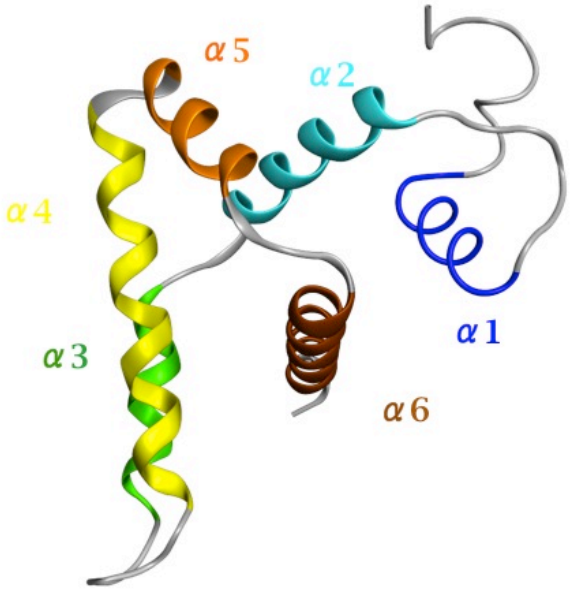

Figure 5.7: Cartoon representation of the α helical core domain of M2-1 protein

RNA binding site

A vast positively charged surface is present in the M2-1 protein that would facilitate electrostatic interactions with the negatively charged RNA and P protein. Several studies[54,57] led to the identification of the M2-1 residues involved in RNA binding: Ser58 and 61, Lys92 and 150, Arg151 and Lys159, which are within the core, but also Arg3 and 4 that are on the N-terminal region. Ser58 and 61 are critical for the protein activity: they are phosphorylated during infection, which reflects a reduced RNA binding ability, thus affecting the antitermination function of the protein.

Moreover, those residues outside and within the core are believed to be essential for RNA binding and, as a consequence, for protein function.

P binding site

A second surface of the M2-1 protein critical for its function is the binding site of the phosphoprotein P. It is suggested that this protein binds to residues of the helices α4, α5, α6. The P region is proximal and partially overlaps with the RNA binding site. By mutagenesis studies, the residues involved in P binding were also confirmed: mutants of Arg126, Thr130, Lys148, Thr160 and Asn163 did not bind P *in vitro* and were related to an M2-1 transcription impairment. A final conclusion can be arisen: binding of both RNA and P is essential for M2-1 transcription antitermination.

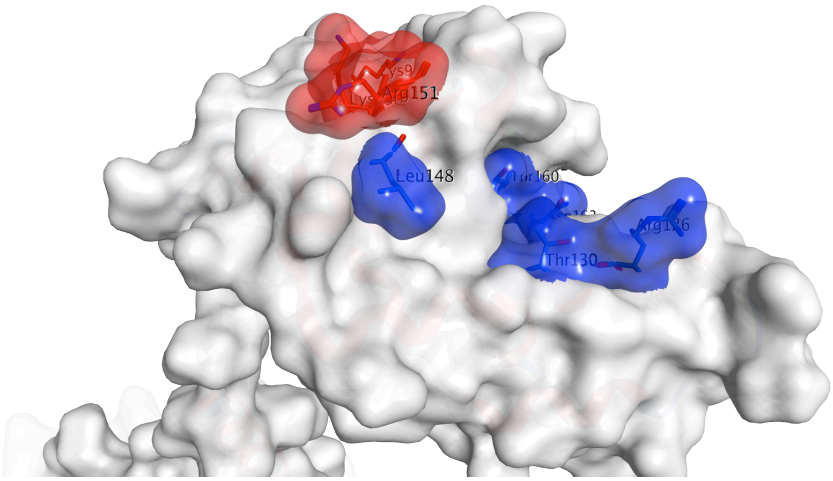

Figure 5.8: Surface representation formed by 8 residues and colored according to the region of the M2-1 they belong: red for the RNA binding and blu for P binding

5.2.2 Mechanism of action

The mechanism of action of M2-1 is still not completely clear, but different hypotheses were postulated. A first scenario could be an increased affinity of the polymerase for the genomic RNA template, while a second hypothesis suggests that the M2-1 protein binds the nascent mRNA transcript and enables the transcription elongation by preventing the mRNA to form certain secondary structures that could make the transcription complex less stable.[7]

5.3 Fusion protein

The process of RSV infection consists in the attachment and fusion of the viral particle to the target cell membrane through envelope glycoproteins. The G protein, in particular, is responsible for the binding to receptors present on the surface of the host cells, while the fusion protein enables the viral genome to enter into the cell through fusion of the viral membrane with the target cell membrane.[60,61,62] Due to its essential role for viral entry, the F protein is an attractive target for drug and vaccine development.

5.3.1 Structure

The fusion protein is a type I transmembrane surface protein[63] and it is synthesised as an inactive precursor, F0,[64] that is activated by proteolytic cleavage to yield two subunits linked by a disulfide bridge: F1 and F2.[65,33] The fusion peptide region, located at the N terminus of the F1 subunit, inserts into the target cellular membrane during the fusion process.[66] The transmembrane region is close to the C terminus of the F1 subunit. Between these two segments, there are two regions containing heptad repeats (HR1 and HR2).[67] A dramatic conformational change in the structure of the F protein occurs when the fusion process is triggered. A pre-hairpin intermediate is formed, in which the fusion peptide region is inserted in the target cell membrane. This intermediate, then, undergoes to a refolding that leads to a highly stable post-fusion structure characterized by a six-helix bundle (6HB) containing heptad repeats HR1 and HR2.[68] The fusion pore finally opens and leads the viral genome to enter the target cell (figure 5.9).

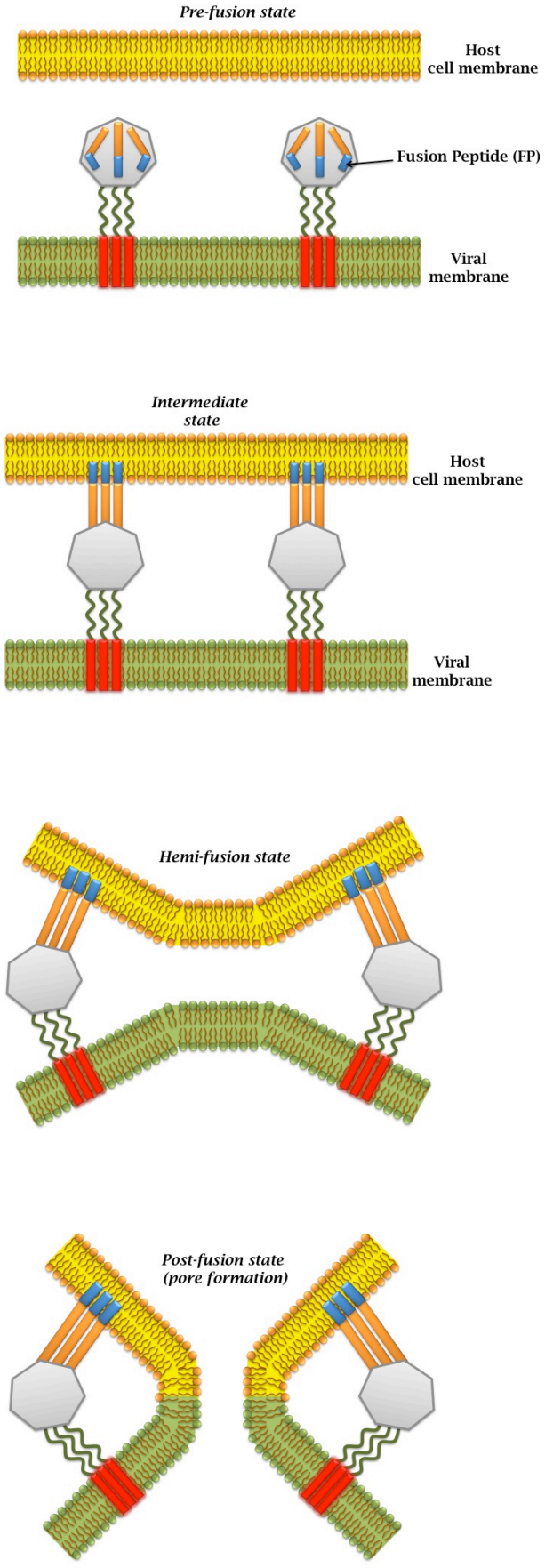

Figure 5.9: Mechanism of viral and cell membrane fusion mediated by F protein

5.3.2 RSV entry inhibitors targeting F protein

The literature describes several small molecules that inhibit the RSV entry by targeting the F protein. To our knowledge, there are currently only two drugs in clinical trials: MDT-637 in Phase I[69] and GS-5806 in Phase 2.[49] Several of these inhibitors (BMS-433771, RFI-641, VP-14637, and BTA-9881) have been stopped at preclinical or Phase 1-2 studies, because of their lack of appropriate pharmaceutical properties. For most of them, the region targeted was a hydrophobic pocket formed by the trimeric coiled-coil. JNJ identified one compound, JNJ-2408068, with an extremely potent anti-RSV activity (EC_{50} = 0.16 nM).[70] Further optimization studies, aiming to improve the low elimination in tissue observed for JNJ-2408068, led to the identification of a very promising drug candidate, TMC-353121 (Figure 5.10), that is under preclinical studies for further development.[71]

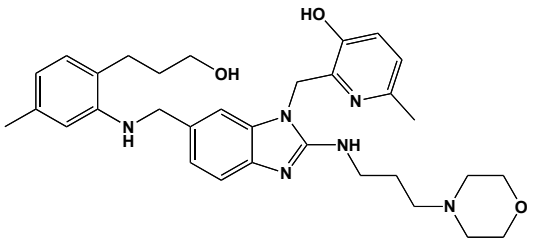

Figure 5.10: Chemical structure of TMC-353121

This compound has been found to bind to the 6-HB and to interact with both the HR1 and HR2 domains.[72] In 2010, the crystal structure of TMC-353121 with a 6HB construct was resolved (PDB ID: 3KPE) in order to understand the binding mode of the compound. It was suggested that the binding of the ligand induces the formation of a distorted 6HB, with the most conformational change involving a partial unwinding of the α-helical backbone of HR2. The rotameric state of three residues (Asp486, Asp200 and Glu487), in particular, was altered by this conformational change in order to have better interactions with the ligand. The crystal structure shows a network of hydrophobic and electrostatic interactions. The molecule nicely anchors the protein through the hydroxypyridine group that is involved in several interactions with HR1, like a hydrogen bond with the carboxylate group of Asp200 and stacking interactions with Tyr198. The ligand interacts also with residues of HR2, e.g. a hydrogen bond with Asp486 and the amino substituent group of the benzimidazole. Additional hydrogen bonds mediated by a molecule of water are established between

Glu487, the hydroxyl group in the hydroxypropyl chain and the hydroxypyridine. A mechanism of action has been hypothesized from the ligand binding mode. Although the compound bound to the protein disrupts the essential interactions between the two heptad-repeats, TMC-353121 increases the stability of the 6HB. However, it could prevent the formation of the appropriate protein conformation for the fusion step.

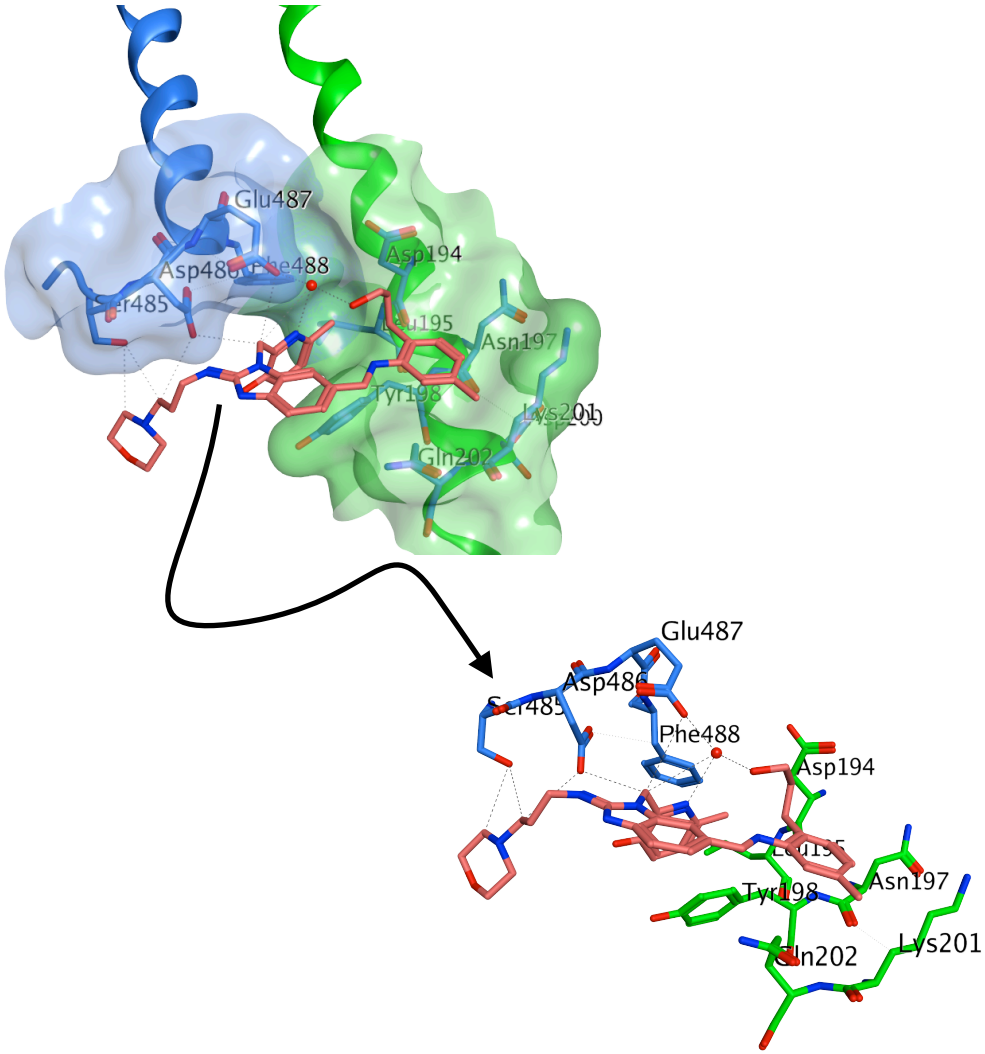

Figure 5.11: Binding mode and close-up interactions of TMC-353121

Results and discussion

5.4 M2-1 protein as a target for drug design of new antivirals

The current research to combat RSV infection is mainly concentrated to develop a safe vaccine for infants, but identifying antiviral compounds that would target specific viral functions, such as the RdRP complex, may represent a promising approach. M2-1 protein is an interesting target for the design of small molecules.[4] In this study, two areas were studied: the zinc binding domain that was evaluated to design and synthesise potential zinc-ejecting compounds, and the surfaces where RNA and P bind, which are critical for the M2-1 function.

5.4.1 Zinc-binding domain of M2-1 protein as a target for *de novo* design

As already described, the zinc binding domain (ZBD) is one of the essential regions of the M2-1 protein. The zinc finger motif is specifically in the N-terminus of the protein and interacts with a proximal protomer, thus increasing the stability of the tetramer. There are evidences that the integrity of this motif represents a key element for maintaining the functionality of M2-1 protein.[60] The sequence of the zinc finger motif (C-X_7-C-X_5-C-X_3-H), which has the Zn^{2+} ion coordinated by three cysteine residues and one histidine, is slightly different if compared to other ZBDs, but resembles the one revealed for the human transcription factor Nup475.

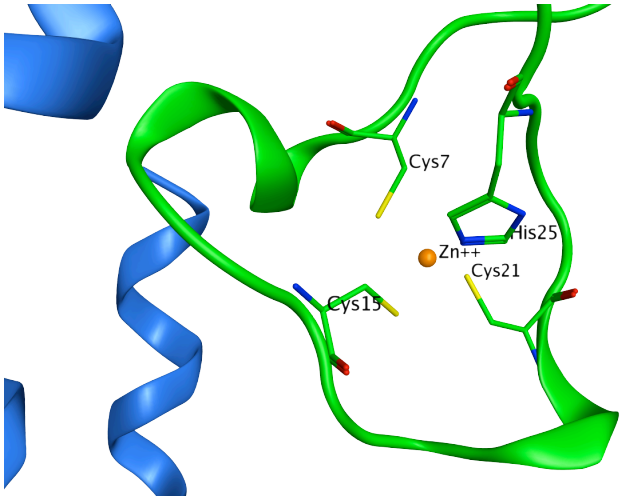

Figure 5.12: Close up of zinc binding domain. Cys_3-His_1 coordinated zinc atoms are shown in green with the N-terminal face of the core of an adjacent monomer represented in blue (PDB ID: 43CB).

Based on a study that described the ability of 2,2'-dithiodipyridine (aldrithiol, AT-2),[73] a known zinc finger reactive compound, to inhibit RSV infectivity due to modifications of the ZBD of M2-1 protein, the aim of this study was to design potential inhibitors of RSV infection that, like AT-2, would act by modifying the zinc finger motif.

Zinc-ejecting compounds

Zinc ejection has been already described in the literature as a method of enzyme inhibition.[74] A successful example of metal chelation by zinc-ejecting compounds is represented by the effect of azodicarbonamides on the HIV nucleocapsid (NCp7) that selectively eject zinc ions.[75,76,77,78,79] One of these NCp7 zinc-ejecting compounds is currently in phase I/II clinical trials against advanced acquired immunodeficiency disease syndrome (AIDS).[80] On the basis of these promising results, the aim of this study was to design new scaffolds containing zinc-chelating moieties to interact with the zinc ion on the M2-1, thus affecting the functionality of the protein.

5.4.2 *De novo* drug design

A computer-aided approach guided the design of a series of zinc-reactive compounds. The ZBD of M2-1 protein is a very tight binding pocket, defined by three cysteine residues and a histidine that have a simple geometry and form a planar ring that surrounds the Zn ion. Due to the delimited region, our approach was to use a library of small fragments that could guide the design of molecules containing a zinc-ejecting group. To do so, a library of 1,611,889 'clean' fragments from the commercially available ZINC database compounds was downloaded.[81] 'Clean' fragments defines a subset of small ligands for which filtering rules were applied, e.g. aldehyes and thiols are removed, logP is less or equal to 3.5, molecular weight less than 250 and rotatable bonds equal or less than 5. The input database was further filtered by molecular weight in order to have a feasible number of small molecules to analyze: only those fragments with a molecular weight less than 150 were taken into account for docking studies. A total of 12,420 ligands was then docked to the binding site, defined by the zinc ion that is encircled by Cys7, Phe9, Glu10, Cys15, Asn17, Cys21, Phe23 and His25 residues. Since the purpose of this analysis is to explore the chemical space and evaluate which fragments could be able to interact with the residues selected, it was not necessary to use

accurate scoring functions, therefore the docking study was performed with MOE. Three sites were specifically targeted: the one in close proximity to Cys_3-His_1 motif and two areas that surrounds the zinc finger.

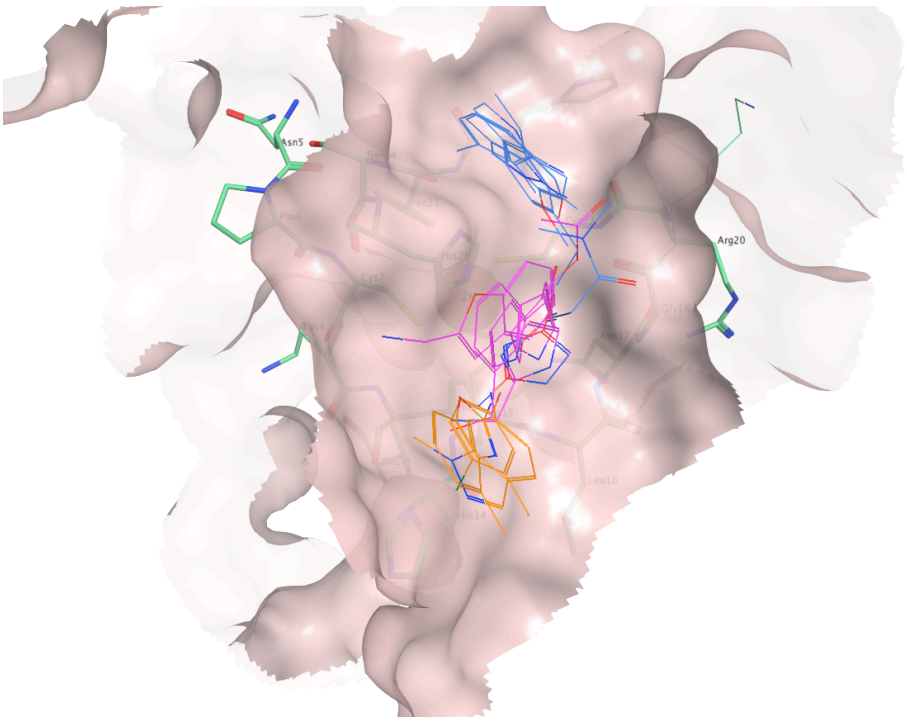

Figure 5.13: Representation of several fragments docked in the zinc binding site. Fragments are differently colored according to the targeted area

According to docking results and the availability of accessible reagents, 7 fragments were selected for the design and synthesis of a new series of compounds.

5.5. Synthesis of aryl dithiocarbamates

Figure 4.14 shows the chemical scaffold of the new derivatives bearing a dithiocarbamate moiety, which is known to have metal ejecting properties.[82]

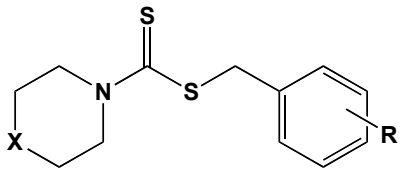

Figure 5.14: chemical scaffolds of designed compounds

According to the results obtained from docking studies, a family of aryl-dithiocarbamates was synthesised by reaction of an heterocyclic amine with aryl chloride or bromide, as shown in sheme 5.1, where the common synthetic pathway applied is reported. Piperazine, N-methyl piperazine, benzyl piperazine, morpholine and piperidine were selected among the secondary amines validated *in silico*, while a set of aryl substituents was selected in order to occupy the space in the pocket and increase the ligand binding.

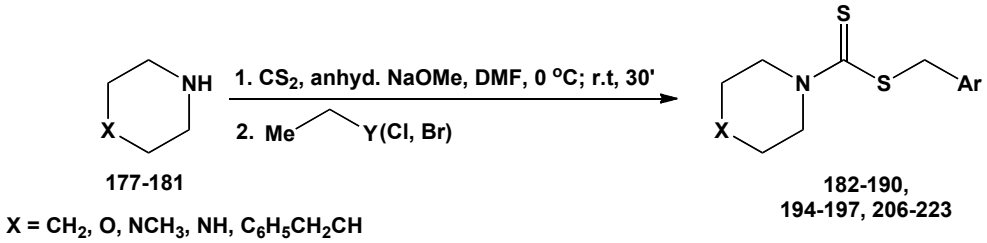

Scheme 5.1: Common synthetic pathway for the synthesis of aryl dithiocarbamates **182-190, 194-197, 206-223**

5.5.1 2-Chloromethyl benzimidazole carbodithioates (182-186)

In this first series of compounds, a benzimidazole moiety was selected in order to synthesise final dithiocarbamates **182-186** (Scheme 5.2), according to a reported procedure.[83]

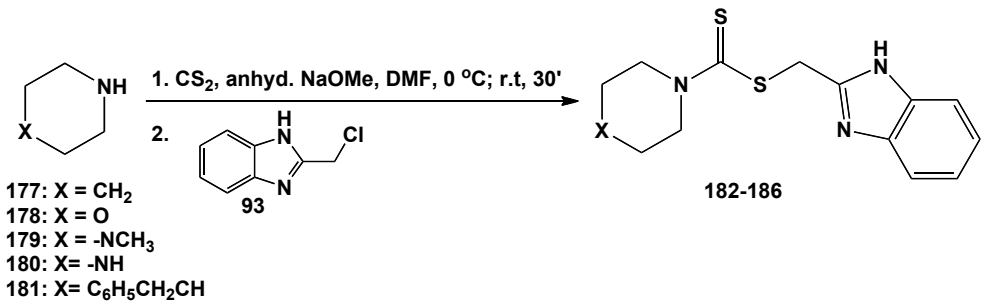

Scheme 5.2: Synthesis of compounds **182-186**

Synthesis of benzyl piperazine (181)

Intermediate **181** (Scheme 5.3) was obtained by adding benzyl bromide to an excess of piperazine **180**, according to a referred procedure,[84] in order to achieve a single nucleophilic displacement on the chloride leaving group. The desired compound was obtained in high yield (89%) and was used for the next step without further purification.

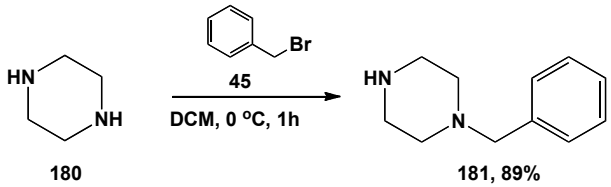

Scheme 5.3: Synthesis of compound **181**

Synthesis of 2-chloromethyl benzimidazole carbodithioates (182-186)

Final compounds **182-186** were prepared in a one-pot reaction according to a general procedure for which an equimolar ratio of the appropriate alicyclic secondary amine (**177-181**) and carbon disulfide were stirred at 0 °C for 30', in the presence of sodium methoxide, in order to get the formation of the dithiocarbamate salt. 2-Chloromethyl benzimidazole **93** was successively added in order to get final compounds **182-186** (TLC analysis) through displacement of the chloride leaving group by the dithiocarbamate salt (scheme 5.4). The reaction conditions were adjusted for the synthesis of the derivative bearing a piperazine group: 0.5 equivalents of carbon disulfide was added to piperazine **180** in order to prevent a double nucleophilic attachment on the two free amino groups.

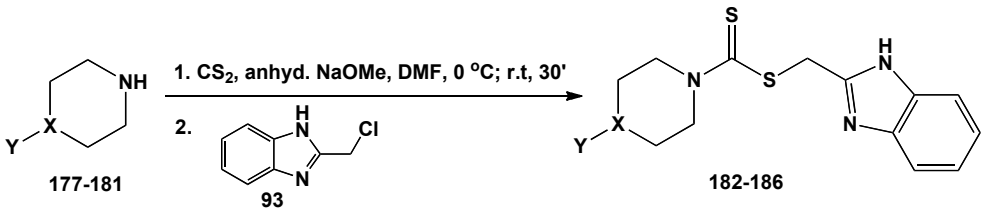

Starting alicyclic secondary amine	X	Y	Product	Yield %
177	CH_2	-	**182**	12.3
178	O	-	**183**	10.2
179	NCH_3	-	**184**	11
180	NH	-	**185**	10.3
181	CH	$C_6H_5CH_2$	**186**	17

Scheme 5.4: Pathway for the synthesis of compounds **182-186**

5.5.2 2-Chloromethyl benzoxazole carbodithioates (187-190)

A second series of dithiocarbamates, **187-190**, was synthesised following the general procedure described above and using this time 2-bromomethyl benzoxazole **193** (Scheme 5.5).

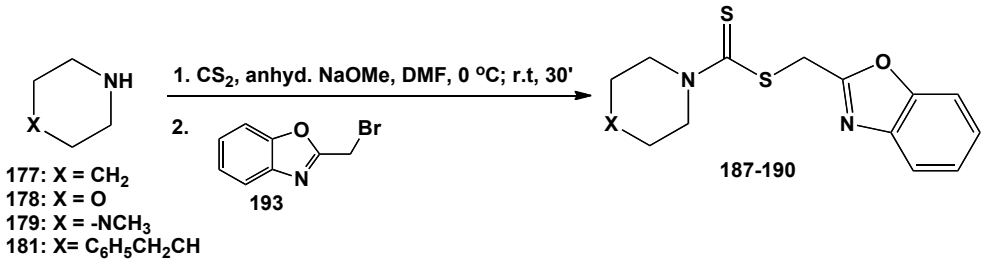

Scheme 5.5: Pathway for the synthesis of compounds **187-190**

Synthesis of 2-bromomethyl benzoxazole (193)

Intermediate **193** was prepared according to a referred procedure (Scheme 5.6) by a condensation reaction between 2-aminophenol **191** and bromoacetic acid **192**, in the presence of an excess of polyphosphoric acid (PPA).[85] The reaction gives the formation of the intermediate 2-bromo-*N*-(2-hydroxyphenyl)acetamide, then the energy given by heating leads to ring closure with the synthesis of intermediate **193**. The desired compound was

isolated from the unreacted intermediate through purification by flash column chromatography.

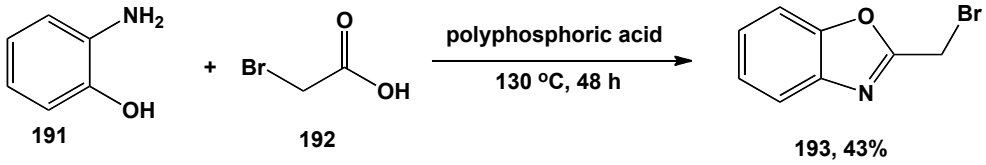

Scheme 5.6: Synthesis of intermediate **193**

Synthesis of chloromethyl benzoxazole carbodithioates (187-190)

Final benzoxazole derivatives **187-190** were obtained following the common synthetic strategy described above.

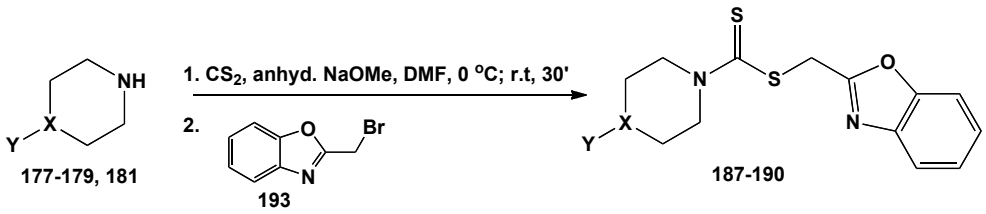

Starting alicyclic secondary amine	X	Y	Product	Yield %
177	CH_2	-	**187**	94
178	O	-	**188**	14
179	NCH_3	-	**189**	19.5
181	CH	$C_6H_5CH_2$	**190**	29

Scheme 5.7: Synthesis of compounds **187-190**

5.5.3 2-Chloromethyl benzothiazole carbodithioates (194-197)

A final series of heterocyclic aromatic compounds, **194-197** (Scheme 5.8), was obtained by reaction of secondary alicyclic amines with 2-chloromethyl benzothiazole.

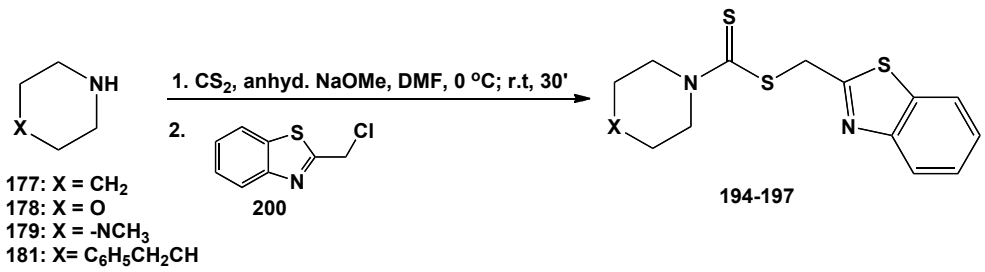

Scheme 5.8: Pathway for the synthesis of compounds **194-197**

Synthesis of 2-chloromethyl benzothiazole (200)

Intermediate **200** was synthesized by condensation reaction between 2-aminothiophenol **198** and chloroacetic acid **199** (Scheme 5.9). The desired compound was obtained with a 50% yield after purification by flash column chromatography.

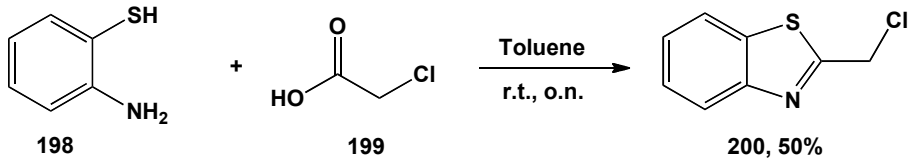

Scheme 5.9 Synthetic pathway for intermediate **200**

Synthesis of 2-chloromethyl benzothiazole carbodithioates (194-197)

Final compounds **194-197** were obtained by the already described pathway, through nucleophilic attack on the chloromethyl benzimidazole by the dithiocarbamate ion (Scheme 5.9).

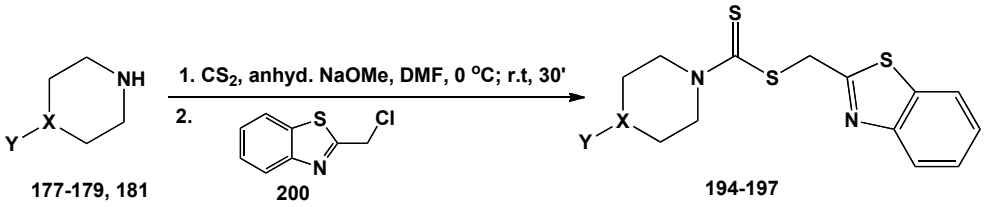

Starting alicyclic secondary amine	X	Y	Product	Yield %
177	CH_2	-	**194**	66
178	O	-	**195**	75
179	NMe	-	**196**	27
181	CH	$C_6H_5CH_2$	**197**	42

Scheme 5.9: Synthesis of compounds **194-197**

5.5.4 Aryl dithioates (196-220)

The same strategy applied for the previous compounds was carried out used for the synthesis of another family of aryl dithioates, **206-220** (Scheme 5.10). Different substituents in the *meta* and/or *para* positions of the aryl bromide were explored, as they were predicted to give interactions with the residues of the ZBD, while on the other side of the molecule the alicyclic amines used before were maintained.

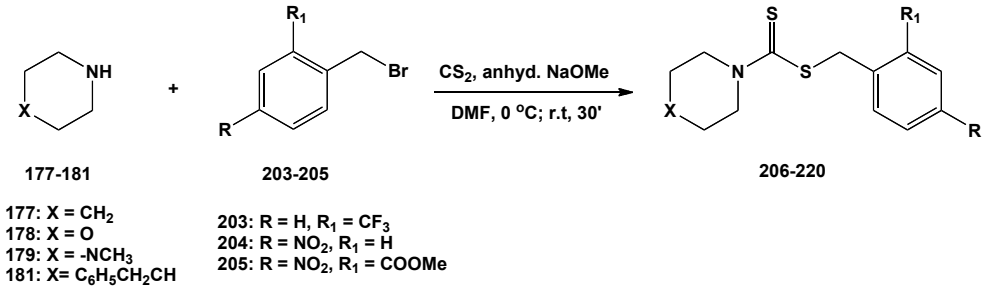

Scheme 5.10: Synthetic pathway for compounds **196-220**

Synthesis of methyl 4-(bromomethyl)-3-nitrobenzoate (202)

The intermediate methyl 4-(bromomethyl)-3-nitrobenzoate **202** was synthesised by reaction of the correspondent carboxylic acid **201** in MeOH (Scheme 5.11).

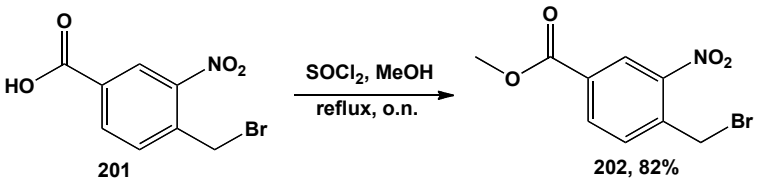

Scheme 5.11: General procedure for the synthesis of intermediate **202**

Synthesis of aryl dithioates (196-220)

According to the described procedure,[14] fifteen new derivatives were prepared (Scheme 5.12).

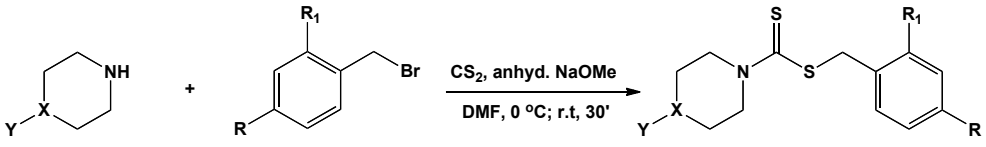

177-181 203-205 206-220

Alicyclic secondary amine	X	Y	Aryl bromide	R	R_1	Product	Yield %
177	CH_2	-	**203**	CF_3	H	**206**	88.5
178	O	-	**203**	CF_3	H	**207**	18.5
179	NMe	-	**203**	CF_3	H	**208**	11.5
180	NH	-	**203**	CF_3	H	**209**	32
181	CH	$C_6H_5CH_2$	**203**	CF_3	H	**210**	16.5
177	CH_2	-	**204**	H	NO_2	**211**	20
178	O	-	**204**	H	NO_2	**212**	29
179	NCH_3	-	**204**	H	NO_2	**213**	14
180	NH	-	**204**	H	NO_2	**214**	16
181	CH	$C_6H_5CH_2$	**204**	H	NO_2	**215**	16
177	CH_2	-	**205**	CO_2Me	NO_2	**216**	83
178	O	-	**205**	CO_2Me	NO_2	**217**	26
179	NCH_3	-	**205**	CO_2Me	NO_2	**218**	33
180	NH	-	**205**	CO_2Me	NO_2	**219**	75.5
181	CH	$C_6H_5CH_2$	**205**	CO_2Me	NO_2	**220**	82.7

Scheme 5.12: Synthetic pathway for final compounds **206-220**

5.5.5 Dithiocarbamate methyl aryl acids (221-224)

Methyl ester derivatives **216-218** and **220** were used for the synthesis of their related acids **221-224** by a base-catalysed hydrolysis with lithium hydroxide, as shown in Scheme 5.13.[86]

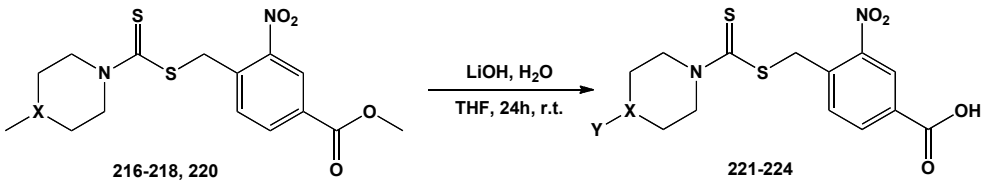

216-218, 220 221-224

Ester derivative	X	Y	Product	Yield %
216	CH_2	-	**221**	94
217	O	-	**222**	14
218	NCH_3	-	**223**	19.5
220	CH	$C_6H_5CH_2$	**224**	10

Scheme 5.13: Synthetic pathway for final compounds **221-224**

5.5.6 Biological evaluation

All designed compounds were kindly tested in cell-based assay by Dr. Ivy Widjaja, under the supervision of Professor Xander den Haan at Utrech University. Activity is expressed for each compound in terms of IC_{50}, that is the inhibitory concentration (μM) of compound required to inhibit RSV replication by 50%. Cytotoxicity is evaluated in terms of CC_{50}, that is the cytostatic/cytotoxic concentration (μM) required to observe 50% of adverse effect on the host cell. The selectivity index, SI, is evaluated by calculating the ratio CC_{50}/IC_{50} (table 5.1, 5.2).

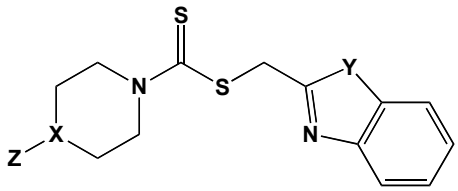

Compound	X	Z	Y	IC_{50} (μM)	CC_{50} (μM)	SI
182	CH_2	-	N	20	130	6.5
183	O	-	N	47	NA	-
184	NMe	-	N	56	NA	-
185	NH	-	N	NI	NA	-
186	CH	$C_6H_5CH_2$	N	18	29	1.6
187	CH_2	-	O	39	NA	-
188	O	-	O	NI	NA	-
189	NMe	-	O	NI	NA	-
190	CH	$C_6H_5CH_2$	O	36	123	3.4
194	CH_2	-	S	NI	NA	-
195	O	-	S	NI	NA	-
196	NMe	-	S	NI	102	-
197	CH	$C_6H_5CH_2$	S	6	NA	-

Table 5.2: Antiviral activity and cytotoxicity of compounds **182-197**; NI= no concentration-dependent inhibition, NA= not affected

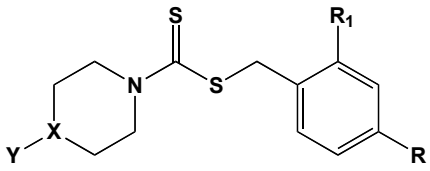

Compound	X	Y	R	R_1	IC_{50} (µM)	CC_{50} (µM)	SI
206	CH_2	-	CF_3	H	25	95	3.8
207	O	-	CF_3	H	43	133	3
208	NCH_3	-	CF_3	H	19	78	4.1
209	NH	-	CF_3	H	NI	NA	-
210	CH	$C_6H_5CH_2$	CF_3	H	30	NA	-
211	CH_2	-	H	NO_2	43	130	3
212	O	-	H	NO_2	20	27	1
213	NCH_3	-	H	NO_2	27	36	1.3
214	NH	-	H	NO_2	NI	NA	-
215	CH	$C_6H_5CH_2$	H	NO_2	26	160	6.1
216	CH_2	-	CO_2Me	NO_2	155	NA	-
217	O	-	CO_2Me	NO_2	42	NA	-
218	NCH_3	-	CO_2Me	NO_2	90	NA	-
219	NH	-	CO_2Me	NO_2	49	44	0.8
220	CH	$C_6H_5CH_2$	CO_2Me	NO_2	27	NA	-
221	CH_2	-	CO_2H	NO_2	36	NA	-
222	O	-	CO_2H	NO_2	NI	NA	-
223	NCH_3	-	CO_2H	NO_2	NI	NA	-
224	CH	$C_6H_5CH_2$		NO_2	99	NA	-

Table 5.2: Antiviral activity and cytotoxicity of compounds **206-220**; NI= no concentration-dependent inhibition, NA= not affected

In general, all the analogues having a piperazine moiety are not associated to antiviral effect, as well the aryl acid derivatives, **221-224**, for which no concentration-dependent inhibition was observed. The most active compound is the benzothiazole carbodithioate derivative **197**, showing a IC_{50} value of 6 µM and no cytotoxic effect on the cells. An antiviral effect

was also observed for two analogues, **215, 220**, sharing the common benzyl piperazine moiety with the derivative **197**.

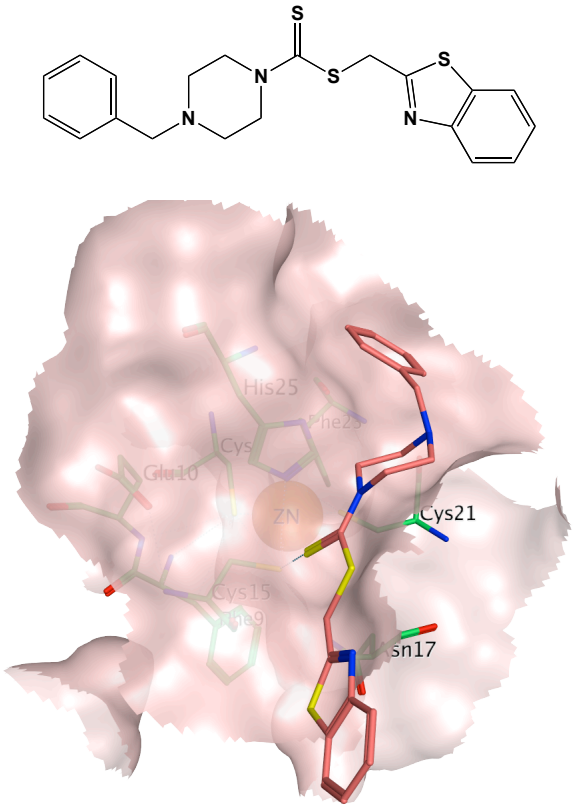

Figure 5.15: Chemical structure and predicted binding mode of compound **197**

Figure 5.15 shows the putative binding mode for compound **197** that occupies the region, lying on the surface of the binding pocket and interacting with Cys15 through a H-bond.

On the other hand, all the other derivatives bearing the 4-benzylpiperazine-1-carbodithioate group, were associated with cytotoxic effect, as in the case of compound **186**, or with an higher IC_{50}, as for compounds **190, 210**. Three more derivatives, **182, 206** and **208** showed a range of activity of 20-25 μM, sharing between each other some common features. Both compounds **182** and **206** contain the piperidine ring, while the derivative **208**, which has a N-methyl piperazine on the level of the alicyclic amine, shares the 4-trifluoromethyl benzyl moiety with the analogue **206**.

5.6 Structure-based virtual screening on the M2-1 protein

A structure-based virtual screening was performed on the M2-1 protein. The target site selected was the dual P/RNA binding site. Although both, P- and RNA-binding sites, are on the surface of the protein, hence solvent exposed, the first one has a cleft that may accommodate a ligand. Due to the essential role demonstrated for Arg126, Thr130, Lys148, Lys150, Arg151, Thr160, and Asn163, the aim was to identify compounds that would be able to bind the region delimited by these residues. A recently published crystal structure of M2-1 protein (PDB ID: 4C3B), with high resolution (2.95 Å), was used for a structure-based virtual screening. The region selected for this computational study is delimited by the already cited residues, of which Thr160 represent a key amino acid, since it buries into the protein domain and can represent a good anchoring point for the molecules.

5.6.1 Pharmacophoric filter and docking methods

A pharmacophore was designed and used to pre-screen the Specs library. As had been previously done for the other studies, a conformational search with MOE2010.10 was performed for the creation of a conformational database of the compounds to be screened.[87] The target residues of the P/RNA binding site were considered in order to build the pharmacophoric query, made by seven features: two acceptor and metal ligator groups to interact, respectively with Arg126 (F1:Acc&ML) and Arg151 (F2:Acc&ML), the latter one being a key amino acid that is on the interface between the RNA and phosphoprotein P binding sites; a donor group to interact with Thr160 (F3:Don) and a hydrophobic atom group to interact with side chains of Asp163 and Thr130 (F4:HydA); a donor & metal ligator group in correspondence to Asn163 (F5: Don&ML) and, finally, two hydrophobic and linker groups to interact with Tyr134 side chain (F6:Hyd&Link) and with Leu148 (F6:Hyd&Link). Excluded volumes were added after selecting the features, of which four were kept as essential and a partial match of 5 was required.

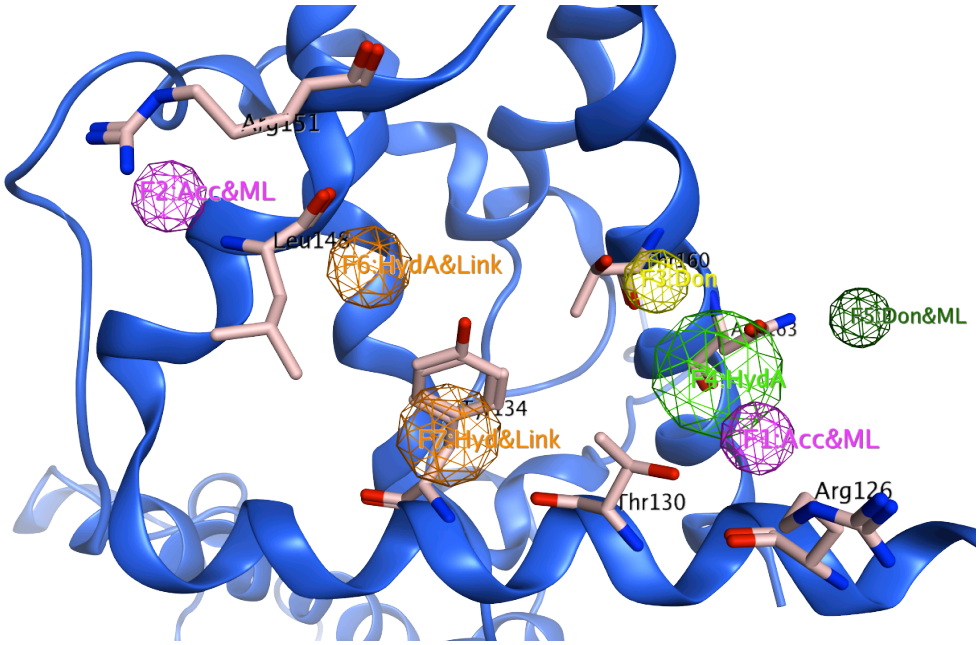

Figure 5.15: Pharmacophoric model based on the 4C3B crystal structure

A pharmacophoric search was run on the conformational database of the Specs compounds and a total of 5636 hit molecules was found and kept for the docking phase. Ligand preparation (LigPrep) was then performed on the output conformational database and two low energy conformations per ligand were produced. As already described in section 2.3.3, the usual docking procedure was followed, running Glide docking standard precision (SP) mode and re-scoring the output database with Plants [88] and FlexX [89] scoring functions, which were combined in a final consensus scoring analysis (section 1.3.5). The 25% best performing structures (1416) were selected and visually inspected to identify which ones could best interact with the selected residues. Fourteen molecules were selected and purchased for biological evaluation (Appendix I). The biological results were performed by Dr. Ivy Widjaja, under the supervision of Professor Xander den Haan at Utrecht University. Some of the selected compounds showed antiviral effect as well as cytotoxicity in cell-based assay. Compound **225** was found to have a good activity profile: the IC_{50} value for RSV replication was 16 µM, with a CC_{50} of 76 µM. Its structure and predicted binding mode are shown in figure 5.16.

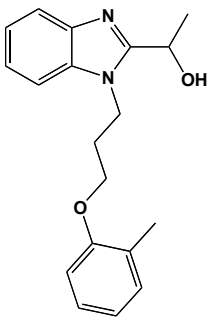

IC_{50} = 16 μM;
CC_{50} = 76 μM;
SI = 4.75

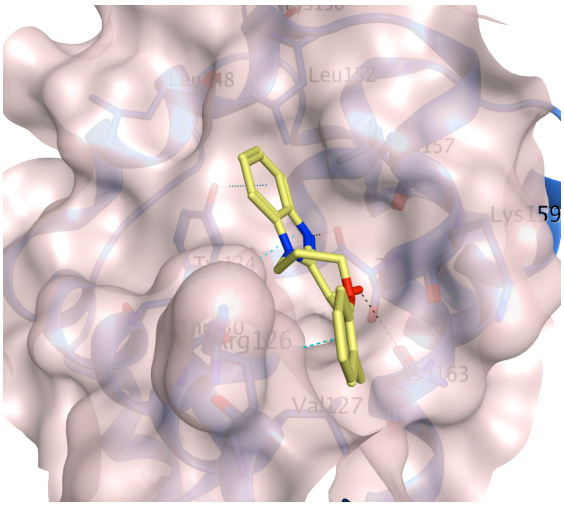

Figure 5.16: Chemical structure of compound **225** and its predicted binding mode

Compound **225** is predicted to be located on the lower part of the binding site, making hydrogen bonds with Lys159 and Thr160, while showing hydrophobic interactions with the side chain of Thr130. Further biological data are required to confirm the preliminary data and to assess the activity of the compound on the M2-1 protein.

5.7 Ligand-based Virtual Screening on the F protein

A ligand-based virtual screening was performed on the crystallized ligand, TMC-353121, with the aim to find new scaffolds that would interact with the binding site of the F protein, by sharing the active conformation of the reference compound. The *iter* followed for this study is the one previously described in section 2.9.1. The conformational database of the SPECS compounds was analysed against the selected conformation of TMC-353121 with the vROCS 3.1.2 software,[90] considering both shape and electrostatics complementarity with the target query for the evaluation of screened structures. In figure 5.17, the queries chosen as essential parameters for the screening are highlighted. They were selected on the base of previous studies that revealed the importance of those functional groups for the activity of the molecule.[42]

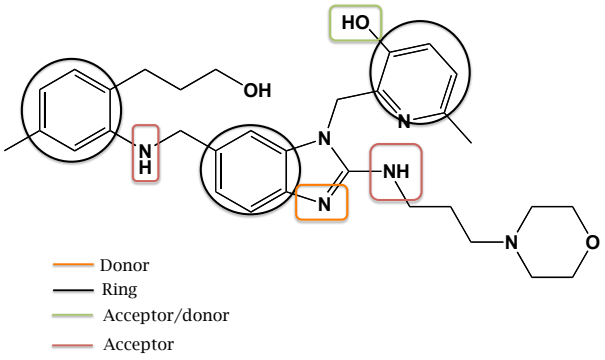

Figure 5.17: Chemical structure of TMC0353121 and its electrostatic features set for the screening.

All screened conformations that answered to the required parameters were analyzed by docking and rescoring procedures. Around 600 molecules were selected from the consensus scoring and were visually inspected in order to reduce the final selection to 7 molecules, purchased and tested in cell-based assays (Appendix I). Among them, two molecules showed antiviral effect at concentration values to be considered for a structure-activity evaluation. However, these compounds were also associated to cytotoxic effect on cell viability assay, thus excluding their chemical structure for further optimization studies.

Compound	Chemical structure	IC_{50} (µM)	CC_{50} (µM)	SI
226	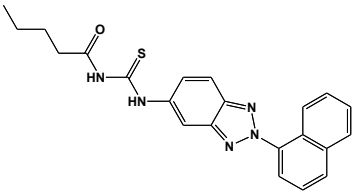	15	36	2.4
227	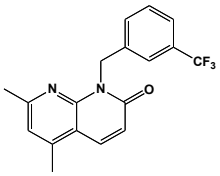	24	48	2

Table 5.3: Antiviral activity and cytotoxicity of compounds **226-227**

Conclusions

Computer-aided approaches were performed, aiming to identify potential RSV inhibitors. Starting from the active conformation of a known inhibitor of the fusion protein, a ligand-based virtual screening led to the selection of seven compounds, of which two were found active with a IC_{50} of 20 µM, but also having cytotoxic effect. In parallel, a structure-based drug design virtual screening was performed on the recently released crystal structure of M2-1 protein. The targeted binding area corresponds to the RNA and P binding sites. Among the 14 chosen compounds, several were associated to antiviral activity but were toxic for the cells. Compound **225** showed a good activity profile, with a IC_{50} of 16 µM, and will represent a valuable starting point for drug optimisation.

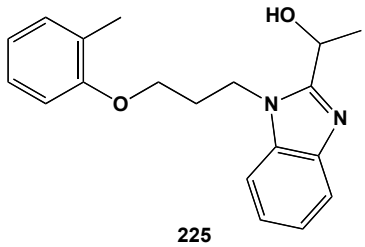

225

An additional study was performed on the zinc-binding domain of the same protein, M2-1, where a *de novo* design approach was applied. Using a library of small fragments that was docked within the active site, a series of 32 compounds, all having a common zinc-ejecting moiety, was designed and synthesized. Preliminary biological data reveal a good activity profile for compound **197**, sharing a common chemical group with derivatives **215** and **220** that were also associated to antiviral effect against RSV.

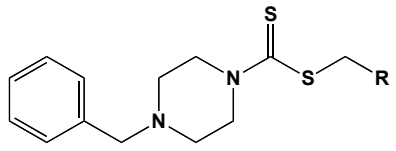

R =

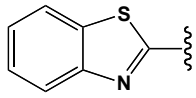

197
IC_{50} = 6 µM
CC_{50} = NA

;

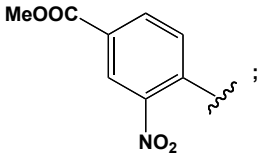

215
IC_{50} = 26 µM
CC_{50} = 160 µM

;

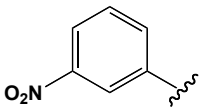

220
IC_{50} = 27 µM
CC_{50} = NA

From these evaluation, it can be inferred that the length of the molecule is important for activity, with longer structures associated with a better antiviral profile and no cytotoxic effect on the cell viability assay, while for a second set of shorter compounds, **182, 206** and **208,** the CC_{50} values, even if still acceptable, were lower than the previous ones, thus reducing their selectivity index.

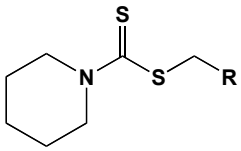

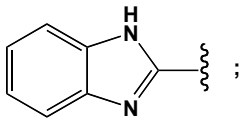

182
IC_{50} = 20 µM; CC_{50} = 130 µM

;

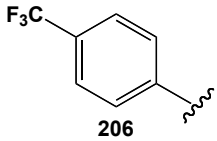

206
IC_{50} = 25 µM; CC_{50} = 95 µM

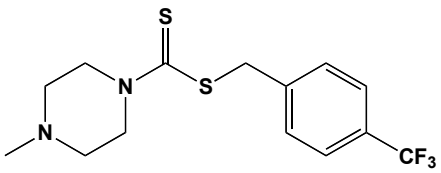

208
IC_{50} = 19 µM; CC_{50} = 78 µM

References

1 Hall, C.B.; Weinberg, G.A.; Iwane, M.K.; Blumkin, A.K.; Edwards, K.M.; Staat, M.A.; Auinger, P.; Griffin, M.R.; Poehling, K.A.; Erdman, D.; Grijalva, C.G.; Zhu, Y.; Szilagyi, P. The Burden of Respiratory Syncytial Virus Infection in Young Children. *N. Engl. J. Med.* **2009**, 360, 588–598.

2 Respiratory Syncytial Virus Infection (RSV). Centers for Disease Control and Prevention. Available from: http://www.cdc.gov/rsv/research/us-surveillance.html. (accessed August 22, 2014)

3 Nair H.; Nokes, D.J.; Gessner, B.D.; Dherani, M.; Madhi, S.A.; Singleton, R.J.; O'Brien, K.L.; Roca, A.; Wright, P.F.; Bruce, N.; Chandran, A.; Theodoratou, W.; Sutanto, A.; Sedyaningsih, E.R.; Ngama. M.; Munywoki, P.K.; Kartasasmita, C.; Simoes, E.A. F.; Rudan, I.; Weber, M.W.; Campbell, H. Global burden of acute lower respiratory infections due to respiratory syncytial virus in young children: a systematic review and meta-analysis. *Lancet* **2010**, 375(9725),1545-1555.

4 Hall, C.B.; Douglas, R.G. Jr. Clinically useful method for the isolation of respiratory syncytial virus. *J. Infect. Dis.* **1975**, 131 (1), 1-5.

5 Collins, P.L.; Crowe, J.E. Jr. Respiratory syncytial virus and metapneumovirus. In: *Fields Virology*, Knipe, D.M.; Howley, P.M. Eds.; Wolters Kluwer-Lippincott Williams & Wilkins, Philadelphia, 2007; 1601-1646.

6 Gardener, P.S.; McQuillin, J.; McGuckin, R. The late detection of respiratory syncytial virus in cells of respiratory tract by immunofluorescence. *J. Hyg. (Lond)* **1970**, 68 (4), 575-80.

7 Levine, S.; Klaiber-Franco, E.; Paradiso, R. Demonstration that glycoprotein G is the attachment protein of Respiratory Syncytial Virus. *J. Gen. Virol.* **1987**, 68, 2521-2524.

8 Walsh, E.E.; Hruska, J. Monoclonal antibodies to respiratory syncytial virus proteins: identification of the fusion protein. *J Virol* **1983**, 47 (1), 171-177.

9 Easton, C.R.; Pringle, C.R. Order Mononegavirales, In: *Virus Taxonomy—Ninth Report of the International Committee on Taxonomy of Viruses*; King, A.M.Q.; Lefkowitz, E.; Adams, M.J.; Carstens, E.B.; London, UK: Elsevier/Academic Press, 2011; 653–657.

10 Mufson, M.A.; Orvell, C.; Rafnar, B.; Norrby, E. Two distinct subtypes of human respiratory syncytial virus. *J. Gen. Virol.* **1985**, 66, 2111–2124.

11 Collins, P.L; Melero, J.A. Progress in understanding and controlling respiratory syncytial virus: still crazy after all these years. *Virus Res.* **2011**, 162, 80 –99.

12 Collins, P.L.; Mink, M.A.; Stec, D.S. Rescue of synthetic analogs of respiratory syncytial virus genomic RNA and effect of truncations and mutations on the expression of a foreign reporter gene. *PNAS* **1991**, 88, 9663–9667.

13 Mink, M.A.; Stec, D.S.; Collins, P.L. Nucleotide sequences of the 3' leader and 5' trailer regions of human respiratory syncytial virus genomic RNA. *Virology* **1991**, 185, 615– 624.

14 Moudy, R.M.; Sullender, W.M.; Wertz, G.W. Variations in intergenic region sequences of Human respiratory syncytial virus clinical isolates: analysis of effects on transcriptional regulation. *Virology* **2004**, 327 (1), 121-133.

15 Liuzzi, M., Mason, S.W., Cartier, M., Lawetz, C., McCollum, R.S., Dansereau, N., Bolger, G., Lapeyre, N., Gaudette, Y., Lagace, L., Massariol, M.J., Do, F., Whitehead, P., Lamarre, L., Scouten, E., Bordeleau, J., Landry, S., Rancourt, J., Fazal, G., Simoneau, B. Inhibitors of respiratory syncytial virus replication target cotranscriptional mRNA guanylylation by viral RNA-dependent RNA polymerase. *J. Virol.* **2005**, 79 (20), 13105–13115.

16 Collins, P.L.; Andrerson, K.; Langer, S.J.; Wertz, G.W. Correct sequence for the major nucleocapsid protein mRNA of respiratory syncytial virus. *Virology* **1985**, 146 (1), 69-77.

17 Collins, P.L.; Hill, M.G.; Cristina, J.; Grosfeld, H. Transcription elongation factor of respiratory syncytial virus, a nonsegmented negative-strand RNA virus. *PNAS* **1996**, 93, 81–85.

18 Yu, Q.; Hardy, R.W.; Wertz, G.W. Functional cDNA clones of the human respiratory syncytial (RS) virus N, P, and L proteins support replication of RS virus genomic RNA analogs and define minimal trans-acting requirements for RNA replication. *J. Virol.* **1995**, 69, 2412–2419.

19 Yunus, A.S.; Collins, P.L.; Samal, S.K. Sequence analysis of a functional polymerase (L) gene of bovine respiratory syncytial virus: determination of minimal trans-acting requirements for RNA replication. *J. Gen. Virol.* **1998**, 79, 2231–2238.

20 Garcia-Barreno, B.; Delgrado, T.; Melero, J.A. Identification of protein regions involved in the interaction of human respiratory syncytial virus phosphoprotein and nucleoprotein: significance for nucleocapsid assembly and formation of cytoplasmic inclusions. *J. Virol.* **1996**, 70 (2), 801-808.

21 Asenjo, A.; Calvo, E.; Villanueva, N. Phosphorylation of human respiratory syncytial virus P protein at threonine 108 controls its interaction with the M2-1 protein in the viral RNA polymerase complex. *J. Gen. Virol.* **2006**, 87, 3637-3642.

22 Curran, J.; Marq, J.B.; Kolakofsky, D. An N-terminal domain of the Sendai paramyxovirus P protein acts as a chaperone for the NP protein during the nascent chain assembly step of genome replication. *J. Virol.* **1995**, 69 (2), 849–855.

23 Fearns, R.; Collins, P.L. Role of the M2-1 transcription antitermination pro- tein of respiratory syncytial virus in sequential transcription. *J. Virol.* **1999**, 73 (7), 5852–5864.

24 Bermingham, A.; Collins, P.L. The M2-2 protein of human respiratory syncytial virus is a regulatory factor involved in the balance between RNA replication and transcription. *PNAS* **1999,** 96 (20), 11259–11264.

25 Levine, S.; Klaiber-Franco, R.; Paradiso, P.R. Demonstration that glycoprotein G is the attachment protein of respiratory syncytial virus. *J. Gen. Virol.* **1987**, 68, 2521-2524.

26 Zhao, X.; Singh, M.; Malashkevich, V.N.; Kim, P.S. Structural characterization of the human respiratory syncytial virus fusion protein core. *PNAS* **2000,** 97 (26), 14172–14177

27 Fuentes, S.; tran, K.C.; Luthra, P.; Teng, M.N.; He, B. Function of the respiratory syncytial virus small hydrophobic protein. *J. Virol.* **2007**, 81, 8361-8366.

28 Henderson, G.; Murray, J.; Yeo, R.P. Sorting of the respiratory syncytial virus matrix protein into detergent-resistant structures is dependent on cell-surface expression of the glycoproteins. *Virology* **2002**, 300 (2), 244–254.

29 Ghildyal, R.; Murray, M.; Vardaxis, N.; Meanger, J. Respiratory syncytial virus matrix protein associates with nucleocapsids in infected cells. *J. Gen. Virol.* **2002**, 83, 753-757.

30 Atreya, P.L.; Peeples, M.E.; Collins, P.L. The NS1 protein of human respiratory syncytial virus is a potent inhibitor of minigenome transcription and RNA replication. *J. Virol.* **1998**, 72 (2), 1452–1461.

31 Bossert, B.; Marozin, S.; Conzelmann, K. K. Nonstructural proteins NS1 and NS2 of bovine respiratory syncytial virus block activation of interferon regulatory factor 3. *J. Virol.* **2003**, 77, 8661-8668.

32 Dickens, L.E.; Collins, P.L.; Wertz, G.W. Transcriptional mapping of human respiratory syncytial virus. *J. Virol.* **1984**, 52,364 –369.

33 Kuo, L.; Fearns, R.; Collins, P.L. Analysis of the gene start and gene end signals of human respiratory syncytial virus: quasi-templated initiation at position 1 of the encoded mRNA. *J. Virol.* **1997**, 71 (7), 4944–4953.

34 Fearns, R.; Peeples, M.E.; Collins, P.L. Mapping the transcription and replication promoters of respiratory syncytial virus. *J. Virol.* **2002**, 76 (4), 1663–1672.

35 Liuzzi, M.; Mason, S.W.; Cartier, M.; Lawetz, C.; McCollum, R.S.; Dansereau, N.; Bolger, G.; Lapeyre, N.; Gaudette, Y.; Lagacé, L.; Massariol, M.J.; Dô, F.; Whitehead, P.; Lamarre, L.; Scouten, E.; Bordeleau, J.; Landry, S.; Rancourt, J.; Fazal, G.; Simoneau, B. Inhibitors of respiratory syncytial virus replication target cotranscriptional mRNA guanylylation by viral RNA-dependent RNA polymerase. *J. Virol.* **2005**, 79, 13105–13115.

36 Mitra, R.; Baviskar, P.; Duncan-Decocq, R.; Patel, D.; Oomens, A.G.P. The Human Respiratory Syncytial Virus Matrix Protein Is Required for Maturation of Viral Filaments. *J. Virol.* **2012**, 86 (8), 4432-4443.

37 Wright, P.F. Progress in the prevention and treatment of RSV infection. *N. Eng. J. Med.* **2014**, 371 (8), 776-777.

38 Faber, T.E.; Jimoen, J.L.; Bont, L.J. Respiratory syncytial virus bronchiolitis: prevention and treatment. *Expert Opin. Pharmaco.* **2008**, 9: 2451–2458.

39 Welliver, R.C. Respiratory syncytial virus infection: therapy and prevention. *Paediatr. Resp. Rev*. **2004**, 5, 127–133.

40 Wainwright, C. Acute viral bronchiolitis in children – a very common condition with few therapeutic options. *Paediatr Respir Rev.* **2010**, 11 (1), 39-45.

41 Hampp, C.; Kauf, T.L.; Saidi, A.S.; Winterstein, A.G. Cost-effectiveness of respiratory syncytial virus prophylaxis in various indications. *Arch. Pediatr. Adolesc. Med.* **2011**, 165 (6), 498-505.

42 Morris, S.K.; Dzolganovski, B.; Beyene, J.; Sung, L. A meta-analysis of the effect of antibody therapy for the prevention of severe respiratory syncytial virus infection. *BMC Infect. Dis.* **2009**, 5 (9), 106.

43 Ventre, K.; Randolph, A.G. Ribavirin for respiratory syncytial virus infection of the lower respiratory tract in infants and young children. *Cochrane Database Syst. Rev.* **2007**, Vol. 1, CD000181.

44 McCoy, D.; Wong, E.; Kuyumjian, A.G.; Wynd, M.A.; Sebti, R.; Munk, G.B. Treatment of respiratory syncytial virus infection in adult patients with hematologic malignancies based on an institution-specific guideline. *Transpl. Infect. Dis.* **2011**, 13 (2), 117–121.

45 http://clinicaltrials.gov/ct2/home/ALN-RSV01 (accessed October 8, 2014).

46 http://clinicaltrials.gov/ct2/rsv-604 (accessed October 8, 2014)

47 Meanwell, N.A.; Krystal, M. Respiratory syncytial virus – the discovery and optimization of orally bioavailable fusion inhibitors. *Drugs Fut. Vol.* **2007**, 32 (5), 441-455.

48 http://clinicaltrials.gov/show/NCT02135614

49 Langley, G.F.; Anderson, L.J. Epidemiology and prevention of respiratory syncytial virus infections among infants and young children. *Pediatr. Infect. Dis. J. Vol.* **2011**, 30 (6), 510-517.

50 Murata, Y. Respiratory syncytial virus vaccine development. *Clin. Lab. Med. Vol.* **2009**, 29 (4), 725-739.

51 Collins, P.L.; Myron, G; Hill, J.C.; Grosfeld, H. Transcription elongation factor of respiratory syncytial virus, a nonsegmented negative-strand RNA virus. *PNAS* **1996**, 93, 81-85.

52 Hardy, R.W; Wertz, G.W.; The product of the respiratory syncytial virus M2 gene ORF1 enhances readthrough of intergenic junctions during viral transcription. *J. Virol.* **1998**, 72, 520-526.

53 Hardy, R.W.; Wertz, G.W. The product of the respiratory syncytial virus M2 gene ORF1 enhances readthrough of intergenic junctions during viral transcription. *J. Virol.* **1998**, 72, 520–526.

54 Tanner, S.J.; Ariza, A.; Richard, C.; Kyle, H.F.; Dods, R.L.; Blondot, M.; Wu, W.; Trincao, J.; Trinh, C.H.; Hiscox, J.A.; Carroll, M.W.; Silman, N.J.; Eleouet, J.; Edwards, T.A.; Barr, J.N. Crystal structure of the essential transcription antiterminator M2-1 protein of human respiratory syncytial virus and implications of its phosphorylation. *PNAS* **2014**, 111 (4), 1580-1585.

55 Cowton, V.M.; McGivern, D.R.; Fearns, R. Unrevealling the complexities of respiratory syncytial virus RNA synthesis. *J. Gen. Virol.*, **2006**, 87, 1805-1821.

56 Tran, T.L.; Castagne, N.; Dubosclard, V.; Noinville, S.; Koch, E.; Moudjou, M.; Henry, C.; Bernard, J.; Yeo, R.P.; Eleouet, J.F. The respiratory syncytial virus M2-1 protein forms tetramers and interacts with RNA and P in a competitive manner. *J. Virol.* **2009**, 83 (13), 6363–6374.

57 Blondot, M-L.; Dubosclard, V.; Fix, J.; Lassoued, S.; Magali, A-N.; Bontems, F.; Eleouet, J-F.; Sizun, C. Structure and functional analysis of the RNA- and viral phosphoprotein-binding domain of respiratory syncytial virus M2-1 protein. *PLoS Pathog.* **2012**, 8 (5), 1-13.

58 Garcia-Barreno, B.; Steel, J.; Paya, M.; Martinez-Sobrido, L.; Delgado, T.; Yeo, R.P.; Melero, J.A. Epitope mapping of human respiratory syncytial virus 22K transcription antitermination factor: role of N-terminal sequences in protein folding. *J. Gen. Virol.* **2005**, 86 (4), 1103-1107.

59 Hardy, R.W.; Wertz, G. The Cys_3-His_1 motif of the respiratory syncytial virus M2-1 protein is essential for protein function. *J. Virol.* **2000**, 74 (13), 5880–5885.

60 Eckert, D.M.; Kim, P.S. Mechanisms of viral membrane fusion and its inhibition. *Annu. Rev. Biochem.* **2001**, 70, 777–810.

61 Weissenhorn, W.; Dessen, A.; Calder, L.J.; Harrison, S.C.; Skehel, J.J.; Wiley, D.C. Structural basis for membrane fusion by enveloped viruses. *Mol. Membr. Biol.* **1999**, 16, 3–9.

62 Peisajovich, S.G.; Shai, Y. New insights into the mechanism of virus-induced membrane fusion. *Trends Biochem. Sci.* **2002**, 27, 183–190.

63 Collins, P.L.; Huang, Y.T.; Wertz, G.W. Nucleotide-Sequence of the gene Encoding the Fusion (F) Glycoprotein of Human Respiratory Syncytial Virus. *PNAS* **1984**, 81, 7683–7687.

64 Calder, L.J.; Gonzalez-Reyes, L.; Garcia-Barreno, B.; Wharton, S.A.; Skehel, L.J.; Wiley, D.C.; Melero, J.A. Electron microscopy of the human respiratory syncytial virus fusion protein and complexes that it forms with monoclonal antibodies. *Virology* **2000**, 271, 122–131.

65 Zhao, X.; Singh, M.; Malashkevich, V.N.; Kim, P.S. Structural characterization of the human respiratory syncytial virus fusion protein core. *PNAS* **2000**, 97 (26), 14172-14177.

66 Collins, P. L., McIntosh, K. & Chanock, R. M. Respiratory Syncytial Virus. In*: Fields Virology*, Vol.1; Knipe, D.M.; Howley, P.M.; Chanock, R.M.; Melnick, J.L.; Monath, T.P.; Roizman, B.; Strauss, S.E. Eds.; Lippincott-Raven Publishers, Philadelphia, 1996; 1313-1351.

67 Chambers, P.; Pringle, C.R.; Easton, A.J. Heptad repeat sequences are located adjacent to hydrophobic regions in several types of virus fusion glycoproteins. *J. Gen. Virol.* **1990**, 71, 3075-3080.

68 Chaiwatpongsakorn, S.; Epand, R.F.; Collins, P.L.; Epand, R.M.; Peeples, M.E. Soluble respiratory syncytial virus fusion protein in the fully cleaved, pretriggered state is triggered by exposure to low-molarity buffer. *J. Virol.* **2011**, 85, 3968–3977.

69 http://clinicaltrials.gov/show/NCT01489306 (accessed October 8, 2014)

70 Andries, K.; Moeremans, M.; Gevers, T.; Willebrords, R.; Sommen, C.; Lacrampe, J.; Jannsens, F.; Wyde, P.R. Substituted benzimidazoles with nanomolar activity against respiratory suncytial virus. *Antiviral Res.* **2003**, 60, 209-219.

71 Bonfanti, J.F.; Roymans, D. Prospects for the development of fusion inhibitors to treat human respiratory syncytial virus infection. *Curr. Opin. Drug Discov. Devel.* **2009**, 12, 479–487.

72 Douglas, J.L.; Panis, M.L.; Ho, E.; Lin, K.Y.; Krawczyk, S.H.; Grant, D.M.; Cai, R.; Swaminathan, S.; Cihlar, T. Inhibition of respiratory syncytial virus fusion by the small molecule VP-14637 via specific interactions with F protein. *J. Virol.* **2003**, 77, 5054–5064.

73 Boukhvalova, M.S.; Prince, G.A.; Blanco, C.G. Inactivation of respiratory syncytial virus by zinc finger reactive compounds. *Virol. J.* **2010**, 7 (20), 1-10.

74 Rice W.G.; Schaeffer C.A.; Harten B.; Villinger F.; South T.L.; Summers M.F.; Henderson L.E.; Bess J.W. Jr.; Arthur L.O.; McDougal J.S.; Orloff, S.L.; Mendeleyev, J.; Kun, E. Inhibition of HIV-1 infectivity by zinc-ejecting aromatic C-nitroso compounds. *Nature* **1993**, 361 (6411), 473-5.

75 Loo, J.L.; Holler, T.P.; Sanchez, J.; Gogliotti, R.; Maloney, L.; Reily, M.D. Biophysical characterization of zinc ejection from HIV nucleocapsid protein by anti-HIV 2,2'-dithiobis[benzamides] and benzisothiazolones. *J. Med. Chem.* **1996**, 39, 4313-4320.

76 Rice, W.G.; Supko, J.G.; Malspeis, L.; Buckheit, R.W.Jr.; Clanton, D.; Bu, M. Graham, L.; Schaeffer, C.A.; Turpin, J.A.; Domagala, J.; Gogliotti, R.; Bader, J.P.; Halliday, S.M.; Coren, L.; Sowder II, R.C.; Arthur, L.O.; Hendelson, L.E. Inhibitors of HIV nucleocapsid protein zinc fingers as candidates for the treatment of AIDS. *Science* **1995**, 270, 1194-7.

77 Rice, W.G.; Turpin, J.A.; Huang, M.; Clanton, D.; Buckheit, R.W.Jr.; Covell, D.G.; Wallqvist, A.; McDonnell, N.B.; DeGuzman, R.N.; Summers, M.F.; Zalkow, L.; Bader, J.P.; Haugwitz, R.D.; Sausville, E.A. Azodicarbonamide inhibits HIV-1 replication by targeting the nucleocapsid protein. *Nat. Med.* **1997**, 3, 341-5.

78 Yu, X.; Hathout, Y.; Fenselau, C.; Sowder, R.C.Jr.; Henderson, LE.; Rice, W.G.; Mendeleyev, J., Kun, E. Specific disulfide formation in the oxidation of HIV-1 zinc finger protein nucleocapsid p7. *Chem. Res. Toxicol.* **1995**, 8, 586-90.

79 Tummino, P.J.; Scholten, J.D.; Harvey, P.J.; Holler, T.P.; Maloney, L.; Gogliotti, R. Domagala, J.; Huoe, D. The in vitro ejection of zinc from human immunodeficiency virus (HIV) type 1 nucleocapsid protein by disulfide benzamides with cellular anti-HIV activity. *PNAS* **1996**, 93, 969-73.

80 Vandevelde, M.; Witvrouw, M.; Schmit, J.C.; Sprecher, S.; De Clercq, E.; Tassignon, J.P. ADA, a potential anti-HIV drug. *AIDS Res. Hum. Retroviruses* **1996**, 12, 567-8.

81 Irwin, J.J.; Sterling, T.; Mysinger, M.M.; Bolstad, E.S.; Coleman, R.G. Zinc: a free tool to discover chemistry from biology. *J. Chem. Inf. Model.* **2012**, 52(7), 1757-1768. http://zinc.docking.org/subsets/fragment-like (accessed April 2014).

82 Burke, T.R.; Bajwa, B.S.; Jacobsen, A.E.; Rice, K.C.; Streaty, R.A.; Klee, W.A. Probes for narcotic receptor mediated phenomena. 7. Synthesis and pharmacological properties of irreversible ligands specific for μ or δ opiate receptors. *J. Med. Chem.* **1984**, 27, 1570-1574.

83 Madalageri, P.M.; Oblennavar, K. Synthesis, DNA protection, and antimicrobial activity of some novel chloromethylbenzimidazole derivatives bearing dithiocarbamates. *J. Chem. Pharma. Res.* **2012**, 4 (5), 2697-2703.

84 Biannic, B.; Bozell, J.J. Efficient Cobalt-Catalyzed Oxidative Conversion of Lignin Models to Benzoquinones. *Org. Lett.* **2013**, 15 (11), 2730-2733.

85 Soares, A.M.S.; Costa, S.P.G.; Goncalves, M.S.T. Oxazole light triggered protecting groups: synthesis and photolysis of fused heteroaromatic conjugates. *Tetrahedron* **2010**, 6 (41), 8189-8195.

86 Grima, P.; Pedro, M.; Aguilar, I.N.; Mir, C.M.; Carrascal, R.M.; Terricabras, B.E. Preparation of 2-aminothiadiazole derivatives as S1P1 receptor agonists. Patent WO 2011069647, 16 Jun 2011.

87 Chemical Computing Group, Montreal, Canad. www.chemcomp.com (accessed February, 2014).

88 Korb, O.; Stützle, T.; Exner, T.E. An ant colony optimization approach to flexible protein–ligand docking. *Swarm Intell.* **2007**, 1, 115-134.

89 BioSolveIT GmbH, Sankt Augustin, Germany. www.biosolveit.de (accessed March, 2014).

90 OpenEye Scientific Software, Santa Fe, NM. www.eyesopen.com (accessed March, 2014).

Conclusions

The main scope of this project was to use *in silico* approaches for the identification of potential antivirals. During the course of this study, different structural proteins of four RNA viruses were investigated. For CVB3, in particular, the homodimer 3A protein was evaluated for a structure-based virtual screening on the two chains of the dimer after building an homology model of the protein. One compound was selected from the *in vitro* assays with a certain antiviral activity, which was taken as a starting point for the design and synthesis of a small series of 10 analogues.

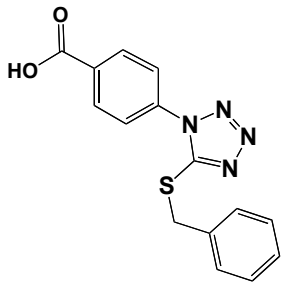

1

The biological evaluation of the new compounds did not reveal an activity improvement. Due to the lack of information on the protein and on the existence of inhibitors of the 3A protein, a second non-structural protein was targeted for drug design. The 3D polymerase was the objective of a second study based on the available information on a novel non-nucleoside inhibitor, GPC-N114 that inhibits the viral replication by competing with an incoming nucleotide. Several computer-aided approaches were used: at first, a structure-based virtual screening on the putative active site; secondly, flexible alignment of six new scaffolds that were designed with the aim to change the central chlorobenzene ring and the two oxygen linker of the GPC-N114 structure.

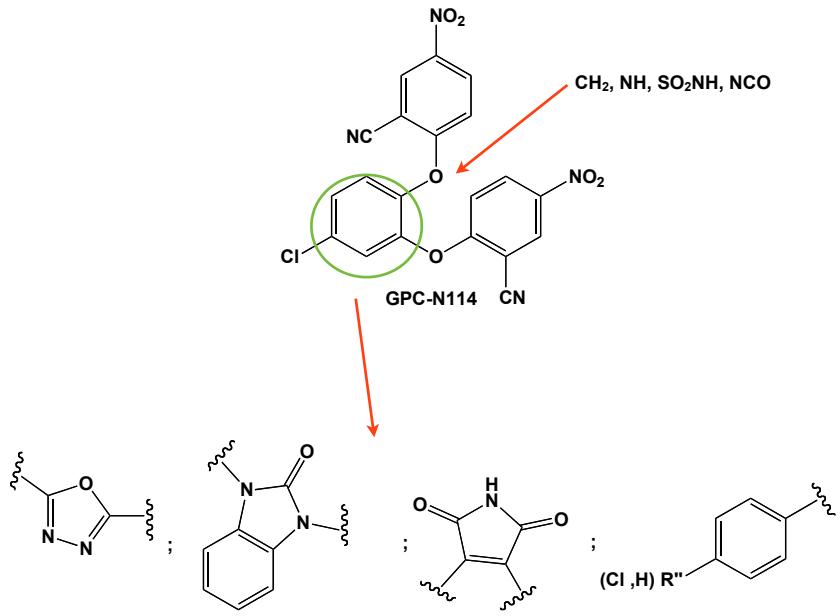

A total of 32 new derivatives were synthesized, of which only compound **52** was associated to antiviral activity, higher than the GPC-N114 compound.

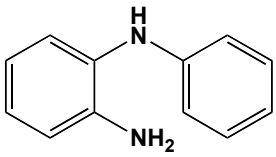

52

Due to the poor antiviral properties, its chemical scaffold was not further investigated. A final attempt was made to use the active conformation of the GPC-N114 compound for a ligand-based virtual screening, from which no new interesting scaffolds were selected. The investigation around GPC-N114 implied also a study on a new virus, FMDV, which belongs to the Picornavirus family, like CVB3. This inhibitor, however, is not active against FMDV but was found to bind the same pocket individuated for CVB3 3D. A structure-based drug design was first attempted in order to find small molecules that could have a better interaction with the residues of the binding site. From the biological results of the selected molecules, no potential inhibitors were identified. A second *de novo* approach was then attempted which led to the selection of a common scaffold bearing a coumarin ring. A small series of 8 compounds was synthesized and tested against FMDV, but no antiviral activity was observed.

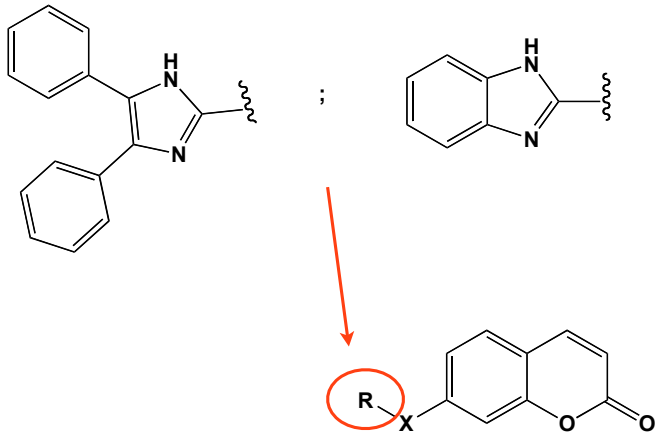

X = CH_2O, NC=O, CH_2S, CH_2S=O, CH_2SO_2

A more classic medicinal chemistry approach was used in the case of Chikungunya virus, for which a novel inhibitor has been previously identified with a structure-based virtual screening on the nsP2 protease. Based on its chemical structure and on the biological results obtained for the novel analogues that followed the discovery of the new inhibitor, four new families of compounds were designed, validated with docking techniques and synthesised in order to establish a SAR study. Of these, the chemical scaffold bearing a thiourea linker seems to be associated to a retained antiviral activity. Additional studies, however, are required to evaluate the activity of these compounds on the target nsP2 protease that was evaluated for *in silico* studies.

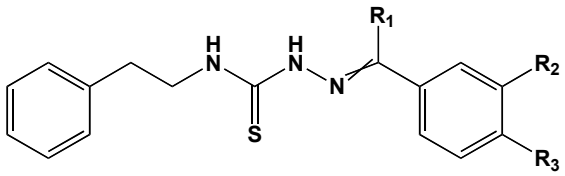

172: R_1 = H; R_2, R_3 = OEt
173: R_1 = Me; R_2 = H; R_3 = C_6H_{11}

Some interesting results were also obtained on a series of studies drove on the M2-1 protein of RSV. From a structure-based virtual screening performed on the surface of the protein where RNA and the phosphoprotein P binds, compound **225** inhibits viral replication.

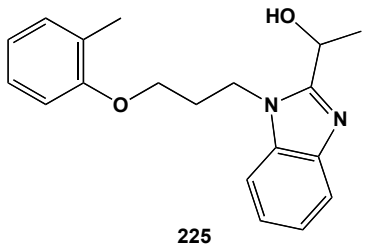

225

On the same crystal structure of M2-1 protein, but targeting the zinc binding domain, a *de novo* drug design guided the selection of a common scaffold bearing a zinc-ejecting moiety that was specifically chosen in order to design and prepare 32 zinc-reactive molecules. Of these, six compounds inhibited RSV replication at low micromolar concentration without substantial effect on cell viability.

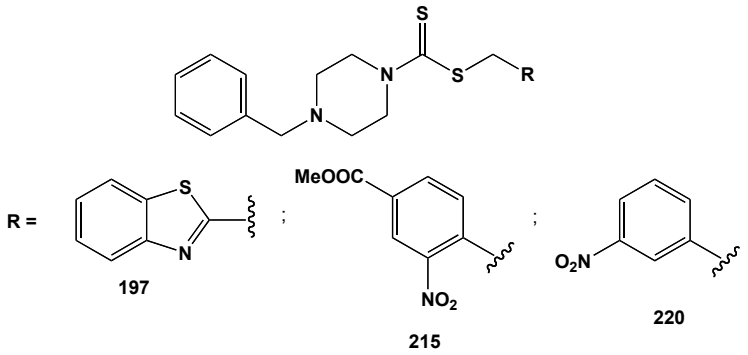

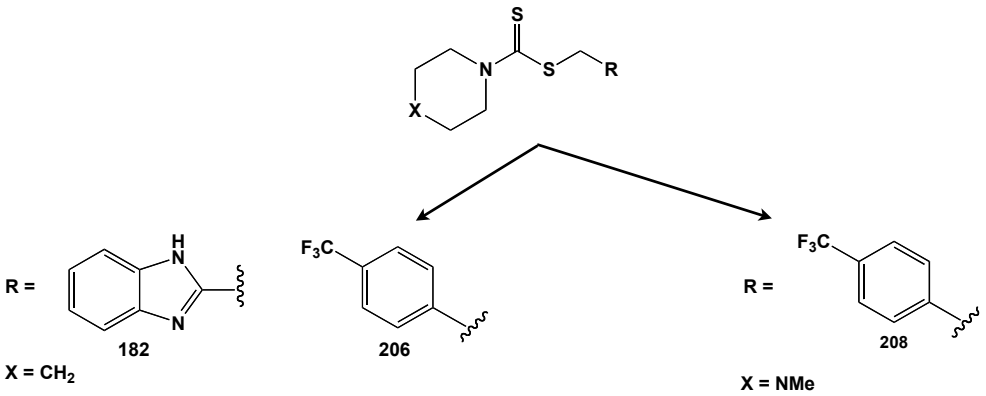

This scaffold represents a promising starting point for future structural modifications. However, additional biological tests have already planned to investigate their mechanism of action of these compounds and see whether the entry or the viral replication is affected. In conclusion, this project confirms the relevance of molecular modelling techniques in drug design: their advantages and the usefulness for the identification of novel, potential active compounds.

Chapter 6

Experimental part

6.1 General information

All chemicals, reagents and solvents were purchased from Aldrich or purified by standard techniques.

Thin Layer Chromatography

Silica gel plates (Merck Kieselgel $60F_{254}$) were used and were developed by the ascending method. After solvent evaporation, compounds were visualised by irradiation with UV light at 254 nm and 366 nm.

Column Chromatography

Glass columns were dry packed in the appropriate eluent under gravity, with Woelm silica (32-63 μm). Samples were applied as a concentrated solution in the same eluent. Fractions containing the product were identified by TLC, combined and the solvent removed under pressure.

NMR Spectroscopy

^{1}H, ^{13}C, NMR spectra were recorded on a Bruker AVANCE 500 spectrometer (500 MHz and 75 MHz respectively) and auto calibrated to the deuterated solvent reference peak. Chemical shifts are given in δ relative to tetramethylsilane (TMS); the coupling constants (J) are given in Hertz. TMS was used as an internal standard (δ = 0 ppm) for ^{1}H NMR and $CDCl_3$ served as an internal standard (δ = 77.0 ppm) for ^{13}C NMR.

Melting Point

Melting points were determined on an electrothermal instrument, Griffin apparatus and are uncorrected.

Mass Spectroscopy

Low resolution mass spectra ES (Electrospray) were recorded on a Micro TOF LC Bruker Daltonic instrument, operating in a positive ion mode.

Microanalysis

Microanalysis data were performed by Medac Ltd., Brunel Centre, Surrey.

6.1.1 Molecular Modelling

Molecular Operating Environment (MOE) 2010.10 and the Maestro platform (Schrodinger version 9.0) were used as molecular modelling softwares.
All minimisations were performed with MOE until RMSD gradient of 0.001

Kcal mol^{-1} $Å^{-1}$ with the AMBER99 force field and the partial charges were automatically calculated.

Pharmacophoric filters were created within MOE 2010.10 choosing the PCH (polar-charged-hydrophobic) scheme.

Docking experiments were carried out with Glide SP mode in Maestro. All molecule databases used for virtual screening were processed with the LigPreP tool in Maestro which enables to make corrections, optimise or eliminate structures. Outputs generated were refined with Glide SP, 'refine-do not score' tool. All refined docking results were re-scored using Plants, FlexX and Glide XP scoring functions. Molecules were selected by a consensus scoring function which combines information from every docking analysis in order to balance errors in single scores. Three functions were searched for every set of docking score. The first quartile value which splits the lowest 25 % of data (negative energy values) representing the best values of the scoring results. The mathematical function sign was calculated in order to define whether a docked pose belongs to the best 25% for every scoring function. A value of '+1' was assigned if that docked pose is among the best 25% solutions and a value of '-1' if not. Finally, the three sign values, each one for every scoring function, was calculated in order to take into account only the ones with a sign sum equal to +3.

The shape-comparison screening was performed with vROCS version 3.1.2. Both shape and colour screen criteria were applied to the query. Output conformations were ranked by the Tanimoto Combo score and the Shape Tanimoto score.

6.2 Synthesis of tetrazole derivatives

6.2.1 General procedures 1-5

General procedure 1: synthesis of aryl isothiocyanates

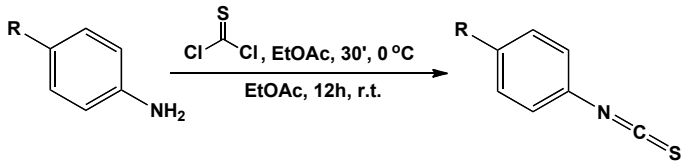

A solution of aryl aniline (1 eq.) and triethylamine (2.2 eq.) in ethyl acetate (5.9 mL/mmol eq.) was treated with thiophosgene (1.09 eq.) in ethyl acetate (4.4 mL/mmol eq.), dropwise over 30 min at 0ºC. After the addition, the cooling bath was removed and the reaction mixture was allowed to gradually warm up to room temperature over 12 h. The reaction mixture was diluted with ethyl acetate, then washed with water (2 x 6.6 mL/mmol eq.) and brine (2 x 6.6 mL/mmol eq.). The organic layer was evaporated at reduced pressure after drying over $MgSO_4$ and the product was purified by flash column chromatography or obtained as pure aryl isothiocyanate.

General procedure 2: synthesis of aryl mercaptotetrazoles

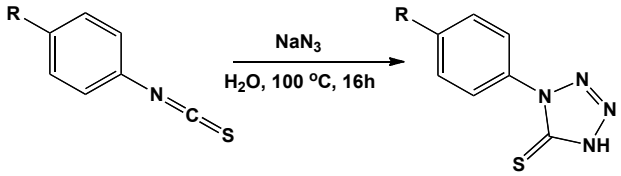

To a sodium azide (3 eq.) solution in water (2 mL/mmol eq.), was added the aryl isothiocyanate (1 eq.). The reaction mixture was heated at 100 ºC for 16 h. The reaction was quenched in an ice-bath with 0.1 M HCl to pH 1 and then extracted with EtOAc (2 x 3.3 mL/mmol eq.). The organic layer was evaporated at reduced pressure after drying over $MgSO_4$ and the product was purified by flash column chromatography or recrystallisation to afford pure 1-aryl mercaptotetrazoles.

General procedure 3: synthesis of (benzylthio)-1-aryl-1*H*-tetrazoles

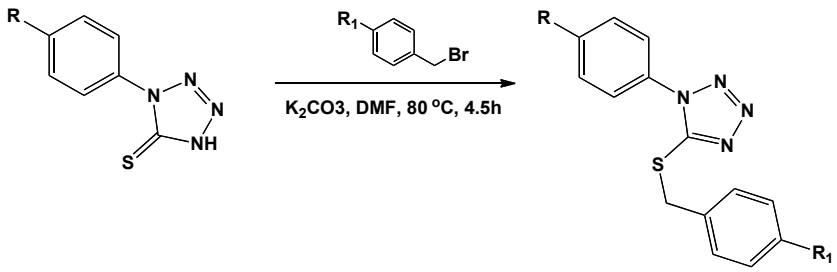

To a mixture of 1-aryl mercaptotetrazole (1 eq.) and K_2CO_3 (1.5 eq.) in dry DMF (3.66 mL/mmol eq.) was added the benzyl bromide (1 eq.) and the reaction was stirred under N_2 at 80°C for 4.5 h. Upon completion, the reaction was suspended in H_20 (2x 10.5 mL/mmol eq.), brine (2x 10.5 mL/ mmol eq.) and dried over $MgSO_4$. The organic layer was removed at reduced pressure and then purified by flash column chromatography or recrystallization to afford the pure 5-(benzylthio)-1-aryl-1H-tetrazole.

General procedure 4: synthesis of (5-(benzylthio)-1*H*-tetrazol-1-*yl*)benzoic acids

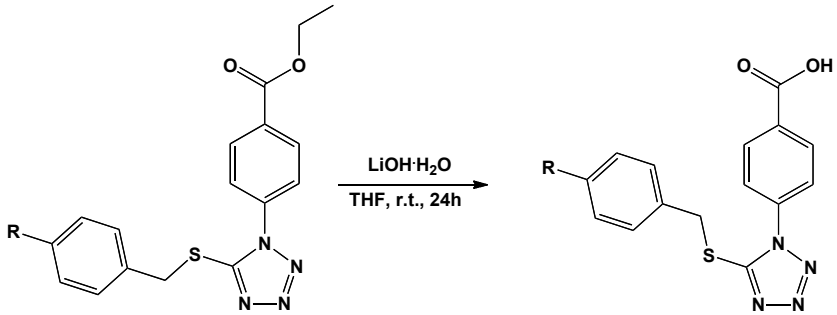

5-(Benzylthio)-1-aryl-1*H*-tetrazole (1 eq.) in THF (36.4 mL/mmol eq.) was treated with LiOH monohydrate (7.26 eq., 0.3 g in 17 mL of water). The mixture was stirred at room temperature for 24 h. Upon completion, the organic solvent was removed at reduced pressure and the residue was washed with EtOAc (2 x 33 mL/mmol eq.). The aqueous layer, cooled in an ice bath, was acidified with 3M HCl to pH 1-2 and stirred until the formation of a white precipitate. The precipitate was filtrated and dried to afford the pure product.

General procedure 5: synthesis of ethyl 4-(5-(benzylthio)-1*H*-tetrazol-1-*yl*)benzoates

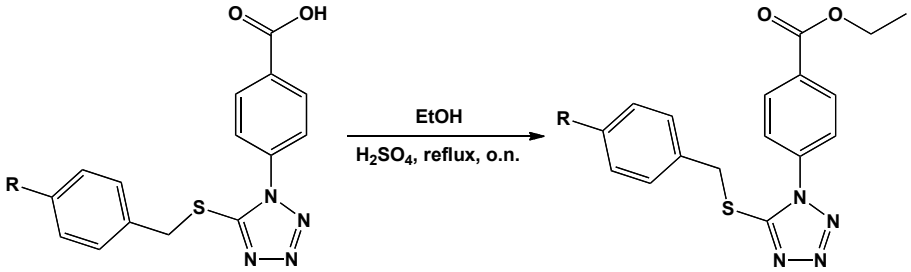

A solution of 4-(5-benzylthio)-1*H*-tetrazol-1-yl)benzoic acid (1eq.) in EtOH (15.4 mL/mmol eq) was treated with sulphuric acid (1.15 mL/mmol eq.) at reflux, overnight. Upon completion, the solvent was removed at reduced pressure and the residue was dissolved in ethyl acetate and saturated aqueous $NaHCO_3$ solution. The combined organic layers were washed with $NaHCO_3$ sat. (2 x 40 mL/mmol eq.) and water (2 x 40 mL/mmol eq.), dried over $MgSO_4$ and concentrated at reduced pressure to afford the pure products.

6.2.2 Aryl isothiocyanates (7-11)

Ethyl-4-isothiocyanatobenzoate (7)[1]
($C_{10}H_9NO_2S$; M.W.= 207.25)

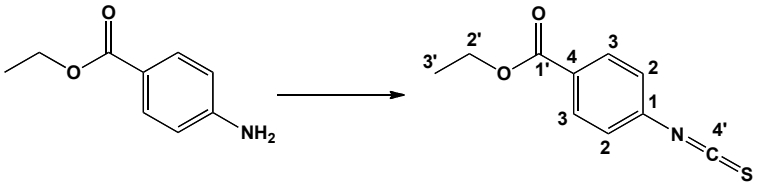

2 7

General procedure: 1;
Reagent: Ethyl 4-aminobenzoate **2** (1 g, 6 mmol);
T.L.C. System: *n*-hexane -EtOAc 9:1 v/v, Rf: 0.43;
Yellow crystals;
Yield: 1.24 g, 99%

^{1}H-NMR ($CDCl_3$), δ: 1.42 (t, J= 7.1 Hz, 3H, H-3'), 4.40 (q, J= 7.1 Hz, 2H, H-2'), 7.29 (d, J= 8.7 Hz, 2H, H-aromatic), 8.06 (d, J= 8.7 Hz, 2H, H-aromatic).

^{13}C-NMR ($CDCl_3$), δ: 14.29 (CH_3, C-3'), 61.32 (CH_2, C-2'), 125.60 (CH, C-aromatic), 129.10 (C, C-aromatic), 131.01 (CH, C-aromatic), 136.9 (C, C-aromatic), 146.9 (C, C-4'), 165.9 (C, C-1').

1-Isothiocyanato-4-nitrobenzene (8)[2]
($C_7H_4N_2O_2S$; M.W.= 180.18)

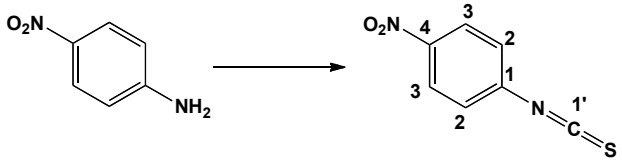

3 8

General procedure 1;
Reagent: 4-nitroaniline **3** (1 g, 7.24 mmol)
T.L.C. System: *n*-hexane -EtOAc 8:2 v/v, Rf: 0.83;
Yellow solid;
Purification by flash column chromatography (*n*-hexane:EtOAc 100:0 v/v, increasing to 96:4 v/v);

Yield: 1.17 g, 90 %

^{1}H-NMR ($CDCl_3$), δ: 7.37 (d, J= 2.1 Hz, 2H, H-aromatic), 8.27 (d, J= 2.1 Hz, 2H, H-aromatic).

^{13}C-NMR ($CDCl_3$), δ: 125.27, 126.35 (CH, C-aromatic), 129.10 (C, C1), 136.9 (C, C-aromatic), 146.9 (C, C-aromatic).

1-Isothiocyanato-4-methylbenzene (9)[3]
(C_8H_7NS; M.W.= 149.21)

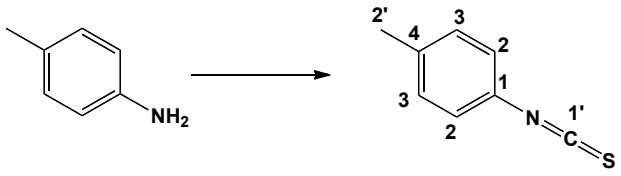

4 **9**

General procedure 1;
Reagent: toluidine **4** (1 g, 9.33 mmol);
T.L.C. System: *n*-hexane -EtOAc 95:5 v/v, Rf: 0.9;
Brown oleum;
Yield: 1.26 g, 90.6 %

^{1}H-NMR ($CDCl_3$), δ: 2.37 (s, 3H, H-aliphatic), 7.15 (d, J= 8.4 Hz, 2H, H-aromatic), 7.17 (d, J= 8.4 Hz, 2H, H-aromatic).

^{13}C-NMR ($CDCl_3$), δ: 21.41 (CH_3, C-2'), 125.86 (CH, C-aromatic), 129.90 (C, C-4), 137.53 (C, C-1), 146.9 (C, C-1').

1-Isothiocyanato-4-methoxybenzene (10)[4]

(C_8H_7NOS; M.W.= 165.21)

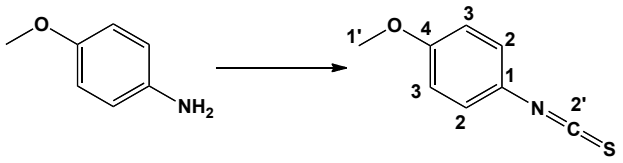

5 **10**

General procedure 1;
Reagent: 4-methoxyaniline **5** (1 g, 8.12 mmol);
T.L.C. System: *n*-hexane -EtOAc 9:1 v/v, Rf: 0.3;
Brown oleum;
Yield: 1.32 g, 98.5 %

^{1}H-NMR ($CDCl_3$), δ: 3.82 (s, 3H, H-1'), 6.86 (d, J= 9.0 Hz, 2H, H-aromatic), 7.18 (d, J= 9.0 Hz, 2H, H-aromatic).

^{13}C-NMR ($CDCl_3$), δ: 55.51 (CH_3, C-1'), 114.23 (CH, C-aromatic), 123.53 (C, C-aromatic), 125.06, 126.48 (CH, C-aromatic), 133.77 (C, C-aromatic), 158.58 (C, C-2').

4-Isothiocyanatophenol (11)[5]

(C_7H_5NOS; M.W.= 151.19)

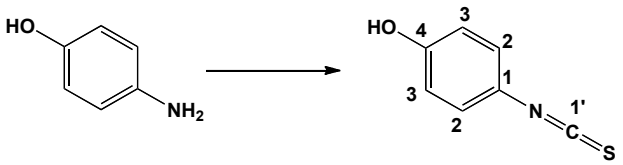

6 **11**

p-Aminophenol **6** (1 g, 9.16 mmol) was stirred with 1M HCl (11 mL) and thiophosgene (0.7 mL, 9.16 mmol) was added dropwise. The mixture was stirred at r.t. for 7 h. The oily product was extracted with diethyl ether (2 x 15 mL) and dichloromethane (2 x 15 mL). The organic layer was dried under $MgSO_4$ to afford the pure product 4-isothiocyanatophenol as brown oleum.

T.L.C. System: EtOAc-MeOH 8:2 v/v, Rf: 0.45;

Yield: 1.37 g, 99 %

^{1}H-NMR ($CDCl_3$), δ: 6.65 (bs, OH), 6.82 (d, J= 8.9 Hz, 2H, H-aromatic), 7.10 (d, J= 8.9 Hz, 4H, H-aromatic).

^{13}C-NMR ($CDCl_3$), δ: 116.40 (CH, C-aromatic), 123.34 (C, C-aromatic), 126.49 (CH, C-aromatic), 133.77, 152.29 (C, C-1').

6.2.3 Aryl mercaptotetrazoles (12-16)

Ethyl 4-(5-thioxo-4,5-dihydro-1*H*-tetrazol-1-*yl*)benzoate (12)
($C_{10}H_{10}N_4O_2S$; M.W.= 250.28)

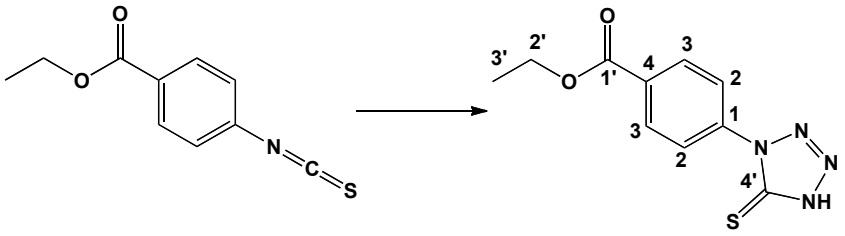

7 **12**

General procedure 2;
Reagent: ethyl 4-isothiocyanatobenzoate **7** (1.24 g, 5.98 mmol);
T.L.C. System: EtOAc-MeOH 9:1 v/v, Rf: 0.4;
Yellow solid;
Purification: flash column chromatography (*n*-n-hexane:EtOAc 100:0 v/v increasing to 50:50 v/v);
Yield: 0.6 g, 40%

^{1}H-NMR ($CDCl_3$), δ: 1.45 (t, J= 7.2 Hz, 3H, H-3'), 4.46 (q, J= 7.2 Hz, 2H, H-2'), 8.20 (d, J= 8.7 Hz, 2H, H-aromatic), 8.27 (d, J= 8.7 Hz, 2H, H-aromatic), 13.2 (bs, H, N<u>H</u>).

^{13}C-NMR ($CDCl_3$), δ: 14.48 (CH_3, C-3'), 61.51 (CH_2, C-2'), 125.76 (C, C-aromatic), 125.79 (CH, C-aromatic), 129.27 (C, C-aromatic), 131.13, (CH, C-aromatic), 166.0, 174.50 (C, C-1', C-4').

1-(4-Nitrophenyl)-1*H*-tetrazole-5(4*H*)-thione (13)[6]
($C_7H_5N_5O_2S$; M.W.= 223.21)

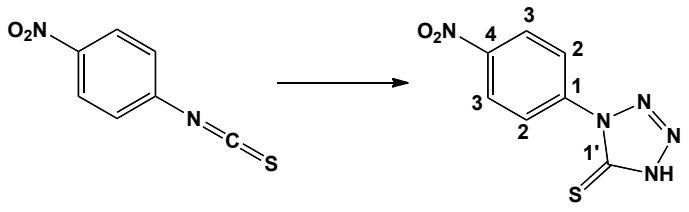

8 **13**

General procedure 2;
Reagent: 1-isothiocyanato-4-nitrobenzene **8** (1.17 g, 6.5 mmol);
T.L.C. System: EtOAc-MeOH 9:1 v/v, Rf: 0.46;
Orange solid;
Purification: flash column chromatography (*n*-hexane:EtOAc 100:0 v/v increasing to 50:50 v/v);
Yield: 0.55 g, 38%

^{1}H-NMR (DMSO-d$_6$), δ: 8.35 (d, J= 9.1 Hz, 2H, H-aromatic), 8.45 (d, J= 9.1 Hz, 2H, H-aromatic).

^{13}C-NMR (DMSO-d$_6$), δ: 125.10, 125.17 (CH, C-aromatic), 138.98 (C, C-aromatic), 146.98 (C, C-aromatic), 164.12 (C, C-1').

1-(*p*-tolyl)-1*H*-tetrazole-5(4*H*)-thione (14)[7]
($C_8H_8N_4S$; M.W.= 192.24)

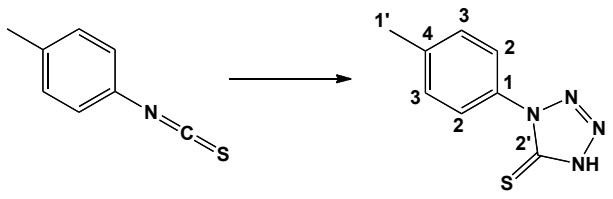

9 **14**

General procedure 2;
Reagent: 1-isothiocyanato-4-methylbenzene **9** (1.26 g, 8.44 mmol);
T.L.C. System: EtOAc-MeOH 9:1 v/v, Rf: 0.54;
White solid;
Purification: recrystallization from MeOH;
Yield: 0.94 g, 58%

^{1}H-NMR ($CDCl_3$), δ: 2.48 (s, 3H, H-1'), 7.40 (d, J= 8.4 Hz, 2H, H-aromatic), 7.81 (d, J= 8.4 Hz, 2H, H-aromatic), 13.98 (bs, N<u>H</u>).

^{13}C-NMR ($CDCl_3$), δ: 21.32 (CH_3, C-1'), 123.77 (CH, C-aromatic), 129.96 (CH, C-aromatic), 131.42 (C, C-aromatic), 140.32 (C, C-aromatic), 174.12 (C, C-1').

1-(4-Methoxyphenyl)-1*H*-tetrazole-5(4*H*)-thione (15)[8]

($C_8H_8N_4OS$; M.W.= 208.24)

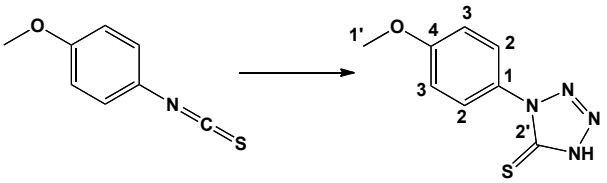

10 **15**

General procedure 2;
Reagent: 1-isothiocyanato-4-methoxybenzene **10** (1.32 g, 7.98 mmol);
T.L.C. System: EtOAc-MeOH 9:1 v/v, Rf: 0.59;
Brown oleum;
Yield: 1.16 g, 70 %

^{1}H-NMR ($CDCl_3$), δ: 3.91 (s, 3H, H-1'), 7.08 (d, J= 9.0 Hz, 2H, H-aromatic), 7.81 (d, J= 9.0 Hz, 2H, H-aromatic).

^{13}C-NMR ($CDCl_3$), δ: 55.68 (CH_3, C-1'), 114.53, 125.65 (CH, C-aromatic), 126.64 (C, C-aromatic), 160.52 (C, C-aromatic), 174.12 (C, C-2').

1-(4-Hydroxyphenyl)-1*H*-tetrazole-5(4*H*)-thione (16)

($C_7H_6N_4OS$; M.W.= 194.21)

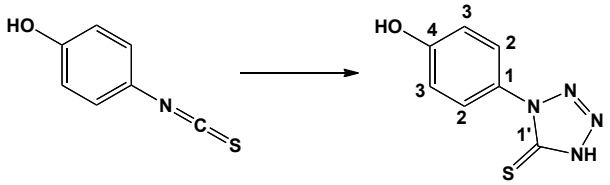

11 **16**

General procedure 2;
Reagent: 4-isothiocyanatophenol **11** (1.37 g, 9.06 mmol);
T.L.C. System: EtOAc-MeOH 9:1 v/v, Rf: 0.54;
White solid;
Purification: recrystallization from MeOH;
Yield: 1.37 g, 78 %

^{1}H-NMR (DMSO-d_6), δ: 6.94 (d, J= 8.8 Hz, 2H, H-aromatic), 7.60 (d, J= 8.8 Hz, 2H, H-aromatic), 10.05 (bs, NH).

^{13}C-NMR (DMSO-d_6), δ: 115.52 (CH, C-aromatic), 126.09 (C, C-aromatic), 126.31 (CH, C-aromatic), 158.40 (C, C-aromatic), 174.12 (C, C-1').

6.2.4 Benzylthio-1-aryl-1*H*-tetrazoles (20-25)

Ethyl 4-(5-(benzylthio)-4,5-dihydro-1*H*-tetrazol-1-*yl*)benzoate (20)
($C_{17}H_{18}N_4O_2S$; M.W.= 340.42)

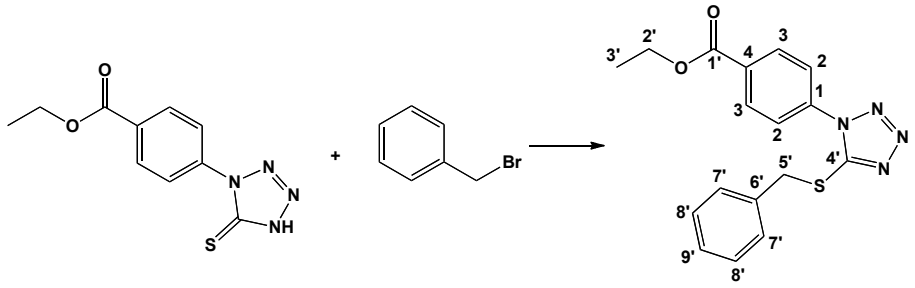

12 **17** **20**

General procedure 3;
Reagent: ethyl 4-(5-thioxo-4,5-dihydro-1*H*-tetrazol-1-yl)benzoate **12** (0.48 g, 1.9 mmol);
T.L.C. System: *n*-hexane -EtOAc: 5:5 v/v, Rf: 0.53;
Yellowish-brown oleum;
Purification: flash column chromatography (*n*-hexane:EtOAc 100:0 v/v, increasing to 80:20 v/v);
Yield: 0.53 g, 83 %

^{1}H-NMR ($CDCl_3$), δ: 1.43 (t, J= 7.1, 3H, H-3'), 4.44 (q, J= 7.1, 2H, H-2'), 4.66 (s, 2H, H-5'), 7.29-7.35 (m, 3H, H-aromatic), 7.43-7.44 (m, 2H, H-aromatic), 7.66 (d, J= 8.8 Hz, 2H, H-aromatic), 8.22 (d, J= 8.8 Hz, 2H, H-aromatic).

^{13}C-NMR ($CDCl_3$), δ: 14.28 (CH_3, C-3'), 37.89 (CH_2, C-2'), 61.61 (CH_2, C-5'), 114.53, 123.33, 128.33, 128.89 (CH, C-aromatic), 130.65 (C, C-aromatic), 131.11 (CH, C-aromatic), 135.05, 135.54, 153.96 (C, C-aromatic), 165.07 (C, C-1').

5-(Benzylthio)-1-(4-nitrophenyl)-4,5-dihydro-1*H*-tetrazole (21)
($C_{14}H_{13}N_5O_2S$; M.W.= 313.35)

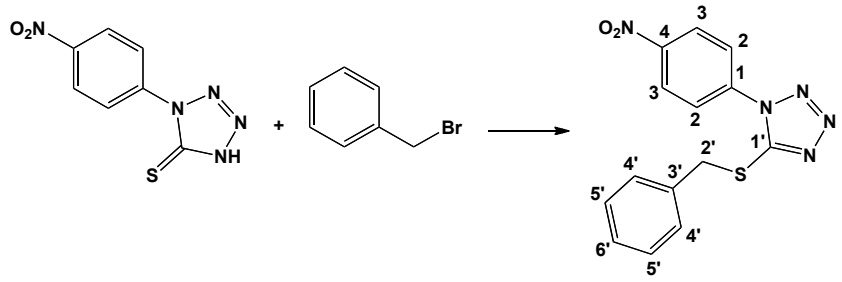

13 **17** **21**

General procedure 3;
Reagent: 1-(4-nitrophenyl)-1*H*-tetrazole-5(4*H*)-thione **13** (0.55 g, 2.46 mmol);
T.L.C. System: *n*-hexane -EtOAc: 7:3 v/v, Rf: 0.94;
Yellow solid;
Purification: recrystallization from MeOH;
Yield: 0.30 g, 38.9%;
Melting point: 69-72 °C;
MS $(ESI)^+$: 313.9 $[M+H]^+$

^{1}H-NMR ($CDCl_3$), δ: 4.70 (s, 2H, H-2'), 7.31-7.39 (m, 3H, H-aromatic), 7.44-7.46 (m, 2H, H-aromatic), 7.84 (d, J= 9.0 Hz, 2H, H-aromatic), 8.43 (d, J= 9.0 Hz, 2H, H-aromatic).

^{13}C-NMR ($CDCl_3$), δ: 38.14 (CH_2, C-2'), 124.10, 125.29, 128.46, 128.97, 129.27 (CH, C-aromatic), 134.77, 138.41, 148.00 (C, C-aromatic), 154.13 (C, C-1').

5-(Benzylthio)-1-(*p*-tolyl)-1*H*-tetrazole (22)

($C_{15}H_{14}N_4S$; M.W.= 282.36)

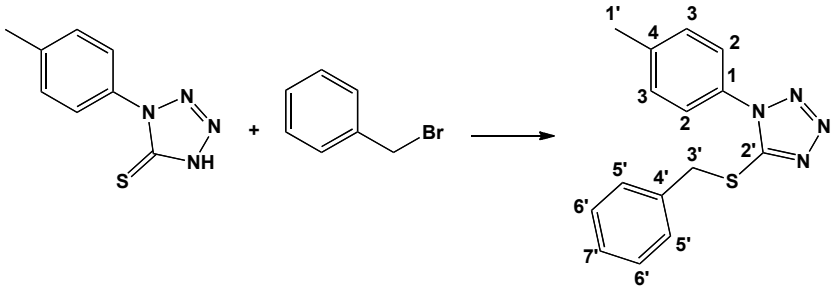

14 **17** **22**

General procedure 3;

Reagent: 1-(*p*-tolyl)-1*H*-tetrazole-5(4*H*)-thione **14** (0.1 g, 0.52 mmol);

T.L.C. System: *n*-hexane -EtOAc: 8:2 v/v, Rf: 0.5;

White solid;

Purification: flash column chromatography (*n*-hexane:EtOAc 100:0 v/v, increasing to 90:10 v/v);

Yield: 0.08 g, 57 %;

Melting point: 43-45 °C;

MS $(ESI)^+$: 282.9 $[M+H]^+$

^{1}H-NMR ($CDCl_3$), δ: 2.43 (s, 3H, H-1'), 4.62 (s, 2H, H-3'), 7.35-7.27 (m, 3H, H-aromatic), 7.41-7.36 (m, 2H, H-aromatic), 7.43-7.41 (m, 2H, H-aromatic).

^{13}C-NMR ($CDCl_3$), δ: 21.26 (CH_3, C-1'), 37.63 (CH_2, C-3'), 128.16, 128.48, 128.82, 129.56 (CH, C-aromatic), 130.30 (C, C-aromatic), 130.53 (CH, C-aromatic), 135.37, 140.54 (C, C-aromatic), 153.91 (C, C-2').

5-(Benzylthio)-1-(4-methoxyphenyl)-1*H*-tetrazole (23)
($C_{15}H_{14}N_4OS$; M.W.= 298.36)

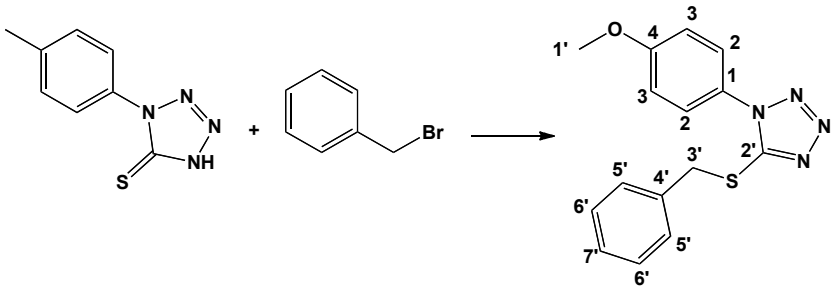

15 **17** **23**

General procedure 3;
Reagents: 1-(4-methoxyphenyl)-1*H*-tetrazole-5(4*H*)-thione **15** (1.16 g, 5.57 mmol);
T.L.C. System: *n*-hexane -EtOAc: 8:2 v/v, Rf: 0.3;
Red wax;
Purification: flash column chromatography (*n*-hexane:EtOAc 100:0 v/v, increasing to 70:30 v/v);
Yield: 0.993 g, 59.6 %;
Melting point: 34-36 °C;
MS $(ESI)^+$: 299.1 $[M+H]^+$

^{1}H-NMR ($CDCl_3$), δ: 3.87 (s, 3H, H-1'), 4.62 (s, 2H, H-3'), 7.02 (d, J= 6.9 Hz, 2H, H-aromatic), 7.30-7.35 (m, 3H, H-aromatic), 7.37-7.44 (m, 4H, H-aromatic).

^{13}C-NMR ($CDCl_3$), δ: 37.57 (CH_2, C-3'), 55.58 (CH_3, C-1'), 125,55 (CH, C-aromatic), 126.26 (C, C-aromatic), 127.59, 128.50, 128.84, 129.07 (CH, C-aromatic), 135.35, 154.07, 160.76 (C, C-aromatic).

Ethyl 4-(5-((4-methylbenzyl)thio)-1*H*-tetrazol-1-*yl*)benzoate (24)
($C_{18}H_{18}N_4O_2S$; M.W.= 354.43)

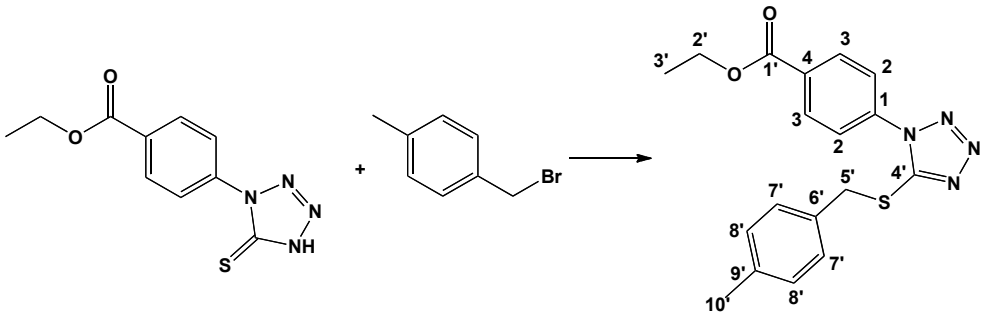

12 **18** **24**

General procedure 3;
Regent: 4-methylbenzyl bromide **17** (0.23 g, 1.2 mmol);
T.L.C. System: *n*-hexane -EtOAc: 8:2 v/v, Rf: 0.70;
White solid;
Purification: recrystallization from MeOH;
Yield: 0.20 g, 47.6 %;
Melting point: 65-68 ^{o}C;
MS $(ESI)^+$: 355.0 $[M+H]^+$

^{1}H-NMR ($CDCl_3$), δ: 1.43 (t, J= 7.0, 3H, H-3'), 4.43 (q, J= 7.0 Hz, 2H, H-2'), 4.61 (s, 2H, H-5'), 7.13-7.24 (m, 2H, H-aromatic), 7.30-7.38 (m, 2H, H-aromatic), 7.63-7.70 (m, 2H, H-aromatic), 8.19-8.25 (m, 2H, H-aromatic).

^{13}C-NMR ($CDCl_3$), δ: 14.1 (CH_3, C-3'), 21.3 (CH_3, C-10'), 34.7 (CH_2, C-5'), 60.9 (CH_2, C-2'), 122.5, 128.8, 129, 129.9 (CH, C-aromatic), 134.1 (C, C-aromatic), 134.27 (CH, C-aromatic), 135.0, 136.8, 137.4, 155.1 (C, C-aromatic), 165.07 (C, C-1').

Ethyl 4-(5-((4-chlorobenzyl)thio)-1*H*-tetrazol-1-*yl*)benzoate (25)
($C_{17}H_{15}ClN_4O_2S$; M.W.= 374.84)

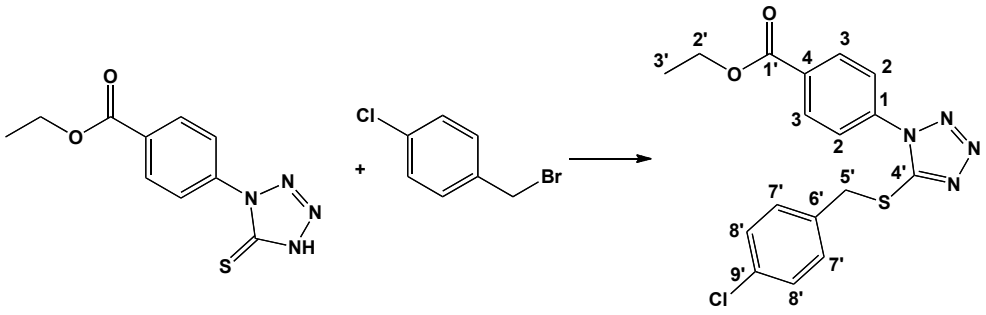

12 **19** **25**

General procedure 3;
Reagent: 1-(bromomethyl)-4-chlorobenzene,**19** (0.21 g, 1.03 mmol);
T.L.C. System: *n*-hexane -EtOAc: 8:2 v/v, Rf: 0.53;
White crystals;
Purification: recrystallization from MeOH;
Yield: 0.056 g, 15 %
Melting point: 160-163 ^{o}C
MS $(ESI)^{+}$: 375.1 $[M+H]^{+}$

^{1}H-NMR ($CDCl_3$), δ: 1.44 (t, J= 7.1, 3H, H-3'), 4.44 (q, J= 7.1 Hz, 2H, H-2'), 4.62 (s, 2H, H-5'), 7.31 (d, J= 8.4 Hz, 2H, H-aromatic), 7.40 (d, J= 8.4 Hz, 2H, H-aromatic), 7.66 (d, J= 8.6 Hz, 2H, H-aromatic), 8.23 (d, J= 8.6 Hz, 2H, H-aromatic).

^{13}C-NMR ($CDCl_3$), δ: 14.27 (CH_3, C-3'), 37.01 (CH_2, C-5'), 61.64 (CH_2, C-2'), 123.31, 129.05, 130.63, 131.16 (CH, C-aromatic), 131.87, 131.91, 133.76, 134.27, 136.88 (C, C-aromatic), 165.07 (C, C-1').

4-(5-(Benzylthio)-1*H*-tetrazol-1-*yl*)phenol (26)
($C_{14}H_{12}N_4OS$; M.W.= 284.34)

4-(5-((4-(benzyloxy)benzyl)thio)-1*H*-tetrazol-1-*yl*)phenol (27) ($C_{21}H_{18}N_4O_2S$; M.W.= 390.46)

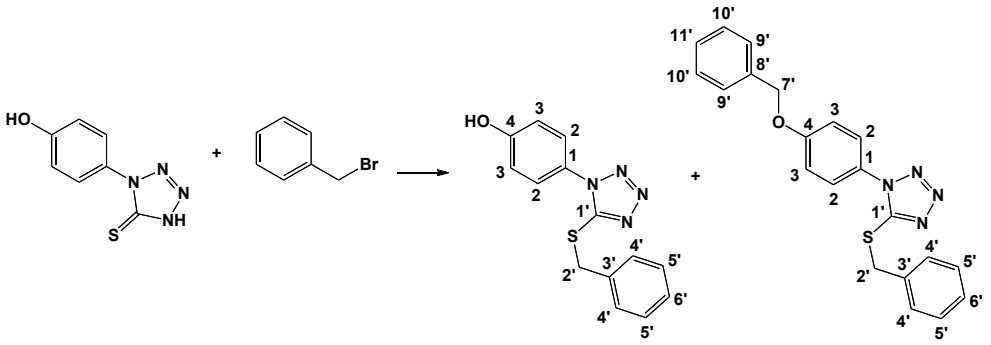

16 **17** **26** **27**

Compound 26:

General procedure 3;
Reagent: 1-(4-hydroxyphenyl)-1*H*-tetrazole-5(4*H*)-thione **16** (1.37 g, 7.05 mmol);
T.L.C. System: *n*-hexane -EtOAc: 7:3 v/v, Rf: 0.4;
White solid;
Purification: flash column chromatography (*n*-hexane:EtOAc 100:0 v/v, increasing to 85:15 v/v) and recrystallization from EtOAc/*n*-hexane;
Yield: 0.43 g, 21.5 %;
Melting point: 85-88 °C;
MS $(ESI)^+$: 284.9 $[M+H]^+$

^{1}H-NMR ($CDCl_3$), δ: 4.61 (s, 2H, H-2'), 6.91 (bs, OH), 7.06 (d, J= 6.4 Hz, 2H, H-aromatic), 7.27-7.46 (m, 7H, H-aromatic).

^{13}C-NMR ($CDCl_3$), δ: 37.64 (CH_2, C-2'), 116.63, 125.79 (CH, C-aromatic), 125.86 (C, C-aromatic), 128.25, 128.87, 129.20 (CH, C-aromatic), 135.06, 154.37, 157.88 (C, C-aromatic).

Compound 27:

General procedure 3;
Reagent: 1-(4-hydroxyphenyl)-1*H*-tetrazole-5(4*H*)-thione **16** (1.37 g, 7.05 mmol);
T.L.C. System: *n*-hexane -EtOAc, Rf: 0.75;
White solid;
Purification: flash column chromatography (*n*-hexane:EtOAc 100:0 v/v, increasing to 75:25 v/v);
Yield: 0.77 g, 28.5 %;
Melting point: 65-68 ^{o}C;
MS (ESI)$^{+}$: 390.9 $[M+H]^{+}$

^{1}H-NMR ($CDCl_3$), δ: 4.63 (s, 2H, H-2'), 5.14 (s, 2H, H-7'), 7.10 (d, J= 7.4 Hz, 2H, H-aromatic), 7.31-7.40 (m, 4H, H-aromatic), 7.41-7.47 (m, 8H, H-aromatic).

^{13}C-NMR ($CDCl_3$), δ: 37.62 (CH_2, C-2'), 70.45 (CH_2, C-7'), 115.76, 125.54 (CH, C-aromatic), 126.53 (C, C-aromatic), 127.48, 128.17, 128.33, 128.75, 128.84, 129.23 (CH C-aromatic), 135.35, 136.07, 154.37, 159.92 (C, C-aromatic).

6.2.5 (5-(Benzylthio)-1*H*-tetrazol-1-*yl*)benzoic acids (1, 28, 29)

4-(5-(Benzylthio)-1*H*-tetrazol-1-*yl*)benzoic acid (1)
($C_{15}H_{12}N_4O_2S$; M.W.= 312.35)

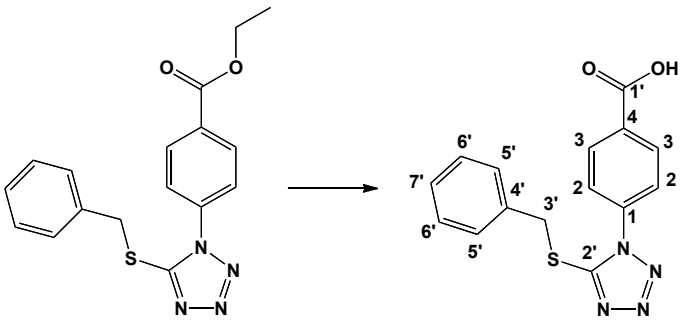

20 **1**

General procedure 4;
Reagent: ethyl 4-(5-(benzylthio)-1*H*-tetrazol-1-*yl*)benzoate **20** (0.32 g, 0.94 mmol);
T.L.C. System: *n*-hexane-EtOAc: 9:1 v/v, Rf: 0.17;
White crystals;
Yield: 0.0942 g, 31.6 %;
Melting point: 149-152 °C;
MS $(ESI)^+$: 312.9 $M+H]^+$

^{1}H-NMR ($CDCl_3$), δ: 4.69 (s, 2H, H-3'), 7.31-7.39 (m, 3H, H-aromatic), 7.74 (d, J= 8.8 Hz, 2H, H-aromatic), 7.45 (d, J= 5.4, 2H, H-aromatic), 8.29 (d, J= 8.8 Hz, 2H, H-aromatic).

^{13}C-NMR ($CDCl_3$), δ: 37.97 (CH_2, C-3'), 123.43, 128.35, 128.92, 129.26 (CH, C-aromatic), 130.30 (C, C-aromatic), 131.80 (CH, C-aromatic), 134.97, 137.79, 153.99 (C, C-aromatic), 168.07 (C, C-1').

4-(5-((4-Methylbenzyl)thio)-1*H*-tetrazol-1-*yl*)benzoic acid (28)
($C_{16}H_{14}N_4O_2S$; M.W.= 326.37)

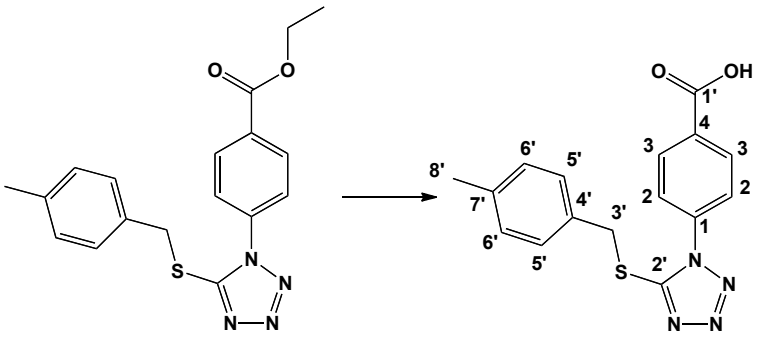

24 **28**

General procedure 4;
Reagent: ethyl 4-(5-((4-methylbenzyl)thio)-1*H*-tetrazol-1-*yl*)benzoate **24** (0.2 g, 0.57 mmol);
T.L.C. System: DCM-MeOH: 9:1 v/v, Rf: 0.14;
White solid;
Yield: 0.064 g, 34 %;
Melting point: 163-165 °C;
MS $(ESI)^+$: 327.1 $[M+H]^+$

^{1}H-NMR (DMSO-d_6), δ: 2.27 (s, 3H, H-8'), 4.58 (s, 2H, H-3'), 7.12 (d, J= 2.0, 2H, H-aromatic), 7.31 (d, J= 2.0, 2H, H-aromatic), 7.74 (d, J=1.9 Hz, 2H, H-aromatic), 8.16 (d, J= 1.9 Hz, 2H, H-aromatic), 13.38 (bs, 1H, -COO<u>H</u>).

^{13}C-NMR (DMSO-d_6), δ: 20.67 (CH_3, C-8'), 36.68 (CH_2, C-3'), 124.35, 129.02, 129.10, 130.87 (CH, C-aromatic), 132.35, 132.84, 136.23, 137.16, 153.97 (C, C-aromatic), 166.11 (C, C-1').

4-(5-((4-Chlorobenzyl)thio)-1*H*-tetrazol-1-*yl*)benzoic acid (29)
($C_{15}H_{11}ClN_4O_2S$; M.W.= 346.03)

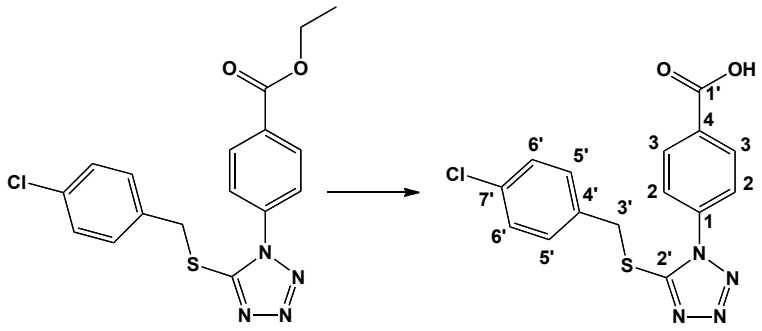

25 **29**

General procedure 4;
Reagent: ethyl 4-(5-((4-chlorobenzyl)thio)-1*H*-tetrazol-1-*yl*)benzoate **25** (0.046 g, 0.11 mmol);
T.L.C. System: DCM-MeOH: 9:1 v/v, Rf: 0.38;
White solid;
Yield: 0.013 g, 33 %;
Melting point: 102-104 °C;
MS $(ESI)^+$: 347.1 $[M+H]^+$

^{1}H-NMR (DMSO-d_6), δ: 4.62 (s, 2H, H-3'), 7.39 (d, J= 8.4, 2H, H-aromatic), 7.48 (d, J= 8.4, 2H, H-aromatic), 7.76 (d, J= 8.7 Hz, 2H, H-aromatic), 8.16 (d, J= 8.7 Hz, 2H, H-aromatic), 13.45 (bs, 1H, -COO<u>H</u>).

^{13}C-NMR (DMSO-d_6), δ: 35.90 (CH_2, C-3'), 124.40, 128.48 (CH, C-aromatic), 130.2 (C, C-aromatic), 130.89, 131.00 (CH, C-aromatic), 132.84, 135.39, 137.16, 155.1 (C, C-aromatic), 166.11 (C, C-1').

6.2.6 Ethyl 4-(5-(benzylthio)-1*H*-tetrazol-1-*yl*)benzoates (30, 31)

Ethyl 4-(5-(benzylthio)-1*H*-tetrazol-1-*yl*)benzoate (30)
($C_{17}H_{16}N_4O_2S$; M.W.= 340.40)

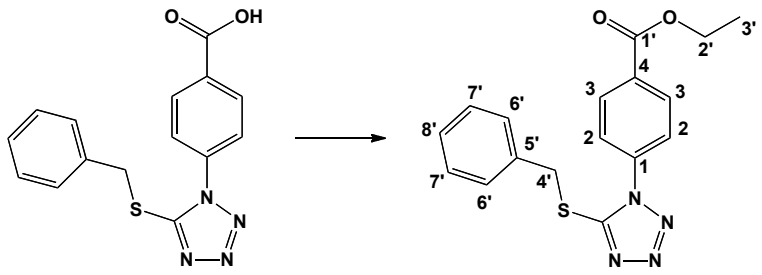

1 **30**

General procedure 5;
Reagent: 4-(5-(benzylthio)-1*H*-tetrazol-1-*yl*)benzoic acid **1** (0.08 g, 0.26 mmol);
T.L.C. System: *n*-hexane -EtOAc: 5:5 v/v, Rf: 0.79;
Brown oleum;
Yield: 0.07 g, 87.5 %;
Melting point: 33-35 °C;
MS (ESI)$^+$: 340.9 $[M+H]^+$

^{1}H-NMR ($CDCl_3$), δ: 1.44 (t, J= 7.1 Hz, 3H H-3'), 4.44 (q, J= 7.1 Hz, 2H, H-2'), 4.67 (s, 2H, H-4'), 7.3-7.38 (m, 3H, H-aromatic), 7.45 (d, J= 6.9, 2H, H-aromatic), 7.67 (d, J= 8.8 Hz, 2H, H-aromatic), 8.23 (d, J= 8.8 Hz, 2H, H-aromatic).

^{13}C-NMR ($CDCl_3$), δ: 14.27 (CH_3, C-3'), 37.90 (CH_2, C-2'), 61.62 (CH_2, C-4'), 123.32, 128.31, 128.90, 129.25, 131.11 (CH, C-aromatic), 131.88, 135.04, 137.4, 155.4 (C, C-aromatic), 165.9 (C, C-1').

Ethyl 4-(5-((4-methylbenzyl)thio)-1*H*-tetrazol-1-*yl*)benzoate (31)
($C_{18}H_{18}N_4O_2S$; M.W.= 354.43)

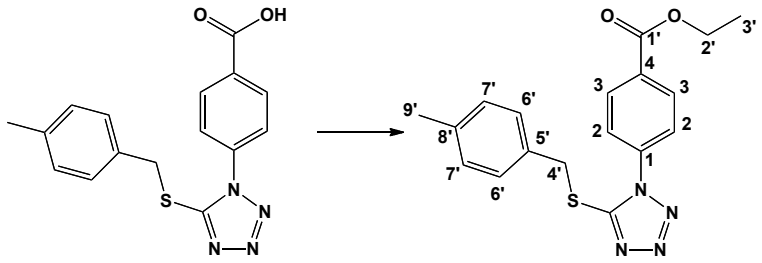

28 **31**

General procedure 5;
Reagent: 4-(5-((4-methylbenzyl)thio)-1*H*-tetrazol-1-*yl*)benzoic acid **29** (0.06 g, 0.18 mmol);
T.L.C. System: *n*-hexane -EtOAc: 5:5 v/v, Rf: 0.81;
White solid;
Yield: 0.016 g, 25.8 %;
Melting point: 65-68 °C;
MS $(ESI)^+$: 355.0 $[M+H]^+$

^{1}H-NMR ($CDCl_3$), δ: 1.44 (t, J= 7.2 Hz, 3H H-3'), 2.35 (s, 3H, H-9'), 4.44 (q, J= 7.2 Hz, 2H, H-2'), 4.64 (s, 2H, H-4'), 7.16 (d, J= 7.9, 2H, H-aromatic), 7.33 (d, J= 7.9, 2H, H-aromatic), 7.67 (d, J= 9.0 Hz, 2H, H-aromatic), 8.22 (d, J= 9.0 Hz, 2H, H-aromatic).

^{13}C-NMR ($CDCl_3$), δ: 14.30 (CH_3, C-3'), 21.19 (CH_3, C-9'), 37.70 (CH_2, C-2'), 61.64 (CH_2, C-4'), (123.29, 129.19, 129.58, 131.11 (CH, C-aromatic), 131.80, 131.91, 137.01, 138.24 , 155.1 (C, C-aromatic), 165.12 (C, C-1').

6.3 Synthesis of 2,5-bis-Aryl-1,3,4-oxadiazoles

6.3.1 General procedures 6-7

General procedure 6: synthesis of aryl acetohydrazide derivatives (38, 39)

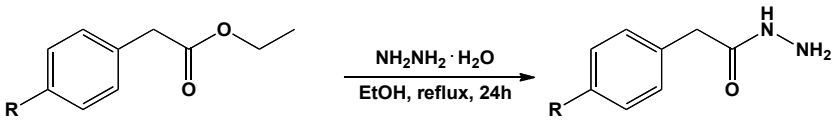

A mixture of arylacetic acid ester (1eq.) and hydrazine monohydrate (3 eq.) was refluxed in EtOH (2.9 mL/mmol eq.) for 24 hours. The mixture was cooled down and put in an ice-bath. The solid separated was filtered and used without further purification.

General procedure 7: 2,5-bis-aryl-1,3,4-oxadiazoles (32, 40)

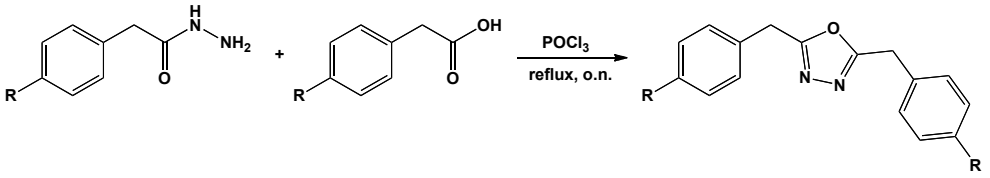

Aryl acetohydrazide (**36, 37**), (1 eq.) and arylacetic acid (**38, 39**) (1 eq.) were dissolved in phosphoryl chloride (8.3 mL/mmol eq.) and heated at reflux over night. The solvent was removed under reduced pressure and the residue was recrystallized to obtain the final product.

6.3.2 2-Phenylacetic acid (39)[9]

($C_8H_8O_2$; M.W.= 136.05)

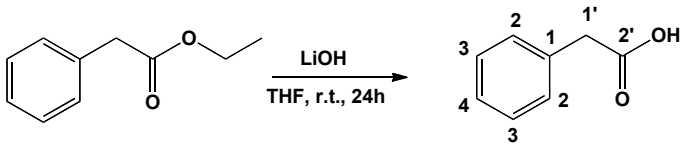

42 **39**

Ethyl 2-phenylacetate **39** (1.08 g, 6.6 mmol) in THF (50 mL) was treated with LiOH monohydrate (2.01 g in 110 mL of water, 48 mmol). The mixture was stirred at room temperature for 24 h. Upon completion, the organic solvent was removed under reduced pressure. The residue was washed with EtOAc (2 x 30 mL). The aqueous layer, cooled in a ice bath, was acidified with 3M HCl to pH 1-2 and stirred until the formation of a white precipitate that was filtrated and dried to afford the pure product.

T.L.C. System: DCM-MeOH: 9:1 v/v, Rf: 0.55;
White solid;
Yield: 0.8 g, 88.8 %;

^{1}H-NMR ($CDCl_3$), δ: 3.68 (s, 2H, H-1'), 7.29-7.34 (m, 3H, H-aromatic), 7.35-7.39 (m, 2H, H-aromatic), 11.1 (bs, 1H, -COO<u>H</u>).

^{13}C-NMR ($CDCl_3$), δ: 41.04 (CH_2, C-1'), 127.37, 128.66, 129.38 (CH, C-aromatic), 133.27 (C, C-1), 177.75 (C, C-2').

6.3.3 Ethyl 2-(4-nitrophenyl)acetate (41)[10]

($C_{10}H_{11}NO_4$; M.W.= 209.20)

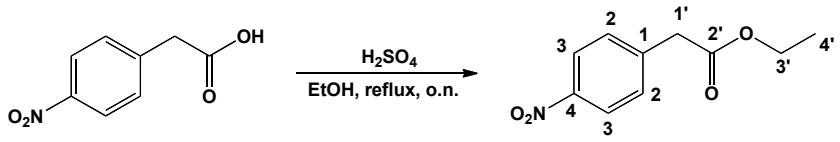

38 **41**

A solution of the 4-nitrophenylacetic acid **39** (0.5g, 2.7 mmol) in ethanol (41.5 mL) was treated with sulphuric acid (6.3 mL) at reflux for 24 h. The reaction was concentrated in vacuo. The residue was dissolved in ethyl

acetate (20 mL) and washed with saturated aqueous bicarbonate solution (3 x 20 mL) and water (3 x 20 mL). The organic ayer was dried over $MgSO_4$, filtered and concentrated in vacuo to give ethyl 2-(4-nitrophenyl)acetate without further purification.

T.L.C. System: *n*-hexane -EtOAc: 5:5 v/v, Rf: 0.54;
White solid;
Yield: 0.29 g, 51.4 %;

^{1}H-NMR ($CDCl_3$), δ: 1.28 (t, J= 7.1, 3H, H 4'), 3.78 (s, 2H, H-1'), 4.20 (q, J= 7.1 Hz, 2H, H-3'), 7.48 (d, J= 8.6 Hz, 2H, H-aromatic), 8.21 (d, J= 8.6 Hz, 2H, H-aromatic).

^{13}C-NMR ($CDCl_3$), δ: 14.12 (CH_3, C-4'), 41.08 (CH_2, C-1'), 61.38 (CH_2, C-3'), 123.73, 130.27 (CH, C-aromatic), 141.45 (C, C-1), 147.22 (C, C-4), 170.16 (C, C-2').

6.3.4 Aryl acetohydrazides (36, 37)

2-(4-Nitrophenyl)acetohydrazide (36)[11]
($C_8H_9N_3O_3$; M.W.= 195.18)

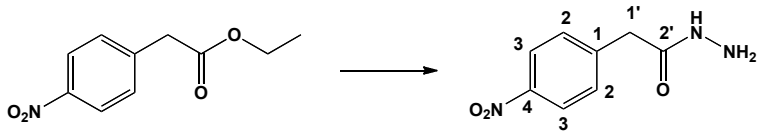

41 **36**

General procedure 6;
Reagent: Ethyl 2-(4-nitrophenyl)acetate **41** (0.3 g, 1.4 mmol);
T.L.C. System: *n*-hexane -EtOAc: 5:5 v/v, Rf: 1;
White solid;
Yield: 0.16 g, 62 %;

^{1}H-NMR (DMSO-d_6), δ: 3.53 (s, 2H, H-1'), 4.26 (bs, 2H, N<u>H</u>$_2$), 7.54 (d, J= 8.8 Hz, 2H, H-aromatic), 8.18 (d, 2H, J= 8.8 Hz, H-aromatic), 9.31 (bs, 1H, N<u>H</u>).

^{13}C-NMR (DMSO-d_6), δ: 40.11 (CH_2, C-1'), 123.28, 130.25 (CH, C-aromatic), 144.31 (C, C-1), 147.22 (C, C-4), 168.34 (C, C-2').

2-Phenylacetohydrazide (37)[12]
($C_8H_{10}N_2O$; M.W.= 150.18)

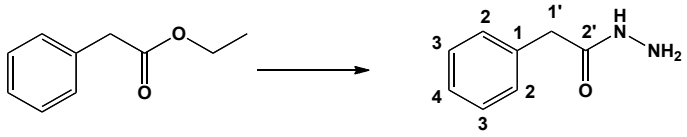

42 **37**

General procedure 6;
Reagent: Ethyl phenylacetate **42** (0.94 mL, 6.6 mmol);
T.L.C. System: *n*-hexane -EtOAc: 5:5 v/v, Rf: 1;
White foam;
Yield: 0.251 g, 25.3 %;

^{1}H-NMR ($CDCl_3$), δ: 3.58 (s, 2H, H-1'), 3.86 (bs, 2H, N<u>H</u>$_2$), 6.75 (bs, 1H, N<u>H</u>), 7.25-7.40 (m, 5H, H-aromatic).

^{13}C-NMR ($CDCl_3$), δ: 41.90 (CH_2, C-1'), 127.49, 129.01, 129.36 (CH, C-aromatic), 134.00 (C, C-1), 171.68 (C, C-2').

6.3.5 2,5-bis-Aryl-1,3,4-oxadiazoles (32, 40)

2,5-bis(4-Nitrobenzyl)-1,3,4-oxadiazole (32)
($C_{16}H_{12}N_4O_5$; M.W.= 340.29)

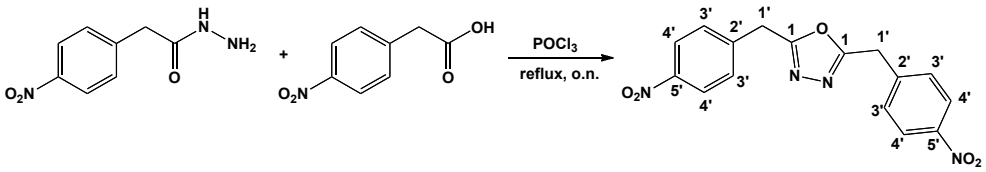

36 **38** **32**

General procedure 7;
Reagent: 4-nitro phenyl acetic acid **36** (0.160 g, 0.82 mmol);
T.L.C. System: *n*-hexane -EtOAc: 5:5 v/v, Rf: 0.44;
Brownish solid;
Purification: recrystallization from EtOH;
Yield: 0.15 g, 53.2 %;
Melting point: 129-131 °C;
MS $(ESI)^+$: 341.1 $[M+H]^+$

^{1}H-NMR ($CDCl_3$), δ: 4.30 (s, 4H, H-1'), 7.49 (d, 4H, J= 8.6 Hz, H-aromatic), 8.22 (d, 4H, J= 8.6 Hz, H-aromatic).

^{13}C-NMR ($CDCl_3$), δ: 31.53 (CH_2, C-1'), 124.17, 129.84 (CH, C-aromatic), 140.60 (C, C-2'), 147.60 (C, C-5'), 164.76 (C, C-1).

2,5-Dibenzyl-1,3,4-oxadiazole (41)[13]
($C_{16}H_{14}N_2O$, M.W.=250.30)

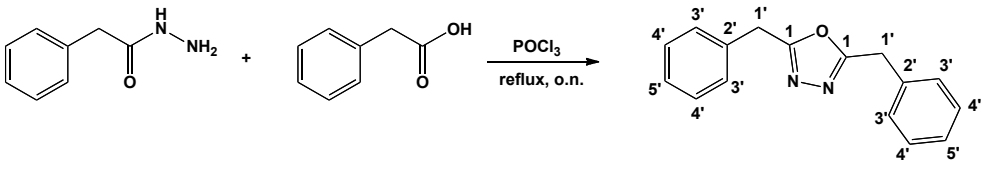

37 **39** **40**

General procedure 7;
Reagent: phenyl acetic acid **40** (0.66 g, 4.84 mmol);
T.L.C. System: *n*-hexane -EtOAc: 5:5 v/v, Rf: 0.66;

White solid;
Purification: recrystallization from EtOH/H_20 ;
Yield: 0.65 g, 54 %;
Melting point: 92-94 ^oC; (lit. 97-99 ^oC)
MS $(ESI)^+$: 251.1 $[M+H]^+$

^{1}H-NMR ($CDCl_3$), δ: 4.16 (s, 4H, H-1'), 7.27-7.32 (m, 6H, H-aromatic), 7.33-7.37 (m, 4H, H-aromatic).

^{13}C-NMR ($CDCl_3$), δ: 31.79 (CH_2, C-1'), 127.51, 128.57, 128.63, 128.69, 128.80, 128.87, 129.19 (CH, C-aromatic), 133.85 (C, C-2'), 165.83 (C, C-1).

6.4 1,3-bis-Aryl-1*H*-benzo[*d*]imidazol-2(3*H*)-ones (34, 46)

6.4.1 General procedure 8: synthesis of 1,3 -bis-aryl-1*H*-benzo[*d*]imidazol-2(3*H*)-ones

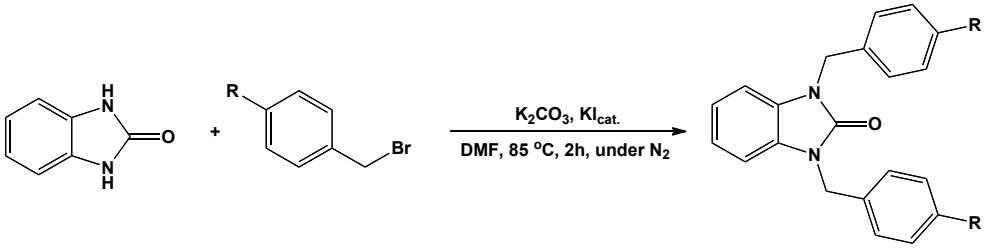

Aryl bromide (1.97 eq.), K_2CO_3 (5.5 eq.) and a catalytic amount of KI were added to a solution of benzoimidazol-2-one (1 eq.) in anhydrous DMF (2.01 mL/mmol eq.) under nitrogen atmosphere. The reaction mixture was heated at 85ºC for 4h. After cooling, the mixture was poured in a solution of water (39.8 mL) and 2N HCl in water (1.8 mL/mmol eq.). The resultant mixture was extracted with ethyl acetate (2x 4.5 mL/mmol eq.) and the combined organic phases were washed with brine and dried under $MgSO_4$. The crude product was purified by recrystallization.

6.4.2 1,3-1*H*-benzo[*d*]imidazol-2(3*H*)-one (43)[14]

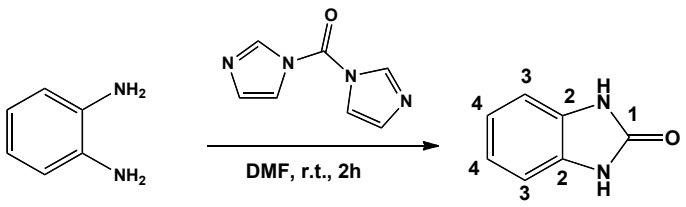

43

Carbonyldiimidazole (1.5 g, 9.24 mmol) was added portionwise over 10-15 min to a stirred solution of *o*-phenylenediamine (1 g, 9.24 mmol) in DMF (13 mL). The reaction mixture was stirred at room temperature for 3h and successively diluted with water (15 mL). The solid was collected by filtration, washed with water and dried under $MgSO_4$ to give the title product as dark brown solid.

T.L.C. System: *n*-hexane -EtOAc: 8:2 v/v, Rf: 0.32;
Yield: 0.74 g, 60 %

^{1}H-NMR (DMSO-d$_6$), δ: 6.90-6.92 (m, 4H, H-aromatic), 10.68 (bs, 2H, N$\underline{H}_2$).

^{13}C-NMR (DMSO-d$_6$), δ: 108.43, 120.36 (CH, C-aromatic), 129.62 (C, C-2), 155 (C, C-1).

6.4.3 1,3-bis-Aryl-1*H*-benzo[*d*]imidazol-2(3*H*)-ones (34, 46)

1,3-bis(4-Nitrobenzyl)-1*H*-benzo[*d*]imidazol-2(3*H*)-one (34)[15]
($C_{21}H_{16}N_4O_5$; M.W.= 404.38)

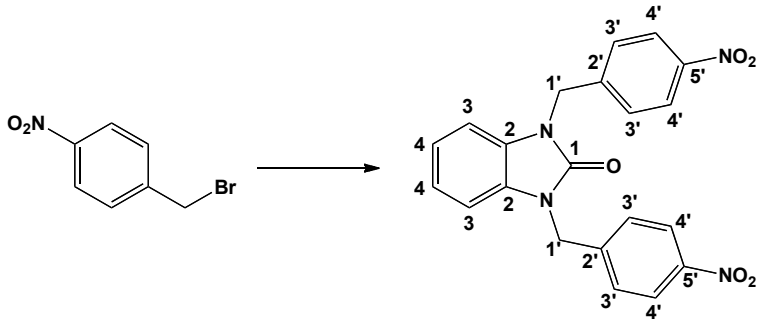

44 **34**

General procedure 6;
Reagent: 4-nitro benzyl bromide **45** (1.28 g, 5.96 mmol);
T.L.C. System: *n*-hexane -EtOAc: 5:5 v/v, Rf: 0.56;
White solid;
Purification: recrystallization from MeOH/*n*-hexane;
Yield: 0.2 g, 16 %;
Melting point: 162-165 °C; (lit. 168-170 °C)
MS $(ESI)^+$: 405.1 $[M+H]^+$

^{1}H-NMR ($CDCl_3$), δ: 6.87-6.92 (m, 2H, H-1'), 7.05-7.11 (m, 2H, H-aromatic), 7.52 (d, J= 8.8 Hz, 2H, H-aromatic), 8.23 (d, 2H, J= 8.8 Hz, H-aromatic).

^{13}C-NMR ($CDCl_3$), δ: 44.46 (CH_2, C-1'), 108.32, 122.24, 124.19, 128.20 (CH, C-aromatic), 128.85, 143.30 (C, C-aromatic), 147.67 (C, C-5'), 154.24 (C, C-1).

1,3-Dibenzyl-1*H*-benzo[*d*]imidazol-2(3*H*)-one (46)[16]

($C_{21}H_{18}N_2O$; M.W.= 314.38)

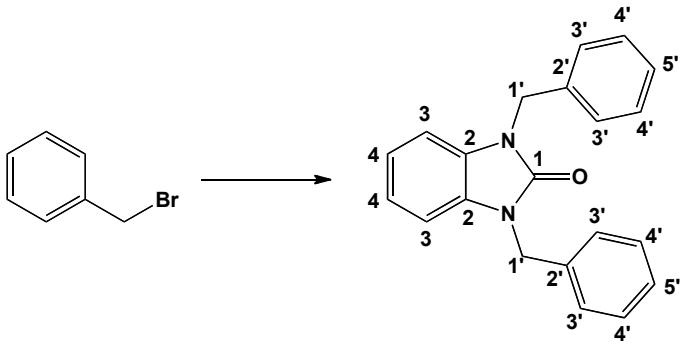

45 **46**

General procedure 6;

Reagent: benzyl bromide **45 (**0.53 mL, 4.4 mmol);

T.L.C. System: *n*-hexane -EtOAc: 5:5 v/v, Rf: 0.75;

White solid;

Purification: recrystallization from MeOH/H_20;

Yield: 0.075 g, 10.7 %;

Melting point: 93-96 °C; (lit. 106-108 °C)

MS $(ESI)^+$: 315.1 $[M+H]^+$

^{1}H-NMR ($CDCl_3$), δ: 5.17 (s, 4H, H-1'), 6.88-6.93 (m, 2H, H-aromatic), 6.97-7.03 (m, 2H, H-aromatic), 7.26-7.32 (m, 2H, H-aromatic), 7.32-7.40 (m, 8H, H-aromatic).

^{13}C-NMR ($CDCl_3$), δ: 45.02 (CH_2, C-1'), 108.35, 121.38, 127.50, 127.72, 128.79 (CH, C-aromatic), 129.31, 136.34 (C, C-aromatic), 154.60 (C, C-1).

6.5 Methyl-3,4-bis(phenylamino)-1*H*-pyrrole-2,5-dione (47)

6.5.1 *N*-Methyl-3,4-dibromomaleimide (49)[17]

($C_5H_3Br_2NO_2$; M.W.= 268.89)

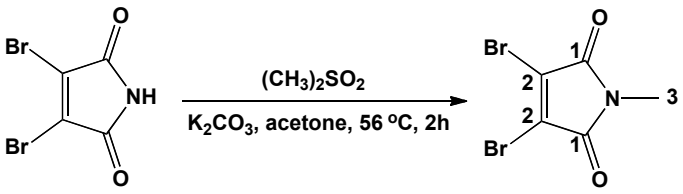

48 **49**

To a stirred solution of 3,4-dibromo-1*H*-pyrrole-2,5-dione **48** (1 g, 3.92 mmol) in fresh-distilled acetone (15 mL), K_2CO_3 (0.6 g, 4.13 mmol) and dimethyl sulfate (0.4 mL, 4.21 mmol) were added. The mixture was stirred and heated at 56°C for 2 h. Upon completion, the solvent was removed in vacuo and the residue was taken up with ethyl acetate (20 mL) and washed with water (2 x 20 mL). The organic phase was dried over $MgSO_4$ and the solvent was removed in vacuo to afford the pure product.

T.L.C. System: *n*-hexane -EtOAc: 9:1 v/v, Rf: 0.28;
Yellowish solid;
Yield: 0.18 g, 54.4 %;

^{1}H-NMR ($CDCl_3$), δ: 3.15 (s, 3H, H-3).

^{13}C-NMR ($CDCl_3$), δ: 25.44 (CH_3, C-3), 129.41 (C, C-2), 164.0 (C, C-1).

6.5.2 3-Bromo-1-methyl-4-(phenylamino)-1*H*-pyrrole-2,5-dione (50)

($C_{11}H_9BrN_2O_2$; M.W.= 281.11)

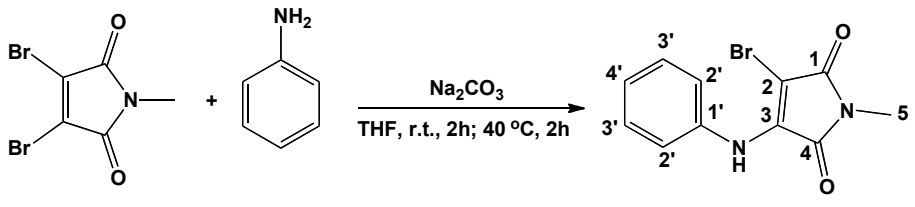

49 **50**

To a mixture of *N*-methyl-3,4-dibromomaleimide **49** (0.15 g, 0.56 mmol) and Na_2CO_3 (0.15g, 1.4 mmol) in THF (8.4 mL), aniline was added (0.11 mL, 1.2 mmol). The reaction mixture was stirred at room temperature for 30 min and up to 2 h. The reaction was then warmed to 40 °C for 2 more h. The solvent was evaporated under reduced pressure and the residue was taken with dichloromethane (2 x 20 mL), washed with water (2x 20 mL) and dried over $MgSO_4$. The solvent was removed in vacuo and the residue was purified by flash column chromatography to afford the title compound.

T.L.C. System: *n*-hexane -EtOAc: 7:3 v/v, Rf: 0.6;
Yellow solid;
Purification by flash column chromatography (*n*-hexane:EtOAc 100:0 v/v, increasing to 95:5 v/v);
Yield: 0.08 g, 53.3 %

^{1}H-NMR ($CDCl_3$), δ: 3.12 (s, 3H, H-5), 7.12 (bs, 1H, NH), 7.20-7.24 (m, 2H, H-aromatic), 7.29-7.31 (m, 1H, H-aromatic), 7.39-7.44 (m, 2H, H-aromatic).

^{13}C-NMR ($CDCl_3$), δ: 24.66 (CH_3, C-5), 97.9 (C, C-aromatic), 124.45, 126.40, 128.78 (CH, C-aromatic), 142.2, 152.1, 164.0 (C, C-aromatic).

6.5.3 1-Methyl-3,4-bis(phenylamino)-1*H*-pyrrole-2,5-dione (47)

($C_{17}H_{15}N_3O_2$; M.W.= 293.32)

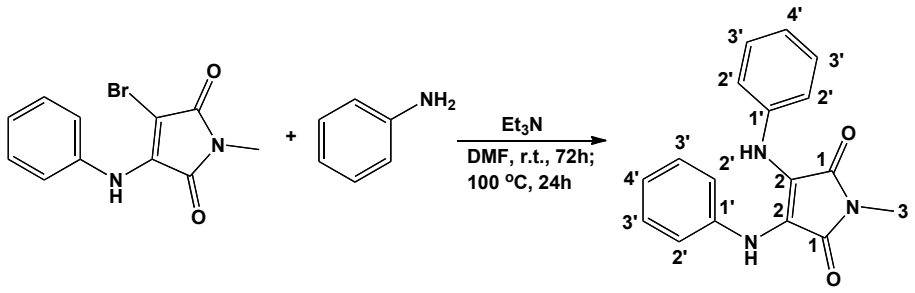

50 **47**

Aniline (0.09 mL, 1.05 mmol) was added dropwise to a stirred solution of bromo-1-methyl-4-(phenylamino)-1H-pyrrole-2,5-dione **50** (0.08 g, 0.28 mmol) in dimethylformamide (0.3 mL) followed by the addition of triethylamine (0.09 mL, 0.64 mmol). The mixture was stirred at room temperature for 72 h, then warmed to 100°C for 24 h. Upon completion,

dichloromethane (10 mL) was added to the mixture and the residue was washed up with water (2 x 10 mL). The organic phase was dried with $MgSO_4$, concentrated in vacuo and then purified by flash column chromatography (*n*-hexane:EtOAc: 100:0 v/v, increasing to 90:10 v/v) and recrystallization from EtOH to afford the title compound as a red solid.

T.L.C. System: *n*-hexane -EtOAc: 7:3 v/v, Rf: 0.5;
Yield: 0.005 g, 6 %;
Melting point: 102-105 °C
MS $(ESI)^+$: 293.9 $[M+H]^+$

^{1}H-NMR ($CDCl_3$), δ: 3.11 (s, 3H, H-3), 6.33 (bs, 2H, NH), 6.67-6.78 (m, 6H, H-aromatic), 6.97 7.05-(m, 4H, H-aromatic).

^{13}C-NMR ($CDCl_3$), δ: 24.02 (CH_3, C-3), 115.35 (C, C-aromatic), 117.68, 121.64, 128.58 (CH, C-aromatic), 140.76 (C, C-aromatic), 169.79 (C, C-1).

6.6 Synthesis of *N*[1]-phenylbenzene-1,2-diamine (52)[18] ($C_{12}H_{12}N_2$; M.W.= 184.242)

To a flask charged with 1,2-diaminobenzene (0.43g, 4 mmol) in 6 mL of DMSO was added CuI (0.15g, 0.8 mmol), L-proline (0.18 g, 1.6 mmol), iodobenzene (4g, 20 mmol) and K_2CO_3 (2.26 g, 16.4 mmol) and was stirred for 18 h at 80 °C. The reaction mixture was cooled down and poured into 20 mL of H_2O and extracted with Et_2O (2 x 20 mL). The organic phase was dried with $MgSO_4$, concentrated in vacuo and then purified by flash column chromatography (*n*-hexane:EtOAc: 100:0 v/v, increasing to 98:2 v/v) and to afford the title compound as a yellow solid.

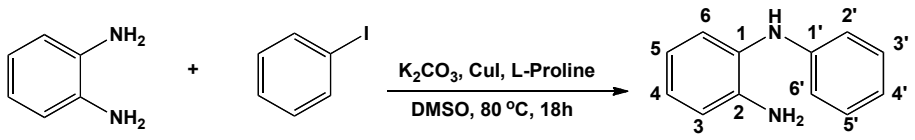

52

T.L.C. System: *n*-hexane -EtOAc: 9:1 v/v, Rf: 0.6;
Yield: 0.137 g, 18.7 %;
Melting point: 75-77 °C (lit. 77-79 °C)[18]
MS $(ESI)^+$: 185.1 $[M+H]^+$

^{1}H-NMR ($CDCl_3$), δ: 3.79 (bs, 2H, N<u>H</u>$_2$), 5.20 (bs, 1H, N<u>H</u>), 6.74-6.81 (m, 3H, H-aromatic), 6.81-6.88 (m, 2H, H-aromatic), 7.01-7.08 (m, 1H, H-aromatic), 7.20-7.27 (m, 2H, H-aromatic).

^{13}C-NMR ($CDCl_3$), δ: 115.24, 116.18, 119.17, 119.34, 124.92, 125.75 (CH, C-aromatic), 128.57 (C, C-aromatic), 129.33 (CH, C-aromatic), 141.97, 145.38 (C, C-aromatic).

6.7 Synthesis of arylsulfonamides

6.7.1 General procedure 9: synthesis of bis-sulfonamido derivatives

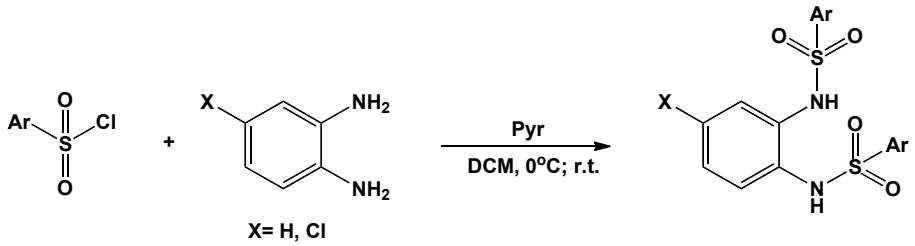

To an ice-cold solution of *o*-phenylenediamine or 4-chloro-*o*-phenylenediamine (0.5 g, 4.62 mmol) and pyridine (0.75 mL, 9.24 mmol) in 12.5 mL of dichloromethane was added portionwise the sulfonyl chloride (9.24 mmol). The reaction mixture was warmed at r.t. and stirred until completion of reaction (TLC analysis). Water (10 mL) was introduced causing the product to precipitate. The solid formed was filtered, washed with H_2O and dried to give a residue which was purified by recrystallization.

***N,N'*-(1,2-Phenylene)dibenzenesulfonamide (61)**[19]
($C_{18}H_{16}N_2O_4S_2$; M.W.= 388.06)

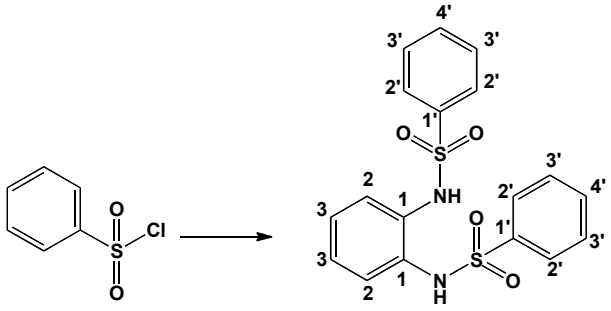

55 **61**

General procedure 9;
T.L.C. System: *n*-hexane -EtOAc: 5:5 v/v, Rf: 0.53;
White solid;
Purification: recrystallization from EtOH;
Yield: 1.2 g, 67.5 %;
Melting point: 180-182 °C; (lit. 192-193 °C)
MS $(ESI)^+$: 411.0 $[M+Na]^+$

H^1 NMR (DMSO-d_6), δ: 6.96-7.02 (m, 2H, H-aromatic), 7.54-7.57 (m, 3H, H-aromatic), 7.70-7.71 (m, 1H, H-aromatic), 7.71-7.72 (m, 1H, H-aromatic), 9.33 (bs, 1H, NH).

^{13}C NMR (DMSO-d_6), δ: 123.40, 125.86, 126.80, 129.27 (CH, C-aromatic), 129.69 (C, C-aromatic), 133.20 (CH, C-aromatic), 139.01 (C, C-1').

***N,N'*-(1,2-Phenylene)bis(4-chlorobenzenesulfonamide) (62)[20]**
($C_{18}H_{14}Cl_2N_2O_4S_2$; M.W.= 455.98)

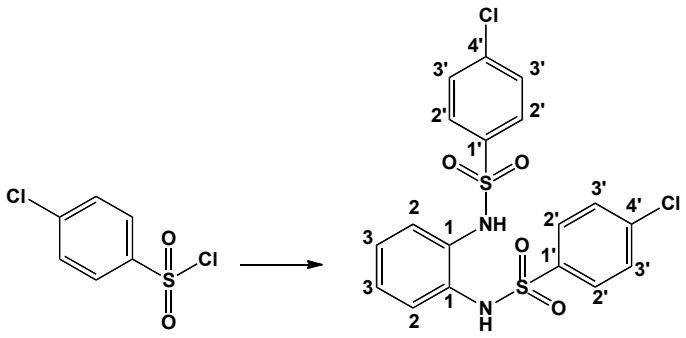

56 **62**

General procedure 9;
T.L.C. System: *n*-hexane -EtOAc: 5:5 v/v, Rf: 0.48;
White fine powder;
Purification: recrystallization with EtOH;
Yield: 0.95 g, 45.2 %;
Melting point: 144-146 °C;
MS $(ESI)^+$: 478.9 $[M+Na]^+$

H^1 NMR ($CDCl_3$), δ: 6.94 (bs, 1H, NH), 6.97-7.01 (m, 1H, H-aromatic), 7.10-7.14, (m, 1H, H-aromatic), 7.44 (d, J= 8.7 Hz, 2H, H-aromatic), 7.65 (d, J= 8.7 Hz, 2H, H-aromatic).

^{13}C NMR ($CDCl_3$), δ: 126.38, 127.89, 129.01, 129.36 (CH, C-aromatic), 130.57 (C, C-1), 136.75 (C, C-4'), 140.00 (C, C-1').

***N,N'*-(1,2-Phenylene)bis(4-nitrobenzenesulfonamide) (63)[19]**

($C_{18}H_{14}N_4O_8S_2$; M.W.= 478.03)

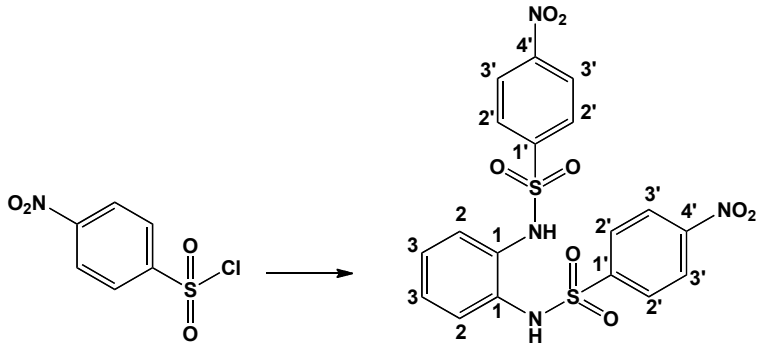

57 **63**

General procedure 9;
T.L.C. System: *n*-hexane -EtOAc: 5:5 v/v, Rf: 0.3;
Off-White powder;
Purification: recrystallization from EtOH;
Yield: 1.13 g, 51.2 %;
Melting point: 240-242 °C; (lit. 255-256 °C)
MS $(ESI)^+$: 501.0 $[M+Na]^+$

H^1 NMR (DMSO-d_6), δ: 6.94-6.98 (m, 1H, H-aromatic), 7.07-7.11 (m, 1H, H-aromatic), 7.97 (d, J= 8.8 Hz, 2H, H-aromatic), 8.38 (d, J= 8.8 Hz, 2H, H-aromatic), 9.68 (bs, 1H, NH).

^{13}C NMR (DMSO-d_6), δ: 124.60, 124.63, 126.80, 128.40 (CH, C-aromatic), 129.98 (C, C-1), 144.87, 149.88 (C, C-aromatic).

***N,N'*-(1,2-Phenylene)bis(4-cyanobenzenesulfonamide) (64)**

($C_{20}H_{14}N_4O_4S_2$; M.W.= 438.05)

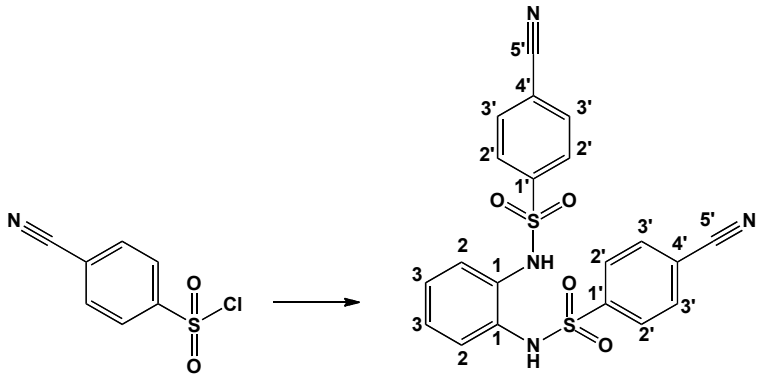

58 **64**

General procedure 9;
T.L.C. System: *n*-hexane-EtOAc: 6:4 v/v, Rf: 0.74;
Pale orange powder;
Purification: recrystallization with EtOH;
Yield: 0.6 g, 30 %;
Melting point: 194-197 °C
MS $(ESI)^+$: 461.0 $[M+Na]^+$

H^1 NMR (DMSO-d_6), δ: 6.92-6.96 (m, 1H, H-aromatic), 7.06-7.10 (m, 1H, H-aromatic), 7.85 (d, J= 8.6 Hz, 2H, H-aromatic), 8.03 (d, J= 8.6 Hz, 2H, H-aromatic), 9.62 (bs, 1H, NH).

^{13}C NMR (DMSO-d_6), δ: 115.53, 117.57 (C, C-aromatic), 124.46, 126.71, 127.53 (CH, C-aromatic), 129.90 (C, C-aromatic), 133.47 (CH, C-aromatic), 143.40 (C, C-1').

***N,N'*-(1,2-Phenylene)bis(4-methoxybenzenesulfonamide) (65)[19]**

($C_{20}H_{20}N_2O_6S_2$; M.W.= 448.08)

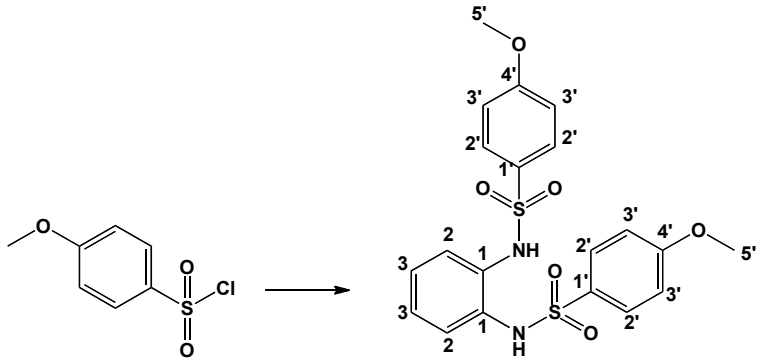

59 **65**

General procedure 9;
T.L.C. System: *n*-hexane -EtOAc: 6:4 v/v, Rf: 0.77;
White spongy powder;
Purification: recrystallization from EtOH;
Yield: 2.07 g, 73.4 %;
Melting point: 129-131 °C (lit. 130-132 °C)[19]
MS $(ESI)^+$: 471.1 $[M+Na]^+$

H^1 NMR ($CDCl_3$), δ: 3,86 (s, 3H, H-5'), 6.90 (bs, 1H, NH), 6.90 (d, J= 9.0 Hz, 2H, H-aromatic); 6.97-7.01 (m, 1H, H-aromatic), 7.04-7.08 (m, 1H, H-aromatic), 7.64 (d, J= 9.0 Hz, 2H, H-aromatic).

^{13}C NMR ($CDCl_3$), δ: 55.62, 114.15, 126.23, 127.33 (CH, C-aromatic), 129.73 (C, C-aromatic), 129.96 (CH, C-aromatic), 130.98, 163.33 (C, C-aromatic).

***N,N'*-(1,2-Phenylene)bis(4-(trifluoromethyl)benzenesulfonamide) (66)[21]**

($C_{20}H_{14}F_6N_2O_4S_2$; M.W.= 524.03)

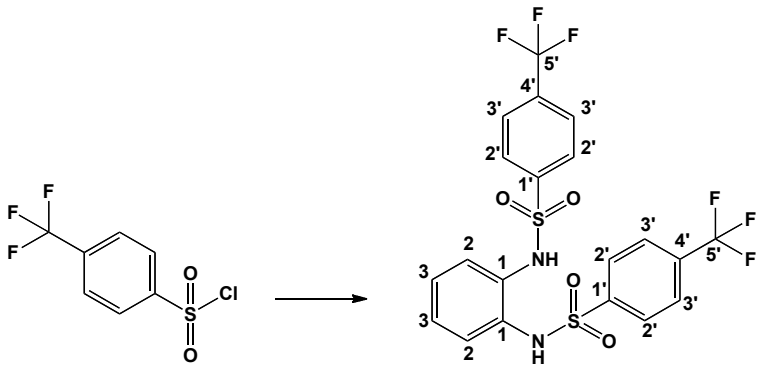

60 **66**

General procedure 9;
T.L.C. System: *n*-hexane -EtOAc: 6:4 v/v, Rf: 0.35;
White powder;
Purification: recrystallization with EtOH;
Yield: 0.5 g, 20.6 %;
Melting point: 135-138 °C;
MS $(ESI)^+$: 547.0 $[M+Na]^+$

H^1 NMR (DMSO-d_6), δ: 6.96-6.99 (m, 1H, H-aromatic), 7.05-7.08 (m, 1H, H-aromatic), 7.92-7.97 (m, 4H, H-aromatic), 9.61 (bs, 1H, NH).

^{13}C NMR (DMSO-d_6), δ: 122.26 (C, C-aromatic), 124.03 (CH, C-aromatic), 124.43 (C, C-aromatic), 126.45, 126.53, 126.56, 127.78 (CH, C-aromatic), 129.77 (C, C-aromatic), 132.34, 132.59, 132.85 (m, C, C-5'), 143.29 (C, C-aromatic).

***N,N'*-(4-Chloro-1,2-phenylene)dibenzenesulfonamide (67)**[22]

($C_{18}H_{15}ClN_2O_4S_2$; M.W.= 422.02)

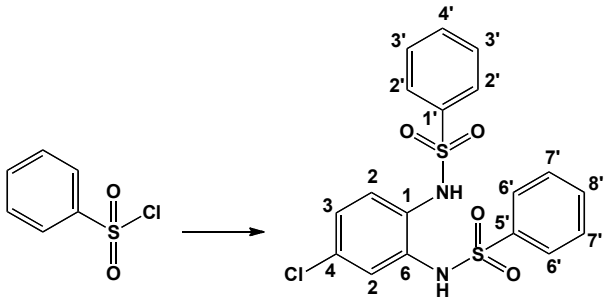

55 **67**

General procedure 9;

T.L.C. System: *n*-hexane -EtOAc: 6:4 v/v, Rf: 0.68;
Off-White powder;
Purification: recrystallization from DCM/Hexane;
Yield: 0.4 g, 20.6 %;
Melting point: 139-142 °C; (lit. 154 °C)[22]
MS $(ESI)^+$: 445.0 $[M+Na]^+$

H^1 NMR (DMSO-d_6), δ: 6.96-7.01 (m, 2H, H-aromatic), 7.06-7.10 (m, 1H, H-aromatic), 7.53-7.62 (m, 4H, H-aromatic), 7.64-7.76 (m, 6H, H-aromatic), 9.49 (bs, 1H, NH), 9.52 (bs, 1H, NH).

^{13}C NMR (DMSO-d_6), δ: 122.14, 125.11, 125.39, 126.80, 126.81 (CH, C-aromatic), 128.13 (C, C-aromatic), 129.37, 129.45 (CH, C-aromatic), 129.62, 131.30 (C, C-aromatic), 133.36, 133.50 (CH, C-aromatic), 138.71, 138.80 (C, C-1', C-5').

***N,N'*-(4-Chloro-1,2-phenylene)bis(4-chlorobenzenesulfonamide) (68)**

($C_{18}H_{13}Cl_3N_2O_4S_2$; M.W.= 489.94)

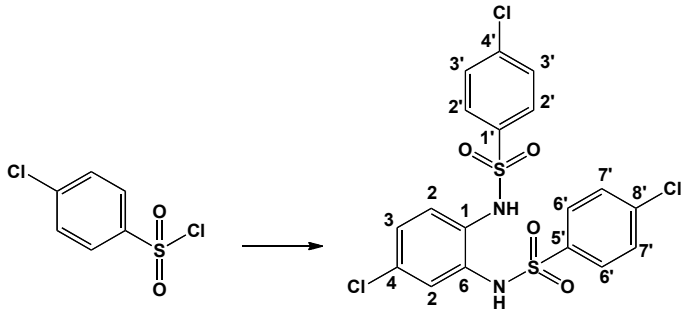

56 68

General procedure 9;
T.L.C. System: *n*-hexane -EtOAc: 6:4 v/v, Rf: 0.9;
White powder;
Purification: recrystallization from EtOH;
Yield: 0.65 g, 28.7 %;
Melting point: 164-167 ^{o}C;
MS $(ESI)^{+}$ 512.9 $[M+Na]^{+}$

H^1 NMR (DMSO-d_6), δ: 6.97 (d, J= 8.6 Hz, 1H, H-aromatic), 7.03 (d, J= 2.4 Hz, 1H, H-aromatic), 7.14 (dd, J_1= 8.8 Hz, J_2= 2.4 Hz, 1H, H-aromatic) 7.65 (d, J= 8.8 Hz, 2H, H-aromatic), 7.67 (d, J= 8.8 Hz, 2H, aromatic), 7.70 (d, J= 8.8 Hz, 2H, aromatic), 7.74 (d, J= 8.8 Hz, 2H, H-aromatic), 9.58 (bs, 2H,- N<u>H</u>).

^{13}C NMR (DMSO-d_6), δ: 122.57, 125.69 (CH, C-aromatic), 128.17 (C, C-aromatic), 128.73, 128.76, 129.52, 129.59 (CH, C-aromatic), 130.08, 137.74, 138.25, 138.37 (C, C-1', C-5').

***N,N'*-(4-Chloro-1,2-phenylene)bis(4-nitrobenzenesulfonamide) (69)**
$C_{18}H_{13}ClN_4O_8S_2$; M.W.= 511.99)

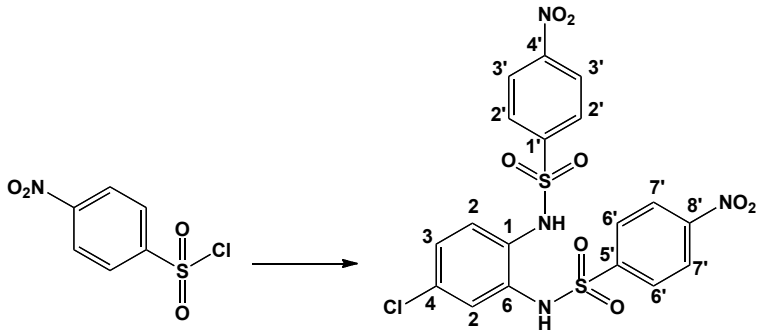

57 69

General procedure 9;
T.L.C. System: *n*-hexane -EtOAc: 6:4 v/v, Rf: 0.6;
White solid;
Purification: recrystallization from EtOH;
Yield: 1.08 g, 45.7 %;
Melting point: 217-219 °C;
MS $(ESI)^+$: 535.0 $[M+Na]^+$

H^1 NMR (DMSO-d_6), δ: 6.92 (d, J= 8.7 Hz, 1H, H-2), 7.05 (d, J= 2.4 Hz, 1H, H-5), 7.14 (dd, J_1= 8.7 Hz, J_2= 2.4 Hz, 1H, H-3), 7.95 (d, J= 8.9 Hz, 2H, H-aromatic), 8.01 (d, J= 8.9 Hz, 2H, H-aromatic), 8.37-8.41 (m, 4H, aromatic), 9.87 (bs, 2H, NH).

^{13}C NMR (DMSO-d_6), δ: 123.04, 124.69, 124.73, 126.06, 126.35 (CH, C-aromatic), 128.26 (C, C-aromatic), 128.38, 128.44 (CH, C-aromatic), 144.61, 149.92, 149.98 (C, C-aromatic).

***N,N'*-(4-Chloro-1,2-phenylene)bis(4-cyanobenzenesulfonamide) (70)[20]**

$C_{20}H_{13}ClN_4O_4S_2$; M.W.= 472.01)

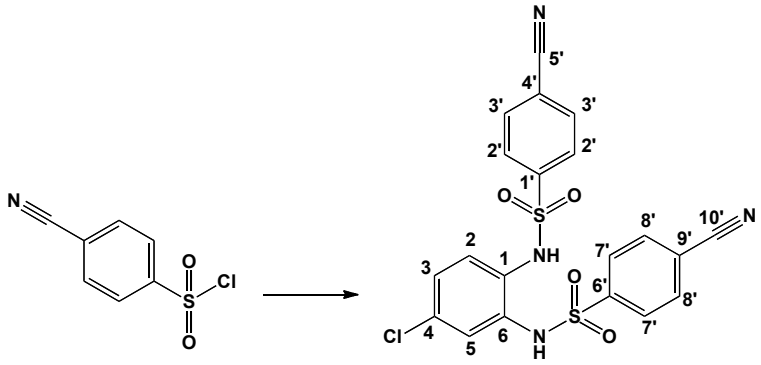

58 **70**

General procedure 9;
T.L.C. System: *n*-hexane -EtOAc: 5:5 v/v, Rf: 0.74;
White solid;
Purification: recrystallization from MeOH;
Yield: 0.52 g, 24 %;
Melting point: 112-115 ^oC;
MS $(ESI)^+$: 495.0 $[M+Na]^+$

H^1 NMR (DMSO-d_6), δ: 6.90 (d, J= 8.6 Hz, 1H, H-2), 7.00 (d, J= 2.3 Hz, 1H, H-5), 7.14 (dd, J_1= 8.6 Hz, J_2= 2.3 Hz, 1H, H-3), 7.86 (d, J= 8.7 Hz, 2H, H-aromatic), 7.91 (d, J= 8.7 Hz, 2H, H-aromatic), 8.04-8.13 (m, 4H, H-aromatic), 9.79, (bs, 2H, N<u>H</u>).

^{13}C NMR (DMSO-d_6), δ: 115.63, 117.55 (C, C-aromatic), 123.05, 126.19, 127.52, 127.56 (CH, C-aromatic), 128.32 (C, C-aromatic), 133.53, 133.58 (CH, C-aromatic), 143.16 (C, C-aromatic).

***N,N'*-(4-Chloro-1,2-phenylene)bis(4-methoxybenzenesulfonamide) (71)**

($C_{20}H_{19}ClN_2O_6S_2$; M.W.= 482.04)

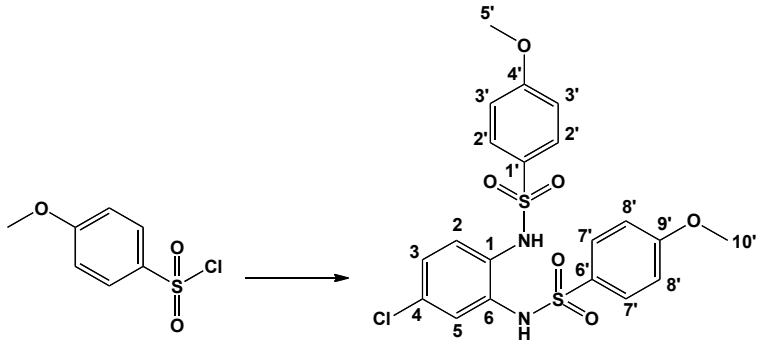

59 **71**

General procedure 9;

T.L.C. System: *n*-hexane -EtOAc: 6:4 v/v, Rf: 0.8;

Off-White powder;

Purification: recrystallization from MeOH;

Yield: 0.87 g, 39 %;

Melting point: 139-142 °C;

MS $(ESI)^+$: 505.0 $[M+Na]^+$

H^1 NMR (DMSO), δ: 3.83 (s, 6H, H-5', H-10'), 6.99 (d, J= 8.6 Hz, 1H, H-2), 7.04-7.11 (m, 6H, H-aromatic), 7.62 (d, J= 8.8 Hz, 2H, H-aromatic), 7.66 (d, J= 8.8 Hz, 2H, H-aromatic), 9.34 (bs, 2H, NH).

^{13}C NMR (DMSO), δ: 55.9 (CH, C-10'), 122.13, 125.09, 125.38, 126.79, 126.81, 128.14, 129.37, 129.45 (CH, C-aromatic), 129.62, 130.2, 138.79, 163.9 (C, C-aromatic).

***N,N'*-(4-Chloro-1,2-phenylene)bis(4-(trifluoromethyl)benzenesulfonamide) (72)[20] ($C_{20}H_{13}ClF_6N_2O_4S_2$; M.W.= 557.99)**

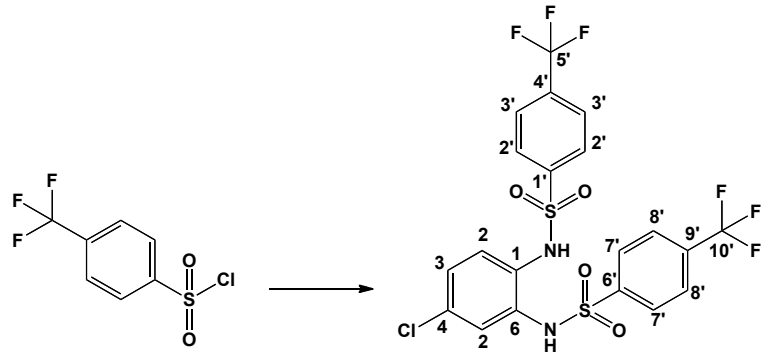

60 **72**

General procedure 9;
T.L.C. System: *n*-hexane -EtOAc: 5:5 v/v, Rf: 0.72;
White, sponge solid;
Purification: recrystallization from DCM/Hexane;
Yield: 0.7 g, 28 %;
Melting point: 140-143 ^{o}C
MS $(ESI)^{+}$: 581.0 $[M+Na]^{+}$

H^1 NMR (DMSO-d_6), δ: 6.97 (d, J= 8.7 Hz, 1H, H-aromatic), 7.01 (d, J= 2.0 Hz, 1H, H-5), 7.14 (dd, J_1= 8.6 Hz, J_2= 2.0 Hz, 1H, H-aromatic), 7.94-7.96 (m, 3H, H-aromatic), 7.97-7.99 (m, 5H, H-aromatic), 9.80, (bs, 2H, NH).

^{13}C NMR (DMSO-d_6), δ: 120.05, 122.20, 122.22 (C, C-aromatic), 122.90 (CH, C-aromatic), 124.37, 124.39 (C, C-aromatic), 125.74, 126.01, 126.57, 126.60, 126.63, 126.66, 127.80 (CH, C-aromatic), 128.30, 130.21, 131.51 (C, C-aromatic), 132.47, 132.59, 132.73, 132.85, 132.99, 133.11, 133.24, 133.36 (C, C-5', C-10'), 142.96, 143.05 (C, C-aromatic).

6.8 Aryl amides

6.8.1 General procedure 10: synthesis of bis-amido derivatives

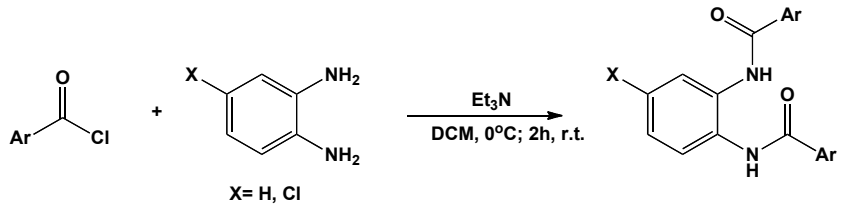

To an ice cold solution of o-phenylenediamine (4.62 mmol) and triethylamine (1.6 mL, 11.55 mmol) in dichloromethane (5 mL), a solution of the desired aryl chloride (9.24 mmol) in dichloromethane (5 mL) was added dropwise under cooling with ice and water. The reaction mixture was allowed to stir for 2h at room temperature. Water (20 mL) was introduced causing the product to precipitate. The solid was filtered and dried under vacuum. The residue collected was purified by recrystallization.

***N,N'*-(1,2-Phenylene)dibenzamide (79)**
($C_{20}H_{16}N_2O_2$; M.W.= 316.12)

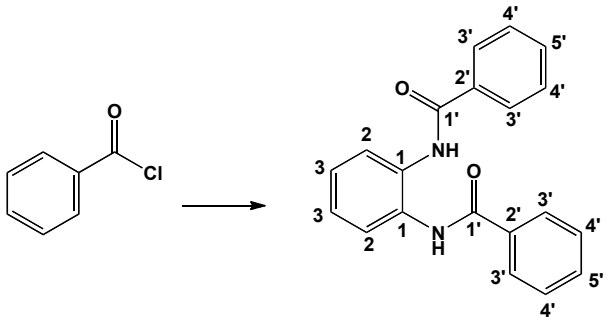

73 **79**

General procedure 10;
T.L.C. System: *n*-hexane -EtOAc: 6:4 v/v, Rf: 0.4;
White powder;
Purification: recrystallization from EtOH;
Yield: 0.82 g, 58.6 %;
Melting point: charring >260 °C; (lit. 298-300 °C)
MS $(ESI)^+$: 339.1 $[M+Na]^+$

H^1 NMR (DMSO-d_6), δ: 7.28-7.33 (m, 1H, H-aromatic), 7.50-7.58 (m, 2H, H-aromatic), 7.57-7.62 (m, 1H, H-aromatic), 7.65-7.69 (m, 1H, H-aromatic), 7.92-7.98 (m, 2H, H-aromatic), 10.06 (bs, 1H, NH).

^{13}C NMR (DMSO-d_6), δ: 125.55, 125.83, 127.46, 128.26 (CH, C-aromatic), 128.55 (C, C-aromatic), 131.29 (CH, C-aromatic), 131.83 (C, C-aromatic), 165.44 (C, C-1').

***N,N'*-(1,2Phenylene)bis(4-chlorobenzamide) (80)[23]**
($C_{20}H_{14}Cl_2N_2O_2$; M.W.= 384.04)

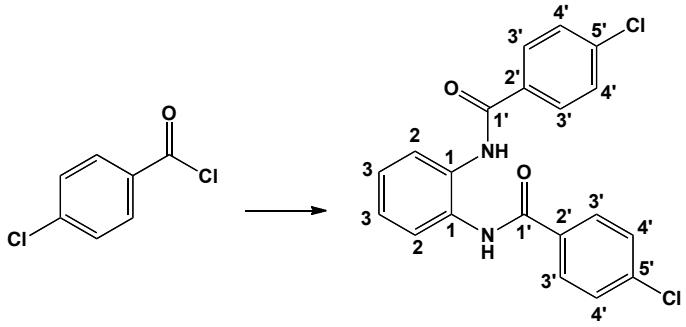

74 **80**

General procedure 10;
T.L.C. System: *n*-hexane -EtOAc: 6:4 v/v, Rf: 0.3;
White powder;
Purification by recrystallization from MeOH;
Yield: 0.7 g, 41 %;
Melting point: charring >260 °C; (lit. 300 °C)[23]
MS $(ESI)^+$: 407.0 $[M+Na]^+$

H^1 NMR (DMSO-d_6), δ: 7.27-7.34 (m, 1H, H-aromatic), 7.61 (d, J= 8.4 Hz, 2H, H-aromatic), 7.63-7.68 (m, 1H, H-aromatic), 7.97 (d, J= 8.4 Hz, 2H, H-aromatic), 10.10 (bs, 1H, NH).

^{13}C NMR (DMSO-d_6), δ: 125.62, 126.00, 128.57, 129.49 (CH, C-aromatic), 131.27, 133.07, 136.57 (C, C-aromatic), 164.46 (C, C-1').

***N,N'*-(1,2-Phenylene)bis(4-nitrobenzamide) (81)[24]**

($C_{20}H_{14}N_4O_6$; M.W.= 406.09)

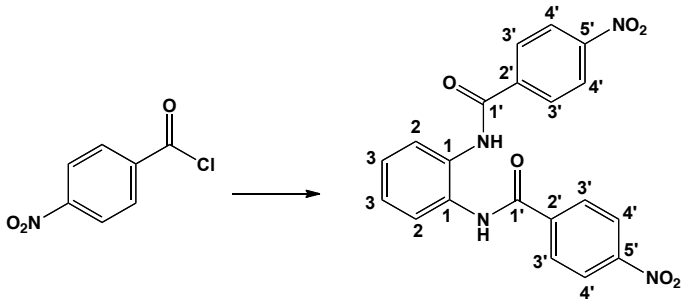

75 **81**

General procedure 10;

T.L.C. System: *n*-hexane -EtOAc: 6:4 v/v, Rf: 0.75;

Fine yellow powder;

Purification by recrystallization from MeOH;

Yield: 1.6 g, 83.7 %;

Melting point: charring >260 °C; (lit. 300 °C)[24]

MS $(ESI)^+$: 407.1 $[M+H]^+$

H^1 NMR (DMSO-d_6), δ: 7.31-7.36, (m, 1H, H-aromatic), 7.66-7.72 (m, 1H, H-aromatic), 8.18 (d, J= 8.8 Hz, 2H, H-aromatic), 8.37 (d, J= 8.8 Hz, 2H, H-aromatic), 10.29 (bs, 1H, NH).

^{13}C NMR (DMSO-d_6), δ: 123.58, 125.88, 126.20, 129.17 (CH, C-aromatic), 131.22, 140.21, 149.17 (C, C-aromatic), 163.99 (C, C-1').

***N,N'*-(1,2-Phenylene)bis(4-cyanobenzamide) (82)**

($C_{22}H_{14}N_4O_2$; M.W.= 366.11)

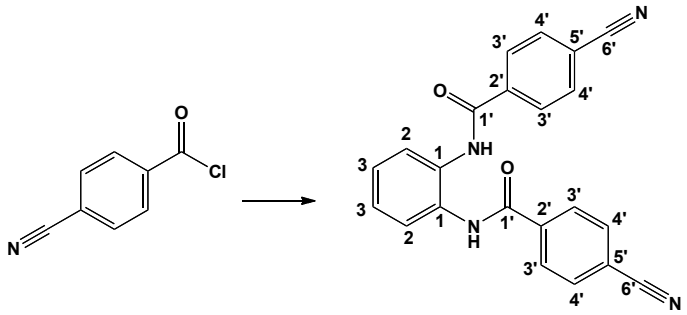

76 **82**

General procedure 10;

T.L.C. System: *n*-hexane -EtOAc: 6:4 v/v, Rf: 0.83;

White powder;

Purification by recrystallization from EtOH;

Yield: 1.1 g, 65.3 %;

Melting point: 264-266 °C;

MS $(ESI)^+$: 367.1 $[M+H]^+$

H^1 NMR (DMSO-d_6), δ: 7.30-7.34 (m, 1H, H-aromatic), 7.64-7.69 (m, 1H, H-aromatic), 8.01 (d, J= 8.4 Hz, 2H, H-aromatic), 8.09 (d, J= 8.4 Hz, 2H, H-aromatic), 10.20 (bs, 1H, NH).

^{13}C NMR (DMSO-d_6), δ: 113.90, 118.23 (C, C-aromatic), 125.81, 126.15, 128.47 (CH, C-aromatic), 140.21, 131.21, 132.48, 138.53 (C, C-aromatic), 164.22 (C, C-1').

***N,N'*-(1,2-Phenylene)bis(4-methoxybenzamide) (83)**[25]

($C_{22}H_{20}N_2O_4$; M.W.= 376.14)

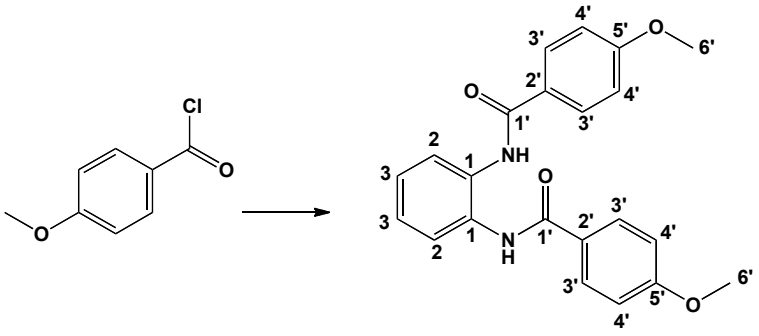

77 **83**

General procedure 10;

T.L.C. System: *n*-hexane -EtOAc: 6:4 v/v, Rf: 0.65;

Fine, white powder;

Purification by recrystallization from MeOH;

Yield: 0.9 g, 53 %;

Melting point: 164-167 °C;

MS $(ESI)^+$: 399.1 $[M+Na]^+$

H^1 NMR (DMSO-d_6), δ: 3.83 (s, 3H, H-6'), 7.06 (d, J= 8.8 Hz, 2H, H-aromatic), 7.27-7.29 (m, 1H, H-aromatic), 7.63-7.66 (m, 1H, H-aromatic), 7.94 (d, J= 8.8 Hz, 2H, H-aromatic), 9.96 (bs, 1H, NH).

^{13}C NMR (DMSO-d_6), δ: 55.44, 113.84, 125.33, 125.69 (CH, C-aromatic), 126.14 (C, C-aromatic), 129.36 (CH, C-aromatic), 131.33, 162.11 (C, C-aromatic), 164.85 (C, C-1').

***N,N'*-(1,2-Phenylene)bis(4-(trifluoromethyl)benzamide) (84)**

($C_{22}H_{14}F_6N_2O_2$; M.W.= 452.10)

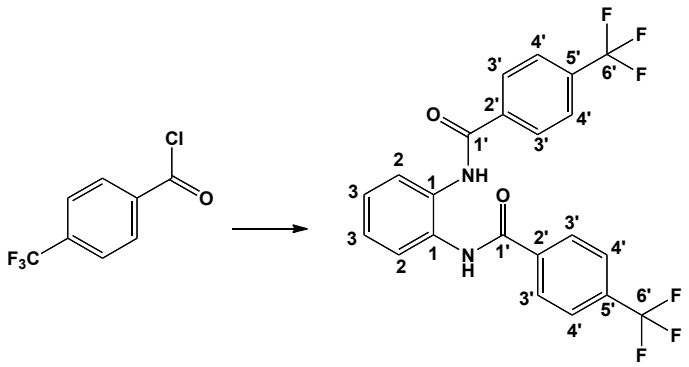

78 **84**

General procedure 10;
T.L.C. System: *n*-hexane -EtOAc: 6:4 v/v, Rf:0.36;
White solid;
Purification: recrystallization from EtOH/H_2O;
Yield: 0.7 g, 33.5 %;
Melting point: 175-177°C;
MS $(ESI)^+$: 475.1 $[M+Na]^+$

H^1 NMR ($CDCl_3$), δ: 6.84-6.88 (m, 1H, H-aromatic), 7.34-7.39 (m, 1H, H-aromatic), 7.83 (d, J= 8.1 Hz, 2H, H-aromatic), 8.15 (d, J= 8.1 Hz, 2H, H-aromatic), 9.58 (bs, 1H, N<u>H</u>).

^{13}C NMR ($CDCl_3$), δ: 125.85, 125.88, 126.63, 128.08 (CH, C-aromatic), 130.39 (C, C-aromatic), 133.92 (C, C-6'), 134.18, 136.54 (C, C-aromatic), 165.26 (C, C-1').

***N,N'*-(4-Chloro-1,2-phenylene)dibenzamide (85)[26]**

$C_{20}H_{15}ClN_2O_2$; M.W.= 350.08)

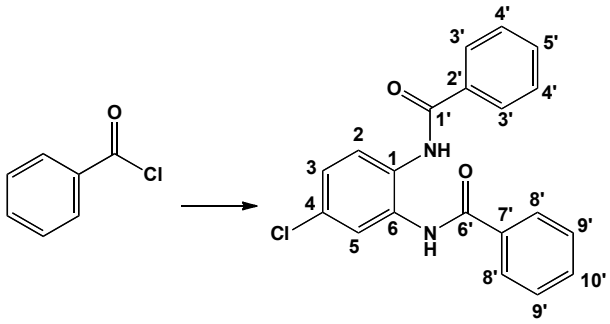

73 **85**

General procedure 10;
T.L.C. System: *n*-hexane -EtOAc: 6:4 v/v, Rf:0.34;
White solid;
Purification: recrystallization from EtOH;
Yield: 0.43 g, 27 %;
Melting point: 220-223 °C; (lit. 227-228 °C)[26]
MS $(ESI)^+$: 373.1 $[M+Na]^+$

H^1 NMR (DMSO-d_6), δ: 7.36 (dd, J_1= 8.7 Hz, J_2= 2.5 Hz, 1H, H-3), 7.50-7.56 (m, 4H, H-aromatic), 7.57-7.63 (m, 2H, H-aromatic), 7.68 (d, J= 8.7 Hz, 1H, H-aromatic), 7.81 (d, J= 2.5 Hz, 1H, H-5), 7.92-7.99 (m, 4H, H-aromatic), 10.08 (bs, 2H, NH).

^{13}C NMR (DMSO-d_6), δ: 125.10, 125.16, 127.42, 127.55, 127.59, 128.52, 128.55 (CH, C-aromatic), 129.14, 130.05 (C, C-aromatic), 131.91, 131.97 (CH, C-aromatic), 132.74, 133.98, 134.01 (C, C-aromatic), 165.55, 165.65 (C, C-1', C-6').

***N,N'*-(4-Chloro-1,2-phenylene)bis(4-chlorobenzamide) (86)**

($C_{20}H_{13}Cl_3N_2O_2$; M.W.= 418.00)

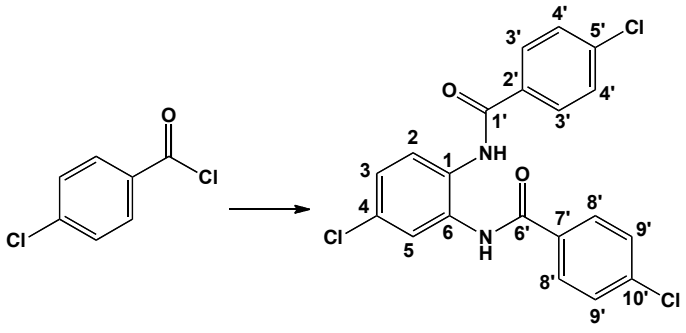

74 86

General procedure 10;
T.L.C. System: *n*-hexane -EtOAc: 6:4 v/v, Rf:0.63;
White solid;
Purification: recrystallization from MeOH;
Yield: 1.5 g, 80 %;
Melting point: 224-227 ^{o}C;
MS (ESI)$^{+}$: 441.0 $[M+Na]^{+}$

H^1 NMR (DMSO-d_6), δ: 7.36 (dd, J_1= 8.9 Hz, J_2= 2.5 Hz, 1H, H-3), 7.58-7.64 (m, 4H, H-aromatic), 7.67 (d, J= 8.9 Hz, 1H, H-2), 7.79 (d, J= 2.5 Hz, 1H, H-5), 7.93-8.01 (m, 4H, H-aromatic), 10.10 (bs, 2H, NH).

^{13}C NMR (DMSO-d_6), δ: 125.25, 125.29, 127.57, 128.54, 128.57, 129.19, 129.59 (CH, C-aromatic), 129.61, 130.01 (C, C-aromatic), 132.68 (CH, C-aromatic), 132.89, 132.92, 136.64, 136.72 (C, C-aromatic), 164.60, 164.64 (C, C-1', C-6').

***N,N'*-(4-Chloro-1,2-phenylene)bis(4-nitrobenzamide) (87)**

($C_{20}H_{13}ClN_4O_6$;M.W.= 440.05)

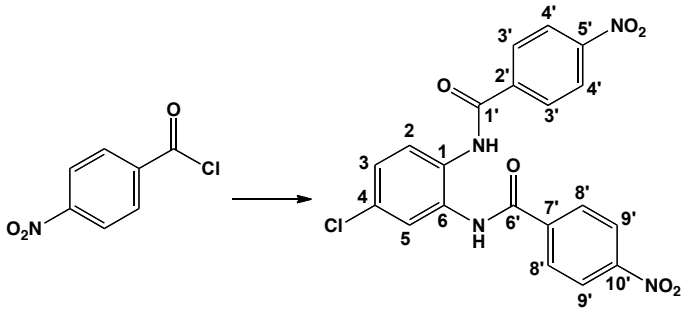

75 **87**

General procedure 10;
T.L.C. System: *n*-hexane-EtOAc: 6:4 v/v, Rf:0.58;
Yellow powder;
Purification: recrystallization from EtOH;
Yield: 1.4 g, 71 %;
Melting point: 259-261 ^{o}C;
MS $(ESI)^{+}$: 463.0 $[M+Na]^{+}$

H^1 NMR (DMSO-d_6), δ: 7.40 (dd, J_1= 8.6 Hz, J_2= 2.5 Hz, 1H, H-3), 7.71 (d, J= 8.6 Hz, 1H, H-2), 7.82 (d, J= 2.5 Hz, 1H, H-5), 8.15-8.21 (m, 4H, H-aromatic), 8.36-8.39 (m, 4H, H-aromatic), 10.35,(bs, 2H, NH).

^{13}C NMR (DMSO-d_6), δ: 123.57, 123.58, 125.54, 127.76 (CH, C-aromatic), 129.28 (C, C-aromatic), 129.42 (CH, C-aromatic), 129.97, 132.58, 139.99, 149.25, 162.33 (C, C-aromatic).

***N,N'*-(4-Chloro-1,2-phenylene)bis(4-cyanobenzamide) (88)**

($C_{22}H_{13}ClN_4O_2$; M.W.= 400.07)

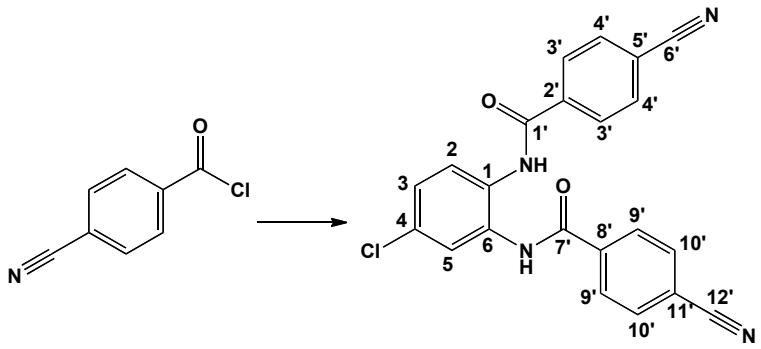

76 **88**

General procedure 10;
T.L.C. System: *n*-hexane -EtOAc: 6:4 v/v, Rf:0.4;
Fine white powder;
Purification by recrystallization from MeOH;
Yield: 0.8 g, 48 %;
Melting point: 162-165 ^{o}C;
MS $(ESI)^{+}$: 423.1 $[M+Na]^{+}$

H^1 NMR (DMSO-d_6), δ: 7.38 (dd, J_1= 8.7 Hz, J_2= 2.5 Hz, 1H, H-3), 7.69 (d, J= 8.7 Hz, 1H, H-2), 7.80 (d, J= 2.5 Hz, 1H, H-5), 8.01-8.03 (m, 4H, H-aromatic), 8.06-8.11 (m, 4H, H-aromatic), 10.25 (bs, 2H, NH).

^{13}C NMR (DMSO-d_6), δ: 113.97, 114.02, 118.2 (C, C-aromatic), 125.46, 127.70, 128.56 (CH, C-aromatic), 129.36, 129.95 (C, C-aromatic), 132.46, 132.48 (CH, C-aromatic), 132.59, 138.33, 138.36, 164.41 (C, C-aromatic).

***N,N'*-(4-Chloro-1,2-phenylene)bis(4-methoxybenzamide) (89)**

($C_{22}H_{19}ClN_2O_4$; M.W.= 410.10)

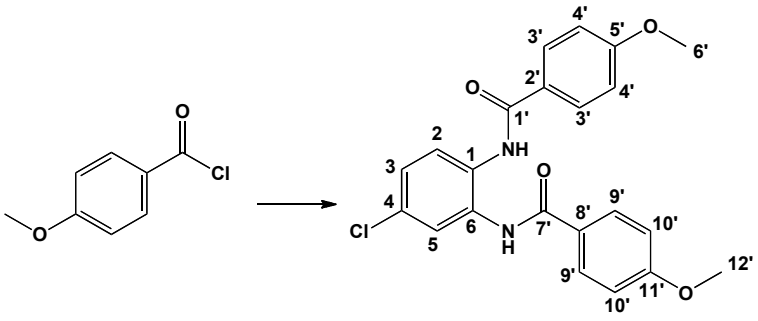

77 89

General procedure 10;
T.L.C. System: *n*-hexane -EtOAc: 6:4 v/v, Rf: 0.38
Fine white powder;
Purification by recrystallization from MeOH;
Yield: 1.3 g, 70 %;
Melting point: 148-150 ^{o}C;
MS $(ESI)^{+}$: 433.1 $[M+Na]^{+}$

H^1 NMR (DMSO-d_6), δ: 3.83 (s, 6H, -H-6', H-12'), 7.07 (d, J= 8.6 Hz, 4H, H-aromatic), 7.33 (dd, J_1= 8.6 Hz, J_2= 2.3 Hz, 1H, H-3), 7.65 (d, J= 8.6 Hz, 1H, H-2), 7.79 (d, J= 2.3 Hz, 1H, H-aromatic), 7.93-7.95 (m, 4H, H-aromatic), 9.97 (bs, 1H, NH), 9.99 (bs, 1H, NH).

^{13}C NMR (DMSO-d_6), δ: 55.46, 113.82, 113.86, 124.93 (CH, C-aromatic), 125.91, 125.95 (C, C-aromatic), 127.27 (CH, C-aromatic), 128.94 (C, C-aromatic), 129.47, 129.52 (CH, C-aromatic), 130.06, 132.78, 162.19, 162.25 (C, C-aromatic), 164.90, 165.07 (C, C-1', C-7').

***N,N'*-(4-Chloro-1,2-phenylene)bis(4-(trifluoromethyl)benzamide) (90)**

($C_{22}H_{13}ClF_6N_2O_2$; M.W.= 486.06)

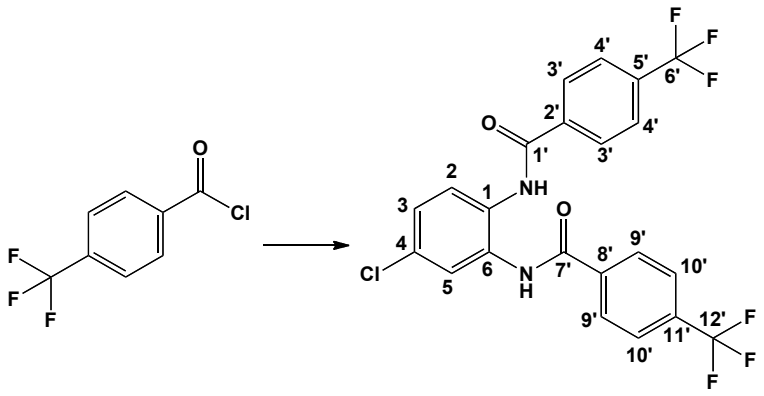

78 **90**

General procedure 10;
T.L.C. System: *n*-hexane -EtOAc: 6:4 v/v, Rf:0.8;
White solid;
Purification by recrystallization from MeOH;
Yield: 2.2 g, 30 %;
Melting point: 189.5 ^{o}C;
MS $(ESI)^{+}$: 509.0 $[M+Na]^{+}$

H^1 NMR (DMSO-d_6), δ: 7.38 (dd, J_1= 8.6 Hz, J_2= 2.5 Hz, 1H, H-3), 7.71 (d, J= 2.5 Hz, 1H, H-5), 7.83 (d, J= 8.6 Hz, 1H, H-2), 7.92 (d, J= 8.4 Hz, 4H, H-aromatic), 8.11-8.16 (m, 4H, H-aromatic), 10.25 (bs, 2H, NH).

^{13}C NMR (DMSO-d_6), δ: 125.41, 125.44, 125.47, 127.67, 128.63 (CH, C-aromatic), 129.32, 129.97, 132.62, 138.0, 138.11, 164.60 (C, C-aromatic).

6.9 Synthesis of aryl coumarin structures

6.9.1 General procedures 11-13

General procedure 11: synthesis of aryl thio methyl-2H-chromen-2-one

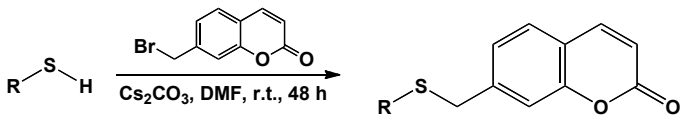

To a solution of the desired arylthiol (4 mmol) in DMF (5 mL), cesium carbonate (1.56 g, 4.8 mmol) was added, followed by the addition of 7-bromomethyl coumarin (1 g, 4.19 mmol). The solution was stirred for 48 h at room temperature. The reaction mixture was poured into ethyl acetate (30 mL) and washed with water (3 x 30 mL) and brine (3 x 30 mL). The organic layer was dried over $MgSO_4$, filtered, concentrated and purified by flash column chromatography and/or recrystallization to give the title compound.

General procedure 12: synthesis of aryl sulfinyl methyl-2H-chromen-2-one

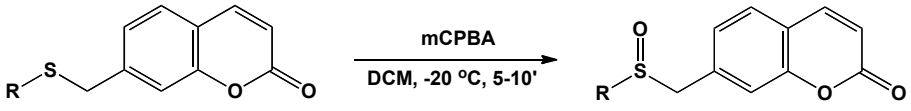

The appropriate aryl thio methyl-2H-chromen-2-one derivative (1eq.) was dissolved in dry DCM (4.13 mL/mmol eq.) and the solution was cooled to -20 °C. *meta*-Chloroperoxybenzoic acid (1.3 eq.) was added portionwise to this solution and the cooling bath was maintained for 5-10' (TLC check). The reaction mixture was poured into 15% Na_2CO_3 (15 mL/mmol eq.), extracted with DCM (15 mL/ mmol eq.), washed with brine (15 mL/ mmol eq.) and dried over $MgSO_4$. The crude product was purified by flash column chromatography to afford the title compound.

General procedure 13: synthesis of aryl sulfonyl methyl-2H-chromen-2-ones

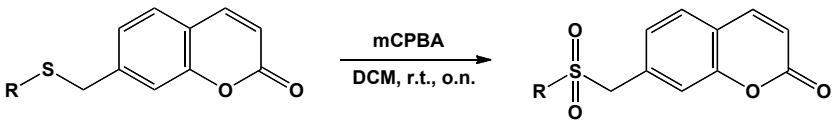

The aryl thio methyl-2H-chromen-2-one derivative (1eq.) was dissolved in dry DCM (5.5 mL/mmol eq.) and the solution was cooled to -0 °C.
meta-Chloroperoxybenzoic acid (3 eq.) was added portion wise to this solution and the cooling bath was removed. The reaction mixture was stirred at room temperature, over night, then was poured into 15% Na_2CO_3 (15 mL/mmol eq.), extracted with DCM (15 mL/mmol eq.), washed with brine and dried over $MgSO_4$. The crude product was purified by flash column chromatography or recrystallization to afford the title compound.

6.9.2 Synthesis of 7-bromomethyl coumarin (102)[27]

($C_{10}H_7BrO_2$; M.W.= 239.07)

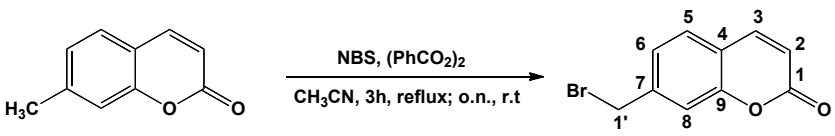

101 **102**

To a stirred solution of 7-methylcoumarin (1 g, 6.24 mmol) in acetonitrile (20 mL) was added N-bromosuccinimide (1.3 g, 7.23 mmol), followed by a catalytic amount of benzoyl peroxide (0.07 g, 0.3 mmol). The mixture was heated at reflux for 3h. After that time, the resulting solution was stirred over night at room temperature which allowed the product to precipitate. A white solid was filtered off, washed with propan-2-ol (20 mL) and dried. The title compound was obtained as a white solid and used without further purification.

T.L.C. System: *n*-hexane -EtOAc: 5:5 v/v, Rf: 0.68;
Yield: 1.09 g, 66.6 %

^{1}H-NMR ($CDCl_3$), δ: 4.54 (s, 2H, H-1'), 6.45 (d, J= 9.5 Hz,1H, H-aromatic), 7.33 (d, J= 7.9 Hz, 1H, H-aromatic), 7.34-7.35 (m, 1H, H-aromatic), 7.49 (d, J= 7.9 Hz, 1H, H-aromatic), 7.71 (d, J= 9.5 Hz, 1H, H-aromatic).

^{13}C-NMR ($CDCl_3$), δ: 31.82 (CH_2, C-1'), 117.15, 117.25 (CH, C-aromatic), 118.71 (C, C-aromatic), 125.20, 128.30 (CH, C-aromatic), 141.99 (C, C-aromatic), 142.82 (CH, C-aromatic), 154.02 (C, C-aromatic), 160.41 (C, C-1).

6.9.3 Synthesis of 6-amino coumarin(96)[28]

($C_9H_7NO_2$; M.W.= 161.16)

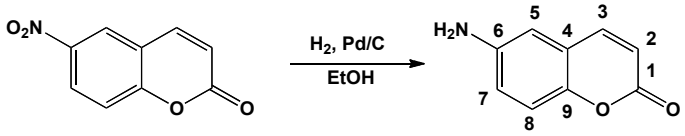

95 **96**

6-Nitrocoumarin (0.3 g, 1.6 mmol) was dissolved in EtOH (14.5 mL) and a catalytic amount of palladium on carbon (0.6 g) was added. Hydrogen was refluxed until the starting material disappeared. The mixture was filtered off through celite to remove the catalyst. The filtered solution was evaporated under pressure to afford the title compound as a brown solid that was used for the following step without further purification.

T.L.C. System: DCM-MeOH: 9:1 v/v, Rf: 0.44;
Yield: 0.23 g, 92 %

^{1}H-NMR (MeOD), δ: 3.75 (bs, 2H, N$\underline{H}_2$), 6.40 (d, J= 9.5 Hz, 1H, H-aromatic), 6.74 (d, J= 2.7 Hz,1H, H-aromatic), 6.89 (dd, J_1= 8.8 Hz, J_2= 2.7 Hz, 1H, H-aromatic), 7.17 (d, J= 8.8 Hz, 1H, H-aromatic), 7.59 (d, J= 9.5 Hz, 1H, H-aromatic).

^{13}C-NMR (MeOD), δ: 112.88, 116.87, 117.99 (CH, C-aromatic), 120.83 (C, C-aromatic), 121.20, 145.84 (CH, C-aromatic), 146.39, 148.02 (C, C-aromatic), 163.67 (C, C-1).

6.9.4 Synthesis of 7-((1H-Benzo[*d*]imidazol-2-*yl*)methoxy)-*2H*-chromen-2-one (91) ($C_{17}H_{12}N_2O_3$; M.W.= 292.29)

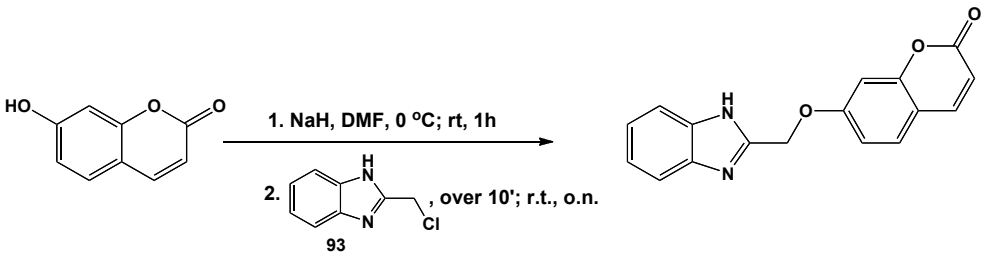

92 **91**

7-Hydroxycoumarin (0.5 g., 3 mmol) was charged in a flask and anhydrous DMF (7 mL) was added. Upon dissolution, the mixture was cooled to 0 °C and allowed to stir for 15 min. NaH (0.072 g, 3 mmol) was then added and the mixture was stirred for 1h.

A solution of 2-(chloromethyl)benzimidazole (0.6 g, 3.6 mmol) in anhydrous DMF (7 mL) was added dropwise over 10 min. The reaction was allowed to warm to room temperature and was stirred overnight. After 12h, the starting material was still present, therefore Et_3N (0.4 mL, 3 mmol) was added and the reaction was stirred for additional 24 h. The reaction mixture was quenched with water (20 mL) and extracted with EtOAc (2 x 20 mL), dried over $MgSO_4$ and concentrated in vacuo. The crude mixture was purified by flash column chromatography (*n*-hexane:EtOAc 100:0 v/v, increasing to 60:40 v/v) and recrystallized from EtOH to give the pure product as a white solid.

T.L.C. System: EtOAc-Hexane: 9:1 v/v, Rf: 0.33;

Yield: 0.09 g, 10.2 %;

Melting point: 150-153 °C;

MS $(ESI)^+$: 293.1$[M+H]^+$

^{1}H-NMR (DMSO-d_6), δ: 5.45 (s, 2H, H-1'), 6.3 (d, 1H, J= 9.4 Hz, H-aromatic), 7.10 (d, 1H, J= 8.6 Hz), 7.15-7.27 (m, 3H, H-aromatic), 7.51 (d, 1H, J= 7.5 Hz, H-aromatic), 7.64 (d, 1H, J= 7.8 Hz, H-aromatic), 7.67 (d, 1H, J= 8.6 Hz, H-aromatic), 8.00 (d, 1H, J= 9.4 Hz, H-aromatic), 12.7 (bs, 1H, N<u>H</u>).

^{13}C-NMR (DMSO-d_6), δ: 64.25 (CH_2, C-1'), 101.71 (CH, C-aromatic), 111.0 (CH, C-aromatic), 112.5 (C, C-aromatic), 112.87, 112.91, 123.0, 129.57 (CH, C-aromatic), 138.9, 144.21(C, C-aromatic), 149.22 (CH, C-aromatic), 155.18,

160.16 (C, C-aromatic), 160.91 (C, C-1).

6.9.5 Synthesis of N-(2-oxo-2H-chromen-7-yl)-1H-benzo[d]imidazole-2-carboxamide (94) ($C_{17}H_{11}N_3O_3$; M.W.=305.29)

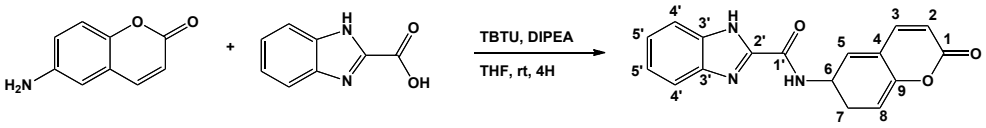

96 **97** **94**

1H-Benzimidazole-2-carboxylic acid (0.54 g 3.7 mmol) and TBTU (1.3 g, 4 mmol) were suspended in anhydrous THF (20 mL) at room temperature. DIPEA (1.35 mL, 7.77 mmol) was added to the reaction mixture, followed by 6-aminocoumarin (0.6 g, 3.36 mmol) and the stirring was maintained for 4h. From the solution, a precipitate was formed which was filtered and washed with THF. The crude product was recrystallized from EtOH to obtain the title compound as a white solid.

T.L.C. System: *n*-hexane -EtOAc: 5:5v/v, Rf: 0.4;
Yield: 0.2, 18 %;
Melting point: 269-271 ºC;
MS $(ESI)^+$: 306.0 $[M+Na]^+$

^{1}H-NMR (DMSO-d$_6$), δ: 6.52 (d, J= 9.5 Hz, 1H, H-aromatic), 7.34-7.40 (m, 2H), 7.46 (d, J= 8.9 Hz 1H, H-aromatic), 7.60-7.63 (m, 1H, H-aromatic), 7.78-7.82 (m, 1H, H-aromatic), 8.07 (d, J= 8.9 Hz 1H, H-aromatic), 8.12 (d, J= 9.5 Hz 1H, H-aromatic), 8.36 (d, J= 2.4 Hz, 1H, H-aromatic), 11.19 (bs, 1H, -CONH), 13.47 (bs, 1H, NH).

^{13}C-NMR (DMSO-d$_6$), δ: 112.70, 116.57, 116.63 (CH, C-aromatic), 118.56 (C, C-aromatic), 119.25, 120.03, 122.81, 124.53, 124.76 (CH, C-aromatic), 134.66 (C, C7), 144.36 (CH, C-aromatic), 145.26, 149.93 (C, C-aromatic), 157.46 (C, C-1'), 159.97 (C, C-1).

6.9.6 Aryl thio methyl 2H-chromen-2-ones (95, 96)

7-(((1*H*-Benzo[*d*]imidazol-2-*yl*)thio)methyl)-*2H*-chromen-2-one (99)
($C_{17}H_{12}N_2O_2S$; M.W.= 308.35)

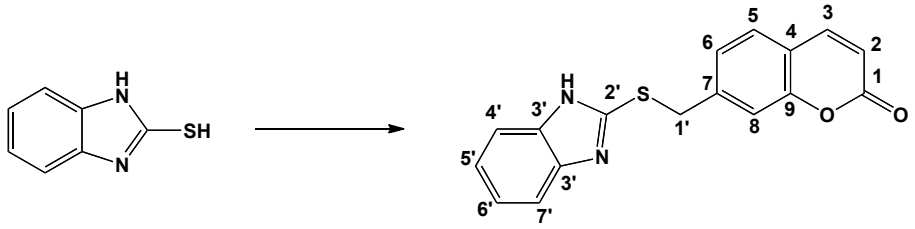

103 **99**

General procedure 11;
T.L.C. System: *n*-hexane -EtOAc: 5:5 v/v, Rf: 0.33;
Off white solid;
Purification: flash column chromatography (*n*-hexane:EtOAc: 100:0 v/v, increasing to 50:50 v/v) and recrystallization from EtOH;
Yield: 0.52 g, 42 %;
Melting point: 135-137 ^oC;
MS $(ESI)^+$: 309.1 $[M+H]^+$

^{1}H-NMR (DMSO-d_6), δ: 4.66 (s, 2H, H-1'), 6.45 (d, 1H, J= 9.5 Hz, H-aromatic), 7.10-7.18 (m, 2H, H-aromatic), 7.34-7.40 (m, 1H, H-aromatic), 7.44 (dd, 1H, J_1= 1.5 Hz, J_2= 7.9 Hz, H-aromatic), 7.50 (s, 1H, H-aromatic), 7.53-7.59 (m, 1H, H-aromatic), 7.65 (d, 1H, J= 8.0 Hz, H-aromatic), 8.01 (d, 1H, J= 9.5 Hz, H-aromatic), 12.62 (bs, 1H, N<u>H</u>).

^{13}C-NMR (DMSO-d_6), δ: 34.51 (CH_2, C-1'), 110.39, 115.92 (CH, C-aromatic), 116.35 (C, C-aromatic), 117.45, 117.80, 121.21, 121.76, 125.11, 128.45 (CH, C-aromatic), 142.81 (C, C-aromatic), 143.51 (CH, C-aromatic), 143.88 (C, C-aromatic), 130.63 (CH, C-aromatic), 149.19, 153.34 (C, C-aromatic), 159.87 (C, C-1).

7-(((4,5-Diphenyl-*1H*-imidazol-2-*yl*)thio)methyl)-*2H*-chromen-2-one (100)
($C_{25}H_{18}N_2O_2S$; M.W.= 410.49)

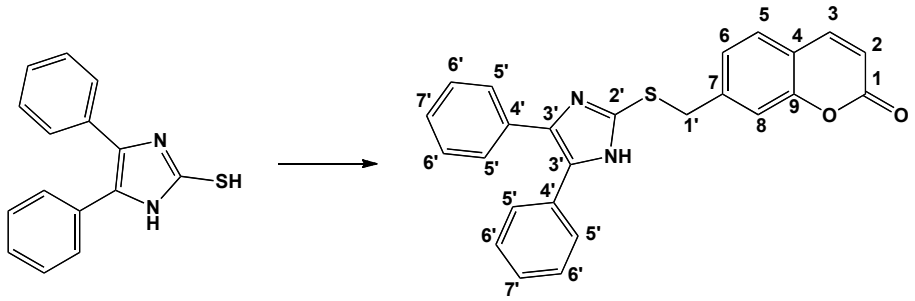

104 **100**

General procedure 11;
T.L.C. System: *n*-hexane -EtOAc: 5:5 v/v, Rf: 0.75;
Off white solid;
Purification: flash column chromatography (*n*-hexane:EtOAc: 100:0 v/v, increasing to 50:50 v/v);
Yield: 0.140 g, 8.5%;
Melting point: 193-195 °C-
MS $(ESI)^+$: 411.1 $[M+H]^+$

^{1}H-NMR (DMSO-d_6), δ: 4.47 (s, 2H, H-1'), 6.46 (d, 1H, J= 9.4 Hz, H-aromatic), 7.18-7.25 (m, 1H), 7.26-7.44 (m, 9H, H-aromatic), 7.47 (d, 2H, J= 7.5 Hz, H-aromatic), 7.66 (d, 1H, J= 7.9 Hz, H-aromatic), 8.03 (d, 1H, J= 9.4 Hz, H-aromatic), 12.60 (bs, 1H, NH).

^{13}C-NMR (DMSO-d_6), δ: 36.51 (CH_2, C-1'), 115.82, 116.45 (CH, C-aromatic), 117.71 (C, C-aromatic), 125.22, 126.58, 126.90, 127.69, 127.80, 128.20, 128.36, 128.66 (CH, C-aromatic), 128.74, 130.63, 134.78, 137.25, 138.60, 143.12, 143.95, 153.34 (C, C-aromatic), 159.92 (C, C-1).

6.9.7 Aryl sulfinyl methyl-2H-chromen-2-ones (105, 106)

7-(((1H-Benzo[*d*]imidazol-2-*yl*)sulfinyl)methyl)-*2H*-chromen-2-one (105)
($C_{17}H_{12}N_2O_3S$; M.W. =324.35)

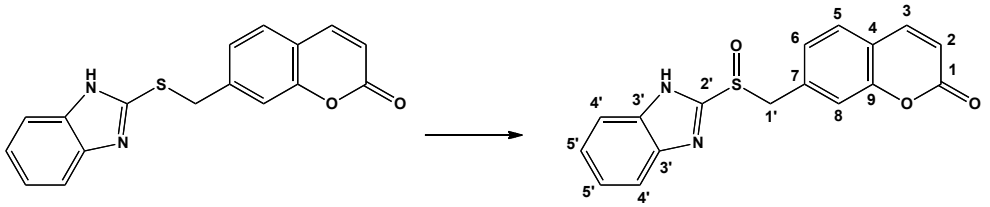

99 **105**

General procedure 12;
Reagent: 7-(((1*H*-benzo[*d*]imidazol-2-*yl*)thio)methyl)-2*H*-chromen-2-one **95** (0.1 g, 0.32 mmol);
T.L.C. System: *n*-hexane -EtOAc: 2:8 v/v, Rf: 0.5;
White solid;
Purification: flash column chromatography (*n*-hexane:EtOAc: 100:0 v/v, increasing to 80:20 v/v);
Yield: 0.18 g, 59.2 %;
Melting point: 171-173 ^{o}C;
MS $(ESI)^+$: 325.1 $[M+H]^+$

^{1}H-NMR (DMSO-d_6), δ: 4.62 (d, 1H, J= 12.7 Hz, H-1'), 4.85 (d, 1H, J= 12.7 Hz, H-1'), 7.10-7.18 (m, 2H, H-aromatic), 6.48 (d, 1H, J= 9.5 Hz H-aromatic), 7.01 (dd, 1H, J_1= 7.8 Hz, J_2= 1.3 Hz, H-aromatic), 7.23 (s, 1H, H-aromatic), 7.28-7.31 (m, 2H, H-aromatic), 7.48-7.52 (m, 1H, H-aromatic), 7.56 (d, 1H, J= 8.0 Hz, H-aromatic), 7.73-7.77 (m, 1H, H-aromatic)., 8.01 (d, 1H, J_2= 9.6 Hz, H-aromatic), 13.35 (bs, 1H, N<u>H</u>).

^{13}C-NMR (DMSO-d_6), δ: 58.91 (CH_2, C-1'), 116.36, 118.13 (CH, C-aromatic), 118.44 (C, C-aromatic), 126.32, 128.20 (CH, C-aromatic), 134.04 (C, C-aromatic), 143.85 (CH, C-aromatic), 153.00, 153.05 (C, C-aromatic), 159.71 (C, C-1).

7-(((4,5-Diphenyl-*1H*-imidazol-2-*yl*)sulfinyl)methyl)-*2H*-chromen-2-one (106) ($C_{25}H_{18}N_2O_3S$; M.W. =426.49)

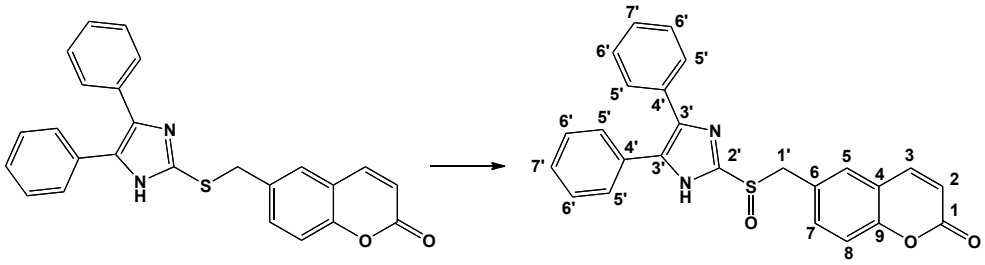

100 **106**

General procedure 12;

Reagent: 7-(((4,5-diphenyl-1*H*-imidazol-2-*yl*)thio)methyl)-2*H*-chromen-2-one **96** (0.5 g, 1.2 mmol);

T.L.C. System: *n*-hexane -EtOAc: 3:7 v/v, Rf: 0.60;

White solid;

Purification: flash column chromatography (*n*-hexane:EtOAc: 100:0 v/v, increasing to 50:50 v/v);

Yield: 0.100 g, 19.6 %;

Melting point: 175-177 ^{o}C;

MS (ESI)$^{+}$: 427.1 $[M+H]^{+}$

^{1}H-NMR (DMSO-d_6), δ: 4.74 (d, J= 12.4 Hz, 1H, H-1'), 4.79 (d, J= 12.4 Hz, 1H, H1'), 6.49 (d, J= 9.5 Hz, 1H, H-aromatic), 7.22 (d, J= 7.8 Hz, 1H, H-aromatic), 7.29 (s, 2H, H-aromatic), 7.32-7.53 (m, 9H, H-aromatic), 7.68 (d, J= 7.8 Hz 1H, H-aromatic), 8.05 (d, J= 9.5 Hz, 1H), 13.58 (bs, 1H, N<u>H</u>).

^{13}C-NMR (DMSO-d_6), δ: 58.53 (CH_2, C-1'), 116.32, 117.97 (CH, C-aromatic), 118.39 (C, C-aromatic), 126.52, 127.15, 127.20, 128.34 (CH, C-aromatic), 128.42 (C, C-aromatic), 128.70 (CH, C-aromatic), 129.79, 130.48, 134.78, 137.86, 143.88, 153.20 (C, C-aromatic), 159.75 (C, C-1).

6.9.8 Aryl sulfonyl methyl-2H-chromen-2-ones (107, 108)

7-(((1H-Benzo[d]imidazol-2-*yl*)sulfonyl)methyl)-2H-chromen-2-one (107)
($C_{17}H_{12}N_2O_4S$; M.W. = 340.35)

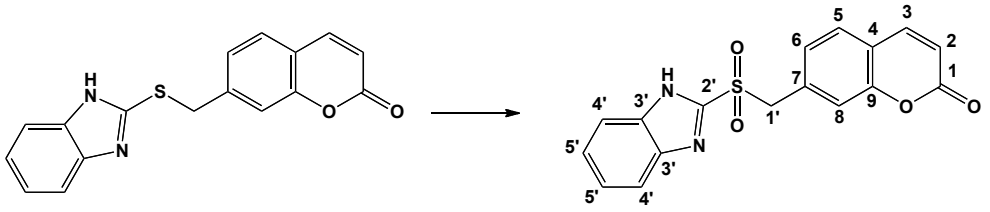

99 **107**

General procedure 13;
Reagent: 7-(((1*H*-benzo[*d*]imidazol-2-*yl*)thio)methyl)-2*H*-chromen-2-one **95** (0.15g, 0.49 mmol);
T.L.C. System: *n*-hexane -EtOAc: 5:5 v/v, Rf: 0.4;
White solid;
Purification: flash column chromatography (*n*-hexane:EtOAc: 100:0 v/v, increasing to 50:50 v/v);
Yield: 0.020 g, 13%;
Melting point: 224-226 ^{o}C;
MS (ESI)$^{+}$: 341.1 $[M+H]^{+}$

^{1}H-NMR (DMSO-d_6), δ: 5.16 (s, 2H, H-1'), 6.51 (d, J= 9.6 Hz, 1H, H-aromatic), 7.14 (d, J= 7.9 Hz, 1H, H-aromatic), 7.32 (s, 1H, H-aromatic), 7.35-7.45 (m, 2H, H-aromatic), 7.62 (d, J= 7.9 Hz, 1H, H-aromatic), 7.69-7.72 (m, 2H, H-aromatic), 8.02 d, J= 9.6 Hz, 1H, H-aromatic).

^{13}C-NMR (DMSO-d_6), δ: 58.86 (CH_2, C-1'), 116.80, 118.80 (CH, C-aromatic), 118.87 (C, C-aromatic), 127.04, 128.33, 143.71 (CH, C-aromatic), 153.05 (C, C-aromatic), 159.60 (C, C-1).

7-(((4,5-Diphenyl-*1H*-imidazol-2-*yl*)sulfonyl)methyl)-*2H*-chromen-2-one (108) ($C_{25}H_{18}N_2O_4S$; M.W.= 442.49)

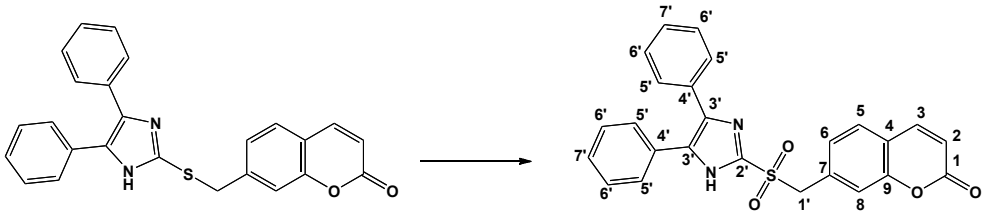

100 **100**

General procedure 13;
Reagent: 7-(((4,5-diphenyl-1*H*-imidazol-2-*yl*)thio)methyl)-2*H*-chromen-2-one **96** (0.12 g, 0.29 mmol);
T.L.C. System: DCM-MeOH 9:1 v/v, Rf: 0.42;
White solid;
Purification: recrystallization from DCM/*n*-hexane;
Yield: 0.05g, 39%;
Melting point:225-227 °C;
MS $(ESI)^+$: 443.1 $[M+H]^+$

^{1}H-NMR (DMSO-d_6), δ: 5.02 (s, 2H, H-1'), 6.52 (d, 1H, J= 9.5 Hz, H-aromatic), 7.19 (d, 1H, J= 8.0 Hz, H-aromatic), 7.24 (s, 1H, H-aromatic), 7.27-7.55 (m, 10H, H-aromatic), 7.71 (d, 1H, J= 7.9 Hz, H-aromatic), 8.07 (d, 1H, J= 9.5 Hz, H-aromatic), 13.86 (bs, 1H, NH).

^{13}C-NMR (DMSO-d_6), δ: 60.32 (CH_2, C-1'), 116.68, 118.67 (CH, C-aromatic), 118.78 (C, C-aromatic), 127.09, 128.28, 128.46 (CH, C-aromatic), 132.13 (C, C-aromatic), 143.79 (CH, C-aromatic), 143.95, 153.07 (C, C-aromatic), 159.64 (C, C-1).

6.10 Synthesis of (2*E*)-*N*'-benzylidene aryl acrylohydrazides

6.10.1 General procedures 14-17

General procedure 14: synthesis of acrylic acids

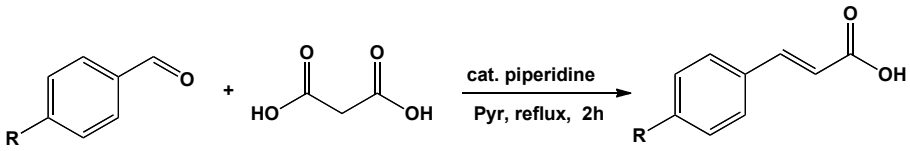

A mixture of malonic acid (1.61g, 11.5 mmol), the desired aldehyde (5.7 mmol) and a catalytic amount of piperidine (0.1 mL) was heated in a solution of pyridine (5 mL) at reflux for 2 h. The resultant mixture was poured into ice and a solution of 2 M HCl aq. was added dropwise. The formed solid was collected by filtration, washed with water and purified by flash column chromatography (*n*-hexane:EtOAc 100:0 v/v, increasing to 80:20 v/v) to give the title compound.

General procedure 15: synthesis of acryloyl chlorides

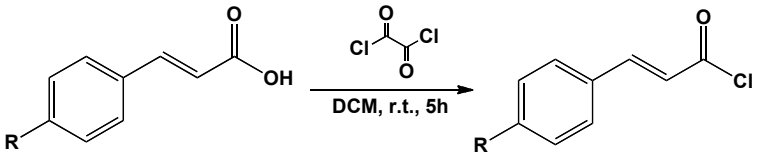

To a stirred solution of acid (6 mmol), in DCM (50 mL) was added oxalyl chloride (1 mL, 12 mmol), and the mixture was stirred at room temperature for 5 h. The resulting solution was concentrated under reduced pressure to give the desired product which was used without further purification.

General procedure 16: synthesis of aryl hydrazones

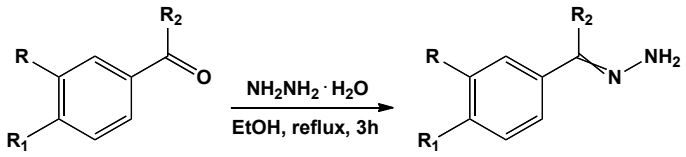

A solution of the corresponding benzaldehyde (1 eq.) in ethanol (1.80 mL/ mmol eq.) was treated with hydrazine monohydrate (1.1 eq.). The mixture was heated under reflux for 3 h and the solvent was evaporated under reduced pressure. The solid residue was washed with hexane, collected by filtration and dried.

General procedure 17: synthesis of (2*E*)-*N*'-benzylidene aryl acrylohydrazides

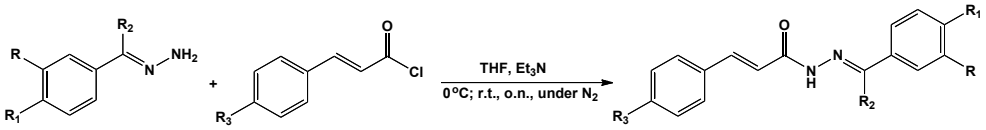

The desired acryloyl chloride (2.5 mmol) was dissolved in dry THF (16 mL) and cooled to 0 ºC. TEA (0.71 mL, 5 mmol) was then added. The hydrazide derivative (2.5 mmol), dissolved in dry THF (14 mL) was then added dropwise at 0 ºC. The solution was stirred for 24 h under nitrogen atmosphere. The reaction was stopped and water (30 mL) were added. The formed solid was filtered, dried and purified by flash column chromatography or recrystallization to afford the title compound.

6.10.2 Aryl acrylic acids (115-118)

(*E*)-3-(4-Isopropylphenyl)acrylic acid (115)[29]
($C_{12}H_{14}O_2$: M.W.= 190.24)

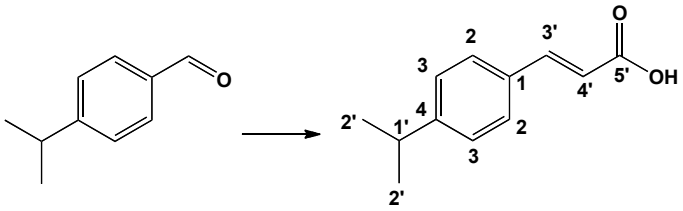

111 **115**

General procedure 14;
T.L.C. system: *n*-hexane -EtOAc 1:1 v/v, Rf: 0.50;
White powder;
Yield: 0.098 g, 91 %

^{1}H-NMR ($CDCl_3$), δ: 1.29 (d, J= 6.9 Hz, 6H, H-2'), 2.93-2.99 (m, 1H, H-1'), 6.44 (d, J= 15.9 Hz, 1H, H-3'), 7.29 (d, J= 8.0 Hz, 2H, H-aromatic), 7.52 (d, J=8.0 Hz, 2H, H-aromatic), 7.81 (d, J= 15.9 Hz, 1H, H-4'), 11.75 (bs, 1H, -COOH).

^{13}C-NMR ($CDCl_3$), δ: 23.74 (CH_3, C-2'), 34.13 (CH, C-1'), 116.18 (CH, C-3'), 127.10, 128.51 (CH, C-aromatic), 131.74 (C, C-aromatic), 147.08 (CH, C-4'), 152.16 (C, C-aromatic), 172.14 (C, C-5').

(*E*)-3-(4-(Trifluoromethyl)phenyl)acrylic acid (116)[40]
($C_{10}H_7F_3O_2$: M.W.=216.16)

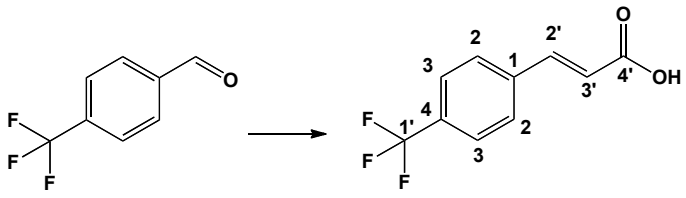

112 **116**

General procedure 14;
T.L.C. system: *n*-hexane -EtOAc 1:1 v/v, Rf: 0.32;
White powder;
Yield: 1.12 g, 91 %

^{1}H-NMR (DMSO-d_6), δ: 6.68 (d, J= 16.0 Hz, 1H, H-2'), 7.66 (d, J= 16.0 Hz, 1H, H-3'), 7.77 (d, J= 8.0 Hz, 2H, H-aromatic), 7.92 (d, J= 8.0 Hz, 2H, H-aromatic), 12.59 (bs, 1H, -COO<u>H</u>).

^{13}C-NMR (DMSO-d_6), δ: 122.16 (CH, C-2'), 125.09 (C, C-4), 125.64, 125.67, 128.80 (CH, C-aromatic), 129.67 (C, C-1'), 138.27 (C, C-1), 142.03 (CH, C-3'), 167.14 (C, C-5').

(*E*)-3-(4-Methoxyphenyl)acrylic acid (117)[40]
($C_{10}H_{10}O_3$: M.W.= 178.18)

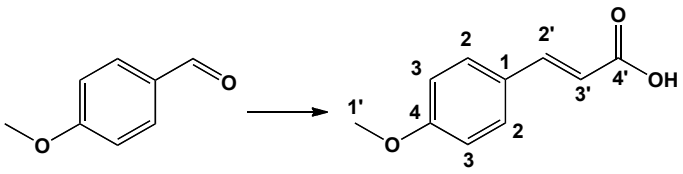

113 **117**

General procedure 14;
T.L.C. system: *n*-hexane -EtOAc 1:1 v/v, Rf: 0.52;
White powder;
Yield: 0.81 g, 80 %

^{1}H-NMR ($CDCl_3$), δ: 3.87 (s, 3H, H-1'), 6.35 (d, J= 15.8 Hz, 1H, H-2'), 6.95 (d, J= 8.8 Hz, 2H, H-aromatic), 7.53 (d, J= 8.8 Hz, 2H, H-aromatic), 7.77 (d, J= 15.8 Hz, 1H, H-3'), 11.50 (bs, 1H, -COO<u>H</u>).

^{13}C-NMR ($CDCl_3$), δ: 55.41 (CH_3, C-1'), 114.42 (CH, C-aromatic), 114.58 (CH, C-2'), 126.85 (C, C-aromatic), 130.09 (CH, C-aromatic), 146.68 (CH, C-3'), 161.77 (C, C-4').

(*E*)-3-(Biphenyl-4-*yl*)acrylic acid (118)[40]

($C_{15}H_{12}O_2$: M.W.= 224.25)

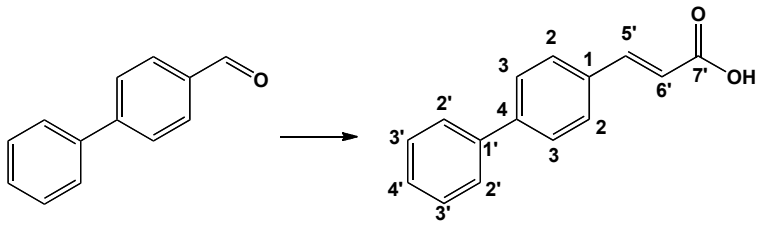

114 **118**

General procedure 14;
T.L.C. system: *n*-hexane -EtOAc 1:1 v/v, Rf: 0.66;
White powder;
Yield: 1.17 g, 92 %

^{1}H-NMR (DMSO-d_6), δ: 6.58 (d, J= 16.0 Hz, 1H, H-5'), 7.40-7.42 (m, 1H, H-aromatic), 7.48-7.50 (m, 2H, H-aromatic), 7.64 (d, J= 16.0 Hz, 1H, H-6'), 7.71-7.74 (m, 4H, H-aromatic), 7.79 (d, J= 8.4 Hz, 2H, H-aromatic), 12.40 (bs, 1H, -COO<u>H</u>).

^{13}C-NMR (DMSO-d_6), δ: 119.20 (CH, C-5'), 126.66, 127.04, 127.90, 128.82, 128.99 (CH, C-aromatic), 133.36, 139.22, 141.68, 143.35 (CH, C-6'), 167.56 (C, C-7').

6.10.3 Aryl acryloyl chlorides (119-122)

(*E*)-3-(4-Isopropylphenyl)acryloyl chloride (119)[30]
($C_{12}H_{13}ClO$: M.W.= 190.14)

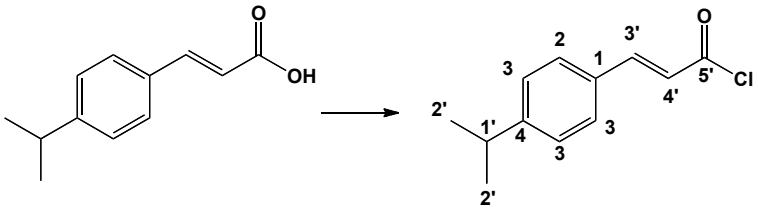

115 **119**

General procedure 15;
T.L.C. system: *n*-hexane -EtOAc 1:1 v/v, Rf: 0.74;
Pale yellow oil;
Yield: 1.1 g, 100 %

^{1}H-NMR ($CDCl_3$), δ: 1.29 (d, J= 6.9 Hz, 6H, H-2'), 2.93-3.02 (m, 1H, H-1'), 6.63 (d, J= 15.4 Hz, 1H, H-3'), 7.32 (d, J= 8.0 Hz, 2H, H-aromatic), 7.53 (d, J= 8.0 Hz, 2H, H-aromatic), 7.85 (d, J= 15.4 Hz, 1H, H-4'),

^{13}C-NMR ($CDCl_3$), δ: 23.65 (CH_3, C-2'), 34.25 (CH, C-1'), 121.29 (CH, C-3'), 127.11, 129.31 (CH, C-aromatic), 130.75 (C, C-aromatic), 150.83 (CH, C-4'), 153.76 (C, C-aromatic), 166.18 (C, C-5').

(*E*)-3-(4-(Trifluoromethyl)phenyl)acryloyl chloride (120)[31]
($C_{10}H_6ClF_3O$: M.W.= 234.60)

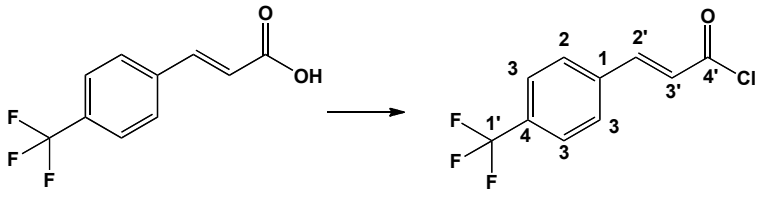

116 **120**

General procedure15;
T.L.C. system: *n*-hexane -EtOAc 1:1 v/v, Rf: 0.40;
Pale yellow powder;
Yield: 1.27 g, 91 %

^{1}H-NMR (DMSO-d_6), δ: 6.69 (d, J= 16.0 Hz, 1H, H-2'), 7.67 (d, J= 16.0 Hz, 1H, H-3'), 7.76 (d, J= 8.0 Hz, 2H, H-aromatic), 7.92 (d, J= 8.0 Hz, 2H, H-aromatic).

^{13}C-NMR (DMSO-d_6), δ: 122.16 (CH, C-2'), 125.09 (C, C-4), 125.64, 125.67, 128.80 (CH, C-aromatic), 129.66, 129.92 (C, C-1'), 138.28 (C, C-1), 142.03 (CH, C-3'), 167.13 (C, C-5').

(*E*)-3-(4-Methoxyphenyl)acryloyl chloride (121)[32]
($C_{10}H_9ClO_2$: M.W.= 196.63)

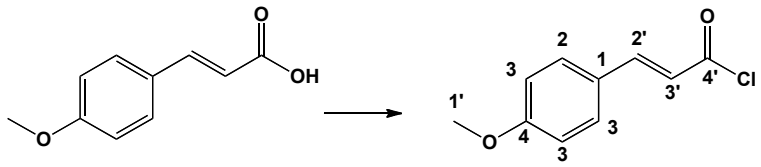

117 **121**

General procedure 15;
T.L.C. system: *n*-hexane -EtOAc 1:1 v/v, Rf: 0.56;
Yellow powder;
Yield: 1.10 g, 94 %

^{1}H-NMR ($CDCl_3$), δ: 3.89 (s, 3H, H-1'), 6.54 (d, J= 15.4 Hz, 1H, H-2'), 6.97 (d, J= 8.7 Hz, 2H, H-aromatic), 7.56 (d, J= 8.7 Hz, 2H, H-aromatic), 7.82 (d, J= 15.4 Hz, 1H, H-3').

^{13}C-NMR ($CDCl_3$), δ: 55.41 (CH_3, C-1'), 114.43 (CH, C-aromatic), 114.58 (CH, C-2'), 126.85 (C, C-aromatic), 130.10 (CH, C-aromatic), 146.72 (CH, C-3'), 161.78 (C, C-4').

(*E*)-3-(Biphenyl-4-yl)acryloyl chloride (122)[33]
($C_{15}H_{11}ClO$: M.W.= 242.70)

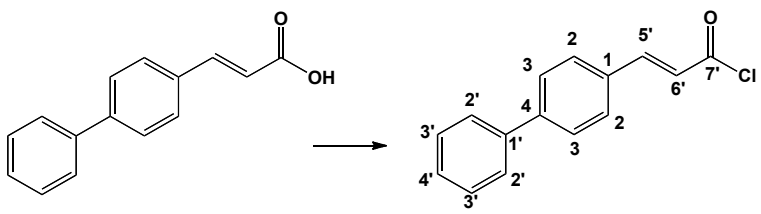

118 **122**

General procedure 15;
T.L.C. system: *n*-hexane-EtOAc 1:1 v/v, Rf: 0.56;
Pale yellow powder;
Yield: 1.42 g, 98 %

^{1}H-NMR (DMSO-d$_6$), δ: 6.58 (d, J= 16.0 Hz, 1H, H-5'), 7.39-7.41 (m, 1H, H-aromatic), 7.48-7.50 (m, 1H, H-aromatic), 7.64 (d, J= 16.0 Hz, 1H, H-6'), 7.71-7.74 (m, 4H, H-aromatic), 7.78 (d, J= 8.4 Hz, 2H, H-aromatic).

^{13}C-NMR (DMSO-d$_6$), δ: 119.16 (CH, C-5'), 126.66, 127.04, 127.89, 128.82, 128.99 (CH, C-aromatic), 133.35, 139.21, 141.68 (C, C-aromatic), 143.37 (CH, C-6'), 167.53 (C, C-7').

6.10.4 Aryl hydrazones (126-128)

(4-Methylbenzylidene)hydrazine (126)[34]
($C_8H_{10}N_2$; M.W.= 134.178)

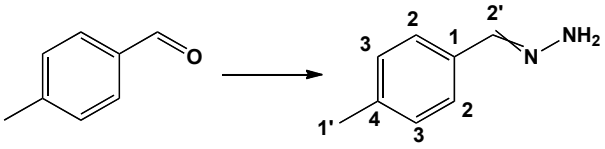

123 **126**

General procedure 16;
Reagent: benzaldehyde () (1 g, 8.32 mmol);
T.L.C. system: *n*-hexane- EtOAc 1:1 v/v, Rf: 0.32
Pale yellow powder;
Yield: 0.851 g, 76 %

^{1}H-NMR (DMSO-d_6), δ: 2.28 (s, 3H, H-1'), 6.62 (bs, 2H, N$\underline{H}_2$), 7.13 (d, J= 8.0 Hz, 2H, H-aromatic), 7.36 (d, J= 8.0 Hz, 2H, H-aromatic), 7.67 (s, 1H, H-2').

^{13}C-NMR (DMSO-d_6), δ: 20.79 (CH_3, C-1'), 125.11, 129.04 (CH, C-aromatic), 133.64, 136.68 (C, C-aromatic).

(3,4-Diethoxybenzylidene)hydrazine (127)
($C_{11}H_{16}N_2O_2$; M.W.= 208.257)

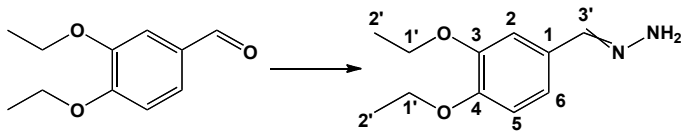

124 **127**

General procedure 16;
Reagent: 3,4-Diethoxybenzaldehyde () (1 g, 5.15 mmol);
T.L.C. system: *n*-hexane -EtOAc 1:1 v/v, Rf: 0.24
Pale yellow powder;
Yield: 0.980 g, 91 %

^{1}H-NMR (DMSO-d_6), δ: 1.30-1.34 (m, 6H, H-2'), 3.99-4.04 (m, 4H, H-1'), 6.49 (bs, 2H, N$\underline{H}_2$), 6.90 (s, 2H, H-aromatic), 7.12 (s, 1H, H-aromatic), 7.62 (s,1H,

H-3').

^{13}C-NMR (DMSO-d$_6$), δ: 14.72 (CH_3, C-2'), 63.55 (CH_2, C-1'), 109.03, 113.14, 118.74 (CH, C-aromatic), 129.38 (C, C-aromatic), 138.82 (CH, C-3'), 148.03, 148.30 (C, C-aromatic).

(1-(4-Cyclohexylphenyl)ethylidene)hydrazine (120)
($C_{14}H_20N_2$; M.W.= 216.322)

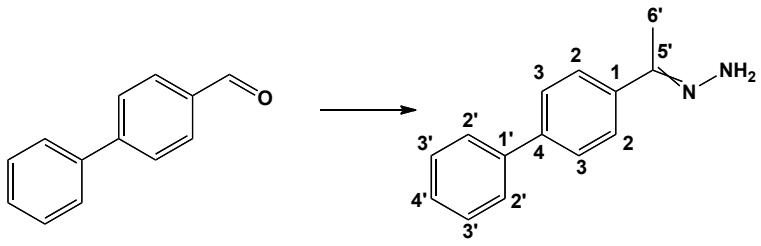

125 **128**

General procedure 16;
Reagent:4′-Cyclohexylacetophenone () (1 g, 4.94 mmol);
T.L.C. system: *n*-hexane- EtOAc 1:1 v/v, Rf: 0.61
Pale yellow powder;
Yield: 1.01 g, 94 %

^{1}H-NMR (DMSO-d$_6$), δ: 1.19-1.27 (m, 1H, H-4'), 1.34-1.41 (m, 4H, CH_2), 1.69-1.71 (m, 1H, H-4'), 1.76-1.80 (m, 4H, CH_2), 2.00 (s, 3H, H-6'), 2.46-2.49 (m, 1H, H-1'), 6.24 (bs, 2H, N$\underline{H}_2$), 7.16 (d, J= 8.3 Hz, 2H, H-aromatic), 7.52 (d, J= 8.3 Hz, 2H, H-aromatic).

^{13}C-NMR (DMSO-d$_6$), δ: 11.34 (CH_3, C-6'), 25.58, 26.32, 33.88 (CH_2), 43.39 (CH, C-1'), 124.73, 126.29 (CH, C-aromatic), 137.51, 142.32, 146.34 (C, C-aromatic).

4-(Hydrazonomethyl)phenol (168)[32]
($C_7H_8N_2O$; M.W.= 136.151)

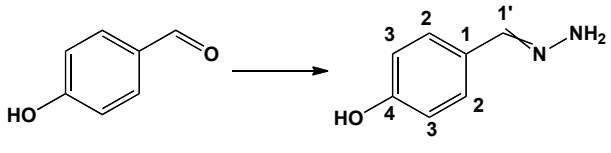

142 **168**

General procedure 16;
Reagent: 4-hydroxybenzaldehyde (**142**) (1 g, 8.19 mmol);
T.L.C. system *n*-hexane- EtOAc 1:1 v/v, Rf: 0.15
Pale yellow powder;
Yield: 1.16 g, 99 %

^{1}H-NMR (DMSO-d$_6$), δ: 6.37 (bs, 2H, N<u>H</u>$_2$), 6.72 (d, J= 8.5 Hz, 2H, H-aromatic), 7.30 (d, J= 8.5 Hz, 2H, H-aromatic), 7.62 (s, 1H, H-1'), 9.36 (bs, 1H, -O<u>H</u>).

^{13}C-NMR (DMSO-d$_6$), δ: 115.30 (CH, C-aromatic), 126.60 (CH, C-aromatic), 127.44 (C, C-aromatic), 139.34 (CH, C-1'), 157.16 (C, C-aromatic).

6.10.5 *N'*-benzylideneacrylohydrazides (121-132)

3-(4-Isopropylphenyl)-*N'*-(4-methylbenzylidene)acrylohydrazide (129) ($C_{20}H_{22}NO_2$; M.W.= 306.40)

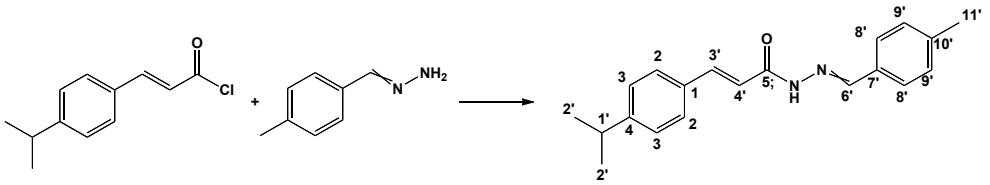

119 **126** **129a,b**

General procedure 17;
T.L.C. system: *n*-hexane -EtOAc 1:1 v/v, Rf: 0.56;
White powder;
Purification: recrystallization from DCM/*n*-hexane;
Yield: 0.441 g, 58 %
Melting point: 157-161 ºC
MS $(ESI)^+$: 307.2 $[M+H]^+$
Two species observed. Major/minor species ratio: 2:1

^{1}H-NMR (DMSO-d_6), δ: (major species, **129a**) 1.21-1.24 (m, 6H, H-2'), 2.35 (s, 3H, H-11'), 2.89-2.97 (m, 1H, H-1'), 6.66 (d, J= 15.6 Hz, 1H, H-3'), 7.27 (d, J= 7.9 Hz, 2H, H-aromatic), 7.60-7.68 (m, 7H, H-aromatic, H-trans), 8.21 (s, 1H, H-6'), 11.57 (bs, s, 1H, H, NH).

^{1}H-NMR (DMSO-d_6), δ: (minor species, **129b**) 1.21-1.24 (m, 6H, H-2'), 2.35 (s, 3H, H-11'), 2.89-2.97 (m, 1H, H-1'), 7.27 (d, J= 7.9 Hz, 2H, H-aromatic), 7.31-7.35 (m, 4H, H-aromatic, H-trans), 7.51-7.58 (m, 4H, H-aromatic, H-trans), 8.03 (s, 1H, H-6'), 11.39 (bs, s, 1H, H, NH).

^{13}C-NMR (DMSO-d_6), δ: 21.01 (CH_3, C-11'), 23.62 (CH_3, C-2'), 33.31 (CH, C-1'), 116.24, 119.29 (CH, C-3'), 126.83, 126.90, 126.94, 127.05, 127.80, 128.25, 129.39 (CH, C-aromatic), 131.49, 131.60, 132.34, 132.53, 139.51, 139.81 (C, C-aromatic), 140.37, 141.95 (CH, C-4'), 143.13, 146.57 (CH, C-6'), 150.47, 150.62 (C, C-aromatic), 161.45, 166.02 (C, C-5').

***N'*-(3,4-Diethoxybenzylidene)-3-(4-isopropylphenyl)acrylohydrazide (130)**
($C_{23}H_{28}N_2O_3$; M.W.= 380.48)

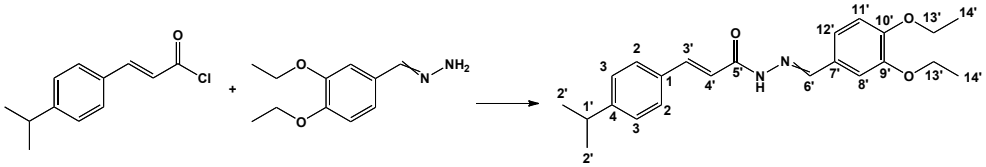

119 **127** **130a,b**

General procedure 17;
T.L.C. system: DCM-MeOH 95:5 v/v, Rf: 0.55;
Yellow powder;
Purification: flash column chromatography (DCM-MeOH 100:0 v/v, increasing to 98:2 v/v);
Yield: 0.120 g, 13 %
Melting point: 118-125 °C
MS $(ESI)^+$: 403.2 $[M+Na]^+$
Two major species observed. Major/minor species ratio: 5:3

^{1}H-NMR (DMSO-d_6), δ: (major species, **130a**) 1.27 (d, J= 1.24 Hz, 6H, H-2'), 1.33-1.39 (m, 6H, H-14'), 2.89-2.97 (m, 1H, H-1'), 4.08 (q, J= 6.9 Hz, 3H, H-13'), 4.12-4.15 (m, 1H, H-13'), 6.65 (d, J= 15.7 Hz, 1H, H-3'), 7.01 (d, J= 8.3 Hz, 1H, H-aromatic), 7.20 (d, J= 8.4 Hz, 1H, H-aromatic), 7.31-7.34 (m, 2H, H-aromatic, H-trans), 7.55 (d, J= 8.1 Hz, 3H, H-aromatic), 7.65 (d, J= 7.4 Hz, 1H, H-aromatic), 8.15 (s, 1H, H-6'), 11.49 (bs, 1H, NH).

^{1}H-NMR (DMSO-d_6), δ: (minor species, **130b**) 1.27 (d, J= 1.24 Hz, 6H, H-2'), 1.33-1.39 (m, 6H, H-14'), 2.89-2.97 (m, 1H, H-1'), 4.08 (q, J= 6.9 Hz, 3H, H-13'), 4.12-4.15 (m, 1H, H-13'), 7.01 (d, J= 8.3 Hz, 1H, H-aromatic), 7.24 (d, J= 8.4 Hz, 1H, H-aromatic), 7.31-7.34 (m, 4H, H-aromatic, H-trans), 7.58-7.60 (m, 1H, H-aromatic), 7.61-7.63 (m, 1H, H-trans), 7.65 (d, J= 7.4 Hz, 1H, H-aromatic), 7.97 (s, 1H, H-6'), 11.36 (bs, 1H, NH).

^{13}C-NMR (DMSO-d_6), δ: 14.62, 14.91 (CH_3, C-2'), 23.61 (CH_3, C-14'), 33.30 (C, C-1'), 63.78, 63.85 (CH_2, C-13'), 110.09, 110.77, 112.76, 112.98, 116.41, 119.41, 120.70, 121.71, 126.92, 127.76, 128.17 (CH, C-aromatic), 132.37, 132.57 (C, C-aromatic), 140.14 , 141.71, 143.10, 146.72 (CH, C-aromatic), 148.36, 149.87, 150.14, 150.40, 150.58 (C, C-aromatic), 161.32, 165.91 (C, C-5').

***N'*-(1-(4-Cyclohexylphenyl)ethylidene)-3-(4-isopropylphenyl)acrylohydrazide (131)**

($C_{26}H_{32}N_2O$; M.W.= 388.55)

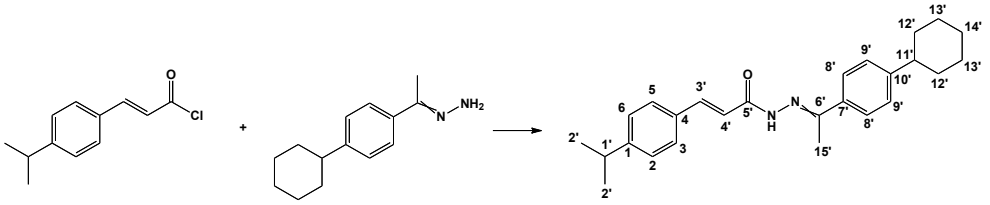

119 **128** **131a,b**

General procedure 17;

T.L.C. system: *n*-hexane -EtOAc 1:1 v/v, Rf: 0.65;

White powder;

Purification: recrystallization from DCM/*n*-hexane;

Yield: 0.178 g, 18.3 %;

Melting point: 186-190 °C;

MS $(ESI)^+$: 389.3 $[M+H]^+$

Two species observed. Major/minor species ratio: 10:7

^{1}H-NMR (DMSO-d_6), δ: (major species, **131a**) 1.22 (d, J= 6.8 Hz, 6H, H-2'), 1.27-1.30 (m, 1H, H-14'), 1.34-1.47 (m, 4H, CH_2), 1.69-1.74 (m, 1H, CH_2), 1.78-1.82 (m, 4H, CH_2), 2.31 (s, 3H, H-15'), 2.55-2.59 (m, 1H, H-11'), 2.90-2.96 (m, 1H, H-1'), 7.00 (d, J= 15.9 Hz, 1H, H-3'), 7.27-7.30 (m, 2H, H-aromatic), 7.33 (d, J= 8.1 Hz, 2H, H-aromatic), 7.54-7.60 (m, 2H, H-aromatic), 7.61-7.69 (m, 1H, H-trans), 7.74 (d, J= 7.9 Hz, 2H, H-aromatic), 10.49 (bs, 1H, NH).

^{1}H-NMR (DMSO-d_6), δ: (minor species, **131b**) 1.22 (d, J= 6.8 Hz, 6H, H-2'), 1.27-1.30 (m, 1H, H-14'), 1.34-1.47 (m, 5H, CH_2), 1.72 (d, J= 13.0 Hz, 1H, CH), 1.80 (d, J= 10.4 Hz, 4H, CH_2), 2.28 (s, 3H, H-15'), 2.90-2.96 (m, 1H, CH), 7.28 (d, J=7.3 Hz, 2H, H-aromatic), 7.33 (d, J= 8.1 Hz, 2H, H-aromatic), 7.50-7.60 (m, 2H, H-aromatic, H-trans), 7.61-7.69 (m, 2H, H-aromatic, H-trans), 7.74 (d, J= 7.9 Hz, 2H, H-aromatic), 10.57 (bs, 1H, NH).

^{13}C-NMR (DMSO-d_6), δ: 12.68, 14.94 (CH_3, C-15'), 23.81, 25.05 (CH_3, C-2'), 26.06, 26.13 (CH_2, C-14'), 26.80, 26.84, 26.86 (CH_2), 34.10 (CH, C-1'), 34.28, 34.33 (CH_2), 44.41, 44.46 (CH, C-14'), 115.76 (CH, C-4'), 126.20, 126.61, 126.80, 126.88, 126.93, 127.01, 128.15, 128.42 (CH, C-aromatic), 132.93,

135.67, 136.21 (C, C-aromatic), 143.44, 143.78 (CH, C-3'), 147.02, 149.66, 149.76, 151.28, 157.62 (C, C-aromatic), 167.65 (C, C-5').

***N'*-(4-Methylbenzylidene)-3-(4-(trifluoromethyl)phenyl)acrylohydrazide (132) ($C_{18}H_{15}F_3N_2O$; M.W.= 332.32)**

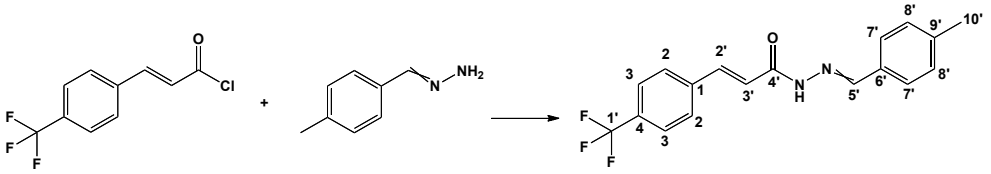

120 **126** **132a,b**

General procedure 17;
T.L.C. system: *n*-hexane -EtOAc 1:1 v/v, Rf: 0.37;
White powder;
Purification: recrystallization from EtOH/H_2O
Yield: 0.05 g, 6 %
Melting point: 166-170 °C
MS $(ESI)^+$: 355.1 $[M+Na]^+$
Two species observed. Major/minor species ratio: 5:4

^{1}H-NMR (DMSO-d_6), δ: (major species, **132a**) 2.36 (s, 3H, H-10'), 6.84 (d, J= 16.0 Hz, 1H, H-2'), 7.26-7.29 (m, 2H, H-aromatic), 7.80 (d, J= 8.2 Hz, 4H, H-aromatic, H-trans), 7.85 (d, J= 8.2 Hz, 2H, H-aromatic), 7.99 (d, J= 8.2 Hz, 1H, H-aromatic), 8.23 (s, 1H, H-5'), 11.68 (bs, 1H, NH).

^{1}H-NMR (DMSO-d_6), δ: (minor species, **132b**) 2.36 (s, 3H, H-10'), 7.26-7.29 (m, 1H, H-aromatic, H-trans), 7.63-7.68 (m, 5H, H-aromatic), 7.71-7.74 (m, 2H, H-aromatic, H-trans), 7.85 (d, J= 8.2 Hz, 1H, H-aromatic), 7.99 (d, J= 8.2 Hz, 1H, H-aromatic), 8.05 (s, 1H, H-5'), 11.54 (bs, 1H, NH).

^{13}C-NMR (DMSO-d_6), δ: 21.01, 21.59 (CH_3, C-10'), 120.13, 123.20 (CH, C-2'), 122.98, 125.14 (C, C-aromatic), 125.73, 125.82, 125.85, 126.94, 128.32, 128.83, 129.39, 129.59 (CH, C-aromatic), 127.15, 131.36, 131.47 (C, C-aromatic), 138.64, 140.17 (CH, C-3'), 138.73, 138.84, 139.66, 139.99 (C, C-aromatic), 143.67, 147.19 (CH, C-5'), 160.84, 165.46 (C, C-4').

***N'*-(3,4-Diethoxybenzylidene)-3-(4-(trifluoromethyl)phenyl)acrylohydrazide (133)**
($C_{21}H_{21}F_3N_2O_3$; M.W.= 406.40)

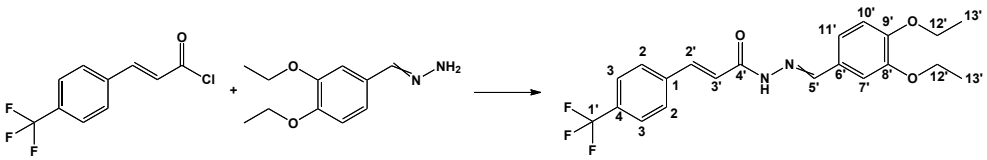

120 **127** **133a,b**

General procedure 17;
T.L.C. system: *n*-hexane -EtOAc 1:1 v/v, Rf: 0.62
Yellow powder;
Purification by flash column chromatography (*n*-hexane:EtOAc 100:0 v/v, increasing to 60:40 v/v);
Yield: 0.050 g, 5 %;
Melting point: 140-144 °C
MS $(ESI)^+$: 429.1 $[M+Na]^+$
Two major species observed. Major/minor species ratio: 10:6

^{1}H-NMR (DMSO-d_6), δ: (major species, **133a**) 1.36 (q, J= 6.7 Hz, 6H, H-13'), 4.06-4.15 (m, 4H, H-12'), 6.84 (d, J= 15.9 Hz, 1H, H-2'), 7.02-7.04 (m, 1H, H-aromatic), 7.22 (d, J= 8.2 Hz, 1H, H-aromatic), 7.34 (d, J= 7.6 Hz, 1H, H-aromatic),7.68 (d, J= 15.9 Hz, 1H, H-3'), 7.73 (s, 1H, H-aromatic), 7.80 (d, J= 8.5 Hz, 2H, H-aromatic), 7.85 (d, J= 8.2 Hz, 1H, H-aromatic), 7.96-7.99 (m, 1H, H-aromatic), 8.17 (s, 1H, H-5'), 11.60 (bs, 1H N<u>H</u>).

^{1}H-NMR (DMSO-d_6), δ: (minor species, **133b**) 1.36 (q, J= 6.7 Hz, 6H, H-13'), 4.06-4.15 (m, 4H, H-12'), 7.02-7.04 (m, 1H, H-trans), 7.26 (d, J= 8.2 Hz, 1H, H-aromatic), 7.34 (d, J= 7.6 Hz, 1H, H-aromatic), 7.80 (d, J= 8.5 Hz, 2H, H-aromatic), 7.85 (d, J= 8.2 Hz, 2H, H-aromatic), 7.96-7.99 (m, 2H, H-aromatic, H-trans), 11.52 (bs, 1H- N<u>H</u>).

^{13}C-NMR (DMSO-d_6), δ: 14.62, 14.70 (CH_3, C-12'), 63.78, 63.87 (CH_2, C-11'), 110.14, 110.98, 112.75, 112.95, 120.34, 120.82, 121.85, 123.33, 125.81 (CH, C-aromatic), 126.81 (C, C-aromatic), 128.29, 128.74, 138.41 (CH, C-aromatic), 138.87 (C, C-aromatic), 139.93, 143.65, 147.38 (CH, C-aromatic), 147.85, 148.36, 150.26 (C, C-aromatic), 160.69 (C, C-4').

***N'*-(1-(4-Cyclohexylphenyl)ethylidene)-3-(4-(trifluoromethyl)phenyl) acrylohydrazide (134)**

($C_{24}H_{25}F_3N_2O$: M.W.= 414.46)

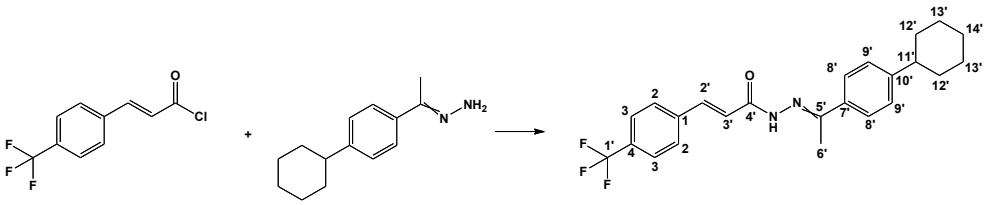

120 **128** **134a,b**

General procedure 17;

T.L.C. system: *n*-hexane- EtOAc 1:1 v/v, Rf: 0.76;

White powder;

Purification by flash column chromatography (*n*-hexane:EtOAc 100:0 v/v, increasing to 75);

Yield: 0.120 g, 12 %;

Melting point: 200-206 ^oC

MS $(ESI)^+$: 437.2 $[M+Na]^+$

Two species observed. Major/minor species ratio: 2:1

^{1}H-NMR (DMSO-d_6), δ: (major species, **134a**) 1.21-1.31 (m, 1H, H-14'), 1.34-1.47 (m, 5H, CH_2), 1.71-1.73 (m, 1H, CH), 1.80-1.82 (m, 4H, CH_2), 2.33 (s, 3H, H-6'), 7.19 (d, J= 15.4 Hz, 1H, H-2'), 7.28 (d, J= 8.3 Hz, 2H, H-aromatic), 7.68 (d, J= 15.4 Hz, 1H, H-3'), 7.75-7.78 (m, 3H, H-aromatic), 7.79-7.87 (m, 2H, H-aromatic), 7.95 (d, J= 7.8 Hz, 1H, H-aromatic), 10.61 (bs, 1H, N<u>H</u>).

^{1}H-NMR (DMSO-d_6), δ: (minor species, **134b**) 1.21-1.31 (m, 1H, H-14'), 1.34-1.47 (m, 3H, CH_2), 1.71-1.73 (m, 1H, CH), 1.80-1.82 (m, 4H, CH_2), 2.31 (s, 3H, H-6'), 2.53-2.57 (m, 2H, CH_2), 7.28 (d, J= 8.3 Hz, 2H, H-aromatic), 7.75-7.78 (m, 2H, H-aromatic, H-trans), 7.79-7.87 (m, 5H, H-aromatic, H-trans), 7.95 (d, J= 7.8 Hz, 1H, H-aromatic), 10.72 (bs, 1H, N<u>H</u>).

^{13}C-NMR (DMSO-d_6), δ: 13.71, 14.06 (CH_3, C-6'), 25.54 (CH_2, C-14'), 26.26, 33.77 (CH_2), 43.51 (CH, C-11'), 120.71 (CH, C-2'), 122.99 (C, C-aromatic), 123.79 125.83, 126.17, 126.41, 126.58, 126.70, 128.23, 128.70 (CH, C-aromatic), 137.75 (C, C-aromatic), 138.30, 140.03 (CH, C-3'), 138.97, 148.36, 148.95, 152.26 (C, C-aromatic), 161.24 (C, C-4').

3-(4-Methoxyphenyl)-*N*'-(4-methylbenzylidene)acrylohydrazide (135)[35]
($C_{18}H_{18}N_2O_2$; M.W.= 294.35)

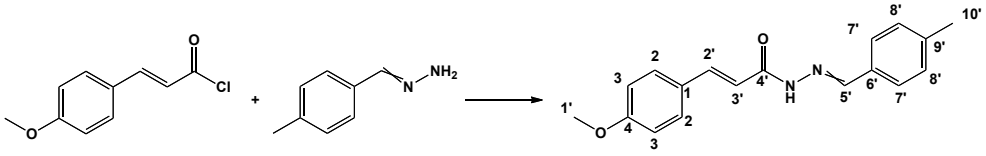

121 **126** **135a,b**

General procedure 17;
T.L.C. system: *n*-hexane -EtOAc 1:1 v/v, Rf: 0.40;
White powder;
Purification: recrystallization from $EtOH/H_2O$;
Yield: 0.405 g, 55 %;
Melting point: 184-188 °C
MS $(ESI)^+$: 295.1 $[M+H]^+$
Two major species observed. Major/minor ratio: 7:5

^{1}H-NMR (DMSO-d_6), δ: (major species, **135a**) 2.35 (s, 3H, H-10'), 3.81 (s, 3H, H-1'), 6.56 (d, J= 15.8 Hz, 1H, H-2'), 7.01 (d, J= 7.5 Hz, 2H, H-aromatic), 7.27 (d, J= 7.5 Hz, 2H, H-aromatic), 7.55-7.66 (m, 3H, H-aromatic, H-trans), 7.71 (d, J= 8.20 Hz, 2H, H-aromatic), 8.20 (s, 1H, H-5'), 11.51 (bs, 1H, NH).

^{1}H-NMR (DMSO-d_6), δ: 2.35 (minor species, **135b**) (s, 3H, H-10'), 3.82 (s, 3H, H-1'), 7.01 (d, J= 7.5 Hz, 2H, H-aromatic), 7.27 (d, J= 7.5 Hz, 2H, H-aromatic), 7.45 (d, J= 15.8 Hz, 1H, H-2'), 7.55-7.66 (m, 5H, H-aromatic, H-trans), 8.02 (s, 1H, H-5'), 11.34 (bs, 1H, NH),

^{13}C-NMR (DMSO-d_6), δ: 21.00 (CH_3, C-10'), 55.28 (CH_3, C-1'), 114.39, 114.44, 114.56 (CH, C-aromatic), 117.69 (CH, C-2'), 126.81, 127.02 (CH, C-aromatic), 127.06, 127.46 (C, C-aromatic), 129.37, 129.87 (CH, C-aromatic), 131.54, 131.66, 139.44, 139.74 (C, C-aromatic), 140.17 (CH, C-aromatic), 141.77 (CH, C-aromatic), 142.93 (CH, C-aromatic), 146.33 (CH, C-5'), 160.62 (C, C-aromatic), 161.64 (C, C-4').

***N'*-(3,4-Diethoxybenzylidene)-3-(4-methoxyphenyl)acrylohydrazide (136)**
($C_{21}H_{24}N_2O_4$; M.W.= 368.43)

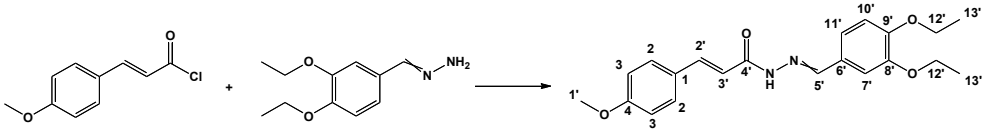

121 **127** **136a,b**

General procedure 17;
T.L.C. system: DCM-MeOH 95:5 v/v, Rf: 0.38;
Pale yellow powder;
Purification: flash column chromatography (DCM-MeOH 100:0 v/v, increasing to 99:1 v/v)
Yield: 0.32 g, 35%
Melting point: 140-146 ºC
MS $(ESI)^+$: 369.2 $[M+H]^+$
Two species observed. Major/minor species: 10:7

^{1}H-NMR (DMSO-d_6), δ: (major species, **136a**) 1.33-1.38 (m, 6H, H-13'), 3.81 (s, 3H, H-1'), 4.08 (q, J= 6.9 Hz, 4H, H-12'), 6.65 (d, J= 15.8 Hz, 1H, H-2'), 7.01 (d, J= 8.5 Hz, 4H, H-aromatic), 7.19 (d, J= 8.2 Hz, 1H, H-aromatic), 7.31-7.33 (m, 1H, H-aromatic), 7.62 (d, J= 15.8 Hz, 1H, H-3'), 7.58 (d, J= 8.2 Hz, 1H, H-aromatic), 8.15 (s, 1H, H-5'), 11.44 (bs, 1H, NH).

^{1}H-NMR (DMSO-d_6), δ: (minor species, **136b**) 1.33-1.38 (m, 6H, H-13'), 3.82 (s, 3H, H-1'), 4.08 (q, J= 6.9 Hz, 2H, H-12'), 4.11-4.15 (m, 2H, H-12'), 7.01 (d, J= 8.5 Hz, 1H, H-aromatic), 7.24 (d, J= 8.2 Hz, 1H, H-aromatic), 7.31-7.33 (m, 1H, H-trans), 7.45 (d, J= 15.8 Hz, 1H, H-2'), 7.53-7.55 (m, 1H, H-trans), 7.58 (d, J= 8.2 Hz, 2H, H-aromatic), 7.69 (d, J= 8.5 Hz, 2H, H-aromatic), 7.96 (s, 1H, H-5'), 11.30 (bs, 1H, NH).

^{13}C-NMR (DMSO-d_6), δ: 14.63, 14.71 (CH_3, C-13'), 55.28 (CH_3, C-1'), 63.78, 63.85 (CH_2, C-12'), 110.08, 110.85, 112.77, 113.00, 114.44, 114.75, 117.81, 120.64, 121.65 (CH, C-aromatic), 126.99, 127.29 (C, C-aromatic), 129.31, 129.79, 139.94, 141.54, 142.92, 146.53, 148.36 (CH, C-aromatic), 148.36, 150.20, 160.58 (C, C-aromatic), 161.50 (C, C-4').

***N'*-(1-(4-Cyclohexylphenyl)ethylidene)-3-(4-methoxyphenyl)acrylohydrazide (137)**
($C_{24}H_{28}N_2O_2$; M.W.= 376.49)

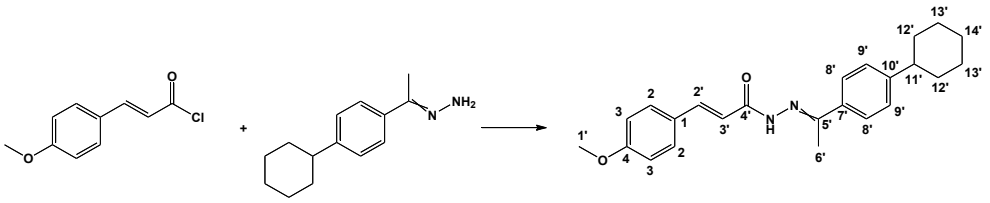

121 **128** **137**

General procedure 17;
T.L.C. system: *n*-hexane -EtOAc 1:1 v/v, Rf: 0.48;
White powder;
Purification: recrystallization from DCM/*n*-hexane;
Yield: 0.085 g, 9 %
Melting point: 194-200 °C;
MS $(ESI)^+$: 377.2 $[M+H]^+$

^{1}H-NMR ($CDCl_3$), δ: 1.26-1.35 (m, 1H, CH_2), 1.41-1.49 (m, 4H, CH_2), 1.77-1.82 (d, J= 12.6 Hz, 2H, CH), 1.86-1.94 (m, 4H, CH_2), 2.27 (s, 3H, H-1'), 2.53-2.61 (m, 1H, CH), 3.87 (s, 3H, H-6'), 6.95 (d, J= 8.6 Hz, 2H, H-aromatic), 7.30 (d, J= 8.0 Hz, 2H, H-aromatic), 7.51 (d, J= 15.9 Hz, 1H, H-2'), 7.61 (d, J= 8.4 Hz, 2H, H-aromatic), 7.74 (d, J= 7.5 Hz, 2H, H-aromatic), 7.84 (d, J= 15.9 Hz, 1H, H-3'), 8.58 (bs, 1H, N<u>H</u>).

^{13}C-NMR ($CDCl_3$), δ: 12.64, 14.10 (CH_3, C-6'), 26.06, 26.13, 26.80, 26.84, 34.28, 34.33 (CH_2), 44.41 (CH, C-11'), 55.37 (CH_3, C-1'), 114.19, 114.22, 114.27, 126.19, 126.61, 127.01, 128.14, 129.96 (CH, C-aromatic), 128.04, 135.69 (C, C-aromatic), 143.11, 143.48 (CH, C-3'), 146.84 (C, C-5'), 149.64, 161.12, 161.23 (C, C-aromatic), 167.70 (C, C-4').

3-(Biphenyl-4-*yl*)-*N*'-(4-methylbenzylidene)acrylohydrazide (138)
($C_{23}H_{20}N_2O$; M.W.= 340.42)

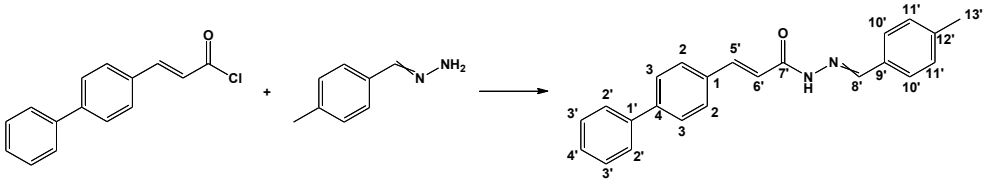

122 **126** **138a,b**

General procedure 17;
T.L.C. system: *n*-hexane -EtOAc 1:1 v/v, Rf: 0.39;
Purification: flash column chromatography (*n*-hexane:EtOAc 100:0 v/v, increasing to 50:50 v/v);
White powder;
Yield: 0.095 g, 10.6 %;
Melting point: 194-197 °C;
MS $(ESI)^+$: 363.1 $[M+Na]^+$
Two species observed. Major/minor species ratio: 5:4

^{1}H-NMR (DMSO-d_6), δ: (major species, **138a**) 2.36 (s, 3H, H-13'), 6.76 (d, J= 15.7 Hz, 1H, H-5'), 7.28 (d, J= 7.8 Hz, 1H, H-aromatic), 7.39-7.43 (m, 1H, H-aromatic), 7.48-7.53 (m, 1H, H-aromatic), 7.61-7.69 (m, 4H, H-aromatic), 7.71-7.79 (m, 6H, H-aromatic, H-trans), 7.86, (d, J= 8.0 Hz, 1H, H-6'), 8.23 (s, 1H, H-8'), 11.61 (bs, 1H, NH).

^{1}H-NMR (DMSO-d_6), δ: (minor species, **138b**) 2.36 (s, 3H, H-13'), 7.28 (d, J= 7.8 Hz, 2H, H-aromatic), 7.39-7.43 (m, 2H, H-aromatic, H-trans), 7.48-7.53 (m, 3H, H-aromatic), 7.61-7.69 (m, 2H, H-aromatic), 7.71-7.79 (m, 5H, H-aromatic, H-trans), 7.86, (d, J= 8.0 Hz, 1H, H-6'), 8.05 (s, 1H, H-8'), 11.45 (bs, 1H, NH).

^{13}C-NMR (DMSO-d_6), δ: 21.02 (CH_3, C-13'), 117.13, 120.27, 126.61, 126.65, 126.87, 127.08, 127.16, 127.85, 128.35, 128.83, 129.0, 129.39 (CH, H-aromatic), 131.47, 131.59, 133.80, 133.97, 139.25 (C, C-aromatic), 139.90, 141.48, 143.28, 146.72 (CH, C-aromatic), 161.33 (C, C-7').

3-(Biphenyl-4-*yl*)-*N*'-(3,4-diethoxybenzylidene)acrylohydrazide (139)
($C_{26}H_{26}N_2O_3$; M.W.= 414.50)

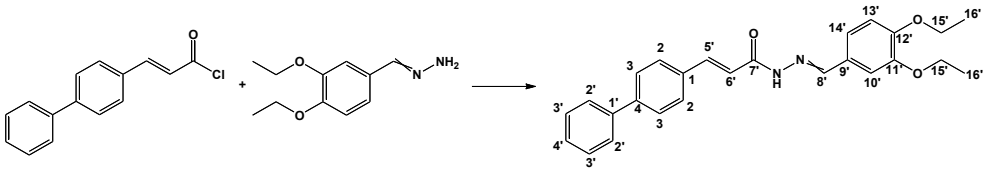

122 **127** **139a,b**

General procedure 17;
T.L.C. system: DCM-MeOH 95:5 v/v, Rf: 0.38;
Pale yellow powder;
Purification: flash column chromatography (DCM-MeOH 100:0 v/v, increasing to 99:1 v/v) and recrystallization from MeOH;
Yield: 0.064 g, 6 %
Melting poiNt: 158-162 °C
MS $(ESI)^+$: 415.2 $[M+H]^+$
Two species observe. Major/minor species ratio: 10:7

^{1}H-NMR (DMSO-d_6), δ: (major species, **139a**) 1.34-1.39 (m, 6H, H-16'), 4.08 (q, J= 6.7 Hz, 3H, H-15'), 4.14 (q, J= 6.7 Hz, 1H, H-15'), 6.75 (d, J= 15.7 Hz, 1H, H-5'), 7.02 (d, J= 8.3 Hz, 1H, H-aromatic), 7.21 (d, J= 8.3 Hz, 1H, H-aromatic), 7.34-7.36 (m, 1H, H-aromatic), 7.38-7.42 (m, 1H, H-aromatic), 7.48-7.52 (m, 2H, H-aromatic), 7.62-7.67 (m, 1H, H-aromatic), 7.70-7.75 (m, 1H, H-trans), 7.77 (d, J= 8.2 Hz, 4H, H-aromatic, H-6'), 7.84 (d, J= 8.2 Hz, 1H, H-aromatic), 8.18 (s, 1H, H-aromatic), 11.53 (bs, s, 1H, NH).

^{1}H-NMR (DMSO-d_6), δ: (minor species, **139b**) 1.34-1.39 (m, 6H, H-16'), 4.08 (q, J= 6.7 Hz, 3H, H-15'), 4.14 (q, J= 6.7 Hz, 1H, H-15'), 7.02 (d, J= 8.3 Hz, 1H, H-aromatic), 7.27 (d, J= 8.3 Hz, 1H, H-aromatic), 7.34-7.36 (m, 1H, H-trans), 7.38-7.42 (m, 1H, H-aromatic), 7.48-7.52 (m, 2H, H-aromatic), 7.62-7.67 (m, 1H, H-aromatic), 7.70-7.75 (m, 6H, H-trans), 7.84 (d, J= 8.2 Hz, 1H, H-aromatic), 7.99 (s, 1H, H-aromatic), 11.41 (bs, 1H, NH).

^{13}C-NMR (DMSO-d_6), δ: 14.63, 14.72 (CH_3, C-16'), 63.79, 63.87 (CH_2, C-17'), 110.14, 112.78, 117.34, 120.40, 120.73, 121.76, 126.60 (CH, C-aromatic), 126.92, 136.94, 139.27 (C, C-aromatic), 139.67, 143.25 (CH, C-aromatic), 148.39, 150.21 (C, C-aromatic), 161.25 (C, C-7').

3-(Biphenyl-4-*yl*)-*N*'-(1-(4-cyclohexylphenyl)ethylidene)acrylohydrazide (140) ($C_{29}H_{30}N_2O$; M.W.= 422.56)

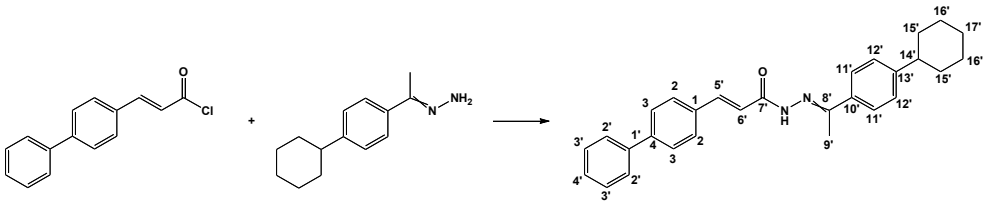

122 **128** **140**

General procedure 17;
T.L.C. system: DCM-MeOH 99:1 v/v, Rf: 0.43;
Pale yellow powder;
Purification: flash column chromatography (DCM-MeOH 100:0 v/v, increasing to 99:1 v/v) and recrystallization from EtOH;
Yield: 0.055 g, 5.3 %
Melting point: 212-220 °C
MS $(ESI)^+$: 445.2 $[M+Na]^+$

^{1}H-NMR ($CDCl_3$), δ: 1.28-1.35 (m, 1H, H-17'), 1.39-1.53 (m, 4H, CH_2), 1.78-1.83 (m, 1H, H-17'), 1.87-1.95 (m, 4H, CH_2), 2.29 (s, 3H, H-9'), 2.55-2.61 (m, 1H, H-14'), 7.31 (d, J= 8.0 Hz, 2H, H-aromatic), 7.38-7.42 (m, 1H, H-aromatic), 7.47-7.51 (m, 2H, H-aromatic, H-trans), 7.64-7.70 (m, 5H, H-aromatic), 7.72-7.78 (m, 4H, H-aromatic), 7.93 (d, J= 15.9 Hz, 1H, H-6'), 8.68 (bs, 1H, NH).

^{13}C-NMR ($CDCl_3$), δ: 12.70 (CH_3, C-9'), 26.13, 26.84, 34.33 (CH_2), 44.42 (CH, C-14'), 116.57 (CH, C-5'), 126.23, 126.60, 127.06, 127.45, 127.49, 127.75, 128.17, 128.82, 128.89 (CH, C-aromatic), 134.22, 135.62, 140.35, 142.79 (C, C-aromatic), 143.31 (CH, C-6'), 147.19, 149.75 (C, C-aromatic), 167.40 (C, C-7').

6.10.6 (*E*)-3-(4-isopropylphenyl)acrylohydrazide (143)

($C_{12}H_{16}N_2O$; M.W.= 204.27)

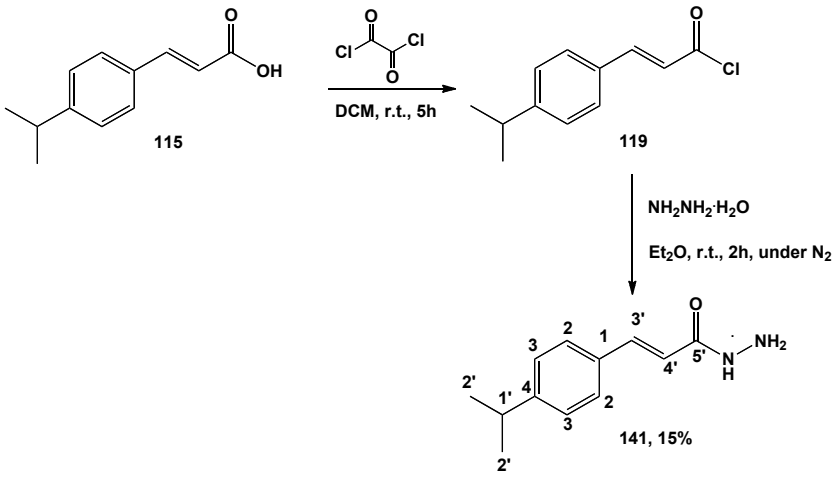

To a solution of (*E*)-3-(4-isopropylphenyl)acrylic acid **115** (1.68 g, 8.83 mmol.) in Et_2O (30 mL) was added oxalyl chloride (0.75 mL, 8.83 mmol) at 0°C under nitrogen atmosphere. The cold bath was removed and the mixture was stirred at room temperature for 3 h. Hydrazine (0.86 mL, 17.66 mmol) was added and the mixture was stirred for additional 2 h. The reaction mixture was diluted with EtOAc (30 mL) and the solid was filtered off by gravity filtration. The organic phase was washed with $NaHCO_3$ sat. solution (2 x 30 mL), Na_2CO_3 sat. solution (2 x 30 mL), brine, dried over $MgSO_4$ and finally evaporated under reduced pressure to give the title compound as a pale yellow powder.

T.L.C. system: *n*-hexane -EtOAc 1:1 v/v, Rf: 0.10;
Yield: 0.250 g, 15 %

^{1}H-NMR (DMSO-d_6, δ: 1.19-1.23 (m, 6H, H-2'), 2.87-2.94 (m, 1H, H-1'), 4.60 (bs, 2H, NH_2), 6.51 (d, J= 15.7 Hz, 1H, H-3'), 7.28 (d, J= 8.2 Hz, 2H, H-aromatic), 7.41 (d, J= 15.7 Hz, 1H, H-4'), 7.47 (d, J= 8.2 Hz, 1H, H-aromatic), 7.53 (d, J= 8.2 Hz, 1H, H-aromatic), 9.30 (bs, 1H, N<u>H</u>).

^{13}C-NMR (DMSO-d_6), δ: 23.63 (CH_3, C-2'), 33.25 (CH, C-1'), 119.31 (CH, C-3'), 126.89, 127.47 (CH, C-aromatic), 132.56, 139.95, 149.91 (C, C-aromatic), 164.59 (C, C-5').

6.10.7 *N'*-(4-Hydroxybenzylidene)-3-(4-isopropylphenyl)acrylohydrazide (143) ($C_{19}H_{20}N_2O_2$; M.W.= 308.37)

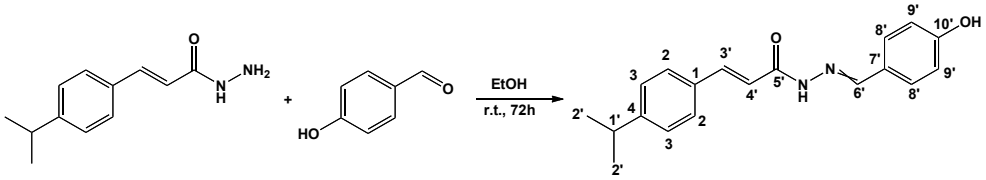

141 **142** **143a,b**

A mixture of (*E*)-3-(4-isopropylphenyl)acrylohydrazide **141** (0.250 g, 1.22 mmol) and 4-hydroxybenzaldehyde **142** (0.180 g, 1.47 mmol) in ethanol (15 mL) was stirred under reflux for 72 hours. The reaction mixture was dried under vacuum and the crude product was purified by flash column chromatography (*n*-hexane:EtOAc 100:0 v/v, increasing to 10:90 v/v) and then recrystallized from ethanol to give the pure (2*E*,*N'E*)-*N'*-(4-hydroxybenzylidene)-3-(4-isopropylphenyl)acrylohydrazide as a pale yellow powder.

T.L.C. system: *n*-hexane -EtOAc 1:1 v/v, Rf: 0.55;
Yield: 0.026 g, 7 %
Melting point: 255-260 ºC
MS (ESI)$^+$: 309.2 $[M+H]^+$
Two species observed. Major/minor species: 5:4

^{1}H-NMR (DMSO-d$_6$), δ: (major species, **143a**) 1.21-1.24 (m, 6H, H-2'), 2.90-2.97 (m, 1H, H-1'), 6.64 (d, J= 15.9 Hz, 1H, H-3'), 6.84 (d, J= 7.8 Hz, 2H, H-aromatic), 7.30-7.34 (m, 3H, H-aromatic), 7.50-7.62 (m, 2H, H-aromatic, H-trans), 7.65 (d, J= 8.0 Hz, 2H, H-aromatic), 8.14 (s, 1H, H-6'), 9.86 (bs, 1H, N<u>H</u>), 9.90 (bs, 1H, N<u>H</u>), 11.42 (bs, 1H, -O<u>H</u>).

^{1}H-NMR (DMSO-d$_6$), δ: (minor species, **143b**) 1.21-1.24 (m, 6H, H-2'), 2.90-2.97 (m, 1H, H-1'), 6.84 (d, J= 7.8 Hz, 2H, H-aromatic), 7.30-7.34 (m, 1H, H-trans), 7.50-7.62 (m, 7H, H-aromatic, H-trans), 7.96 (s, 1H, H-6'), 9.86 (bs, 1H, N<u>H</u>), 11.26 (bs, 1H, -O<u>H</u>).

^{13}C-NMR (DMSO-d$_6$), δ: 23.63 (CH_3, C-2'), 33.30 (CH, C-1'), 115.65, 115.98, 116.46, 118.43, 119.47 (CH, H-aromatic), 125.22, 125.29 (C, C-aromatic), 126.88, 126.93, 127.74, 128.20, 128.55, 128.83 (CH, H-aromatic), 132.40,

132.60 (C, C-aromatic), 140.01, 141.63, 143.29, 146.83 (CH, C-aromatic), 150.36, 150.53, 159.11, 159.36 (C, C-aromatic), 161.24, 165.81 (C, C-5').

6.11 (*E*)-*N*-(1H-Benzo[*d*]imidazol-2-*yl*)-3-(4-*tert*-butylphenyl)acrylamides

6.11.1 General procedures 18-19

General procedure 18: synthesis of 2-aminobenzimidazoles

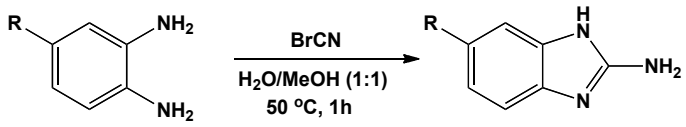

Aryl-1,2-diamine (4.62 mmol) was dissolved in a 1:1 mixture of methanol (40 mL) and water (40 mL). The reaction mixture was treated with BrCN (0.73 mL, 13.86 mmol) and heated at 50 °C for 1 h. After cooling to room temperature, methanol was removed under reduced pressure and the remaining reaction mixture was basified with 1M NaOH aq. to pH=8 and extracted with ethyl acetate (3x 30 mL). The combined organic fractions were washed with water (2x 50 mL), brine (2x 50 mL), dried over $MgSO_4$ and the solvent was removed under reduced pressure to give pure 2-aminobenzimidazole derivatives.

General procedure 19: synthesis of (*E*)-*N*-(1*H*-benzo[*d*]imidazol-2-*yl*)-3-(4-*tert*-butylphenyl)acrylamides

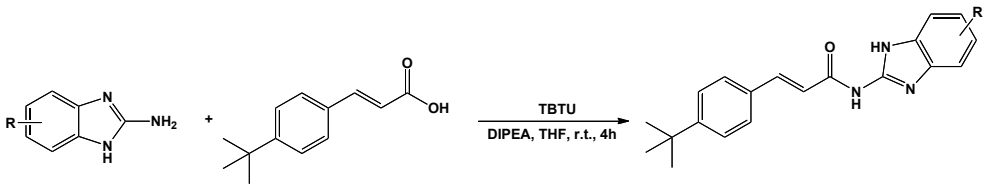

(*E*)-3-(4-*tert*-Butylphenyl)acrylic acid (0.276 g, 1.35 mmol) and TBTU (0.433 g, 1.35 mmol) were suspended in dry THF (7.3 mL) at room temperature. DIPEA (0.49 mL, 2.84 mmol) was then added to the reaction mixture, followed by the desired 2-aminobenzbenzimidazoleimidazole (1.35 mmol). The reaction was stirred for 4 h. The organic solvent was removed under vacuum and the residue was diluted with ethyl acetate (10 mL), then the

organic layer was washed with $NaHCO_3$ (2 x 10 mL) and brine. The crude mixture was purified by flash column chromatography (*n*-hexane:EtOAc 100:0 v/v, increasing to 80:20 v/v) to give the desired compound.

6.11.2 (*E*)-3-(4-*tert*-Butylphenyl)acrylic acid (153)[36]

($C_{13}H_{16}O_2$; M.W.= 204.260)

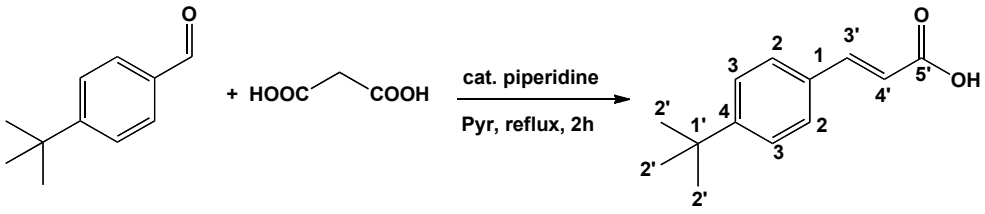

152 **153**

A mixture of malonic acid (12.32 mmol, 2 eq), aldehyde **152** (6.16 mmol) and catalytic amount of piperidine (0.2 mL) was heated in a solution of pyridine (5 mL, 60 mmol) at reflux for 2 h. The resultant solution of pyridine was poured into ice and a solution of 2 M HCl aq. was poured dropwise, which led the crude product to precipitate. The solid was collected by filtration, washed with water and purified by flash column chromatography (*n*-hexane-EtOAc 100:0 v/v, increasing to 80:20 v/v) to give the pure (E)-3-(4-*tert*-butylphenyl)acrylic acid as a white solid.

T.L.C. system: *n*-hexane -EtOAc 6:4 v/v, Rf: 0.28
Yield: 1.060 g, 84 %

^{1}H-NMR ($CDCl_3$), δ: 1.36 (s, 9H, H-2'), 6.45 (d, J= 15.9 Hz, 1H, H-3'), 7.45 (d, J= 8.3 Hz, 2H, H-aromatic), 7.53 (d, J= 8.3 Hz, 2H, H-aromatic), 7.81 (d, J= 15.9 Hz, 1H, H-4'), 11.57 (bs, 1H, COO<u>H</u>).

^{13}C-NMR (DMSO), δ: 25.89 (CH_3, C-2'), 29.70 (C, C-1'), 111.05, 120.70 (CH, C-aromatic), 122.99 (CH, C-3'), 126.09 (C, C-aromatic), 141.72 (CH, C-4'), 149.16 (C, C-aromatic), 166.94 (C, C-5').

6.11.3 Substituted 2-aminobenzimidazoles (150, 151)

1H-Benzo[*d*]imidazol-2-amine (150)[37]
($C_7H_7N_3$: M.W.= 133.15)

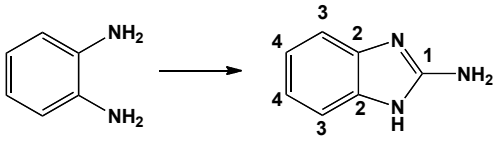

148 **150**

General procedure 18;
T.L.C. system: *n*-hexane -EtOAc 5:5 v/v, Rf: 0.1;
Light brown powder;
Yield: 0.530 g, 87 %

^{1}H-NMR (DMSO-d_6), δ: 6.06 (bs, 2H, N<u>H</u>$_2$), 6.83-6.85 (m, 2H, H-aromatic), 7.08-7.10 (m, 2H, H-aromatic), 10.63 (bs, 1H, N<u>H</u>).

^{13}C-NMR (DMSO-d_6), δ: 111.50, 118.90 (CH, C-aromatic), 115.21 (C, C-aromatic).

5-Methyl-1*H*-benzo[*d*]imidazol-2-amine (143)[38]
($C_8H_9N_3$: M.W.= 147.18)

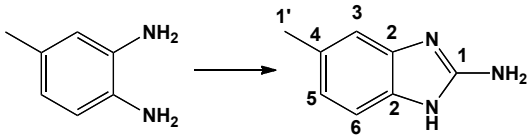

149 **151**

General procedure 18;
T.L.C. system: *n*-hexane -EtOAc 5:5 v/v, Rf: 0.1;
Brown powder;
Yield: 0.59 g, 87 %

^{1}H-NMR ($CDCl_3$), δ: 2.30 (s, 3H, H-1'), 6.01 (bs, s, 2H, N<u>H</u>$_2$), 6.66 (d, J= 7.8 Hz, 1H, H-aromatic), 6.91 (s, 1H, H-aromatic), 6.96 (d, J= 7.8 Hz, 1H, H-aromatic), 10.54 (bs, s, 1H, N<u>H</u>).

^{13}C-NMR ($CDCl_3$), δ: 21.20 (CH_3, C-1'), 111.06, 111.89, 119.85 (CH, C-aromatic), 127.57, 155.04 (C, C-aromatic).

6.11.4 *E*)-*N*-(1*H*-Benzo[*d*]imidazol-2-*yl*)-3-(4-*tert*-butylphenyl)acrylamides (144, 145

(*E*)-*N*-(1*H*-Benzo[*d*]imidazol-2-*yl*)-3-(4-*tert*-butylphenyl)acrylamide (144) ($C_{20}H_{21}N_3O$: M.W.= 319.40)

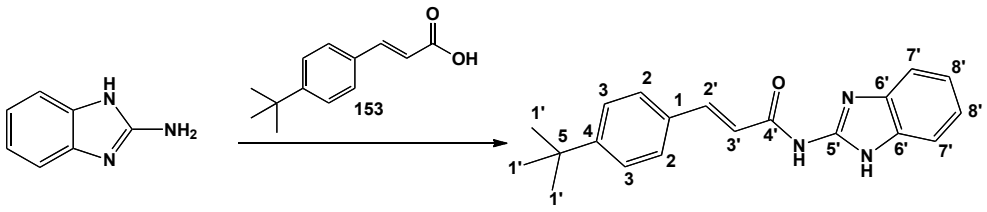

150 **144**

General procedure 19;
T.L.C. system: *n*-hexane -EtOAc 1:1 v/v, Rf: 0.46;
Yield: 0.05 g, 11.6 %
Melting point: 260-261 °C;
MS $(ESI)^+$: 320.2 $[M+H]^+$

^{1}H-NMR (DMSO-d_6), δ: 1.31 (s, 9H, H-1'), 5.75 (s, 1H, H-aromatic), 6.93 (d, J= 15.7 Hz, 1H, H-4'), 7.09-7.11 (m, 2H, H-aromatic), 7.46-7.48 (m, 2H, H-aromatic), 7.50 (d, J= 8.3 Hz, 2H, H-aromatic), 7.59 (d, J= 8.3 Hz, 1H, H-aromatic), 7.71 (d, J= 15.7 Hz, 1H, H-3'), 11.73 (bs, 1H, NH), 12.13 (bs, 1H, NH).

^{13}C-NMR (DMSO-d_6), δ: 30.90 (CH_3, C-1'), 34.61 (C, C-5), 119.67, 121.02, 125.88, 127.82 (CH, C-aromatic), 131.63 (C, C-aromatic), 141.84 (CH, C-aromatic), 143.75, 146.79, 153.18 (C, C-aromatic), 164.43 (C, C-4').

3-(4-*tert*-Butylphenyl)-*N*-(5-methyl-1*H*-benzo[*d*]imidazol-2-*yl*)propanamide (145) ($C_{21}H_{25}N_3O$; M.W.= 333.43)

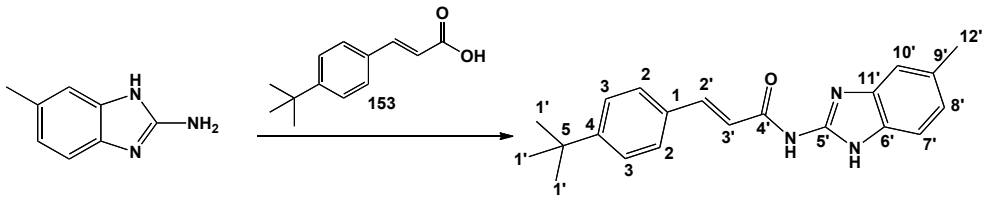

151 **145**

General procedure 19;
T.L.C. system: *n*-hexane -EtOAc 1:1 v/v, Rf: 0.32'
Yield: 0.05 g, 10 %
Melting point: 202-207 °C;
MS (ESI)$^+$: 334.2 $[M+H]^+$

^{1}H-NMR (DMSO-d$_6$), δ: 1.31 (s, 9H, H-2'), 2.38 (s, 3H, H-12'), 6.92-6.97 (m, 2H, H-aromatic, H-trans), 7.29 (s, 2H, H-aromatic), 7.34 (d, J= 7.3 Hz, 1H, H-2'), 7.49 (d, J= 7.5 Hz, 2H, H-aromatic), 7.58 (d, J= 7.5 Hz, 2H, H-aromatic), 7.70 (d, J= 15.7 Hz, 1H, H-4'), 11.83 (bs, 1H, N<u>H</u>), 12.02 (bs, 1H, N<u>H</u>).

^{13}C-NMR (DMSO-d$_6$), δ: 21.28 (CH_3, C-11'), 30.89 (CH_3, C-1'), 34.59 (C, C-1'), 119.76 (CH, C-3'), 122.33, 125.88, 127.79 (CH, C-aromatic), 129.98, 131.64, 139.53, 140.59 (C, C-aromatic), 141.72 (CH, C-4'), 153.15 (C, C-5').

6.12 Synthesis of *N*-(1H-benzo[*d*]imidazol-2-*yl*)-3-(4-*tert*-butylphenyl)propanamides

6.12.1 General procedure 20: synthesis of *N*-(1*H*-benzo[*d*]imidazol-2-*yl*)-3-(4-*tert*-butylphenyl)propanamides

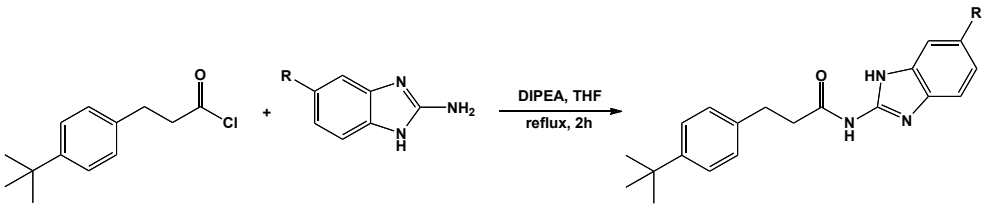

A solution of the desired aryl chloride (1 eq.) and DIPEA (3 eq.) in dry THF (0.5 mL/mmol eq.) was added dropwise to 2-aminobenzimidazole (1 eq.). After stirring at reflux for 2 hours, the reaction mixture was diluted with DCM (5 mL/mmol eq.) and washed with water (5 mL/mmol eq.), $NaHCO_3$ (5 mL/mmol eq.) and brine. The organic layer was dried over $MgSO_4$ and evaporated under reduced pressure. The resulting crude mixture was purified by flash column chromatography and/or recrystallization to give the desired compound.

6.12.2 3-(4-*tert*-Butylphenyl)propanoic acid (154)[39]

($C_{13}H_{18}O_2$; M.W.= 206.28)

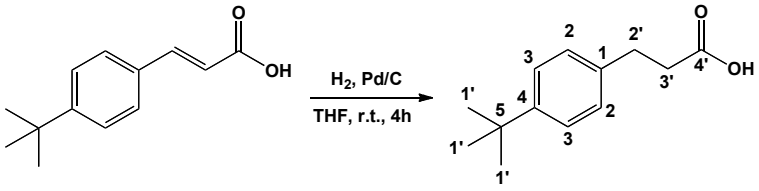

153 **154**

(*E*)-3-(4-*tert*-butylphenyl)acrylic acid (**153**) (0.5 g, 0.5 mmol) was dissolved in dry THF (9.5 mL) and a catalytic amount of 10% Pd/C was added (0.122 g) to carry out the hydrogenation. The reaction mixture was stirred for 5 hours at room temperature under H_2 atmosphere, after that time it was diluted with ethyl acetate (10 mL), filtered through celite and concentrated under reduced pressure to give 3-(4-tert-butylphenyl)propanoic acid as a white powder.

T.L.C. system: *n*-hexane -EtOAc 4:6 v/v, Rf: 0.76;
Yield: 0.5 g, 99 %

^{1}H-NMR ($CDCl_3$), δ: 1.33 (s, 9H, H-1'), 2.71 (t, J= 7.8 Hz, 2H, H-2'), 2.96 (t, J= 7.8 Hz, 2H, H-3'), 7.17 (d, J= 8.0 Hz, 2H, H-aromatic), 7.35 (d, J= 8.0 Hz, 2H, H-aromatic).

^{13}C-NMR ($CDCl_3$), δ: 30.04 (CH_2, C-2'), 31.37 (CH_3, C-1'), 34.39 (C, C-5'), 35.39 (CH_2, C-3'), 125.45, 127.91 (CH, C-aromatic), 137.08, 149.23 (C, C-aromatic), 178.25 (C, C-4').

6.12.3 3-(4-*tert*-Butylphenyl)propanoyl chloride (155)[40]

($C_{13}H_{17}ClO$: M.W.= 224.10)

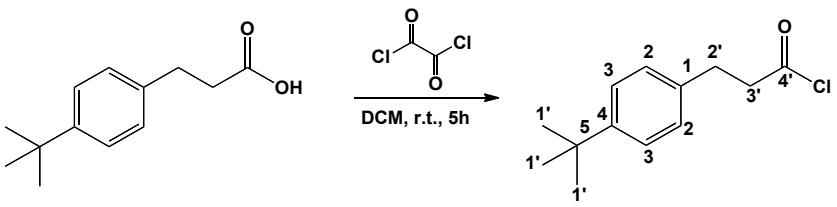

154 **155**

To a stirred solution of 3-(4-*tert*-butylphenyl)propanoic acid **154** (2.94 mmol), in DCM (15 mL) at room temperature was added oxalyl chloride (0.5 mL, 5.88 mmol), and the mixture was stirred for 5 h. The resulting solution was concentrated under reduced pressure to give the desired product which was used without further purification.

T.L.C. system *n*-hexane -EtOAc 7:3 v/v, Rf: 0.76;
Pale yellow oil;
Yield: 0.540 g, 83 %

^{1}H-NMR ($CDCl_3$), δ: 1.34 (s, 9H, H-1'), 3.01 (t, J= 7.5 Hz, 2H, H-2'), 3.22 (t, J= 7.5 Hz, 2H, H-3'), 7.15 (d, J= 8.2 Hz, 2H, H-aromatic), 7.36 (d, J= 8.2 Hz, 2H, H-aromatic).

^{13}C-NMR ($CDCl_3$), δ: 30.47 (CH_2, C-2'), 31.34 (CH_3, C-1'), 34.44 (C, C-aromatic), 48.56 (CH_2, C-3'), 125.65, 127.96 (CH, C-aromatic), 135.54, 149.75 (C, C-aromatic), 173.14 (C, C-4').

6.12.4 Benzoimidazol-4-*tert*-butylphenyl)propanamides (146, 147)

_N_-(1H-Benzo[_d_]imidazol-2-_yl_)-3-(4-_tert_-butylphenyl)propanamide (146) ($C_{20}H_{23}N_3O$; M.W.= 321.42)

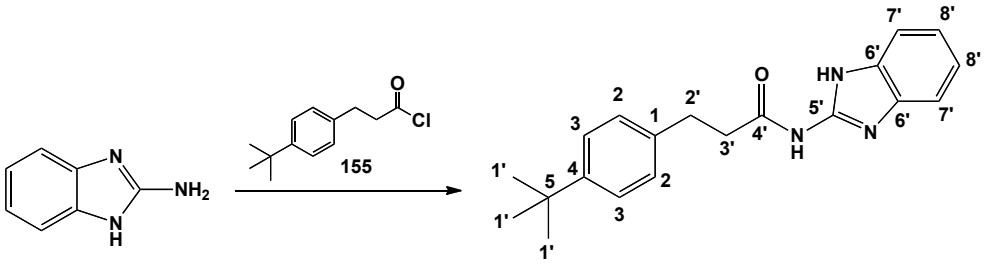

150 **146**

General procedure 20;
Reagent: 1*H*-benzo[*d*]imidazol-2-amine (**150**) (0.17g, 1.28 mmol);
T.L.C. system: *n*-hexane -EtOAc 1:1 v/v, Rf: 0.42;
Yield: 0.02 g, 5 %
Melting point: 248-252 °C
MS (ESI)$^+$: 322.2 $[M+H]^+$

^{1}H-NMR (DMSO-d_6), δ: 1.25 (s, 9H, H-1'), 2.76 (t, J= 7.4 Hz, 2H, H-2'), 2.92 (t, J= 7.4 Hz, 2H, H-3'), 7.07-7.09 (m, 2H, H-aromatic), 7.19 (d, J= 7.8 Hz, 2H, H-aromatic), 7.31 (d, J= 7.8 Hz, 2H, H-aromatic), 7.43-7.48 (m, 2H, H-aromatic), 11.50 (bs, 1H, NH), 12.02 (bs, 1H, NH).

^{13}C-NMR (DMSO-d_6), δ: 29.84 (CH_2, C-2'), 31.16 (CH_3, C-1'), 34.04 (C, C-aromatic), 36.96 (CH_2, C-3'), 120.59, 121.14, 125.04, 127.89 (CH, C-aromatic), 132.46, 137.69, 146.52, 148.27 (C, C-aromatic), 171.70 (C, C-4').

3-(4-_tert_-Butylphenyl)-_N_-(5-methyl-1H-benzo[_d_]imidazol-2-_yl_)propanamide (147) ($C_{21}H_{25}N_3O$: M.W.= 335.44)

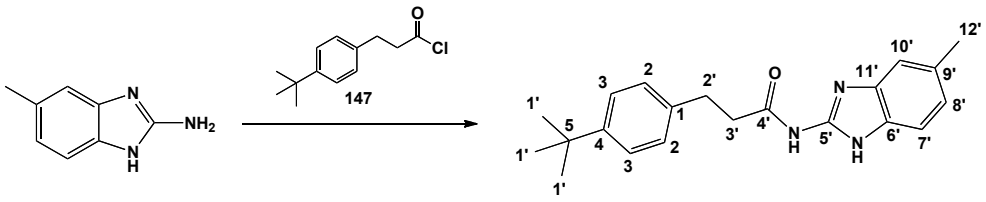

151 **147**

General procedure 20;
Reagent: 5-methyl-1*H*-benzo[*d*]imidazol-2-amine (**151**) (0.42 g, 2.85 mmol);

T.L.C. system: *n*-hexane -EtOAc 1:1 v/v, Rf: 0.45;
White powder;
Yield: 0.05 g, 5.3 %;
Melting point: 206-211 °C
MS $(ESI)^+$:336.2 $[M+H]^+$

^{1}H-NMR (DMSO-d$_6$), δ: 1.25 (s, 9H, H-1'), 2.36 (s, 3H, H-11'), 2.72-2.77 (m, 2H, H-2'), 2.89-2.94 (m, 2H, H-3'), 6.87-6.91 (m, 1H, H-aromatic), 7.16-7.24 (m, 3H, H-aromatic), 7.28-7.32 (m, 3H, H-aromatic), 11.45 (bs, 1H, NH), 11.89 (bs, 1H, NH).

^{13}C-NMR (DMSO-d$_6$), δ: 21.25 (CH_3, C-1'), 29.84 (CH_2, C-2'), 31.15 (CH_3, C-11'), 34.02 (C, C-aromatic), 36.94 (CH_2, C-3'), 122.20, 125.03, 127.88 (CH, C-aromatic), 129.81, 137.69, 146.31, 148.27 (C, C-aromatic), 171.62 (C, C-4').

6.13 Synthesis of 1-Phenethyl-4-*p*-tolyl-1H-1,2,3-triazole

6.13.1 2-(Azidoethyl)benzene (151)[41]

($C_8H_9N_3$: M.W.= 147.18)

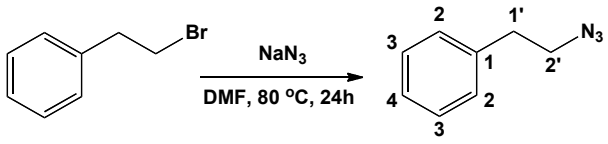

158 **159**

A solution of (2-bromoethyl)benzene (**158)** (0.37 mL, 2.70 mmol) in DMF (10.8 mL) was treated with NaN_3 (0.878 g, 13.5 mmol) under nitrogen atmosphere and the mixture was stirred at 80 °C for 24 h. The reaction mixture was cooled down to room temperature and extracted with DCM (3 x 20 mL). The combined organic layers were washed with water (3 x 20 mL) and brine, dried over $MgSO_4$ and the solvent was removed under reduced pressure to give the pure (2-azidoethyl)benzene as a pale yellow oil.

T.L.C. system: *n*-hexane -EtOAc 9.8:0.2 v/v, Rf: 0.72
Yield: 0.290 g, 73 %

^{1}H-NMR ($CDCl_3$), δ: 2.93 (t, J= 7.2 Hz, 2H, H-1'), 3.54 (t, J= 7.2 Hz, 2H, H-2'), 7.25 (d, J= 7.0 Hz, 2H, H-aromatic), 7.29 (d, J= 7.0 Hz, 1H, H-aromatic), 7.34-7.37 (m, 2H, H-aromatic).

^{13}C-NMR ($CDCl_3$), δ: 35.37 (CH_2, C-1'), 52.48 (CH_2, C-2'), 126.79, 128.66, 128.76 (CH, C-aromatic), 138.04 (C, C-1).

6.13.2 1-Phenethyl-4-*p*-tolyl-1H-1,2,3-triazole (157)[42]

($C_{17}H_{17}N_3$: M.W.= 263.34)

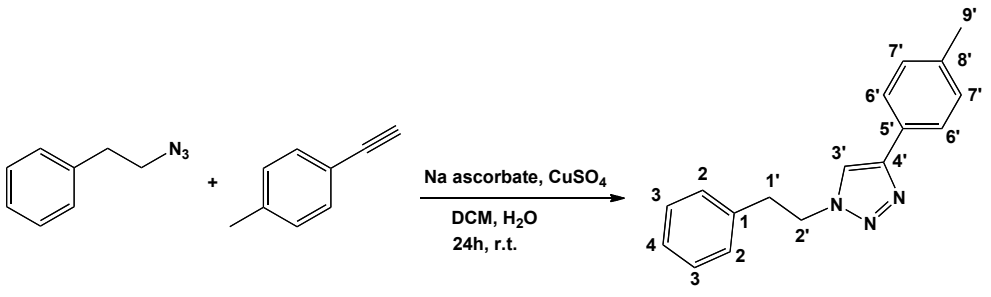

159 **160** **157**

A solution of (2-azidoethyl)benzene (**159**) (0.290 g, 1.97 mmol) and 1-ethynyl-4-methylbenzene (**160**) (0.322 mL, 2.54 mmol) in 4.8 mL of DCM was stirred at r.t. and 3.6 mL of water were added followed by 65 mg of $CuSO_4 \cdot 5H_2O$. Sodium ascorbate (0.177 g, 0.89 mmol) was then added in small portions and the mixture was stirred at room temperature for 24 h. The DCM layer was separated, dried over $MgSO_4$ and removed under reduced pressure. The crude product was then recrystallized from DCM/*n*-hexane to give the pure 1-phenethyl-4-p-tolyl-1H-1,2,3-triazole as a off-whiteoff-white powder.

T.L.C. system: *n*-hexane -EtOAc 1:1 v/v, Rf: 0.74;
Yield: 0.128 g, 25 %;
Melting point: 96-100 °C
MS $(ESI)^+$: 264.1 $[M+H]^+$

^{1}H-NMR ($CDCl_3$), δ: 2.39 (s, 3H, H-9'), 3.27 (t, J= 7.2 Hz, 2H, H-1'), 4.65 (t, J= 7.2 Hz, 2H, H-2'), 7.16 (d, J= 6.6 Hz, 2H, H-aromatic), 7.24 (d, J= 7.5 Hz, 2H, H-aromatic), 7.32 (d, J= 7.5 Hz, 2H, H-aromatic), 7.34-7.38 (m, 1H, H-aromatic), 7.45 (s, 1H, H-3'), 7.68 (d, J= 7.8 Hz, 2H, H-aromatic).

^{13}C-NMR ($CDCl_3$), δ: 21.26 (CH_3, C-9'), 36.82 (CH_2, C-1'), 51.71 (CH_2, C-2'), 119.54, 125.62, 127.13 (CH, C-aromatic), 127.86 (C, C-aromatic), 128.74, 128.85, 129.48 (CH, C-aromatic), 137.12, 137.92, 147.59 (C, C-aromatic).

6.14 Synthesis of (*E*)-2-benzylidene-N-(4-*tert*-butylstyryl)hydrazinecarboxamides

6.14.1 General procedure 21: synthesis of -2-benzylidene-N-(4-*tert*-butylstyryl)hydrazinecarboxamides (154-157)

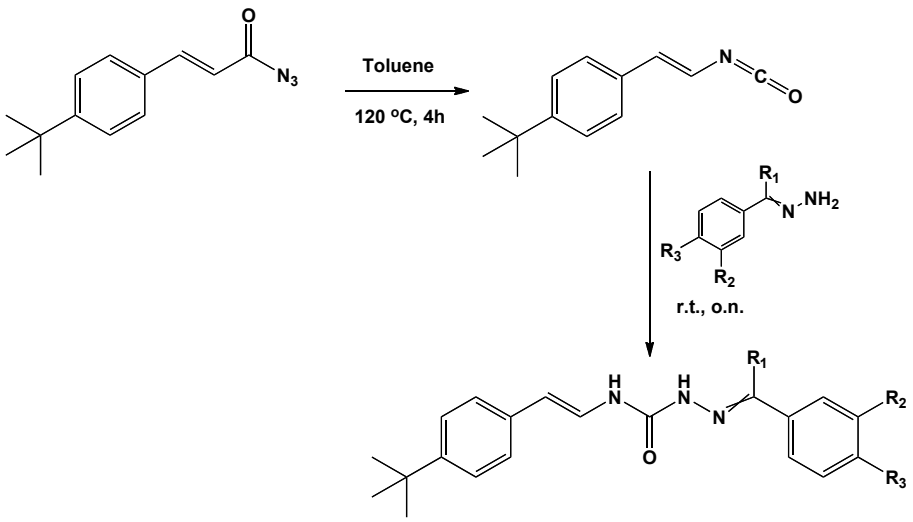

A solution of azide (1 eq.) in toluene (16 mL/mmol eq.) was heated at 120 ºC for 4 h to give the isocyanate derivative that was not isolated. After cooling the reaction to r.t., the amine (1 eq.) was slowly added to the isocyanate solution. The reaction mixture was stirred at room temperature, overnight. The solid was filtered and washed with toluene (7 mL/mmol eq. The crude product was then recrystallized from ethanol to give the title compounds.

6.14.2 (*E*)-3-(4-*tert*-Butylphenyl)acryloyl azide (166)[43]

($C_{13}H_{15}N_3O$; M.W.= 229.278)

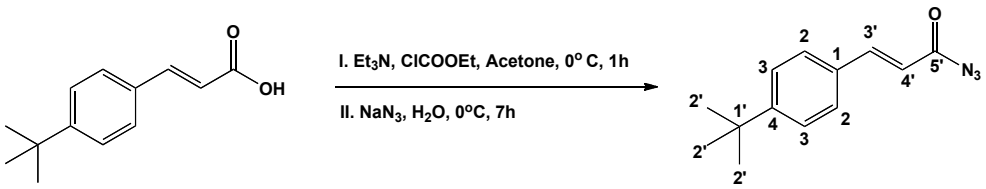

153 **166**

A mixture of 3-(4-*tert*-butylphenyl)acrylic acid (**153**) (0.750 g, 3.67 mmol), Et_3N (0.56 mL, 4.03 mmol) and ethyl-chlorocarbonate (0.7 g, 3.67 mmol) in dry acetone (28.5 mL) was stirred at 0 °C for 1 h under nitrogen atmosphere. Sodium azide (0.22 g, 3.67 mmol) dissolved in 6,4 mL of water was added and stirring was kept at 0 °C for 7 hours. The organic mixture was poured into ice. The obtained precipitate was collected by filtration and washed with water to give the pure (E)-3-(4-tert-butylphenyl)acryloyl azide as a white powder.

T.L.C. system: *n*-hexane -EtOAc 1:1 v/v, Rf: 0.37
Yield: 0.531 g, 63 %

^{1}H-NMR ($CDCl_3$), δ: 1.35 (s, 9H, H-2'), 6.42 (d, J= 15.8 Hz, 1H, H-3'), 7.45 (d, J= 8.4 Hz, 2H, H-aromatic), 7.50 (d, J= 8.4 Hz, 2H, H-aromatic), 7.76 (d, J= 15.8 Hz, 1H, H-4').

^{13}C-NMR ($CDCl_3$), δ: 31.11 (CH_3, C-2'), 35.01 (C, C-1'), 118.18 (CH, C-3'), 126.09, 128.48 (CH, C-aromatic), 131.11 (C, C-aromatic), 146.69 (CH, C-4'), 154.93 (C, C-aromatic), 172.18 (C, C-5').

6.14.3 2-benzylidene-N-(4-*tert*-butylstyryl)hydrazinecarboxamides (162-165)

N-(4-*tert*-Butylstyryl)-2-(4-methylbenzylidene)hydrazinecarboxamide (162) ($C_{21}H_{25}N_3O$; M.W.= 335.443)

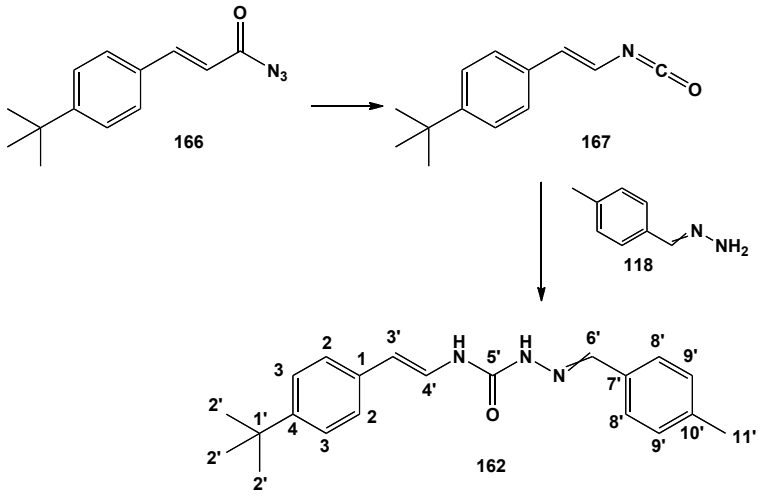

General procedure 21;
T.L.C. system: *n*-hexane -EtOAc 1:1 v/v, Rf: 0.48
White powder;
Yield: 0.332 g, 42.9 %;
Melting point: 205-209 °C
MS $(ESI)^+$: 336.2 $[M+H]^+$

^{1}H-NMR (DMSO-d_6), δ: 1.27 (s, 9H, H-2'), 2.35 (s, 3H, H-13'), 6.39 (d, J= 14.5 Hz, 1H, H-3'), 7.23-7.25 (m, 4H, H-aromatic), 7.31 (d, J= 8.2 Hz, 2H, H-aromatic), 7.37 (dd, J_1= 14.5 Hz J_2= 10.4 Hz, 1H, H-4'), 7.74 (d, J= 8.2 Hz, 2H, H-aromatic), 7.90 (s, 1H, H-6'), 9.17 (d, J= 10.4 Hz, 1H, NH), 10.76 (bs, 1H, NH).

^{13}C-NMR (DMSO-d_6), δ: 6.83 (C, C-1'), 20.99 (CH_3, C-13') , 31.11 (CH_3, C-2'), 109.51 (CH, C-3'), 123.86 (CH, C-4'), 124.40, 125.38, 127.00, 129.15 (CH, C-aromatic), 131.68, 134.43, 139.12, 147.90 (C, C-aromatic), 152.71 (C, C-5').

***N*-(4-*tert*-Butylstyryl)-2-(3,4-diethoxybenzylidene)hydrazinecarboxamide (163) ($C_{24}H_{31}N_3O_3$; M.W.= 409.521)**

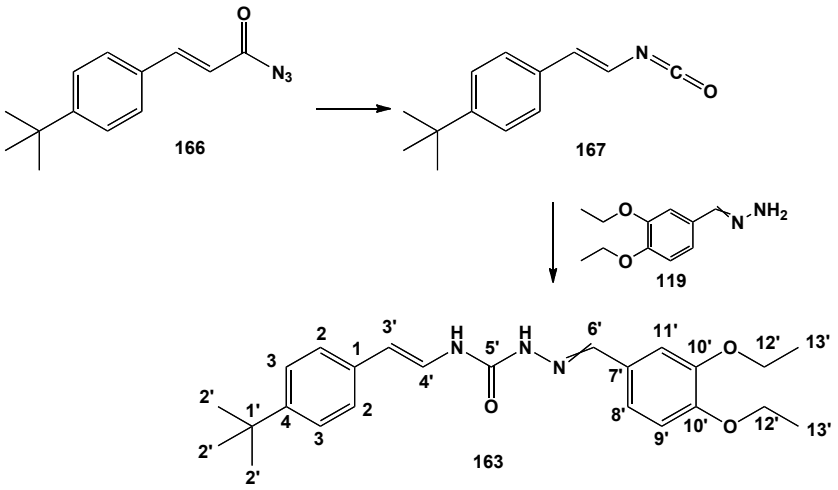

General procedure 21;
T.L.C. system: *n*-hexane -EtOAc 1:1 v/v, Rf: 0.47;
Purification: flash column chromatography (*n*-hexane:EtOAc 100:0 v/v, increasing to 70:30 v/v) and recrystallization from ethanol;
Yield: 0.055 g, 11 %;
Melting point: 145-158 °C
MS $(ESI)^+$: 432.2 $[M+Na]^+$

^{1}H-NMR (DMSO-d_6), δ: 1.27 (s, 9H, H-2'), 1.33-1.38 (m, 6H, H-14'), 4.07 (q, J_1= 6.8 Hz, 2H, H-aromatic), 4.13 (q, J_1= 6.8 Hz, 2H, H-aromatic), 6.36 (d, J= 14.6 Hz, 1H, H-3'), 6.98 (d, J= 8.3 Hz, 1H, H-aromatic), 7.22-7.25 (m, 3H, H-aromatic), 7.30 (d, J= 8.3 Hz, 2H, H-aromatic), 7.39 (dd, J_1= 14.6 Hz, J_2= 10.3 Hz, 1H, H-4'), 7.50 (d, J= 1.7 Hz, 1H, H-aromatic), 7.85 (s, 1H, H-6'), 9.18 (d, J= 10.3 Hz, 1H, NH), 10.69 (bs, 1H, NH).

^{13}C-NMR (DMSO-d_6), δ: 14.66, 14.78 (CH_3, C-14'), 31.11 (CH_3, C-2'), 34.08 (C, C-1'), 63.76, 64.06 (CH_2, C-13'), 109.38, 111.03 (CH, C-aromatic), 112.74 (CH, C-3'), 121.35 (CH, C-4'), 123.92, 124.38, 125.37 (CH, C-aromatic), 127.11, 134.43 (C, C-aromatic), 141.58 (CH, C-6'), 147.87, 148.39, 149.77 (C, C-aromatic), 152.73 (C, C-10').

***N*-(4-*tert*-Butylstyryl)-2-(1-(4-cyclohexylphenyl)ethylidene)hydrazinecarboxamide (164)**
($C_{27}H_{35}N_3O$; M.W.= 417.49)

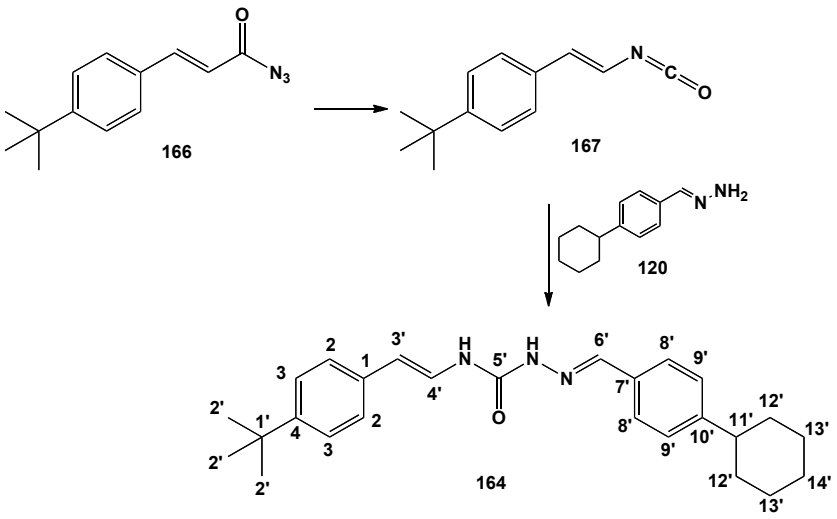

General procedure 21;
T.L.C. system: *n*-hexane -EtOAc 1:1 v/v, Rf: 0.75
Pale yellow powder;
Purification: recrystallization with DCM;
Yield: 0.351 g, 29 %
Melting point: 158-165 °C
MS $(ESI)^+$: 418.3 $[M+H]^+$

^{1}H-NMR (DMSO-d_6), δ**:** 1.25-1.30 (s, 10H, H-2', H-14'), 1.37-1.45 (m, 4H, CH_2), 1.78-1.83 (m, 4H,CH_2), 2.23 (s, 3H, H-7'), 2.53-2.57 (m, 1H, 14'), 6.39 (d, J= 14.9 Hz, 1H, H-3'), 7.23-7.27 (m, 4H, H-aromatic), 7.30 (d, J= 8.0 Hz, 2H, H-aromatic), 7.36-7.42 (m, 1H, H-4'), 7.83 (d, J=7.9 Hz, 2H, H-aromatic), 9.05 (d, J= 10.5 Hz, 1H, N<u>H</u>), 9.84 (bs, 1H, N<u>H</u>).

^{13}C-NMR (DMSO-D_6), δ: 13.75 (CH_3, C-7'), 25.55 (CH_2, C-17'), 26.28 (CH_2, C-aliphatic), 31.11 (CH_3, C-2'), 34.09 (CH_2, C-aliphatic), 34.09 (C, C-aromatic), 43.48 (CH, C-14'), 109.62 (CH, C-3'), 123.78 (CH, C-4'), 124.42, 125.36, 126.41, 126.43 (CH, C-aromatic), 134.42, 135.69, 146.60, 147.90 (C, C-aromatic), 148.32 (C, C-5').

***N*-(4-*tert*-Butylstyryl)-2-(4-hydroxybenzylidene)hydrazinecarboxamide (165) ($C_{20}H_{23}N_3O_2$; M.W.= 337.416)**

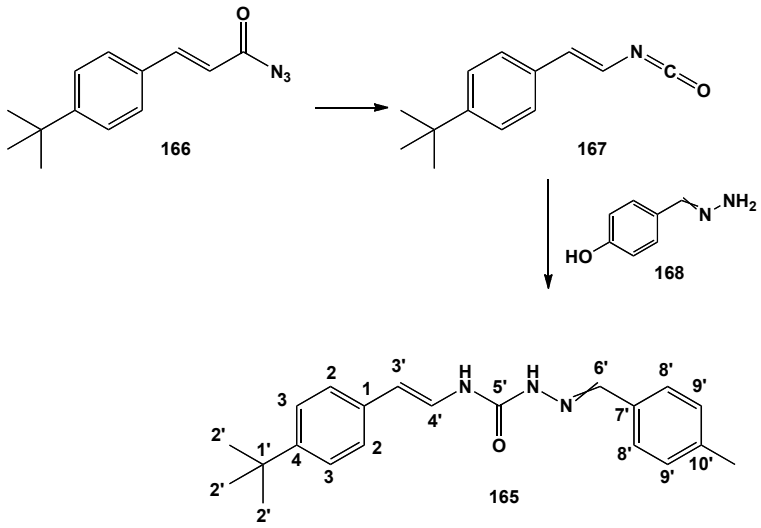

General procedure 21;
T.L.C. system: *n*-hexane -EtOAc 1:1 v/v, Rf: 0.49;
White powder;
Yield: 0.178 g, 40 %
Melting point: 156-160 ^oC
MS $(ESI)^+$: 360.2 $[M+Na]^+$

^{1}H-NMR (DMSO-d_6), δ: 1.27 (s, 9H, H-2'), 6.37 (d, J= 14.6 Hz, 1H, H-3'), 6.81 (d, J= 8.5 Hz, 2H, H-aromatic), 7.23 (d, J= 8.5 Hz, 2H, H-aromatic), 7.30 (d, J= 8.5 Hz, 2H, H-aromatic), 7.35-7.40 (m, 1H, H-4'), 7.67 (d, J= 8.5 Hz, 2H, H-aromatic), 7.83 (s, 1H, H-6'), 9.10 (d, J= 10.4 Hz, 1H, N<u>H</u>), 9.79 (bs, 1H, N<u>H</u>), 10.61 (bs, 1H, -O<u>H</u>).

^{13}C-NMR (DMSO-d_6), δ: 31.11 (CH_3, C-2'), 109.26 (CH, C-3'), 115.40 (CH, C-aromatic), 123.91 (CH, C-4'), 124.36, 125.37 (CH, C-aromatic), 125.45 (C, C-aromatic), 128.69 (CH, C-aromatic), 134.48 (C, C-aromatic), 141.48 (CH, C-6'), 147.85, 152.75 (C, C-aromatic), 152.75 (C, C-5'), 158.84 (C, C-10')

6.15 Synthesis of 2-arylidene-*N*-phenetylhydrazinecarbothioamides

6.15.1 General procedure 22: synthesis of 2-arylidene-*N*-phenetylhydrazinecarbothioamides

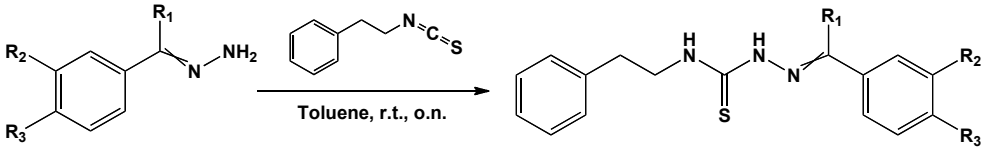

A solution of (2-isothiocyanatoethyl)benzene (0.4 g, 5.16 mmol) in toluene (30 mL) was stirred for few minutes to dissolve the isothiocyanate and then the aryl aldehyde azines (5.16 mmol) was slowly added to the solution. The reaction mixture was stirred at room temperature overnight. The reaction was stopped, the solvent removed under reduced pressure and the obtained solid was collected by filtration and dried. The solid purified by flash column chromatography or recrystallization to give the title compounds.

6.15.2 (2-Isothiocyanatoethyl)benzene (176)[44]

(C_9H_9NS; M.W.= 149.213)

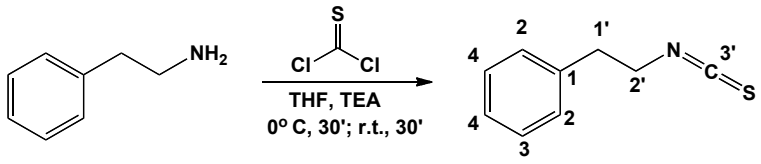

175 **176**

Thiophosgene (0.32 mL, 4.13 mmol) was added dropwise to a solution of 2-phenylethanamine (**175**) (0.52 mL, 4.13 mmol) and TEA (1.72 mL, 12.37 mmol) in THF (50 mL). The mixture was stirred for 30 min at 0 °C, then the cold bath was removed and the stirring was continued for another 30 min. The mixture was extracted with ethyl acetate (2 x 50 mL) and water (2 x 50 mL). The organic layers were combined, washed with brine, dried over $MgSO_4$ and the organic solvent was removed under reduced pressure to give the pure (2-isothiocyanatoethyl)benzene as a brown oil.

T.L.C. system: *n*-hexane -EtOAC 1:1 v/v, Rf: 0.92
Yield: 0.770 g, 100 %

^{1}H-NMR ($CDCl_3$), δ: 3.02 (t, J= 6.9 Hz, 2H, H-1'), 3.75 (t, J_2= 6.9 Hz, 2H, H-2'), 7.24 (d, J= 6.8 Hz, 2H, H-aromatic), 7.30-7.32 (m, 1H, H-aromatic), 7.35-7.39 (m, 2H, H-aromatic).

^{13}C-NMR ($CDCl_3$), δ: 36.37 (CH_2, C-1'), 45.84 (CH_2, C-2'), 126.44, 127.21, 128.78 (CH, C-aromatic), 137.00 (C, C-1).

6.15.3 2-Arylidene-*N*-phenetylhydrazinecarbothioamides (171-174)

2-(4-Methylbenzylidene)-N-phenethylhydrazinecarbothioamide (171)
($C_{17}H_{19}N_3S$: M.W.= 297.42)

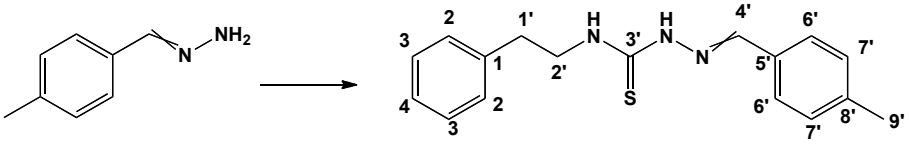

118 **171**

General procedure 22;
T.L.C. system: *n*-hexane -EtOAc 1:1 v/v, Rf: 0.98;
Off-White powder;
Yield: 0.23 g, 15 %
Melting point: 121-130 °C
MS $(ESI)^+$: 298.1 $[M+H]^+$

^{1}H-NMR (DMSO-d_6), δ: 2.34 (s, 3H, H-9'), 2.91-2.95 (m, 2H, H-1'), 3.75-3.80 (m, 2H, H-2'), 7.21-7.26 (m, 3H, H-aromatic), 7.27-7.30 (m, 2H, H-aromatic), 7.31-7.35 (m, 2H, H-aromatic), 7.65 (d, J= 8.0 Hz, 2H, H-aromatic), 8.03 (s, 1H, H-4'), 8.48 (t, J= 7.7 Hz, 1H, NH), 11.44 (bs, s, 1H, NH).

^{13}C-NMR (DMSO-d_6), δ: 21.01 (CH_3, C-9'), 34.86 (CH_2, C-1'), 44.95 (CH_2, C-2'), 126.16, 127.13, 128.43, 128.58, 129.25 (CH, C-aromatic), 131.44, 139.24, 139.61 (C, C-aromatic), 142.01 (CH, C-4'), 176.86 (C, C-3').

2-(3,4-Diethoxybenzylidene)-*N*-phenethylhydrazinecarbothioamide (172)
($C_{20}H_{25}N_3O2S$: M.W.= 371.50)

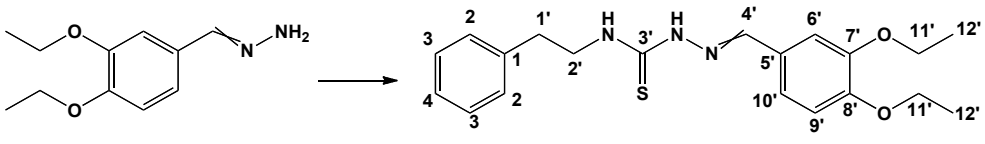

119 **172**

General procedure 22;
T.L.C. system: *n*-hexane -EtOAc 1:1 v/v, Rf: 0.75
Purification: flash column chromatography (*n*-hexane-EtOAc 100:0 v/v, increasing to 70:30 v/v);
White powder;

Yield: 0.2 g, 10.5 %
Melting point: 88-91 °C
MS (ESI)$^+$: 372.2 $[M+H]^+$

^{1}H-NMR (DMSO-d$_6$), δ: 1.35 (q, J= 7.0 Hz, 6H, H-12'), 2.93 (t, J= 7.6 Hz, 2H, H-1'), 3.76-3.81 (m, 2H, H-2'), 4.00-4.11 (m, 4H, H-11'), 6.98 (d, J= 8.4 Hz, 1H, H-aromatic), 7.17-7.24 (m, 2H, H-aromatic), 7.28-7.34 (m, 4H, H-aromatic), 7.37 (d, J= 1.6 Hz, 1H H-aromatic), 7.97 (s, 1H, H-4'), 8.40 (t, 1H, NH), 11.38 (bs, 1H, NH).

^{13}C-NMR (DMSO-d$_6$), δ: 14.62 (CH_3, C-12'), 34.70 (CH_2, C-1'), 45.02 (CH_2, C-2'), 63.78 (CH_2, C-11'), 110.98, 112.77, 121.74, 126.43 (CH, C-aromatic), 126.75 (C, C-aromatic), 128.39, 128.56 (CH, C-aromatic), 139.25, 140.37, 142.38, 150.13 (C, C-aromatic), 176.69 (C, C-3').

2-(1-(4-Cyclohexylphenyl)ethylidene)-*N*-phenethylhydrazinecarbothioamide (173)
($C_{23}H_{29}N_3S$: M.W.= 379.56)

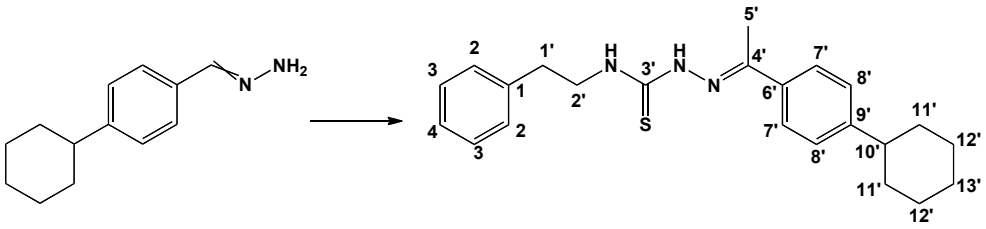

120 **173**

General procedure 22;
T.L.C. system: *n*-hexane -EtOAc 1:1 v/v, Rf: 0.78;
Purification: flash column chromatography (*n*-hexane:EtOAc 100:0 v/v, increasing to 70:30 v/v);
White powder;
Yield: 0.2 g, 10.2 %
Melting point: 87-92 °C
MS (ESI)$^+$: 380.2 $[M+H]^+$

^{1}H-NMR (DMSO-d$_6$), δ: 1.24-1.31 (m, 1H, H-13'), 1.34-1.48 (m, 4H, CH_2), 1.70-1.74 (m, 1H, H-13'), 1.78-1.82 (m, 4H, CH_2), 2.28 (s, 3H, H-5'), 2.54-2.57 (m, 1H, H-10'), 2.91-2.94 (m 2H, H-1'), 3.80 (q, J= 8.1 Hz, 2H, H-2'), 7.24-7.26 (m, 3H, H-aromatic), 7.28-7.30 (m, 2H, H-aromatic), 7.32-7.34 (m, 2H, H-

aromatic), 7.74 (d, J= 8.4 Hz, 2H, H-aromatic), 8.39 (t, J= 5.7 Hz, 1H, NH), 10.23 (bs, 1H, NH).

^{13}C-NMR (DMSO-d$_6$), δ: 14.06 (CH_3, C-5'), 25.52, 26.27, 33.75 (CH_2, C-11', 12', 13'), 34.70 (CH_2, C-1'), 43.49 (CH, C-10'), 45.02 (CH_2, C-2'), 126.18, 126.51, 128.45, 128.59 (CH, C-aromatic), 135.35, 139.22, 147.93, 148.85 (C, C-aromatic), 177.81 (C, C-3').

2-(4-Hydroxybenzylidene)-*N*-phenethylhydrazinecarbothioamide (174)
($C_{16}H_{17}N_3OS$: M.W.= 299.39)

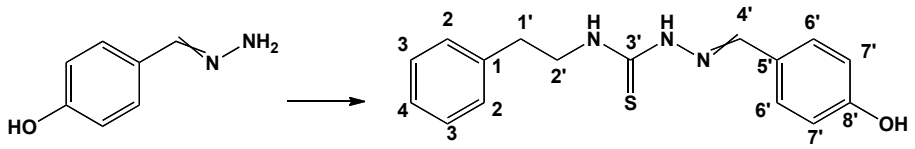

168 **174**

General procedure 22;
T.L.C. system: *n*-hexane -EtOAc 1:1 v/v, Rf: 0.83
Pale yellow powder;
Purification: flash column chromatography (*n*-hexane:EtOAc 100:0 v/v, increasing to 70:30 v/v);
Yield: 0.24 g, 16 %
Melting point: 121-128 °C
MS (ESI)$^+$: 300.1 $[M+H]^+$

^{1}H-NMR (DMSO-d$_6$), δ: 2.90-2.94 (m, 2H, H-1'), 3.73-3.79 (m, 2H, H-2'), 6.8 (d, J= 8.6 Hz, 2H, H-aromatic), 7.21-7.25 (m, 2H, H-aromatic), 7.27-7.29 (m, 2H, H-aromatic), 7.31-7.35 (m, 2H, H-aromatic), 7.58 (d, J= 8.6 Hz, 2H, H-aromatic), 7.96 (s, 1H, H-4'), 8.38 (t, J= 5.8 Hz, 1H, NH), 9.87 (bs, 1H, NH), 11.31 (bs, 1H, -OH).

^{13}C-NMR (DMSO-d$_6$), δ: 34.93 (CH_2, C-1'), 44.89 (CH_2, C-2'), 115.53 (CH, C-aromatic), 125.12 (C, C-aromatic), 126.15, 128.43,), 128.57, 128.90 (CH, C-aromatic), 139.27, 142.33, 159.23 (C, C-aromatic), 176.59 (C, C-3').

6.16 Synthesis of dithiocarbamate structures

6.16.1 General procedure 23-24

General procedure 23: synthesis of dithiocarbamates

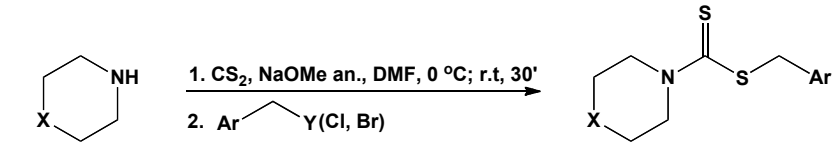

X = CH_2, O, -NCH_3, -NH, $C_6H_5CH_2$

To a solution of amine (6 mmol) in DMF (4 mL) was added dropwise carbon disulphide (0.46 g, 6 mmol) and anydrous sodium methoxide (0.1 g, 2 mmol) at 0 ºC. The resulting mixture was stirred at room temperature for 30 min. The aryl methyl bromide/chloride (3 mmol) was added by one portion and the stirring was continued. After completion of the reaction (monitored by TLC) the mixture was diluted with ice-cold water (20 mL) and the precipitate was filtered. The collected solid was purified by column chromatography and/or recrystallization to give the desired product.

General procedure 24: synthesis of dithiocarbamate methyl aryl acids

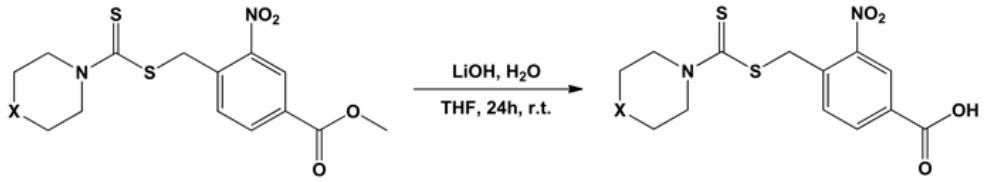

X = CH_2, O, N-CH_3, NH, $C_6H_5CH_2$

The appropriate methyl ester derivative (1 eq.) was dissolved in THF (30.4 mL/mmol eq.) and LiOH (7.3 eq.) in water (2.42 mL/mmol eq.). The mixture was stirred for 24 h, at room temperature. The organic layer was evaporated, then the residue was acidifed by the addition of a 2N HCl solution. The resulting precipitate was filtrated, washed with water and dried. The crude residue was purified by flash column chromatography and/or recrystallization to give the title compound.

6.16.2 Benzyl piperazine ($C_{11}H_{16}N_2$; M.W.= 176.26) (181)[45]

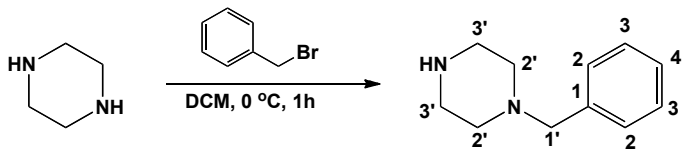

180 **181**

Benzyl bromide (2 g, 11.7 mmol) was added dropwise at 0 °C to a solution of piperazine (**180**) (5.03 g, 58 mmol) in dry DCM (25 mL). The reaction mixture was stirred at the same temperature for 1h, rinsed with $NaHCO_3$ (20 mL), dried over Na_2SO_4 and concentrated under vacuum. The crude product was used in the next step without further purification.

T.L.C. System: *n*-hexane -EtOAc: 5:5 v/v, Rf: 0.29;
Pale, yellow oil;
Yield: 1.85 g, 89.8%

^{1}H-NMR ($CDCl_3$), δ: 2.29-2.36 (m, 4H, CH_2), 2.81 (t, J= 4.8 Hz, 4H, piperidine), 3.42 (s, 2H, H-1'), 3.43 (bs, 1H, NH), 7.14-7.19 (m, 2H, H-aromatic), 7.21-7.24 (m, 3H, H-aromatic).

^{13}C-NMR ($CDCl_3$), δ: 46.12 (CH_2, C-1'), 53.10, 53.15, 62.99, 63.08 (CH_2, C-2', C-3'), 126.97, 127.00, 128.17, 129.13, 129.22 (CH, C-aromatic), 138.11 (C-1).

6.16.3 2-(Bromomethyl)benzo[*d*]oxazole (193)[46]
(C_8H_6BrNO; M.W.= 212.04)

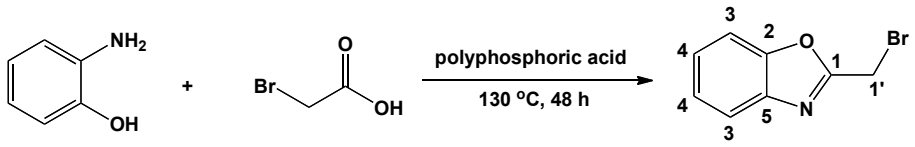

191 **192** **193**

To a mixture of 2-aminophenol (**191**) (0.5 g, 4.58 mmol) in polyphosphoric acid (4.6 g, 13.8 mmol), bromoacetic acid (**192**) (0.95 g, 6.87 mmol) was added and stirred at 130 °C for 48 h. The reaction mixture was diluted with water (25 mL) and extracted with DCM (2x 20 mL). The organic layer was separated, dried over Na_2SO4 and evaporated under pressure. The crude

product was purified by flash column chromatography (*n*-hexane:EtOAc 100:0 v/v, increasing to 90:10 v/v) to give a pale, yellow oil.

T.L.C. System: *n*-hexane -EtOAc: 8:2 v/v, Rf: 0.64;
Yield: 0.21g, 43.2%

^{1}H-NMR ($CDCl_3$), δ: 4.62 (s, 2H, H-1'), 7.37-7.44 (m, 2H, H-aromatic), 7.56-7.58 (m, 1H, H-aromatic), 7.74-7.77 (m, 1H, H-aromatic).

^{13}C-NMR ($CDCl_3$), δ: 20.60 (CH_2, C-1'), 110.88, 120.53, 124.85, 126.00 (CH-aromatic), 143.25, 151.18, 155.63 (C, C-aromatic).

6.16.4 2-(Chloromethyl)benzo[d]thiazole (200) (C_8H_6ClNS, M.W.=183.66)[47]

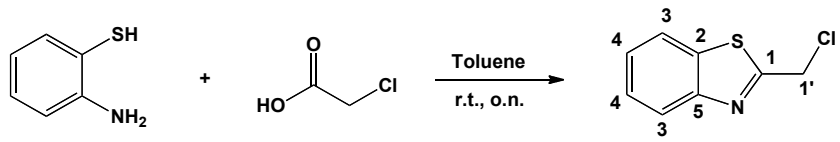

198 **199** **200**

To a solution of 2-aminothiophenol (**198**) (1.02 g, 10 mmol) in toluene (30 mL), chloroacetic acid (**199**) (0.88 mL, 11 mmol) was added dropwise with continuous stirring, over 15 min. The mixture was stirred for 24h at room temperature and then partitioned in H_2O (20 mL) and EtOAc (20 mL). The organic layer was separated, washed with H_2O, brine and dried over $MgSO_4$. The crude mixture was purified by flash column chromatography (*n*-hexane:EtOAc 100:0 v/v, increasing to 90:10 v/v) to give a colourless oil.

T.L.C. System: *n*-hexane -EtOAc: 2:8 v/v, Rf: 0.7;
Yield: 1.5g, 50 %

^{1}H-NMR ($CDCl_3$), δ: 4.87 (s, 2H, H-1'), 7.35 (td, 1H, J_1= 7.6 Hz, J_2= 1.3 Hz, H-aromatic), 7.43 (td, 1H, J_1= 7.6 Hz, J_2= 1.3 Hz, H-aromatic), 7.81-7.83 (m, 1H, H-aromatic), 7.94-7.96 (m, 1H, H-aromatic).

^{13}C-NMR ($CDCl_3$), δ: 42.06 (CH_2, C-1'), 121.80, 123.47, 125.77, 126.49 (CH-aromatic), 135.83, 152.81, 166.80 (C, C-aromatic).

6.16.5 Methyl 4-bromo-3-nitrobenzoate (202)[48]

($C_8H_6BrNO_4$; M.W.= 274.07)

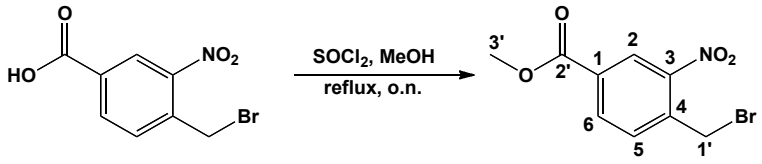

201 **202**

A mixture of 4-(bromomethyl)-3-nitrobenzoic acid (**201**) (1 eq, 5.76 mmol) and thionyl chloride (2.1 eq., 12.4 mmol) in MeOH (9.6 mL) was refluxed overnight. The reaction mixture was then cooled to room temperature and dried under pressure. The remaining residue was washed with cold MeOH and dried.

T.L.C. System: *n*-hexane -EtOAc: 7:3 v/v, Rf: 0.47;
Orange oil;
Yield: 0.45 g, 82 %

^{1}H-NMR ($CDCl_3$), δ: 4.01 (s, 3H, H-3'), 5.03 (s, 2H, H-1'), 7.85 (d, J= 8.1 Hz, 1H, H-aromatic), 8.32 (d, J= 8.1 Hz, 1H, H-aromatic), 8.71 (s, 1H, H-2).

^{13}C-NMR ($CDCl_3$), δ: 42.35 (CH_2, C-1'), 52.86 (CH_3, C-3'), 126.28, 131.65 (CH, C-aromatic), 131.77 (C, C-aromatic), 134.18 (CH, C-aromatic), 136.67, 158.9 (C, C-aromatic), 165.9 (C, C-2').

6.16.6 2-Chloromethyl benzoimidazol carbodithioates (182-186)

(1*H*-Benzo[*d*]imidazol-2-*yl*)methyl piperidine-1-carbodithioate (182)[49]
($C_{14}H_{17}N_3S_2$; M.W.= 291.43)

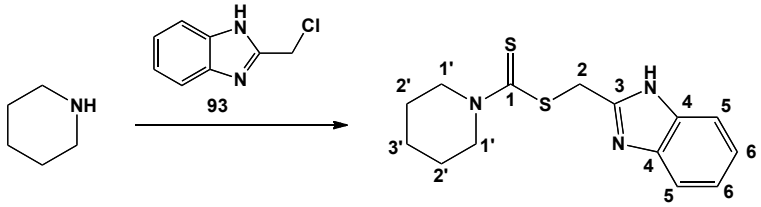

177 **182**

General procedure 23;
T.L.C. System: DCM-MeOH: 9:1 v/v, Rf: 0.62;
Off-white solid;
Purification: recrystallization from EtOH/H_2O;
Yield: 0.107 g, 12.3%;
Melting point: 170-173 ºC; (lit. 184 ºC)
MS $(ESI)^+$: 292.1 $[M+H]^+$
Microanalysis: Calculated for $C_{14}H_{17}N_3S_2$ (291.43); Theoretical: %C = 57.70, %H = 5.88, %N = 14.41; Found: %C = 57.47, %H = 5.93, %N = 14.42.

^{1}H-NMR ($CDCl_3$), δ: 1.69-1.79 (m, 6H, CH_2), 3.88-3.94 (m, 2H, CH_2), 4.33-4.42 (m, 2H, CH_2), 4.94 (s, 2H, H-2), 7.24-7.26 (m, 2H, H-aromatic), 7.41-7.44 (m, 1H, H-aromatic), 7.71-7.74 (m, 1H, H-aromatic), 10.49 (bs, 1H, N<u>H</u>).

^{13}C-NMR ($CDCl_3$), δ: 24.06, 25.54, 26.02 (CH_2), 33.80 (CH_2, C-2), 52.01, 54.06 (CH_2-), 122.63 (CH-aromatic), 151.90 (C, C-aromatic), 195.08 (C, C-1).

(1H-Benzo[*d*]imidazol-2-yl)methyl morpholine-4-carbodithioate (183)[50]
($C_{13}H_{15}N_3OS_2$; M.W.= 293.41)

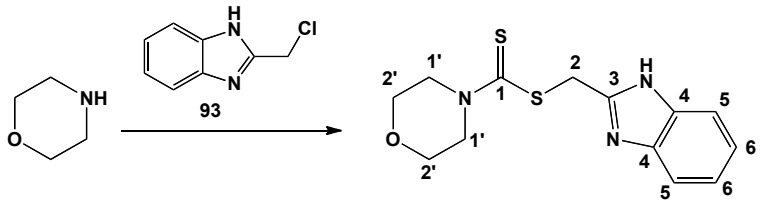

178 **183**

General procedure 23;
T.L.C. System: DCM-MeOH 9:1;
Dark yellow solid;
Purification: flash column chromatography (DCM:MeOH: 100:0 v/v, increasing to 99:1 v/v) and recrystallization from DCM/*n*-hexane;
Yield: 0.09 g, 10.2 %;
Melting point: 165-168 °C; (lit. 178 °C)
MS (ESI)$^+$: 294.1 $[M+H]^+$
Microanalysis: Calculated for $C_{13}H_{15}N_3OS_2$ (293.41); Theoretical: %C = 53.22, %H = 5.15, %N = 14.32; Found: %C = 52.84, %H = 4.99, %N = 14.19.

^{1}H-NMR ($CDCl_3$), δ: 3.73-3.86 (m, 4H, CH_2), 3.92-3.99 (m, 2H, CH_2), 4.39-4.46 (m, 2H, CH_2), 4.96 (s, 2H, H-2), 7.25-7.27 (m, 2H, H-aromatic), 7.41-7.80 (m, 2H, H-aromatic), 10.38 (bs, 1H, N<u>H</u>).

^{13}C-NMR ($CDCl_3$), δ: 33.63 , 50.91, 52.36, 65.87 (CH_2), 66.45 (CH_2, C-2) 122.77 (CH-aromatic), 148.2, 151.33 (C, C-aromatic), 197.11 (C, C-1).

(1*H*-Benzo[*d*]imidazol-2-yl)methyl 4-methylpiperazine-1-carbodithioate (184) ($C_{14}H_{18}N_4S_2$; M.W.= 306.45)

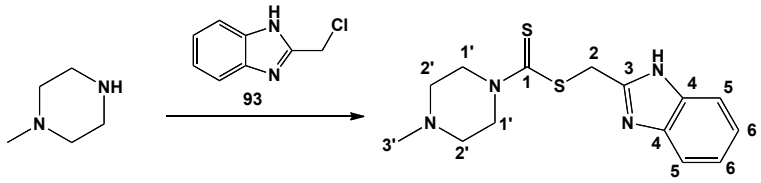

179 **184**

General procedure 23;
T.L.C. System: DCM-MeOH: 9:1 v/v, Rf: 0.47;
Yellow solid;
Purification: flash column chromatography (DCM:MeOH: 100:0 v/v, increasing to 99:1 v/v) and recrystallization from DCM/*n*-hexane;
Yield: 0.1 g, 11 %;
Melting point: 154-156 °C;
MS (ESI)$^+$: 307.1 $[M+H]^+$
Microanalysis: Calculated for $C_{14}H_{18}N_4S_2$ (306.10); Theoretical: %C = 54.87, %H = 5.92, %N = 14.28; Found: %C = 54.50, %H = 5.52, %N = 17.87.

^{1}H-NMR ($CDCl_3$), δ: 2.34 (s, 3H, H-3'), 2.47-2.59 (m, 4H, CH_2), 3.92-3.98 (m,

2H, CH_2), 4.41-4.72 (m, 2H, CH_2), 4.94 (s, 2H, H-2), 7.27 (m, 2H, H-aromatic), 7.47-7.75 (m, 2H, H-aromatic), 10.44 (bs, 1H, NH).

^{13}C-NMR ($CDCl_3$), δ: 33.77 (CH_2), 45.53 (CH_3, C-3'), 50.38, 52.25 (CH_2), 54.31 (CH_2, C-2), 122.65 (CH-aromatic), 151.58, 154.9 (C, C-aromatic), 196.50 (C, C-1).

(1H-Benzo[*d*]imidazol-2-*yl*)methyl piperazine-1-carbodithioate (185)[50]
($C_{13}H_{16}N_4S_2$; M.W.= 292.42)

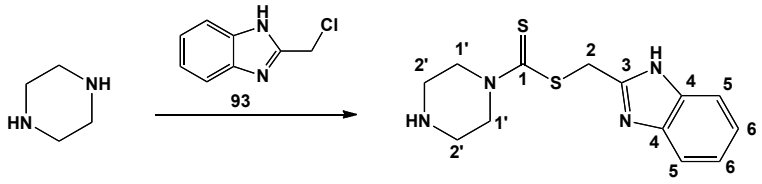

180 **185**

General procedure 23;
T.L.C. System: DCM-MeOH: 9:1 v/v, Rf: 0.5;
Whitish solid;
Purification: flash column chromatography (DCM:MeOH: 100:0 v/v, increasing to 99:1 v/v) and recrystallization from MeOH;
Yield: 0.09 g,10.3 %;
Melting point: 165-167 ^oC; (lit. 179 ^oC)
MS $(ESI)^+$: 293.1 $[M+H]^+$
Microanalysis: Calculated for $C_{13}H_{16}N_4S_2$ (292.42); Theoretical: %C = 53.40, %H = 5.51, %N = 19.16; Found: %C = 53.21, %H = 5.16, %N = 18.99.

^{1}H-NMR (DMSO-d_6), δ: 3.32-3.35 (m, 4H, CH_2), 4.14-4.21 (m, 2H, CH_2), 4.35-4.40 (m, 2H, CH_2), 4.80 (s, 2H, H-2), 7.13-7.18 (m, 2H, H-aromatic), 7.46 (d, J=7.2 Hz, 1H, H-aromatic), 7.55 (d, J=7.2 Hz, 1H, H-aromatic), 12.38 (bs, 1H, N<u>H</u>).

^{13}C-NMR (DMSO-d_6), δ: 34.34, 47.59, 49.65, 54.87 (CH_2), 58.02 (CH_2, C-2), 111.25, 118.39, 121.24, 122.12 (CH-aromatic), 143.15, 149.36 (C, C-aromatic) 194.21 (C, C-1).

(1H-Benzo[d]imidazol-2-*yl*)methyl 4-benzylpiperazine-1-carbodithioate (186) ($C_{20}H_{22}N_4S_2$; M.W.= 382.55)

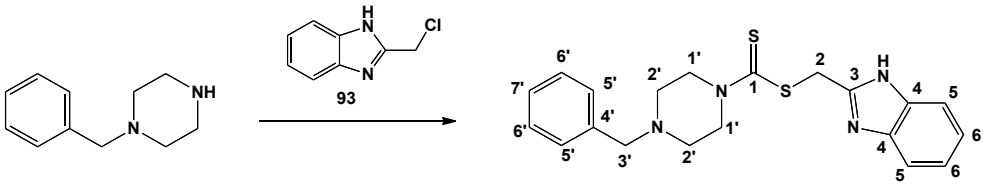

181 **186**

General procedure 23

T.L.C. System: *n*-hexane -EtOAc: 5:5 v/v, Rf: 0.5;

Brown solid;

Purification: recrystallization from EtOH;

Yield: 0.19 g, 17%;

Melting point: 104-106°C;

MS $(ESI)^+$: 383.1 $[M+H]^+$

Microanalysis: Calculated for $C_{20}H_{22}N_4S_2$ (382.55); Theoretical: %C = 62.79, %H = 5.80, %N = 14.65; Found: %C = 62.50, %H = 5.57, %N = 14.53.

^{1}H-NMR ($CDCl_3$), δ: 2.51-2.55 (m, 2H, CH_2), 2.60-2.63 (m, 2H, CH_2), 3.56 (s, 2H, CH_2, H-3'), 3.92-3.95 (m, 2H, CH_2), 4.41-4.45 (m, 2H, CH_2), 4.94 (s, 2H, CH_2, H-2), 7.23-7.27 (m, 2H, H-aromatic), 7.29-7.37 (m, 5H, H-aromatic), 7.41-7.43 (m, 1H, H-aromatic), 7.71-7.74 (m, 1H, H-aromatic), 10.40 (bs, 1H, NH).

^{13}C-NMR ($CDCl_3$), δ: 33.73 (CH_2, C-3'), 50.56, 52.34 (CH_2), 62.39 (CH_2, C-2), 127.50, 128.44, 129.09 (CH-aromatic), 137.17 (C, C-aromatic), 149.3, 151.63 (C, C-aromatic), 196.29 (C, C-1).

6.16.7 2-Chloromethyl benzo[*d*]oxazol carbodithioates (187-190)

Benzo[*d*]oxazol-2-*yl*-methyl piperidine-1-carbodithioate (187)
($C_{20}H_{22}N_4S_2$; M.W.= 292.42)

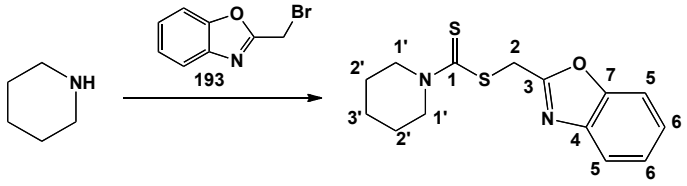

177 **187**

General procedure 23;
T.L.C. System: *n*-hexane -EtOAc-: 8:2 v/v, Rf: 0.53;
Yellow wax;
Purification: flash column chromatography (*n*-hexane:EtOAc: 100:0 v/v, increasing to 80:20 v/v);
Yield: 0.81 g, 93.8 %;
Melting point: 53-55 ^oC;
MS $(ESI)^+$: 293.1 $[M+H]^+$
Microanalysis: Calculated for $C_{14}H_{16}N_2OS_2$ (292.42); Theoretical: %C = 57.50, %H = 5.52, %N = 9.58; Found: %C = 57.61, %H = 5.60, %N = 9.72.

^{1}H-NMR ($CDCl_3$), δ: 1.73-1.75 (m, 6H, CH_2), 3.93-3.99 (m, 2H, CH_2), 4.29-4.35 (m, 2H, CH_2), 4.96 (s, 2H, H-2), 7.32-7.35 (m, 2H, H-aromatic), 7.52-7.54 (m, 1H, H-aromatic), 7.71-7.73 (m, 1H, H-aromatic).

^{13}C-NMR ($CDCl_3$), δ: 24.21, 25.40, 26.11, 34.23, 51.57 (CH_2), 53.71 (CH_2, C-2), 110.64, 120.05, 124.38, 125.07 (CH-aromatic), 141.26, 141.23, 151.08, 162.41 (C, C-aromatic), 192.84 (C, C-1).

Benzo[*d*]oxazol-2-yl-methyl morpholine-4-carbodithioate (188)
($C_{13}H_{14}N_2O_2S_2$; M.W.= 294.39)

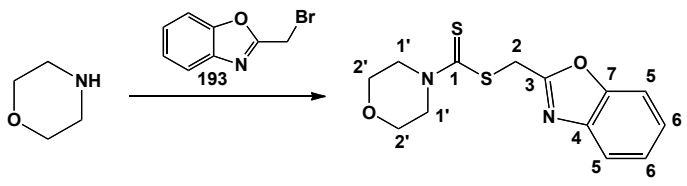

178 **188**

General procedure 23;
T.L.C. System: *n*-hexane -EtOAc-: 5:5 v/v, Rf: 0.7;
White solid;
Purification: recrystallization from EtOH;
Yield: 0.12 g, 13.6 %;
Melting point: 61-64 °C;
MS (ESI)$^+$: 295.1 $[M+H]^+$
Microanalysis: Calculated for $C_{13}H_{14}N_2O_2S_2$ (294.39); Theoretical: %C = 53.04, %H = 4.79, %N = 9.52; Found: %C = 52.92, %H = 4.60, %N = 9.29.

^{1}H-NMR ($CDCl_3$), δ: 3.79-3.82 (m, 4H, CH_2), 3.98-4.08 (m, 2H, CH_2), 4.31-4.41 (m, 2H, CH_2), 4.96 (s, 2H), 7.34-7.36 (m, 2H, H-aromatic), 7.53-7.55 (m, 1H, H-aromatic), 7.72-7.74 (m, 1H, H-aromatic).

^{13}C-NMR ($CDCl_3$), δ: 33.92, 25.40 (CH_2), 66.20 (CH_2, C-2), 110.65, 120.10, 124.47, 125.19 (CH-aromatic), 141.20, 141.23, 151.08, 162.02 (C, C-aromatic), 194.73 (C, C-1).

Benzo[*d*]oxazol-2-*yl*-methyl 4-methylpiperazine-1-carbodithioate (189)
($C_{14}H_{17}N_3OS_2$; M.W.= 307.43)

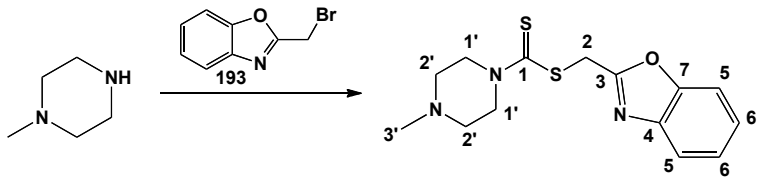

179 **189**

General procedure 23;
T.L.C. System: *n*-hexane -EtOAc-: 5:5 v/v, Rf: 0.4;
Whitish sponge;
Purification: recrystallization from DCM;
Yield: 0.18 g, 19.5 %;
Melting point: 55-58 °C;
MS (ESI)$^+$: 308.1 $[M+H]^+$
Microanalysis: Calculated for $C_{14}H_{17}N_3OS_2$ (307.43); Theoretical: %C = 54.69, %H = 5.57, %N = 13.67; Found: %C = 54.51, %H = 5.20, %N = 13.42.

^{1}H-NMR ($CDCl_3$), δ: 2.35 (s, CH_3, H-3'), 2.52-2.55 (m, 4H, CH_2), 3.97-4.06 (m,

2H, CH_2), 4.35-4.43 (m, 2H, CH_2), 4.96 (s, 2H, H-2), 7.33-7.36 (m, 2H, H-aromatic), 7.52-7.55 (m, 1H, H-aromatic), 7.71-7.74 (m, 1H, H-aromatic).

^{13}C-NMR ($CDCl_3$), δ: 34.13 (CH_2), 45.52 (CH_3, C-3'), 54.36 (CH_2, C-2), 110.64, 120.08, 124.42, 125.13 (CH-aromatic), 141.23, 141.07, 162.17 (C, C-aromatic), 194.12 (C, C-1).

Benzo[*d*]oxazol-2-*yl*-methyl 4-benzylpiperazine-1-carbodithioate (190)
($C_{20}H_{21}N_3OS_2$; M.W.= 383.53)

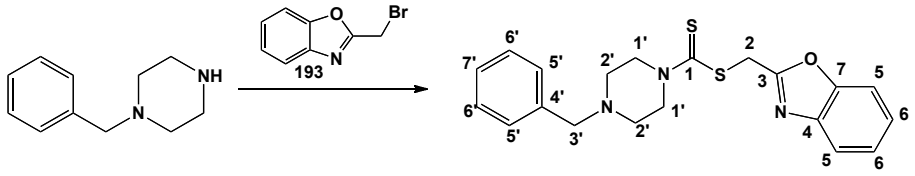

181 **180**

General procedure 23;
T.L.C. System: *n*-hexane -EtOAc-: 8:2 v/v, Rf: 0.53;
Fine, white powder;
Purification: flash column chromatography (*n*-hexane:EtOAc: 100:0 v/v, increasing to 70:30 v/v) and recrystallization from EtOH;
Yield: 0.33 g, 28.7 %;
Melting point: 86-88 ^{o}C;
MS (ESI)$^{+}$: 384.1 $[M+H]^{+}$
Microanalysis: Calculated for $C_{20}H_{21}N_3OS_2$ (383.11); Theoretical: %C = 62.63, %H = 5.52, %N = 10.96; Found: %C = 62.64, %H = 5.55, %N = 10.80.

^{1}H-NMR ($CDCl_3$), δ: 2.56-2.59 (m, 4H, CH_2), 3.57 (s, 2H, H-3'), 3.96-4.05 (m, 2H,CH_2), 4.32-4.42 (m, 2H, CH_2), 4.96 (s, 2H, H-2), 7.29-7.33 (m, 1H, H-aromatic), 7.32-7.36 (m, 6H, H-aromatic), 7.52-7.54 (m, 1H, H-aromatic), 7.71-7.73 (m, 1H, H-aromatic).

^{13}C-NMR ($CDCl_3$), δ: 34.11 (CH_2, C-2), 52.35 (CH_2), 62.47 (CH_2, C-3'), 110.64, 120.07, 124.42, 125.12, 127.46, 128.43, 129.11 (CH-aromatic), 139.65, 141.23, 162.21 (C, C-aromatic), 193.93 (C, C-1).

6.16.8 2-Chloromethyl benzo[*d*]thiazol carbodithioates (194-197)

Benzo[*d*]thiazol-2-*yl*-methyl piperidine-1-carbodithioates (194)

($C_{14}H_{16}N_2S_3$; M.W.= 308.49)

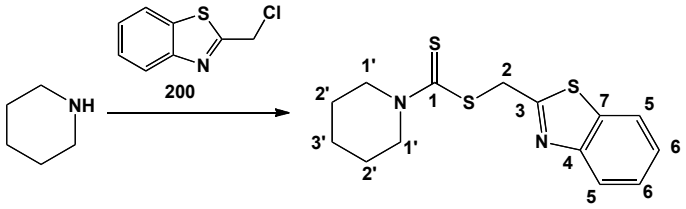

177 **194**

General procedure 23;

T.L.C. System: *n*-hexane -EtOAc-: 5:5 v/v, Rf: 0.58;

Fine, white powder;

Purification: recrystallization from EtOH;

Yield: 0.61 g, 66 %;

Melting point: 81-84 ^{o}C;

MS (ESI)$^{+}$: 309.1 $[M+H]^{+}$

Microanalysis: Calculated for $C_{14}H_{16}N_2S_3$ (308.49); Theoretical: %C = 54.51, %H = 5.23, %N = 9.08; Found: %C = 54.58, %H = 5.49, %N = 8.77.

^{1}H-NMR ($CDCl_3$), δ: 1.72-1.76 (m, 6H, CH_2), 3.90-3.95 (m, 2H, CH_2), 4.32-4.36 (m, 2H, CH_2), 5.15 (s, 2H, H-2), 7.36-7.39 (m, 1H, H-aromatic), 7.45-7.47 (m, 1H, H-aromatic), 7.83-7.85 (m, 1H, H-aromatic), 7.99-8.02 (m, 1H, H-aromatic).

^{13}C-NMR ($CDCl_3$), δ: 24.23, 25.48, 26.17 (CH_2), 39.11 (CH_2, C-2), 51.68, 53.84 (CH_2), 121.61, 122.86, 125.18, 126.02 (CH-aromatic), 135.75, 152.72, 168.19 (C, C-aromatic), 193.15 (C, C-1).

Benzo[*d*]thiazol-2-*yl*-methyl morpholine-4-carbodithioate (195)
($C_{13}H_{14}N_2OS_3$; M.W.= 310.46)

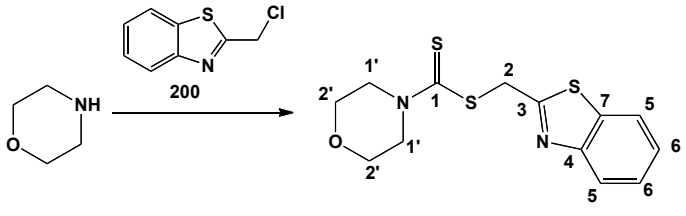

178 **195**

General procedure 23;
T.L.C. System: *n*-hexane -EtOAc-: 5:5 v/v, Rf: 0.76;
Fine, white powder;
Purification: recrystallization from EtOH;
Yield: 0.65 g, 75 %;
Melting point: 80-82 ^oC;
MS $(ESI)^+$: 311.1 $[M+H]^+$
Microanalysis: Calculated for $C_{13}H_{14}N_2OS_3$ (310.03); Theoretical: %C = 50.30, %H = 4.55, %N = 9.02; Found: %C = 49.90, %H = 4.57, %N = 8.91.

^{1}H-NMR ($CDCl_3$), δ: 3.79-3.82 (m, 4H, CH_2), 3.95-4.12 (m, 2H, CH_2), 4.29-4.45 (m, 2H, CH_2), 5.15 (s, 2H, C-2), 7.36-7.39 (m, 1H, H-aromatic), 7.47-7.49 (m, 1H, H-aromatic), 7.84-7.86 (m, 1H, H-aromatic), 8.00-8.02 (m, 1H, H-aromatic).

^{13}C-NMR ($CDCl_3$), δ: 38.79 (CH_2), 66.41 (CH_2, C-2), 121.63, 122.92, 125.32, 126.14 (CH-aromatic), 135.68, 152.68, 167.46 (C, C-aromatic), 195.10 (C, C-1).

Benzo[*d*]thiazol-2-*yl*-methyl 4-methylpiperazine-1-carbodithioate (196)
($C_{14}H_{17}N_3S_3$; M.W.= 323.50)

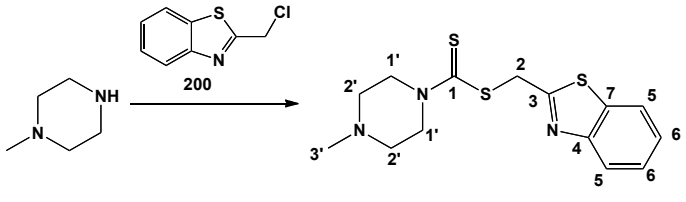

179 **196**

General procedure 23;
T.L.C. System: *n*-hexane -EtOAc-: 2:8 v/v, Rf: 0.56;
Fine, whitish powder;
Purification: recrystallization from EtOH;
Yield: 0.26 g, 27 %;
Melting point: 61-64ºC;
MS (ESI)$^+$: 324.1 $[M+H]^+$
Microanalysis: Calculated for $C_{14}H_{17}N_3S_3$ (323.50); Theoretical: %C = 51.98, %H = 5.30, %N = 12.99; Found: %C = 51.95, %H = 6.31, %N = 12.58.

^{1}H-NMR ($CDCl_3$), δ: 2.35 (s, 3H, H-3'), 2.51-2.55 (m, 4H, CH_2), 3.97-4.02 (m, 2H, CH_2), 4.39-4.44 (m, 2H, CH_2), 5.14 (s, 2H, C-2), 7.37-7.39 (m, 1H, H-aromatic), 7.47-7.49 (m, 1H, H-aromatic), 7.84-7.86 (m, 1H, H-aromatic), 8.00-8.02 (m, 1H, H-aromatic).

^{13}C-NMR ($CDCl_3$), δ: 39.04 (CH_2), 45.57 (CH_3, C-3'), 54.38 (CH_2, C-2), 121.60, 122.91, 125.23, 126.06 (CH-aromatic), 135.74, 152.74, 167.69 (C, C-aromatic), 194.54 (C, 1).

Benzo[*d*]thiazol-2-*yl*-methyl 4-benzylpiperazine-1-carbodithioate (197) ($C_{20}H_{21}N_3S$; M.W.= 399.60)

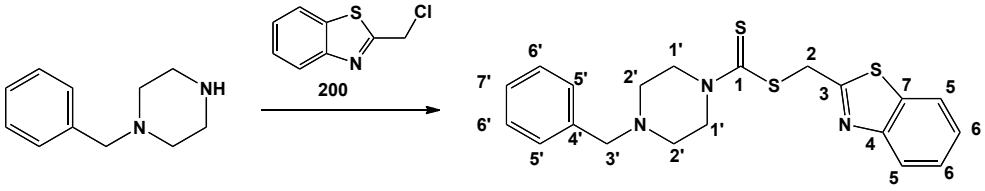

181 **197**

General procedure 23;
T.L.C. System: *n*-hexane -EtOAc-: 5:5 v/v, Rf: 0.45;
White crystals;
Purification: flash column chromatography (*n*-hexane:EtOAc: 100:0 v/v, increasing to 70:30 v/v) and recrystallization from EtOH;
Yield: 0.5 g, 42 %;
Melting point: 59-61 ºC;
MS (ESI)$^+$: 400.1 $[M+H]^+$
Microanalysis: Calculated for $C_{20}H_{21}N_3S_3$ (399.60); Theoretical: %C = 60.11,

%H = 5.30, %N = 10.52; Found: %C = 60.15, %H = 5.54, %N = 10.11.

^{1}H-NMR ($CDCl_3$), δ: 2.54-2.60 (m, 4H, CH_2), 3.57 (s, 2H, H-3'), 3.95-4.01 (m, 2H, CH_2), 4.36-4.43 (m, 2H, CH_2), 5.14 (s, 2H, H-2), 7.29-7.35 (m, 4H, H-aromatic), 7.36-7.40 (m, 2H, H-aromatic), 7.46-7.50 (m, 1H, H-aromatic), 7.85 (d, J= 8.1 Hz, 1H, H-aromatic), 8.01 (d, J= 8.1 Hz, 1H, H-aromatic).

^{13}C-NMR ($CDCl_3$), δ: 38.97 (CH_2), 52.40 (CH_2, C-2), 62.48 (CH_2, C-3'), 121.62, 122.89, 125.24, 126.07, 127.46, 128.44, 129.13 (CH-aromatic), 137.28, 140.6, 152.8, 168.0 (C, C-aromatic), 196.8 (C, C-1).

6.16.9 Aryl carbodithioates (206-220)

4-(Trifluoromethyl)benzyl piperidine-1-carbodithioate (206)[51]
($C_{14}H_{16}F_3NS_2$; M.W.= 319.41)

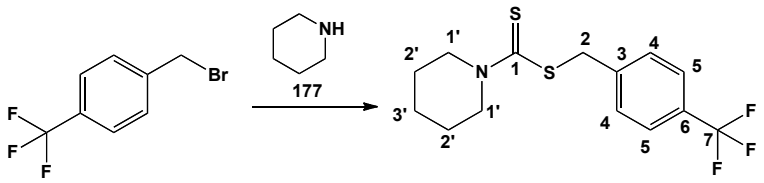

203 **206**

General procedure 23;
T.L.C. System: *n*-hexane -EtOAc: 9:1 v/v, Rf: 0.57;
Off-White solid;
Purification: recrystallization from MeOH;
Yield: 0.084 g, 88.5%;
Melting point: 49-51 °C;
MS $(ESI)^+$: 320.1 $[M+H]^+$
Microanalysis: Calculated for $C_{14}H_{16}F_3NS_2$ (319.41); Theoretical: %C = 52.64, %H = 5.05, %N = 4.39; Found: %C = 52.37, %H = 5.15, %N = 4.37.

^{1}H-NMR ($CDCl_3$), δ: 1.69-1.76 (m, 6H, CH_2), 3.87-3.94 (m, 2H, CH_2), 4.29-4.36 (m, 2H, CH_2), 4.69 (s, 2H, H-2), 7.53 (d, 2H, J= 8.2 Hz, H-aromatic), 7.58 (d, 2H, J=8.2 Hz, H-aromatic).

^{13}C-NMR ($CDCl_3$), δ: 24.26 (CH_2, C-3'), 25.45, 26.08 (CH_2), 41.15 (CH_2, C-2), 51.43, 53.28 (CH_2), 124.18 (q, J= 270.2 Hz, C-7), 125.44 (q, J= 3.7 Hz, CH, C-5), 129.41 (C, C-6), 129.64 (CH, C-6), 140.94 (C, C-3), 194.36 (C, C-1).

4-(Trifluoromethyl)benzyl morpholine-4-carbodithioate (207)[51]
($C_{13}H_{14}F_3NOS_2$; M.W.= 321.38)

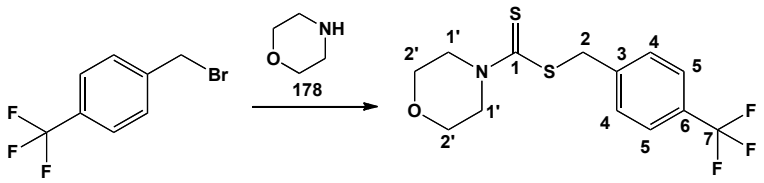

203 **207**

General procedure 23;
T.L.C. System: *n*-hexane -EtOAc: 9:1 v/v, Rf: 0.56;
White sponge;
Purification: recrystallization from MeOH
Yield: 0.178 g, 18.5%;
Melting point: 57-59 °C;
MS (ESI)$^+$: 322.1 $[M+H]^+$
Microanalysis: Calculated for $C_{13}H_{14}F_3NOS_2$ (321.38); Theoretical: %C = 48.58, %H = 4.39, %N = 4.36; Found: %C = 48.37, %H = 4.86, %N = 4.35.

^{1}H-NMR ($CDCl_3$), δ: 3.77-3.80 (m, 4H, CH_2), 3.92-4.09 (m, 2H, CH_2), 4.25-4.41 (m, 2H, CH_2), 4.68 (s, 2H, H-2), 7.53 (d, 2H, J=8.1 Hz, H-aromatic), 7.59 (d, 2H, J=8.1 Hz, H-aromatic).

^{13}C-NMR ($CDCl_3$), δ: 40.08 (CH_2, C-2), 66.11 (CH_2), 125.31 (q, J= 271.3, C-7), 125.51 (q, J= 3.7 Hz, CH, C-5), 129.58 (CH, C-aromatic), 129.72 (q, J= 32.0 Hz, C, C-6), 140.53 (C, C-3), 196.30 (C, C-1).

4-(Trifluoromethyl)benzyl 4-methylpiperazine-1-carbodithioate (208)[50]
($C_{14}H_{17}F_3N_2S_2$; M.W.= 334.42)

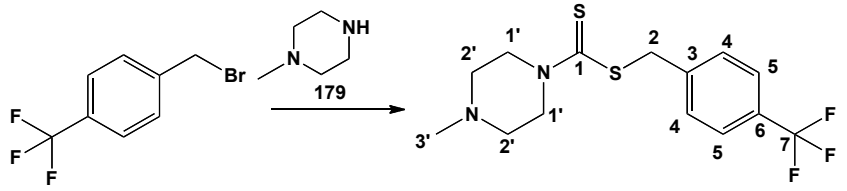

203 **208**

General procedure 23;
T.L.C. System: DCM-MeOH: 9:1 v/v, Rf: 0.34;
White solid;
Purification: recrystallization from EtOH/H_2O;
Yield: 0.112 g,11.2%;
Melting point: 57-60 °C;
MS (ESI)$^+$: 335.1 $[M+H]^+$
Microanalysis: Calculated for $C_{14}H_{17}F_3N_2S_2$ (334.42); Theoretical: %C = 50.28, %H = 5.12, %N = 8.38; Found: %C = 50.23, %H = 5.39, %N = 8.39.

^{1}H-NMR ($CDCl_3$), δ: 2.35 (s, 3H, H-3'), 2.49-2.53 (m, 4H, CH_2), 3.93-4.02 (m, 2H, CH_2), 4.32-4.43 (m, 2H, CH_2), 4.66 (s, 2H, H-2), 7.53 (d, 2H, J=8.2 Hz, H-aromatic), 7.58 (d, 2H, J=8.2 Hz, H-aromatic).

^{13}C-NMR ($CDCl_3$), δ: 41.07 (CH_2), 45.62 (CH_3, C-3'), 54.39 (CH_2, C-2), 124.14 (q, J= 272.2, C-7), 125.42 (q, J= 3.7 Hz, CH, C-C-5), 129.70 (q, J= 32.0 Hz, C, C-6), 140.72 (C, C-3), 195.73 (C, C-1).

4-(Trifluoromethyl)benzyl piperazine-1-carbodithioate (209)
($C_{13}H_{15}F_3N_2S_2$; M.W.= 320.40)

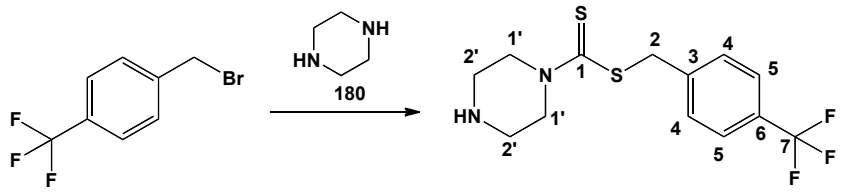

193 **200**

General procedure 23;
T.L.C. System: *n*-hexane -EtOAc: 3:7 v/v, Rf: 0.4;
Off-white, fine powder;
Purification by recrystallization from MeOH;
Yield: 0.308 g, 32%;
Melting point: 154-156° C;
MS $(ESI)^+$: 321.1 $[M+H]^+$
Microanalysis: Calculated for $C_{13}H_{15}F_3N_2S_2$ (320.40); Theoretical: %C = 48.73, %H = 4.72, %N = 8.74; Found: %C = 39.31, %H = 5.28, %N = 8.91.

^{1}H-NMR (DMSO-d_6), δ: 2.91 (bs, 1H, NH), 3.02-3.04 (m, 2H, CH_2), 4.10-4.13 (m, 2H, CH_2), 4.32-4.36 (m, 2H, CH_2), 4.55-4.58 (m, 2H, CH_2), 4.70 (s, 2H, H-2), 7.63 (d, J= 8.1 Hz, 2H, H-aromatic), 7.69 (d, J= 8.1 Hz, 2H, H-aromatic).

^{13}C-NMR (DMSO-d_6), δ: 39.02, 43.03 CH_2), 45.54 (CH_2-H-2), 125.20, 125.23 (CH, C-aromatic), 125.30 (C, C-7), 127.44 (C, C-6), 127.63 (C, C-aromatic), 129.89 (CH, C-aromatic), 141.82 (C, C-aromatic), 194.5 (C, C-1).

4-(Trifluoromethyl)benzyl 4-benzylpiperazine-1-carbodithioate (210)
($C_{20}H_{21}F_3N_2S$; M.W.= 410.52)

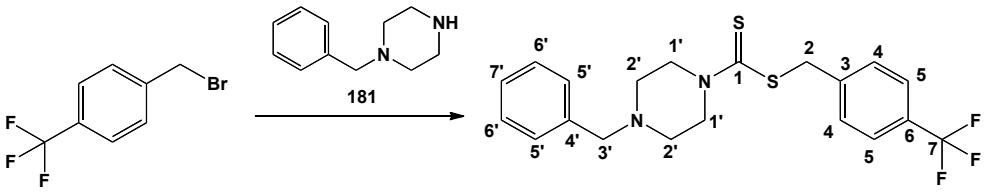

203 **210**

General procedure 24;
T.L.C. System: DCM-MeOH: 95:5 v/v, Rf: 0.82;
White solid;
Purification: recrystallization from EtOH/H_2O;
Yield: 0.2 g, 16.2 %;
Melting point: 65-68 ^oC;
MS $(ESI)^+$: 411.1 $[M+H]^+$
Microanalysis: Calculated for $C_{20}H_{21}F_3N_2S_2$ (410.52); Theoretical: %C = 58.51, %H = 5.16, %N = 6.82; Found: %C = 58.57, %H = 4.91, %N = 6.70.

^{1}H-NMR ($CDCl_3$), δ: 2.52-2.59 (m, 4H, CH_2), 3.57 (s, 2H, CH_2, H-2), 3.89-3.99 (m, 2H, CH_2), 4.33-4.42 (m, 2H, CH_2), 4.66 (s, 2H, CH_2, H-3'), 7.31-7.38 (m, 5H, H-aromatic), 7.52 (d, J= 8.0 Hz, 2H, H-aromatic), 7.58 (d, J= 8.0 Hz, 2H, H-aromatic).

^{13}C-NMR ($CDCl_3$), δ: 41.05 (CH_2), 52.37 (CH_2, C-2), 62.49 (CH_2, C-3'), 125.44, 125.47, 127.45, 128.42, 129.11, 129.62 (CH-aromatic), 140.75, 157.2, 168.5, 184.6 (C, C-aromatic), 195.54 (C, C-1).

3-Nitrobenzyl piperidine-1-carbodithioate (211)
($C_{13}H_{16}N_2O_2S_2$; M.W.= 296.41)

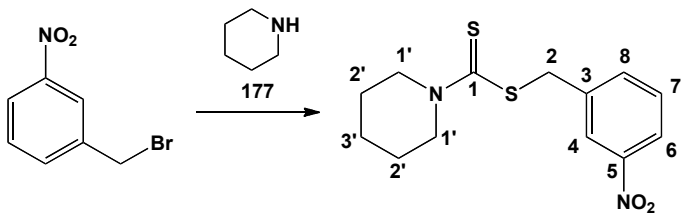

204 **211**

General procedure 23;
T.L.C. System: *n*-hexane -EtOAc-: 8:2 v/v, Rf: 0.5;
Fine, white powder;
Purification: recrystallization from EtOH;
Yield: 0.17 g, 20 %;
Melting point: 78-81 °C
MS (ESI)$^+$: 319.1 $[M+Na]^+$
Microanalysis: Calculated for $C_{13}H_{16}N_2O_2S_2$ (296.41); Theoretical: %C = 52.68, %H = 5.44, %N = 9.45; Found: %C = 52.78, %H = 5.36, %N = 9.26.

^{1}H-NMR ($CDCl_3$), δ: 1.70-1.75 (m, 6H, CH_2), 3.88-3.95 (m, 2H, CH_2), 4.27-4.35 (m, 2H, CH_2), 4.72 (s, 2H, H-2), 7.47-7.49 (m, 1H, H-aromatic), 7.78 (d, 1H, J= 8.3 Hz, H-aromatic), 8.12 (d, 1H, J= 8.3 Hz, H-aromatic), 8.27 (s, 1H, H-aromatic).

^{13}C-NMR ($CDCl_3$), δ: 24.23, 25.38, 26.07 (CH_2), 40.55 (CH_2, C-2), 51.49, 53.40 (CH_2), 122.32, 124.15, 129.29, 135.48 (CH, C-aromatic), 139.38 (C, C-3), 148.32 (C, C-5), 193.85 (C, C-1).

3-Nitrobenzyl morpholine-4-carbodithioate (212)[51]
($C_{12}H_{14}N_2O_3S_2$; M.W.= 298.38)

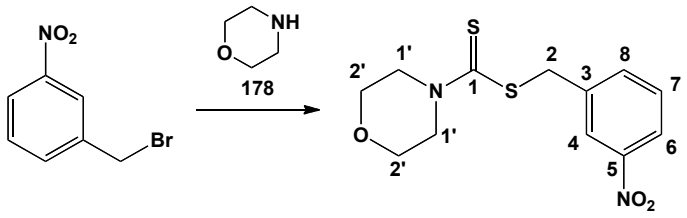

204 **212**

General procedure 23;
T.L.C. System: *n*-hexane -EtOAc-: 8:2 v/v, Rf: 0.26;
Fine, white powder;
Purification: recrystallization from EtOH;
Yield: 0.26 g, 29.2 %;
Melting point: 83-85 °C;
MS (ESI)$^+$: 321.1 $[M+Na]^+$
Microanalysis: Calculated for $C_{12}H_{14}N_2O_3S_2$ (298.38); Theoretical: %C = 48.30, %H = 4.73, %N = 9.38; Found: %C = 48.43, %H = 4.63, %N = 9.17.

^{1}H-NMR ($CDCl_3$), δ: 3.78-3.81 (m, 4H, CH_2), 3.93-4.06 (m, 2H, CH_2), 4.28-4.40 (m, 2H, CH_2), 4.73 (s, 2H, H-2), 7.48-7.50 (m, 1H, H-aromatic), 7.77 (d, 1H, J= 7.6 Hz, H-aromatic), 8.14 (d, 1H, J= 8.2 Hz, H-aromatic), 8.27 (s, 1H, H-aromatic).

^{13}C-NMR ($CDCl_3$), δ: 40.28 (CH_2), 66.23 (CH_2, C-2), 122.48, 124.17, 129.36, 135.46 (CH, C-aromatic), 138.96 (C, C-3), 148.34 (C, C-5), 195.76 (C, C-1).

3-Nitrobenzyl 4-methylpiperazine-1-carbodithioate (213)
($C_{13}H_{17}N_3O_2S_2$; M.W.= 311.42)

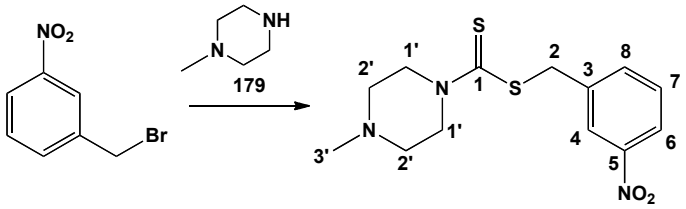

204 **213**

General procedure 23;
T.L.C. System: DCM-MeOH: 9:1 v/v, Rf: 0.2;
Fine, pale yellow powder;
Purification: recrystallization from EtOH;
Yield: 0.13 g, 14 %;
Melting point 78-81 ^oC;
MS $(ESI)^+$: 312.1 $[M+H]^+$
Microanalysis: Calculated for $C_{13}H_{17}N_3O_2S_2$ (311.42); Theoretical: %C = 50.14, %H = 5.50, %N = 13.49; Found: %C = 50.24, %H = 5.44, %N = 13.64.

^{1}H-NMR ($CDCl_3$), δ: 2.25 (s, 3H, H-3'), 2.41-2.44 (m, 4H, CH_2), 3.84-3.92 (m, 2H, CH_2), 4.24-4.33 (m, 2H, CH_2), 4.62 (s, 2H, H-2), 7.38-7.40 (m, 1H, H-aromatic), 7.67 (d, 1H, J= 7.8 Hz, H-aromatic), 8.02-8.04 (m, 1H, H-aromatic), 8.17 (s, 1H, H-aromatic).

^{13}C-NMR ($CDCl_3$), δ: 40.45, 45.65 (CH, C-3'), 49.90, 51.57 (CH_2), 54.38 (CH_2, C-2), 122.45, 124.18, 129.36, 135.54 (CH, C-aromatic), 139.09 (C, C-3), 148.27 (C, C-5), 195.11 (C, C-1).

3-Nitrobenzyl piperazine-1-carbodithioate (214)

($C_{12}H_{15}N_3O_2S_2$; M.W.= 297.40)

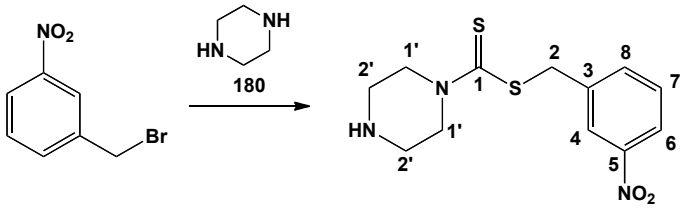

204 **215**

General procedure 23;

T.L.C. System: *n*-hexane -EtOAc: 7:3 v/v, Rf: 0.54;

Fine, grey yellow powder;

Purification: flash column chromatography (DCM-MeOH: 100:0 v/v, increasing to 90:10 v/v) and recrystallization from EtOAc/*n*-hexane;

Yield: 0.14 g, 15.7 %;

Melting point: 139-141 ^{o}C;

MS $(ESI)^+$: 298.1 $[M+H]^+$

Microanalysis: Calculated for $C_{12}H_{15}N_3O_2S_2$ (297.06); Theoretical: %C = 48.46, %H = 5.08, %N = 14.13; Found: %C = 48.24, %H = 5.22, %N = 14.02.

^{1}H-NMR (DMSO-d_6), δ: 2.54-2.58 (m, 4H, CH_2), 4.10-4.11 (m, 2H, CH_2), 4.33-4.37 (m, 2H, CH_2), 4.77 (s, 2H, H-2), 7.62-7.64 (m, 1H, H-aromatic), 7.88 (d, J= 7.5 Hz, 1H, H-aromatic), 8.11-8.14 (m, 1H, H-aromatic), 8.29-8.30 (m, 1H, H-4).

^{13}C-NMR (DMSO-d_6), δ: 38.98, 39.96, 40.03, 47.57 (CH_2), 47.89 (CH_2, C-2), 122.20, 123.66, 129.84, 135.89 (CH, C-aromatic), 139.56 (C, C-3), 147.64 (C, C-5), 194.35 (C, C-1).

3-Nitrobenzyl 4-benzylpiperazine-1-carbodithioate (215)

($C_{19}H_{21}N_3O_2S_2$; M.W.= 387.52)

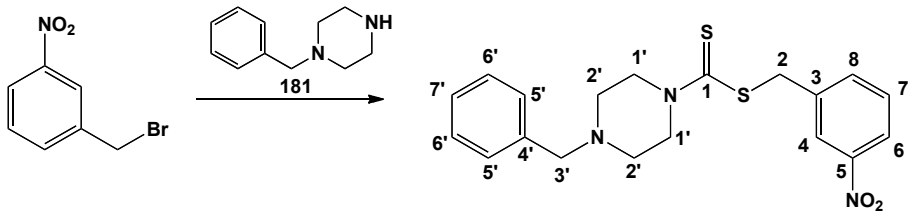

204 **214**

General procedure 23;

T.L.C. System: DCM-MeOH: 95:5 v/v, Rf: 0.62;

Whitish solid;Yield: 0.18 g, 16.2 %;

Purification: flash column chromatography (DCM-MeOH: 100:0 v/v, increasing to 99:1 v/v) and recrystallization from EtOH;

Melting point: 63-65°C;

MS $(ESI)^+$: 388.1 $[M+H]^+$

Microanalysis: Calculated for $C_{19}H_{21}N_3O_2S_2$ (387.52); Theoretical: %C = 58.89, %H = 5.46, %N = 10.84; Found: %C = 58.62, %H = 5.31, %N = 10.57.

^{1}H-NMR ($CDCl_3$), δ: 2.46-2.62 (m, 4H, CH_2), 3.54 (s, 2H, CH_2, H-3'), 3.83-4.02 (m, 2H, CH_2), 4.22-4.38 (m, 2H, CH_2), 4.61 (s, 2H, CH_2, H-2), 7.20-7.29 (m, 5H, H-aromatic), 7.38-7.40 (m, 1H, H-aromatic), 7.66 (d, J= 7.6 Hz, 1H, H-aromatic), 8.04 (d, J= 8.3 Hz, 1H, H-aromatic), 8.17 (s, 1H, H-4).

^{13}C-NMR ($CDCl_3$), δ: 40.50 (CH_2), 52.17 (CH_2, C-2), 62.32 (CH_2, C-3'), 122.14, 124.14, 128.58, 129.35, 135.47 (CH-aromatic), 139.03, 146.6 (C, C-aromatic), 148.33 (C, C-5), 195.3 (C, C-1).

Methyl 3-nitro-4-(((piperidine-1-carbonothioyl)thio)methyl)benzoate (216) ($C_{15}H_{18}N_2O_4S_2$; M.W.= 354.44)

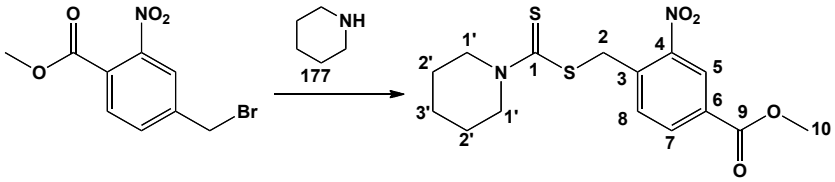

205 **216**

General procedure 23;
T.L.C. System: *n*-hexane -EtOAc: 8:2 v/v, Rf: 0.56;
Yellow wax;
Purification: flash column chromatography (*n*-hexane:EtOAc 100:0 v/v, increasing to 85:15 v/v)
Yield: 0.87 g, 83%;
Melting point: 50-52 °C;
MS $(ESI)^+$: 356.1 $[M+2H^+]$
Microanalysis: Calculated for $C_{15}H_{18}N_2O_4S_2$ (354.44); Theoretical: %C = 50.83, %H = 5.12, %N = 7.90; Found: %C = 50.70, %H = 4.88, %N = 7.77.

^{1}H-NMR ($CDCl_3$), δ: 1.66-1.72 (m, 6H, CH_2), 3.85-3.91 (m, 2H, CH_2), 3.98 (s, 3H, H-10), 4.23-4.31 (m, 2H, CH_2), 5.07 (s, 2H, H-2), 7.98 (d, J= 8.0 Hz, 2H, H-aromatic), 8.20 (dd, J_1= 8.0 Hz, J_2= 1.7 Hz, 1H, H-aromatic), 8.64 (d, J= 1.7 Hz, 1H, H-aromatic).

^{13}C-NMR ($CDCl_3$), δ: 24.19 (CH_2), 38.01 (CH_2, C-2), 52.69 (CH_3, C-10), 126.03 (CH-aromatic), 127.94, 130.58 (C, C-aromatic), 133.17, 133.64 (CH, C-aromatic), 138.23 (C, C-aromatic), 164.83 (C, C-9), 193.82 (C, C-1).

Methyl 4-(((morpholine-4-carbonothioyl)thio)methyl)-3-nitrobenzoate (217) ($C_{14}H_{16}N_2O_5S$; M.W.= 356.42)

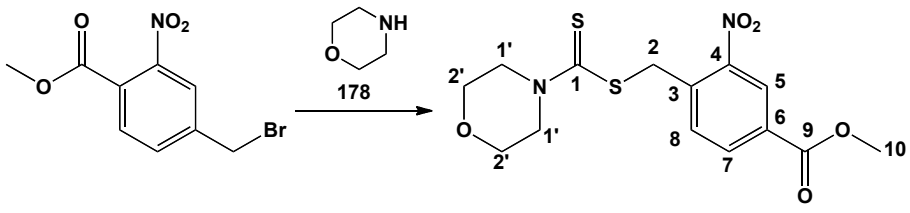

205 **217**

General procedure 23;
T.L.C. System: *n*-hexane -EtOAc: 8:2 v/v, Rf: 0.65;
Fine, off-white powder;
Purification: flash column chromatography (*n*-hexane:EtOAx: 100:0 v/v, increasing to 80:20 v/v) and recrystallization from EtOH;
Yield: 0.27 g, 26 %;
Melting point: 67-70 ^{o}C;
MS (ESI)$^{+}$: 379.1 $[M+Na]^{+}$
Microanalysis: Calculated for $C_{14}H_{16}N_2O_5S_2$ (356.42); Theoretical: %C = 47.18, %H = 4.52, %N = 7.86; Found: %C = 47.32, %H = 4.55, %N = 7.55.

^{1}H-NMR ($CDCl_3$), δ: 3.74-3.79 (m, 6H, CH_2), 3.98 (s, 3H, H-10), 4.21-4.38 (m, 2H, CH_2), 5.08 (s, 2H, H-2), 7.96 (d, J= 8.0 Hz, 1H, H-aromatic), 8.21 (dd, J_1= 8.0 Hz, J_2= 1.9 Hz, 1H, H-aromatic), 8.66 (d, J= 1.9 Hz, 1H, H-aromatic).

^{13}C-NMR ($CDCl_3$), δ: 37.86 (CH_2), 52.73 (CH_3, C-10), 59.35 (CH_2, C-2), 126.13 (CH-aromatic), 130.81 (C, C-aromatic), 133.20, 133.71 (CH, C-aromatic), 137.73, 148.7 (C, C-aromatic), 164.75 (C, C-9), 195.79 (C, C-1).

Methyl 4-(((4-methylpiperazine-1-carbonothioyl)thio)methyl)-3-nitrobenzoate (218) ($C_{15}H_{19}N_3O_4S_2$; M.W.= 369.46)

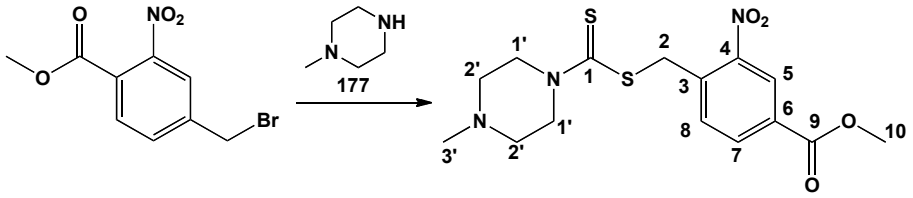

205 **218**

General procedure 23;
T.L.C. System: DCM-MeOH: 9:1 v/v, Rf: 0.32;
White solid;
Yield: 0.36 g, 32.7 %;
Purification: recrystallization from EtOH;
Melting point: 70-72 ^{o}C;
MS (ESI)$^{+}$: 370.1 $[M+H]^{+}$
Microanalysis: Calculated for $C_{15}H_{19}N_3O_4S_2$ (369.08); Theoretical: %C = 48.76, %H = 5.18, %N = 11.37; Found: %C = 48.65, %H = 4.87, %N = 11.31.

^{1}H-NMR ($CDCl_3$), δ: 2.33 (s, 3H, H-3), 2.48-2.51 (m, 4H, CH_2), 3.88-3.95 (m, 1H, CH_2), 3.96-4.00 (m, 4H, H-10, $C\underline{H}_2$), 4.28-4.48 (m, 2H, CH_2), 5.07 (s, 2H, H-2), 7.97 (d, J= 8.0 Hz, 1H, H-aromatic), 8.20 (d, J= 8.0 Hz, 1H, H-aromatic), 8.65 (s, 1H, H-aromatic).

^{13}C-NMR ($CDCl_3$), δ: 37.99 (CH_2), 45.57 (CH_3, C-3'), 52.71 (CH_3, C-10), 54.35 (CH_2, C-2), 126.08 (CH-aromatic), 130.70 (C, C-aromatic), 133.18, 133.68 (CH, C-aromatic), 137.94, 148.7 (C, C-aromatic), 164.78 (C, C-9), 195.15 (C, C-1).

Methyl 3-nitro-4-(((piperazine-1-carbonothioyl)thio)methyl)benzoate (219) ($C_{14}H_{17}N_3O_4S_2$; M.W.= 355.43)

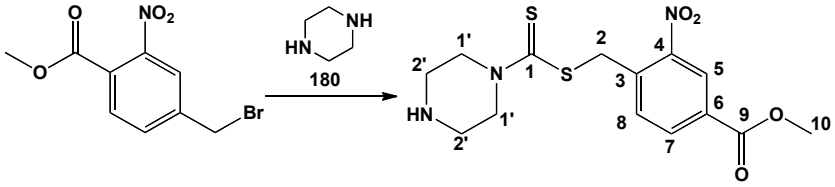

205 **219**

General procedure 23;
T.L.C. System: *n*-hexane -EtOAc: 7:3 v/v, Rf: 0.45;
White solid;
Yield: 0.83 g, 75.4 %;
Purification: recrystallization from MeOH;
Melting point: 145-148 ^oC;
MS $(ESI)^+$: 357.1 $[M+2H]^+$
Microanalysis: Calculated for $C_{14}H_{17}N_3O_4S_2$ (355.07); Theoretical: %C = 47.31, %H = 4.82, %N = 11.82; Found: %C = 47.15, %H = 4.58, %N = 11.79.

^{1}H-NMR (DMSO-d_6), δ: 3.30-3.31 (m, 4H, CH_2), 3.91 (s, 3H, H-10), 4.07-4.11 (m, 2H, CH_2), 4.28-4.32 (m, 2H, CH_2), 4.97 (s, 2H, H-2), 7.93 (d, J= 8.2 Hz, 1H, H-8), 8.22 (dd, J_1= 8.2 Hz, J_2= 1.7 Hz, 1H, H-7), 8.45 (d, J= 1.7 Hz, 1H, H-5).

^{13}C-NMR (DMSO-d_6), δ: 36.87 (CH_2), 47.98, 49.74 (CH_2, C-2), 52.77 (CH_3, C-10), 125.16 (CH-aromatic), 129.96 (C, C-aromatic), 133.04, 133.48 (CH, C-aromatic), 137.22, 148.63 (C, C-4), 164.25 (C, C-9), 193.82 (C, C-1).

Methyl 4-(((4-benzylpiperazine-1-carbonothioyl)thio)methyl)-3-nitrobenzoate (220) ($C_{21}H_{23}N_3O_4S_2$; M.W.= 445.56)

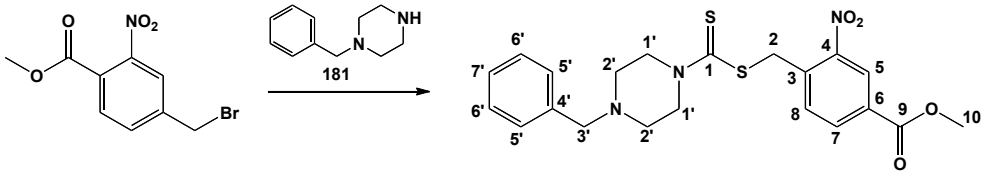

205 **220**

General procedure 23;
T.L.C. System: *n*-hexane-EtOAc: 8:2 v/v, Rf: 0.26;
Yellow oil;
Yield: 1.1 g, 82.7 %;
Purification: flash column chromatography (*n*-hexane:EtOAx: 100:0 v/v, increasing to 60:40 v/v);
MS-$(ESI)^+$: 446.1 (M+H);

^{1}H-NMR ($CDCl_3$), δ: 2.51-2.57 (m, 4H, CH_2), 3.55 (s, CH_2, C-3'), 3.86-3.95 (m, 1H, CH_2), 3.98 (s, 3H, H-10), 4.01-4.16 (m, 1H, CH_2), 5.07 (s, 2H, H-2), 7.30-7.37 (m, 5H, H-aromatic), 7.96 (d, J= 8.0 Hz, 1H, H-aromatic), 8.20 (d, J= 8.0 Hz, 1H, H-aromatic), 8.65 (s, 1H, H-aromatic).

^{13}C-NMR ($CDCl_3$), δ: 37.97 (CH_2, C-3'), 51.96, 52.33, 52.71 (CH_2), 53.42 (CH_3, C-10), 62.44 (CH_2, C-2), 126.07, 127.44, 128.41, 129.10 (CH-aromatic), 130.68 (C, C-aromatic), 133.18, 133.68 (CH, C-aromatic), 137.25, 137.97 (C, C-aromatic), 148.57 (C, C-4), 164.79 (C, C-9), 194.95 (C, C-1).

6.16.10 Dithiocarbamate methyl aryl acids (221-224)

3-Nitro-4-(((piperidine-1-carbonothio*yl*)thio)methyl)benzoic acid (221)
($C_{14}H_{16}N_2O_4S_2$; M.W.= 340.42)

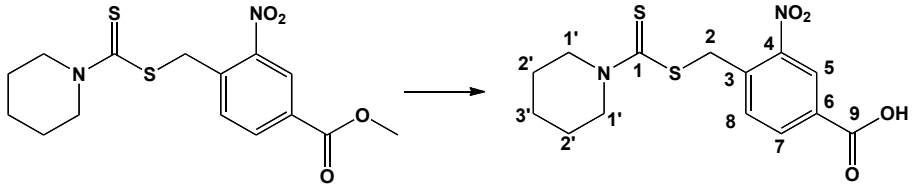

216 **221**

General procedure 24;
Reagent: Methyl 3-nitro-4-(((piperidine-1-carbonothioyl)thio)methyl)benzoate **216** (0.28 g, 0.79 mmol);
Pale, yellow powder;
Purification: recrystallization from EtOH/H_2O;
Yield: 0.135 g, 50.3 %;
Melting point: 162-164 ºC;
MS $(ESI)^+$: 341.1 $[M+H]^+$
Microanalysis: Calculated for $C_{14}H_{16}N_2O_4S_2$ (340.42); Theoretical: %C = 49.40, %H = 4.74, %N = 8.23; Found: %C = 49.01, %H = 4.66, %N = 8.37.

^{1}H-NMR ($CDCl_3$), δ: 1.67-1.76 (m, 6H, CH_2), 3.85-3.94 (m, 2H, CH_2), 4.25-4.33 (m, 2H, CH_2), 5.10 (s, 2H, H-2), 8.04 (d, J= 7.1 Hz 1H, H-aromatic), 8.26 (d, J= 7.1 Hz, 1H, H-aromatic), 8.71 (s, 1H, H-5), 10.84 (bs, 1H, -COO<u>H</u>).

^{13}C-NMR ($CDCl_3$), δ: 24.18 (CH_2), 37.18 (CH_2, C-2), 126.63 (CH-aromatic), 129.54 (C, C-aromatic) 133.37, 134.10 (CH-aromatic), 139.29, 148.7 (C, C-aromatic), 168.91 (C, C-9), 193.70 (C, C-1').

4-(((Morpholine-4-carbonothio*yl*)thio)methyl)-3-nitrobenzoic acid (222)
($C_{13}H_{14}N_2O_5S_2$; M.W.= 342.39)

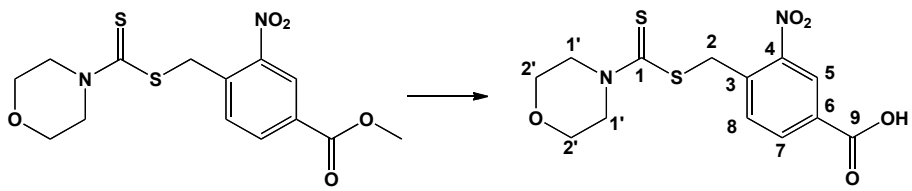

217 **222**

General procedure 24;

Reagent: Methyl 4-(((morpholine-4-carbonothioyl)thio)methyl)-3-nitrobenzoate **217** (0.18 g, 0.5 mmol);

Off-White solid;

Purification: recrystallization from EtOH/H_2O;

Yield: 0.05 g, 29.4 %;

Melting point: 166-168 ºC;

MS $(ESI)_+$: 365.1 $[M+Na]^+$

Microanalysis: Calculated for $C_{13}H_{14}N_2O_5S_2$ (342.39); Theoretical: %C = 45.60, %H = 4.12, %N = 8.18; Found: %C = 45.65, %H = 4.22, %N = 7.90.

^{1}H-NMR (DMSO-d_6), δ: 3.64-3.68 (m, 4H, CH_2), 3.88-3.97 (m, 2H, CH_2), 4.15-4.24 (m, 2H, CH_2), 4.97 (s, 2H, H-2), 7.90 (d, J= 7.9 Hz, 1H, H-aromatic), 8.20 (dd, J_1= 7.9 Hz, J_2= 1.5 Hz, 1H, H-aromatic), 8.43 (d, J= 1.5 Hz, 1H, H-aromatic), 13.61 (bs, 1H, -COO<u>H</u>).

^{13}C-NMR (DMSO-d_6), δ: 36.86 (CH_2), 65.48 (CH_2, C-2), 125.21 (CH-aromatic), 131.33 (C, C-aromatic) 132.87, 133.62 (CH-aromatic), 136.73, 148.7 (C, C-aromatic), 165.23 (C, C-9), 194.05 (C, C-1).

4-(((4-Methylpiperazine-1-carbonothio*yl*)thio)methyl)-3-nitrobenzoic acid (223) ($C_{14}H_{17}N_3O_4S_2$; M.W.= 355.43)

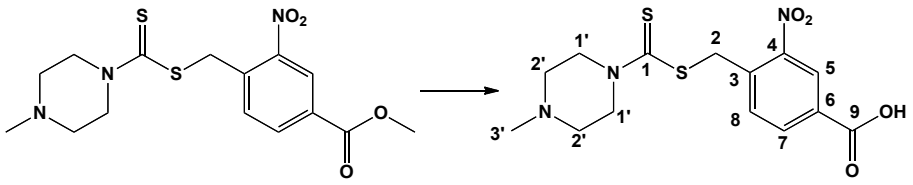

218 **223**

General procedure 24;

Reagent: methyl 4-(((4-methylpiperazine-1-carbonothioyl)thio)methyl)-3-nitrobenzoate **218** (0.12 g, 0.32 mmol);

White solid;

Purification: recrystallization from DCM;

Yield: 0.035 g, 30.9 %;

Melting point: 206-209 ºC;

MS $(ESI)^+$: 356.1 $[M+H]^+$

Microanalysis: Calculated for $C_{14}H_{17}N_3O_4S_2$ (355.43); Theoretical: %C = 47.31, %H = 4.82, %N = 11.82; Found: %C = 46.93, %H = 5.20, %N = 11.57.

^{1}H-NMR (DMSO-d_6), δ: 2.22 (s, 3H, H-3'), 2.40-2.43 (m, 4H, CH_2), 3.86-3.93 (m, 2H, CH_2), 4.17-4.23 (m, 2H, CH_2), 4.94 (s, 2H, H-2), 7.88 (d, J= 8.0 Hz, 1H, H-aromatic), 8.19 (dd, J_1= 8.0 Hz, J_2= 1.7 Hz,1H, H-aromatic), 8.42 (d, J= 1.7 Hz, 1H, H-aromatic).

^{13}C-NMR (DMSO-d_6), δ: 37.02 (CH_2), 44.86 (CH_3, H-3'), 49.51, 51.16 (CH_2), 53.81 (CH_2, C-2), 125.20 (CH-aromatic), 131.76 (C, C-aromatic) 132.79, 133.63 (CH-aromatic), 136.58, 148.59 (C, C-aromatic), 165.33 (C, C-9), 194.57 (C, C-1).

4-(((4-Benzylpiperazine-1-carbonothioyl)thio)methyl)-3-nitrobenzoic acid (224) ($C_{20}H_{21}N_3O_4S_2$; M.W. = 431.53)

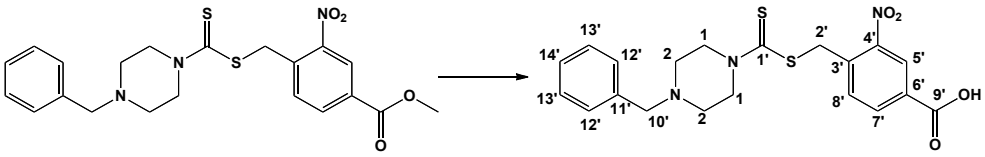

220 **224**

General procedure 24;
Reagent: methyl 4-(((4-benzylpiperazine-1-carbonothioyl)thio)methyl)-3-nitrobenzoate **220** (0.3 g, 0.67 mmol);
Yellow, fine powder;
Yield: 29.5 g, 10.4 %;
Purification: recrystallization from EtOH/H_2O;
MS (ESI)$^+$: 432.1 $[M+H]^+$
Microanalysis: Calculated for $C_{20}H_{21}N_3O_4S_2$ (431.10); Theoretical: %C = 55.67, %H = 4.91, %N = 9.74; Found: %C = 55.70, %H = 4.73, %N = 9.41.

^{1}H-NMR ($CDCl_3$), δ: 3.38-3.44 (m, 4H, CH_2), 3.58 (s, CH_2, C-10'), 3.89-3.96 (m, 2H, CH_2), 4.18-4.29 (m, 2H, CH_2), 4.94 (s, 2H, H-2), 7.32-7.36 (m, 5H, H-aromatic), 7.87-7.91 (m, 1H, H-aromatic), 8.18-8.21 (m, 1H, H-aromatic), 8.42-8.43 (s, 1H, H-aromatic).

^{13}C-NMR ($CDCl_3$), δ: 37.09 (CH_2, C-10'), 40.03 (CH_2), 49.51, 51.16 (CH_2), 61.02 (CH_2, C-2), 125.20, 127.28, 128.26, 129.07 (CH-aromatic), 131.30 (C, C-aromatic) 132.85, 133.61 (CH-aromatic), 136.75 (C, C-aromatic), 148.64 (C, C-4'), 165.24 (C, C-9'), 193.51 (C, C-1).

References

1 Carpenter, R.D.; Andrei, M.; Aina, O.H.; Lau, E.Y.; Lightstone, F.C.; Liu, R.; Lam, K.S.; Kurth, M.J. Selectively Targeting T- and B-Cell Lymphomas: A Benzothiazole Antagonist of α4β1 Integrin. *J. Med. Chem.* **2009**, 52(1), 14-19.

2 Li, Z.; Ma, H.; Han, C.; Xi, Hai-T.; Meng, Q.; Chen, X.; Sun, X. Synthesis of isothiocyanates by reaction of amines with phenyl chlorothionoformate via one-pot or two-step process. *Synthesis* **2013**, 12, 1667-1674.

3 Khatik, G.L.; Pal, A.; Mobin, S.M.; Nair, V. A.Stereochemical studies of 5-methyl-3-(substituted phenyl)-5-[(substituted phenyl) hydroxy methyl]-2-thiooxazolidin-4-ones. *Tetrahedron Lett.* **2010**, 51(28), 3654-3657.

4 Munch, H.; Hansen, J.S.; Pittelkow, M.; Christensen, J.B.; Boas, U. A new efficient synthesis of isothiocyanates from amines using di-*tert*-butyl dicarbonate. *Tetrahedron Lett.* **2008**, 49(19), 3117-3119.

5 Liu, P.; Li, C.; Zhang, J.; Xu, X. Facile and versatile synthesis of alkyl and aryl isothiocyanates by using triphosgene and cosolvent. *Synthetic Communications* **2013**, 43(24), 3342-3351.

6 Sakai, Y.; Ikeuchi, K.; Yamada, Y.; Wakimoto, T.; Kan, T. Modified Julia-Kocienski reaction promoted by means of m-NPT (nitrophenyltetrazole) sulfone. *Synlett* **2010**, 5, 827-829.

7 Han, S.Y.; Lee, J.W.; Kim, H.; Kim, Y.; Lee, S.; Gyoung, Y.S. A facile one-pot synthesis of 1-substituted tetrazole-5-thiones and 1-substituted 5-alkyl(aryl)sulfanyltetrazoles from organic isothiocyanates. *Bull. of the Korean Chem. Soc.* **2012**, 33(1), 55-59.

8 Hrabalek, A.; Kunes, J.; Pour, M.; Waisser, K. [1-Alkyl(aryl)tetrazol-5-ylthio]acetic acids. Russian *J. Org. Chem.* **2000**, 36(5), 761-762.

9 Wang, X-D.; Wei, W.; Wang, P-F.; Tang, Y-T.; Deng, R-C.; Li, B.; Zhou, S-S.; Zhang, J-W.; Zhang, L.; Xiao, Z-P.; Ouyang, H.; Zhu, H-L. Novel 3-arylfuran-2(5H)-one-fluoroquinolone hybrid: design, synthesis and evaluation as antibacterial agent. *Bioorg. & Med. Chem.* **2014**, 22(14), 3620-3628.

10 Andrews, M.D.; Bagal, S.K.; Gibson, K.R.; Omoto, K.i; Ryckmans, T.; Skerratt, S.E.; Stupple, P.A. Pyrrolo[2,3-d]pyrimidine derivatives as inhibitors of tropomyosin-related kinases and their preparation and use in the treatment of pain. Patent WO 2012137089, 11 Oct, 2012.

11 Elsinghorst, P.; Haertig, W.; Goldhammer, S.; Grosche, J.; Guetschow, M. A gorge-spanning, high-affinity cholinesterase inhibitor to explore β0amyloid plaques. *Org. & Biomol. Chem.* **2009**, 7(19), 3940-3946.

12 Murty, M.S.R.; Ram, K.R.; Rao, B.R.; Rao, R.V.; Katiki, M.R.; Rao, J.V.; Pamanji, V.:.R. Synthesis, characterization, and anticancer studies of S and N alkyl piperazine-substituted positional isomers of 1,2,4-triazole. *Med. Chem. Res.* **2014**, 23(4), 1661-1671.

13 Chiriac, C.I. Phosphorous acid-iodine as reagent for the synthesis of 1,3,4-oxadiazoles from diacylhydrazines. *Revue Roumaine de Chimie* **1986**, 31(2), 159-162.

14 Kim, Y.J.; Varma, R.S. Microwave-assisted preparation of cyclic ureas from diamines in the presence of ZnO. *Tetrahedron Lett.* **2004**, 45(39), 7205-7208.

15 Frank, R.; Sundermann, B.; Schick, H.; Sonnenschein, H. Preparation of substituted cyclic urea derivatives and the use thereof as vanilloid receptor 1 modulators. Patent WO 2006111346, 26 Oct, 2006.

16 Li, J.; Huang, Y. Xie, M. Qu, G.; Niu, H.; Wang, H.; Qin, B.; Guo, H. One-Pot Synthesis of 7,9-Dialkylpurin-8-one Analogues: Broad Substrate Scope. *J. Org. Chem.* **2013**, 78(24), 12629-12636

17 Zhang, H.; Jia, H.; Zhao, S. Synthesis of 2-bromo-3-(1H-indol-3-yl)-N-methylmaleimide. *Hecheng Huaxue*, **2008**, 16(1), 105-106, 109.

18 Sun, Q.; Wu, R.; Cai, S.; Lin, Y.; Sellers, L.; Sakamoto, K.; He, B.; Peterson, B.R. Synthesis and biological evaluation of analogues of AKT (protein kinase B) inhibitor-IV. *J. Med. Chem.* **2011**, 54(5), 1126-1139.

19 Proust, N.; Gallucci, J.C.; Paquette, L.A. Effect of Sulfonyl Protecting Groups on the Neighboring Group Participation Ability of Sulfonamido Nitrogen. *J.Org. Chem.* **2009**, 74(7), 2897-2900.

20 Todd, A.; Anderson, R.J.; Small, D.A.P.; Groundwater, P.W.; Benton, M.R. Preparation of bis sulfonamides as thioredoxin reductase inhibitors. Patent WO 2014096864, 26 June, 2014.

21 Amendola, V.; Fabbrizzi, L.; Mosca, L.; Schmidtchen, F-P. Urea- , Squaramide- , and Sulfonamide- Based Anion Receptors: A Thermodynamic Study. *Chemistry -A European Journal* **2011**, 17(21), 5972-5981.

22 Madge, D.; Wishart, G.; Dolman, M.; Maunder, P. Preparation of bissulfonamide derivatives as inhibitors of dehydroquinate synthetase and type II dehydroquinase enzymes. Patent WO 2001028537 26 Apr, 2001.

23 Laknhan, R.; Bimal, P. a-Oxonitrile as potential acylating agent. *Indian J. Chem.* **1999**, 38B (8), 979-981.

24 Keurulainen, L.; Salin, O.; Siiskonen, A.; Kern, J.M.; Alvesalo, J.; Kiuru, P.; Maass, M.; Yli-Kauhaluoma, J.; Vuorela, P. Design and synthesis od 2-arylbenzimidazoles and evaluation of their inhibitory effect against Chlamydia pneumoniae. *J. Med. Chem.* **2010**, 53 (21), 7664-7674.

25 Koshio, H.; Hirayama, F.; Ishihara, T.; Shiraki, R.; Shigenaga, T.; Taniuchi, Y.; Sato, K.; Moritani, Y.; Iwatsuki, Y.; Yoshiyuki, K.; Seiji, K.N.; Kawasaki, T.; Matsumoto, Y.; Sakamoto, S.; Tsukamoto, S-I. Synthesis and biological activity of novel 1,2-disubstituted benzene derivatives as factor Xa inhibitors. *Bioorg. & Med. Chem.* **2005**, 13(4), 1305-1323.

26 Yajnanarayana, J.H.R.; Harry, G.W. Synthesis of 2- cyano- 1, 3-dibenzoyl- 2, 3- dihydrobenzimidazole: a novel Reissert compound from benzimidazole. *J. Org. Chem.* **1991**, 56(2), 865-7.

27 Leonetti, F.; Favia, A.; Rao, A.; Aliano, R.; Paluszcak, A.; Hartmann, R.W.; Carotti, A. Design, Synthesis, and 3D QSAR of Novel Potent and Selective Aromatase Inhibitors. *J. Med. Chem.* **2004**, 47(27), 6792-6803

28 Datta, P.; Mukhopadhyay, A.P.; Manna, P.; Tiekink, E.R.T.; Parames, C.; Sinha, C. Structure, photophysics, eectrochemistry, DFT calculation, and in-vitro antioxidant activity od coumarin Schiff base complexes of group 6 metal carbonyls. *J. Inorg. Biochem.* **2011**, 105(4), 577-588.

29 Germain, A.R.; Carmody, L.C.; Nag, P.P.; Morgan, B.; VerPlank, L.; Fernandez, C.; Donckele, E.; Feng, Y.; Perez, J.R.; Dandapani, S.; Palmer, M.; Lander, E.S.; Gupta, P.B.; Shreiber, S.L.; Munoz, B. Cinnamides as selective small- molecule inhibitors of a cellular model of breast cancer stem cells. *Bioorg. & Med. Chem. Lett.* **2013**, 23(6), 1834-1838.

30 Parmenopoulou, V.; Kantsadi, A.L.; Tsirkone, V.G.; Chatzileontiadou, D.S.M.; Manta, S.; Zographos, S.E.; Molfeta, C.; Archontis, G.; Agius, L.; Hayes, J.M.; Leonidas, D.D.; Komiotis, D. Structure-based inhibitor design targeting glycogen phosphorylase b. Vritual screening, synthesis, biochemical and biological assessment of novel N-acyl-β-D-glucopyranosylamines. *Bioorg. & Med. Chem.* **2014**, 22(17), 4810-4825.

31 Kamal, A.; Reddy, C.R.; Vishnuvardhan, M.V.P.S.; Mahesh, R.; Lakshma, N.V.; Prabhakar, S.; Reddy, C.S. Synthesis and biological evaluation of cinnamido linked benzophenone hybrids as tubulina polymerization inhibitors and apoptosis inducine agents. *Bioorg. & Med. Chem. Lett.* **2014**, 24(10), 2309-2314.

32 Varadi, A.; Hosztafi, S.; Le Rouzic, V.; Toth, G.; Urai, A.; Noszal, B.; Pasternak, G.W.; Grinnell, S.G.; Majumdar, S. Novel 6-acylaminomorphinans with analgesic activity. *Europ. J. Med. Chem.* **2013**, 69, 786-789.

33 Hoveyda, H.; Zoute, L.; Lenoir, F. Azepanes, azocanes and related compounds as GPR43 modulators and their preparation and used for the treatment of inflammatory, gastrointestinal and metabolic disorders. Patent WO 2011151436, 8 Dec 2011.

34 Das, V.K.; Das, S.; Thakur, A.J. Protection and deprotection chemistry catalyzed by zirconium oxychloride octahydrate (ZrOCl2 ·8H2O). *Green Chem. Lett. and Rev.* **2012**, 5(4), 577-586.

35 Chatrabhuji, P.M.; Vyas, K.B.; Nimavat, K.S.; Undavia, N.K. Synthesis and antibacterial activity of some new thiazolidines. *Elixir Org. Chem.* **2013**, 54A, 12778-12780.

36 Zhang, P.; Hu, H-R; Bian, S-H.; Huang, Z-H.;Chu, Y.; Ye, D-Y. Design, synthesis and biological evaluation of benzothiazepinones (BTZs) as novel non-ATP competitive inhibitors of glycogen synthase kinase-3β (GSK-3β). *Europ. J. Med. Chem.* **2013**, 61, 95-103.

37 Garg, K.; Bansal, Y.; Bansal, G.; Goel, R. K. Design, synthesis, and PASS- assisted evaluation of novel 2- substituted benzimidazole derivatives as potent anthelmintics. *Med. Chem. Res.* **2014**, 23 (5), 2690-2697.

38 Adam, W.; Zhao, C-G.; Jakka, K. Dioxirane oxidations of compounds other that alkenes. In: *Organic Reactions*; 2008, 69 (1), 1-346; DOI: 10.1002/0471264180.or069.01

39 Yang, G.; Lindovska, P.; Zhu, D.; Kim, J.; Wang, P.; Tang, R-Y.; Movassaghi, M.; Yu, J-Q.; Pd(II)- catalyzed meta-C-H olefination, arylation, and acetoxylation of indolines using a U- shaped template. *J. Am. Chem. Soc.* **2014**, 136, 10807-10813.

40 Codd, E.; Dax, S.; Flores, C.; Jetter, M.; Youngman, M. Biaryl derived amides as modulators of vanilloid VR1 receptor and their preparation, pharmaceutical compositions and use in treatment and prevention of diseases. Patent WO 2006102645 28 Sept, 2006.

41 Hattori, T.; Tsubone, A.; Sawama, Y.; Monguchi, Y.; Sajiki, H. Systematic evaluation of the palladium-catalyzed hydrogenation under flow conditions. *Tetrahedron* **2014**, 70(32), 4790-4798.

42 Yamada, Y.M.A.; Sarkar, S.M.; Uozumi, Y. Amphiphilic self-assembled polymeric copper catalyst to parts per million levels: click chemistry. J. Am. Chem. Soc. 2012, 134(22), 9285-9290.

43 Clark, R.D.; Caroon, J.M.; Harrison, I.T.; Kluge, A.F.; Unger, S.H.; Spires, H.R.; Mathews, R. Synthesis and evaluation of ureido and vinylureidopenicillins as inhibitors of intraruminal lactic acid production. *J. Med. Chem.* **1981**, 24 (10), 1250-1253.

44 Patel, S.R.; Rahul, G.; Abhay, T.S.; Rahul, J. Synthesis, biological evaluation and 3D-QSAR study of hydrazie, semicarbazide and thiosemicarbazide derivatives of 4-(adamantan-1-yl)quinoline as anti-tubercolosis agents. *Europ. J. Med. Chem.* **2014**, 85, 255-267.

45 Berenger, B.; Bozell, J.J. Efficient cobalt-catalyzed oxidative conversion of lignin models to benzoquinones. *Org. Lett.* **2013**, 15(11), 2730-2733.

46 Soares, A.M.S.; Costa, S.P.G.; Goncalves, M.S.T. Oxazole light triggered protecting groups: synthesis and photolysis of fused heteroaromatic conjugates. *Tetrahedron* **2010**, 6 (41), 8189-8195.

47 Vlahakis, J.Z.; Vukomanovic, D.; Nakatsu, K.; Szarek, W.A. Selective inhibition of heme oxygenase-2 activity by analogs of 1-(4-chlorobenzyl)2-(pyrrolidin-1-ylmethyl)-1H-benzimidazole (clemizole): exploration of the effects of substituents at the N-1 position. *Bioorg. & Med. Chem.* **2013**, 21(21), 6788-6795.

48 Lopes, M.S.; Pietra, R.C.C. de Souza; Borgati, T.F.; Romeiro, C.F.D.; Junior, P.A.S.; Romanha, A.J.; Alves, R.J.; Souza-Fagundes, E.M.; Fernandes, AnP.S.M.; de Oliveira, R.B. Synthesis and evaluation of the anti parasitic activity of aromatic nitro compounds. *Europ. J. Med. Chem. 2011*, 46(11), 5443-5447.

49 Madalageri, P.M.; Oblennavar, K. Synthesis, DNA protection, and antimicrobial activity of some novel chloromethylbenzimidazole derivatives bearing dithiocarbamates. *J. Chem. and Pharma. Res.* **2012**, 4(5), 2697-2703.

50 Altintop, M.D.; Gurkan-Alp, A.S.; Oezkay, Y.; Kaplancikli, Z.A. Synthesis and biological evaluation of a series of dithiocarbamates as new cholinesterase inhibitors. *Archiv. der Pharmazie* (Weinheim, Germany), **2013**, 346(8), 571-576.

51 Li, R-T.; Ge, Z-M.; Cheng, T-M.; Cai, M-S. New synthetic method for dithiocarbamates. *Gaodeng Xuexiao Huaxue Xuebao* **1999**, 20(12), 1897-1902.

Appendix

Structure and biological evaluation for purchased compounds

The tables below contain all the compounds selected by virtual screening studies from Specs database that were tested for their antiviral activity in cytostatic assays at Rega Institute in Leuven, Belgium.

Virtual screening on 3A protein

Compound number	Chemical structure	EC_{50} (µM)	EC_{90} (µM)	CC_{50} (µM)
228	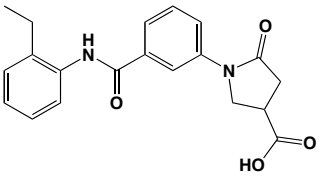	>200	>200	-
229	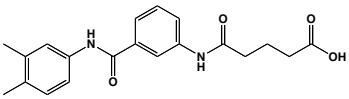	>100	>100	-
230	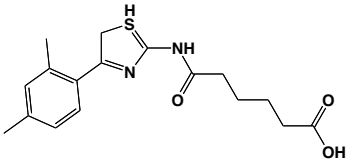	>100	>100	-
231	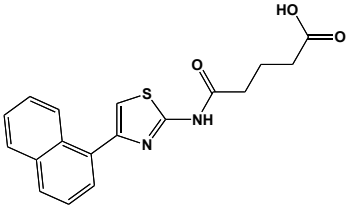	>100	>100	-
232	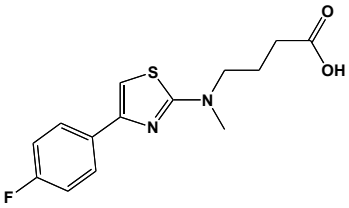	>100	>100	-
233	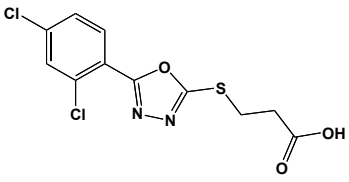	>100	>100	-
234	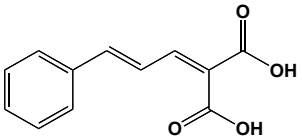	>100	>100	-

Compound number	Chemical structure	EC_{50} (µM)	EC_{90} (µM)	CC_{50} (µM)
235	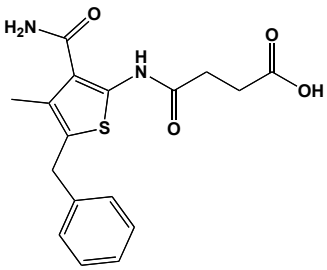	>100	>100	-
236	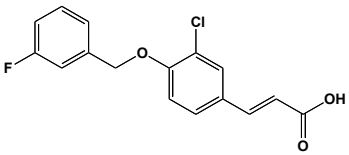	>100	>100	-
237	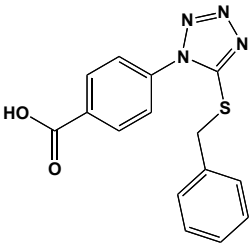	130	216	-
238	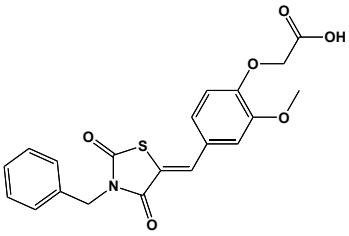	>100	>100	-
239	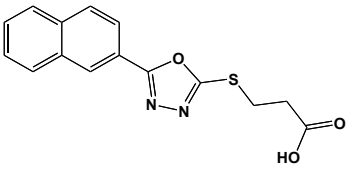	>100	>100	-
240	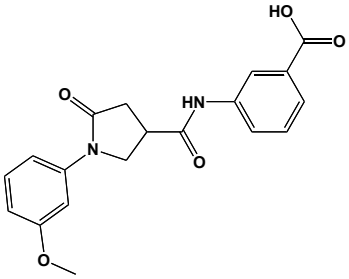	>100	>100	-
241	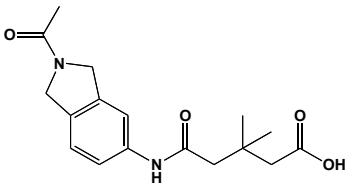	>100	>100	-

Compound number	Chemical structure	EC_{50} (µM)	EC_{90} (µM)	CC_{50} (µM)
242	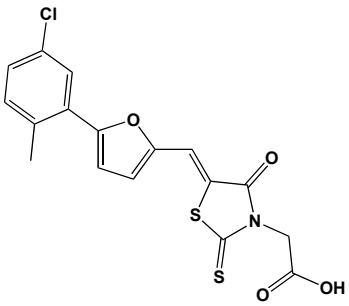	>25	>25	-
243	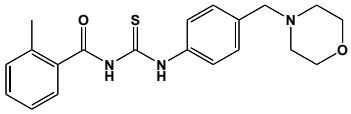	>100	>100	-
244	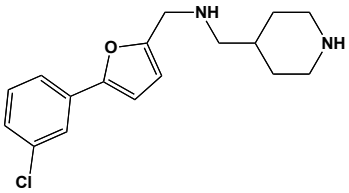	>100	>100	-
245	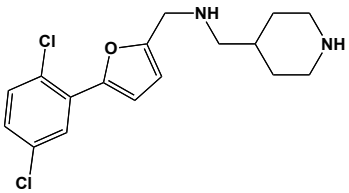	>100	>100	-
246	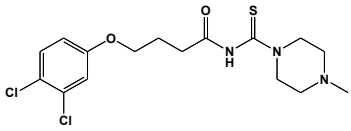	>100	>100	-
247	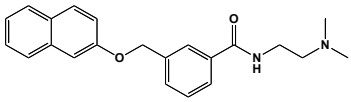	>100	>100	-

Purchased analogues of hit compound 1

Compound number	Chemical structure	EC_{50} (µM)	EC_{90} (µM)	CC_{50} (µM)
248	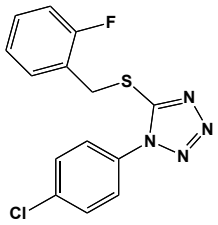	>200	>200	-
249	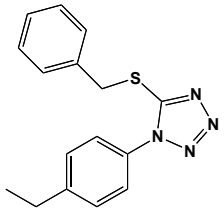	>200	>200	-
250	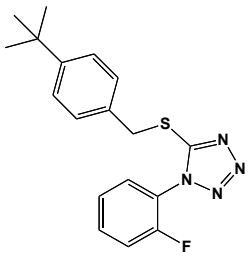	>200	>200	-
251	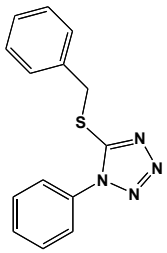	>200	>200	-
252	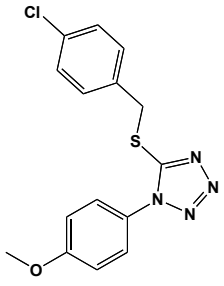	>200	>200	-
253	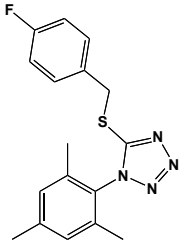	>200	>200	-

Compound number	Chemical structure	EC_{50} (µM)	EC_{90} (µM)	CC_{50} (µM)
254	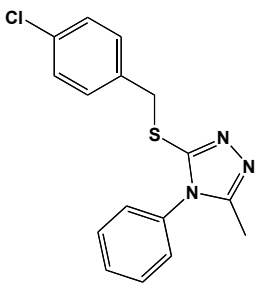	>200	>200	-
255	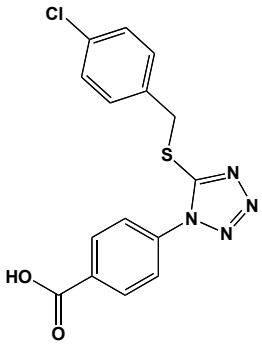	>200	>200	-
256	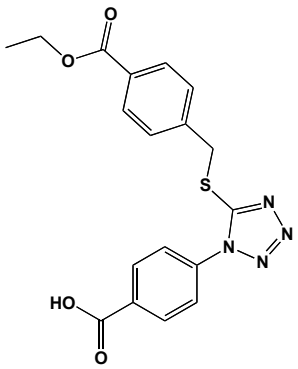	>200	>200	-
257	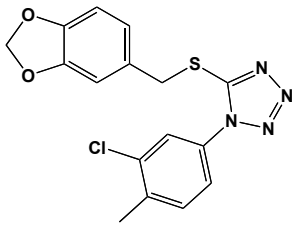	>200	>200	-
258	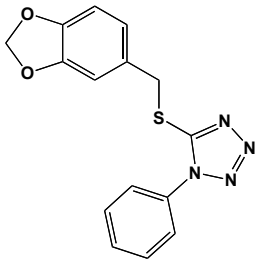	>200	>200	-

Compound number	Chemical structure	EC_{50} (µM)	EC_{90} (µM)	CC_{50} (µM)
259	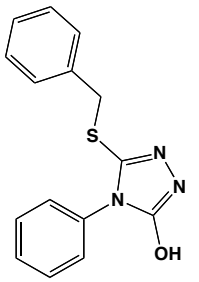	>200	>200	-
260	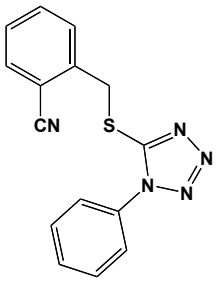	>200	>200	-
261	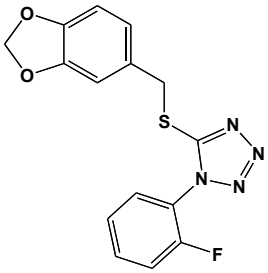	>200	>200	-
262	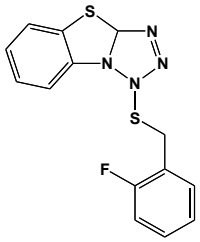	>200	>200	-
263	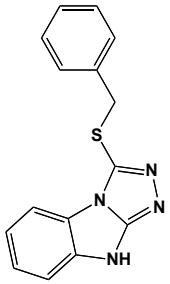	>200	>200	-
264	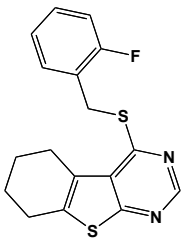	>200	>200	-

Compound number	Chemical structure	EC_{50} (µM)	EC_{90} (µM)	CC_{50} (µM)
265	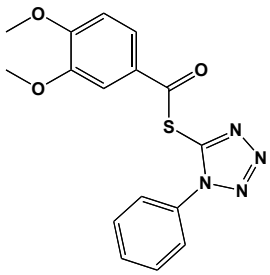	>200	>200	-
266	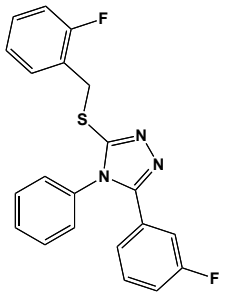	>200	>200	-

Structure-Based Virtual Screening on the CVB3 3D polymerase

Compound number	Chemical structure	EC_{50} (µM)	EC_{90} (µM)	CC_{50} (µM)
267	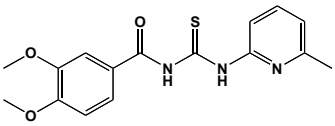	>200	>200	-
268	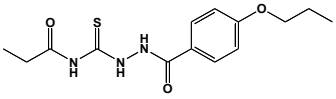	>200	>200	-
269	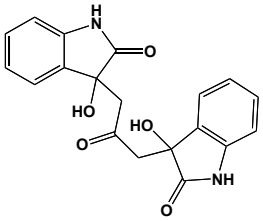	>200	>200	-
270	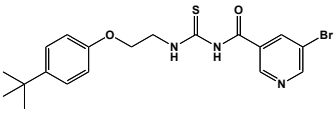	>200	>200	-
271	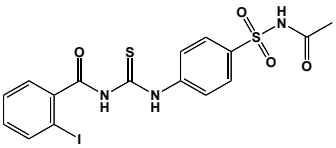	>200	>200	-
272	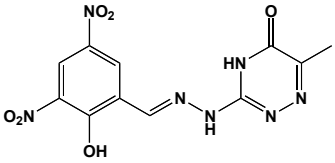	>200	>200	-
273	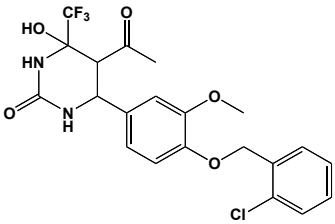	>200	>200	-
274	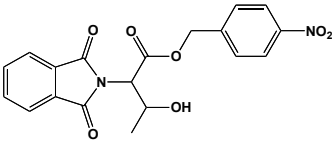	>200	>200	-

Compound number	Chemical structure	EC_{50} (µM)	EC_{90} (µM)	CC_{50} (µM)
275	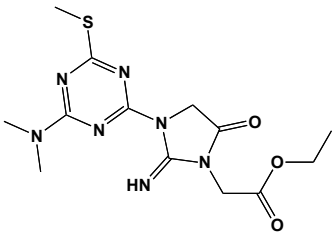	>200	>200	-
276	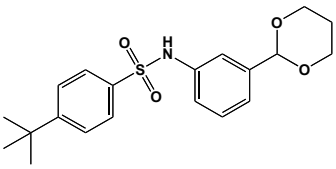	>200	>200	-
277	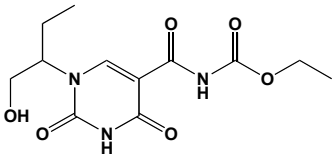	>200	>200	-
278	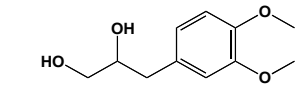	>200	>200	-
279	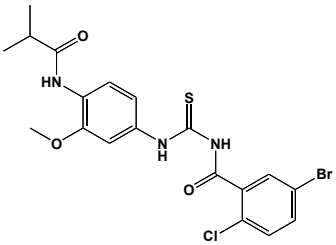	>200	>200	-
280	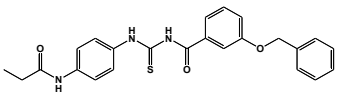	>200	>200	-
281	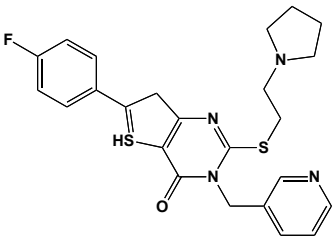	>200	>200	-
282	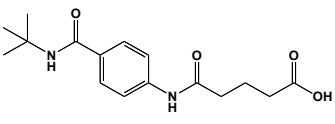	>200	>200	-

Compound number	Chemical structure	EC_{50} (µM)	EC_{90} (µM)	CC_{50} (µM)
283	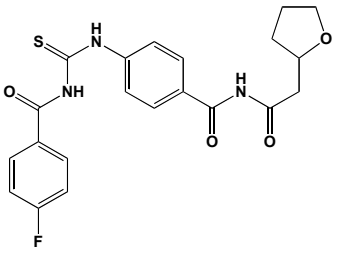	>200	>200	-
284	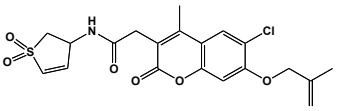	>200	>200	-

Ligand-Based Virtual Screening on GPC-N114

Compound number	Chemical structure	EC_{50} (µM)	EC_{90} (µM)	CC_{50} (µM)
285	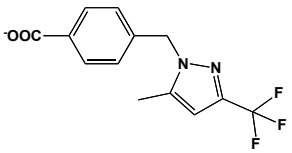	>200	>200	-
286	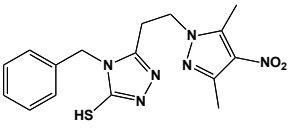	>200	>200	-
287	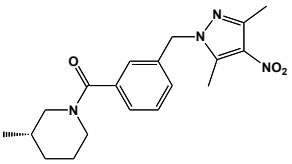	>200	>200	-
288	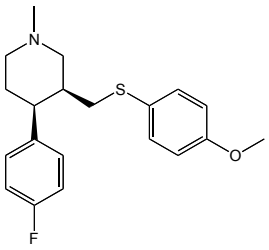	>200	>200	-
289	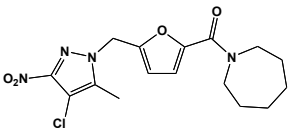	>200	>200	-

Compound number	Chemical structure	EC_{50} (µM)	EC_{90} (µM)	CC_{50} (µM)
290	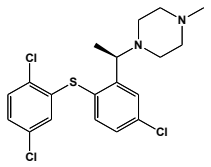	>200	>200	-
291	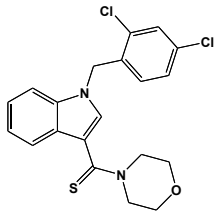	>200	>200	-
292	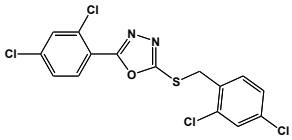	>200	>200	-
293	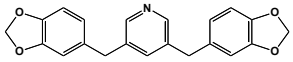	>200	>200	-
294	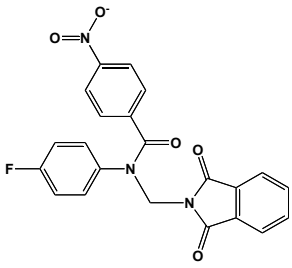	>200	>200	-
295	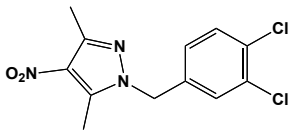	>200	>200	-
296	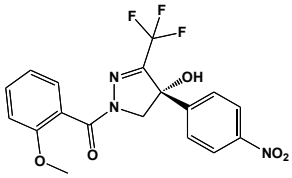	>200	>200	-
297	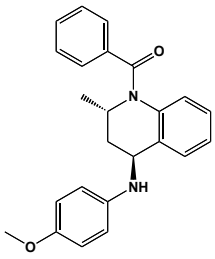	>200	>200	-

Compound number	Chemical structure	EC_{50} (µM)	EC_{90} (µM)	CC_{50} (µM)
298	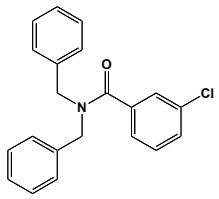	>200	>200	-
299	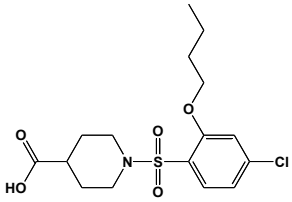	>200	>200	-
300	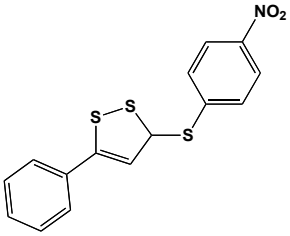	>200	>200	-

Structure-based virtual screening on the FMDV 3D polymerase

Compound number	Chemical structure	EC_{50} (µM)	EC_{90} (µM)	CC_{50} (µM)
301	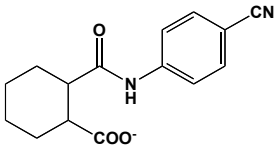	>200	>200	-
302	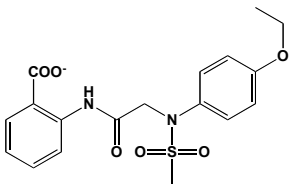	>200	>200	-
303	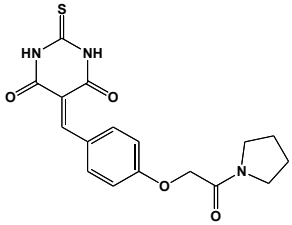	>200	>200	-
304	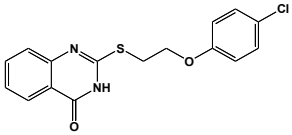	>200	>200	-
305	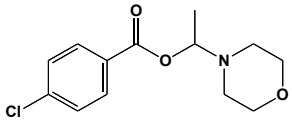	>200	>200	-
306	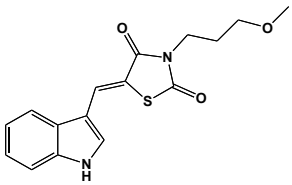	>200	>200	-
307	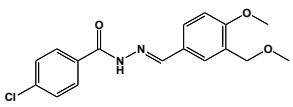	>200	>200	-
308	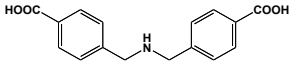	>200	>200	-
309	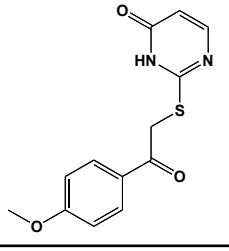	>200	>200	-

Compound number	Chemical structure	EC_{50} (μM)	EC_{90} (μM)	CC_{50} (μM)
310	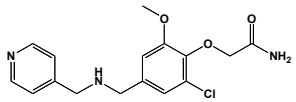	>200	>200	-

Structure-based virtual screening on the M2-1 protein

Compound number	Chemical structure	IC_{50} (μM)	CC_{50} (μM)
311	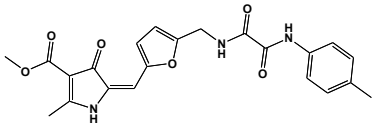	57	NA*
312	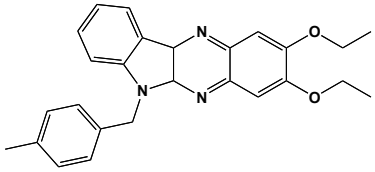	-	-
313	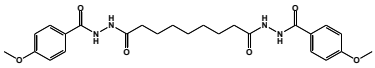	NI**	NA
314	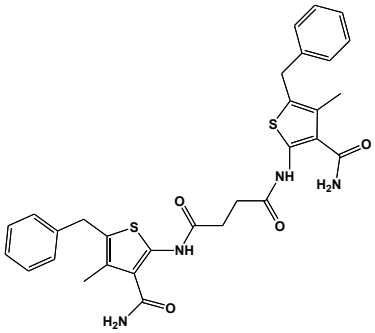	NI	44
315	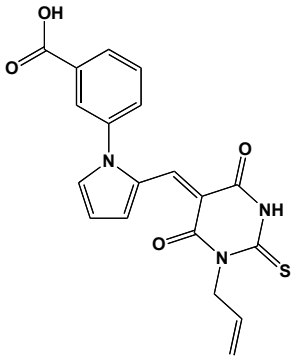	NI	22

Compound number	Chemical structure	IC_{50} (µM)	CC_{50} (µM)
316	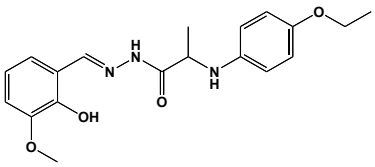	17	22
317	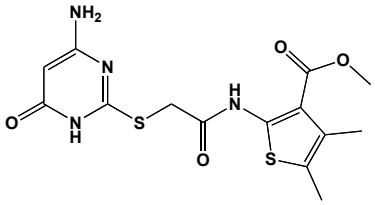	NI	NA
318	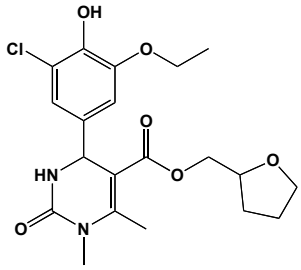	70	NA
319	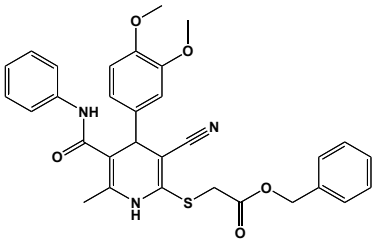	NI	95
320	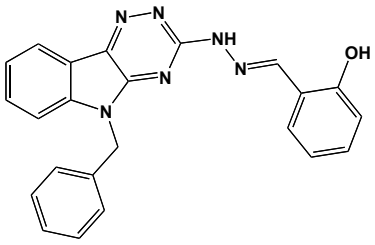	-	-
321	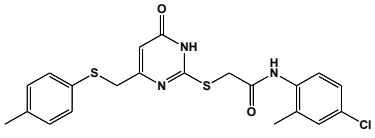	37	39

Compound number	Chemical structure	IC_{50} (µM)	CC_{50} (µM)
322	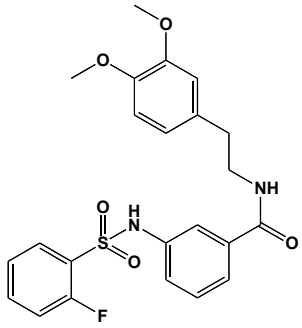	NI	NA
323	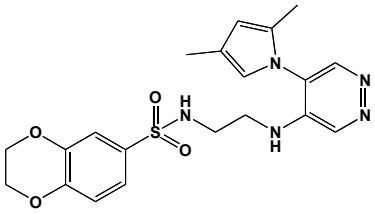	NI	NA
324	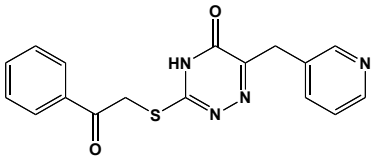	NI	101
325	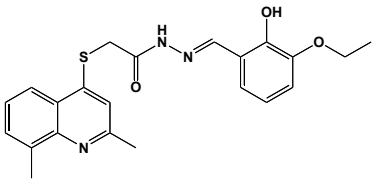	12	28
326	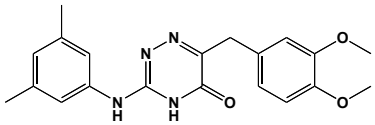	21	30
327	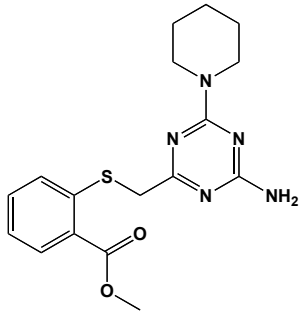	6	39

***NA:** not affected

**** NI:** no concentration-dependent inhibition

Ligand-based virtual screening on the TMC-353121

Compound number	Chemical structure	EC_{50} (µM)	CC_{50} (µM)
328	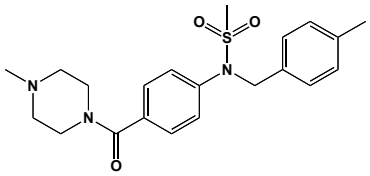	NI*	NA**
329	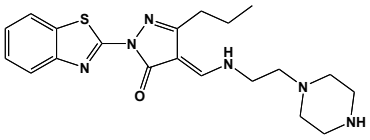	NI	NA
330	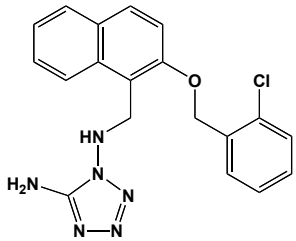	52	54

* **NI:** no concentration-dependent inhibition

** **NA:** not affected